Nanomedicine and Nanotoxicology

Surender Kumar Sharma
Hamed Nosrati
Taras Kavetskyy *Editors*

Harnessing Materials for X-ray Based Cancer Therapy and Imaging

Springer

Nanomedicine and Nanotoxicology

Series Editor

V. Zucolotto, Institute of Physics São Carlos, University of São Paulo,
São Carlos, São Paulo, Brazil

"Nanomedicine and Nanotoxicology" is a book Series dedicated to the application of Nanotechnology to achieve breakthroughs in healthcare as well as its risks and impact on the human body and environment. This book Series welcomes manuscripts on in vivo and in vitro diagnostics to therapy including targeted delivery, magnetic resonance imaging (MRI) and regenerative medicine; interface between nanomaterials (surfaces, particles, etc.) or analytical instruments with living human material (cells, tissue, body fluids); new tools and methods that impact significantly existing conservative practices; nanoparticles interaction with biological systems, and their risk assessments; among others. To submit a proposal or request further information, please contact Dr. Mayra Castro, Editor Applied Sciences, via mayra.castro@springer.com

More information about this series at https://link.springer.com/bookseries/10620

Surender Kumar Sharma · Hamed Nosrati ·
Taras Kavetskyy
Editors

Harnessing Materials for X-ray Based Cancer Therapy and Imaging

Springer

Editors
Surender Kumar Sharma
Central University of Punjab
Bathinda, India

Taras Kavetskyy
John Paul II Catholic University of Lublin
Lublin, Poland

Hamed Nosrati
Zanjan Pharmaceutical Biotechnology
Research Center
Zanjan University of Medical Sciences
Zanjan, Iran

ISSN 2194-0452 ISSN 2194-0460 (electronic)
Nanomedicine and Nanotoxicology
ISBN 978-3-031-04070-2 ISBN 978-3-031-04071-9 (eBook)
https://doi.org/10.1007/978-3-031-04071-9

This Springer imprint is published by the registered company Springer Nature Switzerland AG
The registered company address is: Gewerbestrasse 11, 6330 Cham, Switzerland

Contents

X-rays Based Bioimaging Techniques and Scintillating Materials

Gopal Niraula, Jason J. A. Medrano, Mohan C. Mathpal, Jero-R Maze, Jose A. H. Coaquira, and Surender K. Sharma

Abstract X-ray scintillators are broadly connected in cancer radiotherapy, warm treatment, and clinical diagnosis as therapeutic imaging materials since of their astonishing penetration control in tissues and organs. These X-ray energized scintillators can be focused on in cancer-site which retain and change over X-rays into unmistakable light outflows and diminishes the chance of overdose X-ray presentation to the typical cells. A few X-ray-based strategies have been illustrated for non-invasive high-resolution imaging of thick natural examples. These methods are undertaking to enhance our understanding and in situ natural chemistry and illness pathology examinations. In this chapter, we show those X-ray-based procedures and as of late outlined X-ray energized scintillators to offer an outline of such materials for the therapeutic diagnosis, imaging, and treatment.

G. Niraula · S. K. Sharma (✉)
Department of Physics, Federal University of Maranhao, Sao Luis, MA 65080-805, Brazil
e-mail: surender.sharma@ufma.br; surender.sharma@cup.edu.in

G. Niraula · J. A. H. Coaquira
Laboratory of Magnetic Materials, NFA, Institute of Physics, University of Brasilia, Brasilia, DF 70910-900, Brazil

J. J. A. Medrano
Institute of Physics, University of Brasilia, Brasilia, DF 70910-900, Brazil

M. C. Mathpal · J.-R. Maze
Instituto de Física, Pontificia Universidad Católica de Chile, Casilla 306, 7820436 Santiago, Chile

S. K. Sharma
Department of Physics, Central University of Punjab, Bathinda, Punjab 151401, India

S. K. Sharma et al. (eds.), *Harnessing Materials for X-ray Based Cancer Therapy and Imaging*, Nanomedicine and Nanotoxicology,
https://doi.org/10.1007/978-3-031-04071-9_1

1 Introduction

Since the development of nanoscience and its application in technology, so-called 'nanotechnology', from industry to biomedicine, nanomaterials and the relevant instrumental devices are the centered point of research. The advancement in each technology is a natural process in research which gives more precise, accurate and updated information's, and the methods to apply to the practical use. In particular, biomedical imaging is a focal technique at the in-vivo anatomic, structural, and functional visualization of inside-organs in a non or minimally invasive way. X-ray imaging is established as a strong imaging technique since the discovery of X-rays in 1895. Since then, a novel imaging techniques based on X-rays, such as radiography, fluoroscopy, computed tomography (CT), and single-photon computed tomography (SPCT) are developed which requires extremely sensitive materials/scintillators to enhance the image quality while minimizing radiation induced health risks to patients [1–5]. Recently, positron emission tomography (PET) showed its highly sensitive nature at the picomolar level that allows in-vivo molecular-imaging-based precise diagnosis.

Scintillators are energy conversion materials which absorb and translate X-rays radiations into the visible light region. Control Synthesis of novel X-rays induced scintillators tuning their luminescence properties is a rising field of current research. In this scenario, the idea of integrating the quick response toward X-rays with big absorption cross-section stemming from the thickness and relatively high mass density exhibited a good sensitivity in single-crystal perovskite-based scintillators under keV X-ray radiation. The lead-halide perovskite single crystal scintillators display a short absorption length and high detection efficiency to X-rays [6]. On the other hand, organic scintillators are observed having a weak detection of high-energy radiations because of their relatively low density of chemical constituents [7]. Organic crystals like naphthalene, stilbene and anthracene showed very weak detection capacity of higher-energy X-rays [8, 9]. However, they possess high attenuation constants that help them to act as excellent scintillator candidates for β rays and hot neutrons. To enhance their detection, heavy metal ions can be adopted to construct organic–inorganic based scintillators because of high energy resolution and energy-conversion efficiency of these metal ions [10]. Thus, this chapter presents a brief overview of techniques used in medical imaging, namely, radiography, fluoroscopy, angiography, and computed tomography as well as recent developed X-ray detectors/scintillators which show convincing results in terms of sensitivity and serve as an excellent candidate for medical imaging.

2 An Overview of X-ray: Discovery and Road Towards Biomedical Imaging

With the discovery of X-rays on 8 November 1895, the great revolution in the cognition of physical world is started. The discovery of X-rays was interesting as it was found incidentally while Wilhelm Conrad Rontgen was studying the behavior of cathode rays in Hittorf-Geissler-Crookes (HGC) tubes at his own laboratory. While busy with his experiments, unknowingly one day he observed that some crystals lying close to the HGC tube had become intensely fluorescent produced by a hitherto unknown radiation. After the spent myriad of breathless night, he confirmed that this could not be due to cathode rays; cathode rays are fully absorbed either by the glass wall of the tube, or by the air and thus introduced as an X-rays. The fluorescence stimulation in different crystals depends upon the voltage used, for instance, fluorite is a fine and suited crystal for 'soft' cathode rays, whereas barium platino cyanide fluorescing strongly under the bombardment of 'hard' cathode rays. The high energy X-rays, also referred as 'hard' X-rays, contain the component of short wavelength that amplify the penetration into thick objects or those with large object densities. Similarly, the low energy X-rays, referred as 'soft X-rays' component comprises the longer-wavelength X-rays which enhance the image contrast. The 'soft X-rays' are responsible to produce beam hardening corrections that can be applied to reduce their effects on the resulting X-ray image [11, 12]. The X-rays was the first in a series of three discoveries; X rays, uranium rays, and the electron, i.e., the study of the discharge of electricity in gases. These three physical discovery have immense contribution on the transformation of physical world of nanoscience and nanotechnology. The X-rays originate from the bright fluorescence on the tube where the cathode rays strike the glass and spread out. The point of origin of the X-rays moves in straight lines by a magnetic field, and their absorption depends on the material through which they pass, but the X-rays themselves are insensitive to the magnet. In principle, X-rays are produced by ionizing a target source, such as tungsten, with an electron beam at very high speed and retarded instantly. In this process, the electrons are discharged from a cathode and accelerated toward an anode by a high voltage potential between the cathode and anode. once the electrons strike with the anode, they start to decelerate accompanying by the emission of electromagnetic radiation. The energy spectrum emitted from the X-ray tube is a function of the voltage potential, target material, the angle at which the electron beam strikes with the target, the angle at which the X-rays are observed, and the material used for the X-ray tube window [13–15].

After the discovery of X-rays and its experimental verification, Roentgen's and Dr. Henry W. Cattell, Demonstrator of Morbid Anatomy at the University of Pennsylvania have demonstrated the X rays to locate bullets in human flesh and photograph broken bones and confirmed their importance for the diagnosis of kidney stones and cirrhotic livers, stating that "The surgical imagination can pleasurably lose itself in devising endless applications of this wonderful process." This was the key step to move forward the application of X-rays in medical sciences. Röntgen

demonstrated the medical use of X-rays with taking a picture of his wife's hand on a photographic plate formed. It was the first photograph of a human body part using X-rays. The first use of X-rays for a surgical operation was implemented on February 14, 1896 [16]. This success of the first medical applications contributes not only to the lives of humanity but also open the industrial possibility in medical science and technology. Imaging techniques is one of the great and finest achievement of physical science which provides an interface between vision and intuition. Especially, biological imaging has taken a wide space in human lives, not only to understand the fundamental biology in nature but also due to extensive use in medical science, i.e., biomedical imaging in view of its ability to aid analysis and diagnosis through X-ray images at the molecular and cellular levels [5, 17]. X-ray imaging is a noninvasive measurement techniques used extensively for the evaluation of static objects, visualize and characterize the complex internal structures. The several techniques can be used to detect an X-rays. Initially, it was detected through film-based techniques; however, with the time, researcher successfully designed a new system where digital detection can be achieved through electronic detector [18]. There are two types of detectors: direct conversion and indirect conversion detectors. In case of direct conversion detectors, X-ray photons are directly converted into an electrical charge with the help of an X-ray photoconductor (e.g., amorphous selenium). On the other hand, in case of indirect conversion detectors, first a scintillator converts incident X-rays to visible light, and then this obtained light is converted to an electrical signal through a photodetector. In both cases, the output signal from these devices is sensed by an electronic readout mechanism with an analog-to-digital converter to yield digital image. The X-ray imaging systems, for example, old computed tomography systems, scintillators are used to convert X-rays to visible light; the visibility of light depends on the X-ray energy. The linear scintillator simply facilitates for the electronic absorption of individual signal to quantify the X-ray intensity of a fan beam through a horizontal plane [19, 20].

3 X-ray Imaging and Application in Medicine

The use of X-ray in medical imaging is under two categories: structural imaging, which reveals anatomical structure i.e. imaging of bone, teeth, microcalcinations, lungs, and orthopedic devices, and functional imaging which track the main changes in biological function, such as metabolism, blood flow, regional chemical composition and biochemical processes. However, endogenous soft tissue types are difficult to distinguish using conventional X-ray projection imaging. Distinguishing tissue types for functional imaging requires either exogenous contrast agents (e.g., radiopaque agents to view vasculature and flow in angiography), or technique that are more sensitive to tissue differences (or both).

3.1 Radiography

Radiography is an application of X-ray imaging used in medical science. The foremost aim of radiography is the inspection of ruptures, cracks the internal structures of the body and their effects/changes in the skeletal system. In addition, this technique is used to perceive the changes of a bone's consistency or density, e.g., in case of osteoporosis or bone cancer. Radiography creates two dimensional projection images by exposing an anatomy of interest to X-rays and record the photograph of the X-ray attenuation map of an object when passes through the object. X-ray images are processed in a similar way of conventional photographic film in which shadow of an object are analogized. The lighter shadow images are related to the object areas of greatest density. The X-ray attenuation map of an object/materials has great role on the development of contrast in the radiograph and hence better images quality. The obtained contrast in the radiograph usually reduced by the consequence of the X-ray absorption and X-ray scattering. The X-ray absorption is always varying with the X-ray energy level, whereas X-ray scatter cause a general fogging of the image; as a consequence, reduces the brightness and sharpness, clear contrast, and the resolution. Such scattering is possible to reduce by passing the X-ray through a metal filter before to reach the object of interest that, obviously, lessen the quantity of soft X-rays reaching to the object [15]. On the other hand, advance digital detectors use to capture the X-ray intensity that produce images. Digital radiography improved the sensing capacity of 2D sensor arrays and computer power of receiving, processing, and displaying the large data sets. The advantages of digital radiography, as compared to the conventional film, is the speed of image obtained and the pliability in manipulating and accumulating those images.

There are several techniques of radiography imaging process which are used for a specific purpose from industrial technology to nanomedicine; among them, X-ray radiography for flow visualization (XRFV) and Flash X-ray radiography (FXR) are widely used. The XRFV is extensively used in myriad industrial applications, such as power generation, pharmaceutical production, fuel production, and mineral and powder processing. The working mechanism is based on gas/liquid flowing through a granular bed at an ample velocity to suspend the particles, where these granular beds have ability of uniform mixing, low pressure drop, high heat and mass transfer rates. On the other hand, the flash X-ray radiography (FXR) is an imaging process where strong burst of irradiation is induced for a second that records a high-speed events obscured by light. In addition, FXR helps to seize the images of voids inside opaque objects that are scrap of these dynamic events. These FXR are often used in medical imaging for biological studies [21–23].

3.2 *Fluoroscopy*

The fluoroscopy technique is a very essential in minimally invasive intercessions, where the different tool such as catheters and endoscopes need to be guided to operate the system without direct visual contact to the intercession region. Moreover, this is the technology to visualize internal organs/vessels, for instance arteries or veins using scintillators as a contrast agent; as a result, fluoroscopy is also referred as a positive contrast technique having a low background and highly sensitive to low elemental concentrations [24, 25]. In principle, during the absorption of X-ray photon by an atom, small part of its energy reemit as a secondary X-ray fluorescence (XRF). In this process, binding energy and nuclear charge are key factors; the binding energy is proportional to the square of nuclear charge and the emitted photon energy is characteristic of each element. The scanning of the specimen and acquisition of X-ray yields quantitative topographical maps for a wide range of elements, that allow the quantitative elemental analysis, including most biologically relevant transition metals. Taking an advantage of the elemental quantification/composition using nuclear charge of elements [26], this technique is applying to find the metal toxicity [26, 27], uptake and distribution of metallopharmacueticals [28], intracellular elemental distributions in biological samples[2, 29–31], and in vivo to non-invasively evaluate the concentration in the bones, human skin, and iodine in the thyroid [32–34]. The image from a fluoroscopy sequence can be depicted by the placement of the two electrodes and wires of a heart pacemaker. A precise and accurate clinical setup is very essential for a minimally invasive surgery where the X-ray imaging unit is given by a C-arm scanner that can be freely positioned around the patient. Conventional radiography typically refers to the acquisition of a single or small number of X-ray projection images for a specified view. In contrast, fluoroscopy describes a sequence of radiographic images acquired periodically at a certain frame rate. The X-ray source can either be triggered for each frame or simply provide a constant radiation exposure to the region of interest. Potential X-ray detectors can be image intensifiers. The frame rate is typically limited by the acquisition speed of the detection system. For image intensifiers, it is given by the inertia of the final fluorescent screen. In practice, frame rates of 30 frames per second are possible. However, rates are often reduced for dose reasons. In brief, fluoroscopy is a promising procedure because it is less invasive, substantially reducing the risk of infection or skin injury due to iatrogenic radiation, compared to conventional surgical procedures, being able to use dose metrics to develop adequate follow-up and management plans for the patient [35].

The use of the fluoroscopic technique came after the discovery of X-rays, where in the beginning the operating mechanisms of these equipment was limited due to technological factors: such as low-quality film emulsions and X-ray tubes that were not very reliable in their functioning. For this reason, fluoroscopy appeared as a more promising and probably more important alternative than radiographic techniques. Subsequently, the equipment improved and fluoroscopy began to occupy an extremely important role in imaging examinations and that it is still in force today, in other words, the study and detection of moving parts, dynamic examinations, interventionism, angiography, make this technique be of great acceptance

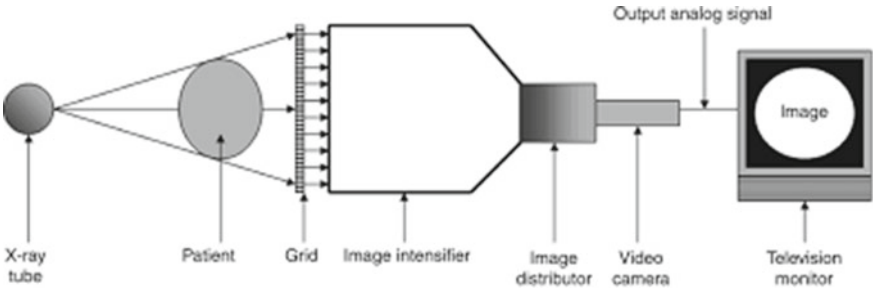

Fig. 1 Representation of a fluoroscopy equipment with image intensifier. Reprinted with permission of Ref. [38]

[24, 25, 36]. The main difference between radiography and fluoroscopy is that the latter uses a much lower X-ray fluency rate, but for a much longer time. Through this technique a continuous image is produced allowing the observer to see dynamic changes within the patient such as moving organs or flow of contrast media through blood vessels, digestive system. The principle of fluoroscopic imaging is in the ability of X-rays to cause fluorescence in a phosphor-like material. A fluoroscope basically consists of two components: An X-ray tube and a fluoroscopic screen. The tube and the screen are mounted facing each other in an aligned way, (see Fig. 1). In this way the operator moves the fluoroscopic screen along the patient and the tube follows the screen. X-ray photons that pass through the patient interact with the screen, producing photons of light that reach the observer [37].

Certain limitations must be considered due to this arrangement, such as, for example: images with a very low brightness, three or four orders of magnitude lower than that of a conventional radiograph. The possibility of increasing the X-ray rate is not feasible either because this would mean doses that are clearly intolerable for patients and also very high for the observer himself. Therefore, the fluoroscopic image can only be viewed without ambient lighting, in the dark, with the consequent loss due to the vision characteristics of the human eye and the inconvenience of adaptation to darkness. The result is a very poor quality image. The only way to significantly improve this quality without excessively increasing the doses to patients is by using a system that amplifies the light from the screen: the image intensifier.

Fluoroscopy is demonstrated in several types of experiment including cardiac catheterization [39], lumbar puncture, arthrography, placement of intravenous catheters, and biopsies. Further applications of fluoroscopy include foreign body localization, injecting image-driven anesthesia into the spine, and in percutaneous vertebroplasty [40]. The use of nanoparticles have shown very promising results that suffused into bio-degradable filters made up of poly-p-dioxanone (PPDO) could amend device radiopacity without any unexpected effects on device efficacy and safety, in swine models [41]. This demonstrates the continuous effort to improve procedures and add the use of new nanomaterials to optimize results. The most common applications are:

In Diagnosis:

- Digestive system: swallowing studies, esophagograms, intestinal transit, laparoscopies, barium enema, transcutaneous liver biopsies, enteroclysis.
- Urology: cystography, diagnostic percutaneous nephrostomy, percutaneous excretory urogram.
- Gynecology: hysterosalpingography.
- Neurology: myelograms.
- Cardiology: angiograms of vessels of the lower extremities, heart and brain; intracardiac electrophysiological study (EPS).
- Traumatology: arthrography, post-surgical control.

In Treatment:

- Placement of endoprostheses: esophageal, biliary, urethral stents, intravascular stents.
- Infiltrations: especially common in intra and periarticular drug infiltration (anesthetics, corticosteroids, contrast solutions).
- Dilation of vascular, digestive or urological stenosis.
- Guided surgery: biopsies, vertebroplasties, tumor removal (especially in delicate locations), kidney surgery, nephrostomy, placement of pacemakers and cardiac defibrillators, angioplasties, urological surgery (especially in retrograde pyelography).

The use of fluoroscopy is usually considerable in regards of safety concerns. However, the risks arise due to the accumulated radiation from number of X-ray test or treatments for a long period [42]. For a fluoroscopy patient, it is important to consider whether the patient suffers from any type of allergies to the substance to be administered or any history of allergic reactions. Patients who are allergic to any remedy, iodine, latex, or contrast environments are at a higher risk of developing an allergic reaction. It is not recommended that pregnant women be exposed to this type of procedure with fluoroscopy due to the risk that it can affect the fetus.

3.3 Angiography

Angiography is a technique that consists of filling the vessels of the circulatory system with a contrast agent, that is, a good absorber of radiation that produces a visible shadow in the image. This substance is injected into the area to be explored, using needles or guiding a catheter under fluoroscopic control. To perform the test, anesthesia is applied to the site where the catheter will be inserted, which is a small tube that is directed by the doctor to the site where you want to see the blood vessels, which is usually inserted in the groin or neck. After the catheter is inserted into the site to be tested, a contrast agent is injected and then several X-rays are taken on the X-ray machine. The contrast liquid, when exposed to X-rays, will be shown on the monitor image with a different color from the images taken, which allows observing the

patient's circulatory system. During the exam, the patient remains awake, but since it is necessary to remain as still as possible, the doctor may apply medication to sedate the patient. This procedure can take about an hour. After this time, the patient does not necessarily need hospitalization, since general anesthesia is not used. In some cases, it may also be necessary to suture and place a dressing where the catheter was inserted. At present we can find more modern equipment, where characteristics such as road mapping (in which the interventional doctor can use images with contrast and digital subtraction previously acquired to use them as a way to introduce catheters with diameters less than 1 mm without using more contrast), have greatly facilitated angiographic and interventional procedures [43, 44].

Another advantage currently used is the use of pulsed fluoroscopy, where the duration of the examination is much shorter and also the amount of dose administered to the patient is less, thus obtaining a good quality image.

In general, this equipment consists of a C-arm suspended from the ceiling or anchored to the ground that incorporates the X-ray tube and the image receptor system. This arch can be moved in almost all directions to allow as many views of the patient as possible. This is placed on a lifting table, with a flat, floating and sliding tabletop that allows easy access to the patient. A mobile device with two or more TV monitors allows the specialist to follow the image in real time while performing the examination or to view the dynamic series previously obtained (see Fig. 2).

Currently there are high-end models where the use of dynamic flat panels as image receptors has notably improved the performance of this equipment, considerably improving the quality and contrast of the image, in addition to the fact that the mass and volume lightening of the arc allows a remarkable agility with faster and more precise movements. Relatively recent developments such as so-called rotational angiography in which the image receptor-tube assembly (or assemblies) rotates around the patient at high speed, taking pulsed images while a contrast medium is injected into the patient, have been incorporated into current teams. In this way the images are processed and displayed as a video sequence with the advantage that the vascular tree can be seen from different orientations with a single injection of contrast [46, 47]. One step further is the possibility of performing a 3D reconstruction of the vascular tree. In recent years, the equipment has incorporated the possibility of obtaining tomographic sections, as well as those obtained with a computerized tomography, using the digital image detector itself.

In a large number of surgeries, fluoroscopy or X-ray imaging is required during the surgeries. The transfer of the patient to obtain an X-ray, or the installation of a permanent X-ray equipment, being unfeasible, which can make interventions in which X-rays are not required due to space issues. For this situation where the use of fluoroscopy is necessary to guide a catheter or an endoscope, there are mobile radio surgical arches. They are so named because of the appearance of the X-ray tube and image receptor as a C-arc (See Fig. 3), with both parts always aligned and at a fixed distance (90–100 cm). In this way, the patient can be positioned between the tube and the intensifier and access to the examination site is relatively free. This arch is mounted at the end of an extendable arm anchored to the foot of the equipment that includes the X-ray generator and the console with the controls. Said foot has wheels

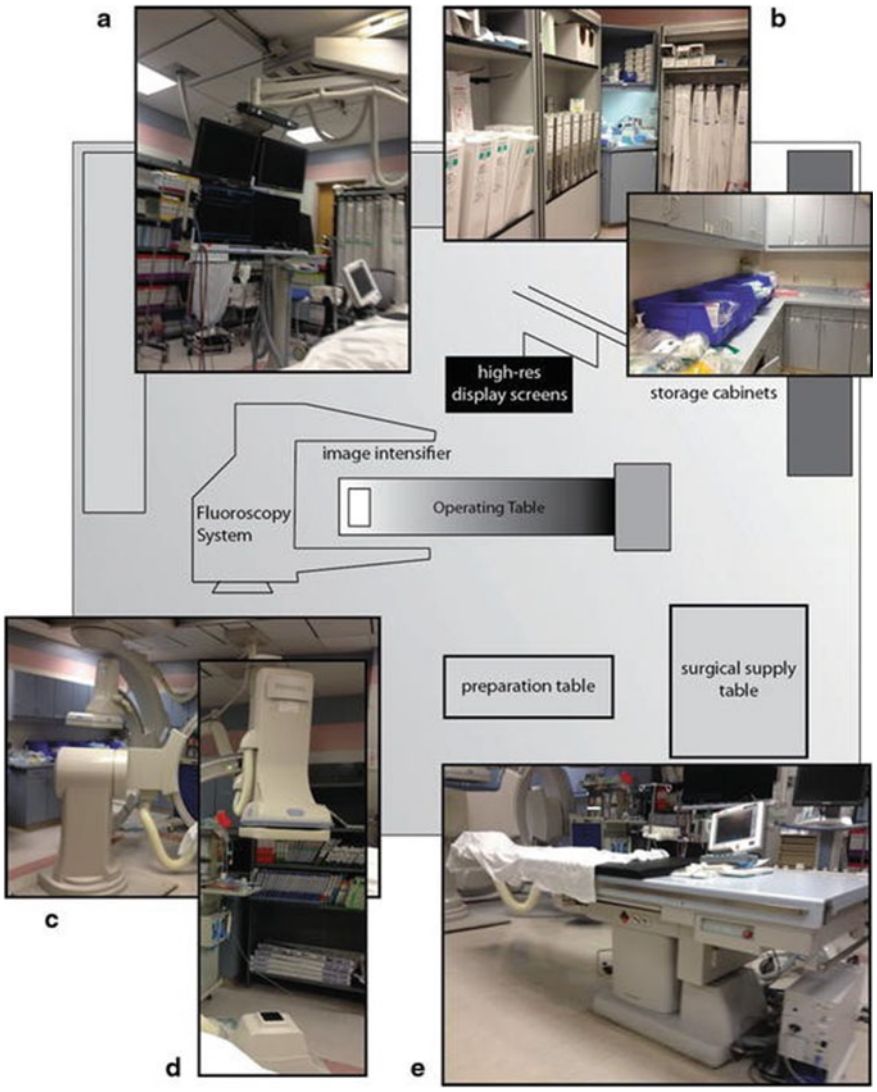

Fig. 2 Representation of an angiography equipment. Reprinted with permission of Ref. [45]

which allow the movement of the whole equipment. Due to the need for space and their good performance, all current arches incorporate high-frequency generators, which also allows the use of pulsed fluoroscopy.

The use of nanomaterials is increasingly present in biomedical applications. Composite of nanoscale zero-valent iron in ordered mesoporous carbon (nZVI@C) are being used in trials to improve image quality in Magnetic Resonance Angiography studies. In addition, this material did not show deleterious effects on cells [49].

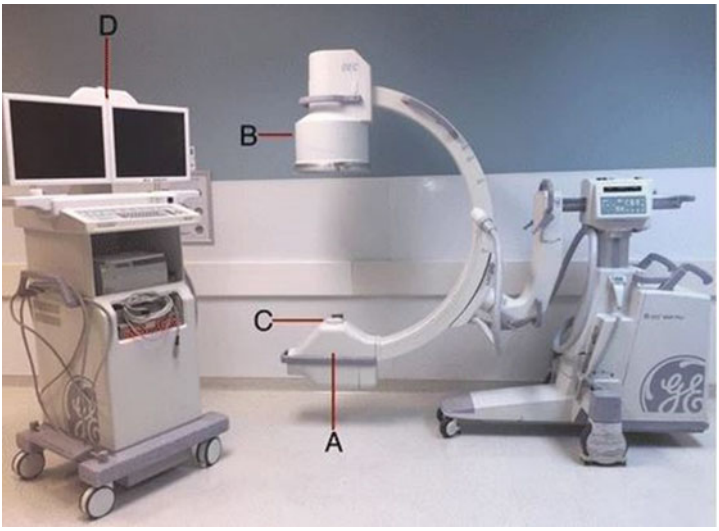

Fig. 3 Mobile C-Arm used in angiography; **A** X-ray Tube; **B** Image Intensifier; **C** Collimator; **D** Display Monitor. Reprinted with open access permission Ref. [48]

Currently some kind of ferrites like as $ZnFe_2O_4$ are explored as the contrast agent for magnetic resonance angiography, due to his higher transverse relaxation time. First assays are being in rats. Results show an increase in image contrast using nanoparticles $ZnFe_2O_4$ smaller than 6 nm [50]. Procedures that use angiography range from intravenous or arterial injections to angioplastic techniques that use balloons, stents, and other devices to unclog blood vessels and reinforce the internal structure of damaged arteries. Modern angiography units are equipped with a variety of the latest developments in fluoroscopic imaging technology including C-arms with fully movable image receiver and tube and a complete digital image acquisition system. In the hemodynamic units in which the coronary tree of the heart is explored, it is usual to use very high fluoroscopy and acquisition rates (25 images per second and even higher) to avoid the loss of spatial resolution due to the movement of the heart. On the contrary, in vascular radiology equipment the acquisition rate is not so critical, but the size of the image receptor (intensifier or flat panel in the most modern equipment), since many of the examinations are performed in the abdominal area or in the trunk of the patient. The most common risk from this test is an allergic reaction to the contrast medium that is inserted; however, the doctor usually has medications ready to inject if this happens. In addition, bleeding at the catheter insertion site or kidney problems may also occur due to the contrast medium (nephropathy) [51].

3.4 Computed Tomography

X-ray computed tomography (CT) can provide unmatched information on the internal structure of materials non-destructively from meter scales to tens of nanometers in length. It takes advantage of the penetrating power of X-rays to obtain a series of two-dimensional (2D) radiographs of the object seen from many different directions. This process is sometimes called a CT scan [52]. CT should not be confused with conventional X-ray radiology, which also allows two-dimensional visualization, but with much less detail, because the different structures of the body are superimposed on the same image, because the radiation is emitted from a single image. diffuse shape. On the other hand, for CT a very well-directed beam is used and with a certain thickness, which depends on the size of the structure to be studied, and can vary from 0.5 mm to 20 mm. The development of new, more sophisticated equipment obeyed a need, since with the first scanners for clinical use, data was acquired, for example, from the brain in approximately 4 min, two contiguous sections, and the calculation time was about 7 min per image. Shortly afterwards, scanners applicable to any part of the body were developed; First they were axial scanners, with a single row of detectors, and from these it was moved to helical or spiral scanners, which later allowed the use of equipment with multiple rows of detectors, whose clinical use has reached wide diffusion today [52, 53].

Today, specially designed CT scanners are available for certain clinical applications. Thus, there are specific CT equipment for planning radiotherapy treatments. Another current example is the integration of CT scanners in applications that include various imaging techniques; for example, by hybridizing a CT scanner with a positron emission tomography (PET), or with a single photon emission tomography (SPECT) [54].

Axial computed tomography is the first equipment used or called “first generation”, they use parallel beam geometry and a translation-rotation movement. The X-ray beam is highly collimated and, after passing through the section of interest of the patient, it strikes a pair of scintillation detectors each coupled to a photomultiplier tube. The emitter-detector assembly, integrally joined, moves through 160 positions, thus obtaining different measurements [55]. The most recent equipment is often described as “rotation only” or “rotation-stationary”, since it is now only the X-ray tube that rotates around the patient while the detectors, which cover the entire 360° space, remain immobile during cutting (see Fig. 4).

Helical computed tomography has greatly improved CT performance. Some of the advantages of helical CT: scan time is shortened, and more consistent information is obtained to reproduce 3D images of the scanned volume. The main disadvantage of helical CT was the appearance of some associated artifacts (windmills, etc.) [57, 58]. Helical acquisition made it possible to obtain data from a large volume of the apnea patient, which was a prerequisite for the development of high-quality CT angiography. The displacement of the stretcher is generally expressed in relation to the nominal width of the beam (equal to the width of cut in single cutters); the quotient between the displacement of the stretcher in a 360° rotation of the tube

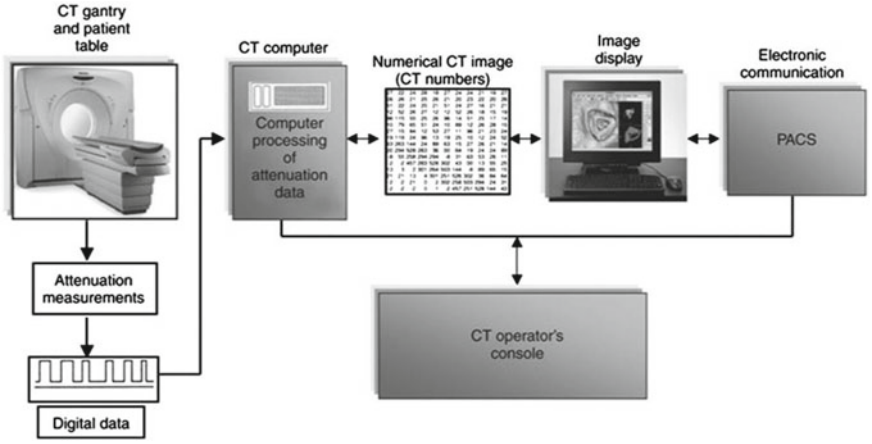

Fig. 4 Representation of computed tomography. Reprinted with permission of Ref. [56]

and the nominal width of the beam is called the pitch factor. Obviously, continuous scanning considerably reduces the exploration time, while allowing a more efficient use of the X-ray generating system. In return, as can be seen, the data collected in a complete revolution does not correspond exactly to any complete axial section, but the section moves continuously with the movement, also continuous, of the stretcher.

Multi-slice computed tomography, ten years after the introduction of helical CT, with the introduction of rapidly rotating multi-detector scanners, there was an enormous advance in CT technology that facilitated the emergence of new clinical applications. The first teams with 4 contiguous rows of active detectors, gave way to those with 16 and 64 rows respectively, which made possible the simultaneous acquisition of profiles of a large number of sections. In addition, the rotation time was reduced from 1–2 s, typical in single cutting equipment, to much lower values (0.3–0.4 s). Consequently, under these conditions it is possible to scan practically the entire body of an adult on inspiration with slice thicknesses well below 1 mm. With multi-detector CT equipment, acquisitions are usually made in helical mode. Exceptions are for high-resolution CT of, for example, lungs, and sequential acquisition on cardiac CT, either for coronary calcium calculation or for coronary CT angiography [59, 60].

An obvious difference between the different types of tomography can be observed in Fig. 5. It is possible to see the difference in tones in the images obtained, which allows more detailed information on the area of interest, allowing the doctor a decision on the most convenient treatment.

CT is used in diagnosis and in patient follow-up studies, in planning radiotherapy treatments. Diagnose different diseases and minor changes in various sectors of the human body. For example, a CT scan can evaluate a head injury or, because of its quick results, help find strokes. In addition, the procedure helps to detect tumors and infectious processes of different organs. The exam also detects important

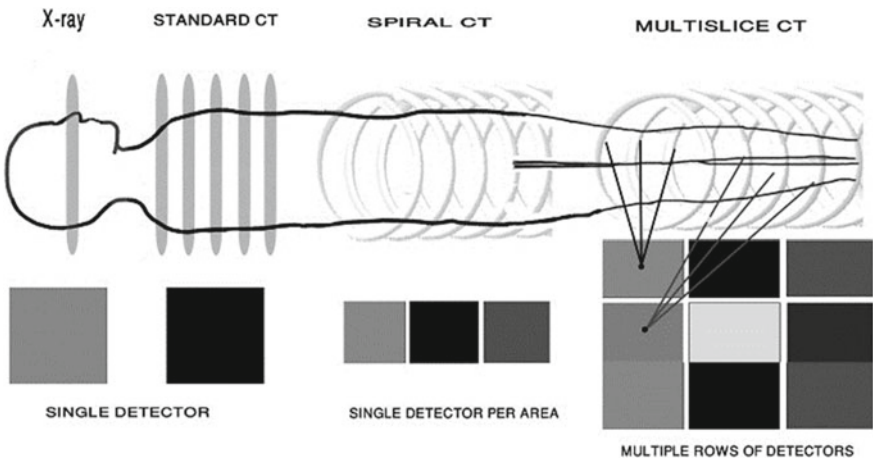

Fig. 5 Difference between techniques using computed tomography and X-ray. Reprinted with open access permission Ref. [61]

warning signs, such as bleeding, aneurysms, perforation of intestinal loops, and even heart attacks. It is well known that there is a growing concern for the care of the environment, this reflects efforts in nanobiotechnology, that is developing new processes for the synthesis of nanoparticles (green synthesis). Was reported the use of aqueous leaf extract of barley leaves during process of synthetic to obtained new gold nanoparticles (BL-Au), taking advantage of the fact that the extract of barley leaves has properties that act as a reducing agent during the synthesis process. Results of this assay using BL-Au nanoparticles in computed tomography with zebra fish showed Brightness image was still much stronger than Ultravist (component usually used in this process) [62]. Another interesting work used Au nanoparticles as contrast agent for computed tomography in mice, with different sizes of nanoparticles and found that larger Au nanoparticles provided strong liver and spleen contrast [63].

All X-rays deliver ionizing radiation, which has the potential to cause natural impacts within the human body. For patients, these biological impacts can run from an expanded hazard of cancer at some point in life, to conceivable unfavorably susceptible responses or kidney disappointment from contrast media. Beneath a few uncommon circumstances of delayed presentation to expansive dosages, x-rays can cause unfavorable wellbeing impacts such as blushing of the skin (erythema), harm to skin tissue, hair misfortune, cataracts, or birth abandons (in the event that they consider is carried out). carried out amid a pregnancy). For this reason, it is critical that CT checks are constrained to as it were those cases where the advantage that can be gotten essentially outweighs the increased hazard. This is often particularly genuine for children, who are more sensitive to ionizing radiation and have longer life anticipation and so have a generally higher chance of creating cancer than adults [64].

4 High Energy X-ray Sensitive Materials for Medical Applications

The strong penetrating power of invisible high energy X-rays allows them to scan the object and display the internal parts/structure/composition in medical imaging [65, 66]. In X-ray based imaging, Image contrast results from the variable signal detected when rays are absorbed, preventing the receptivity of the various organs/subjects to the radiation. Albeit, such rays are hardly perceived by ordinary photographic substrates, so studies are devoted to the search of scintillating materials with the properties of efficiently absorbing these rays and converting the absorbed X-rays into photon radiation emitted in the visible light range. Scintillators are special energy conversion materials that can absorb X-rays/γ-rays and convert them into the visible light range [67]. Although scintillators are unable to produce medical X-ray images straightly, they are advantageous due to their ability to reduce the radiation dose required for imaging. It is clear from the definition of 'high energy' that higher atomic numbers (Z) metals ion are needed to achieve high stopping power and noteworthy scintillation performance since they have high energy resolution and energy-conversion efficiency [10, 68].

4.1 Perovskite-Based Sensitive Materials

Perovskite-based nanomaterials (PNMs), such as $CaTiO_3$ and its diverse composition (ABX_3 where A and B represent as cations and X as anion) have been investigated persuasively in the last decades due to their tunable photoelectric properties, luminescent and electrical performance which allow these materials to be used in wide range of medical imaging [69–71]. Different energy conversion phenomena can be discussed in such X-ray perovskite-based detectors; in scintillator based detector, energy conversion takes place from X-ray to UV–Vis photon via down-conversion [72]. In addition, the absorption material has limited carrier diffusion length by which these materials are recommended to avoid in X-ray based scintillators [73, 74]. Considering those materials which exhibit limited/short absorption length but high detection efficiency to X-rays, Lead-halide based perovskite single-crystals are promising scintillators. The quick reaction toward X-rays with large absorption cross-section originated via physical factors, such as, thickness and relatively high mass density, made perovskite scintillators promising materials to enhancing the detection efficiency under keV X-ray radiation [6]. However, these materials show their better performance only on low temperature since they are sensitive to open environment, i.e., air and humidity since they are sensitive to these factor (air and humidity) [10, 75]. As compared to bulk perovskites, perovskites nano-scale materials have been demonstrated as a better processing capability for the fabrication of multifunctional thin films, flexible devices [76]. Furthermore, they exhibit a superior optical and electromagnetic properties because of their quantum effect and small-size effect

[77]. The use of high energy scintillators varies on the required fields. Particularly in X-ray imaging, following points should have to be considered: (a) high absorption coefficient which provides a considerable quality of imaging with reducing the dose amount, (b) highly luminescence yield which reduces the noise signal, (c) decay time should adjust in the range of CT scanners in $\geq$10 kHz, (d) absence of afterglow that causes sickle artifacts in the imaging, and (e) Low temperature dependence of the LY.

Several pattern of Pb-halide perovskites such as bulk crystals, thin films, nanoparticles and quantum dots can be prepared by chemical routes instead of ultra-high vacuum technique; which minimizes the cost within a reasonable range. As it is established, however, that Pb element is toxic that led towards the health threats in biomedical use. Besides, low resistance to the humidity and temperature reduces their sensitivity that evidently limit the application of interest. Recently, organic–inorganic hybrid Pb-halide perovskite-has been prepared that exhibits an excellent scintillator in view of their low preparation cost, high light yield, short decay time in the nanosecond range, and low inherent trap density [6]. Methylammonium Pb based perovskites (MAPbX3) have demonstrated a significant scintillating performance for luminous devices and high-sensitive detectors in the visible range [78–80]. Saidaminov et al. [81] have reported the novel hybrid organo-lead tri-halide perovskites, MAPbBr3 and MAPbI3 in hot solutions, prepared by controlling the solvent, temperature and other parameters. They found that these material show carrier transport properties similar to those grown by the usual cooling or anti-solvent vapor-assisted crystallization techniques. The authors stated the 'quantum leap' in crystal growth rates of these scintillators presents a major breakthrough in the research area of perovskite single crystals enabling the wide applications from medical imaging to industrial technology. Moreover, Wei et al. [82] have synthesized sensitive $MAPbBr_3$ single-crystal X-ray detectors with a record $\mu\tau$ product of 1.2×10^{-2} cm^2 V^{-1} and the lowest surface recombination velocity of 64 cm s^{-1}. Impressively, this material exhibited an excellent optoelectronic property as compared with those for CdZnTe. It was synthesized by the solution growth method which take an advantages of low cost, large scale and faster growth rates than the conventional routes, i.e., vapor deposition method adopted for CdZnTe crystal growth. The performed experiment of a charge collection efficiency up to ~33–42% for UV–vis light, and ~16.4% for hard X-ray photons which facilitates the ability to direct conversion of high-energy X-ray into collectable charges with a high sensitivity of 80 μC G y_{air}^{-1} cm^{-2} and a lowest detectable dose rate of 0.5 $\mu Gy_{air} s^{-1}$, which meets the practical needs of medical diagnostics. They believed that these findings offer an effective way to engineer the trap density of the hybrid perovskite material to increase the device charge collection efficiency for photodetectors. Later following this work, Wei W. and co-workers [83] designed the Si-integrated $MAPbBr_3$ through low-temperature solution-processed molecular bonding method in cooperation with brominated APTES (3-aminopropyl triethoxysilane) molecules. The insertion idea of this layer was to reduce the dark current which is crucial for a detector to sense very low X-ray. It is found, as anticipated, that a momentous lessening in dark current at higher bias, detecting a really low X-ray (8 keV) measurements rate of <0.1 μGy_{air} s^{-1} with a high affectability of 2.1×10^4 μC G y_{air}^{-1} cm^{-2}. Further, they appeared that the X-ray dosage to patients utilizing the

created direct finder cluster can be drastically decreased by 15–120-fold. The result gotten here is a few orders of magnitude superior than the state-of-the-art commercial α-Se X-ray locators, clearing the way for the commercialization of perovskite X-ray finders for therapeutic applications. This strategy gives an effortless way to coordinate MAPbBr3 single gems onto different by and largely utilized substrates at moo temperatures in arrangement, which opens an unused road for the application of perovskite materials in much broader areas, such as active-matrix flat-panel imagers and flat-panel shows.

The lanthanides with proper energy state, i.e., the rare earth (RE) doped scintillators have exhibited satisfactory properties [84]. Recently, scintillators of CaI_2: Eu^{2+} with doping RE [85] and LuI_3: Ce^{3+} [86] have achieved ray output of more than 100,000 photons per MeV. Similarly, Sr^{2+}, Ca^{2+} co-doped $LaBr_3$: Ce^{3+} scintillator show an ultrahigh energy-resolution [87], while some scintillators, for example, Ce^{3+} doped $PrBr_3$ [88] and Nd^{3+} doped LaF_3 have very short scintillating decay time of 6 ns. Interestingly, these scintillators emit photons in the range of ultraviolet, visible, or near-infrared when excited by X-rays/γ-rays, so that are considered as potential scintillating materials for medical imaging [89]. Likewise, to use lanthanide-based scintillators for CT imaging, Tb^{3+} doped LaF_3-Rose Bengal (RB) scintillators are functionalized with a silica layer for the pathologic diagnosis of cancer [90]. It is observed that the shell-thickness of the silica layer was controllable which given a uniform measure, great biocompatibility, colloidal soundness, and photostability. It is found that once the nano-scintillator infused into the tumor location, the flag escalated expanded significantly. The measured X-ray constriction control outperforms the commercial CT differentiate instrument (Ultravist® 300), which makes it a perfect CT differentiate specialist for deep-tumor determination. In spite of the fact that promising in CT imaging, more tests are still required to encourage confirm the photodynamic restorative efficacy of the Tb^{3+} doped LaF3-RB scintillating fabric by X-ray actuation. Investigating multiplexed scintillators has gotten to be an inquire about hotspot for the development of double show imaging devices.

5 Highly Sensitive X-ray Detector: Organic and Inorganic Materials

Xu et al. [3] have developed a new zero dimensional (0D) organic manganese (II) halide hybrid $(C_{38}H_{34}P_2)MnBr_4$ which exhibit highly efficient green emission upon photo and X-ray excitations. It is observed that the X-ray image of $(C_{38}H_{34}P_2)MnBr_4$ single crystal is more brighter than Ce:LuAG indicating that $C_{38}H_{34}P_2MnBr_4$ is more sensitive to X-ray irradiation than Ce: LuAG. Further, the scintillator response to X-ray dose rate, the radio-luminescence (RL) intensities have been investigated under various X-ray dose rates for $(C_{38}H_{34}P_2)MnBr4$ and Ce:LuAG. This single crystal scintillator shows discernible scintillation properties with amazing reaction linearity to dosage rate, tall light abdicates, and low detection limits. Interestingly,

the X-ray scintillation properties were found to be prevalent to those of metal halide perovskite nanocrystals and most of today's commercially accessible scintillators. X-ray imaging was moreover effectively illustrated with tall determination. The low-cost, simple planning, ecologically neighborly, and state-of-the craftsmanship glitter execution make this natural manganese (II) half breed $(C_{38}H_{34}P_2)MnBr_4$ an exceedingly promising scintillator for commercial applications. The authors believed that this work could be a new way to explore new low-cost, high-performance eco-friendly hybrid materials for radiation scintillators. Although, scintillators have a tunable properties in visible region owing to their abundant electronic states, adjustable bandgap, high detection efficiency and relatively lower reabsorption to X-rays [91–93], pristine perovskites exhibit some intrinsic deficiency. For instance, some halide PNMs have demonstrated a limited adaptability of optical and electrical performances in addition to poor stability for light, heat, oxygen, humidity and aggregation and phase transition [94]. Researchers are still trying to add external doping ions into PNMs to overcome these drawbacks [70].

The design of novel scintillators which allow the medical detections under lower X-ray radiation dose with faster evaluation is still challenging and large area of investigation still need to be addressed. Organic nanocrystals such as stilbene, naphthalene and anthracene showing high attenuation-constant which can be used as scintillating materials for β-ray; however, they show a poor efficiency on X-ray detections [8, 9]. Based on organic framework, metal organic frameworks (MOFs) scintillators exhibit noteworthy energy conversion efficiency to X-rays which opens tunable platform for several application [95]. The organic emitters allow them to respond quickly to X-rays as compared to conventional available inorganic scintillators [96]. The strong green light emission actuated by the charge-transfer from ligand to metal, advocates that the UVI materials are anticipated as a proficient scintillating candidate for X-ray detection and the perceptible light emission in a uranyl-organic system (SCU-9) are exceptionally promising highlights for down to earth applications in therapeutic imaging areas. SCU-9 assist appears the prevalence of decreasing the non-radiative unwinding within the prepare of excitation, which advance makes strides the transformation productivity. The emission escalated appears a basically direct relationship with the uncovered X-ray measurements, and this parameter is comparable to that of the commercial scintillator CsI:Tl. In expansion, SCU-9 moreover shows diminished hydroscopicity, improved X-ray radiation resistance, and decreased effectiveness [97].

Thirimanne et al. [98] have synthesized a hybrid 'inorganic in organic' X-ray detector which demonstrated promising sensitivities of 1712 and 58 $\mu C\ mGy^{-1}\ cm^{-3}$ for soft and hard X-rays respectively. In addition to this, due to the flexibility of the detectors, they show a high sensitivity of 300 $\mu C\ mGy^{-1}\ cm^{-3}$, recommending its potential for dosimetry and bio-imaging in non-planar architectures. The made strides X-ray affectability could be a result of affect ionization, and an upgraded way length due to Mie diffusing and the proficient division, and transport of these by the BHJ-NP engineering coming about in high-charge collection efficiencies (>60%). Based on this concept, a preparatory level board imager has moreover been illustrated. The strategy of coordinate discovery and imaging, combined with low fetched,

adaptability and versatility for large-area fabricate, makes strides on current strong state X-ray finder execution by 2–3 orders of magnitudes, beneath low voltages, whereas conveying novel properties reasonable for an extend of current and already unexplored discovery and imaging applications.

Lee and co-workers [99] have studied organic–inorganic X-ray detectors by adding inorganic quantum dots (QDs) to the organic active layer which results the improved sensitivity due to combined interface properties, i.e., excellent physico-chemical stability, excellent carrier mobility, and efficient photon absorption on the organic polymer interface. The inner organic active layer consisted of a conjugated polymer P3HT and fullerene derivatives PC70BM to which indium phosphide (InP) QDs were added by changing the size and amount of InP) QDs. The sensitivity of the detector was extracted during X-ray exposure according to the QD size change (4–12 nm in diameter). It was observed that the sensitivity decreased with the increased QDs size. Moreover, the absorbance of the active layer decreased when the size of QDs exceeded 4 nm which reduces the solubility and dispersion of the QDs in the organic active layer. Therefore, the detector with the P3HT:PC70BM:InP QDs (4 nm diameter) showed the highest sensitivity, of 2.01 mA/Gy·cm2, showing that the sensitivity was improved by 44.60% over that of the P3HT:PC70BM detector. On the other hand, there is another way to further improve the sensitivity by varying the amount of QDs keeping the QDs size fixed to 4 nm in diameter. It was observed that the most noteworthy affectability of 2.26 mA/Gy·cm^2 gotten from the finder P3HT:PC70BM:InP QDs (1 mg) dynamic layer. In expansion, the most noteworthy versatility, of 1.69×10^{-5} cm^2/V·s, was gotten from the same locator. The changed sum of InP QDs within the P3HT:PC70BM natural dynamic layer changed the surface morphology, subsequently expanding the charge eras by moving forward the light-absorbing surface range. In expansion, the well-formed arrange between inorganic InP QDs and natural P3HT:PC70BM dynamic layer were diminished RS and moved forward the portability, since it makes a difference charge exchange and charge collection. The frequency response of the detector without the scintillator was evaluated using a pulsed green LED (emission peak at 540 nm).

6 Conclusion and Future Perspectives

The combination of developed X-ray techniques and synthesis of X-ray activated scintillators have offered excellent technology in medical radiography, diagnosis, and deep-tumor therapy. The nanoscale scintillators serve as a contrast medium in low dosage CT imaging. Owing to the boundless infiltration profundity of X-ray, the comparing scintillator shows extraordinary potential for the focus on the treatment of profound situated tumors. The high X-ray attenuation coefficient reduces the possibility of destruction of healthy tissues and organs in radiotherapy. However, the new materials with optimization of X-ray activated nanoscintillator will always remain and very essential for the progress of radiographic and therapeutic facilities for the diagnosis and treatment of deep-tumor in clinical level. For this, work

in incredible collaborations and near co-operation between researchers, engineers, doctors, and drug specialists are direly required within the precise assessment of the treatment viability and side impacts of the intra-tumor infused scintillators, which is exceptionally vital for assist progressing the remedy rate of cancer and extraordinarily dragging out the life of the patients. We have to appreciate the work done and the efforts made so far which brought a lots of achievement and the possibility for the X-ray activated scintillators in biomedical scenario. However, the theoretical understanding to find the accurate band structures, and the mechanisms of charge and energy transfer, is on centered which need to be tackled before experiment that obviously helps to improve the photoluminescence (PL) performances and may open the broad applications.

Acknowledgements GN and SKS are very thankful to funding agencies CAPES, CNPq and FAPEMA, Brazil; SKS is also very thankful to PPGF-UFMA for motivation to work on this book project. JAHC thanks the CNPq and FAPDF, Brazil for the financial support. Dr. Mohan C. Mathpal greatly acknowledges the funding from FONDECYT program (N ° 3190316) to support the research activity. J.R.M and M.C. acknowledge the support from ANID Fondequip EQM140168.

References

1. Nikl M, Yoshikawa A (2015) Recent R&D trends in inorganic single-crystal scintillator materials for radiation detection. Adv Opt Mater 3:463–481. https://doi.org/10.1002/ADOM.201400571
2. De Jonge MD, Vogt S (2010) Hard X-ray fluorescence tomography-an emerging tool for structural visualization. Curr Opin Struct Biol 20:606–614
3. Xu L-J, Lin X, He Q, Worku M, Ma B (2020) Highly efficient eco-friendly X-ray scintillators based on an organic manganese halide. Nat Commun 111(11):1–7. https://doi.org/10.1038/s41467-020-18119-y
4. Wei H, Bruns OT, Kaul MG, Hansen EC, Barch M, Wiśniowska A, Chen O, Chen Y, Li N, Okada S, Cordero JM, Heine M, Farrar CT, Montana DM, Adam G, Ittrich H, Jasanoff A, Nielsen P, Bawendi MG (2017) Exceedingly small iron oxide nanoparticles as positive MRI contrast agents. Proc Natl Acad Sci USA 114:2325–2330. https://doi.org/10.1073/pnas.1620145114
5. James ML, Gambhir SS (2012) A molecular imaging primer: Modalities, imaging agents, and applications. Physiol Rev 92:897–965
6. Birowosuto MD, Cortecchia D, Drozdowski W, Brylew K, Lachmanski W, Bruno A (2016) Soci C (2016) X-ray Scintillation in Lead Halide Perovskite Crystals. Sci Reports 61(6):1–10. https://doi.org/10.1038/srep37254
7. Bertrand GHV, Hamel M, Sguerra F (2014) Current status on plastic scintillators modifications. Chem A Eur J 20:15660–15685. https://doi.org/10.1002/CHEM.201404093
8. Buck C, Yeh M (2016) Metal-loaded organic scintillators for neutrino physics. J Phys G Nucl Part Phys 43. https://doi.org/10.1088/0954-3899/43/9/093001
9. Kharzheev YN (2015) Scintillation counters in modern high-energy physics experiments (Review). Phys Part Nucl 464(46):678–728. https://doi.org/10.1134/S1063779615040048
10. Dujardin C, Auffray E, Bourret-Courchesne E, Dorenbos P, Lecoq P, Nikl M, Vasil'Ev AN, Yoshikawa A, Zhu RY (2018) Needs, trends, and advances in inorganic scintillators. IEEE Trans Nucl Sci 65:1977–1997. https://doi.org/10.1109/TNS.2018.2840160

11. Hsieh J (2009) Computed tomography principles, design, artifacts, and recent advances. SPIE, Bellingham, WA
12. Ketcham RA, Carlson WD (2001) Acquisition, optimization and interpretation of x-ray computed tomographic imagery: applications to the geosciences. Comput Geosci 27:381–400. https://doi.org/10.1016/S0098-3004(00)00116-3
13. Grassler T, Wirth KE (2000) X-ray computer tomography-potential and limitation for the measurement of local solids distribution in circulating fluidized beds. Chem Eng J 77:65–72. https://doi.org/10.1016/S1385-8947(99)00133-3
14. The Fundamentals of X-ray and radium physicsthe fundamentals of X-ray and radium physics (1954) By SelmanJoseph, M.D., Director, School for X-ray Technicians, Tyler Junior College; Chief of Radiology, Mother Frances Hospital; Director, Radiology Department, Medical Center Hospital; Consultant in Radiology, East Texas Tuberculosis Hospital, Tyler, Texas. A volume of 340 pages, with 174 illustrations and 8 tables. Published by Charles C Thomas, Springfield, Ill.1954 Price $8.50 Radiology 63:264–265. https://doi.org/10.1148/63.2.264b
15. Cartz L (1995) Nondestructive testing. ASM International, Material Park, OH
16. Kudryashov YB (2008) Radiation biophysics ionizing radiations. Nova Science Pub Inc
17. Kherlopian AR, Song T, Duan Q, Neimark MA, Po MJ, Gohagan JK, Laine AF (2008) A review of imaging techniques for systems biology. BMC Syst Biol 2
18. Chotas HG, Dobbins JT, Ravin CE (1999) Principles of digital radiography with large-area, electronically readable detectors: a review of the basics. Radiology 210:595–599
19. Seeger A, Kertzscher U, Affeld K, Wellnhofer E (2003) Measurement of the local velocity of the solid phase and the local solid hold-up in a three-phase flow by X-ray based particle tracking velocimetry (XPTV). Chem Eng Sci 58:1721–1729. https://doi.org/10.1016/S0009-2509(03)00010-1
20. Heindel TJ, Gray JN, Jensen TC (2008) An X-ray system for visualizing fluid flows. Flow Meas Instrum 19:67–78. https://doi.org/10.1016/j.flowmeasinst.2007.09.003
21. Johnson Q, Pellinen D (1979) Flash X-ray. Sagamore Army Mater Res Conf Proc 117–150. https://doi.org/10.1007/978-1-4613-2952-7_6
22. Jamet F, Thomer G (1976) Flash radiography 192
23. Heindel TJ (2011) A review of X-ray flow visualization with applications to multiphase flows. J Fluids Eng Trans ASME 133. https://doi.org/10.1115/1.4004367/456290
24. Shalom NE, Gong GX, Auster M (2020) Fluoroscopy: an essential diagnostic modality in the age of high-resolution cross-sectional imaging. World J Radiol 12:213. https://doi.org/10.4329/WJR.V12.I10.213
25. Covello B, McKeon B (2022) Fluoroscopic angiography assessment, protocols, and interpretation. StatPearls Publishing
26. McRae R, Bagchi P, Sumalekshmy S, Fahrni CJ (2009) In situ imaging of metals in cells and tissues. Chem Rev 109:4780–4827. https://doi.org/10.1021/cr900223a
27. Fahrni CJ (2007) Biological applications of X-ray fluorescence microscopy: exploring the subcellular topography and speciation of transition metals. Curr Opin Chem Biol 11:121–127
28. Shimura M, Saito A, Matsuyama S, Sakuma T, Terui Y, Ueno K, Yumoto H, Yamauchi K, Yamamura K, Mimura H, Sano Y, Yabashi M, Tamasaku K, Nishio K, Nishino Y, Endo K, Hatake K, Mori Y, Ishizaka Y, Ishikawa T (2005) Element array by scanning X-ray fluorescence microscopy after cis-diamminedichloro-platinum(II) treatment. Cancer Res 65:4998–5002. https://doi.org/10.1158/0008-5472.CAN-05-0373
29. Ortega R, Devès G, Carmona A (2009) Bio-metals imaging and speciation in cells using proton and synchrotron radiation X-ray microspectroscopy. J Royal Soc Interface Royal Soc 6: S469-S658
30. Miqueles EX, De Pierro AR (2010) Exact analytic reconstruction in x-ray fluorescence CT and approximated versions. Phys Med Biol 55:1007–1024. https://doi.org/10.1088/0031-9155/55/4/007
31. Marmorato P, Ceccone G, Gianoncelli A, Pascolo L, Ponti J, Rossi F, Salomé M, Kaulich B, Kiskinova M (2011) Cellular distribution and degradation of cobalt ferrite nanoparticles in Balb/3T3 mouse fibroblasts. Toxicol Lett 207:128–136. https://doi.org/10.1016/j.toxlet.2011.08.026

32. Milakovic M, Berg G, Eggertsen R, Nyström E, Olsson A, Larsson A, Hansson M (2006) Determination of intrathyroidal iodine by X-ray fluorescence analysis in 60 to 65 year olds living in an iodine-sufficient area. J Intern Med 260:69–75. https://doi.org/10.1111/j.1365-2796.2006.01660.x
33. Studinski R, O'Meara J, McNeill F (2008) The feasibility of in vivo measurement of arsenic and silver by x-ray fluorescence. X-ray Spectrom 37:51–57. https://doi.org/10.1002/xrs.1010
34. Hoppin JA, Aro ACA, Williams PL, Hu H, Ryan PB (1995) Validation of K-XRF bone lead measurement in young adults. Environ Health Perspect 103:78–83. https://doi.org/10.1289/ehp.9510378
35. Mach JC, Omar A, Barone HE, Harb A, Abujudeh H (2021) Fluoroscopy and MRI induced skin injuries: a review of diagnostic, management, and preventative principles. Curr Radiol Reports 91(9):1–10. https://doi.org/10.1007/S40134-020-00376-W
36. Green JD, Omary RA, Schirf BE, Tang R, Lu B, Gehl JA, Huang JJ, Carr JC, Pereles FS, Li D (2005) Comparison of X-ray fluoroscopy and interventional mri for the assessment of coronary artery stenoses in swine. Magn Reson Med 54:1094. https://doi.org/10.1002/MRM.20699
37. Wang J, Blackburn TJ (2000) The AAPM/RSNA physics tutorial for residents. 20:1471–1477. https://doi.org/10.1148/radiographics.20.5.g00se181471
38. Seeram E (2019) Digital Fluoroscopy. Digit Radiogr 95–110. https://doi.org/10.1007/978-981-13-3244-9_6
39. Graham MT, Assis F, Allman D, Wiacek A, Gonzalez E, Gubbi MR, Dong J, Hou H, Beck S, Chrispin J, Bell MAL (2020) Photoacoustic image guidance and robotic visual servoing to mitigate fluoroscopy during cardiac catheter interventions. 11229:80–85. https://doi.org/10.1117/12.2546910
40. Yang Y, Tian Q, Wang D, Yi F, Song H, Li W, Wu C (2021) Percutaneous vertebroplasty for C1 osteolytic lesions via lateral approach under fluoroscopic guidance . J Pain Res 14:2121–2128. https://doi.org/10.2147/JPR.S318236
41. Huang SY, Damasco JA, Tian L, Lu L, Perez JVD, Dixon KA, Williams ML, Jacobsen MC, Dria SJ, Eggers MD, Melancon AD, Layman RR, Whitley EM, Melancon MP (2020) In vivo performance of gold nanoparticle-loaded absorbable inferior vena cava filters in a swine model. Biomater Sci 8:3966–3978. https://doi.org/10.1039/D0BM00414F
42. Bohari A, Hashim S, Mohd Mustafa SN (2020) Scatter radiation in the fluoroscopy-guided interventional room. Radiat Prot Dosimetry 188:397–402. https://doi.org/10.1093/RPD/NCZ299
43. Kimura M, Castillo M (2013) Basic principles of computed tomography angiography (CTA). Vasc Imaging Cent Nerv Syst Phys Princ Clin Appl Emerg Tech 67–82. https://doi.org/10.1002/9781118434550.CH4
44. Ivancevic MK, Geerts L, Weadock WJ, Chenevert TL (2009) Technical principles of MR angiography methods. Magn Reson Imaging Clin N Am 17:1–11. https://doi.org/10.1016/J.MRIC.2009.01.012
45. Htyte N, Jenkins JS (2014) Diagnostic cerebral and peripheral angiography. Pan Vascular Med 1–55. https://doi.org/10.1007/978-3-642-37393-0_39-1
46. Ishihara S, Ross IB, Piotin M, Weill A, Aerts H, Moret J (2000) 3D rotational angiography: recent experience in the evaluation of cerebral aneurysms for treatment. Interv Neuroradiol 6:85. https://doi.org/10.1177/159101990000600202
47. Van Rooij WJ, Sprengers ME, De Gast AN, Peluso JPP, Sluzewski M (2008) 3D rotational angiography: the new gold standard in the detection of additional intracranial aneurysms. AJNR Am J Neuroradiol 29:976–979. https://doi.org/10.3174/AJNR.A0964
48. Kaplan DJ, Patel JN, Liporace FA, Yoon RS (2016) Intraoperative radiation safety in orthopaedics: a review of the ALARA (As low as reasonably achievable) principle. Patient Saf Surg 101(10):1–7. https://doi.org/10.1186/S13037-016-0115-8
49. Nimi N, Saraswathy A, Nazeer SS, Francis N, Shenoy SJ, Jayasree RS (2018) Biosafety of citrate coated zerovalent iron nanoparticles for magnetic resonance angiography. Data Br 20:1829–1835. https://doi.org/10.1016/J.DIB.2018.08.157

50. Islam K, Haque M, Kumar A, Hoq A, Hyder F, Hoque SM (2020) Manganese Ferrite Nanoparticles ($MnFe_2O_4$): size dependence for hyperthermia and negative/positive contrast enhancement in MRI. Nanomater 10:2297. https://doi.org/10.3390/NANO10112297
51. Tavakol M, Ashraf S, Brener SJ (2012) Risks and complications of coronary angiography: a comprehensive review. Glob J Health Sci 4:65. https://doi.org/10.5539/GJHS.V4N1P65
52. Withers PJ, Bouman C, Carmignato S, Cnudde V, Grimaldi D, Hagen CK, Maire E, Manley M, Du Plessis A (2021) Stock SR (2021) X-ray computed tomography. Nat Rev Methods Prim 11(1):1–21. https://doi.org/10.1038/s43586-021-00015-4
53. Garvey CJ, Hanlon R (2002) Computed tomography in clinical practice. BMJ Br Med J 324:1077. https://doi.org/10.1136/BMJ.324.7345.1077
54. Bockisch A, Freudenberg LS, Schmidt D, Kuwert T (2009) Hybrid imaging by SPECT/CT and PET/CT: proven outcomes in cancer imaging. Semin Nucl Med 39:276–289. https://doi.org/10.1053/J.SEMNUCLMED.2009.03.003
55. Ter-Pogossian MM (1977) Basic principles of computed axial tomography. Semin Nucl Med 7:109–127. https://doi.org/10.1016/S0001-2998(77)80013-5
56. Seeram E (2010) Computed tomography: physical principles and recent technical advances. J Med Imaging Radiat Sci 41:87–109. https://doi.org/10.1016/J.JMIR.2010.04.001
57. Novelline RA, Rhea JT, Rao PM, Stuk JL (1999) Helical CT in emergency radiology. Radiology 213:321–339. https://doi.org/10.1148/RADIOLOGY.213.2.R99NV01321
58. Silverman PM, Cooper CJ, Weltman DI, Zeman RK (1995) Helical CT: practical considerations and potential pitfalls. Radiographics 15:25–36. https://doi.org/10.1148/RADIOGRAPHICS.15.1.7899611
59. Sun ZH, Cao Y, Li HF (2011) Multislice computed tomography angiography in the diagnosis of coronary artery disease. J Geriatr Cardiol 8:104. https://doi.org/10.3724/SP.J.1263.2011.00104
60. Goldman LW (2008) Principles of CT: multislice CT. J Nucl Med Technol 36:57–68. https://doi.org/10.2967/JNMT.107.044826
61. Tawfik HA, Abdelhalim A, Elkafrawy MH (2012) Computed tomography of the orbit - A review and an update. Saudi J Ophthalmol Off J Saudi Ophthalmol Soc 26:409–418. https://doi.org/10.1016/J.SJOPT.2012.07.004
62. Xue N, Zhou C, Chu Z, Chen L, Jia N (2020) Barley leaves mediated biosynthesis of Au nanomaterials as a potential contrast agent for computed tomography imaging. Sci China Technol Sci 642(64):433–440. https://doi.org/10.1007/S11431-019-1546-3
63. Dong YC, Hajfathalian M, Maidment PSN, Hsu JC, Naha PC, Si-Mohamed S, Breuilly M, Kim J, Chhour P, Douek P, Litt HI, Cormode DP (2019) Effect of gold nanoparticle size on their properties as contrast agents for computed tomography. Sci Reports 91(9):1–13. https://doi.org/10.1038/s41598-019-50332-8
64. Fayngersh V, Passero M (2009)Estimating radiation risk from computed tomography scanningLung 187:143–148. https://doi.org/10.1007/S00408-009-9143-9
65. Cui Y, Zhang J, He H, Qian G (2018) Photonic functional metal–organic frameworks. Chem Soc Rev 47:5740–5785. https://doi.org/10.1039/C7CS00879A
66. Wei H, Huang J (2019) Halide lead perovskites for ionizing radiation detection. Nat Commun 101(10):1–12. https://doi.org/10.1038/s41467-019-08981-w
67. Nikl M (2016) Nanocomposite, ceramic, and thin film scintillators, 1st edn. Jenny Standard Publishing
68. Wang Y, Yin X, Chen J, Wang Y, Chai Z, Wang S (2020) Gleaming uranium: an emerging emitter for building X-ray scintillators. Chem A Eur J 26:1900–1905. https://doi.org/10.1002/CHEM.201904409
69. Wei Y, Cheng Z, Lin J (2019) An overview on enhancing the stability of lead halide perovskite quantum dots and their applications in phosphor-converted LEDs. Chem Soc Rev 48:310–350. https://doi.org/10.1039/C8CS00740C
70. Zhu H, Zhang P, Dai S (2015) Recent advances of lanthanum-based perovskite oxides for catalysis. ACS Catal 5:6370–6385. https://doi.org/10.1021/ACSCATAL.5B01667

71. Shamsi J, Urban AS, Imran M, De TL, Manna L (2019) Metal halide perovskite nanocrystals: synthesis, post-synthesis modifications, and their optical properties. Chem Rev 119:3296–3348. https://doi.org/10.1021/ACS.CHEMREV.8B00644
72. Nikl M (2006) Scintillation detectors for x-rays. Meas Sci Technol 17:R37. https://doi.org/10.1088/0957-0233/17/4/R01
73. Drozdowski W, Wojtowicz AJ, Łukasiewicz T, Kisielewski J (2006) Scintillation properties of LuAP and LuYAP crystals activated with cerium and molybdenum. Nucl Instr Meth Phys Res Sect A Accel Spectr Detect Assoc Equip 562:254–261. https://doi.org/10.1016/J.NIMA.2006.01.127
74. Birowosuto MD, Dorenbos P (2009) Novel γ- and X-ray scintillator research: on the emission wavelength, light yield and time response of Ce^{3+} doped halide scintillators. Phys status solidi 206:9–20. https://doi.org/10.1002/PSSA.200723669
75. Cao F, Yu D, Ma W, Xu X, Cai B, Yang YM, Liu S, He L, Ke Y, Lan S, Choy K-L, Zeng H (2019) Shining emitter in a stable host: design of halide perovskite scintillators for X-ray imaging from commercial concept. ACS Nano 14:5183–5193. https://doi.org/10.1021/ACSNANO.9B06114
76. Phung N, Abate A (2018) The impact of nano- and microstructure on the stability of perovskite solar cells. Small 14:1802573. https://doi.org/10.1002/SMLL.201802573
77. Pan G, Bai X, Yang D, Chen X, Jing P, Qu S, Zhang L, Zhou D, Zhu J, Xu W, Dong B, Song H (2017) Doping lanthanide into perovskite nanocrystals: highly improved and expanded optical properties. Nano Lett 17:8005–8011. https://doi.org/10.1021/ACS.NANOLETT.7B04575
78. Tan Z-K, Moghaddam RS, Lai ML, Docampo P, Higler R, Deschler F, Price M, Sadhanala A, Pazos LM, Credgington D, Hanusch F, Bein T, Snaith HJ, Friend RH (2014) Bright light-emitting diodes based on organometal halide perovskite. Nat Nanotechnol 99(9):687–692. https://doi.org/10.1038/nnano.2014.149
79. Chondroudis K, Mitzi DB (1999)Electroluminescence from an organic−inorganic perovskite incorporating a quaterthiophene dye within lead halide perovskite layersChem Mater 11:3028–3030https://doi.org/10.1021/CM990561T
80. Dou L, Yang Y (Micheal), You J, Hong Z, Chang W-H, Li G, Yang Y (2014) Solution-processed hybrid perovskite photodetectors with high detectivity. Nat Commun 51(5):1–6. https://doi.org/10.1038/ncomms6404
81. Saidaminov MI, Abdelhady AL, Murali B, Alarousu E, Burlakov VM, Peng W, Dursun I, Wang L, He Y, Maculan G, Goriely A, Wu T, Mohammed OF, Bakr OM (2015) High-quality bulk hybrid perovskite single crystals within minutes by inverse temperature crystallization. Nat Commun 23955. https://doi.org/10.1038/ncomms8586
82. Wei H, Fang Y, Mulligan P, Chuirazzi W, Fang H-H, Wang C, Ecker BR, Gao Y, Loi MA, Cao L, Huang J (2016). Sensitive X-ray detectors made of methylammonium lead tribromide perovskite single crystals. https://doi.org/10.1038/NPHOTON.2016.41
83. Wei W, Zhang Y, Xu Q, Wei H, Fang Y, Wang Q, Deng Y, Li T, Gruverman A, Cao L, Huang J (2017) Monolithic integration of hybrid perovskite single crystals with heterogenous substrate for highly sensitive X-ray imaging. Nat Photonics 11. https://doi.org/10.1038/NPHOTON.2017.43
84. Dorenbos P (2019) (Invited) The quest for high resolution γ-ray scintillators. Opt Mater X 1:100021. https://doi.org/10.1016/J.OMX.2019.100021
85. Cherepy NJ, Payne SA, Asztalos SJ, Hull G, Kuntz JD, Niedermayr T, Pimputkar S, Roberts JJ, Sanner RD, Tillotson TM, Van Loef E, Wilson CM, Shah KS, Roy UN, Hawrami R, Burger A, Boatner LA, Choong WS, Moses WW (2009) Scintillators with potential to supersede lanthanum bromide. IEEE Trans Nucl Sci 56:873–880. https://doi.org/10.1109/TNS.2009.2020165
86. Birowosuto MD, Dorenbos P, van Eijk CWE, Krämer KW, Güdel HU (2006) High-light-output scintillator for photodiode readout: LuI^3:Ce^{3+}. J Appl Phys 99:123520. https://doi.org/10.1063/1.2207689
87. Alekhin MS, de Haas JTM, Khodyuk IV, Krämer KW, Menge PR, Ouspenski V, Dorenbos P (2013) Improvement of γ-ray energy resolution of $LaBr_3$:Ce^{3+} scintillation detectors by Sr^{2+} and Ca^{2+} co-doping. Appl Phys Lett 102:161915. https://doi.org/10.1063/1.4803440

88. Birowosuto MD, Dorenbos P, van Eijk CWE, Krämer KW, Güdel HU (2007) Thermal quenching of Ce^{3+} emission in PrX_3 (X = Cl, Br) by intervalence charge transfer. J Phys Condens Matter 19:256209. https://doi.org/10.1088/0953-8984/19/25/256209
89. Osakada Y, Pratx G, Hanson L, Solomon PE, Xing L, Cui B (2013) X-ray excitable luminescent polymer dots doped with an iridium(III) complex. Chem Commun 49:4319–4321. https://doi.org/10.1039/C2CC37169C
90. Elmenoufy AH, Tang Y, Hu J, Xu H, Yang X (2015) A novel deep photodynamic therapy modality combined with CT imaging established via X-ray stimulated silica-modified lanthanide scintillating nanoparticles. Chem Commun 51:12247–12250. https://doi.org/10.1039/C5CC04135J
91. Wang L, Song Q, Zhao Z, Liu Y, Alsaadi FE (2019) Synchronization of two nonidentical complex-valued neural networks with leakage delay and time-varying delays. Neurocomputing 356:52–59. https://doi.org/10.1016/J.NEUCOM.2019.04.068
92. Zhang Y, Sun R, Ou X, Fu K, Chen Q, Ding Y, Xu L-J, Liu L, Han Y, Malko AV, Liu X, Yang H, Bakr OM, Liu H, Mohammed OF (2019) Metal halide perovskite nanosheet for X-ray high-resolution scintillation imaging screens. ACS Nano. https://doi.org/10.1021/ACSNANO.8B09484
93. Duan J, Wei J, Tang Q, Li Q (2020) Unveiling the interfacial charge extraction kinetics in inorganic perovskite solar cells with formamidinium lead halide ($FAPbX_3$) nanocrystals. Sol Energy 195:644–650. https://doi.org/10.1016/J.SOLENER.2019.12.001
94. Zheng C, Bi C, Huang F, Binks D, Tian J (2019) Stable and strong emission $CsPbBr_3$ quantum dots by surface engineering for high-performance optoelectronic films. ACS Appl Mater Interfaces 11:25410–25416. https://doi.org/10.1021/ACSAMI.9B07818
95. Lu J, Xin X-H, Lin Y-J, Wang S-H, Xu J-G, Zheng F-K, Guo G-C (2019) Efficient X-ray scintillating lead(II)-based MOFs derived from rigid luminescent naphthalene motifs. Dalt Trans 48:1722–1731. https://doi.org/10.1039/C8DT04587A
96. Srm II, Golafale ST, Bacsa J, Steiner A, Ingram CW, Doty FP, Auden E, Hattar K (2017) Mesoporous stilbene-based lanthanide metal organic frameworks: synthesis, photoluminescence and radioluminescence characteristics. Dalt Trans 46:491–500. https://doi.org/10.1039/C6DT03755K
97. Wang Y, Yin X, Liu W, Xie J, Chen J, Silver MA, Sheng D, Chen L, Diwu J, Liu N, Chai Z, Albrecht-Schmitt TE, Wang S (2018) Emergence of uranium as a distinct metal center for building intrinsic X-ray scintillators. Angew Chemie Int Ed 57:7883–7887. https://doi.org/10.1002/ANIE.201802865
98. Thirimanne HM, Jayawardena KDGI, Parnell AJ, Bandara RMI, Karalasingam A, Pani S, Huerdler JE, Lidzey DG, Tedde SF, Nisbet A, Mills CA, Silva SRP (2018) High sensitivity organic inorganic hybrid X-ray detectors with direct transduction and broadband response. Nature Commun. https://doi.org/10.1038/s41467-018-05301-6
99. Lee J, Liu H, Kang J (2020) A study on an organic semiconductor-based indirect X-ray detector with Cd-free QDs for sensitivity improvement. Sensors20:6562–6562.https://doi.org/10.3390/S20226562

Radiosensitizers in Radiation-Induced Cancer Therapy

Hamid Rashidzadeh, Faezeh Mozafari, Hossein Rahimi, Mohammadreza Ghaffarlou, Ali Ramazani, Morteza Abazari, Mohammad-Amin Rahmati, Hossein Danafar, Hafeez Anwar, Surender K. Sharma, and Taras Kavetskyy

Abstract Radiation therapy (RT) has established as a very auspicious tool to tackle cancer, but its efficacy has encountered with some challenges. As we all know, in the case of cancer therapy by RT, high doses of radiation is required to fully eradicate tumor cells and shrink them as well. However, this auspicious tool is far from being faultless, as its enhancement in maximally killing tumor cells while minimally causing severe adverse effects to normal cells have always been unresolved clinical problems and challenges. To address these drawbacks, researchers have conducted a lot of research studies, among them, radiosensitizers have shown great potential to improve the bottleneck of RT for cancer therapy. Radiosensitizers are chemical or

These authors contribute equally to this work

H. Rashidzadeh · F. Mozafari · H. Rahimi · M. Abazari · M.-A. Rahmati · H. Danafar
Zanjan Pharmaceutical Biotechnology Research Center, Zanjan University of Medical Sciences, Zanjan, Iran
e-mail: danafar@zums.ac.ir

H. Rashidzadeh · F. Mozafari · A. Ramazani · H. Danafar
Cancer Gene Therapy Research Center, Zanjan University of Medical Sciences, Zanjan, Iran

M. Ghaffarlou
Department of Chemistry, Hacettepe University, 06800 Beytepe, Ankara, Turkey

H. Anwar
Department of Physics, University of Agriculture, 38040 Faisalabad, Pakistan

S. K. Sharma
Department of Physics, Central University of Punjab, 151401 Bathinda, India

Department of Physics, Federal University of Maranhao, 65080-805 Sao Luis, MA, Brazil

T. Kavetskyy (✉)
Joint Ukraine-Azerbaijan International Research and Education Center of Nanobiotechnology and Functional Nanosystems, Drohobych, Ukraine, Baku, Azerbaijan
e-mail: kavetskyy@yahoo.com

Department of Materials Engineering, The John Paul II Catholic University of Lublin, 20-950 Lublin, Poland

Drohobych Ivan Franko State Pedagogical University, 82100 Drohobych, Ukraine

S. K. Sharma et al. (eds.), *Harnessing Materials for X-ray Based Cancer Therapy and Imaging*, Nanomedicine and Nanotoxicology,
https://doi.org/10.1007/978-3-031-04071-9_2

pharmacologic agents that makes tumor cells more vulnerable to RT by augmenting free radical formation and assisting DNA damage. Over the last decades, many attempts have been devoted to design and fabricate radiosensitizers that are highly efficient in tumor therapy and characterized with low toxicity. In this review, we classified and summarized the emerging strategies as three main types including nanomaterials, macromolecules, and small molecules based on their structure. Additionally, the development states of radiosensitizers, their mechanisms and how to harness their power to improve radiosensitizers sensibility are presented. We also summarize all exciting advances approaches and emerging smart strategies accossiated with fabrication of radiosensitizers as well as prospects and challenges for clinical translation of these agents in oncotherapy are reviewed.

Keywords Radiosensitizers · Cancer therapy · Radiotherapy · Nanomedicine · Small molecules · Macromolecules

1 Introduction

Radiation therapy (RT) has established as a very auspicious tool to tackle cancer, but its effectiveness has diminished by broad range of impediments, such as cancer complications, metabolic alterations, vasculogenesis and angiogenesis, tumor heterogeneity, and cancer stem cells [1–3]. Therefore, it seems that this useful tool alone is not able to completely eliminate cancer without causing severe side effects. Accordingly, there is a gap in clinical practice for boosting the differential effect of radiation in healthy and tumor tissues. A highly promising approach to address the aforementioned obstacles is enhancing the efficacy of RT by implementation of radiosensitizers, which are chemical or pharmacologic agents that makes tumor cells more vulnerable to RT. Accordingly, these agents increase the effects of radiation to achieve greater anti-tumor properties than the additive effect of each modality [4]. Any radiosensitizers which take into account for clinical practice has to be specific for tumor or damaged tissue. If activity of any genes which are responsible for repairing the double-strand break is restricted by any therapeutic agents would be considered as a radiosensitizer, but to be effective, they should acts only on the tumor tissue as tumor cells have surrounded with normal cells. Therefore, radiosensitizers have to be more effective toward tumor cells, unless this, there will be little to no therapeutic gain. Unfortunately, these requirements are too challenging to accomplish. Nevertheless, substantial progress has been made and considerable efforts have been devoted to this field. Radiosensitizers were classified into five main categories by Adams, one of the earliest pioneers in the field of RT. These five main categories of radiosensitizers are as follow: oxygen mimics that possess electrophilic activity, any analogs of thymine that can incorporate into DNA, inhibitors of repair of biomolecules, generation of cytotoxic agents through radiosensitizer radiolysis, and suppression of intracellular (–SH) sulfhydryl or other endogenous radioprotective agents [5, 6]. The above classification of radiosensitizers was based on two mechanisms: DNA repair and DNA damage as well as, specified the direction for these

agents at the early stage. However, with the advent of new technologies, a great number of agents and therapeutics with radiosensitization features are considered as radiosensitizers. These progress in technologies not only have broaden the horizon of this field but also facilitate the development of radiosensitizers [7, 8]. Furthermore, the radiosensitization mechanism of these agents have been also exploited in details [9, 10]. As shown in Fig. 1, RT can destroy tumor tissue and cancer cells through direct and indirect mechanisms. In the case of direct mechanism, radiation could directly induce both DNA single and double strand breaks, which leads to the termination of cell proliferation and division, or even cell apoptosis and necrosis. In the context of indirect mechanism, radiation could induce the generation of reactive oxygen species (ROS) and free radicals, resulting in the induction of cellular stress in, and injure biomolecules, and ultimately alter cellular signaling pathways.

Based on the structures of radiosensitizers, researchers have classified them into three categories, namely small molecules (Fig. 2), macromolecules (Table 1) and nanostructures. Of note, due to the unique properties and diversity of nanostructure materials, the role of nanomaterials as radiosensitizers will be discussed in more details in a distinct chapter.

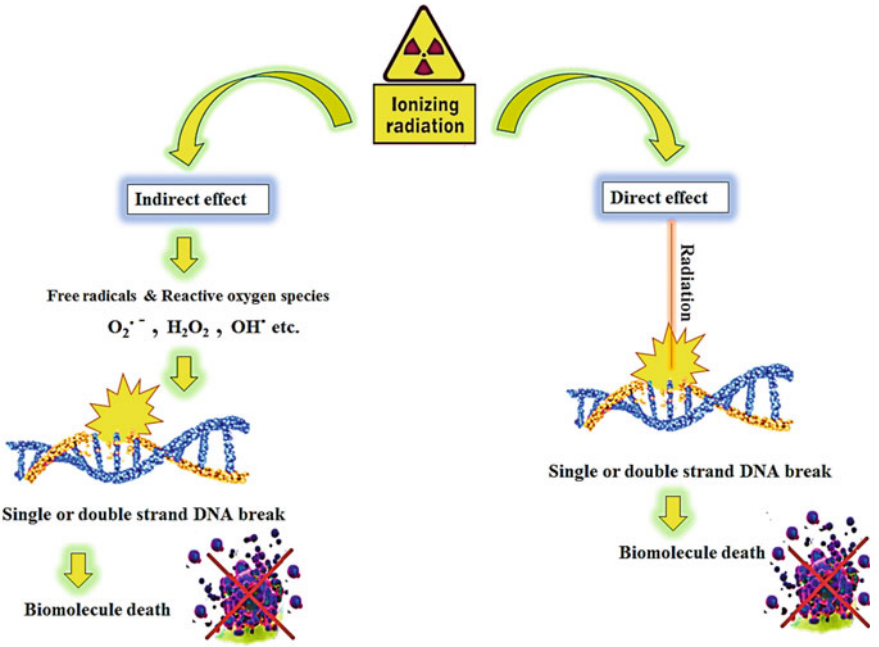

Fig. 1 Schematic representation of direct and indirect DNA damage caused by ionizing radiation (IR) in RT. The direct DNA damage caused by the directly radiation of IR with cellular DNA. In the context of indirect DNA damage, the radiation can indirectly damage DNA through generation of ROS and free radicals which derived from the radiolysis of the water

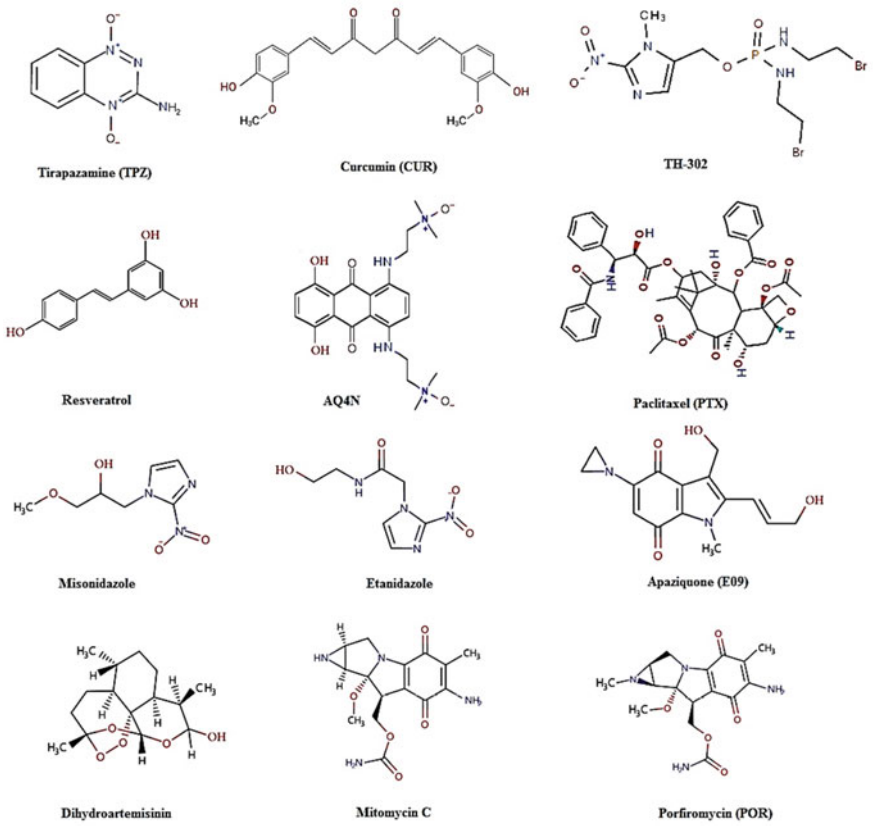

Fig. 2 Chemical structure of different small-molecules for radiosensitization

2 Small Molecules

One of the most distinguished features of solid tumors is hypoxia (low oxygen perfusion), which leads to an impaired response to radiotherapy. Under hypoxia condition, the tumor cells become more resistant to radiotherapy, aggressive and ultimately resistant to death [11, 12]. Thereby, cancer- associated hypoxia cause evolution of radioresistance both through changing patterns of gene expression and increasing free radical scavenging. In radiobiology, oxygen enhancement effect (OEF) or oxygen enhancement ratio (OER) generally refers to the enhancement of the radiological sensitivity of the cells which eventually leads to an increase in effectiveness of radiation, this positive effect is mainly attributed to the presence of oxygen [13]. This favorite response to radiation is most noteworthy once cells are exposed to an ionizing radiation dose. Oxygen as a propitious radiosensitizer can promote formation of the free radicals via its inimitable electronic configuration and acts through a mechanism of damage fixation based on its electron affinity Fig. 3 [14, 15]. It is worth to note that

Table 1 Some macromolecular-based nanoradiosensitizers and their potential in radiosensitization of tumors

Types of macromolecular-based nanoradiosensitizers	Termed/Name	Radiosensitization mechanism of macromolecules/brief results	References
Oligonucleotides	^{111}In–Match–AuNP–Tat	Induced DNA double-strand breaks and inhibiting hTR	[67]
	AuNP-NUAP-STAT3d	Induced cell DNA damage	[85]
	^{111}In-Match oligonucleotides	Induction of DNA damage and telomerase inhibition	[63]
	PSASODN	Induction of DNA damage and and telomerase inhibition, cell apoptosis through the activation of apoptosisassociated proteins	[64]
siRNAs	GLUT-1 siRNA	Increasing apoptosis, inhibiting DNA repair capability as well as inducing a redistribution of cell cycle phases	[86]
	Combination of GLUT1 siRNA with curcumin	Induction of autophagy and apoptosis	[74]
	AuNPs-si-SP1	Inhibiting SP1 to upregulate GZMB	[87]
	ECO/siDNApk-cs NPs	Targeting and inhibiting DNA damage repair	[88]
	tGd–GNMs$_{siRNA}$	Supressed the expression of VEGF gene and generation of ROS	[89]
Peptides and proteins	PETyr-I^{131}	Induction of DNA damage and cell apoptosis along with generation of ROS	[90]
	Phosphorylated peptides derived from Gli2	Diminished Gli2 transcriptional activator activity and induction of apoptosis	[91]
	Co-assembled peptide hydrogel	Impeding cyclooxygenase-2 arresting the cell cycle as well as promoting the number of Pt–DNA adducts	[92]
	AuNP-PTP	Induced apoptosis and increased the targeting efficiency	[93]

(continued)

Table 1 (continued)

Types of macromolecular-based nanoradiosensitizers	Termed/Name	Radiosensitization mechanism of macromolecules/brief results	References
	ANTP-SMACN7	Diminished clone formation and induced apoptosis by activation of caspase-9 and caspase-3 and inhibition of the X-linked inhibitor of apoptosis protein	[94]
	Hsp90 inhibitor NVP-AUY922	Enhancing G2/M arrest and DNA double strand breaks	[95]
	ANTP-SmacN7 fusion peptide	Induction of double-stranded DNA rupture and induction of caspase activation	[96]
	c(RGDyC)-AuNCs	Selectively targeted tumor and increased tumor accumulation of fabricated nano-system	[97]
	pHLIP-αKu80(γ)	Selectively diminished the expression of KU80 and suppressed tumor growth	[84]
	peptide BAL	By selective targeting and linking to the DNA Ligase IV and Artemis leading to inhibition the DNA repair	[98]
	PROM1-NP	Restrict cell proliferation and suppressed tumor growth	[99]
	TP508	Suppressed the upregulation of some checkpoint kinases involved in cell cycle repair and arrest, as well as prevent activation of DNA repair molecule	[100]
	pHLIP-GdNP	Selective tumor targeting ability and promote the effect of short-range Auger electrons and radiosensitizing photoelectrons	[101]

Fig. 3 Mechanism of damage repair/fixation based on oxygen electron affinity, where –SH represents thiols and O. represents biomolecule radicals

oxygen as the most electrophilic cellular molecule could be readily reduced by electrons generation through the incident radiation. Once oxygenated tumor are exposed to an ionizing radiation dose, energy transfer leads to water radiolysis along with the initial generation of ion radicals. These ion radicals then reacts with another water molecule to generate the highly reactive hydroxyl radical. Then unstable peroxide is generated by reaction of hydroxyl radical with oxygen molecule which eventually results in permanent DNA and cellular damage Fig. 4 [11].

Generally, the salubrious effect of typical RT is accomplished with the indirect role of free radicals which produced through water radiolysis, followed by death of cells/or biomolecules. However, the reductant agents such as thiols (–SH, an electron-donating group) could repair the biomolecule lesions by neutralizing radicals inside biomolecules. Whereas, in the presence of O_2 not only the damage is fixed but also the efficacy of RT is boosted. Accordingly, oxygen mimics as radiosensitizers are mainly nitro-containing compounds (with high electron affinity) could fix the cell damage in a manner similar to oxygen. The functions of fixing and repairing are simply interpreted by following equations.

In the tumor tissue, as the cancer cells rapidly growth, the surrounding vasculatures can not supply adequate oxygen to feed the whole tumor new cells, and gradually tumor mass becomes heterogeneous, and ultimately resulted in necrosis and ischemia. Generally, p53 pathway is responsible for apoptosis of cancer cells, but some heterogeneous cells can survive under hypoxic microenvironment through activation of hypoxia-inducible factor-1α (HIF-1α) pathway [16–18]. It has been reported that HIF-1α was connected with various signaling pathways including glycolysis pathway, glucose transport and vascular endothelial growth factor (VEGF) signaling pathway, which all of them involved in generation of the tumor vasculature [19–21]. Under hypoxic microenvironment tumor cells become more resistant to RT, aggressive and ultimately resistant to death through altering gene expression patterns as well as augmenting free radical scavenging [11, 12]. In recent years various approaches and research have been put forward to surpass hypoxia drawbacks, from using the oxygen-carrying blood substitute and high-pressure O_2 cylinder, to using elaborate, truthful strategies that proportionated differences in partial oxygen pressure (PO_2) between healthy and tumors tissue [22, 23]. In order to ameliorate cancer- associated hypoxia, hyperbaric oxygen as a direct method is widely employed, but this method is not convenient and in some cases it may cause complications [24, 25]. However, in the presence of oxygen the therapeutic or noxious effect of ionizing radiation were enhanced. Furthermore, oxygen due to its unique electronic configuration could promote the formation of free radical as well [26]. Several molecules

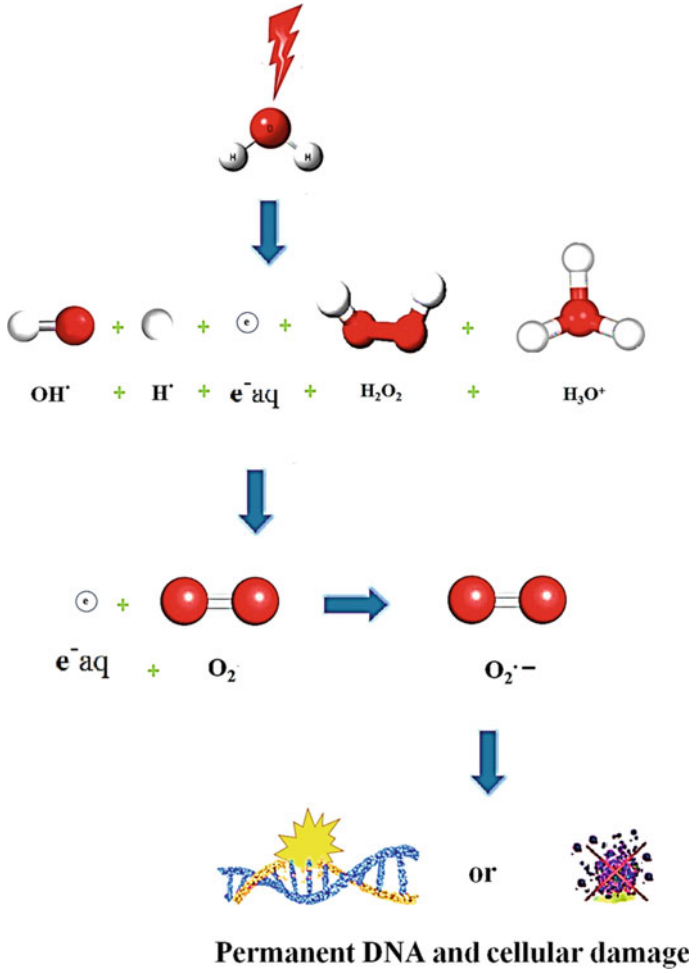

Fig. 4 Radiolyss of water and its mechanism followed by permanent cell or DNA damage

with the similar function and same features are under development as radiosensitizers. Accordingly, some of these agents have been researched into the preclinical and even into clinical. As reported previously, the main pitfall of the most common types of solid tumors is hypoxia which significantly restrict the effect of RT. Accordingly, oxygen and its mimics should be employed as radiosensitizers to enhance the efficacy of RT [27]. Due to the instability of free radicals their reaction with other compounds is very quick, thus oxygen mimetic radiosensitisers should be present at the instant of irradiation. Oxygen mimetics possess the same chemical properties as the oxygen molecule, but exhibited better diffusion properties to oxygen-deficient tissue and greater electron affinity than oxygen as well. According to the Fig. 3, oxygen mimetics similar to oxygen can practically "fix" radiation-induced

damage, which eventually leads to nonrepairable and biomolecule death. Hence, these mimetics of oxygen regards as "true radiosensitizers". Nitric oxide (NO) and nitro- containing compounds, in particular, considered as well studied and representative oxygen mimetics [28, 29]. Nitrobenzene is the most common pattern of electron-affinity radiosensitizers, however afterwards researchers have shifted their focus on nitroimidazole and its derivatives [30]. Nitroimidazoles or nitroaromatic compounds as new class of radiation-induced redox reactions or enzyme-catalysed reactions are inherently inactive, they becomes active once they exposed to the ionizing radiation to fix DNA damage in tumor hypoxic cells [31]. 2-nitroimidazole or misonidazole was found to be the earliest stablished nitroimidazoles. Furthermore, preclinical investigations in the majority of solid murine tumors have revealed that misonidazole possessed superior radiosensitization effect compared to metronidazole (Flagyl®) [32, 33]. Regardless of this unique feature, the collected data from clinical trials associated with misonidazole were failed to show benefits, as it exhibited sever neurotoxicity [34, 35]. Metronidazole, a known nitroimidazole derivatives possesses less electron affinity and was considered as a poor radiosensitizer agent [30, 36]. Indeed, due to the dose-limiting toxicity, both metronidazole and misonidazole are from being perfect for implementation in RT [37]. Accordingly, substantial efforts have been put forward to modulate the pharmacokinetic features of nitroimidazoles and its derivatives. In order to diminish the neurotoxicity associated with nitroimidazole, novel generation of nitroimidazole derivatives such nimorazole or etanidazole have been developed, these agents owing to its suitable hydrophilicity can restrict neurotoxicity. For instance, etanidazole represented superior hydrophilicity in comparison with misonidazole, this is attributed to the presence of hydroxyl groups in side chain of this agent [38]. It is worth noting that etanidazole exhibited no significant assistance in treatment of patients suffer from head and neck cancer [39]. In contrary, nimorazole another nitroimidazole derivatives (5-nitroimidazole) has shown promising out comes in Denmark for treatment of head and neck cancers. Of note, this potential therapeutic agent has been further exploited for its efficacy in an EORTC international trial [40–46]. Interestingly, the DAHANCA 28 trial revealed that treatment of patients with hyper-fractionated, accelerated RT accompanied by nimorazole and cisplatin (HART-CN) resulted in positive outcomes with satisfactory tumor control [47]. Several nitro-based agents have been investigated for its potential in radiosensitization of tumor hypoxia cells as well. It has been well documented that dinitroazetidine, RRx-001, regarded as a potent radiosensitization agent and this low toxic agent has been exploited for its effectiveness in the NCT02871843 clinical trial recently [48].

NO or nitrogen oxides as a known radiosensitizer operates through various mechanism from direct to indirect one. In a similar manner to the oxygen, nitrogen oxides through nitrosative stress pathways can also damage the DNA of the cells by "fixing" or stabilizing radiation-induced DNA damage [28]. Both nitrosative stress and oxidative stress pathways are responsible for the formation of reactive species. For instance, it was found that nitric acid, peroxynitrite and nitrous acid exhibited cytotoxic effects through several mechanisms such as inhibition of mitochondrial respiration, glutathione depletion, protein nitrosylation and cross-linking of DNA [49–52].

Since nitrogen oxides are neutral and have no charges, it can readily and freely diffuse through cell membranes. Accordingly it can regulate vascular physiology by linking to soluble guanylate cyclase (sGC) to induce cyclic GMP production [53–55]. Several studies has shown that both sanazole and nimorazole (5-nitroimidazoles) could release nitrogen oxides [56, 57]. There are some controversial results regarding nitrogen oxides in clinical trials, in one study at a phase of I, results revealed that administration of nitrogen oxides to the non-small-cell lung cancer (NSCLC) patients promoted tumor perfusion and resulted in augmented tumor growth [58]. In contrary, in another study at phase of II of clinical trial results showed that introducing low-dose of nitrogen oxides to the prostate cancer patients resulted in no direct cytotoxic effect, whereas, interestingly low-dose of nitrogen oxides could diminish tumor hypoxia by enhancing blood flow in tumor microenvironment [59]. Several approved chemotherapeutic agents by FDA such as etaracizumab, sorafenib and bevacizumab operates through blocking the VEGF pathway [60]. It was found that overexpression of VEGF under hypoxia condition may lead to neovascularization as well as proliferation of endothelial cell. It has been widely accepted that in angiogenesis in order to maintain the vascular homeostasis, there is a positive and negative feedback regulation association between of nitrogen oxides and VEGF [61]. Moreover, Liebmann and colleagues confirmed that pretreatment of mice with of nitrogen oxides can protect mice and prolong their survival rate after irradiation [62]. Besides advancement in development of novel radiosensitizers, other strategies such as hyperbaric oxygen, Oxygen carriers (perfluorocarbons) have been applied as well. Intratumorally administration of hydrogen peroxide to tumor tissue leads to local generation of oxygen and thereby the effectiveness of irradiation is boosted. Some chemicals developed from the start point of free radicals have shown promising prospects or have already been used clinically.

3 Macromolecules

Besides the above mentioned radiosensitizers, macromolecules such as oligonucleotides, peptides, proteins and miRNAs, are competent enough for regulating radiosensitivity and have been widely exploited as a potential radiotherapeutics for development of novel radiosensitizers. The schematic representation of mechanisms of macromolecules is shown in Fig. 5.

4 Oligonucleotides

Oligonucleotides are potential candidates for regulating gene expression owing to their ease of design and synthesis, and recently antisense oligonucleotides have attracted wide interest of researchers for use as a potent radiosensitizer [4]. It has been well documented that telomerase is upregulated or reactivated in the vast majority

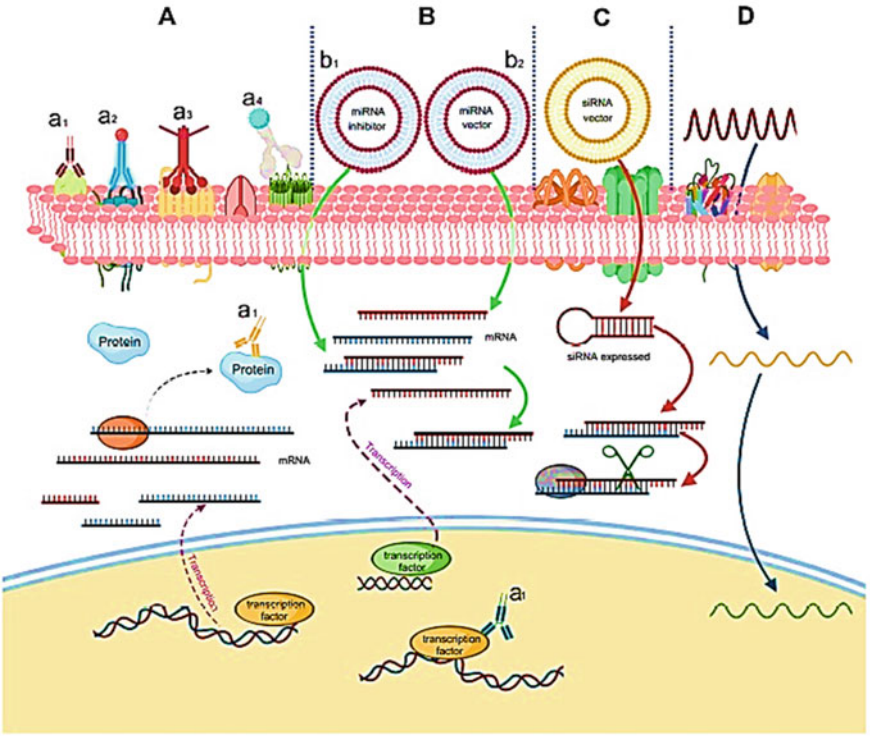

Fig. 5 Schematic illustration of radiosensitization mechanism of macromolecules, **A** Peptides and proteins. **a1** Interaction of key proteins in a direct way. **a2** Radioactive seeds carrying and loading. **a3** Delivery of radiosensitizers. **a4** Nanomaterials decorated with radiosensitizers. **B** Binding of miRNAs with mRNAs in order to accomplish radiosensitization. **b1** Expression was suppressed by inhibitors. **b2** Overexpression. **C** Radiosensitivity was boosted by siRNAs through binding and degrading complementary mRNAs. **D** Radiosensitivity was potential improved by Oligonucleotides through complementary binding with DNAs. Reproduced with permission from Ref. [13] with the permission of the Creative Commons Attribution—Non Commercial (unported, v3.0) License (https://creativecommons.org/licenses/by-nc/3.0/). Copyright 2021, Dove Medical Press Limited

of tumors (>85%), whereas its expression is highly limited in healthy tissue. More recent evidence reveals that the radiolabeled oligonucleotides as a potent radiosensitizer could successfully regulate and inhibit the expression of telomerase by targeted the RNA subunit of telomerase and subsequently induction of DNA damage in telomerase-positive tumor cells [63]. At the same time, it has been reported that the antisense oligonucleotides modified with phosphorothioate against a subunit of telomerase called human telomerase reverse transcriptase (hTERT) could effectively enhance the radiotherapy effect in liver cancer [64]. In the last few years, much more information on oligonucleotides has become available. In this respect, Park and coworkers highlighted that cyclic AMP response element-directed transcription inhibition via decoy oligonucleotides which enhanced tumor cell sensitization to irradiation

[65]. Furthermore, Yu and co-workers reported that the radiosensitivity of nasopharyngeal carcinoma cells were enhanced by antisense oligonucleotides targeted human telomerase RNA (hTR ASODN) [66]. Bavelaar and colleagues fabricated nano-based multiplatform for theranostic radionuclides delivery, radiosensitization and synchronous inhibition of telomerase. Accordingly, gold nanoparticels (AuNPs) were decorated with various moieties including ^{111}In-labeled oligonucleotidesto, Tat and PEG800-SH to obtain nano-based multi-platform in which Tat is cell-penetrating peptide and targeting agent, PEG800-SH reduced aggregation of nanoparticles and ^{111}In-labeled oligonucleotidesto augmented the DNA double-strand break (DSBs) Fig. 6.

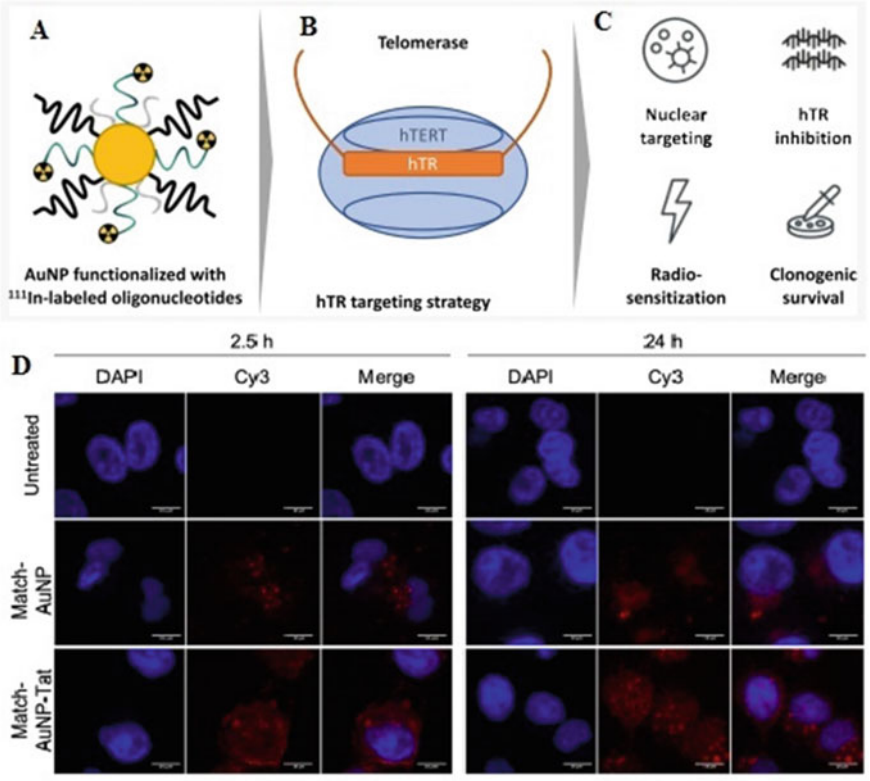

Fig. 6 Schematic representation of fabricated multiplatform based on AuNPs (**A**), hTR targeting strategy (**B**), Nuclear targeting, hTR inhibition, radiosensitization and survival of clonogenic (**C**), AuNPs subcellular distribution in MDA-MB-435 cells during 2.5 or 24 h incubation (**D**). Reproduced with permission from Ref. [67]. Copyright 2021, with permission from ACS

5 SiRNAs

Small interfering RNA (siRNA) also known as silencing RNA or short interfering RNA, are a class of 20–25 nucleotide-long double-stranded RNA molecules in which they operate within the RNA interference (RNAi) pathway similar to miRNA [68]. In the context of DNA double-strand breaks reparation after irradiation, NBS1 complex plays a vital role. Accordingly, targeting of NBS1 complex by siRNA is a highly promising approach which could increase radiation sensitivity of tumor cells [69]. S100A4 is a member of the S100 family which regulate different activities of cancer cells and play an important role in cancer progression through different mechanisms. Furthermore, it has been shown that implementation of short siRNA against S100A4 has sensitized human A549 cells to irradiation [70]. HuR is a protein that reduces radiation-induced DNA damage and lead to evolution of resistance to radiotherapy, thereby, knocking down of this protein using siRNA could boost the radiosensitivity and suppress the radiotherapy resistance [71]. More and more proteins have been identified as targeting sites for knocking down via siRNA to enhance the radiosensitivity of cancer cells. At the same time, surviving, a member of the inhibitor of apoptosis (IAP) protein family is highly expressed in many malignant tumor cells involved in therapy resistance and aggressiveness of tumours. Accordingly, survivin siRNA can be served as potential strategy which make neck and head squamous cell carcinoma more sensitive to radiation and thus overcoming the radiotherapy resistance [72]. In this respect, numerous siRNAs have been developed as radiosensitizers for silencing or down regulating genes related to radioresistance. Moreover, it has been reported that Glucose Transporter-1 (GLUT-1) is great targeting for overcoming radioresistance in malignant tumors since it regards as an intrinsic marker of hypoxia, therefore inhibition of GLUT-1 expression by nanotechnology based siRNA is a very promising option. Miao et al. developed Chitosan-conjugated stearic acid nanoparticles decorated with GLUT-1 siRNA (CSSA/siRNA) to downregulate the expression of GLUT-1. It was found that fabricated nanoparticle exhibited superior cell internalization and great safety compared to Lipofectamine^{TM}2000. They proposed developed polymeric nanoparticles as promising vector for effectively transfection of siRNA to potentiate the radiosensitivity of tumor cells [73].

Similarly, Die and colleagues applied curcumin (CUR), GLUT-1 siRNA and combination of these two modalities to enhance radiosensitivity of laryngeal carcinoma. It was found that combination therapy based on CUR and GLUT-1 exhibited strongest in vivo sensitization through both autophagy and apoptosis [74].

6 Proteins and Peptides

In addition to other medication such as antibody drugs which concurrently employed with RT, several attempts have been made to investigate the potential usage of peptides and proteins as radiosensitizers. Peptides and proteins, such as short peptides

and antibodies, display great affinity to receptors/antigens that are overexpressed in many tumors [75]. For instance, Sym004, a mixture of two recombinant monoclonal antibodies (futuximab and modotuximab) could effectively improve the radiosensitivity in tumor cells thorough two mechanisms: inducting apoptosis by down-regulation of MAPK signaling and inhibiting DNA double strand breaks repair [76]. At the same time, the titer of hepatocyte growth factor (HGF) is upregulated in the most common type of cancer. It has been reported that HGF also known as polypeptide growth factor met signaling pathway which mediates repair of DNA double-strand break, thereby monoclonal antibodies against such a polypeptide growth factor regards as an effective approach for increasing tumor-cell radiosensitivity. Accordingly, Buchanan et al. in their study increases the radiosensitivity of glioblastoma multiforme via inhibiting HGF-mediated repair of DNA damage using a monoclonal antibody of AMG102 [77]. In a major advance in 2019, Bourillon and co-workers reveals that DNA damage repair could be inhibited through inducing cell arrest in the G2/M phase. In this respect they employed HER3-ADC, a maytansine-based antibody–drug conjugate targeting HER3 and consequently the radiosensitivity of HER3-positive pancreatic tumor cells were improved as well [78]. Some similar studies were conducted by González et al. they showed radiosensitizing effect on human epidermal-like A431 cells by inducing DNA damage and apoptosis using nimotuzumab and cetuximab [77]. Furthermore, peptides and proteins in serum, such as paraoxonase-2 [79], HSP [80], and C-reactive peptide [81] have contributed to diminish radioresistance and could be employed as radiotherapy targets. Macrophage inflammatory protein derivative ECI301, can display an essential role in enhancing the effect of radiotherapy by assisting HMGB1 and HSP-70 [80]. Some similar proteins such as NKTR-214 [82] and DNAzyme (DZ1) [83] can improve the effect of radiotherapy as well. Furthermore, Kaplan and colleagues fabricated a novel therapeutic agent based on pH-low insertion peptides (pHLIP)–peptide nucleic acid (PNA) conjugate in which pHLIP could specifically diminish the DNA repair factor KU80 expression in tumors as well as assist selective radiosensitization of tumor cells. Overall they claimed that developed pH-sensitive peptides conjugate with PNA (pHLIP-aKu80 (γ)) are practically safe and nontoxic and could be considered as radiosensitizing agent for selective tumors [84].

Herein we summarized some recent advances in the development macromolecular-based nanoradiosensitizers in Table 1.

7 Nanomaterials

Over the past few decades, emergence of nanotechnology based radiosensitizers have provided a variety of potential therapeutic approaches and expanded the horizon of radiosensitizers development for cancer radiation therapy. In more particular, High-Z nanomaterials have drawn more attention as promising radiosensitizers in recent years owing their unique features of emitting, scattering and absorbing radiation energy. It was also found that heavy metal nanomaterials with high atomic number

(Z) values could be readily developed with tunable structure, size, shape and desirable components and features. In order to restrict the toxicity associated with heavy-metal nanoparticles, several nano-sized materials with particle size of smaller than that of kidney filtration threshold (particle size of less than 5.5 nm) have been fabricated that could be easily removed by urinary system resulted in potential in vivo use with diminished toxicity and accumulation [102, 103]. Besides these, low toxicity, rapid distribution and favorable kinetic profiles are other matchless features of metallic nanomaterials, such as silver and gold nanoclusters /nanoparticles which makes them promising candidates for biological application [104–108]. It has been shown that nanomaterials could effectively accumulate within tumor sites due to the enhanced permeation and retention (EPR) effect [109–111]. Moreover, modification, functionalization, surface coating, composition, shape and particle size of nanomaterials can be readily tuned to improve the EPR effect, and consequently enhance the nanomaterial accumulation within cancers cells resulted in superior therapeutic efficacy [108, 112–117]. In addition to these, nanomaterails have shown various impacts on cells, like inducing cell gaps, hampering motility [118], impacting cellular junctions [119] and prompting morphology changes as well [120]. The aforementioned influences on cells caused by nanoparticles are called nanomaterial-induced endothelial leakiness for which intensity and size regards as crucial elements [121]. Nanomaterial-induced endothelial leakiness enable the nanoparticles to accumulate in tumor tissue even without aid of EPR effect [119, 122]. In addition, there are several promising strategies to promote accumulation of nanomaterials in tumors, including functionalization of nanomaterials surface with desired targeted moieties as well as inducing oxidative stress in endothelial cells [123–125]. There has been substantial interest in development and fabrication of several chemical radiosensitizers based on nanomaterials or delivered by nanovehicles to improve cellular uptake in tumor sites. Hence, nanotechnology based approach holds a promising route to hasten the development of novel and efficient radiosensitizers.

8 Metal-Based Nanomaterials as an Effective Radiosensitizers

Metal-based nanomaterials in particular AuNPs exhibited great radiosensitization features in several cancers owing to its low toxicity, high biocompatibility and sufficient chemical stability (Fig. 7) [126–128]. Additionally, other potent metal-based nanoparticles with high Z value, such as bimetallic nanoparticles and silver nanoparticles (AgNPs), have been exploited in details [129, 130]. In order to enhance the efficacy of RT, metal-based nanoparticles interact with ionizing radiation (IR) and cell components and molecules at various stages such as biological, chemical, and physical aspects [131, 132].

One of the most important interactions in RT is an inelastic scattering of a photon by a charged particle (usually an electron) called Compton scattering. In the context of physical processes, metal-based nanoparticles with high Z value possesses great

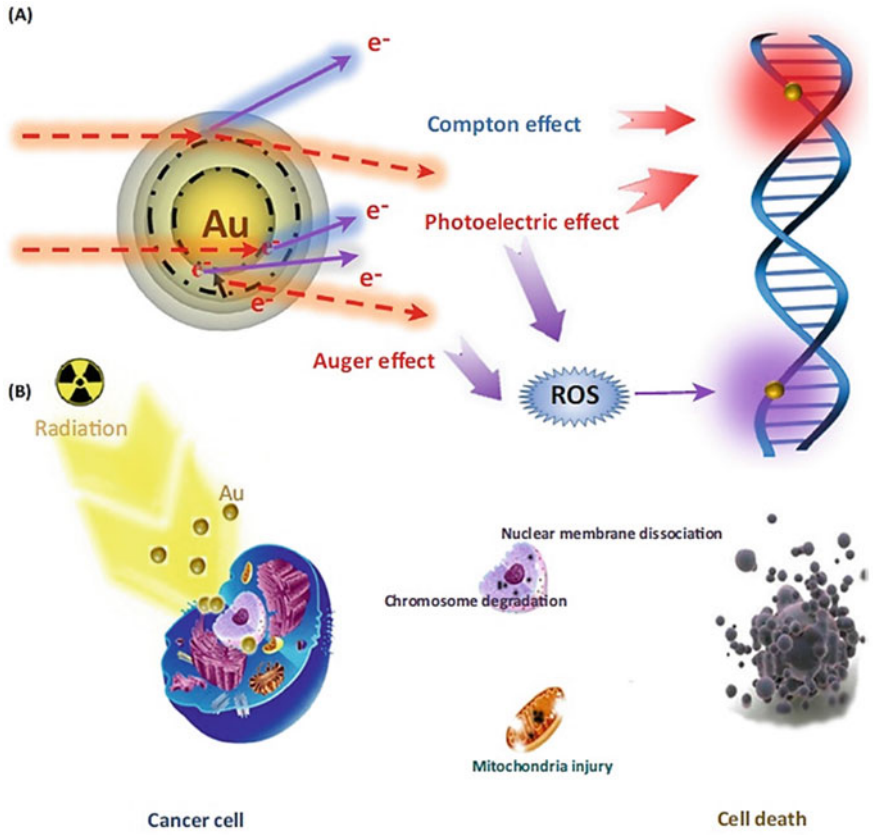

Fig. 7 Possible Mechanisms metal-based nanoparticles for instance AuNPs and its interaction with biomolecules and IR in various ways. The interaction AuNPs with IR dose resulted in DNA damage by Auger effect photoelectric effect and Compton effect (**B**) Metal-based nanomaterials in particular AuNPs can sensitize the cancer cells and enhance the generation of reactive oxygen species (ROS) and biological effects, such as exertion of the bystander effect, restriction of DNA repair and regulation of the cell cycle, which ultimately resulted in cell death. Reproduced with permission from Ref. [4]. Copyright 2018, with permission from Elsevier

competences for absorbing IR and emitting secondary electrons, resulted in augment the local dose, generally through photoelectric effect or the Compton scattering. This may occurs by reduction in energy of the incident photon through collision with electrons and accordingly deposition of the IR energy at the local site is achieved. Moreover, absorbing the energy of incident IR by electrons within a certain atom shell lead to emission of some electrically charged particles to ionize the adjacent cells or biological component called photoelectric effect. Both Compton scattering and photoelectric effect, along with others, e.g. coherent scattering, electron pairs and generation of Auger electrons facilitate nanomaterials with high Z value to boost the IR dose at local sites of tumors [133–135]. Overall, nanomaterials have improved the

RT efficacy through binding to DNA, boosting oxidative stress as well as enhancing the generation of ROS [136]. The latter one is commonly occurs because of the potential catalytic activity regarding to the surface of the nanomaterials. Regardless of inertness of Au, AuNPs represented great catalytic activity on the surface, which under exposure to IR can potentially promote the ROS formation [137, 138]. It has been reported that AuNPs with mean particle size of less than 5 nm due to its high surface area could potentially produce superoxide radicals by transferring electrons from donor groups present on its surface to oxygen molecules [139]. In addition to the above-mentioned advantages associated with AuNPs, this potent agent when its surface charge is positive could effectively sensitize the DNA via direct binding [140]. There have been several theories in the context of biological mechanisms of nanomaterials with high Z value including bystander effect, inhibition of DNA repair, and the cell cycle effect which have been extensively exploited to clarify the biological process of radiosensitization. One of the main factor in radiosensitivity of the tumor cells is the cell cycle, since it has been revealed that most cells are radiosensitive in both mitotic phases and the late G2 while radioresistant in the late S phase [141]. Hence, cell cycle regulation can be considered as an alternative option with positive outcomes in radiation-induced tumor therapy. In this case, metal-based nanomaterials holds a great potential as they can modulate the cell cycle phases in the favor of enhanced radiosensitivity [142–144]. IR may cause several types of DNA lesions namely base damage, double-strand breaks (DSB) and single-strand breaks (SSB), in this condition cancer cells endeavor to repair these damages to prevent tumor cell death. Therefore, this could be an effective approach for radiosensitization of tumor cells by inhibition of DNA repair. In this context, several studies have revealed that metal-based nanoparticles could effectively improve the radiosensitization of tumor cells through inhibition of DNA repair under IR [145, 146]. During treatment of cancer, several signaling molecules, ROS, miRNAs and cytokines released from tumor cells and simulate the adjacent cells to respond similarly, known as a bystander effect. Metal-based nanoparticles have shown their potential in modulating the bystander signaling, and mathematical models have been also developed to clarify nanomaterials could mediate this effect, and obtained data revealed that bystander effect play an important role in the radiosensitization of metal-based nanoparticles [147–150]. A great number of studies in literatures have demonstrated that nanomaterilas have potential capacity of being used either as a carrier or nanoradiosensitizer agents with beneficial influences in radiation-induced tumor therapy, herein we summarized some recent advances in the development of metal-based nanoradiosensitizers in Table 2.

Nosrati and colleagues developed bimetallic theranostic nanoparticles termed Bi_2S_3@BSA-Au-BSA-MTX-CUR for complete eradication of tumors. It was found that by introducing a single dose of fabricated bimetallic multifunctional theranostic nanoparticles along with a one-time X-ray irradiation, the tumors of mice completely vanished after around 3 weeks (Fig. 8) [156].

Hatoyama et al. fabricated AuNPs decorated with anti-human epidermal growth factor receptor type 2 (HER2) antibody using PEG chains called AuNP-PEG-HER2ab. The results indicated that this nanoparticle could potentially internalized

Table 2 Some recent advances of metal-based nanomaterials as radiosensitizers

Selected nanoparticles	Size (nm)	Cancer/cell lie	Brief outcomes	References
AuNPs-si-SP1	~12.8	CCK-8, A549	promote the radiosensitivity of A549 cells through inhibition of SP1 to upregulate GZMB	[87]
Mix of AuNPs/AuNRs	33.9	MCF-7	Exhibited high radiosensitivizaion and superior antiproliferative effects through regulation the expressions of Bim and Noxa gene	[151]
Fe_3O_4–Au–BSA–FA–CUR	~160	4T1	Exibited great biocompatibility, X-ray-induced DNA damage, ROS generation and radiosensitizing ability	[130]
+ AuNPs or -AuNPs	~30	–	+ AuNPs exhibited superior DNA damage compared to -AuNPs	[152]
AuNP-PEG-HER2ab	~30	SK-OV3	AuNP-PEG-HER2ab could potential localized within tumor deep tissue	[153]
GO-SPIO-Au NFs	40	CT26	A promising multipaltforms as theranostic nanostructures exhibited superior therapeutic efficacy	[154]
Au–Ag@HA NPs	~17.8	4T1	Represented effective tumor radiosensitization through selective tumor targeting and generation of hydroxykl radicals	[155]

(continued)

Table 2 (continued)

Selected nanoparticles	Size (nm)	Cancer/cell lie	Brief outcomes	References
Bi_2S_3@BSA-Au-BSA-MTX-CUR	8.5	4T1	Accomplish complete eradication of tumors in in vivo mouse model just via an injection of single-dose and one-time irradiation	[156]
AuNPs	2–19	PC3flu and PC3pip	Enhanced cellular uptake and therapeutic efficacy	[157]
Bi_2S_3@BSA-MTX NPs	~140	SW480	Improve radiosensitizer efficacy in vitro and exhibited superior therapeutic outcomes	[158]
Bi_2S_3-Au-BSA-FA hybrids	182.7	4T1	Suppress the tumor using developed nano-system along with X-ray irradiation	[159]
Bi_2S_3@BSA–Bio–MTX NPs	107.6	4T1	Showed excellent anticancer activity, in particular when treatment is accompanied by X-ray radiation	[160]
Bi_2S_3@BSA@CUR HNPs	103	HT-29	in vitro results showed enhanced chemo-radiation combination therapy potential	[161]
F-Au-BSA-MTX-CUR	138.4	4T1	Excellent anti-tumor activity in mice and combination therapy showed synergistic effects along with favorable results	[159]
Fe_3O_4-Au-BSA hybrid	<50	–	Excellent biocompatibility	[162]
Bi_2S_3@BSA-FA-CUR	170.9	4T1	Potentiate the efficacy of chemoradiation therapy and suppressed mice tumors in approximately within 3 weeks	[163]

(continued)

Table 2 (continued)

Selected nanoparticles	Size (nm)	Cancer/cell lie	Brief outcomes	References
PEGylated AgNPs (PNPs)	~33.3	C6 glioma	Inducing excellent apoptotic effects and proposed as a potential nano-radiosensitizer for glioma targeting treatment	[164]
PAA-Ag@TiO_2 NPs	49.2	JA774A.1 and HCT	The dose enhancement factors (DEFs) revealed that fabricated nanoparticles are more effective for the radiation dose enhancement at low energy X-rays (80 kV)	[165]
AgNPs	5–40	HepG-2	Green synthesis of silver nanoparticles presented promising radiosensitization and anticancerous activities	[129]

into the cells through endocytosis mechanism which had no effect on radiosensitization efficacy of developed AuNPs. Furthermore, administration of AuNP-PEG-HER2ab mice bearing tumors resulted in localization of these nano-system to both the tumor deep tissue and the periphery of the tumor tissue which potentially augments the radiosensitization efficacy in vivo [153].

Chong et al. synthesized hyaluronic acid-modified Au–Ag alloy nanoparticles termed Au–Ag@HA NPs with efficient cancer cells radiosensitization through selective tumor targeting and generation of ROS in particular hydroxyl radical. Interestingly, peroxidase-like activity of Au–Ag@HA NPs along with the IR promote the release of toxic silver ion (Ag+) and generation of hydroxyl radicals (•OH) in the tumor tissue, consequently resulted in favorable cancer treatment outcomes (Fig. 9) [155].

9 Conclusions and Prospects

It is worth noting that most of the improvements in cancer treatment owe much to the combination treatment modalities, in which RT remains as a cornerstone and is

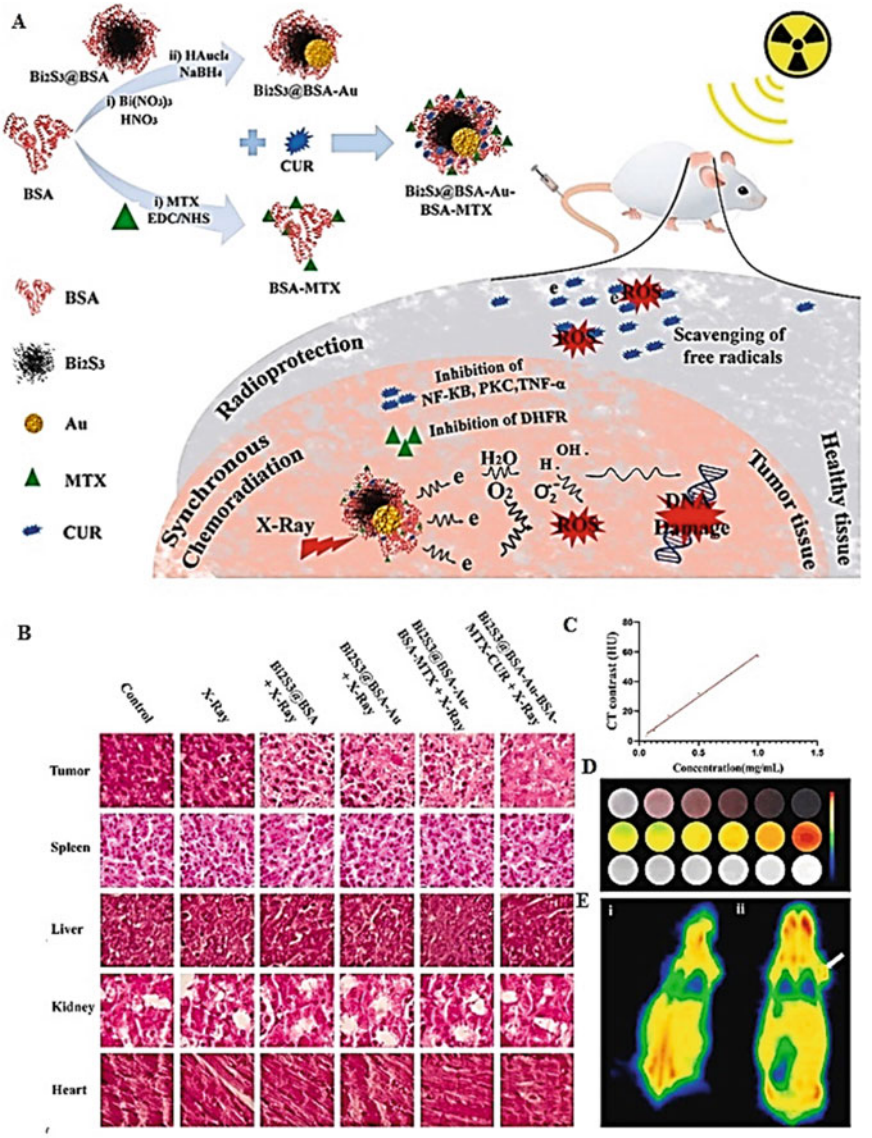

Fig. 8 **A** Schematic representation of fabricated Bi2S3@BSA-Au-BSA-MTX-CUR and its mechanism of action, **B** Histological analysis of the isolated organs and tumors which received various treatments. **C** X-ray attenuation of intensity in Hounsfield units (HU) of developed nano-system. **D** The CT images of different concentration; and **E** The CT images of mice bearing 4T1 tumor recorded at (i) pre and (ii) post intravenous injection of Bi2S3@BSA-Au-BSA-MTX-CUR. Reproduced from Ref. [156] with the permission of the Creative Commons Attribution 4.0 International License (http://creativecommons.org/licenses/by/4.0/). Copyright 2022. Elsevier

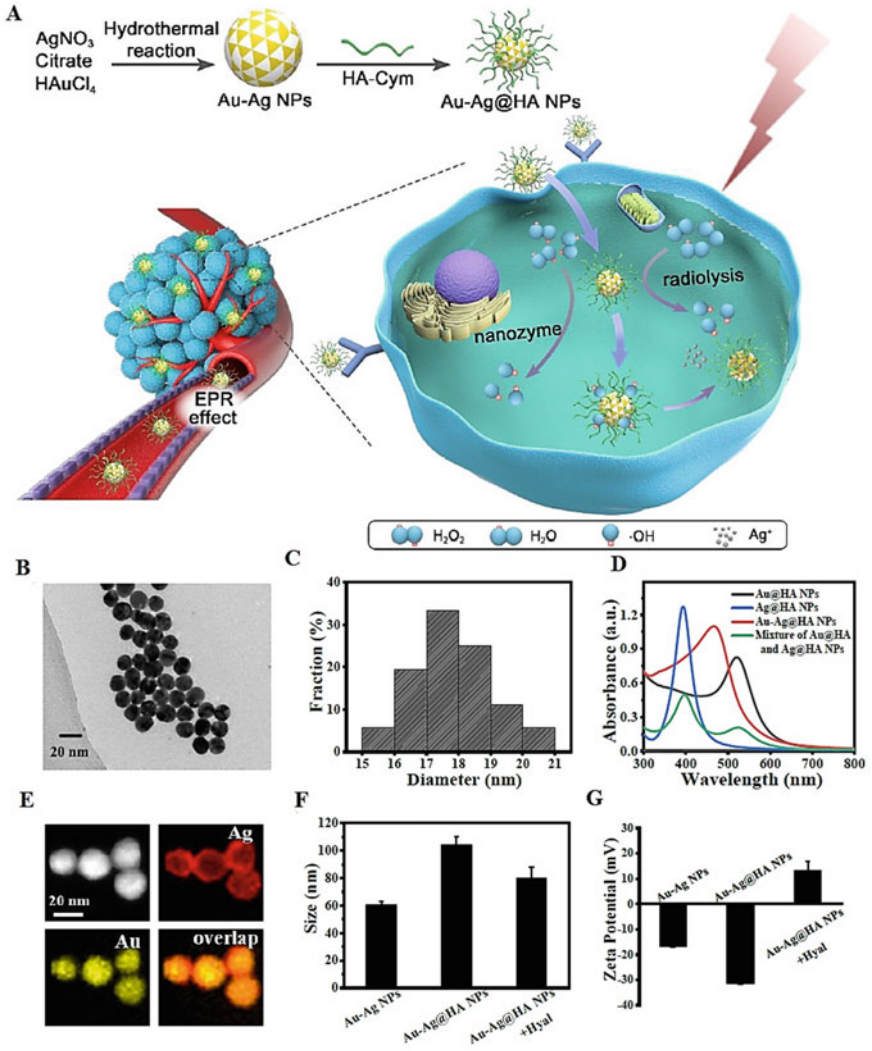

Fig. 9 **A** Schematic representation of synthetic route of Au–Ag@HA NPs and its mechanism of action. **B** TEM images of Au–Ag@HA NPs. **C** Size distribution of of Au–Ag@HA NPs. **D** UV–vis absorption spectra of different groups. **E** STEM-EDX elemental mapping images of Au- Ag@HA NPs, yellow and red colors refer to Au and Ag element, respectively **F** Hydrodynamic size and **G** zeta potential of different NPs. Reproduced with permission from Ref. [155]. Copyright 2020, with permission from ACS

delivered with curative intent in 50% of cancer patients. Of note, numerous clinical trials have revealed that approximately 70% of patients need to receive RT, and even in some [163] cases RT is the only treatment option for fighting against cancer. Recently, RT has received great attention due to its effectiveness in cancer therapy by destroying cancerous cells and shrinking tumors. However, healthy tissue damages induced by RT have remained dose-limiting factors in cancer radiotherapy and this is continue to be true in spite of all technological achievements and recent advances in this field. Furthermore, by increasing in the number of long-term cancer survivors, the patients' quality of life has significantly reduced on account of the emergence of unacceptable complications. The complications vary noticeably among patients from imperceptible to highly disabling levels. On the other hand, radiation-induced developmental disability [166] extensively relies on intrinsic factors, i.e. presence of comorbidity factors along with individual radiation sensitivity as well as extrinsic factors i.e. large variations in delivered doses and changes in the dose fractionation or treatment volume [167, 168]. This means that there are still some problems related to RT worldwide and cancer radiotherapy is far from being perfect. Systemic side effects are accounted as a known feature of common chemotherapy, whereas RT causes local/or loco-regional side effects and the latter one has been divided into early and late side-effects. Typical side effects are dry or moist desquamation of the skin, skin erythema, headaches, mucositis, edema, diarrhea or nausea in the case of early side effects which appear within a few weeks after treatment or occur during the time-course of the RT. Late side-effects are usually appear after latent periods of months to years after treatment, and include neural damage, vascular damage, atrophy and radiation-induced fibrosis which have a great impact on quality of life of cancer survivors [169]. Accordingly, clinicians and patients expect discovery of safe and novel options for the therapeutic management of healthy tissue damage and radiation-induced complications. An advanced understanding of the pathophysiological, molecular and cellular processes governing healthy tissue damage has enabled researchers worldwide to make and invent novel potent therapeutics which not only could minimize radiation-induced side-effects but also improve the efficacy of RT. In addition to the aforementioned obstacles associated with RT, most of the cancers, i.e. lymphoma, prostate, cervix, head and neck have displayed good response to RT, whereas there are still numerous cancers which display intrinsic radioresistance such as melanoma, sarcoma, etc. Hypoxia-induced radioresistance is another distinct problem related to RT which dramatically diminished the efficacy of cancer radiotherapy. Therapeutic ratio can be widened by using agents that selectively sensitize the tumor cells to radiation while protecting the normal tissues from radiation. In this regard, nanotechnology based materials hold great potential in fabrication and development of desirable radiosensitizers and can also provide a new opportunity for researchers to fined highly effective radiosensitizers to address the above-mentioned restriction. In fact, nanomaterials with ease of functionalization, good biocompatibility, low cytotoxicity and well-developed method of preparation, regards as an auspicious radiosensitizers for use in cancer eradication. As combination therapy has shown superior efficacy than monotherapy, development of nanomaterials that can carry drugs in addition to their radiosensitizers properties as

multifunctional platforms can potentiate the treatment efficacy of cancer. Furthermore, focusing on interdisciplinary approaches may also facilitate the development of effective and novel radiosensitizers with positive outcomes. Overall, there are several promising approaches in development of radiosensitizers that showed potential therapeutic effects, however cancer therapy with aid of radiosensitizers is still in its infancy and endeavors should be continued to hasten the clinical application of these systems. We believe that in the near future researchers will fabricate more efficient radiosensitizer and exploiting multitarget radiosensitizers would be an interesting future areas of research.

References

1. Lalla RV et al (2017) Oral complications at 6 months after radiation therapy for head and neck cancer. Oral Dis 23(8):1134–1143
2. Krause M et al (2017) Cancer stem cells: radioresistance, prediction of radiotherapy outcome and specific targets for combined treatments. Adv Drug Deliv Rev 109:63–73
3. Peitzsch C et al (2014) Hypoxia as a biomarker for radioresistant cancer stem cells. Int J Radiat Biol 90(8):636–652
4. Wang H et al (2018) Cancer radiosensitizers. Trends Pharmacol Sci 39(1):24–48
5. Adams G (1973) Chemical radiosensitization of hypoxic cells. Brit Med Bull 29(1):48–53
6. Fowler JF, Adams GE, Denekamp J (1976) Radiosensitizers of hypoxic cells in solid tumours. Cancer Treat Rev 3(4):227–256
7. Kunz-Schughart LA et al (2017) Nanoparticles for radiooncology: mission, vision, challenges. Biomaterials 120:155–184
8. Goel S, Ni D, Cai W (2017) Harnessing the power of nanotechnology for enhanced radiation therapy. ACS Nano 11(6):5233–5237
9. Garibaldi C et al (2017) Recent advances in radiation oncology. Ecancermed Sci 11:785
10. Wen P et al (2018) dbCRSR: a manually curated database for regulation of cancer radiosensitivity. Database 2018:1–8
11. Oronsky BT, Knox SJ, Scicinski J (2011) Six degrees of separation: the oxygen effect in the development of radiosensitizers. Trans Oncol 4(4):189–198
12. Harrison LB et al (2002) Impact of tumor hypoxia and anemia on radiation therapy outcomes. Oncologist 7(6):492–508
13. Gong L et al (2021) Application of radiosensitizers in cancer radiotherapy. Int J Nanomed 16:1083
14. Richardson RB, Harper M-E (2016) Mitochondrial stress controls the radiosensitivity of the oxygen effect: implications for radiotherapy. Oncotarget 7(16):21469
15. Zheng L, Kelly CJ, Colgan SP (2015) Physiologic hypoxia and oxygen homeostasis in the healthy intestine. A review in the theme: cellular responses to hypoxia. Am J Physiol Cell Physiol 309(6):C350–C360
16. Zhu H, Zhang S (2018) Hypoxia inducible factor-1α/vascular endothelial growth factor signaling activation correlates with response to radiotherapy and its inhibition reduces hypoxia-induced angiogenesis in lung cancer. J Cell Biochem 119(9):7707–7718
17. Zhang Q et al (2021) Role of hypoxia inducible factor-1 in cancer stem cells (Review). Mol Med Rep 23(1):17
18. Bel Aiba RS et al (2006) The role of hypoxia inducible factor-1 in cell metabolism–a possible target in cancer therapy. Expert Opin Ther Targets 10(4):583–599
19. Maxwell PH (2005) The HIF pathway in cancer. in Seminars in cell & developmental biology. Elsevier

20. George Boyle R, Travers S (2006) Hypoxia: targeting the tumour. Anti Cancer Agents Med Chem (Formerly Current Medicinal Chemistry Anti-Cancer Agents) 6(4):281–286
21. Verdegem D et al (2014) Endothelial cell metabolism: parallels and divergences with cancer cell metabolism. Cancer Metab 2(1):19
22. Hardavella G et al (2019) Oxygen devices and delivery systems. Breathe 15(3):e108–e116
23. Cabrales P, Intaglietta M (2013) Blood substitutes: evolution from non-carrying to oxygen and gas carrying fluids. ASAIO J 59(4):337–354
24. Stępień K, Ostrowski RP, Matyja E (2016) Hyperbaric oxygen as an adjunctive therapy in treatment of malignancies, including brain tumours. Med Oncol 33(9):1–9
25. Choudhury R (2018) Hypoxia and hyperbaric oxygen therapy: a review. Int J General Med 11:431
26. Rockwell S et al (2009) Hypoxia and radiation therapy: past history, ongoing research, and future promise. Curr Mol Med 9(4):442–458
27. Spiess BD (2020) Oxygen therapeutic agents to target hypoxia in cancer treatment. Curr Opin Pharmacol 53:146–151
28. Zhou X et al (2020) Near-infrared light-responsive nitric oxide delivery platform for enhanced radioimmunotherapy. Nanomicro Lett 12(1):100
29. Lin YJ et al (2020) Biomimetic engineering of a scavenger-free nitric oxide-generating/delivering system to enhance radiation therapy. Small 16(23):2000655
30. Wardman P (2018) Nitroimidazoles as hypoxic cell radiosensitizers and hypoxia probes: misonidazole, myths and mistakes. Br J Radiol 92(1093):20170915
31. Spisz P et al (2019) Why does the type of halogen atom matter for the radiosensitizing properties of 5-halogen substituted 4-thio-2′-deoxyuridines? Molecules 24(15):2819
32. Brown JM (1984) Clinical trials of radiosensitizers: what should we expect? Int J Radiat Oncol Biol Phys 10(3):425–429
33. Brown JM (1975) Selective radiosensitization of the hypoxic cells of mouse tumors with the nitroimidazoles metronidazole and Ro 7–0582. Radiat Res 64(3):633–647
34. Urtasun R et al (1978) Peripheral neuropathy related to misonidazole: incidence and pathology. Br J Cancer Suppl 3:271
35. Dische S et al (1979) Misonidazole—a drug for trial in radiotherapy and oncology. Int J Radiat Oncol Biol Phys 5(6):851–860
36. Bonnet M et al (2018) Next-generation hypoxic cell radiosensitizers: nitroimidazole alkyl-sulfonamides. J Med Chem 61(3):1241–1254
37. Rosenberg A, Knox S (2006) Radiation sensitization with redox modulators: a promising approach. Int J Radiat Oncol Biol Phys 64(2):343–354
38. Coleman CN et al (1990) Final report of the phase I trial of the hypoxic cell radiosensitizer SR 2508 (etanidazole) radiation therapy oncology group 83–03. Int J Radiat Oncol Biol Phys 18(2):389–393
39. Brown JM, Wilson WR (2004) Exploiting tumour hypoxia in cancer treatment. Nat Rev Cancer 4(6):437–447
40. Toustrup K et al (2012) Gene expression classifier predicts for hypoxic modification of radiotherapy with nimorazole in squamous cell carcinomas of the head and neck. Radiother Oncol 102(1):122–129
41. Thomson D et al (2014) NIMRAD–a phase III trial to investigate the use of nimorazole hypoxia modification with intensity-modulated radiotherapy in head and neck cancer. Clin Oncol 26(6):344–347
42. Saksø M et al (2019) A prospective, multicenter DAHANCA study of hyperfractionated, accelerated radiotherapy for head and neck squamous cell carcinoma. Acta Oncol 58(10):1495–1501
43. Bentzen J et al (2015) Locally advanced head and neck cancer treated with accelerated radiotherapy, the hypoxic modifier nimorazole and weekly cisplatin. Results from the DAHANCA 18 phase II study. Acta Oncol 54(7):1001–1007
44. Metwally MAH, Frederiksen KD, Overgaard J (2014) Compliance and toxicity of the hypoxic radiosensitizer nimorazole in the treatment of patients with head and neck squamous cell carcinoma (HNSCC). Acta Oncol 53(5):654–661

45. Overgaard J et al (2005) Plasma osteopontin, hypoxia, and response to the hypoxia sensitiser nimorazole in radiotherapy of head and neck cancer: results from the DAHANCA 5 randomised double-blind placebo-controlled trial. Lancet Oncol 6(10):757–764
46. Overgaard J et al (1998) A randomized double-blind phase III study of nimorazole as a hypoxic radiosensitizer of primary radiotherapy in supraglottic larynx and pharynx carcinoma. Results of the Danish Head and Neck Cancer Study (DAHANCA) Protocol 5–85. Radiother Oncol 46(2):135–146
47. Saksø M et al (2020) DAHANCA 28: a phase I/II feasibility study of hyperfractionated, accelerated radiotherapy with concomitant cisplatin and nimorazole (HART-CN) for patients with locally advanced, HPV/p16-negative squamous cell carcinoma of the oropharynx, hypopharynx, larynx and oral cavity. Radiother Oncol 148:65–72
48. Oronsky B et al (2016) RRx-001, A novel dinitroazetidine radiosensitizer. Invest New Drugs 34(3):371–377
49. Meffert MK, Premack BA, Schulman H (1994) Nitric oxide stimulates Ca2+-independent synaptic vesicle release. Neuron 12(6):1235–1244
50. Nelson EJ, Connolly J, McArthur P (2003) Nitric oxide and S-nitrosylation: excitotoxic and cell signaling mechanism. Biol Cell 95(1):3–8
51. Bonavida B et al (2006) Therapeutic potential of nitric oxide in cancer. Drug Resist Updates 9(3):157–173
52. Edfeldt NF et al (2004) Solution structure of a nitrous acid induced DNA interstrand cross-link. Nucleic Acids Res 32(9):2785–2794
53. Rogers NM et al (2014) Regulation of soluble guanylate cyclase by matricellular thrombospondins: implications for blood flow. Front Physiol 5:134
54. Lundberg JO, Gladwin MT, Weitzberg E (2015) Strategies to increase nitric oxide signalling in cardiovascular disease. Nat Rev Drug Discovery 14(9):623–641
55. Tsai EJ, Kass DA (2009) Cyclic GMP signaling in cardiovascular pathophysiology and therapeutics. Pharmacol Ther 122(3):216–238
56. Girard M et al (1993) 5-Nitroimidazoles. II: unexpected reactivity of ronidazole and dimetridazole with thiols. Canadian J Chem 71(9):1349–1352
57. Kondakova IV et al (2004) Production of nitric oxide by hypoxic radiosensitizer sanazole. Exp Oncol 26(4):329–333
58. Ng Q-S et al (2007) Effect of nitric-oxide synthesis on tumour blood volume and vascular activity: a phase I study. Lancet Oncol 8(2):111–118
59. Siemens DR et al (2009) Phase II study of nitric oxide donor for men with increasing prostate-specific antigen level after surgery or radiotherapy for prostate cancer. Urology 74(4):878–883
60. Libert N et al (2010) Inhibitors of angiogenesis: new hopes for oncologists, new challenges for anesthesiologists. J Am Soc Anesthesiol 113(3):704–712
61. Pandey AK et al (2018) Mechanisms of VEGF (vascular endothelial growth factor) inhibitor–associated hypertension and vascular disease. Hypertension 71(2):e1–e8
62. Liebmann J et al (1994) In vivo radiation protection by nitric oxide modulation. Cancer Res 54(13):3365–3368
63. Jackson MR et al (2019) Radiolabeled oligonucleotides targeting the RNA subunit of telomerase inhibit telomerase and induce DNA damage in telomerase-positive cancer cells. Cancer Res 79(18):4627–4637
64. Cao F et al (2017) Phosphorothioate-modified antisense oligonucleotides against human telomerase reverse transcriptase sensitize cancer cells to radiotherapy. Mol Med Rep 16(2):2089–2094
65. Park SI et al (2016) Inhibition of cyclic AMP response element-directed transcription by decoy oligonucleotides enhances tumor-specific radiosensitivity. Biochem Biophys Res Commun 469(3):363–369
66. Yu C et al (2015) Antisense oligonucleotides targeting human telomerase mRNA increases the radiosensitivity of nasopharyngeal carcinoma cells. Mol Med Rep 11(4):2825–2830
67. Bavelaar BM et al (2021) Oligonucleotide-functionalized gold nanoparticles for synchronous telomerase inhibition, radiosensitization, and delivery of theranostic radionuclides. Mol Pharmaceutics 18(10):3820–3831

68. Gu J et al (2017) Knockdown of HIF-1α by siRNA-expressing plasmid delivered by attenuated Salmonella enhances the antitumor effects of cisplatin on prostate cancer. Sci Rep 7:7546
69. Ohnishi K et al (2006) siRNA targeting NBS1 or XIAP increases radiation sensitivity of human cancer cells independent of TP53 status. Radiat Res 166(3):454–462
70. Qi R, Qiao T, Zhuang X (2016) Small interfering RNA targeting S100A4 sensitizes non-small-cell lung cancer cells (A549) to radiation treatment. Onco Targets Ther 9:3753
71. Mehta M et al (2016) HuR silencing elicits oxidative stress and DNA damage and sensitizes human triple-negative breast cancer cells to radiotherapy. Oncotarget 7(40):64820
72. Khan Z et al (2016) Growth inhibition and chemo-radiosensitization of head and neck squamous cell carcinoma (HNSCC) by survivin-siRNA lentivirus. Radiother Oncol 118(2):359–368
73. Miao J et al (2021) Chitosan-based glycolipid conjugated sirna delivery system for improving radiosensitivity of laryngocarcinoma. Polymers 13(17):2929
74. Dai LB et al (2021) Radiosensitizing effects of curcumin alone or combined with GLUT1 siRNA on laryngeal carcinoma cells through AMPK pathway-induced autophagy. J Cell Mol Med 25(13):6018–6031
75. Lhuillier C et al (2019) Radiation therapy and anti-tumor immunity: exposing immunogenic mutations to the immune system. Genome Med 11(1):1–10
76. Saker J et al (2013) EGFR targeting antibody SYM004 causes radiosensitization in tumor cells expressing wild-type K-Ras via modulation of MAPK signaling. Cancer Res 73(8_Supplement):1027
77. González JE et al (2012) Radiosensitization induced by the anti-epidermal growth factor receptor monoclonal antibodies cetuximab and nimotuzumab in A431 cells. Cancer Biol Ther 13(2):71–76
78. Bourillon L et al (2019) An auristatin-based antibody-drug conjugate targeting HER3 enhances the radiation response in pancreatic cancer. Int J Cancer 145(7):1838–1851
79. Krüger M et al (2016) The anti-apoptotic PON2 protein is Wnt/β-catenin-regulated and correlates with radiotherapy resistance in OSCC patients. Oncotarget 7(32):51082
80. Kanegasaki S et al (2014) Macrophage inflammatory protein derivative ECI301 enhances the alarmin-associated abscopal benefits of tumor radiotherapy. Cancer Res 74(18):5070–5078
81. Nieder C et al (2016) Palliative radiotherapy in cancer patients with increased serum C-reactive protein level. In Vivo 30(5):581–586
82. Walker JM et al (2020) NKTR-214 immunotherapy synergizes with radiotherapy to stimulate systemic CD8+ T cell responses capable of curing multi-focal cancer. J Immunother Cancer 8(1):e000464
83. Cao Y et al (2014) Therapeutic evaluation of Epstein-Barr virus-encoded latent membrane protein-1 targeted DNAzyme for treating of nasopharyngeal carcinomas. Mol Ther 22(2):371–377
84. Kaplan AR et al (2020) Ku80-Targeted pH-sensitive peptide–PNA conjugates are tumor selective and sensitize cancer cells to ionizing radiation. Mol Cancer Res 18(6):873–882
85. Zhang S et al (2018) Dual radiosensitization and anti-STAT3 anti-proliferative strategy based on delivery of gold nanoparticle-oligonucleotide nanoconstructs to head and neck cancer cells. Nanotheranostics 2(1):1
86. Zhong J-T et al (2019) GLUT-1 siRNA enhances radiosensitization of laryngeal cancer stem cells via enhanced DNA damage, cell cycle redistribution, and promotion of apoptosis in vitro and in vivo. Onco Targets Ther 12:9129
87. Zhuang M et al (2021) Radiosensitizing effect of gold nanoparticle loaded with small interfering RNA-SP1 on lung cancer: AuNPs-si-SP1 regulates GZMB for radiosensitivity. Trans Oncol 14(12):101210
88. Lee JA et al (2020) Improving radiation response in glioblastoma using ECO/siRNA nanoparticles targeting DNA damage repair. Cancers 12(11):3260
89. Li X et al (2021) Aminopeptidase N targeting nanomolecules assisted delivery of VEGF siRNA to potentiate antitumour therapy by suppressing tumour revascularization and enhancing radiation response. J Mater Chem B 9(36):7530–7543

90. Liu J et al (2020) Development of injectable thermosensitive polypeptide hydrogel as facile radioisotope and radiosensitizer hotspot for synergistic brachytherapy. Acta Biomater 114:133–145
91. Han L et al (2018) Enhanced radiosensitization of human glioblastoma multiforme cells with phosphorylated peptides derived from Gli2. Neuropeptides 70:87–92
92. Wang Q et al (2020) A coassembled peptide hydrogel boosts the radiosensitization of cisplatin. Chem Commun 56(85):13017–13020
93. Dong W et al (2020) Radiotherapy enhancement for human pancreatic carcinoma using a peptide-gold nanoparticle hybrid. J Biomed Nanotechnol 16(3):352–363
94. Xie Y (2021) ANTP-SMACN7 fusion peptide alone induced high linear energy transfer irradiation radiosensitization in non-small cell lung cancer cell lines. Cancer Biol Med 18(2):1–12
95. Schilling D et al (2017) The Hsp70 inhibiting peptide aptamer A17 potentiates radiosensitization of tumor cells by Hsp90 inhibition. Cancer Lett 390:146–152
96. Zhang R et al (2020) ANTP-SmacN7 fusion peptide-induced radiosensitization in A549 cells and its potential mechanisms. Thoracic Cancer 11(5):1271–1279
97. Liang G et al (2017) RGD peptide-modified fluorescent gold nanoclusters as highly efficient tumor-targeted radiotherapy sensitizers. Biomaterials 144:95–104
98. Zhu C et al (2021) Developing a peptide that inhibits DNA repair by blocking the binding of Artemis and DNA Ligase IV to enhance tumor radiosensitivity. Int J Radiat Oncol Biol Phys 111(2):515–527
99. Chen JLY et al (2017) Prominin-1-Specific binding peptide-modified apoferritin nanoparticle carrying irinotecan as a novel radiosensitizer for colorectal cancer stem-like cells. Part Part Syst Charact 34(5):1600424
100. Moya SM (2017) Radiosensitizing effects of thrombin peptide TP508 on medulloblastoma cancer stem cells. PhD Thesis, The University of Texas Medical Branch
101. Liu W et al (2020) Tumor-targeted pH-low insertion peptide delivery of theranostic gadolinium nanoparticles for image-guided nanoparticle-enhanced radiation therapy. Trans Oncol 13(11):100839
102. Choi HS et al (2010) Design considerations for tumour-targeted nanoparticles. Nat Nanotechnol 5(1):42–47
103. Choi HS et al (2007) Renal clearance of quantum dots. Nat Biotechnol 25(10):1165–1170
104. Luo D et al (2021) Recent development of gold nanoparticles as contrast agents for cancer diagnosis. Cancers 13(8):1825
105. Zhao J et al (2021) Increasing the accumulation of aptamer AS1411 and verapamil conjugated silver nanoparticles in tumor cells to enhance the radiosensitivity of glioma. Nanotechnology 32(14):145102
106. Abdulsahib SS (2021) Synthesis, characterization and biomedical applications of silver nanoparticles. Biomedicine 41(2):458–464
107. Chen Y et al (2020) Gold nanoparticles as radiosensitizers in cancer radiotherapy. Int J Nanomed 15:9407
108. Nosrati H et al (2018) Preparation, characterization, and evaluation of amino acid modified magnetic nanoparticles: drug delivery and MRI contrast agent applications. Pharm Dev Technol 23(10):1156–1167
109. Mikada M et al (2017) Evaluation of the enhanced permeability and retention effect in the early stages of lymph node metastasis. Cancer Sci 108(5):846–852
110. Kang H et al (2020) Size-dependent EPR effect of polymeric nanoparticles on tumor targeting. Adv Healthcare Mater 9(1):1901223
111. Ding Y et al (2020) Investigating the EPR effect of nanomedicines in human renal tumors via ex vivo perfusion strategy. Nano Today 35:100970
112. Yoozbashi M et al (2022) Magnetic nanostructured lipid carrier for dual triggered curcumin delivery: Preparation, characterization and toxicity evaluation on isolated rat liver mitochondria. J Biomater Appl 36(6):1055–1063

113. Rahmati M-A et al (2022) Self-assembled magnetic polymeric micelles for delivery of quercetin: Toxicity evaluation on isolated rat liver mitochondria. J Biomater Sci Polym Ed 33(3):279–298
114. Rashidzadeh H et al (2021) pH-sensitive curcumin conjugated micelles for tumor triggered drug delivery. J Biomater Sci Polym Ed 32(3):320–336
115. Abazari M et al (2022) A systematic review on classification, identification, and healing process of burn wound healing. Int J Low Extrem Wounds 21(1):18–30
116. Fattahi N et al (2021) Enhancement of the brain delivery of methotrexate with administration of mid-chain ester prodrugs: in vitro and in vivo studies. Int J Pharm 600:120479
117. Rezaei SJT et al (2020) pH-triggered prodrug micelles for cisplatin delivery: preparation and in vitro/vivo evaluation. React Funct Polym 146:104399
118. Tay CY et al (2014) Nanoparticles strengthen intracellular tension and retard cellular migration. Nano Lett 14(1):83–88
119. Setyawati M et al (2013) Titanium dioxide nanomaterials cause endothelial cell leakiness by disrupting the homophilic interaction of VE–cadherin. Nat Commun 4(1):1–12
120. Ma X et al (2017) Colloidal gold nanoparticles induce changes in cellular and subcellular morphology. ACS Nano 11(8):7807–7820
121. Tay CY, Setyawati MI, Leong DT (2017) Nanoparticle density: a critical biophysical regulator of endothelial permeability. ACS Nano 11(3):2764–2772
122. Setyawati MI et al (2015) Understanding and exploiting nanoparticles' intimacy with the blood vessel and blood. Chem Soc Rev 44(22):8174–8199
123. Karkossa I et al (2021) Nanomaterials induce different levels of oxidative stress, depending on the used model system: comparison of in vitro and in vivo effects. Sci Total Environ 801:149538
124. Liu M et al (2021) Functionalized mos2-based nanomaterials for cancer phototherapy and other biomedical applications. ACS Mater Lett 3(5):462–496
125. Rashidzadeh H et al (2021) Recent advances in targeting malaria with nanotechnology-based drug carriers. Pharm Dev Technol 26(8):807–823
126. Cui L et al (2017) Radiosensitization by gold nanoparticles: will they ever make it to the clinic? Radiother Oncol 124(3):344–356
127. Morozov KV et al (2020) Radiosensitization by gold nanoparticles: impact of the size, dose rate, and photon energy. Nanomaterials 10(5):952
128. Penninckx S et al (2020) Gold nanoparticles as a potent radiosensitizer: a transdisciplinary approach from physics to patient. Cancers 12(8):2021
129. Jyoti K et al (2020) Cytotoxic and radiosensitizing potential of silver nanoparticles against HepG-2 cells prepared by biosynthetic route using Picrasma quassioides leaf extract. J Drug Delivery Sci Technol 55:101479
130. Nosrati H et al (2021) Iron oxide and gold bimetallic radiosensitizers for synchronous tumor chemoradiation therapy in 4T1 breast cancer murine model. J Mater Chem B 9(22):4510–4522
131. Rosa S et al (2017) Biological mechanisms of gold nanoparticle radiosensitization. Cancer Nanotechnol 8(1):2
132. Ghita M et al (2017) A mechanistic study of gold nanoparticle radiosensitisation using targeted microbeam irradiation. Sci Rep 7:44752
133. Martin RF, Feinendegen LE (2016) The quest to exploit the Auger effect in cancer radiotherapy–a reflective review. Int J Radiat Biol 92(11):617–632
134. Cline B, Delahunty I, Xie J (2019) Nanoparticles to mediate X-ray-induced photodynamic therapy and Cherenkov radiation photodynamic therapy. Wiley Interdiscipl Rev Nanomed Nanobiotechnol 11(2):e1541
135. Goswami N et al (2017) Engineering gold-based radiosensitizers for cancer radiotherapy. Mater Horiz 4(5):817–831
136. Cheng NN et al (2012) Chemical enhancement by nanomaterials under X-ray irradiation. J Am Chem Soc 134(4):1950–1953
137. Misawa M, Takahashi J (2011) Generation of reactive oxygen species induced by gold nanoparticles under x-ray and UV Irradiations. Nanomed Nanotechnol Biol Med 7(5):604–614

138. Mikami Y et al (2013) Catalytic activity of unsupported gold nanoparticles. Catal Sci Technol 3(1):58–69
139. Hvolbæk B et al (2007) Catalytic activity of Au nanoparticles. Nano Today 2(4):14–18
140. Yao X et al (2015) Chemical radiosensitivity of DNA induced by gold nanoparticles. J Biomed Nanotechnol 11(3):478–485
141. Pawlik TM, Keyomarsi K (2004) Role of cell cycle in mediating sensitivity to radiotherapy. Int J Radiat Oncol Biol Phys 59(4):928–942
142. Kumar CG, Poornachandra Y, Chandrasekhar C (2015) Green synthesis of bacterial mediated anti-proliferative gold nanoparticles: inducing mitotic arrest (G2/M phase) and apoptosis (intrinsic pathway). Nanoscale 7(44):18738–18750
143. Liu Y et al (2016) Dynamically-enhanced retention of gold nanoclusters in HeLa cells following X-rays exposure: a cell cycle phase-dependent targeting approach. Radiother Oncol 119(3):544–551
144. Uz M, Bulmus V, Alsoy Altinkaya S (2016) Effect of PEG grafting density and hydrodynamic volume on gold nanoparticle–cell interactions: an investigation on cell cycle, apoptosis, and DNA damage. Langmuir 32(23):5997–6009
145. Kievit FM et al (2015) Nanoparticle mediated silencing of DNA repair sensitizes pediatric brain tumor cells to y-irradiation. Mol Oncol 9(6):1071–1080
146. Choi J et al (2020) Radiosensitizing high-Z metal nanoparticles for enhanced radiotherapy of glioblastoma multiforme. J Nanobiotechnol 18:122
147. Lobachevsky P et al (2021) Synchrotron X-ray radiation-induced bystander effect: an impact of the scattered radiation, distance from the irradiated site and p53 cell status. Front Oncol 11:685598
148. Zainudin NHM et al (2020) Investigation of the bismuth oxide nanoparticles on bystander effect in MCF-7 and hFOB 1.19 cells. J Phys Conf Ser 1497:012017
149. Rostami A et al (2016) The effect of glucose-coated gold nanoparticles on radiation bystander effect induced in MCF-7 and QUDB cell lines. Radiat Environ Biophys 55(4):461–466
150. Zainudin NHM et al (2020) Influence of bismuth oxide nanoparticles on bystander effects in MCF-7 and hFOB 1.19 cells under 10 MV photon beam irradiation. Radiat Phys Chem 177:109143
151. Nakhla S et al (2020) Radiosensitizing and phototherapeutic effects of AuNPs are mediated by differential Noxa and Bim gene expression in MCF-7 breast cancer cell line. IEEE Trans Nanobiosci 20(1):20–27
152. Yogo K et al (2021) Effect of gold nanoparticle Radiosensitization on plasmid DNA damage induced by high-dose-rate brachytherapy. Int J Nanomed 16:359
153. Hatoyama K et al (2019) Quantitative analyses of amount and localization of radiosensitizer gold nanoparticles interacting with cancer cells to optimize radiation therapy. Biochem Biophys Res Commun 508(4):1093–1100
154. Beik J et al (2021) Multifunctional theranostic graphene oxide nanoflakes as MR imaging agents with enhanced photothermal and radiosensitizing properties. ACS Appl Bio Mater 4(5):4280–4291
155. Chong Y et al (2020) Hyaluronic acid-modified Au–Ag alloy nanoparticles for radiation/nanozyme/Ag^+ multimodal synergistically enhanced cancer therapy. Bioconjug Chem 31(7):1756–1765
156. Nosrati H et al (2022) Complete ablation of tumors using synchronous chemoradiation with bimetallic theranostic nanoparticles. Bioactive Mater 7:74–84
157. Luo D et al (2019) Prostate-specific membrane antigen targeted gold nanoparticles for prostate cancer radiotherapy: does size matter for targeted particles? Chem Sci 10(35):8119–8128
158. Faghfoori MH et al (2020) Anticancer effect of X-Ray triggered methotrexate conjugated albumin coated bismuth sulfide nanoparticles on SW480 colon cancer cell line. Int J Pharm 582:119320
159. Abhari F et al (2020) Folic acid modified bismuth sulfide and gold heterodimers for enhancing radiosensitization of mice tumors to X-ray radiation. ACS Sustain Chem Eng 8(13):5260–5269

160. Azizi S et al (2020) Preparation of bismuth sulfide nanoparticles as targeted biocompatible nano-radiosensitizer and carrier of methotrexate. Appl Organomet Chem 34(1):e5251
161. Nosrati H et al (2019) Multifunctional nanoparticles from albumin for stimuli-responsive efficient dual drug delivery. Bioorg Chem 88:102959
162. Nosrati H et al (2019) Bovine serum albumin stabilized iron oxide and gold bimetallic heterodimers: synthesis, characterization and stereological study. Appl Organomet Chem 33(10):e5155
163. Nosrati H et al (2019) Tumor targeted albumin coated bismuth sulfide nanoparticles (Bi_2S_3) as radiosensitizers and carriers of curcumin for enhanced chemoradiation therapy. ACS Biomater Sci Eng 5(9):4416–4424
164. Zhao J et al (2019) Enhancement of radiosensitization by silver nanoparticles functionalized with polyethylene glycol and aptamer as1411 for glioma irradiation therapy. Int J Nanomed 14:9483
165. Rehman AU et al (2021) In vitro and in vivo biocompatibility study of polyacrylate TiO_2@ Ag coated nanoparticles for the radiation dose enhancement. Artificial Cells Nanomed Biotechnol 49(1):185–193
166. Bentzen SM (2006) Preventing or reducing late side effects of radiation therapy: radiobiology meets molecular pathology. Nat Rev Cancer 6(9):702–713
167. Wang K et al (2021) Prostate stereotactic body radiation therapy: an overview of toxicity and dose response. Int J Radiat Oncol Biol Phys 110(1):237–248
168. Bourgier C et al (2012) Pharmacological strategies to spare normal tissues from radiation damage: useless or overlooked therapeutics? Cancer Metastasis Rev 31(3):699–712
169. Schlaak RA et al (2020) Advances in preclinical research models of radiation-induced cardiac toxicity. Cancers 12(2):415

Emerging Nanomaterials as Radio-Sensitizer in Radiotherapy

Ifrah Kiran, Naveed Akhtar Shad, Muhammad Munir Sajid, Hafiz Zeeshan Mahmood, Yasir Javed, Mehwish Hanif, Riffat Ali, Muhammad Sarwar, Hamed Nosrati, Hossein Danafar, and Surender K. Sharma

Abstract Radiotherapy has been involved in treating 50% of the cancer patients in the world and is based on the direct energy deposition into tumor tissues. The major constraint in radiotherapy is the adverse effect of deposited energy on the surrounded healthy tissues. The improved radiotherapeutic tactics involve the use of

I. Kiran · Y. Javed (✉) · M. Hanif · R. Ali
Magnetic Materials Laboratory, Department of Physics, University of Agriculture, Faisalabad, Pakistan
e-mail: myasi60@hotmail.com

N. A. Shad (✉) · M. Sarwar
National Institute of Biotechnology and Genetic Engineering, Government College University, Jhang Road, Faisalabad, Pakistan
e-mail: naveed77.shad@gmail.com

M. Munir Sajid
Henan Key Laboratory of Photovoltaic Materials, School of Physics, Henan Normal University, Xinxiang 453007, China

H. Zeeshan Mahmood
University of Central Punjab, Faisalabad campus, Faisalabad, Pakistan

H. Nosrati
ERNAM—Nanotechnology Research and Application Center, Erciyes University, Kayseri 38039, Turkey

H. Nosrati · H. Danafar
Zanjan Pharmaceutical Biotechnology Research Center, Zanjan University of Medical Sciences, Zanjan, Iran

Joint Ukraine-Azerbaijan International Research and Education Center of Nanobiotechnology and Functional Nanosystems, Drohobych, Ukraine

Joint Ukraine-Azerbaijan International Research and Education Center of Nanobiotechnology and Functional Nanosystems, Baku, Azerbaijan

S. K. Sharma
Department of Physics, Central University of Punjab, Bathinda 151401, India

Department of Physics, Federal University of Maranhao, Sao Luis, MA 65080-805, Brazil

S. K. Sharma et al. (eds.), *Harnessing Materials for X-ray Based Cancer Therapy and Imaging*, Nanomedicine and Nanotoxicology,
https://doi.org/10.1007/978-3-031-04071-9_3

novel nanoparticles as radio-sensitizers. The nanoparticles, due to their high biocompatibility and optical properties, provide the enhanced localized damaging effect with the radiations targeted on the tumor site. There are different nanomaterials which offered enormous potential as radio-sensitizer and showed enhanced response with radiotherapy. In this chapter, we have discussed radio-sensitizing mechanisms and then different emerging nanomaterials being used as radio-sensitizer agents in radiotherapy.

Keywords Cancer treatment · Radiotherapy · Nano-radio-sensitizer · Metals · Metal oxide · Quantum dots

1 Introduction

To improve radio-therapeutic effectiveness, nanotechnology has broadened and unlocked cancer therapeutics and diagnostics window within the prospects of radiotherapy based on nanoparticles (NPs). Radiation therapy is a technique that destroys cancer cells or slows down their growth by destroying the DNA [1]. Radiation therapy also referred to as radiotherapy, is a cancer cure procedure in which high doses of radiation are used to kill cancer cells and suppress tumors. Nanoparticle-based radio-sensitization is widely used to improve the effectiveness of tumor radio-therapeutics [2]. Nanoparticle-based radio-sensitization is a method used to improve the tumor cells' susceptibility by using NPs (approximately 1–100 nm in size) [3] with ionizing radiations to achieve a higher radiotherapy ratio. Nanoscale size has ameliorated the ability to penetrated materials used for treatment and diagnosis at a lower risk compared to traditional drugs in cancer treatment.

NPs distribution in the body can be affected by distinctive parameters, e.g. shape, size, size distribution, surface charge, and ability to use the features of the cancerous cell for its inactivation [4]. However, radio-sensitizers are agents which when exposed to ionizing radiation; increased the tumor tissue susceptibility to injury/damage by the quick damage of DNAand by producing free radicals [5]. Therefore, NPs used for radio-sensitization may be therapeutic agents (e.g., NPs based on drugs which include polymeric drug-encapsulated, based on platinum, or an inert therapeutic agent such as gold NPs) [6] which enhance ionizing radiation effects. Without ionizing radiations, therapeutic NPs (e.g., carboplatin, oxaliplatin, or cisplatin NPs) may destroy and sensitize cancerous cells, however, enhanced the therapeutic efficacy due to their higher atomic numbers when combined with the ionizing radiations [7]. Therefore, it is possible to use a therapeutic agent through encapsulating or attaching drugs to high-Z number NPs inclusive of gold NPs. Besides, with increasing NPs concentration in the tumor, the radiation dose enhancement factor increases [8]. There has been a quick ascent in research enthusiasm for NPs and different micro-particles in the biomedical field, for instance, in the drug delivery, liposomes, dendrimers, quantum dots, metal NPs, biodegradable polymeric NPs, super-paramagnetic Fe_2O_3 NPs, lipid NPs, and non-metal NPs (e.g., fullerene and Si), are utilized as transporters of various drugs

containing agents of chemotherapy [9]. In this chapter, we have discussed different NPs such as gold, silver, quantum dots, hafnium, and gadolinium, mostly used in radiotherapy to increase radio-therapeutic efficacy.

2 Mechanism of NPs Based Sensitization

Different types of interactions depend upon the energy of the ionizing photon. The photoelectric effect is a predominant process in the range of 10–500 keV [10]. Electrons, auger electrons, and characteristics X-rays are produced as the result of this principal process. The photoelectric interaction occurs between metal NPs and photons [11]. Photoelectric absorption occurred due to vacancy in K, L, M shell, and de-excitation are achieved as a result of photoelectric absorption either by Auger electrons emission or characteristics X-rays [12]. The fluorescence yield gives the relative probability of these de-excitation processes. Fluorescent yield for light atoms is small and vice versa, because it is based on atomic number. Compton scattering and excitation occur above 500 keV for photons [19] (Fig. 1). The Compton scattering is observed when an atom is re-excited and Compton electrons are produced as a result of the photoelectric effect [13]. When an atom is excited and emission of phonon occurs then photon emission is stopped completely by the selection of certain rules. The flow of excitation energy as low-grade heat into the host lattice is occurred during phonon emission and is known as the quenching effect [14]. A lot of phonons and fewer photons can be induced by the high-energy excitation in metal NPs. When energy higher than 1.02 meV is used then positron and electron pairs are produced in the pair production process [15]. Besides Compton, all of these interactions depend upon atomic number. In the case of silver NPs, the phenomenon of radio-sensitization is not completely determined [16], and different studies proposed the radio-sensitization process of Ag NPs. Xu et al. [17] used different sizes of silver NPs i.e. 100, 50, and 20 nm in SHG-44, human U251, and rat C6 to test the radio-sensitization effects. Radiations induced a higher level of necrosis in glioma cells in the presence of silver NPs. The radiation sensitivity of U251 human cells was weaker in the case of 100 nm, while stronger for both 50 nm and 20 nm Ag NPs. The same processes were used to find the size-dependent radiation sensitization effect for SHG-44 and C6 glioma cells. Thereafter, researchers confirmed the radio-sensitization effect of silver NPs on A549 lung cancer cells, MGC803 gastric cells, and U231 breast cancer cells. The positive silver cations released from silver NPs are capable to capture the electrons, that's why act as an oxidative agent. Another factor that affects radio-sensitization is surface functionalization [18]. Surface ligands with different molecular weights induce different sensitization levels. The complementary factors are radiation energy and concentration. However, a higher concentration can produce toxicity and homogenous distribution of NPs is required for optimum results.

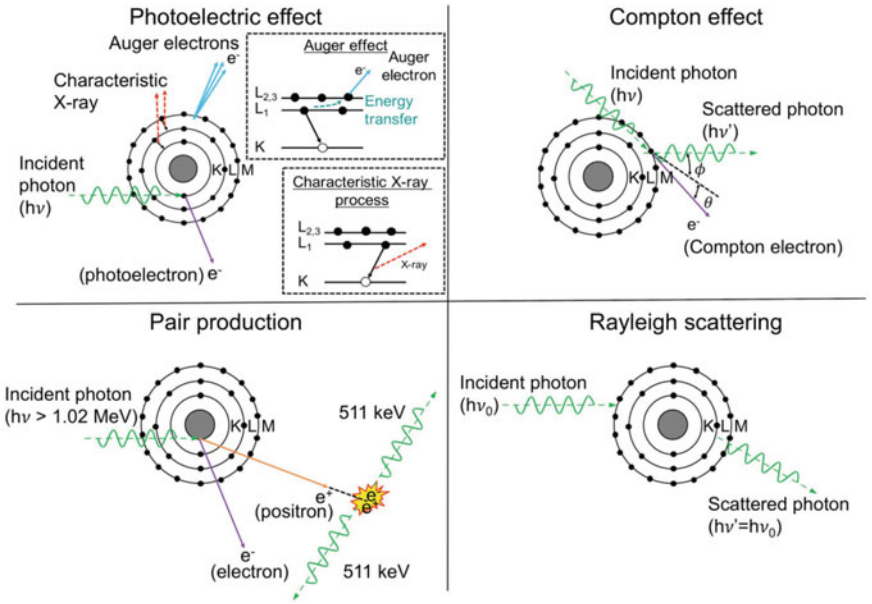

Fig. 1 Interaction mechanisms of photons with matter: Photoelectric effect occurs by colliding incident photon with inner shell electrons of the atom. Compton Effect refers to the collision between the photon and outer shell electrons of the atom and resultantly removes the electron from the atom. Pair production is caused by the passing of high-energy photon (more than 1.02 meV) near the nucleus at some angle which causes mass production and formation of Electron–positron pair (dominated above 10 meV, that's why rarely observed in cancer treatment). Rayleigh scattering does not affect dose enhancement and is usually negligible at high energies, however, high-Z materials with low energy photons can induce more Rayleigh scattering. Reprinted with permission from [19]

3 Nanomaterials Used as Radio-Sensitizer

3.1 Gold NPs

Gold is a chemically inert and good infrared reflector. Gold NPs' versatile surface chemistry enables them to be coated with small molecules [20], biological recognition molecules, and polymers, resultantly, extending their range of applications. Gold NPs with spherical morphology offer different colors of suspensions (from blue to purple-red) depend on the size of the particles [21]. The morphology i.e. size, shape, and aggregation status dictate the optical properties of gold NPs [22]. These particles can be tuned to suit a wide range of applications by concisely engineering different aspects e.g. surface chemistry, dimension, shape, etc. which can make them an efficient diagnostic and treatment tool [23]. The surface of gold NPs can easily be functionalized with proteins, antibodies, and peptides that provide specificity for both in vitro and in vivo cellular targets. Furthermore, oligonucleotide alteration of

the surface allows them to be used for genetic detection. Their use in bio-imaging, biosensors, immunohistochemistry, lateral flow experiments, drug delivery vehicles [24], and cellular probes are some common applications.

Gold NPs can scatter and absorb light with remarkable efficacy. The intense light interactions occur when atoms are excited by light of a specific wavelength, conduct collective oscillations on the metal surface called Plasmon resonance and generate higher scattering and absorption intensities of gold as compared to identical sized non-plasmonic NPs [25]. This causes the dissipation and assimilation forces of gold NPs to be a lot more noteworthy. To ablate breast cancer cells, the gold nanoshell-antibody complexes can be used [26]. The utilization of gold NPs in low doses as radio-sensitizing agents along with I-125 brachytherapy seeds in gamma radiation therapy improved the therapeutic efficacy from 70–130% [27]. The advancements in the field proposed a multifunctional nano-platform containing alginate hydrogel co-stacked through cisplatin and gold NPs for photo-thermal, radio- and chemo-therapy triple mix treatment. The hydrogel therapeutic potential was tested against KB human carcinoma cells in combination with a 532 nm laser and 6 MV X-ray radiation. The findings suggested that as compared to therapies based on mono or bi-modality, higher anticancer effectiveness of gold incorporated hydrogel in tri-modal thermo-chemo-radio therapy was persuaded. The amount of intracellular reactive oxygen species (ROS) was 4.4-fold increased relative to control cells [28] (Fig. 2). Bax pro-apoptotic factor up-regulation and Bcl-2 anti-apoptotic factor down-regulation were shown in the gene expression study. Massive cell damage and the presence of morphological attributes of apoptosis were clear in the KB cells' micrographs taken after radio-thermo-chemo treatment. Consequently, the gold incorporated nano-complexes could provide an affording chance to fight radio- and chemo-resistant tumors.

Zhang et al. [29] investigated the impact of gold NPs under gamma irradiation (2–10 kR) and cytotoxicity against K562 human cells using the Titre-GloTM Cell assay. There were no apparent size and instability changes in gold NPs caused by gamma radiations. Gold NPs exhibited exceptional radiation stability with a conversion factor of 9.491 rad/R. Meanwhile, after gamma irradiation (2–10 kR), the surface plasmon resonance of gold NPs was also improved. Cytotoxicity subsequently demonstrated that a higher concentration of gold NPs might cause a sharp increase in the viability of K562 cells, whereas a lower concentration of gold NPs had no apparent effect on cells. Hainfeld et al. [30] injected gold NPs intravenously in the mouse brain tumor to investigate the enhancement in the efficiency of radiotherapy and X-ray imaging. The sample tumor cells were irradiated with a high dose of X-ray radiation after 15 h of the intravenous injection of gold NPs. The gold NPs uptake was 19:1 from tumor-bearing to normal brain. The intravenously injected gold NPs crossed the blockage of tumor cells, however, could not cross blood brain barrier. The NPs provided high resolution CT tumor imaging. The enrichment of gold NPs along with the radiotherapy dose resulted significantly improved survival rate i.e. 53% as compared to the 9% for the radiation dose alone. The approach offered a new modality towards the treatment of human brain tumors and other tumor ailments. Zhang et al. [31] developed an

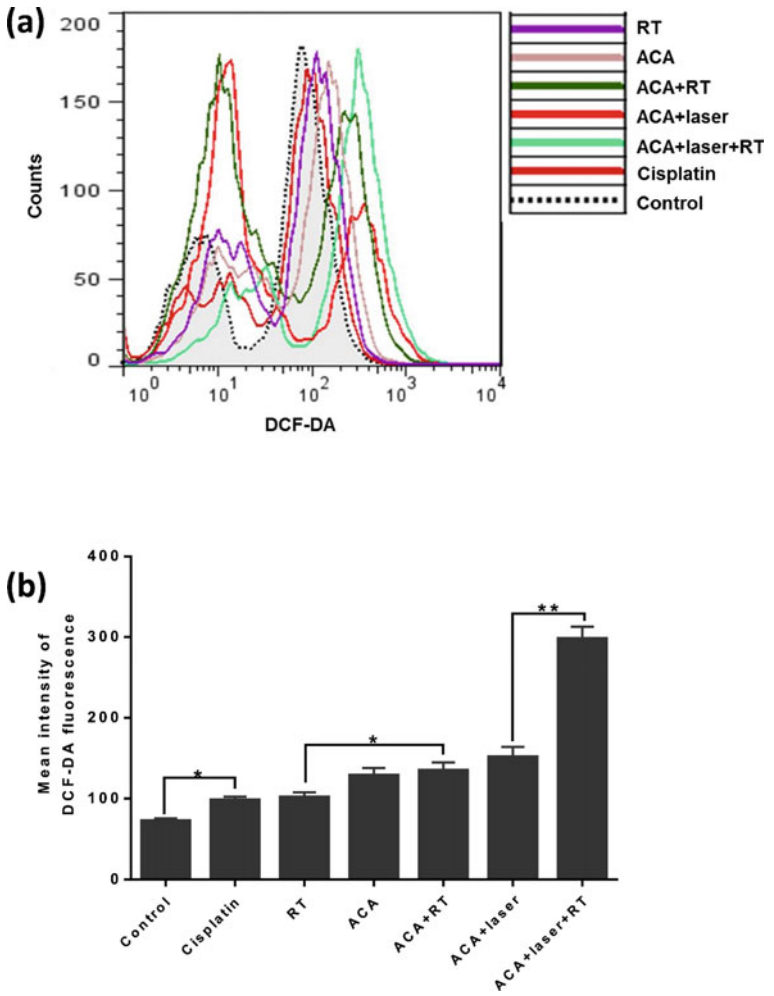

Fig. 2 Intracellular ROS release: **a** Flow cytometric histogram indicates ROS release using different treatments for KB cells, **b** Mean fluorescence intensity in KB cells after different treatments. Reprinted with permission from [28]

innovative radio-sensitizer based on acidic-induced gold NPs aggregates. The aggregation system is comprised of small gold NPs adapting various charged peptides on the surface. Upon injection of gold NPs in tumors, the surface charge of NPs was changed due to charge reversal property and interacted electrostatically with the negatively charged gold NPs to produce large sized gold NPs aggregates. The gold aggregates showed better tumor retention ability and accumulation in the tumor cells. The radio-sensitization effect showed an improved DNA breakage and the comet assay also revealed better radio-therapeutic effects. The sensitization enhancement ratio measured for the gold aggregates with MCF-7 tumor cells was much higher

than the separated gold NPs. The improved enhancement ratio resulted in reduction of the amount of radiation dose to avoid the healthy tissues damage. The gold aggregates displayed quick blood clearance and low phagocytosis. The in vitro analysis also exhibited the enhancement of MCF-7 tumor cells sensitivity to radiotherapy. The in vivo photoacoustic imaging displayed improved signal of the gold aggregates as compared to the small gold NPs.

3.2 Hafnium Oxide NPs

Hafnium has a lustrous silvery-gray presence in its elemental state and does not exist as a free element in nature. Hafnium is mostly part of superalloys [32] and circuits used in the manufacturing of semiconductor devices. The deposition of energy dose in the cancer cells can be increased by the introduction of hafnium oxide NPs [33]. Among different high-k and high index materials, hafnium oxide (HfO_2) has a moderately high dielectric constant [34], broad band gap, and strong chemical and thermal stability. Because of its high refractive index [35], the spectral range is from the mid to far-IR region [36] of the electromagnetic spectrum (250–1200 cm^{-1}). HfO_2 is used for optical coating and is regarded as a refractory material [37] because of its high melting point. The cubic phase of hafnium oxide with low thermal conductivity [38] is used in jet and diesel engines as a thermal barrier coating. As radiosensitizers, HfO_2 NPs are also used to improve the dosage and effectiveness of radiotherapy in tumors without causing any harm to the healthy tissues surrounding them [39]. The extremely small size of the HfO_2 NPs helps them to accumulate when injected into the body for cancer treatment. Hafnium activated Radiotherapy kills cancer cells more efficiently than radiotherapy alone [40] and greatly increases immune cell infiltration in both untreated and treated distant tumors by creating a CD8 + lymphocyte T cell-dependent abscopal impact [41]. An innovative research demonstrated radiotherapy-activated by hafnium oxide NPs and outcomes a significant improvement in HCT116 cell death than radiotherapy alone. The cGAS-STING pathway can be initiated by radiation-induced DNA damage, the ways to increase its activation in cancer cells could give huge therapeutic advantages to patients because of its important function in the activation of anti-cancer immunity. It was observed that, in a human colorectal cancer model, Hafnium oxide (NBTXR3) activated radiotherapy improves cell destruction, micronuclei formation, DNA double-strand breaks, and cGAS-STING pathway activation. Remarkably, results also revealed a dose-dependency that recommended pathway activation equivalent to that acquired through a higher dose of radiotherapy alone [43] (Fig. 3). These results indicated that where radiotherapy dose reduction is paramount, NBTXR3 could be used to improve radiotherapy without altering the radiotherapy-induced tumor cell death effectiveness. Shiryaeva et al. [42] reported a unique approach for radio-sensitizing experimental simulations of the NPs impact in the biomimetic system. It was observed that with the increasing contents of HfO_2 NPs, the number of radicals derived from methanol increased linearly at the same exposure period.

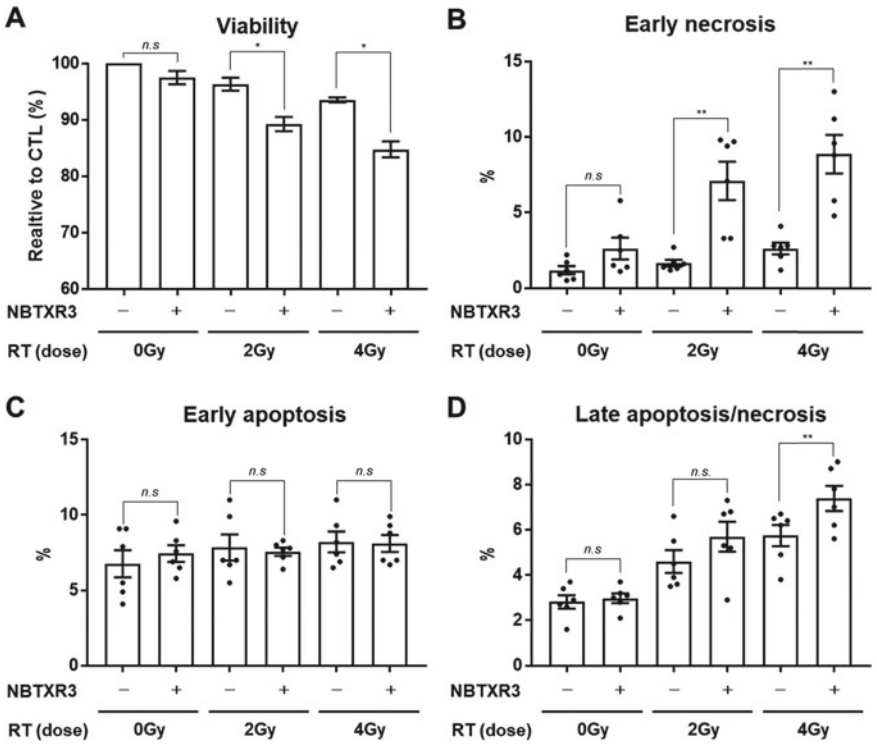

Fig. 3 HCT116-Dual cell death by HfO_2 activated radiotherapy: percentage (**A**) viability, (**B**) early necrosis, (**C**) early apoptosis, and (**D**) late apoptosis (48 h after radiotherapy). Different radiation doses (0–4 Gy) were employed. Reprinted from [43]

Monte Carlo simulations had used as a function of NPs concentration in the studied systems to calculate the absorbed dose. The calculated enhancement factor of the radical formation was lower than measured from absorbed dose, which may be justified by partial self-absorption of secondary electrons partial self-absorption produced inside hafnium oxide NPs.

Li et al. [44] studied intravenously injectable hafnium oxide nano-assembly to increase the efficacy of radiotherapy. Due to the enhanced sensitivity of breast cancer cells, hafnium oxide showed improved free-radical generation to destroy cancer cells upon X-ray irradiation. In a model of breast tumor 4T1, PEGylated hafnium oxide nano-assemblies showed effective tumor-homing capability by intravenous injection and demonstrated enhanced CT imaging. Excellent efficacy of tumor-killing was accomplished by both intravenous and intra-tumoral inoculation treatment using the radiation sensitization feature of hafnium oxide nano-assemblies. Finally, it is advantageous that hafnium oxide nano-assemblies could be degraded and excreted successfully in a living body and inhibited enduring toxicity.

Maggiorella et al. [45] designed different strategies to investigate the proper interaction of hafnium oxide NPs with the suitable ionizing radiation The materials were exposed to a monochromatic energy source by implementing the Monte Carlo Simulations and observed approximately nine-fold dose enhancement as compared to water. These NPs activated for radiotherapy, exhibited a high energy deposit rate in the tumor cells, and proved to be beneficial by eradicating the probable health hazards, due to their chemical inertness in cellular and subcellular systems. The NPs demonstrated adequate dispersion and perseverance in the tumor cells and formed clusters inside the cytoplasm of tumor cells demonstrating their anisotropic dispersion in tumors. The deficiency of pre-existing anti-tumor immune response used to be a challenging feature in the cancer therapeutic effects. Hafnium oxide NPs (NBTXR3) were manufactured by Zhang et al. [46] to enhance the energy dose deposit in the tumor cells. A mouse colorectal cancer model was used. The synthesized NPs were radiotherapy activated and their role in producing the abscopal effect and improving the anti-tumor immune response was investigated. The results revealed a significant increase in the local control over the tumor growth through activating the immune response system. The radiotherapy-activated NBTXR3 NPs ensued high immune cell infiltrates in both the treated and untreated tumor cells. The NPs also generated an abscopal effect mediated by CD8 + lymphocyte T cells. Hence, the NPs proved to be beneficial for being used as an immunotherapeutic agent with radiotherapy for providing improved results. Le Tourneau et al. [47] took under consideration the complications in the survival of older carcinoma (LA HNSC) patients and utilized hafnium oxide (NBTXR3). The NBTXR3 was injected by intra-tumoral single injection to the stage III-IV LA HNSC patients. After the allocation of all the doses at different levels and times, the CT images displayed better dispersion of NBTXR3 in the specific tumor areas. The preliminary efficiency was enhanced by NBTXR3. The NBTXR3 showed low toxicities and high intra-tumoral bioavailability with an enhanced survival rate.

3.3 Gadolinium NPs

Gadolinium NPs are categorized as toxic [48] which may ignite spontaneously and emit flammable gases when in contact with water. Gadolinium is a lanthanide rare earth element [49] that has interesting characteristics beneficial for applications such as tuning of semiconductor materials [50], and the shielding of nuclear reactors [51]. It is used both as phosphors and scintillator crystals [52] due to higher magnetic moment (7.94 μB), also used as a contrast agent in MRI [53] by making complexes with EDTA ligand. In the non-invasive evaluation of cardiovascular pathologies, gadolinium-based imaging has become a significant tool. Its recent use ranges from detecting ischemia, determining viability, cardiomyopathy, and non-invasive angiography [54]. It is known that NPs containing high-Z numbers boost the effectiveness of radiotherapy [55]. Gd is especially suitable as it is a positive MRI contrast agent that enables imaging [56] to be used simultaneously to delineate the tumor and to

guide irradiation. Ultra-small gadolinium NPs induce both a positive contrast in MRI and an effect of radio-sensitization [57]. Utilization of these features contributes to an increased lifespan of rats with brain tumors, as X-ray micro-beams can cause the radio-sensitizing effect due to Gd NPs. Gd is an adequately powerful radio-sensitizing agent for the tumor [58], therefore, offer exciting potential for image-guided radiotherapy. Gadolinium-based NPs were utilized by Kotb et al. [59] and observed that some NPs persisted within the tumor cells over 24 h after intravenous injection into animals carrying B16F10 tumor and demonstrated that single administration of NPs could be adequate for many irradiation cycles. Gadolinium-based NPs through radiation treatment expand tumor cell damage and increases the animal's life expectancies bearing numerous brain melanoma metastases. A novel research work resulted Hyaluronic acid-coated gadolinium oxide (HA-Gd_2O_3) NPs through the hydrothermal process for improving the MRI-guided radiotherapy [60] (Fig. 4). These HA functionalized NPs were 105 nm in diameter and exhibited remarkable properties involving low cytotoxicity, exceptional biocompatibility, and dispersibility

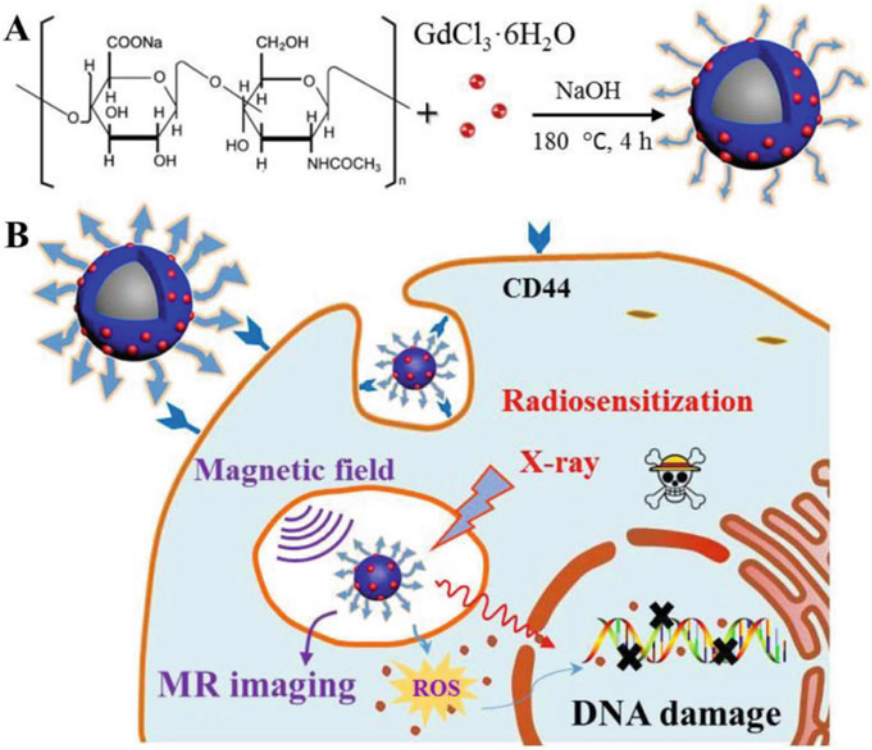

Fig. 4 **A** Hydrothermal Synthesis process of Hyaluronic acid-Gd_2O_3 NPs, **B** possible biomedical applications. Reprinted from [60]

in water. The NPs were transported into the cytoplasm of the tumor cells. The HA-Gd_2O_3 NPs showed high longitudinal relaxivity and produced significant improvement in the radio-sensitization in the manner of material dosage by instigating cell apoptosis.

3.4 Silver NPs

Silver NPs have vital potential in biomedical applications due to their antimicrobial nature [61] and minimal toxicity [62]. Silver NPs have distinctive optical characteristics [63] as they support the surface Plasmon resonances similar to gold NPs. The surface plasmon resonance effect is so intense [64] that it enables the use of a traditional dark field microscope to image individual NPs as small as 20 nm size. Liu et al. [65] assessed effectiveness of silver NPs on the hypoxic glioma cells as radio-sensitizers. For hypoxic cells (U251 and C6), silver NPs have maximum inhibitory concentration values of 27.53 and 30.32 g/mL respectively. The sensitization enhancement ratio showed greater radio-sensitization potential in hypoxic cells as compared to normoxic cells. The basic mechanism of radio-sensitization using silver NPs in hypoxic cells was based on apoptosis and autophagy. This study recommended that silver NPs might be utilized for the therapy of hypoxic glioma as an efficient nano-radio-sensitizer. A new dosimeter gel based on silver nitrate was introduced and studied in gamma radiation therapy ranging from 3–100 Gy. Exposing gel to gamma beams yielded plasmon resonance absorption due to silver NPs at 450 nm. With the rise in the absorbed dose to 100 Gy, the band intensity linearly increased. Silver NPs stability in the dark was strong at 6 °C. In the 5–100 Gy dose range, the total gel dosimeter uncertainty was calculated as approximately 4.65% [66] (Fig. 5).

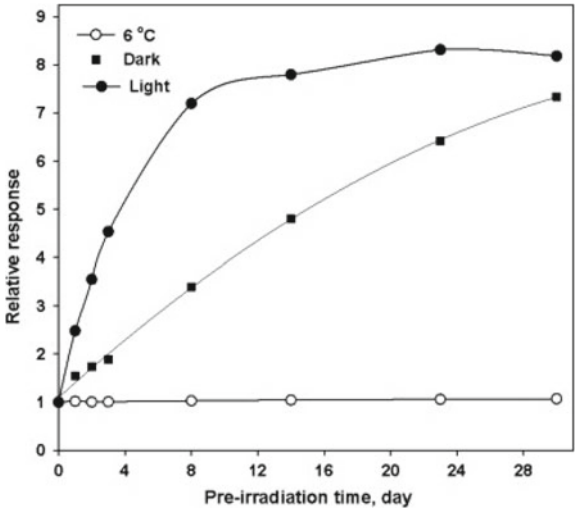

Fig. 5 Stability behavior of silver nitrate gel at different conditions 6 °C, dark and light, and analysis at 450 nm for the different time intervals. Reprinted with permission from [66]

Salih [67] used a colloidal solution of conjugated silver NPs in combination with irradiation of high-energy gamma photons (6 meV) for treating breast cancer. The silver NPs showed high biocompatibility and high mass-energy absorption coefficient. This resulted in the improved generation of free radicals and breakage of DNA causing the enhanced cross-section and dose deposited in tissues. The small doses demonstrated the maximum damage because the distinct silver NPs could induce ROS inside the tumor cells. The in vivo studies of silver NPs showed the efficient detection as well as the targeting of tumor cells simultaneously. Therefore, silver NPs worked as a remarkable photo-absorbing agent to offer major advances in radiotherapy. Abdul wahid and Ali [68] combined the multifunctional silver NPs with high-energy photons to reduce the number of cycles of radiotherapy. The photons of energy ranging from 2–15 meV were used with silver NPs and provided a high sensitivity enhancement ratio due to their high efficiency and small size. The enhancement ratio was increased with the increase in photon energy and yielded more number of destroyed tumor cells. The results showed that silver NPs increased the cross-section and stimulated the photon absorption in the tumors without damaging the healthy tissues in the vicinity. The mass absorption coefficient of the NPs was very high and it increased the absorption of the ionizing zone of the tumor cells. The results revealed that the destruction of the tumor cells was higher at the same photon energy as compared to the radiotherapy performed without injecting silver NPs. The application of the silver NPs resulted in precise tumor targeting and reduction of the radiotherapy cycles from 30–50%, thus, result in less probability of fatigue and exhaustion in the patient.

3.5 Quantum Dots (QDs)

The improved effects of radio-sensitization are effectively evaluated by analyzing the cell cycle of colorectal carcinoma and the degree of apoptosis [69]. Carbon QDs' cooperative behavior for ionizing radiation energy [70] could discernibly increase cell G2/M stage capture, prevent cell replication and promote apoptosis. This is principally because of the overproduction of ROS through carbon QDs and ionizing radiations [71]. This initiates the regulating proteins associated with apoptosis and results in tumor cell apoptosis. Consequently, carbon QDs in tumor radiotherapy offer another nano-radio-sensitizer agent [72].

An adaptable nanomaterial based on MoS2 QDs showed great potential not only to boost the photo-acoustic imaging/X-ray beam processed signals of tomography but also to perform proficient cancer radiotherapy/photo-thermal treatment. In vivo tumor could be correctly mugged and completely wiped out under the photoacoustic/X-ray CT image-guided combinational therapy upon intravenous injection of MoS_2@PANI hybrid NPs. These flexible nano-hybrids showed great potential to encourage double modular imaging and synergetic photothermal/radiotherapy to acknowledge improved anticancer proficiency [73]. Another potential nano-radiosensitizer is cadmium QDs. Semiconductor QDs and NPs made out of metals, polymers or lipids

had developed with favorable uses for early cancer detection and treatment. QDs with interesting optical properties were normally made of Cd confined semiconductors. Cadmium is potentially hazardous, and the toxicity of such types of QDs is not still investigated extensively. Therefore, the search for lesser harmful materials with comparative targeting and optical characteristics was of greater importance. However, it is pertinent to investigate luminescence NPs as light sources for the treatment of cancer.

The diagnosis of patients with cancer glioma is improved, in recent years, due to advancements in neurosurgery and radiotherapy [74]. Multifunctional nanomedicine based on tungsten sulfide QDs (WS2 QDs) synthesized via physical grinding and ultrasonication by a simple and green process is reported. In addition to X-ray computed tomography/photoacoustic imaging signal enhancement, the as-synthesized tungsten sulfide QDs have notable synergistic effects of photothermal/radiotherapy for tumor treatment. After intravenous injection, the tumor was efficiently detected and completely annihilated with tungsten sulfide QDs by combinational treatment. Staining, blood hematology and biochemistry study of hematoxylin and eosin showed no significant toxicity of WS_2 QDs in vivo, indicating that WS_2 QDs have strong biocompatibility. In order to achieve better therapeutic efficacy, such multifunctional NPs might play a vital role in promoting simultaneous synergistic treatment and multimodal imaging combining photothermal and radiotherapy [76] (Fig. 6). Du et al. [75] introduced unique gadolinium-doped

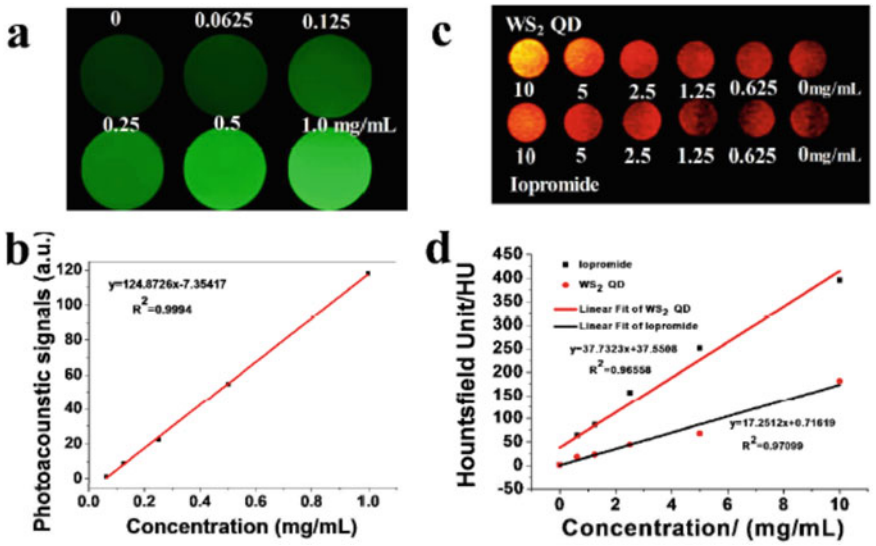

Fig. 6 **a** In vitro Photoacoustic images, **b** Graph of tungsten sulfide quantum dots as a function of concentrations. **c** Comparison of X-ray CT images using Iopromide and tungsten sulfide quantum dots at different concentrations. **d** Hounsfield Unit values of commercially available Iopromide and tungsten sulfide dots at different concentrations. Reprinted (adapted) with permission from [76]. Copyright {2015} American Chemical Society

carbon dots for dealing with the issue of radio-resistance and providing effective MRI-guided radiotherapy. The Gd-doped carbon dots were synthesized by a hydrothermal approach with an average size of 18 nm. The NPs demonstrated high water dispersibility and high photoluminescence stability. The doped carbon dots were injected at the tumor sites and showed a long circulation time and effective tumor targeting. The carbon dots were resided in the kidney from where these NPs were eliminated easily through the bladder. The NPs showed exceptional biocompatibility and resulted in an enhanced longitudinal relaxivity rate with radio-sensitization improvements. The long circulation time and increased longitudinal relaxation efficiency helped in providing better target delineation, pathophysiologic and anatomical tumor detection and accurate location for MRI-guided radiotherapy.

4 Conclusion

In this chapter, we have discussed the advancement of radiotherapy with the use of groundbreaking radiosensitizers. The key parameters of different nanomaterials i.e. radio-sensitizing power, biocompatibility, biodistribution and interaction of NPs with irradiation used and ROS generation play vital role in upgrading the destructive ability of radiotherapy. The innovative radiosensitizers have been used to improve the target selectivity of radiotherapy and reduce the adverse effects of radiation on the healthy tissues. This can be concluded that efficiency depends on the radiation energy and the NPs used as radiosensitizer. The NPs promisingly serve as drug delivery vehicles and enhance the cellular uptake of drugs by functionalizing with targeting molecules. The dose enhancement effect of NPs also generates valuable tumor destruction in radiotherapy. The radiosensitizers thus, offer a potential approach of improved targeted radiotherapy.

References

1. Malik A et al (2016) Role of natural radiosensitizers and cancer cell radioresistance: an update Anal Cell Pathol (Amst). 2016:6146595
2. Shetake NG, Kumar A, Pandey BN (1863) Iron-oxide nanoparticles target intracellular HSP90 to induce tumor radio-sensitization. Biochimica et Biophysica Acta (BBA) General Subjects 1863(5):857–869
3. Shinde NC, Keskar NJ, Argade PD (2012) Nanoparticles: advances in drug delivery systems. Res J Pharm Biol Chem Sci 3:922–929
4. Albanese A, Tang PS, Chan WC (2012) The effect of nanoparticle size, shape, and surface chemistry on biological systems. Annu Rev Biomed Eng 14:1–16
5. Shirai H et al (2013) Parg deficiency confers radio-sensitization through enhanced cell death in mouse ES cells exposed to various forms of ionizing radiation. Biochem Biophys Res Commun 435(1):100–106
6. Yallapu MM et al (2010) Curcumin induces chemo/radio-sensitization in ovarian cancer cells and curcumin nanoparticles inhibit ovarian cancer cell growth. J Ovarian Res 3(1):1–12

7. Al Zaki A et al (2017) Increasing the therapeutic efficacy of radiotherapy using nanoparticles. Increasing the therapeutic ratio of radiotherapy. Springer, pp 241–265
8. Zabihzadeh M, Arefian S (2015) Tumor dose enhancement by nanoparticles during high dose rate 192 Ir brachytherapy. J Canc er Res Therap 11(4):752
9. Wohlfart S, Gelperina S, Kreuter J (2012) Transport of drugs across the blood–brain barrier by nanoparticles. J Control Rel 161(2):264–273
10. Gobet F et al (2006) Absolute energy distribution of hard x rays produced in the interaction of a kilohertz femtosecond laser with tantalum targets. Rev Sci Instrum 77(9):093302
11. Choi J et al (2020) Radiosensitizing high-Z metal nanoparticles for enhanced radiotherapy of glioblastoma multiforme. J Nanobiotechnol 18(1):1–23
12. Fink R et al (1966) Atomic fluorescence yields. Rev Mod Phys 38(3):513
13. Lu L et al (2021) High energy X-ray radiation sensitive scintillating materials for medical imaging, cancer diagnosis and therapy. Nano Energy 79:105437
14. Begum M et al (2017) The effect of different dopant concentration of tailor-made silica fibers in radiotherapy dosimetry. Radiat Phys Chem 141:73–77
15. Brivio D, Sajo E, Zygmanski P (2021) Gold nanoparticle detection and quantification in therapeutic MV beams via pair production. Phys Med Biol 66(6):064004
16. Fathy MM (2020) Biosynthesis of silver nanoparticles using thymoquinone and evaluation of their radio-sensitizing activity. Bio Nano Science 10(1):260–266
17. Xu L et al (2020) Silver nanoparticles: synthesis, medical applications and biosafety. Theranostics 10(20):8996–9031
18. Yuan Y-G et al (2018) Silver nanoparticles potentiates cytotoxicity and apoptotic potential of camptothecin in human cervical cancer cells. Oxid Med Cell Longev 2018:6121328
19. Pelletier M L et al (2018), Gold Nanoparticles in Radiotherapy and Recent Progress in Nanobrachytherapy. Adv. Healthcare Mater. 7(16): 1701460
20. Burrows ND et al (2016) Surface chemistry of gold nanorods. Langmuir 32(39):9905–9921
21. Dinda E, Biswas M, Mandal TK (2011) morphological transition during reversible aqueous and organic phase transfer of gold nanostructures synthesized by tyrosine-based amphiphiles. J Phys Chem C 115(38):18518–18530
22. Aizpurua J et al (2003) Optical properties of gold nanorings. Phys Rev Lett 90(5):057401
23. Pedrosa P et al (2015) Gold nanotheranostics: proof-of-concept or clinical tool? Nanomaterials 5(4):1853–1879
24. Mir M et al (2017) Nanotechnology: from In Vivo imaging system to controlled drug delivery. Nanoscale Res Lett 12(1):500
25. Picardi G et al (2016) Spectral shift of the plasmon resonance between the optical extinction and absorption of gold and aluminum nanodisks. J Phys Chem C 120(45):26025–26033
26. Carpin LB et al (2011) Immunoconjugated gold nanoshell-mediated photothermal ablation of trastuzumab-resistant breast cancer cells. Breast Cancer Res Treat 125(1):27–34
27. Cho SH, Jones BL, Krishnan S (2009) The dosimetric feasibility of gold nanoparticle-aided radiation therapy (GNRT) via brachytherapy using low-energy gamma-/x-ray sources. Phys Med Biol 54(16):4889–4905
28. Alamzadeh Z et al (2020) Gold nanoparticles promote a multimodal synergistic cancer therapy strategy by co-delivery of thermo-chemo-radio therapy. Eur J Pharm Sci 145:105235
29. Zhang X-D et al (2009) Irradiation stability and cytotoxicity of gold nanoparticles for radiotherapy. Int J Nanomed 4:165
30. Hainfeld JF et al (2013) Gold nanoparticle imaging and radiotherapy of brain tumors in mice. Nanomedicine 8(10):1601–1609
31. Zhang Y et al (2019) Enhanced radiosensitization by gold nanoparticles with acid-triggered aggregation in cancer radiotherapy. Adv Sci 6(8):1801806
32. Kotval PS, Venables JD, Calder RW (1972) The role of hafnium in modifying the microstructure of cast nickel-base superalloys. Metall Mater Trans B 3(2):457–462
33. Chajon E et al (2018) A phase I/II trial of hafnium oxide nanoparticles activated by radiotherapy in hepatocellular carcinoma and liver metastasis. Ann Oncol 29:v92

34. Kang AY, Lenahan PM, Conley JF (2002) The radiation response of the high dielectric-constant hafnium oxide/silicon system. IEEE Trans Nucl Sci 49(6):2636–2642
35. Vargas M, Murphy NR, Ramana CV (2014) Tailoring the index of refraction of nanocrystalline hafnium oxide thin films. Appl Phys Lett 104(10):101907
36. Modreanu M et al (2006) Investigation of thermal annealing effects on microstructural and optical properties of HfO_2 thin films. Appl Surf Sci 253(1):328–334
37. Fadel M et al (1998) A study of some optical properties of hafnium dioxide (HfO_2) thin films and their applications. Appl Phys A 66(3):335–343
38. Curtis CE, Doney LM, Johnson JR (1954) Some properties of hafnium oxide, hafnium silicate, calcium hafnate, and hafnium carbide. J Am Ceramic Soc 37(10): 458–465
39. Babaei M, Ganjalikhani M (2014) The potential effectiveness of nanoparticles as radio sensitizers for radiotherapy. Bioimpacts 4(1):15–20
40. Bonvalot S et al (2019) NBTXR3, a first-in-class radioenhancer hafnium oxide nanoparticle, plus radiotherapy versus radiotherapy alone in patients with locally advanced soft-tissue sarcoma (Act.In.Sarc): a multicentre, phase 2–3, randomised, controlled trial. Lancet Oncol 20(8):pp 1148–1159
41. Buchwald ZS et al (2020) Tumor-draining lymph node is important for a robust abscopal effect stimulated by radiotherapy. J Immunother Cancer 8(2):e000867
42. Shiryaeva ES et al (2019) Hafnium oxide as a nanoradiosensitizer under x-ray irradiation of aqueous organic systems: a model study using the spin-trapping technique and monte carlo simulations. J Phys Chem C 123(45):27375–27384
43. Marill J, Mohamed Anesary N, Paris S (2019) DNA damage enhancement by radiotherapy-activated hafnium oxide nanoparticles improves cGAS-STING pathway activation in human colorectal cancer cells. Radiother Oncol 141: 262–266
44. Li Y et al (2020) Gram-scale synthesis of highly biocompatible and intravenous injectable hafnium oxide nanocrystal with enhanced radiotherapy efficacy for cancer theranostic. Biomaterials 226:119538
45. Maggiorella L et al (2012) Nanoscale radiotherapy with hafnium oxide nanoparticles. Future Oncol 8(9):1167–1181
46. Zhang P et al (2020) Radiotherapy-activated hafnium oxide nanoparticles produce abscopal effect in a mouse colorectal cancer model. Int J Nanomed 15:3843
47. Le Tourneau C et al (2020) Phase I trial of hafnium oxide nanoparticles activated by radiotherapy in cisplatin-ineligible locally advanced HNSCC patients. American Society of Clinical Oncology
48. Chen R et al (2015) Parallel comparative studies on mouse toxicity of oxide nanoparticle- and gadolinium-based t1 mri contrast agents. ACS Nano 9(12):12425–12435
49. Trapasso G et al (2021) What do we know about the ecotoxicological implications of the rare earth element gadolinium in aquatic ecosystems? Sci Total Environ 781:146273
50. Che Ani N et al (2016) Investigation of the structural, optical and electrical properties of gadolinium-doped zinc oxide films prepared by sol-gel method. Adv Mater Res 1133:424–428
51. Shamshad L et al (2017) A comparative study of gadolinium based oxide and oxyfluoride glasses as low energy radiation shielding materials. Prog Nucl Energy 97:53–59
52. Hammami S, Boudjada NC, Megriche A (2018) Structural study of europium doped gadolinium polyphosphates $LiGd(PO_3)_4$ and its effect on their spectroscopic, thermal, magnetic, and optical properties. Int J Anal Che 4371064
53. Ghaghada KB et al (2009) New dual mode gadolinium nanoparticle contrast agent for magnetic resonance imaging. PLoS ONE 4(10):e7628
54. Liu A et al (2016) Adenosine stress and rest T1 mapping can differentiate between ischemic, infarcted, remote, and normal myocardium without the need for gadolinium contrast agents. JACC Cardiovas Imaging 9(1):27–36
55. Hao Y et al (2015) Potential for enhancing external beam radiotherapy for lung cancer using high-Z nanoparticles administered via inhalation. Phys Med Biol 60(18):7035–7043
56. Arifin DR et al (2011) Trimodal gadolinium-gold microcapsules containing pancreatic islet cells restore normoglycemia in diabetic mice and can be tracked by using US, CT, and positive-contrast MR imaging. Radiology 260(3):790–798

57. Li F et al (2019) Ultra-small gadolinium oxide nanocrystal sensitization of non-small-cell lung cancer cells toward X-ray irradiation by promoting cytostatic autophagy. Int J Nanomed 14:2415–2431
58. Kanick SC, Eiseman JL, Parker RS (2008) Pharmacokinetic modeling of motexafin gadolinium disposition in mouse tissues using optical pharmacokinetic system measurements. Photodiagn Photodyn Ther 5(4):276–284
59. Kotb S et al (2016) Gadolinium-based nanoparticles and radiation therapy for multiple brain melanoma metastases: proof of concept before phase I trial. Theranostics 6(3):418–427
60. Wu C et al (2020) Hyaluronic acid-functionalized gadolinium oxide nanoparticles for magnetic resonance imaging-guided radiotherapy of tumors. Nanoscale Res Lett 15(1):94
61. Burduș A-C et al (2018) Biomedical applications of silver nanoparticles: an up-to-date overview. Nanomaterials 8(9):681
62. Santoro CM, Duchsherer NL, Grainger DW (2007) Minimal in vitro antimicrobial efficacy and ocular cell toxicity from silver nanoparticles. NanoBiotechnology 3(2):55–65
63. Pinchuk A et al (2004) Substrate effect on the optical response of silver nanoparticles. Nanotechnology 15(12):1890–1896
64. Wulandari P et al (2018) Surface plasmon resonance effect of silver nanoparticles on the enhanced efficiency of inverted hybrid organic–inorganic solar cell. J Nonlinear Opt Phys Mater 27(02):1850017
65. Liu Z et al (2018) Enhancement of radiotherapy efficacy by silver nanoparticles in hypoxic glioma cells. Artificial Cells Nanomed Biotechnol 46(3):S922–S930
66. Soliman YS (2014) Gamma-radiation induced synthesis of silver nanoparticles in gelatin and its application for radiotherapy dose measurements. Radiat Phys Chem 102:60–67
67. Salih NA (2013) The enhancement of breast cancer radiotherapy by using silver nanoparticles with 6 MeV gamma photons. Synthesis 26
68. Abdulwahid TA, Ali IJA (2019) Investigation the effect of silver nanoparticles on sensitivity enhancement ratio in improvement of adipose tissue radiotherapy using high energy photons. In: IOP conference series: materials science and engineering. IOP Publishing
69. Ruan J et al (2018) Graphene quantum dots for radiotherapy. ACS Appl Mater Interfaces 10(17):14342–14355
70. Zhou T et al (2020) Carbon quantum dots modified anatase/rutile TiO_2 photoanode with dramatically enhanced photoelectrochemical performance. Appl Catal B 269:118776
71. Li M et al (2019) Review of carbon and graphene quantum dots for sensing. ACS Sensors 4(7):1732–1748
72. Iravani S, Varma RS (2020) Green synthesis, biomedical and biotechnological applications of carbon and graphene quantum dots a review. Environm Chem Lett 18(3):703–727
73. Wang J et al (2016) MoS2 quantum dot@ polyaniline inorganic–organic nanohybrids for in vivo dual-modal imaging guided synergistic photothermal/radiation therapy. ACS Appl Mater Interfaces 8(37):24331–24338
74. Juzenas P et al (2008) Quantum dots and nanoparticles for photodynamic and radiation therapies of cancer. Adv Drug Deliv Rev 60(15):1600–1614
75. Du F et al (2017) Engineered gadolinium-doped carbon dots for magnetic resonance imaging-guided radiotherapy of tumors. Biomaterials 121:109–120
76. Yong Y et al (2015) Tungsten sulfide quantum dots as multifunctional nanotheranostics for in vivo dual-modal image-guided photothermal/radiotherapy synergistic therapy. ACS Nano 9(12):12451–12463

Nanoradiosensitzers: Preparation, Characterization and Their Performance

Hafeez Anwar, Beenish Abbas, Maryam Khalid, Kamila Yunas, Hamed Nosrati, Hossein Danafar, and Surender K. Sharma

Abstract Nanoradiosensitizers are attracting great interest of scientific community due to their therapeutic benefits for the treatment of malignant tumors. This book chapter is organized into three major parts. Firstly, it covers an introduction of nanoradiosensitizers and related biological processes. In second part, detail of synthesis approaches of various nanoradiosensitizers is discussed. The last part is focused on their characterization and highlights their application and performance in radiotherapy.

1 Introduction

Worldwide, cancer is currently one of the most challenging issues for human health. Radiotherapy (RT) is one of the most widely used treatments for cancer. In some cases, the only effective treatment option is RT. The use of nanoparticles with high atomic numbers as selective radiosensitizers has gained increasing attention in recent years. Radiosensitization of biological cells by heavy nanoparticles is attributed to

H. Anwar (✉) · B. Abbas · M. Khalid · K. Yunas
Department of Physics, University of Agriculture, Faisalabad 38040, Pakistan
e-mail: hafeez.anwar@gmail.com; hafeez.anwar@uaf.edu.pk

H. Nosrati
ERNAM—Nanotechnology Research and Application Center, Erciyes University, Kayseri 38039, Turkey

H. Nosrati · H. Danafar
Zanjan Pharmaceutical Biotechnology Research Center, Zanjan University of Medical Sciences, Zanjan, Iran

Joint Ukraine-Azerbaijan International Research and Education Center of Nanobiotechnology and Functional Nanosystems, Drohobych, Ukraine, Baku, Azerbaijan

S. K. Sharma
Department of Physics, Central University of Punjab, Bathinda 151401, India

Department of Physics, Federal University of Maranhao, Sao Luis 65080-805, MA, Brazil

S. K. Sharma et al. (eds.), *Harnessing Materials for X-ray Based Cancer Therapy and Imaging*, Nanomedicine and Nanotoxicology,
https://doi.org/10.1007/978-3-031-04071-9_4

a combination of physical and chemical effects caused by radiation [1]. Clinicians use various cancer treatment methods, including radiotherapy, chemotherapy, and surgery. In radiotherapy, ionizing radiation destroys cancer cells by damaging their DNA. It can be used as a standalone treatment or in conjunction with other therapies. Radiation therapy is one of the most effective treatments for cancer, but it has inherent drawbacks such as toxic side effects to the human body and radiation resistance in cancer cells. The combination of radiotherapy and radiosensitizers offers great potential for increasing treatment efficacy and broadening the therapeutic window for cancer patients Therefore, radiosensitizers are being further investigated to enhance the effectiveness of radiotherapy [2].

The current understanding regarding NP-induced radiosensitization via multiple biological pathways. Regulatory properties of nanoparticles in cancer cells have been examined, which may provide the basis for nanoradiosensitizer development in the future [3].

There are many applications for nanoparticles (NPs), including consumer goods, energy, and biomedicine [4]. In various types of cancer cells, NPs have been shown to reduce resistance to radiotherapy, both from their intrinsic radiosensitizing characteristics and loading capacity for drugs and siRNAs. NPs are also able to control other biological processes such as oxidative stress, DNA damage, cell cycle arrest, apoptosis, and autophagy which are discussed in the following section [5].

1.1 Oxidative Stress

The oxidative stress phenomenon can result from reactive oxygen species (ROS). ROS can cause potentially damaging biological effects. A lack of metabolic regulatory activity results in an imbalance between the production of reactive oxygen species and the capacity of a biological system to detoxify the reactive intermediates or repair the damage. An excess ROS response can be overcome by cells activating enzymatic as well as nonenzymatic antioxidant systems [6]. The hierarchical model of oxidative stress was proposed as a model of NP-mediated oxidative stress [7]. This model posits that cells and tissues respond to increasing levels of oxidative stress through antioxidant enzyme systems during NP exposure. An unopposed nuclear factor (erythroid-derived 2)-like 2 (Nrf2) induces phase II antioxidant enzyme transcription under conditions of mild oxidative stress. A proinflammatory response is produced at a subclinical level by mitogen-activated protein kinase (MAPK) cascades and nuclear factor kappa-light-chain enhancer of activated B-cells (NF-B). Furthermore, extreme amounts of oxidative stress damage mitochondrial membranes, leading to electron chain dysfunction and cell death. A key factor promoting the oxidative properties of engineered NM is either the decreased amount of antioxidants or the increased release of reactive oxygen species (ROS). An altered redox state leads to production of peroxide to toxic levels and they can damage the genetic material, proteins, lipids, DNA, and other components of the cell [8]. Because of its chemical reactivity, oxidative stress can lead to DNA damage, lipid peroxidation, and the activation of signaling networks

Table 1 Summary of nanoradiosensitizers based on oxidative stress mechanism

Composition	Size (nm)	Surface chemistry	Cell line/model	Source energy	[a]DEF/SER/Effect	References
Gold	14	Thio-glucose	SK-OV-3	90 kVp, 6 MV	Increased cytotoxicity	[12]
Gold	3	Histidine	U14	6 Gy	1.54	[11]
Gold-TiO2	18	Triphenylphosphine (TPP)	MCF-7/4T1 tumor-bearing Balb/c mouse	4, 6 Gy	Tumor volume inhibition	[13]
Silver	15	Polyvinylpyrrolidone	U251	4 Gy	Increased cell death	[14]
Iron oxide	10	Cetuximab	U87MGEGFRvIII	10 Gy	Increased cell death	[15]
Silicon	<5	2-methyl 2-propenoic acid methyl ester	Rat glioma C6 cells	0–3 Gy	Promoted ROS production	[16]

[a] DEF, dose enhancement factor; SER, sensitization enhancement ratio; Ref., references

responsible for loss of cell growth, fibrosis, and carcinogenesis [9]. As well as cell damage, ROS can result from interactions of NP with several biological targets as a result of cell respiration, metabolism, and other factors [10]. The oxygen desaturation that occurs as a result of occupational NM exposures as well as experimental challenge with various NP causes swelling of the airway and interstitial fibrosis [11]. We summarize the radiosensitization effect of NPs based on this oxidative stress mechanism in (Table 1).

1.2 Nanoradiosensitizers Based on Oxidative Stress

A new radiosensitizer based on gold-based nanomaterials has been extensively studied as a cancer radiotherapy agent. Gold nanoparticles adorned in different ways can lead to the sensitization of cancer cells to radiation through oxidative stress. For example, in both PEG-functionalized GNPs (s20 nm) and amino-PEG-functionalized GNPs (10 nm) oxidative stress radiosensitizes cancer cells [17]. Gold-levonorgestrel nanoclusters (2 nm) consisting of Au8(C21H27O2)8 (Au8NC) showed bright luminescence (58.7% quantum yield) and satisfactory biocompatibility in a human esophageal squamous cancer cell line (EC1) and in EC1 tumor-bearing nude mice [18]. Glutathione overexpression in tumors impaired radiotherapy effects. Gold nanoclusters with histidine caps (AuNCs@His) (3 nm) enabled radiotherapy effects by depleting intracellular GSH in U14 cells [11].

Radiosensitization effects generated by GNPs are better if cellular uptake is increased. Thioglucose decoration on GNPs increased cellular uptake by approximately 31% in human ovarian cancer cells (SK-OV-3) in comparison to naked GNPs, and the former resulted in increased ROS production and enhanced radiotherapy. By

Table 2 Summary of nanoradiosensitizers based on DNA damage mechanism

Composition	Size (nm)	Surface chemistry	Cell line/model	Source energy	DEF/SER/Effect	References
Gold	14	Polyethylenimine	A712	80 mGy/min	Increased cell death	[22]
Gold	12	PEG	U251	4 Gy (in vitro), 20 Gy (in vivo)	1.3	[23]
Silver	20	Epidermal growth factor receptor-specific antibody	nasopharyngeal carcinoma epithelial (CNE) cells	0, 2, 4, 6, 8 Gy	1.4	[24]
Iron-oxide	10	Oleic acid	WEHIh-164	2 Gy	Inhibited cell proliferation	[25]
ZnO	7	N.A	SKLC-6	2 Gy	1.23 (10 μg/mL), 1.31 (20 μg/mL	

modifying GNP-PEG with positively charged peptides, we were able to significantly increase the uptake of GNP and ROS production in LS180 colorectal cancer cells, which led to enhanced radiosensitivity [19].

1.3 DNA Damage

Cells are continuously subjected to different types of damage to DNA, and they have developed ingenious mechanisms to restore the damage [20]. The damage to DNA leads to many diseases, including cancer. Cancer treatment often hinges on the risk of DNA damage which may be induced by radiation [21]. NPs are able to radiosensitize DNA damage mechanisms. The physicochemical properties of NPs regulate DNA damage in cancer cells, which has important implications for designing nanoradiosensitizers. Radiosensitization by nanoparticles and DNA damage mechanisms are summarized in Table 2.

1.4 Nanoradiosensitizers Based on DNA Damage

It has been shown that the interactions between GNPs and DNA regulate radiosensitization effects. The DNA of plasmids can undergo single-strand breaks under radioactivity because of the binding of GNPs (five nanometers). Those GNPs that have the shortest possible linkers exhibit the greatest radiosensitization effect, while those with the longest linkers exhibit the lowest radiosensitization effect [26].

Table 3 Summary of nanoradiosensitizers based on cell-cycle arrest mechanisms

Composition	Size (nm)	Surface chemistry	Cell line/model	Source energy	DEF/SER/Effect	References
Gold	11	Glucose	DU-145	2 Gy	Growth inhibition	[28]
Gold-silver	150	l-ascorbic acid	HepG2	0–10 Gy	1.8	[29]
Graphene	Lateral size: 18	N.A	SW620, HCT116 c	3, 6 Gy	Increased cell death	[30]
Iron-oxide	10	Oleic acid	WEHI-164	2 Gy	Inhibited cell proliferation	[25]
TiO2	45	SN-38, nucleus-targeting moieties	4T1-Luc	4, 6 Gy	Inhibited cell proliferation	[31]

GNP-induced DNA damage could contribute to radiosensitization effects on cells. Radiation sensitization of MDA-MB-231 breast cancer cells is induced by DNA damage induced by GNPs of 2 nm pore size. In human GBM-derived cell lines treated with PEG-decorated GNPs, DNA damage increased under irradiation with cells coated in PEG and animals bearing an orthotopic GBM tumor survived better [23]. An increase of two-fold in the number of DNA damage sites (DSBs) in GBM cells after gold and superparamagnetic iron oxide nanoparticle-loaded micelles (GSMs, 100 nm) were shown when combined with radiation therapy [27]. A combination of Au@Se NP treatment with irradiation caused DNA damage by increasing the production of ROS and the phosphorylation of related proteins, including ATM etc.

1.5 Cell-Cycle Arrest

Unlike other cell cycles, the G2/M phase is most sensitive to radiation. The cells cycle goes through four phases: G1, S, G2, and M phases. The radiotherapy effects of NPs that can cause cell-cycle arrest during the G2/M phase are enhanced. Radiation sensitization has been observed to be induced by different types of nanoparticles through cells being inhibited from cell cycle progression. They are summarized in Table 3.

1.6 Nanoradiosensitizers Based on Cell-Cycle Arrest

The receptors in GNPs can increase the sensitivity of cancer cells to radiation during cell-cycle arrest. GNPs (5 nm) combined with neutron/ irradiation, for example, it inhibited cell invasion and migration by arresting cell cycle at the G2/M phase in Huh7

and HepG2 cells [32]. It was found that the combination of radiotherapy and gold nanoparticles (50 nm) significantly increased melanoma cell percentage in G2/M phase, thus enhancing the results of the next radiation treatment [33]. Radiation-resistant human prostate cancer cells DU-145 have been reported to undergo G2/M arrest with glucose nanoparticles (Glu-GNPs, 11 nm) upon activation of CDK1 and CDK2, thus becoming susceptible to radiation. GNPs that are decorated with targeting moieties enhance their radiosensitivity. RGD-GNRs sensitized melanoma A375 cells through suppression of radiation-induced integrin v3 and cell-cycle arrest in the G2/M phase. The anti-EGFR/HGNs (55 nm) coated with the EGFR antibody were internalized more efficiently by HeLa cells than naked HGNs. A greater number of cells arrested in the G2/M phase following EGFR/HGN induction. In the presence of anti-EGFR/HGNs, megavoltage irradiation boosted apoptosis more than irradiation alone [34].

Amounts of GNP impacted radiosensitizing effects of cell-cycle arrest. In MDA-MB-231 cells, for example, the size of Glu-GNPs influenced radiosensitization effects. The smaller GNPs internalized easier and induced greater levels of G2/M cellular arrest. It was found that NP surface structures played a key role in enhancing radiosensitizing effects, as reported by Cho et al. Nanoparticles shaped like day-flowers, with a large surface area, induced significantly more ROS production in HepG2 cells, arrested the cells during the G2/M stage, and exhibited radiosensitization. Although spherical night-flower-like nanoparticles have a small surface area, they do not change cell-cycle distribution and are not radiosensitizing [29].

1.7 Apoptosis

Among the types of apoptosis, there are extrinsic and intrinsic kinds. Apoptosis resulting from extrinsic factors is triggered by activated death receptors on the cell membrane. The intrinsic apoptosis pathway is triggered by mitochondrial or endoplasmic reticulum-related mechanisms [35]. This mechanism of radiosensitization of NPs is based on apoptosis is summarized in Table 4.

1.8 Nanoradiosensitizers Based on Apoptosis

The radiosensitization effects of GNPs are based on apoptosis. At first, GNPs alone significantly increase apoptosis rates of cancer cells [40]. In addition, GNPs conjugated to targeting adjuvants also exhibit excellent radiosensitization effects, leading to apoptosis induction. For example, gold@Fe_2O_3 nanoparticles (44 nm) exhibited radiosensitization effects in KB cells by increasing the apoptosis rate [41]. After irradiation, hollow gold nanospheres (EGFR/HGN, 55 nm) coated with EGFR antibodies induced the downregulation of Bcl-2 and the elevation of caspase 3, Bax, and Bad in HeLa cells. The RGD decoration of breast cancer cells significantly increased their

Table 4 Nanoradiosensitizers based on apoptosis mechanism

Composition	Size (nm)	Surface chemistry	Cell line/model	Source energy	DEF/SER/Effect	References
Gold	20	Cyclic RGD	NCI-H446 tumor-bearing mice	5 Gy	Inhibited tumor growth	[36]
Silver	15	Citrate	U251	4 Gy	1.64	[37]
Silica	40	Hyperbranched polyamidoamine	SK-BR3	0–8 Gy	Inhibited tumor growth	[38]
Gold	55	EGFR antibody	HeLa	5, 10 Gy	Increased cell death	[34]
Selenium	80	PEG	A549	N.A	Increased cell death	[39]

cellular uptake of GNRs@$mSiO_2$ through a receptor-mediated mechanism, resulting in an enhanced apoptosis rate and reduced tumor growth after radiation [34]. Irradiating mice with GNPs conjugated with cyclic RGD (20 nm) induced higher apoptosis rates than irradiating mice with irradiation alone. In combination with radiotherapy, long-term exposure to cRGD-GNPs inhibited tumor tissue growth significantly [36].

The size of the GNP can change the radiosensitisation effect. BSA-GNPs exhibited no cytotoxicity in the hepatocellular carcinoma model without exposure to radiation. Small BSA-GNPs induced the highest caspase-3 and Bax levels in mouse tumor tissues and the lowest Bcl-2 level [42].

1.9 Autophagy

Various types of autophagy exist, including microautophagy, macroautophagy, and chaperone-mediated autophagy [43]. In cells, autophagy is associated with the degradation of dysfunctional and unnecessary components. Autophagy plays an important role in the pathogenesis of cancer, which has been demonstrated. Moreover, cytostatic autophagy contributes to cancer cell death [44]. The radiosensitization effect of NPs can be explained in terms of the autophagy mechanism is shown in Table 5.

1.10 Nanoradiosensitizers Based on Autophagy

Several types of nanoparticles can trigger autophagy, which can induce radiation-sensitized cancer cells. AgNPs combined with irradiation led to autophagy on hypoxic glioma cells. By inhibiting autophagy, 3-MA decreased cytotoxicity, suggesting autophagy plays a key role in radiosensitization effects [47]. Furthermore, Fe_3O_4@Ag nanoparticles (11 nm) were found to exhibit radiosensitization in U251

Table 5 Nanoradiosensitizers based on autophagy mechanism

Composition	Size (nm)	Surface chemistry	Cell line/model	Source energy	DEF/SER/Effect	References
Copper cysteamine	N.A	N.A	SW620	1–4 Gy	Increased cell death	[45]
CuO	5.4	N.A	MCF-7 cells, U14 tumor-bearing nude mice	0–8 Gy	Increased cell death	[46]
Silver	27	N.A	U251	0–8 Gy	1.78	[47]

cells by inhibiting protective autophagy and eventually increasing calcium-dependent apoptosis [48]. Nanoparticles of gadolinium oxide (2–5 nm) sensitized NSCLC cells (A548, NH1299, and NH165) to radiation and instigate autophagy [49]. In SW620 colorectal cells, copper cysteamine nanoparticles reduced mitochondrial membrane potential and increased autophagy by lowering the mitochondrial membrane potential and triggering autophagy when exposed to X-ray irradiation. It was observed that CuO nanoparticles (5.4 nm) induced destructive autophagy in MCF-7 cells, as well as in U14 tumor-bearing nude mice. Nanosheets containing FePt inhibited proliferation of NSCLC cells H1975 and enhanced their sensitivity to radiation. ROS production and autophagy are likely responsible for radiosensitization mechanisms [50].

2 Synthesis of Radiosensitizers

Tumor cells are made prone to radiations by making use of complementary ways like Radiosensitizers. These substances enhance are designed to improve tumor cell cancer cells eradication without affecting normal cells adversely. Multiple elements and compounds have been discovered as Radiosensitizers. A lot of work has been done in order to create novel and improve the capability of previously known bio-radiosensitizers. Substances ranging between 1–100 nm are termed as nanoparticles (NPs). These substances exhibit less hazardous and enhanced infiltration range for normal and cancerous cells respectively. For a very long period of time nanoparticles have been a focus of main research in order to declare them as novel bio-randiosensitizers, like natural, metallic, CNTs and Gold NPs. Some of the most studied synthesis methods are listed below.

2.1 Gold Based Nanoparticles

Recently cancer radiotherapy is usually being done by using different bio-radiosensitizers e.g. gold NPs, etc. These NPs exhibit various properties like adaptable surface and biocompatibility, marking them as a powerful contender to be utilized as radiosensitizers. Various animals and cell lines have been used as subjects to determine sensitizing capabilities of these NPs. Various aspects has been studied enthusiastically like various cell lines, concentrations, size, sources and ratios. Cellular response exhibiting sensitivity levels of living cells sepnds upon multiple factors like NPs type, size, quantity and irradiation vigor. Two main factors involve in NPs improvement to be used as radiosenstizers are enhanced reactive oxygen level and cell cycle variations. Some of the studies synthesis mechanisms are listed below.

Zhang et al. [51] devised a new strategy in order to combine chemotherapy by creating a shrewd self-aggregating and double pH-responsive matrix of gold NPs (Au@PAH-Pt/DMMA), acknowledging pH release and self-amassing of cytoplasmic prodrug by utilizing "charge-reversal like" methodology. Gold NPs were synthesized by using sodium citrate reduction methodology. 6 mL of $AuCl_4H_7O_3$ (10 mg/mL) and water (144 mL) was added, boiled and condensed for 30 min to reflux, 17 mL of $Na_3C_6H_5O_7$ solution (11.5 mg mL^{-1}) was added instantly. Solution was stirred continuously while keeping heat off after 30 min to form solution-I. Forty mg of LA-PAH-Pt/DMMA and ten mL of distilled water [PAH] = 3.4 mg/mL^{-1} was added to form a solution-II. Solution-I and Solution-II was added with continuous stirring in volume ratio of 1:5. Later on sodium hydroxide solution was mixed in a volume ratio of 1:1 instantly resulting in wine red solution, lasting for 4 h. Resultant product was centrifuged at 14,000 rpm for 35 min. Precipitates were dried at 4 °C.

Kunoh et al. [52] explained gold NPs (AuNPs) synthesis methodology by utilizing acid guanidinium thiocyanate—phenol—hloroform (GTPC) fraction in $HAuCl_4$ solution. Solution was mixed for 4 h creating its color to change from clear yellow to turbid brown, after 16 h stirring precipitates were formed and collected. Gold NPs of size 5 nm diameter exhibiting spherical shape were obtained.

Ahmed et al. [53] utilized hydrothermal and chemical reduction methodology using $Na_3C_6H_5O_7$ as reducing agent manufacturing spherical Au, Ag and Au–Ag NPs with size 4–70 nm. $HAuCl_4$ reduction by $Na_3C_6H_5O_7$ and $AgNO_3$ reduction by $Na_3C_6H_5O_7$ in gold and Ag aquos solution are usually done these days to fabricate Au and Au NPs respectively. Bimetallic Au–Ag NPs were manufactured by fraternization and keeping its components uninterrupted for 1 day. Synthesized nanoparticles were proven to be novel radiosensitizing agents with radiation dosage up to 50 times for curing malicious living cells.

Zheng et al. [54] reduced $KAuCl_4$ by suing $NaBH_4$ to synthesize Au nanoparticles. 10 mL of $NaBH_4$ (I8 mM) and 10 ml of $KAuCl_4$ (3 mM) was added and stirred until bubbles vanished in solution for almost 10 min at room temperature. Resultant product was kept in dark at 5 °C. Plasmid DNA extracted from *E. coli* pellet was dissolved in distilled water. Agarose gel electrophoresis revealed various configurations of plasmid DNA like purified as 95% in supercoiled arrangement, same DNA

sequences in twisted strands as 4% and nickec spherical structure as 1%. A mixture of DNA and Au NPs resulted in Au-DNA complexes by using various ratios like 1:30, 2:5, 1:1, 4:3 and 2:1. Now a days single Au NPs per DNA molecule is desirable to maximize their affectively on malignant tumor cells. Hence, marking Au NPs a powerful candidate to be applied as radiosensitizers agent.

Jim et al. [55] did pre functionalization of Gold@DTDTPA NPs utilizing near infrared radiations to better understand the relationship between NPs radiosensitizng characteristics and movement between cells and tumor cells. As DTDTPA provides attachment places for covalent bonding of aminated derivative of Cy_5(Cy_5-NH_2) as it contains 3 carboxylic acid groups. Carboxylic acid condensation resulting in amide bonds formation functionalizing gold@DTDTPA NPs via Cy_5-NH_2. Whole process took place in aqueous form. Dialysis of acidic aqueous solution resulting in colloids formations which were further processed to be used in chemotherapy.

Ma et al. [56] reacted $HAuCl_4$ and silver NPs via galvanic replacement reaction by decreasing silver nanoparticle solution about 5 mL in 140 μL of $HAuCl_4$ 1% aqueous solution to prepare Au Nano spikes by continuous stirring. Prepared mixture was then added with 1 mL LAA solution. Resultant solution changed its color from yellow to navy blue as a result of continuos stirring instantly indicating gold nano spikes formation. 500 μg of HS-PEG was further added in prepared solution in order to enhance dispensability and stability of fabricated gold NSs. Prepared mixture helped in coating GNSs via gold—S coupling, resulting in methoxyl-PEG altered gold nano structures. Surface modification of GNSs was done and its effect on X-ray radiotherapy was also investigated (Fig. 1).

Zhang et al. [57] prepared Au NPs micro disks (MDs) by using PDMS stamp containing collection of micro pillars embedded in polyelectrolyte solution in order to impregnate polyetrolytes in solution for twelve minutes, followed by washing with deionized water. Resultant solution utilized in manufacturing MDs had 1 wt% of PAH-FITC (pH 5), PSS (pH 5.8), PAH (pH 4.3) and PDAC (pH 4.6), also NaCl as

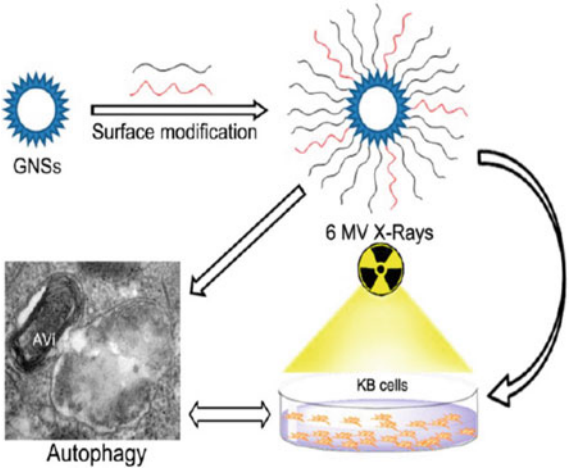

Fig. 1 Surface Modification of GNSs and their effects on X-ray radiotherapy. Reproduced with the permission from [56]

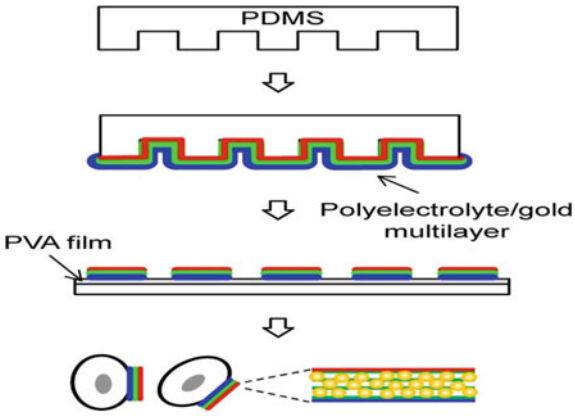

Fig. 2 Gold NPs-loaded MDs for enhanced radiation therapy. Reproduced with the permission from [57]

150 mM. Stamp was prepared by dispersing 0.5 mL of synthesized NPs and left for forty-five minutes, later on washed with deionized water for one minute. Reputation of previously mentioned steps resulted in various layers deposition on stamp which was later dealt with H_2O vapors in water bath at 37 °C for five seconds followed by interaction between glass substrate glazed with polyvinyl acetate film. Prepared stamp was separated from substrate after 45 s and processed in water bath for 25 s at 37 °C to discharge MDs. MDs were mixed with cells and stirred mildly to attach MDs on cells (Fig. 2).

Yi et al. [58] used Turkevich method to synthesize Au NPs. As per this method, refulxion of $HAuCl_4$ 1% weight/volume of 1 and 100 mL of distilled water for 5 min was done. $Na_3C_6H_5O_7$ 1% w/v (1.3 mL) was mixed and boiled for 30 min. resultant NPs were improved by LA-PEG, by 30 min sonication followed by and 6 h stirring, providing us with PEG coated Au NPs. 100 mL of prepared NPs were mixed in 42 mg of potassium permanganate with constant magnetic stirring for 5 min. A solution of 50 mg of PAH and 1 mL of deionized water was added in previously prepared solution dropwise, until its color changes from violet to yellow and then black. Attained gold@MnO_2 NPs were obtained by centrifuging the solution and further processed by LBL polymer coating procedure. Particular amount of poly acrylic acid (PAA) almost 30 mg added in previously prepared solution and sonicated for 30 min, maintaining pH of solution at 8. In order to create cross-networking between PAA and PAH EDC was mixed of 5 mg. Solution was stirred and centrifuged for 6 h at 8,000 rpm in order to remove extra PAA for 10 min while discarding supernatants. Later on, 50 mg of $mPEGNH_2$ was mixed with 1 mL of water. This solution was slowly added in gold@MnO_2 solution. Prepared solution went through ultra-sonication while adding 10 mg of EDC by 2 equal amounts, with 2 h continuous stirring. In order to remove extra PEG solution was centrifuged for 10 min at 8000 rpm. Yielded NPs were kept and stored at 4 °C.

Nicol et al. [59] prepared gold nanoparticles by using Turkevitch/Frens technique. Reduction of 400 mL of 0.01 wt.% $HAuCl_4$ was done in order to produce citrate capped nanoparticles (AuNP-C). PEG capped gold NPs (AuNP-P) were prepared

by dissolving imL of distilled water and 10.68 μg/mL of PEG-SH, followed by AuNP-C. Resultant solutionwas stirred at room temperature creating citerate/PEG cross-linking. Extra PEG was separated by centrifuging the solution for 90 min at 12,000 rcf.

Moreau et al. [60] utilized PVD process to synthesize Au NPs. This technique involves accumulation of atoms in free phase, where single, un-aggregated NPs having lesser size distribution on plane matrix are produced in argon gas envoirment by magnetic sizzling of gold source. Sodium chloride substrate mounted gold nanoparticles in water were used to provide consequent transfer. Repititive coating cycle resulted in extra yield of gold nanoparticles.

Li et al. [61] utilized vapor deposition technique and fabricated gold NPs to specifically aim malignant tumor cells and enhancing their radiosensitizing capabilities with proton illumination of gold NPs deposited by plasma polymerized allylamine. Yielded composites were distributed in CH_3COOH buffer maintaining pH at 5 followed by sonication for 10 min. Extra amount of NaCl and plasma-polymerized allylamine was removed by intermittent diafilteration using an MWCO of 10,000 g/mol as centrifugal concentrators. A solution of 17 mg of Ctxb and 17 ml of phosphate buffered saline was prepared and termed as solution-I. Another solution containing 30.5 mg of and 20.4 mL of PBS was added in solution–I. prepared solution was stirred for 15 min at 25 °C, followed by the addition of Au NPs with water keeping gold concentration at 1.12 $mg{\cdot}ml^{-1}$. Prepared solution was stirred for 4 h while maintaining the temperature at 25 °C for 4 h. synthesized solution was removed of unnecessary components by using centrifugal concentrator of MWCO of 300,000 g/mol using deionized water.

Liang et al. [62] prepared fluorescent Au nanoclusters (NCs) by using one step technique involving template of cyclic arginine-glycine-aspartic acid (c(RGDyC)) peptide. Cyclic arginine-glycine-aspartic acid /gold NPs were prepared by continuous stirring of 100 mL of chloroauric acid in aqueous phase and 1.5 mL of peptide solution. pH of prepared solution was maintained at 12–13 by using 100 mL of sodium hydroxide after 2 min. Resultant product was kept at 50 °C. Reaction was further processed for 20 h. The reaction was allowed to proceed for more than 20 h. yielded NCs were cleansed for 2 h by dialysis against 25 mM of HEPES buffer having pH = 7.8. Execution of unwanted ions and peptides was done by previous step overnight using HEPES (pH 7.8). Purified NPs were kept at 4 °C for future applications in radiation enhancement (Fig. 3).

Fathy et al. [63] studied therapeutic effectiveness by fabricating Chitosan Capped Au NPs encumbered with Doxorubicin (CS-GNPs-DOX) lessening hazardous aftermaths of chemo radiations on living cells while using 100 ml of chitosan (0.05%) and 1% acetic acid solution. Solution was stirred until it starts boiling. Later on 200 μL of $HAuCl_4{\cdot}3H_2O$/ml was added changing its color to dark red showing creation of Au NPs. Supernatant was removed by centrifuging the solution for 30 min at 14,000 rpm removing extra chitosan. Initially used Au weight (4.9 mg) was used to determine Au concentration. For every mL CS-GNPs solution 125 μg of DOX-hydrochloride was used. Prepared solution was shaked whole night kept it incubated. Excess contents were removed by centrifuging the solution for 30 min at 14,000 rpm.

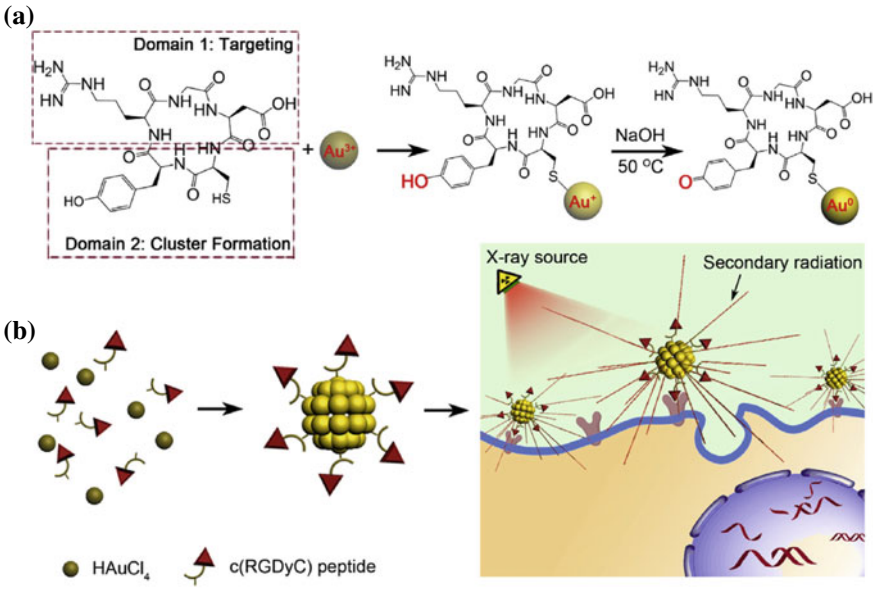

Fig. 3 **a** Capturing of Au^{3+} by Tyr and Cys residues and its reduction into AuNCs **b** c(RGDyC)-AuNCs accumulation in positive tumor cells interacting with incoming radiation, producing secondary radiation causing radiation enhancement effect. Reproduced with the permission from [62]

Mulgaonkar et al. [64] prepared HAuNPs introducing them as novel radiosensitizing particles for breast cancer treatment. Where NPs were fabricated using template of H_2 Nano bubbles (NBs). These NBs were produced electrochemically. Gold clusters were formed from Au+ ions in bubble borderline of high concentration of H_2. Obtained gold clusters sped up $Na_3Au(SO_3)_2$ autocatalytic disproportionation reaction, yielding gold shell formation surrounding hydrogen bubble. A sponge like matrix of metal gold was created from NPs. Synthesized NPs were gathered using anodic aluminum oxide (AAO) membranes having channels of 300 nm diameter, forming NBs and NPs along AAO membrane walls.

2.2 Sulfonamides Based Radiosensitizers

Sulfonamides are considered good radiosensitizing agents especially Heterocyclic rings containing ones are termed as one of the more effective CA inhibitors. A lot of research has been done on sulfonamide and its derivative leading to some new heterogeneous compounds exhibiting enhanced characteristics marking them useful and more applicable. Some of the examples of sulfonamides are benzothiazole, pyrazine, pyrazoline, thiazole, etc. Sulfonamides possesses numerous biological

properties like anti-thyroid, antibacterial, carbonic anhydrase inhibitory and carbonic anhydrase inhibitory. Some of the major work on sulfonamides and their application against tumor cells treatment are listed below.

Ghorab et al. [65] fabricated sulfapyridine or sulfathiazole containing 5-phenyl-pyrrolo[2,3-d]pyrimidine derivatives 7–10, 19–24 and 2-substituted-3-cyano-4-phenyl-pyrrole 5, 6, 11–18 series possessing Pyrroles and pyrrolo [2,3-d]pyrimidines.

Ella et al. [66] fabricated 14 derivatives bearin sulfonamide moiety and a series of thiazolopyrane 5a–d, 11–13 and thiazolopyranopyrimidine 6–10, 7b, 8b. 2-chloro-N-(4-sulfamoylphenyl) acetamide 2, sulfanilamide 1 and chloroacetyl chloride were interacted, when treated with ammonium thiocyanate, resulted in product 4-(4-oxo-4, 5-dihydrothiazol-2-ylamino) benzenesulfonamide 3 to be dealt with in a step by step manner. Various arylidine malononitriles 4a–d were reacted with compound 3 resulting in equivalent thiazolopyrane derivatives 5a–d. On application, these compounds applicating the synthesized compound enhances in activities upon being irradiated with gamma radiations (Fig. 4).

Ghorab et al. [67] synthesized sulfonamide moieties having novel pyrimidine 17–19 and pyrazole 10–16 derivatives. They reacted multiple nucleophiles and various sulfonamides like sulfaquinoxaline, sulfapyridine and sulfadimidine to achieve pyrimidine and pyrazole derivatives resulting in derivatives 4–9. On reaction with hydrazine hydrate corresponding pyrazole were obtained. In comparison with the reference medicine i.e. doxorubicin, it proved itself to be more effective in human liver cell ($HEPG_2$) and less effective in breast cell lines (MCF7) (Fig. 5).

Ghorab et al. [68] studied human liver tumor cell line and synthesized various sulfonamide derivatives containing different moieties like thiophene, pyridine, thiophene and benzothiophene. Targeted derivatives (4a,b-26) were fabricated from N-(4-acetyl-N-(P-substituted) phenyl benzenesulfonamide (3a,b). two separate ways were utilized to synthesize targeted samples utilizing various acetyl group. In the first strategy, compounds 3a,b was reacted with nitrogen nucleophile 2-cyanoacetohydrazide resulting in (E)-N-(4-(1-(2-(2-cyanoacetyl) hydrazono) ethyl)-N-(P-substituted) phenyl benzenesulfonamide 4a,b (Scheme 12a). compound 4a, b and malononitrile in dioxane were reacted by uusing ring-closure strategy to get (Z)-4-(1-((4,6-diamino-3-cyano-2-oxopyridin-1(2H)-yl)imino)ethyl)-N-p-substituted-phenyl-benzenesulfonamide (5a,b) yielding target compounds 5e13. Similarly, malononitrile in dioxane and compounds 4a, b were reacted along with absolute ethanol and elemental sulfur having 3 drops of triethyl amine resulting in thiophene derivatives 6a, b (Scheme 1) (Fig. 6).

DMF-DMA addition on 4b xylene resulted in N-(4-((Z)-1-(2-((E)-2-cyano-3-(dimethylamino) acryloyl) hydrazono) ethyl) phenyl)-4-methylbenzenesulfonamide 7. Under DFM having potassium hydroxide envoirment, reaction of 4b with CS2 resulted in compound (Z)-2-cyano-3-(2-(1-(4-(4-methylphenylsulfonamido) phenyl) ethylidene) hydrazinyl)-3-oxopropanedithioic acid 8. (Z)-N-(4-(1-(2-(3-amino-4,5,6,7-tetrahydrobenzo[b]thiophene- 2-carbonyl) hydrazono) ethyl) phenyl)-4-methyl benzenesulfonamide 9 were yielded upon reacting 4b with sulphur and cyclohexanone (Scheme 2). In the presence of dioxane and pepridine as catalyst

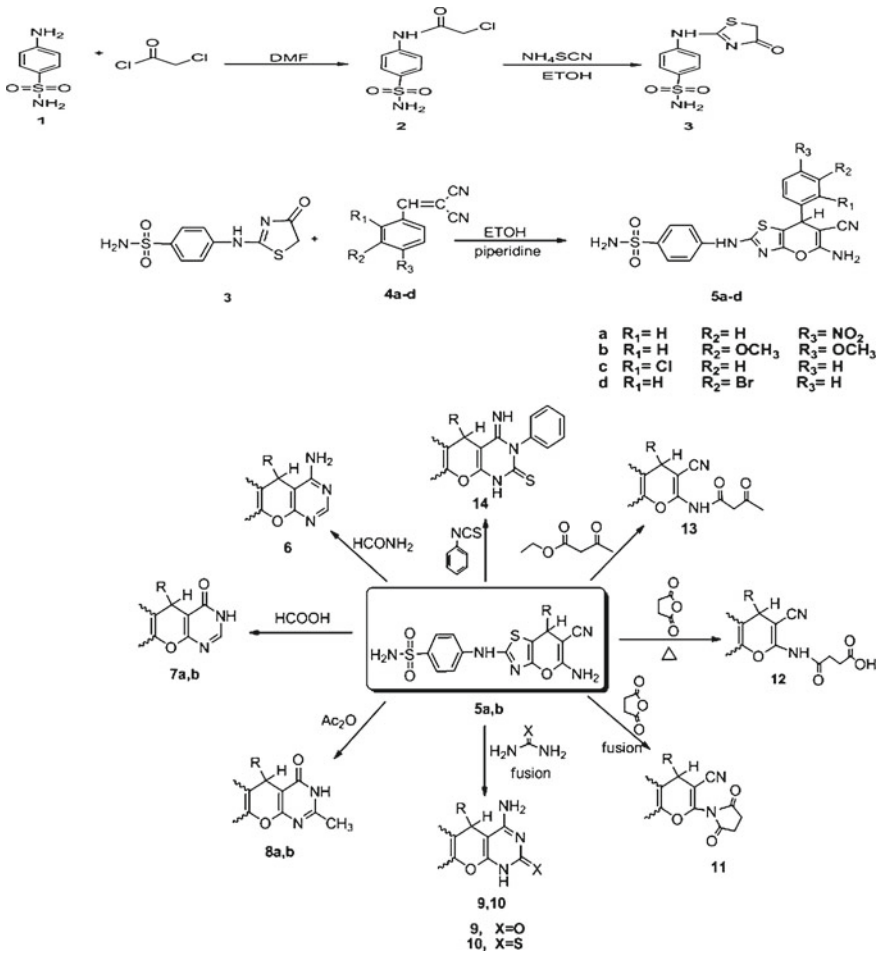

Fig. 4 Complete synthesis scheme of thiazolopyranopyrimidine derivatives starting from sulfonamide moities. Reproduced with the permission from [66]

aromatic benzylidine malononitriles 10 and 12 and 4b were reacted and yielded in dicyanopyridinone derivatives 11 and 13 (Scheme 2).

Aromatic aldehydes and acetophenone derivative 3b were recated under KOH envoirment in ethanol using Claisene Schmidt condensation yielding chalcones 14e19 (Scheme 3). Main aim of the study was to investigate synthesis process and configuration of sulfonamide calcones while reacting with malignant tumor cells. In potassium hydroxide and ethanol presence, hydroxylamine hydrochloride and chalcone 18 were reacted resulting in oxime derivative 20 (Scheme 3). Non isolable hydrazones were manufactured during the reaction procedure of various hydrazine derivatives in plain forms and compound 18. (Scheme 3) Compounds 4a, 4b, 5a, 6a,

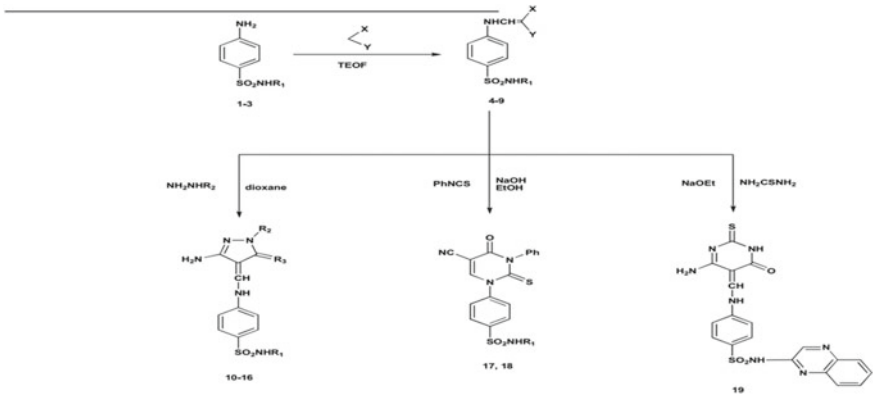

Fig. 5 Sulfonamide moieties containing pyrimidine 17–19 and pyrazole 10–16 derivatives. Reproduced with the permission from [67]

6b, 8, 9, 11, 13, 18 and 19 exhibited strong anti-cancer activity against tumor cells and turned out to be more effective than reference drug doxorubicin.

Gul et al. [69] investigated the fabricating strategy of 4-[3-(aryl)-5-substitutedphenyl-4,5-dihydro-1H-pyrazole-1-yl]benzensulfonamides (19–36) compounds 4-[3-(aryl)-5-substitutedphenyl-4,5-dihy dro-1H-pyrazole-1-yl] benzene sulfonamides (19–36) as shown in Scheme 1. polymethoxylated benzaldehyde and ketones were reacted by Claisen- Schmidt condensation using base as catalyst to initial chalcones, 1-aryl-3-substitutedphenyl-2-propen-1-ones (1–18) compound. Detailed synthesis procedure and spectral data polymethoxylated chalcones 4 and 10 was investigated for the very time in this study. Appropriate chalcone, 1-aryl-3-substitutedphenyl-2-propen-1-ones (1–18) were reacted followed by maintaining acidic envoirment, addition of 4-hydrazinobenzensulfonamide hydrochloride resulted in obtaining targeted compounds 4-[3-(aryl)-5-substitutedphenyl-4,5-dihy dro-1H-pyrazole-1-yl]benzensulfonamides (19–36) (Fig. 7).

Soliman et al. [70] investigated benzoquinazolinones 5–18 synthesis procedure: 0.001 M 2-chloro-N-substituted acetamide and 4 and 0.138 g of K_2CO_3 along with 30 mL of dry acetone was reacted to form a solution by constant stirring for 10 h. Resultant crystals were obtained after washing with ethanol to provide 5–18 compounds. 4-isothiocyanatobenzenesulfonamide 2 and 3-amino-2-naphthoic acid 3 to form 4-(2-mercapto-4-oxobenzo[g]quinazolin-3(4H)-yl) benzenesulfonamide 4 serving as a starting materials. N-(substituted)-2-[(4-oxo-3-(4-sulfamoylphenyl)-3,4-dihydrobenzo[g]quinazolin-2-yl)thio]acetamides 5–18 i.e. a targeted compound was synthesized by reacting 2-chloro-N-substituted acetamide derivatives and 4 in anhydrous K_2CO_3 enviorment having uquimolar dry acetone (Scheme 1) (Fig. 8).

2.3 Zinc Based Radiosensitizers

Elements with higher atomic numbers shows greater photoelectric effects as compared to soft tissues being irradiated with gamma radiations, marking them as powerful entities to maximize radiation therapy effectiveness. NPs possessing magnetic properties offers tumor cells imaging, treatment of targeted tumor cells while keeping normal cells unbothered during medication. A category of NPs known as spinal ferrites exhibiting less poisonousness are playing a vital role in multiple

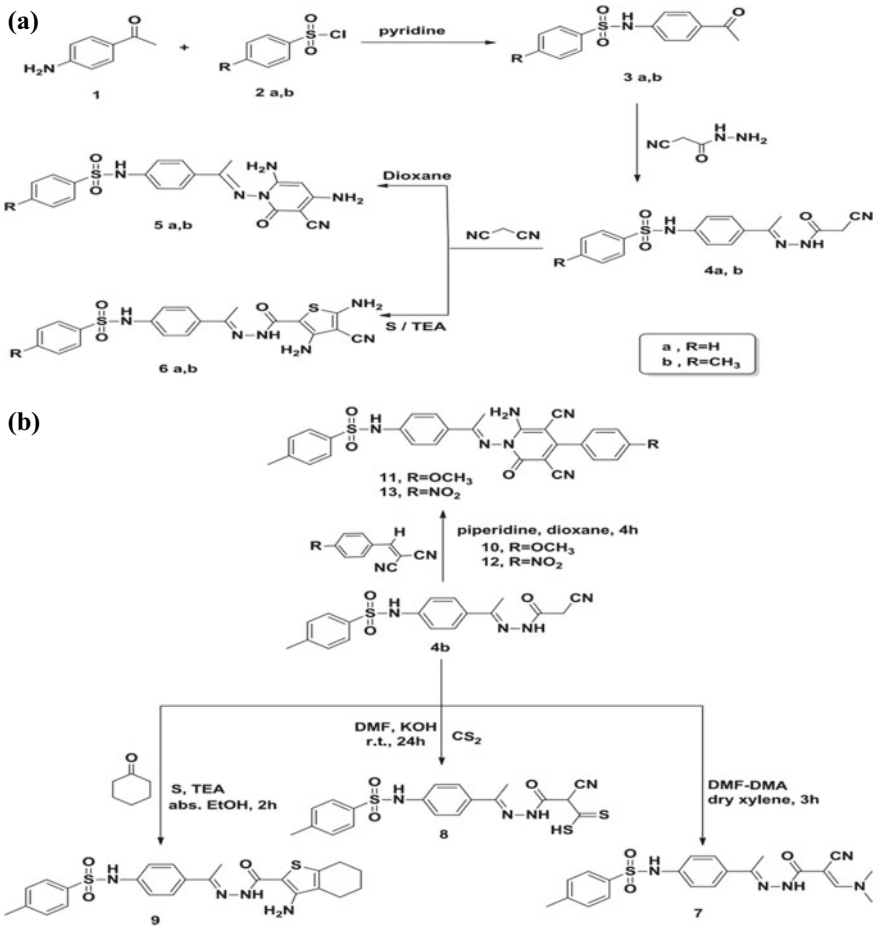

Fig. 6 **a** Compounds 3a,b-6a,b preparation trails. **b** Schametic diagram of reaction between 4b and CS2 having potassium hydroide in DFM yielding compound (Z)-2-cyano-3-(2-(1-(4-(4-methylphenylsulfonamido) phenyl) ethylidene) hydrazinyl)-3-oxopropanedithioic acid 8. **c** Synthetic trails for compounds dicyanopyridinone derivatives. Reproduced with the permission from [68]

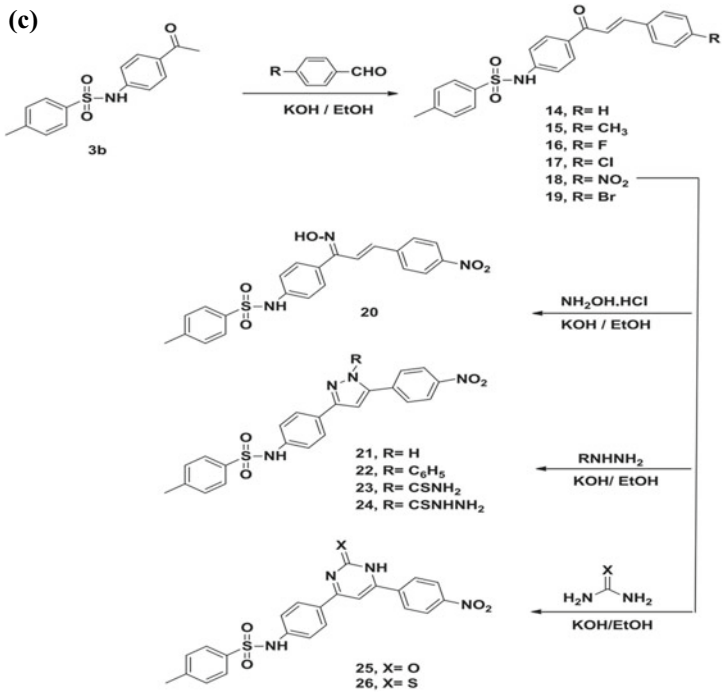

Fig. 6 (continued)

areas like MRI, DNA separation, drug delivery, in treating hyperthermia. One of the most important type of these ferrites is zinc ferrites, exhibiting spinal configuration, represented by $(Zn)[Fe_2]O_4$. This type of ferrites is marked more useful owing to its small band gap ~1.9 eV, behavior like paramagnets at low temperatures, acting like anti-ferromagnetic ground state at Néel temperature i.e. ~10 K.

Meidanchi et al. [71] used hydrothermal reduction procedure synthesizing $ZnFe_2O_4$ NPs using them for cancer therapy. A solution was formed by mixing 80 mL of ethanol, 808 mg of $Fe(NO_3)_3{\cdot}9H_2O$ and 298 mg of $Zn(NO_3)_2{\cdot}6H_2O$. Formed mixture was stirred for 30 min at 400 rpm. Prepared mixture was placed in furnace for 12 h at 180 °C after sealing it in a Teflon-lined stainless steel autoclave. After cooling it down at room temperature, $ZnFe_2O_4$ was purified by washing it multiple times with DI water, and kept for 24 h to dry at 60 °C.

Generalov et al. [72] synthesized two solutions in order to form ZnO/SiO_2 NPs. Solution-I was prepared by using 40 mL of ethanol (75%) to mix 3.3×10^{-3} mol $PEG(COOH)_2$ and 5.36×10^{-3} mol $Zn(AcAc)_2$. Using the same ethanol concentration, another solution was formed having 7.5×10^{-3} mol of sodium hydroxide. After placing Solution-I in flaks having a condenser attached to it, was stirred magnetically at 80 °C. Solution-II was added in solution-I slowly with continuous stirring maintain its temperature for 30 min. Resultant precipitates were cooled down at room temperature, centrifuging the mixture afterwards in order to remove extra ethanol. Wahab

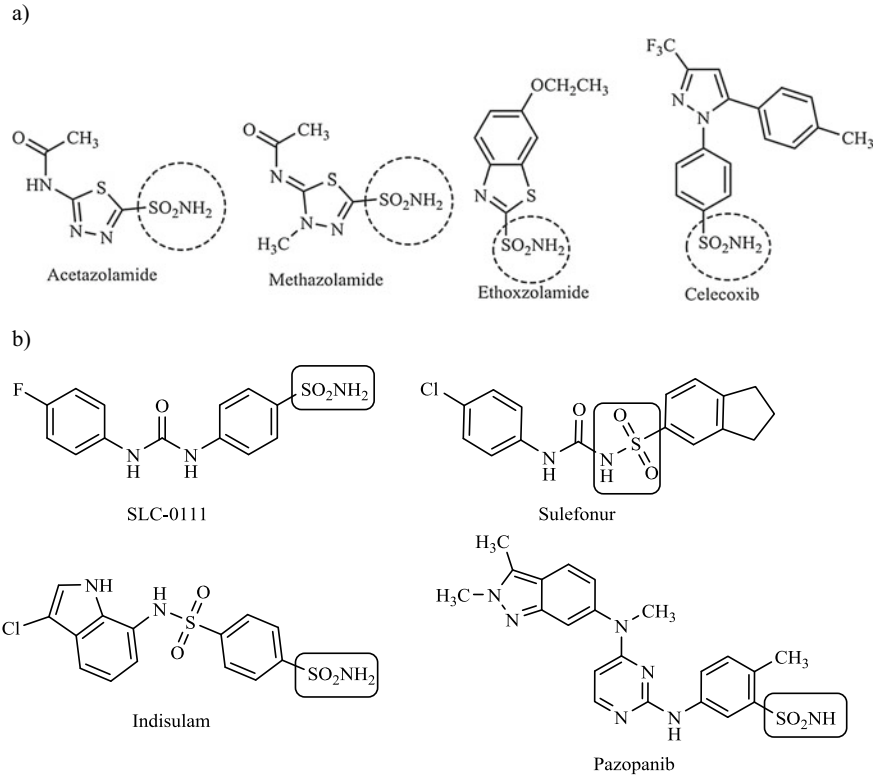

Fig. 7 **a**) Chemical structures of several sulfonamides as CA inhibitors **b**) Sulfonamide derivatives application in malignant tumor cells treatment. Reproduced with the permission from [69]

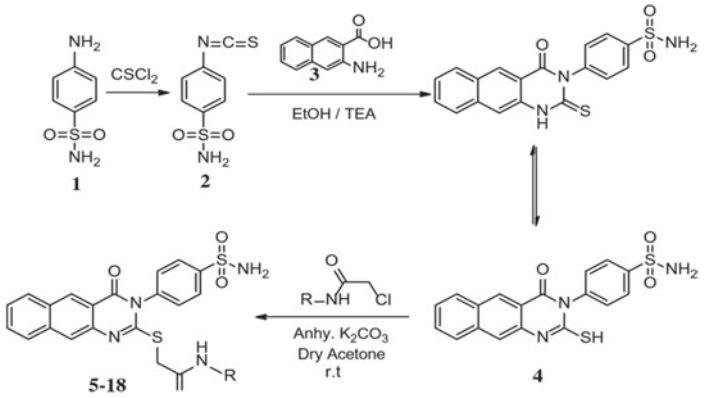

Fig. 8 Synthesis of series of sulfonamide benzoquinazolinones. Reproduced with the permission from [70]

et al. [73] used p-xylene ($C_6H_4(CH_3)_2$). And zinc acetate dihydrate ($Zn(Ac)_2{\cdot}2H_2O$) to prepare zinc oxide NPs. MeOH 100 mL wased to dilute 0.3 M of Zn while stirring it constantly for 30 min. 20 mL of p-Xylene was added in the solution to obtain the pH level of solution at ~6.76. Prepared solution was refluxed by placing it in a 3 necked pot while refluxing at 60 °C. after refluxing for 5 h, solution became translucent, while we needed a white suspension. After 6 h of suspension white suspension was finally achieved. Resultant compounds were purified via centrifuge at 4000 rpm/minutes at10 mins. Yielded precipitates were washed and dried with methanol and placed in a petri dish at room temperature respectively.

2.4 Iron Based Radiosensitizers

IO-MNPs also known as Iron oxide magnetic nanoparticles are termed as perfect radiosensitizing agent because of its two main remarkable properties. First one is behaving like a super paramagnet, can be controlled to reach at targeted cells by making use of externally applied magnetic field. Second one is bio compatibility. But there are some limitations hindering its prevalence in its application in medical field, like accumulation owing to greater surface energy. As a result of which Iron oxide NPs coatings results in making them envoirment friendly possessing multiple properties like enhanced stability, hydrophilicity, etc. some of the novel fabrication technique are listed below.

Klein et al. [74] explained two fabricating techniques to manufacture both citrate coated and uncoated super-paramagnetic iron oxide nanoparticles (SPIONs) for treating human breast cancer cells. First method was Massart´s method where ferrous and ferric chloride co-precipitation at lowest temperatures. Second one involves one pot strategy at greater temperatures having alkaline co-precipitation at 22 °C in diethylene glycol trailed by ligand exchange.

Fathy et al. [75] utilized co precipitation technique in order to fabricate Silica-coated super iron oxide nanoparticles (*SIO-MNPs).* 80 mL of DI water was used to dissolve 0.02 M of $FeCl_3{\cdot}\ 6H_2O$ and 0.01 M of $FeCl_2{\cdot}\ 4H_2O$ with continuous stirring. Reaction was processed for another 30 min at 80 °C with constant stirring while slowly adding 10 mL of ammonia solution. Magnetic characteristic carrying NPs were extracted from solution by suing a magnet and purified by washing with DI water and ethanol. Si shell coated iron ocide magnetic NPs were synthesized by using ethanol DI water (4:1, v/v) solution for dispersing 100 mg of iron oxide magnetic nanoparticles by sonicating the mixture for 15 min. Stirring the mixture continuously, 2 mL of TEOS and 4.6 mL of NH_3 (28 wt%) solution was added. Prepared mixture was further mixed fo another 24 h, followed by washing with DI water and ethanol and finally drying for 10 h at 80 °C.

Klein et al. [76] used co precipitation dtrategy to synthesiz SPIONs also known as Super-paramagnetic iron oxide nanoparticles. Massart's method was used to form ferrous and ferric chloride co precipitates without oxygen atmosphere at 0 °C temperature. Massart [77] explained this method, which involved 500 mL NH_3 solution to

disperse 10 mL of ferrous (2 M, in HC1 2 M) and 40 mL of ferric chloride (1 M). After centrifuge and magnetic decantation, jelly like precipitates were obtained. Yielded precipitates were dealt in two various ways. First one is *alkaline sol:* 1 M of $C_4H_{12}N^+$ hydroxide was used to peptize alkaline Ferro fluid. Second is *Acidic sol: 2 M* $HClO_4$ was stirred with prepared precipitates to prepare acidic solution, peptizing it with adding minute amount of DI water.

2.5 Curcumin Based Radiosensitizers

Turmeric i.e. rhizome curcuma longa roots are the main source of curcumin, exhibiting multiple natural properties like home grown normal polyphenol, which has various natural exercises, including cancer prevention agent, mitigating, neuro-protective, cardioprotective, as well as antitumor limits. Radioprotective impact may be predominantly because of its capacity to lessen oxidative stress, gene transcript and provocative reactions.

Girdhani et al. [78] used human breast tumor cells MCF-7 to study the joint studied the combined results of chemo radiations and curcumin, by treating malignant cells with curcumin before irradiating cells with gamma rays. Natural combination of curcumin mimicking commercially presented ones was utilized possessing following compounds in various ratios: bisdemethoxycurcumin and Dimethoxy curcumin, Curcumin C_3 conjugat (Bis-demethoxycurcumin 4.45%, Curcumin 73.75% and Demethoxycurcumin 21.80%).

Sebastià et al. [79] used antioxidant polyphenols and naturally obtained Curcumin possessing radio modulatory characteristics like protection of normal cells while being irradiated with gamma radiations acting like a shield to save living cells interaction with radiation therapy. Application of previously mentioned strategy involved synthesizing curcumin and antioxidant polyphenols reagents Stock solutions and storing it for 24 h before treatment in the absence of light at low room temperature like ~20 °C. 2.2 to 220 μM trans-resveratrol utlizing G_0 lymphocytes, 0.14 to 7 μM curcumin was used. While, blood cultures having enthused lymphocytes were dealt via 2.2–220 μM of trans-resveratrol and 1.4–140 μM of curcumin.

Xu et al. [80] treated colorectal cancer cells by using self-aggregating small peptide formation strategy against ionizing rays by creating Cur-SNF also known as curcumin-based supramolecular nanofiber as shown in the figure blow (Figs. 9 and 10).

Minafra et al. [81] used ethanolic precipitation strategy synthesizing with and without curcumin based solid NPs also known as Cur-SLN to enhance curcumin radiosensitizing accessibility trailed ultraturrax homogenization. Melted lipids (ML) were formed by heating Precirol ATO as 118 mg at 5–10 °C. For NPs preparation 20 mg of curcumin was mixed with MLs. Another solution was prepared by using 200 mg of Pluronic F_{68}, 30 mg of dimethyldioctadecyl-ammonium bromide creating ethanolic solution. 2 mL of prepared solution was added in MLs. 100 mL of DI water at 1 ± 80 °C was used to suspend synthesized mixture and resultant solution was

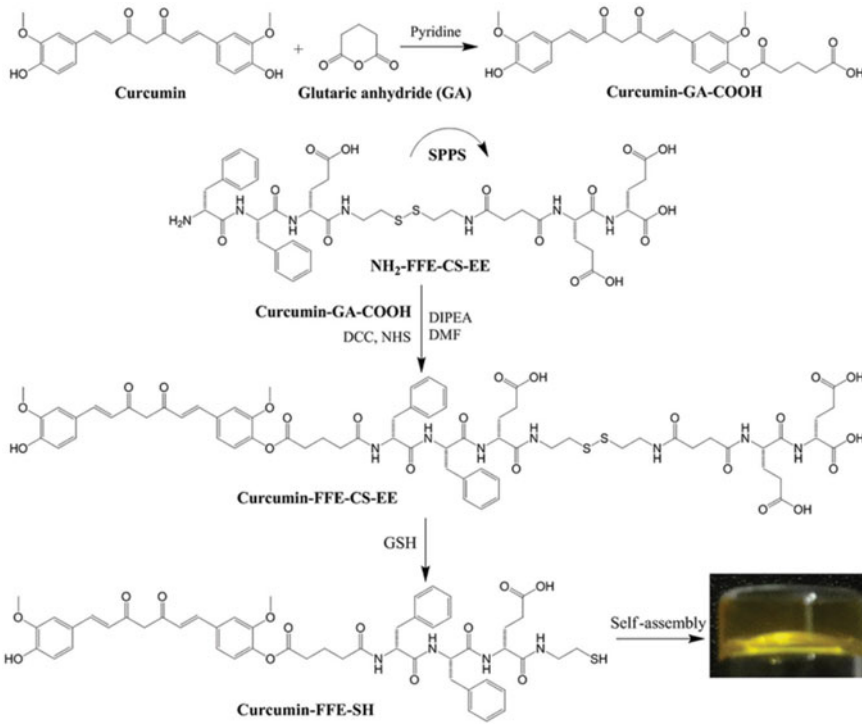

Fig. 9 Preparatory pathways of Curcumin-FFE-CS-EE. Reproduced with the permission from [80]

centrifuged for 10 min at 17, 500 rpm. Prepared solution was removed of excess heat by using 30 min ice bath folwed by purification via dialysis. Yielded NPs were prevented from agglomeration by using NPs suspension named as cryoprotector (trehalose) in a ratio of 1:2 (w/w). In last steps fabricated NPs were dried by freezing and kept in the dark.

2.6 Nitrogen Based Radiosensitizers

Hypoxic cells in comparison with aerobic cells are approximately threefold extra resilient to radiation. Recognizing and categorizing novel approaches to deal with ration interaction with tumor cells are the topics of keen interests in clinical radiation oncology these days. Howard and Flanderss showed that nitric oxide gas efficiently radio sensitize hypoxiz bacterial cells to ionize radiations. A few synthsis methods of nitrogen based radiosensitizers are listed below.

Pietzsch [82] developed two novel coxibs based on a (pyrazolyl) benzenesulfonamide lead with a NO-releasing moiety (Fig. 11) using a direct NO-coupling. There is

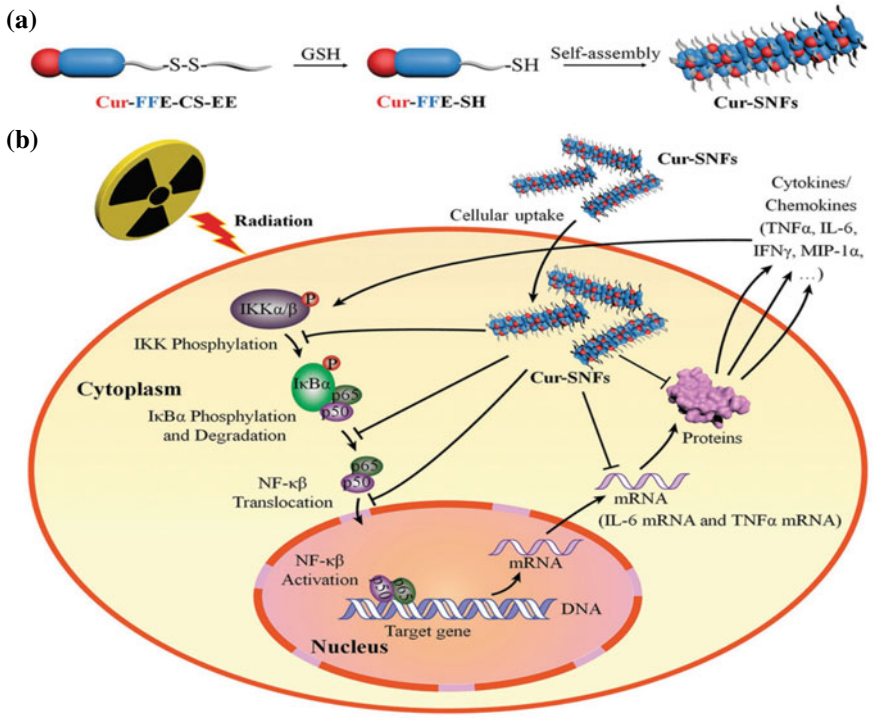

Fig. 10 Graphic representation of **a** self-aggregation methodology for Cur-SNFs preparationvia self-assembly **b** pictoral depiction of molecular interaction between gamma radiations and tumor cells in the presence of Cur-SNFs NPs. Reproduced with the permission from [80]

experimental and clinical evidence that coxibs, like celecoxib, valdecoxib, and NS-398, exhibit promising radiosensitizing properties. A nitric oxide-releasing coxib (NO-coxib) would target two 'hallmarks' of cancer radioresistance, tumor inflammation and hypoxia, concurrently. The free radical Nitric Oxide (NO) provides an additional reaction partner for the formation of reactive oxygen/ nitrogen species, like peroxynitrite (ONOO), which contribute, e.g., to fixation of radiation-induced DNA-lesions even in highly radioresistant hypoxic tumor areas. Moreover, NO enhances radiosensitivity via reduction of hypoxic conditions by increasing tumor perfusion (Fig. 11).

Pietzsch [82] used NO as radiosensitizing agent in treating hypoxie mammalian tumor cell. Sodium hydroxide (0.02 M) was used to prepare Diethanolamine/nitric oxide solution confirming concentration using 8000 M/cm of extinction coefficient at 247 nm absorbance band. Reaction indicated that oxygen content does not affect Diethanolamine /NO decomposition releasing NO. Tumor cells interaction with DEA/NO composites happened by using 10 mM^4-(2-hydroxyethyl)-l-piperazineethanesulfonic acid buffer with pH = 7.0. Resultant effects indicated pH variations from of 7.1–7.3.

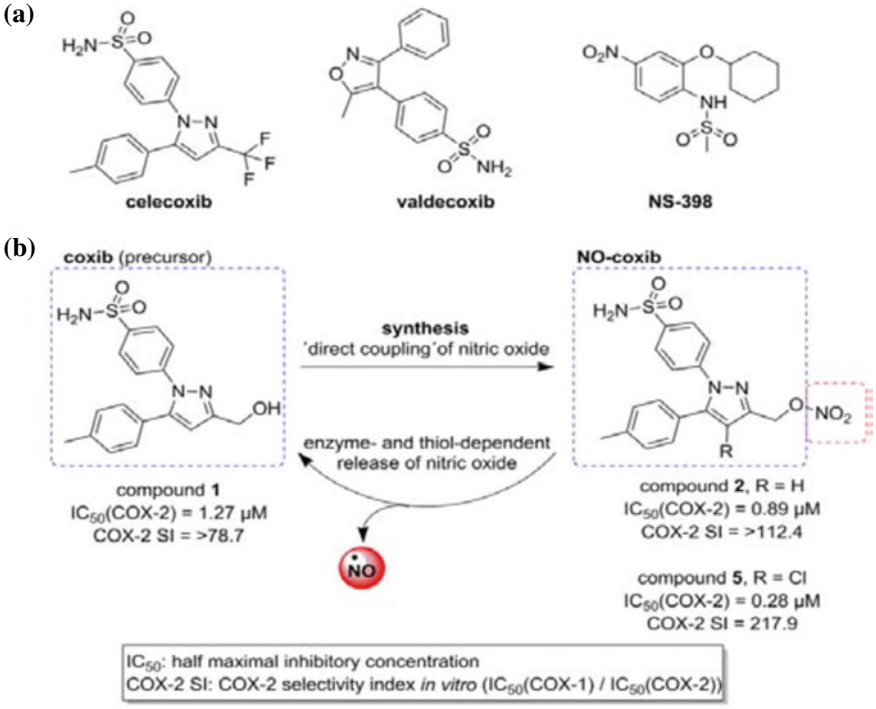

Fig. 11 Chemical structure **a** of selective COX-2 inhibitors used as potential radiosensitizers and **b** of the novel NO-coxibs 2 and 5 as well as the corresponding coxib 1 formed after NO-release. Reproduced with the permission from [82]

Cook et al. [83] used *S*-nitroso-*N*acetyl penicillamine (SNAP) as nitric oxide donor and utilized it in multiple experiments impersonating iNOS gene transfer effects. *S*-nitroso-*N*acetyl penicillamine functioned as negative terminal after being oxidized for 7 days by keeping it at 37 °C, providing us with human iNOS gene (AdiNOS).

Korde et al. [84] purified and cloned NOS_1 or nNOS from neuronal tissue for the very first time. Chromosome site 12q24.2–24.31 contain its gene. 26 exon gene residing in chromosome site 7q35-36NOS3 identified as an isoform of eNOS. iNOS also known as NOS_2 is derivable, residing on chromosome 17q35 to 17q11 site. Previously mentioned NOS types were obtained by molecular O_2 and L-arginine. NOS enzymes preparation requires multiple other factors like Flavin mononucleotide, tetrahydrobiopterin, nicotinamide adenine dinucleotide phosphate.

Munaweera et al. [85] treated lung cancer tumor cells by synthesizing NO and cisplatin releasing Si NPs. 0.3000 g of urea (5.0 mmol) and 0.5000 g of Cetylpyridinium bromide (0.5000 g) and 0.3000 g of urea (5.0 mmol) was added in 10 mL in DI water. Later on previously mentioned solution was mixed with 0.46 mL of iso-propanol and 15 mL of cyclohexane. Prepared mixture was further processed by

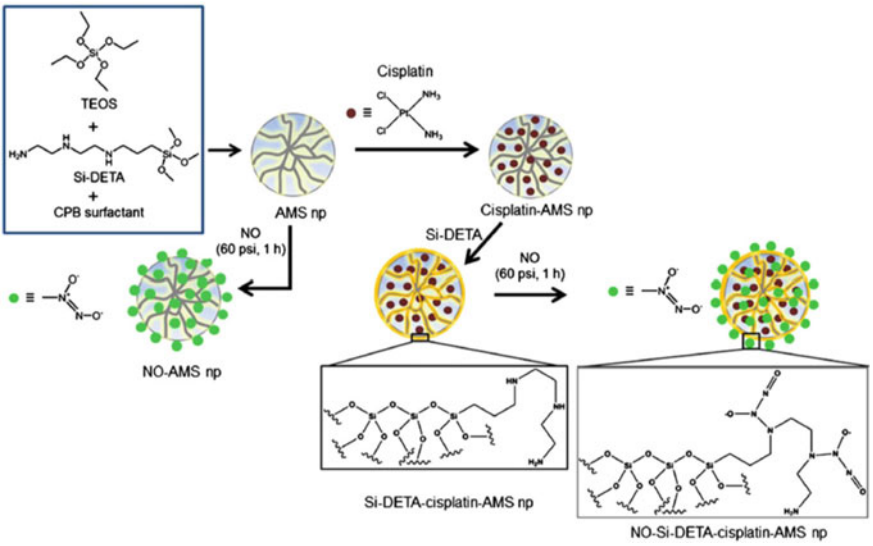

Fig. 12 Schematic diagram of synthetic trails of cisplatin- and NO- loaded AMS. Reproduced with the permission from [85]

0.4639 mL 3-triethoxysilylpropyldiethylenetriamine (Si-DETA) and 0.9378 mL of TEOS slowly with constant stirring for 30 min. Afterwards solution was heated for 24 h at 70 °C, followed by washing with ethanol and purification by centrifuging the mixture. In the last step template was extracted by dispersing synthesized mixture again in 50 mL of ethanol at 70 °C for 24 h (Fig. 12).

2.7 Other Radiosensitizers

Researchers have been doing a lot of work in the field of radiation therapy in order to prepare novel, biocompatible, cost-effective and more effective bio radiosensitizers. Nanopartoicles have been termed as powerful contenders to be used in this field. Novel research have created a wide range of new composites to be used as effective radiosensititizers for various malignant tumor cell enhancing the effect of radiation therapy. Many other synthesis approaches of NPs based bio-radiosensitizers are discussed below.

Jiang et al. [86] used instant precipitation technique to synthesize cupric oxide showing autophagy creating capability after being interacted with malignant tumor cells. Autosis of tumor cells was detected owing to extra autophagy levels after being irradiated with X-rays as shown in the figure below (Fig. 13).

Rajaee et al. [87] utilized sol gel process for synthesizing and imaging bismuth gadolinium oxide NPs to be used in tumor cells treatment. A solution of 6 mL EG

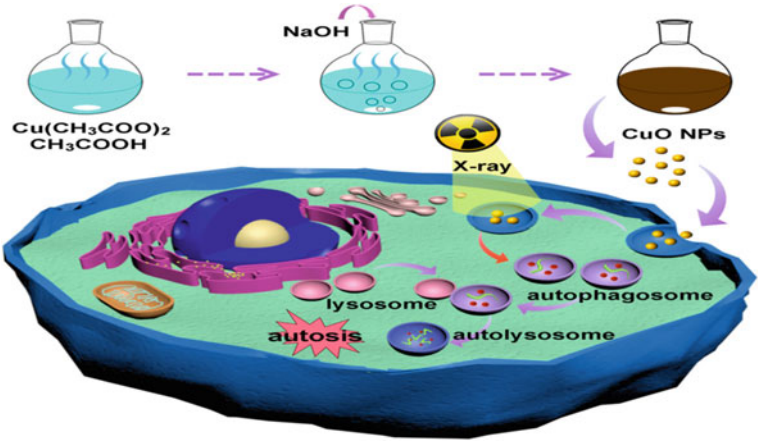

Fig. 13 Synthetic routes and applicatory effects of copper oxide nanoparticles. Reproduced with the permission from [86]

and 3 mmol of Gd $(NO_3)_3{\cdot}6H_2O$ and Bi $(NO_3)_3{\cdot}5H_2O$ was formed with constant stirring until it became translucent. Solution was further stirred for 6 h by adding equal ratios of tartaric acid to be as 1:1. A dried gel was obtained by stirring the solution and maintaining the temperature at 120 °C, which is further processed in powder. Formed powder was dried by keeping it in a furnace at 450 °C for 2 h and was further hardened for 2 h by keeping the temperature at 800 °C until powder turned orange. Synthesized powder was washed several times and centrifuged and dried at 60 °C in vacuum.

Nosrati et al. [88] prepared a solution of 8 mL of bovine serum albumin (BSA) with 31.25 mg/mL concentration. Another solution containing 1 mL HNO_3 and $Bi(NO_3)_3$ with 50 mM share of 2 M concentration was synthesized. Now BSA solution was accommodated by $Bi(NO_3)_3$ solution under constamnt magnetic stirring. Sodium hydroxide was added to bio mineralize Bi_2S_3 and BSA under constant stirring for 12 h. As the process of bio mineralization completed, solution turned back to black, as BSA and Bi_2S_3 were normalized. Resultant product was termed as BSA coated Bi_2S_3 which went through dialysis against water in order to purify it for 48 h providing us with Bi_2S_3@BSA composites. NHS and EDC was done for Formic acid functionalization on previously prepared composite in order to provide activation sites for covenant bonding with Bi_2S_3@BSA. Secondly, Bi_2S_3@BSA and BSA amine groups were reacted, while in the last step, dialysis of obtained composite was done to purify it. 2.4 mg of N-Hydroxy-succinimide and 18 mg of ethylene dichloride was used to activate 1 mL share of formic acid with 10 mg/mL concentration in alkaline DMSO. Synthesized solution was mixed dropwise with Bi_2S_3@BSA solution having 10 mg/mL concentration. 3 M of sodium hydroxide was used to create an alkaline media. Solution was stirred for 24 h by keeping it in dark, further passed thorough

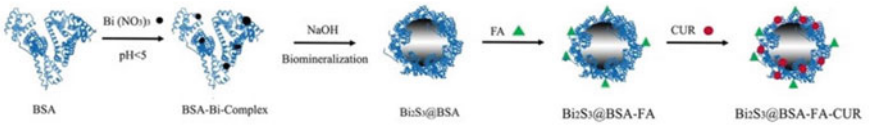

Fig. 14 schematic diagram of Bi2S3@BSA-FA-CUR synthetic gateway. Reproduced with the permission from [88]

dialysis against water. CUR loading on Bi_2S_3@BSA-FA forming Bi_2S_3@BSA-FA-CUR was done by mixing 2.8 mL of DI water, 10 mg Bi_2S_3@BSA-FA further accompanied by another solution containing 200 μL acetone and 2.5 mg CUR. Resultant solution was kept in dark under constant stirring for whole night. Prepared solution now termed as Bi_2S_3@BSAFA-CUR went through repetitive washing and centrifuge at 18,000 rpm (Fig. 14).

3 Characterization and Performance of Various Nanoradiosentizer

3.1 Gold-Based Nanoradiosentizer

Liang et al. [89] reported that the characterization of hollow gold nanospheres (HGNs) and anti-c-Met/HGNs. In Fig. 15a show that morphology was homogeneous of the HGNs and has the diameter 56.25 ± 6.13 nm and the thickness of the wall was 6.56 ± 1.33 nm which was measured by using the TEM. In Fig. 15b clearly shown that the red shift of the plasma resonance which were occurred by the modification of the HGNs. In Fig. 15c the cells of the CaSki anti-c-HGNs was more affected as compared to the HGNs at each interval of time. Peak of both HGNs and anti-c-HGNs was observed for 24 h and find the average numbers of nanoparticles by each cells were 5,378 ± 401 for the HGNs and 8,681 ± 742 for the anti-c-Met/HGNs. Overexpression of the c-Met was observed in different types of pathological in cancer cells. In the analysis of immunofluorescence, the presence of the green fluorescent layer on the cell membrane of CaSki cells can be seen clearly (Fig. 15d).

Teraoka et al. [90] reported that the different effects of 5 nm Au nanoparticles without X-ray treatment in the human head and neck carcinoma cell line (HSC-3). From Fig. 16a, it was clearly shown that there were no significant results shown between the cells of control and the treated cells such as 0.1, 0.4, 1.0 and 10.0 nM Au nanoparticles. On the other hand, in Fig. 16b clearly show that lower radiation dose has cytotoxicity was 4 Gy. However, the dose of radiation 4 Gy was selected for this experiment. By using the X-ray irradiation, the effects of Au nanoparticles were enhanced on the total numbers of cells. Without using the Au nanoparticles, the cells were reduction by using the X-ray irradiation and when combined the Au

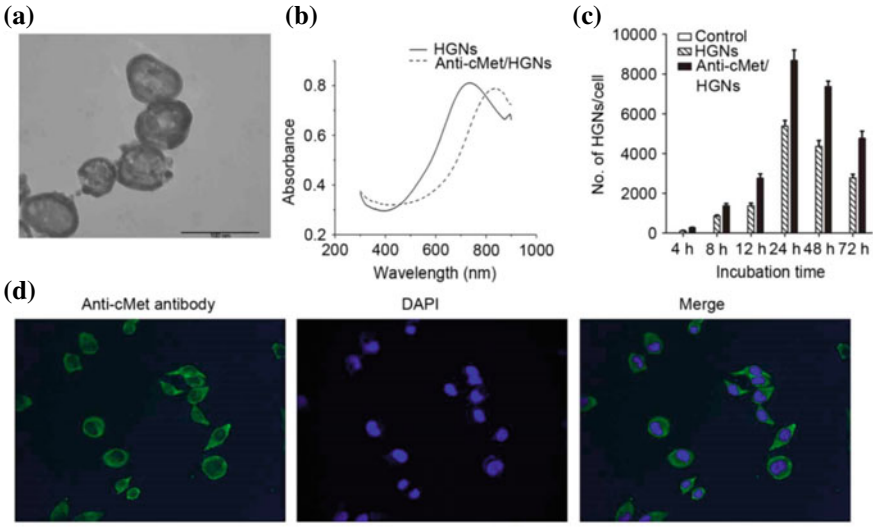

Fig. 15 The characteristics of HGNs and CaSki cells. **a** TEM images of HGNs. **b** peak shifting HGNs **c** Inductively coupled plasma atomic emission spectroscopy was used to count the number of nanospheres endocytosed by each cell. **d** In immunofluorescence, cMet was overexpressed on cell membranes in CaSki cells. Reproduced with the permission from [89]

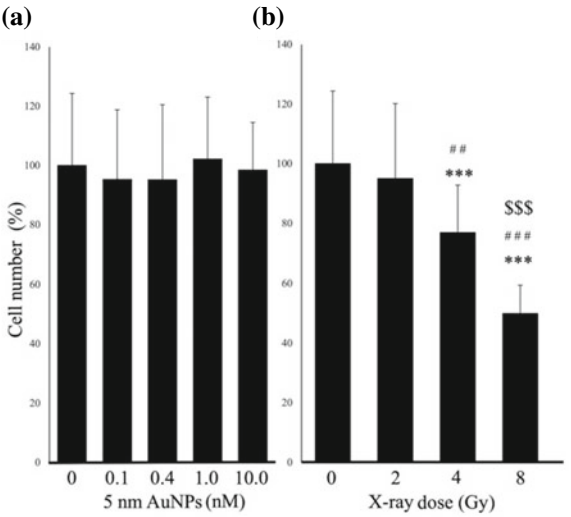

Fig. 16 Effect of single treatment with AuNPs or X-ray irradiation on HSC-3 cell number. **a** HSC-3 cells were used 5-nm AuNPs **b** Different dose was used such as 4 and 8 Gy X-ray irradiation. Reproduced with the permission from [90]

nanoparticles were apparent due to the induction of the apoptosis, but there was no shown the inhibition of cell proliferation.

Ngwa et al. [91] reported that the in Fig. 17a, b. residual γH2AX florescence images was shown for the incubated cells with and without the Au nanoparticles.

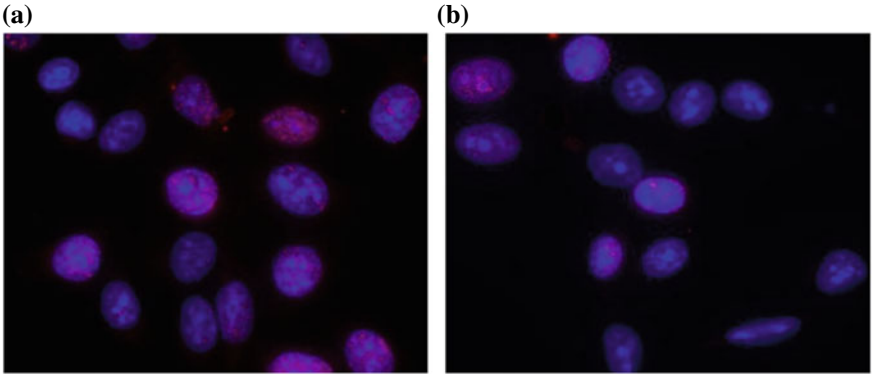

Fig. 17 Fluorescence images which is obtained from the Residual γH2AX **a** with AuNP and **b** without AuNP. Reproduced with the permission from [91]

The results showed that the cells were smaller with the Au nanoparticles, which was enhanced by unrepaired radiation damage.

In Fig. 18, the residual DNA damage enhancement factor (rDEF) plot was shown in which four irradiation experiments as well non-irradiation control samples. In the non-irradiated samples such as 0 Gy, there were no shown any biological effects of Au nanoparticles. The Au nanoparticle was shown minimum effects on the cells in the absence of radiation. Furthermore, the results of the irradiated samples shown in different range such as 1.7 to 2.3. So that, this results were indicate that the more unrepaired radiation damage almost 70–130% which is greater for the incubator cells with the Au nanoparticles which was consider as a significant radio sensitization by the Au nanoparticles.

Penninckx et al. [92] reported that the two different parameters were plotted according to the gold weight percent which shown in Fig. 19. This figure was high-

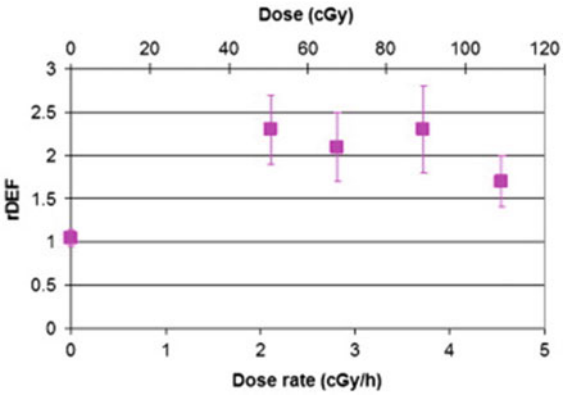

Fig. 18 With and without using AuNP for the HeLa cells. the rDEF is shown four different sets and also one is no irradiation. Reproduced with the permission from [91]

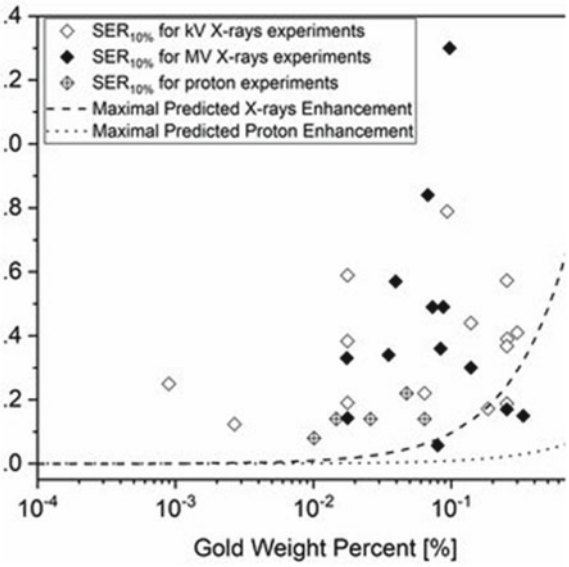

Fig. 19 Comparison of observed in vitro experimental sensitization enhancement ratio (SER) with predicted dose enhancement values for GNPs studies. Reproduced with the permission from [92]

lights in three main deviations from the dose of enhancement of the physical predications. Firstly, many scientists were reported the significant effects of the radio sensitization on the cells which contain less than 0.1 weight percentage. Secondly, it was very interesting that radio sensitization effects were reported that by using the proton beam calculation of the physical predication was enhanced only when the increasing of dose was neglected. Finally, the overserved that the values were enhanced generally than the predication ones as illustrated. Meanwhile, the correlation between the dose of enhancement and observation of the radio sensitization was not significant.

Ma et al. [93] reported that the in Fig. 20a, b was shown that the dose dependent radiation which enhanced the effects of modified GNSs in the KB cells. In the results, the GNSs was shown enhanced radio sensitization and also the fraction of the cells was decreased by increasing the radiation dose with and without the treatment of modified GNSs. The curve of the fraction was shown in Fig. 20c nonlinear fitting which calculated by using the multitarget single hit model. When the dose was 4 Gy than the X-ray radiation only decreased the cell viability at 48%. Moreover, the vibility of the cells were reduced 42% to 24% in the presence of the GNSs, NH2-GNSs, FA-GNSs, and TAT-GNSs, respectively. The SERs was calculated such as 1.34, 1.57, 1.84, and 2.30 for the GNSs-, NH2-GNSs-, FA-GNSs-, and TAT-GNSs-treated, respectively. After 50 to 60 h, it was shown that in Fig. 20d, the viability of the cells was decreased in the groups without X-ray radiation treatment.

Zhang et al. [94] reported that the cells irradiated on the microdisks with X-rays and without nanoparticles (Fig. 21a). It showed weak green fluorescence and

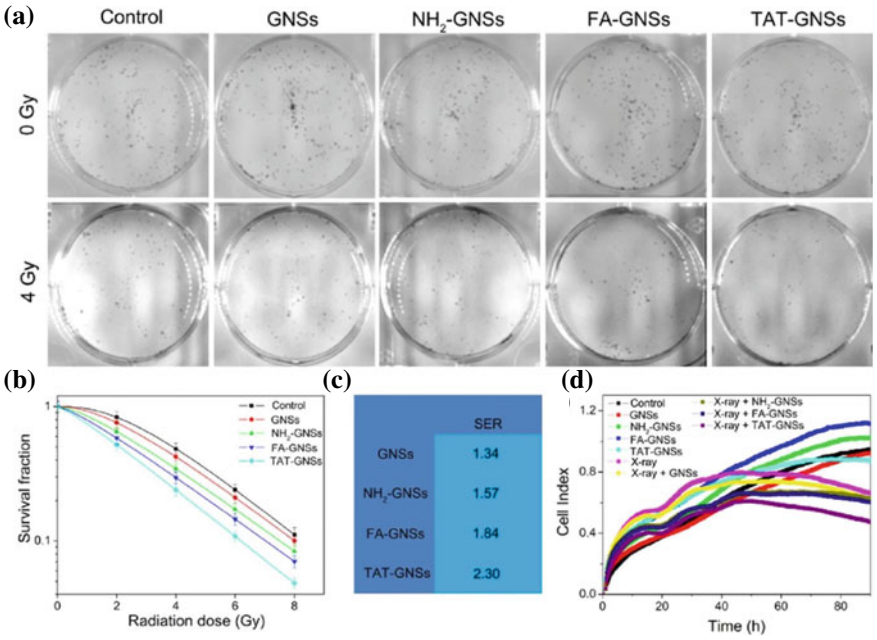

Fig. 20 Effects of different GNSs on radiosensitivity in KB cells. **a** KB cell colony formation with and without Au, but the concentration of the metal is the same. **b** Radiation dose-dependent survival fractions of KB cells before and after treatments with various GNSs. **c** Multitarget single-hit calculates the ratio of different sensitizations. **d** After different treatments as indicated and Cell proliferation curves of KB cells. Reproduced with the permission from [93]

blue color due to the DAPI which was staining of DNA and small amount of γ-H2AX. From Fig. 21b, It showed the strong expression of the γ-H2AX. The signal of fluorescence was artificially decreased from the DAPI and DNA due to the green color. The intensities of the green fluorescence were quantified with the 96 well reader plates. Figure 21c showed that the intensities of the fluorescence in the cells on the microdisks with nanoparticles and without X-rays radiation. Cells radiation on the mirodisks with X-rays was less micronuclei shown in Fig. 21d. The arrows in the Fig. 21e was show that the micronucleus from the cells after irradiation. Figure 21f showed the number of nuclei per 2000 cells and the cells attached to the microdisks with 0, 1, 2, 3 and 4 layers of the nanoparticles. Figure 21g showed that the cells attached on the microdisks have not nanoparticles, the green color showed that the cells were alive. Figure 21h shows the cells was attached on the microdisks and also have nanoparticles and the red colors cells were dead but some microdisks have not cells attached. In Fig. 21i shown the cell viability ratio of 97.2 ± 2.5% at 36 h. the indicate that the cells were killed due to the combined effects of X-ray and nanoparticles.

Li et al. [95] reported that the in Fig. 22. Show exponential was decreased in the fraction for the cells irradiated by using the beam of proton of 25 keV μm^{-1}.

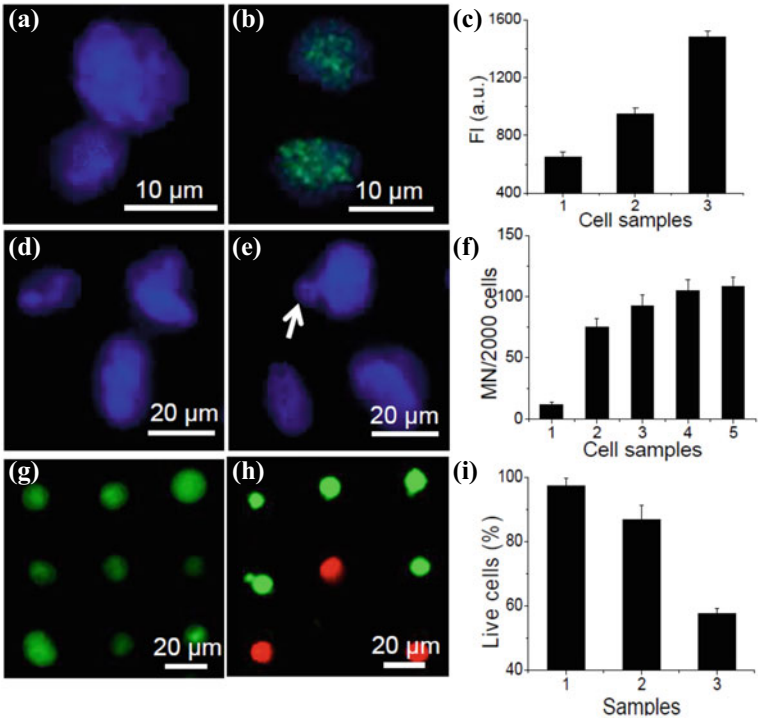

Fig. 21 (**a**) Microdisks with attached cells in fluorescence **b** and Nanoparticles are attached to microdisks containing cells (**c**), after X-ray radiation and staining with DAPI and FITC-labeled γ-H2AX antibody (**d**); Fluorescence images of cells without microdisks or cells attached (**e**) Cells attached to microdisks that contain nanoparticles (**f**), after X-ray radiation and staining with DAPI for micronucleus analysis (**g**) cells attached on microdisks without nanoparticles and with X-ray (**h**) cells attached on microdisks with nanoparticles and X-ray (**i**) cell viabilities in three samples. Reproduced with the permission from [94]

The cells of MDA-MB-453 cells and preincubated was not show the same trend with Ctxb–AuNPs. The curve of the A431 was higher as compared with their control cells. At 2 Gy was observed that the fraction of the cells significant decreased due to the relevant radiation dose. The efficiency of the Ctxb–AuNPs to increase by radiation induced A431 cells were dead by calculated the SER at the 10%. However, the cancer cell- targeting Ctxb–AuNPs was developed and the SER higher as compered the Au nanoparticles. The curve of the cell survival was fitted by using the linear quadratic model.

Liang et al. [96] reported that the cytotoxicity was determined by using the assay of CCK8. In Fig. 23A, 6 Gy irradiation was used to find the survival rate 85.6% for the HeLa cells c(RGDyC)-AuNCs (60 mM Au). It was show that the enhanced effects of radiation and also cell survival rate was decreased at the 54.8%. The factor of radiation was enhanced, defined the ration of eradication cells without and with radio sensitizers, was determined the 1.73 for the c(RGDyC)- AuNCs which was

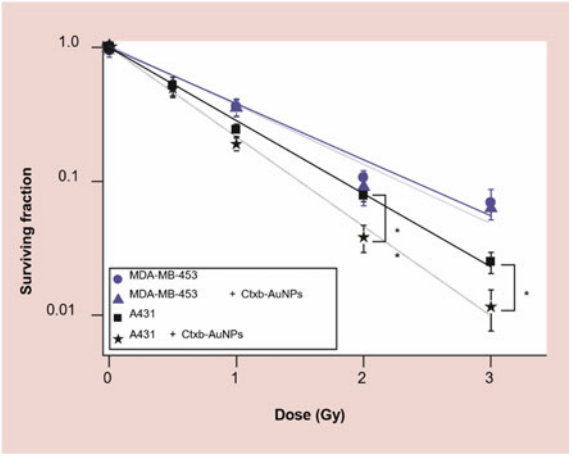

Fig. 22 Survival curves of MDA-MB-453 cells and A431 cells without using gold nanoparticles. Reproduced with the permission from [95]

higher from the c(RADyC)-AuNCs and CMNa. Different irradiation does was used to compare the c(RGDyC)-AuNCs and CMNa. It was illustrating that c(RGDyC)-AuNCs stronger radiation as compared to CMNa under the radiation dose tested shown in Fig. 23b. After 15 days, 6 Gy X-rays induced and shown the cells survival was decreased show in Fig. 23c. Meanwhile, 40% of HeLa cells was still survived after the radiation with the dose of 8 Gy. The cells of c(RGDyC)-AuNCs, by using the same dose the cells of HeLa were not completely dead. Using the multitarget single model, to fit the curve of cell survival and also find the SER of the (RGDyC)-AuNCs was alomost 2.04 which was higher than the c(RADyC)-AuNCs and CMNa 1.33 and 1.63, respectively shown in Fig. 23d. which was suggested the c(RGDyC)-AuNCs in the cells more active and also enhanced the radiation of sensitivity, and to kill the 50% cell the radiation doses were required. To test this hypothesis, cellular DNA was exposure radiation and performed DNA ladder assay shown in Fig. 23e. the results were shown that without radiation and any treatment, no DNA ladder was observed in the cells. It was suggested that only nanoclusters were not significant for the damage the cellular DNA.

Mahmoud and Elshemey [97] reported that the to evaluate the synergistic effects of chemo-radiotherapy by using the different concentration of CS-GNPs-DOX against MCF-7 cancer cells, netural red cell viability assay was used. With the external radiation, all the concentrations of CS-GNPs and viability percentages of the MCF-7 cells were almost 70%, which was suitable for the biocompatibility for the synthesized nano formulation shown in Fig. 24a. The rates of sensitization at different concentration was carried out to examine the relationship between the radiation dose, concentration of nanoparticles and sensitization effects of CS-GNPs-DOX. In Fig. 24b and d was show the cells viability with radiation at doses of 0.5, 1 and 3 Gy was 73%, 45% and 25%, respectively. Once CS-GNPs-DOX was delivered in

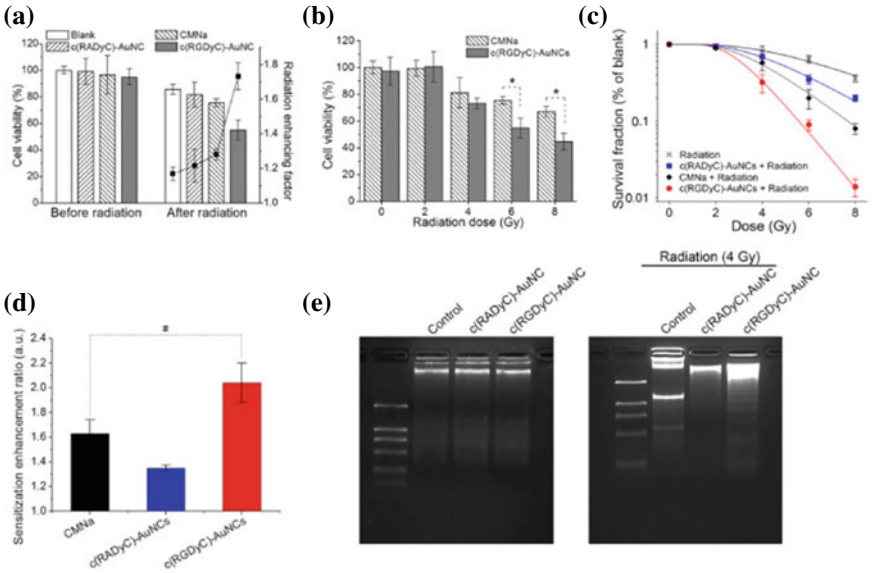

Fig. 23 Radiosensitizing effect of c(RGDyC)-AuNCs. **a** Cell viability and radiation for HeLa cells treated with c(RGDyC) **b** under different doses radiation to Compare the radiosensitizing effect between c(RGDyC)-AuNCs and CMNa **c** using one-fourth of dose ration for Clonogenic survival curves of c(RGDyC)-AuNCs, c(RADyC)-AuNCs, and CMNa **d** SER of CMNa, c(RADyC)-AuNCs and c(RGDyC)-AuNCs **e** with and without irradiation ofDNA fragmentation assay. Reproduced with the permission from [96]

the tumor cells at the lower concentration, it was enhanced the effects of radiations damage as 2 foldes which was compared the cells treated with radiation only at different doses. From Fig. 24c, at low concentration up to 1 Gy, it was shown that the combined therapy regimen (CS-GNPs-DOX + radiation) show more effects on the cancer cells as compared alone CS-GNPs + radiation. It was clearly suggested the chemo-radiotherapy treatment was more effective than the single therapy regimen. So that the effects of radio sensitization were predominates over the chemotherapy effects. There was no significant difference between the cell viability and treated with CS-GNPs-DOX or CS-GNPs which was exposure the different doses of radiation shown in Fig. 24d. The results suggested that CS-GNPs-DOX was efficient for drug delivery, local dose and simultaneously at MV energy range of radiation [10].

Zhu et al. [98] reported that the clonogenic assay was used for the HepG2 cells with X-ray alone or combining X-ray with either GNPs or GAL-PEG-GNPs. The results were show Fig. 25 that cell viability decreased by increasing the radiation dose in three groups. In GAL-PEG-GNPs/X-ray treated group was show lower radiation in 2 groups from 1 to 8 Gy, which was show enhancement radiation sensitivity of HepG2 cells to X-ray. Due to the fitting cell survival curve, found by D0, the SERs of GNPs/X-ray group and GAL-PEG- GNPs/X-ray group were 1.46, and 1.95, respectively.

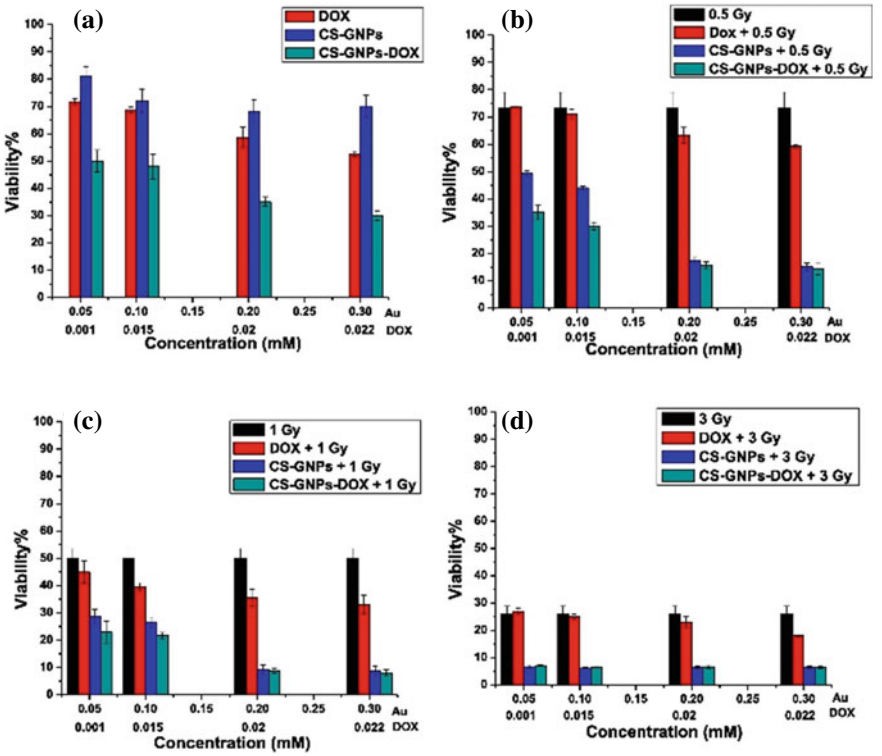

Fig. 24 (**a**–**d**) The synergistic inhibition for MCF-7 cell at different radiation doses and concentrations. Reproduced with the permission from [97]

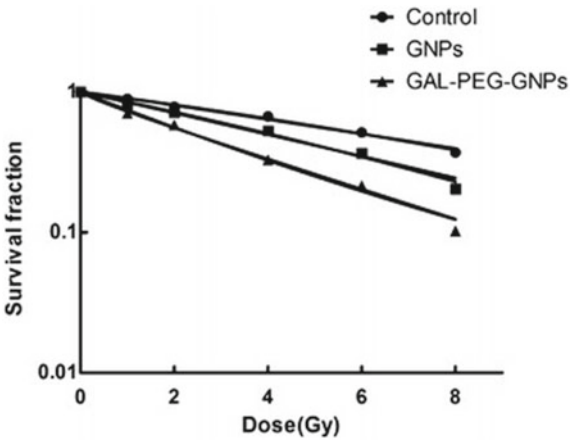

Fig. 25 Clonogenic assays show that GNPs and GALPEGGNPs radiosensitize HepG2 cells. Reproduced with the permission from [98]

Moradi et al. [99] reported that the WST-1 assay was used for calculated the significant differences in cell viability between single treatment cells and control. The results showed that there was no significant difference at the 70 μM gold nanoparticle (GNP) concentration shown in Fig. 26. In the study of double treatment of irradiation (Ir), GNP and 17-allylamino-17-demethoxygeldanamycin (17-AAG) show higher cytotoxic effects as compared the single treatments show in Fig. 27. However,

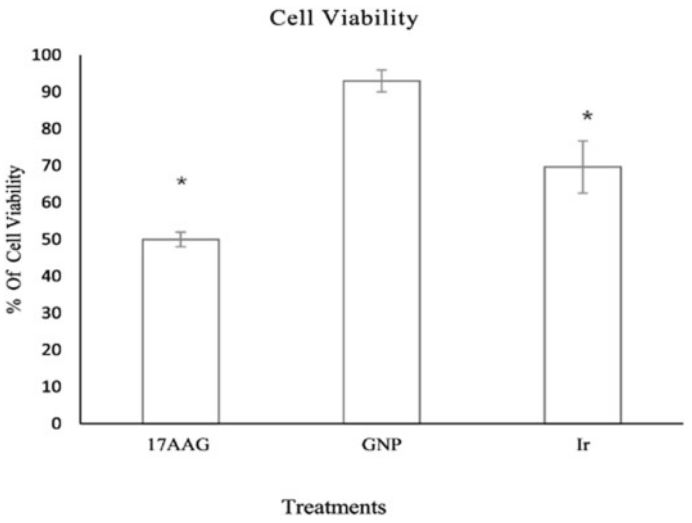

Fig. 26 WST-1 from single treatment of (17-AAG, GNP and Ir) with untreated control cells. Reproduced with the permission from [99]

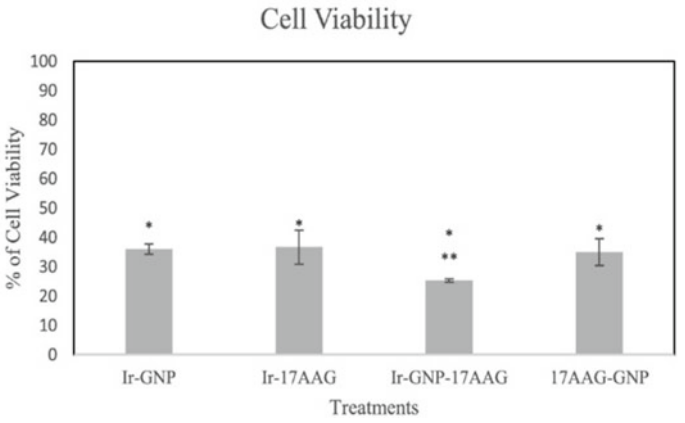

Fig. 27 WST-1 from double treatments (GNP, Ir/Ir,17-AAG/ GNP,17-AAG) with double treatments. Reproduced with the permission from [99]

it concluded that at the lower concentrations, 17-AAG and GNP act as a radio sensitizer with the combination of Ir. 17-AAG and GNP, cell viability was decreased as compared to the single treatments. In triple combination, GNP, Ir and 17-AAG after 24 h was shown higher cell viability as compared the double combination. Moreover, the effects of anti-proliferative of the GNP with X-ray Ir double combinations were decreased as compered the GNP, Ir and 17-AAG in the triple combinations.

Zhang et al. [100] reported that the HeLa cells treated with the $Cu_2(OH)PO_4$@PAAS nanocomposites under the X-ray irradiation which was show the strongest green fluorescence signal as compared to the groups of other treated $Cu_2(OH)PO_4$@PAAS nanocomposites along with X-ray irradiation shown in Fig. 28a. On the other hand, the Fenton-like reaction which was based on the $Cu_2(OH)PO_4$@PAAS nanocomposites in this regard the level of H_2O_2 was evaluated. Firstly, it was reported that concentration of H_2O_2 in the tumor cells was higher as compared to the normal cells. In Fig. 28b show that the irradiation with X-ray on the human cancer cells was improved of the intercellular H_2O_2 level at the different intensities of the X-ray. In Fig. 28c the result indicated that the $Cu_2(OH)PO_4$@PAAS nanocomposites have the ability to kill the tumor cells due to the higher concentration of the H_2O_2 level in the tumor cells as compared to the normal cells. The cytotoxicity of the $Cu_2(OH)PO_4$@PAAS nanocomposites with different concentrations on the human cancer cells were evaluated by using the assay of CCK-8 which is known as counting Kit-8 shown in Fig. 28d. The results were found that no decreased cell viability to human cancer cells at different concentrations, which indicated $Cu_2(OH)PO_4$@PAAS nanocomposites was unable to trigger the Feton-like reactions. After the combination of the X-ray irradiation, cell viability to the human cancer cells were decreased with the increasing of $Cu_2(OH)PO_4$@PAAS nanocomposites. The human cancer cells were incubated with the hypoxia-mimic cobalt chloride show the low cell viability at the same concentration of $Cu_2(OH)PO_4$@PAAS nanocomposites by using the X-ray irradiation. To evaluate the radiotherapeutic efficacy was used for the cancer cells. Assay of clonogenic was used and observed the efficacy on HeLa cells shown in Fig. 28e. To compare the X-ray irradiation, the formation rates of the human cancer cells were decreased from 66.44% to 24.03% under the treatment of $Cu_2(OH)PO_4$@PAAS nanocomposites and also it was indicated the $Cu_2(OH)PO_4$@PAAS nanocomposites was capable of inhibition of cancer cells proliferation shown in Fig. 28f and g. As shown in Fig. 28h the group treatment with $Cu_2(OH)PO_4$@PAAS nanocomposites by using X-ray irradiation shown significant higher results as compared to others groups. In Fig. 28i, no results of γ-H2AX immuno-fluorescent spots were observed in the control and other groups only show in the treated groups with $Cu_2(OH)PO_4$@PAAS nanocomposites. However, the γ-H2AX immuno-fluorescent spots were considered as a higher in the group treated with $Cu_2(OH)PO_4$@PAAS nanocomposites by using the X-ray irradiation, which was more than 1.89-fold higher as compared to other groups with X-ray irradiation shown in Fig. 28j. In these results were indicate that the $Cu_2(OH)PO_4$@PAAS nanocomposites have the efficacy to kill the tumor cells through to control the X-ray-triggered Feton-like reactions.

Yamaguchi et al. [101] reported that in Fig. 29 show the combination of control,

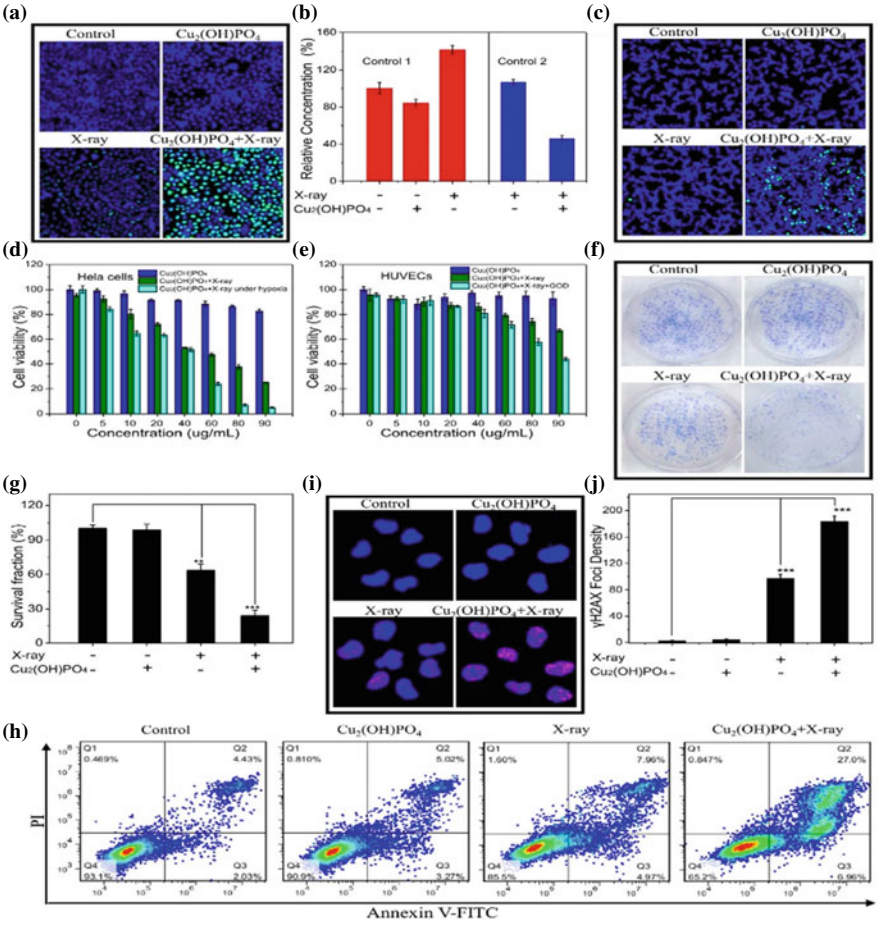

Fig. 28 The efficacy of Cu(OH)PO4@PAAS NCs in vitro. **a** Images of HeLa cells stained **b** H_2O_2 level of HeLa cells with different treatments. **c** Images of HUVECs staining **d** The cytotoxicity of $Cu_2(OH)PO_4$@PAAS NCs on HeLa cells with different treatments **e** Different treatments increased Cu2(OH)PO4@PAAS NC cytotoxicity in HUVECs. **f** Colony formation assay of HeLa cells with $Cu_2(OH)PO_4$@PAAS NCs and irradiation X-ray. **g** With different treatments, the corresponding survival fraction of HeLa cells **h** Flow cytometric analysis of HeLa cells with different treatments **i** X-ray irradiated Cu2(OH)PO4@PAAS-induced DNA double-strand damage. Immunofluorescence images. **j** The corresponding number of γ-H2AX immuno-fluorescent spots at different treatments. Reproduced with the permission from [100]

Silica and PAMAM-coated silica nanoparticles (PCSNs) probes which was caused the apoptosis in the cell of SK-BR3. It was reported that the nanoparticles of silica were induced apoptosis in many types of cells. The combination of radiation and PCSN probes both was caused the cell growth inhibition and death of cells in the lysosomal membrane. Moreover, humanized monoclonal antibody, Trastuzumab,

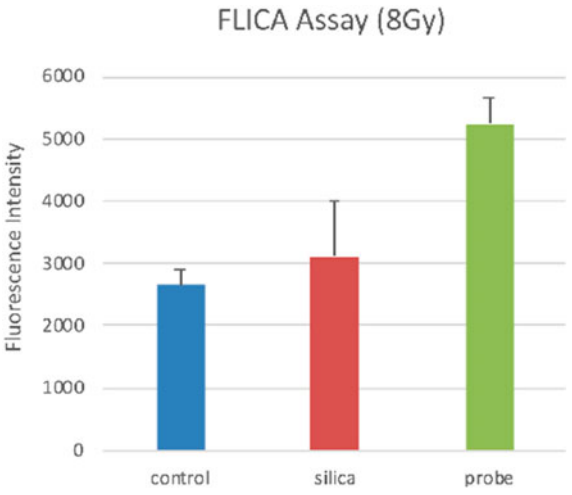

Fig. 29 An 8-Gy Irradiation using PCSN probes. Reproduced with the permission from [101]

selectively binds to the extracellular domain of the HER2 receptor. Trastuzumab triggers HER2 internalization and degradation by promoting tyrosine kinase activity.

Generalov et al. [102] reported that Nanoparticles has the ability to increase the reactions in the cells. The Zinc and silica dioxide nanoparticles were increased the radiation induces and killed the cells shown in Fig. 30. To compare the effects between the nanoparticles-free and containing the nanoparticles samples, the calculation of the radiation was increased the ratio almost twofold for the LNCaP cells and almost 1.5 fold for the Du145 cells. In some literature, the radiation induced effects in the

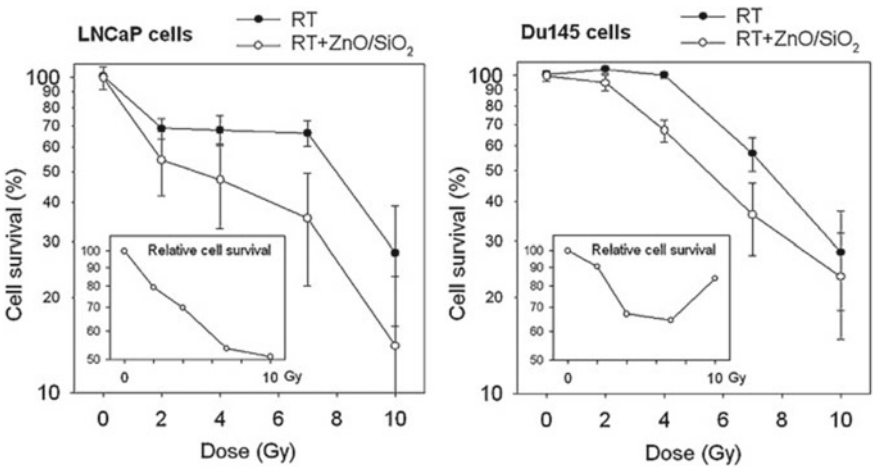

Fig. 30 After radiotherapy with and without nanomaterials (RT, 200kVp) and ZnO/SiO2 nanoparticles, survival of the LNCaP and Du145 cells was studied. Reproduced with the permission from [102]

silica dioxide was the main reason for the augmentation of radiotoxicity. In silica dioxide, the formation of ionization and excitation was occur through the radiolysis.

Press [103] reported that the assay of clonogenic was used to determine the improvement of radio sensitization in the pGNRs@ $mSiO_2$-RGD. The curves were show in the Fig. 31. Such as pGNRs@ $mSiO_2$-RGD treated and pGNRs@ $mSiO_2$-RGD treated with the MDA-MB-231 cells which was combined with the megavoltage RT. By using the single hit multi target model to calculate the RT biology parameters in each groups. Both types of the gold nano probes was induced in the radio sensitization, but the effects of the pGNRs@ $mSiO_2$-RGD nanoprobes were better as compared to the pGNRs@$mSiO_2$. To evaluate the clinical potential, it was very important to assess the cytotoxicity in the GNPs. The cell viability of normal cells such as MCF-10A was used to exposed in the pGNRs@mSiO2 and pGNRs@$mSiO_2$ –RGD nano probes were determined through CCK-8 assay. In the control groups, the cell viability was found 100% but in the remaining groups were found 90% after the incubation at different concentration of the gold nanoprobes, which was shown that gold nanoprobes has low cytotoxicity.

Fathy et al. [75] reported that the MTT assay was used to examine the radio sensitizing effects of IO-MNPs and SIO-MNPs against the breast cancer cells such as MCF7. In Fig. 32a–f, survival curves which were shown the radiation effects on the cancer cells after incubated with different concentrations ratios such as 0, 5, 10, 20, 40 and 80 μg/ml of the IO-MNPs and SIO-MNPs. The results were indicated the cell viability of the treated cells only on the doses of 0.5, 1, 2, and 4 Gy was 80%, 60%, 50% and 47% respectively. After 24 h, the incubation of cancer cells at the different concentration of the IO-MNPs and SIO-MNPs. It was shown the damaging effects and compared with the cells treated. At the lower doses such as 0.5 and 1 Gy, the cell viability was decreased with increasing the concentration in the IO-MNPs and SIO-MNPs compared to cells treated with radiation only. The values of the DFF were found with different concentration in the IO-MNPs and SIO-MNPs were exposed to 0.5 Gy such as 1.08, 1.12, 1.23, 1.37 and 1.64. At the higher doses such as 2 and 4 Gy, there was no significant effects of concentration variation and

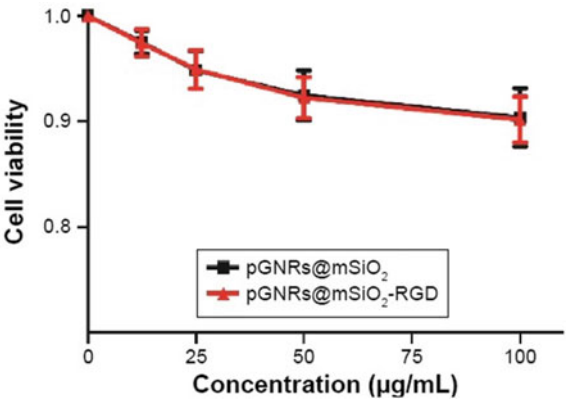

Fig. 31 McF-10a normal cells were incubated with various concentrations of pGNRs@mSiO2 and pGNRs@$mSiO_2$ –RGD nanoprobes. Reproduced with the permission from [103]

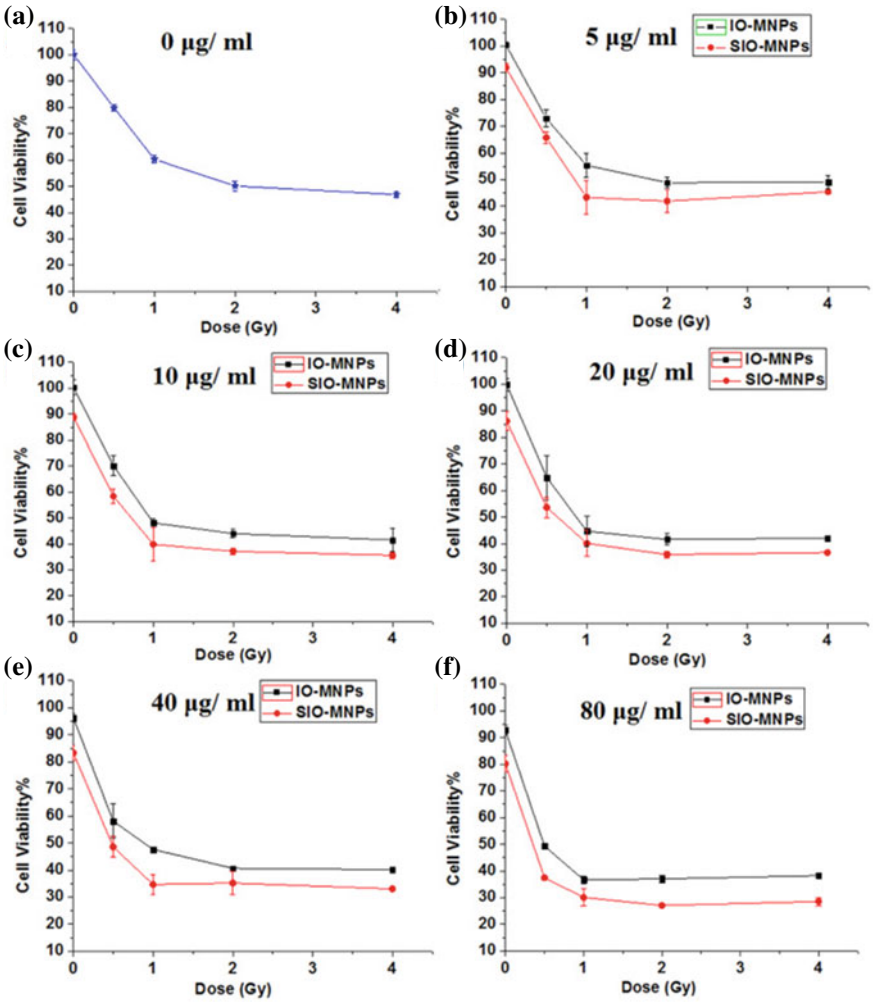

Fig. 32 The survival curves of MCF-7 cells exposed to various drugs (**a**-**f**). Reproduced with the permission from [75]

the values of the DFF were lower in the IO-MNPs and SIO-MNPs. At the low doses 0.5 and 1 Gy, the cell viability in the MCF7 cells tested were decreased almost 25% in cell treated with SIO-MNPs at the same concentrations. Due to the higher doses, the effects in the radio sensitizer were enhancement. With the same concentration in the IO-MNPs, almost 1.3 folds' cell treated was increased. In the other curves, the effects of both IO-MNPs and SIO-MNPs were as a dose modifier. The values of DFF was increased with increasing the concentration in the IO-MNPs and SIO-MNPs and decreased with the radiation dose increased. Overall, each dose and concentration, the values of the DFF of SIO-MNPs was almost 1.3 folds higher than the IO-MNPs. The

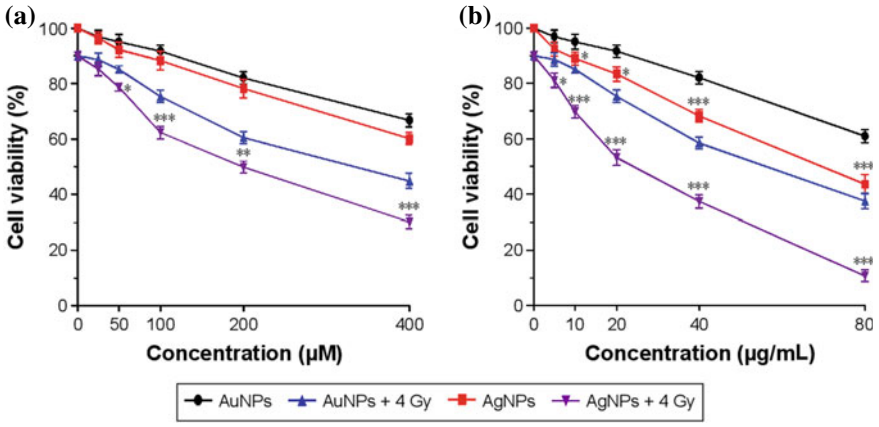

Fig. 33 AuNPs and AgNPs affect U251 cell viability, with or without radiation. Reproduced with the permission from [37]

results were suggested that there was enhancement in the radio therapeutic effects of IO-MNPs and SIO-MNPs.

Press [37] reported that the effects of au and ag nanoparticles on the cell viability shown in Fig. 33a and b. The physicochemical properties were shown in different nanoparticles which had various biological effects and cytotoxicity. By using the CCK-8 cell viability assay, to evaluate the differential growth inhibitions effects and toxicity in the AuNPs and AgNPs on U251 cells. The results were indicated the both AuNPs and AgNPs on U251 cells were dose dependent but show miner effects on the noncancerous cell line. at the same concentration, there was no significant results were shown. Moreover, at the same concentration of mass, AgNPs was increased the growth inhibition in the glioma cells as compared to the AuNPs at the 10% concentration. It was found that AgNPs found toxic and theirs effects were anti-proliferative against the cancer cells. In literature survey, AuNPs was shown anticancer and antimetastic properties without any functionalization while in the current study, AuNPs was shown significant stronger inhibition effects on the U251 glioma cells. Therefore, the deposition of the metal nanoparticles inside the nucleus was effective in the division of the cells and also main caused directly DNA damaging, modification of the nuclear targeted. Both of AuNPs and AgNPs were explored as a new route which improved the treatment of outcome cancer cells.

Klein et al. [104] reported that the by using the MTT assay, to find the biocompatibility of the NH_2-Si nanoparticles and silicon nanoparticles for the MCF-7 and 3T3 shown in Fig. 34 A and B. The value of the cell viability in the SiNPs or NH_2-SiNPs was compared to the medium TOAB and APTES. The value of APTES has been 92% in the MCF-7 and 97% in the 3T3. On the other hand, the value of TOAB has been 23% in the MCF-7 and 38% in the 3T3 which was caused the larger cellular damage in the cell membrane and permeability. The lower values were found for the SiNPs in the 3T3 and MCF-7 cells. They were damage the DNA due to the penetration of

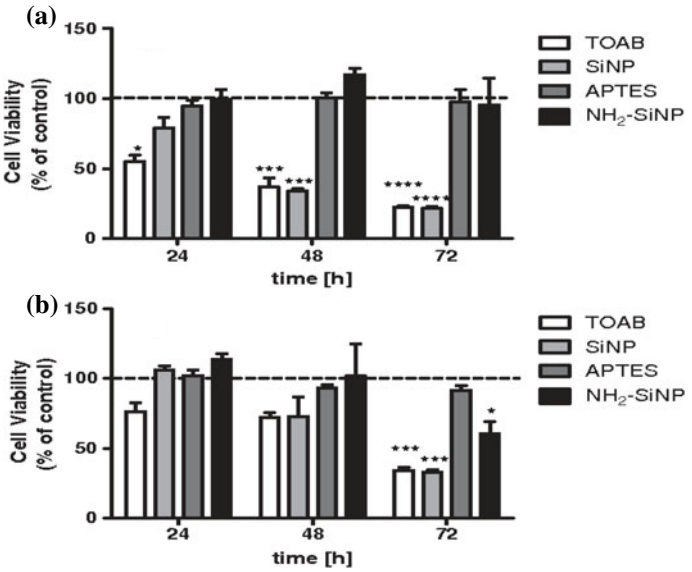

Fig. 34 SiNPs were tested for biocompatibility using the MTT assays (**a**) MCF-7 (**b**) cells with TOAB, APTES, SiNPs or NH2-SiNPs. Reproduced with the permission from [104]

the Si nanoparticles in the nucleus cells. The NH_2-SiNPs were slightly toxic for the 3T3 almost 95% at 72 h but it was less biocompatible for the MCF-7 cells such as 70% at 72 h.

Wardman [105] reported that to measure the oxygen tensions with relevant dose in one model shown in Fig. 35. It was clear show that tumours cells with the fraction cells and oxygen concentration which was raised the radio sensitivity and also improved the tumour oxygenation in the hypoxic subpulations. In the hypoxic cells, the potential gain of radio sensitizing was increased. By using 2 to 3 time higher radiation dose caused the killing of the cells. Today hyperbaric oxygen is not used with the X-ray radiations, it's just used to treat late radiation damage is attracting attention. Oxygen carriers were used to enhance the solubility parameters of the perfluorocarbons which was compare with blood plasma and they showed mixed results. Moreover, new approaches were developed, advanced in nanotechnology, and also it was reasonable prospects for the development of new carries of oxygen which have value in radiotherapy.

Mina et al. [106] reported that the results of this assay revealed the properties of antioxidant in the curcumin. In which three lines of cells were analyzed. In which observed that oxidative stress was increased with X-ray radiation but treatment with curcumin and antioxidant properties of the curcumin. However, treatment with curcumin and combination with the IR was able for the lower level in the cellular oxidative stress as compare to the value of untreated cells. Moreover, in the combination of treatments, the level of oxidative stress was lower which observed in the samples of subjected only irradiation, and also the efficacy of the curcumin was also

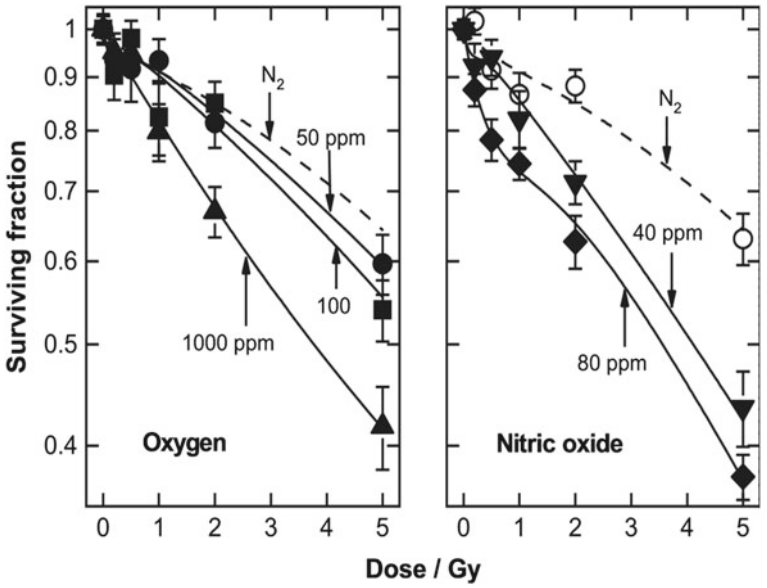

Fig. 35 Oxygen and nitric oxide at very low concentrations radiosensitize hypoxic fibroblastlike cells of the Chinese hamster V79-379A. Reproduced with the permission from [105]

lower in the ROS levels which was produced following administration of IR. GEP data was obtained to analysis on MCF10A, MCF7and MDA-MB-231 cell of breast lines which was treated with 2.5 μM Cur-SLN and irradiation with the beam of photon using the IR dose of 2 Gy. MCF10A samples were treated with the Cur-SLN changed the level of expression such as 657 up regulated and 189 down regulated. On the other hand, 1265 DEGs was selected in MCF BC cells with Cur-SLN treated in which 513 were down regulated and 752 were up regulated. Overall, in MDA-MB-231 BC cell lines have 846 genes in which 657 were up regulated and 189 were down regulated which was treated with the Cur-SLN and 2301 DEGs was selected 1179 up regulated and 112 were down regulated shown in Fig. 36.

Nosrati et al. [107] reported that the by used the vitro uptake analysis for the enhancement the X-ray radiotherapy shown in Fig. 37a-e. The results showed that the FA-conjugation particles were used as folate receptor-mediated endocytosis in to the cells. Therefore, these particles increased the conjugation of the FA. In this regards, the efficacy of the Bi_2S_3@BSA was higher than the Bi_2S_3@BSA-FA and Bi_2S_3@BSA-FA-CUR. These results were shown that the conjunction of the FA enhanced in to the cancer cells for using these particles. MTT assay was used to enhance the X-ray radiotherapy which was designed by the radio sensitizer. The effects of inhibitory on the Bi_2S_3@BSA as a4T1 cells was show this designed radio sensitizer, Bi_2S_3@BSA and also show no significant toxicity. The effect of the inhibitory was increased by loading the CUR, but their difference was not significant. The cells were not treated with the designed radio sensitizer but they irradiated

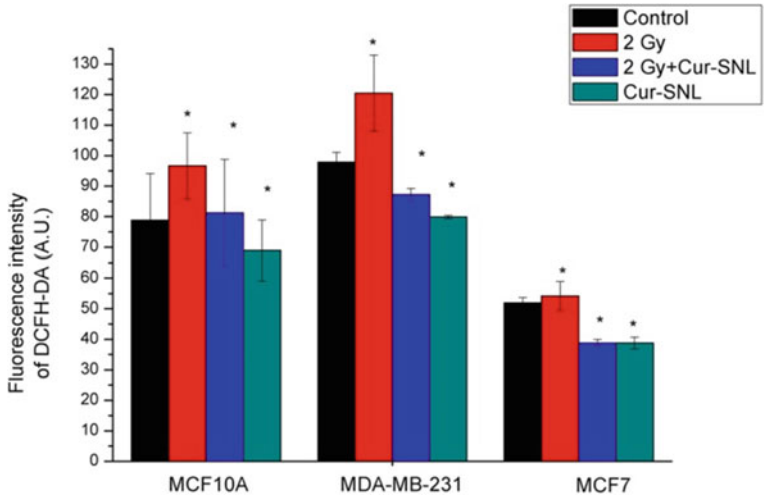

Fig. 36 Determination of intracellular ROS production. Reproduced with the permission from [106]

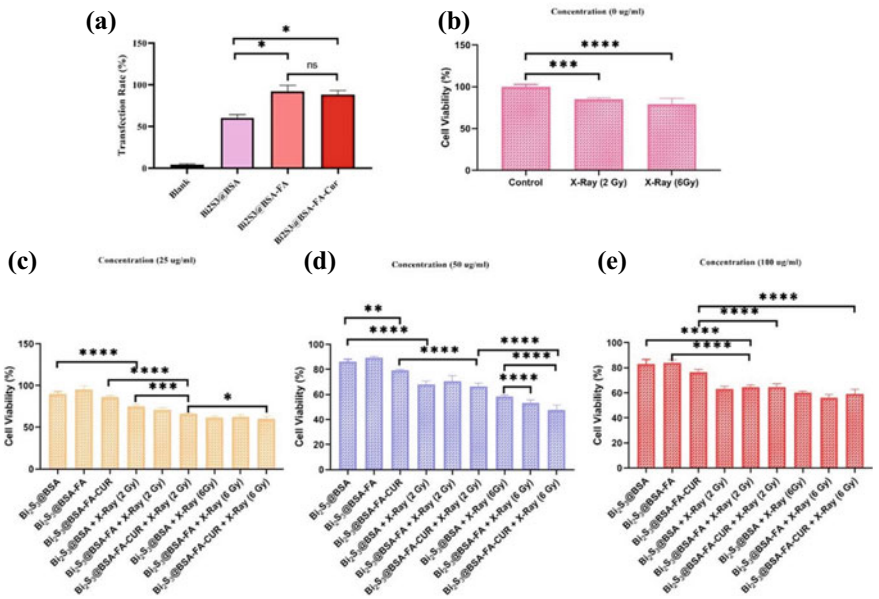

Fig. 37 **a** Transfection rates of Bi_2S_3@BSA, Bi_2S_3@BSA-FA, and Bi_2S_3@BSA-FA-CUR analyzed by flow cytometry **b** 0 **c** 25 **d** 50 and **e** 100 μg/mL concentrations on the 4T1 cell line. Reproduced with the permission from [107]

with X-ray at 2 and 6 Gy. By using the 2 Gy radiation dose, the value of the cell viability was almost 85%. The results were shown no significant differences between with or without irradiated groups. After X-ray radiation, the result of the MTT assay was confirmed that the cell viability was decreased. At the dose of 6 Gy, the results were shown that were not irradiated. To enhance the ability of X-ray radio therapy and the radio sensitizer, Bi_2S_3@BSA, Bi_2S_3@BSA-FA and Bi_2S_3@BSA-FA-CUR, the cells were irradiated with X-ray at the dose of 2 and 6 Gy. The results were suggested that the treated groups such as Bi_2S_3@BSA, Bi_2S_3@BSA-FA and Bi_2S_3@BSA-FA-CUR after used the radiation at different dose 2 and 6 Gy was showed the significant differences with or without irradiated groups. X-ray radiation of the bismuth nanoparticles were generating the electrons such as secondary and Auger. Which was ionized the water molecules and produced the ROS by including the hydroxyl radicals and shown the results DNA damage in the cancer cells.

Sebastià et al. [108] reported that different concentration of trans resveratrol 2.2–220 μM and curcumin 0.14–7 μM was used to test the radio protective potential but the effect was not dose dependent. Under the different experimental conditions were plotted by used the radiation induced chromosome fragments shown in Fig. 38. The results were obtained by using the model of liner multiple regressions. Solvent was not shown toxic effects and radio protective activity in the samples were not shown significant statistically effects in the PCCs cells. In the PCCs cells were not increased and also it was clearly observed the lymphocytes through only the curcumin and trans resveratrol. Therefore, in the presence of the polyphenols, radiation was applied than chromosome was damage alomost −1.37 to −1.28 per Gy.

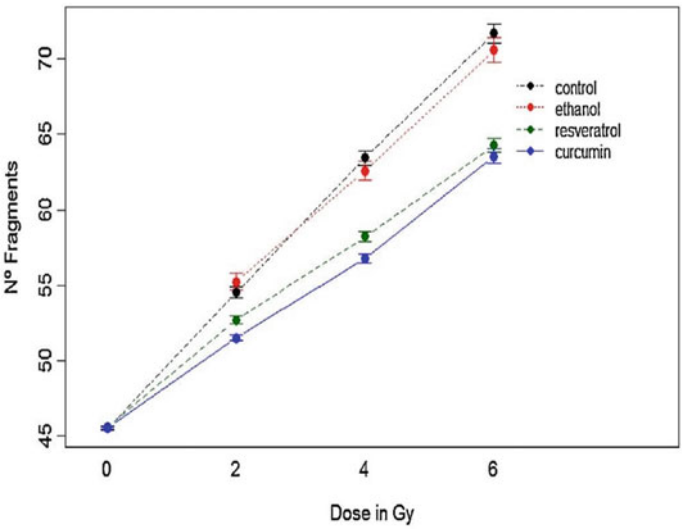

Fig. 38 A dose-dependent radioprotective effect of curcumin and trans-resveratrol on peripheral blood lymphocytes. Reproduced with the permission from [108]

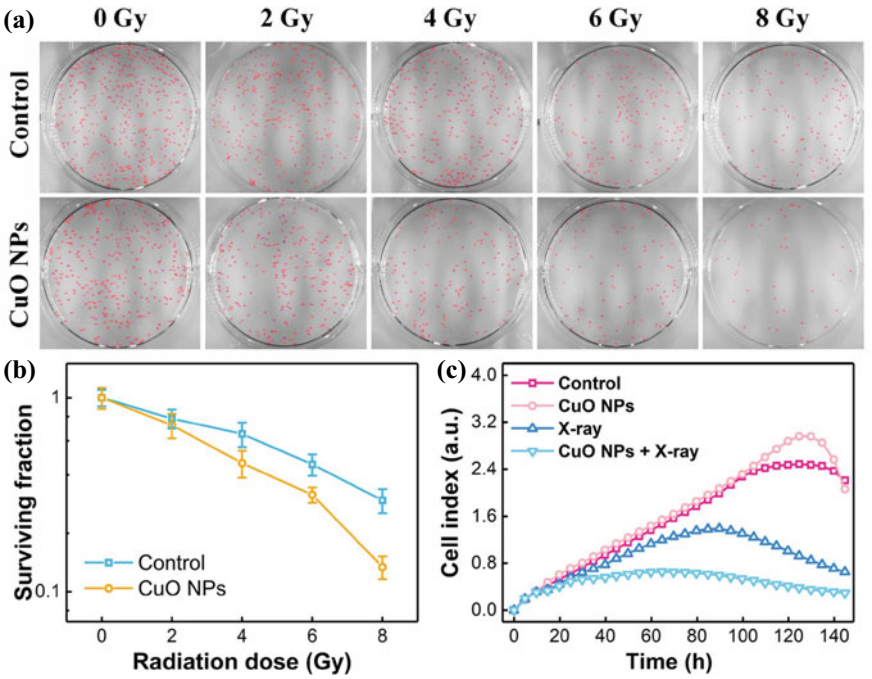

Fig. 39 Radiosensitization evaluation for CuO NPs. **a** Photographs of colonies formed by MCF-7 cells exposed to X-rays and treated with either CuO NPs or without **b** cell surviving fractions of the samples **c** Growth results of MCF-7 cells after different treatments as indicated. Reproduced with the permission from [109]

Jiang et al. [109] reported that the X-ray irradiation assay was used to confirm the results of CuO nanoparticles at the concentration of 10 μg/ml. The radiosensitizers effects of the CuO nanoparticles was carried out by using the assay of colony formation. As shown in Fig. 39a and b was confirmed the cell survival fraction was decrease with increased the X-ray irradiation dose, after the introduction of the CuO nanoparticles, the survival fraction effects was decrease which indicated the enhancement of radio sensitizations. The analysis of real time (RTCA) was confirmed the cell proliferation in the label free, manner of real time which was used for the noninvasive electrical impedance monitoring. After X-ray irradiation, the results of the RTCA showed that the cells proliferation was significant, especially when the CuO nanoparticles were combined. As shown Fig. 39c without using X-ray irradiation there was no effects shown in the inhibition of CuO nanoparticles.

Klein et al. [110] reported that the main objective of this experiment was to understand and quantify the radio enhancing of the HT-SPIONs and LT. so that, X-ray irradiation was used on the tumor cells for enhanced the formation of the ROS, the concentration of the ROS was used in the MCF-7 cells to measure the efficiency of the SPIONs for the ROS formation. However, the cells of MCF-7 were coated or uncoated with the HT-SPIONs and LT and it was exposed to X-ray irradiation at the

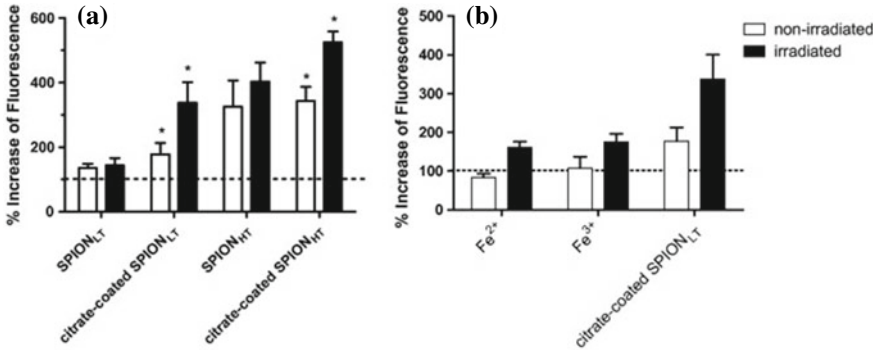

Fig. 40 Analyses of ROS levels in MCF-7 cells exposed to X-rays and non-irradiated cells loaded with citrate-coated and uncoated SPIONs **a** X-ray irradiated and nonirradiated MCF-7 cells loaded with Fe^{2+} , Fe^{3+} or citrate-coated LT-SPIONs were compared to determine relative ROS levels **b** using the DCFH-DA assay. Reproduced with the permission from [110]

single dose of 3 Gy or left it for non-irradiated shown in Fig. 40a. the concentration of the ROS was measured through the intensity of the fluorescence of DCF which was emerges due to the quantitative oxidation of internalized non-fluorescent DCFH per mole ROS. The results were shown that intensity of the fluorescence was 100% in the MCF-7 cells without coated SPIONs. The white bar was shown the value of the relative fluorescence of non-irradiated in the MCF-7 cells by using the SPIONs, but the black bar was shown the MCF-7 cells cultivated with the coated SPIONs species and also exposed the X-ray fluorescence intensity. Therefore, all the species which was coated with the SPIONs showed the improvement of ROS formation and also it was increased the effects the X-ray treatment. On the other hand, the species were coated with citrate LT-SPIONs in the X-ray treated in MCF-7 cells were shown fluorescence intensity almost 340%, which indicated the enhancement in the formation of ROS almost 240% and it was compared with the X-ray treated cells without internalized SPIONs. Moreover, LT-SPIONs species was internalized in the non-irradiated cells which caused a relative increased the concentration of ROS up to 77%. This results confirmed that SPIONs was not only to enhance the efficiency of X-ray on the formation of ROS. It was also act as a surface catalyst for the cycle of Haber–Weiss and Fenton reaction which was contributed in releasing iron ions to generate the ROS through the Haber–Weiss and Fenton reaction. As shown Fig. 40b the non-irradiated MCF-7 cells was contained the Fe^{2+} and Fe^{3+} ions which was shown the lower ROS concentration shown in black bar when it was compared with the references of the MCF-7 cells. It was clearly confirmed that the relative concentration of ROS was increased such as 60–75% shown in black bars. The relative concentration of the ROS in MCF-7 cells with internalized the citrate coated LT-SPIONs was fourfold greater than the non-irradiated MCF-7 cells with internalized Fe^{2+} ions.

Klein et al. [111] reported that analogous experiment was used with Caco-2 cells via malate coated and citrate coated SPIONs, it was stored under the conditions of

ambient for using different time periods shown in Fig. 41. From 1 to 3 weeks, the time of storage was increased by coating the SPIONs, the concentration of the ROS was measured which was lower almost 150% for the malate coating and for the citrate ligands it was 70%. However, in the surface of the SPIONs, the oxidations ions such as Fe^{2+} and Fe^{3+} were produced. Due to the Fenton reaction, Fe^{2+} ions was produced and the formation of the hydroxyl radical stored the SPIONs which was partially lost their activity of catalytic and also increased the formation of ROS with reduced the extent.

Meidanchi et al. [112] reported that the destruction of cell was designed to check the MTT cytotoxicity of the nanoparticles shown in Fig. 42. Up to 100 μgmL^{-1} for the nanoparticles such as $ZnFe_2O_4$, there was not observed the cytotoxicity. However, these nanoparticles were not completely responsible for the destruction

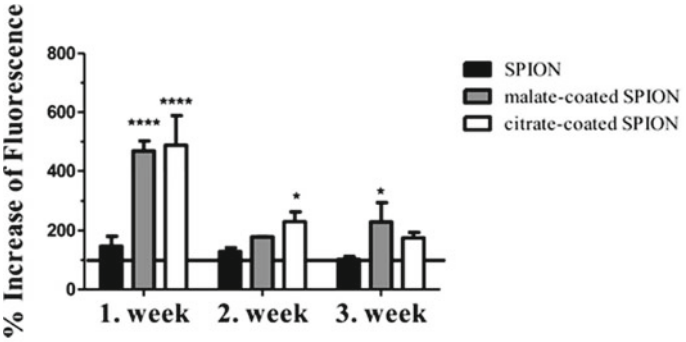

Fig. 41 DCF fluorescence as a measure of ROS concentration in X-ray-irradiated and nonirradiated Caco-2, MCF-7, and 3T3 cells loaded with citrate- or malate-coated or uncoated SPIONs. Reproduced with the permission from [111]

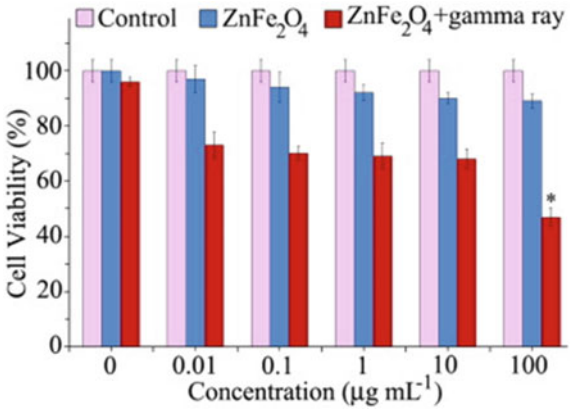

Fig. 42 Viability of LNCaP cells exposed to ZnFe2O4 nanoparticles with and without gamma irradiation. Reproduced with the permission from [112]

of cancer cells. MTT assay of cell viability of the LNCaP cells was exposed to the gamma irradiation with the $ZnFe_2O_4$ nanoparticles at different concentrations shown in Fig. 42. Without using these nanoparticles, no significant cell destruction was found through 2 Gy gamma irradiations. It was also confirmed that the radio resistance of the LNCaP cells against the irradiation of gamma. When the concentration was increased of these nanoparticles from 0.01 to 100 μgmL^{-1}, almost 10% cells were inactivated. Cell viability was decreased almost 53% for these nanoparticles at the concentration of the 100 μgmL^{-1} by using the 2 Gy gamma irradiation. By statistical analysis, it was clearly revealed that the significant effects of synergistic were due to the higher concentration of 100 μgmL^{-1}. The efficacy of the cancer cells by using these nanoparticles was 17 times greater by using the only gamma irradiation. The efficiency of the cell destruction was increased and also assigned the effects of photoelectric, generated the low energy Auger electron by using the $ZnFe_2O_4$ nanoparticles as a sensitizer through gamma irradiation.

Mirrahimi et al. [113] reported that the to evaluate the radiotherapy only to the death cell by using the KB and L929 cells, it was exposed the radiation dose of 2 and 4 Gy, and the X-ray irradiated 6 MV, and their toxicity was examined by using the assay of MTT. It was observed that both cells not different but also when the irradiation dose was increased there seemed no significant effect on the reducing cell viability shown in Figs. 43 and 44. To show the effects of synergistic of the RT with the FA-Au@Fe_2O_3 at the concentration of 20 μM and then irradiated with the 2 and 4 Gy. The death cells were deepened on the increasing dose with the FA-Au@Fe_2O_3 and also shown significant average rate. In the KB cells, the result was shown that the FA-Au@Fe_2O_3 exposed with 2 and 4 Gy and the irradiation was decreased from

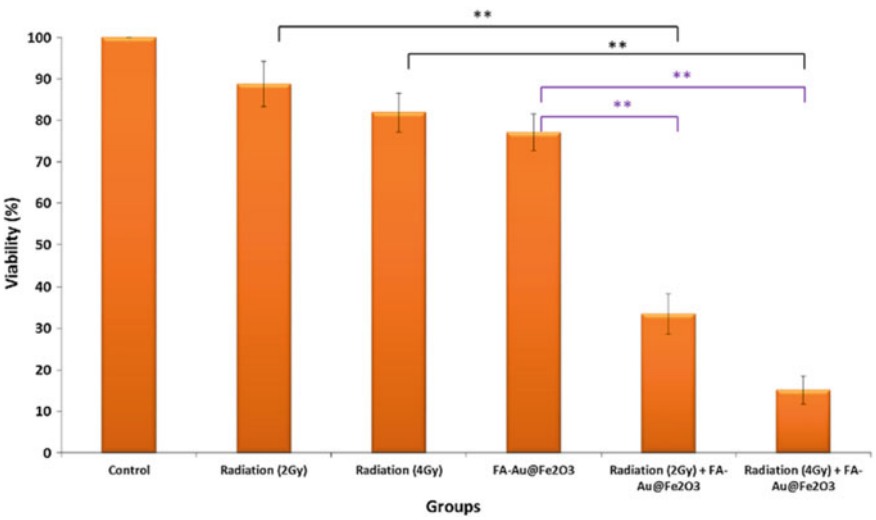

Fig. 43 Treatments of nanoparticles and radiation gave KB cancer cells varying levels of viability. Reproduced with the permission from [113]

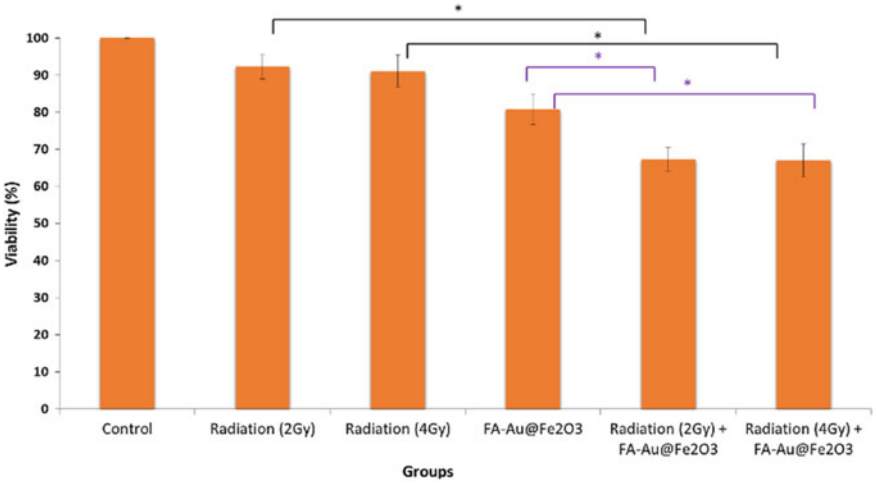

Fig. 44 The viability of healthy L929 cells after being treated with nanoparticles and radiation. Reproduced with the permission from [113]

33.53 to 15.13% which was completely staking. Overall, in the case of L929 cells, it was show that the enhancement of dose on the reeducation cells was not considerable. The cells survival was decreased from 67.23 to 66.96% which was not significant.

4 Conclusion

At present, nanoradiosensitizers have developed tremendously in the last decade thus providing new research approaches to enhance the therapeutic benefits. These benefits mainly include good radiosensitivity of tumour cells and radiation dose reduction. These are also in limelight due to their good biocompatibility and their capability as multi drug carriers. Excellent targeting, easy functionalization and good biocompatibility of nanoradiosensitizers solve the difficulties of traditional radiotherapy. It is worth mentioning that size, morphology and functionalization of these nanoradiosensitizers affect their performance and efficiency towards treatment of tumours. Research on the radiation sensitization mechanism will provide targets for new radiation sensitizers, and interdisciplinary research will promote the further development of nanoradiosensitizers. In summary, radiotherapy sensitizers can considerably improve the effect of radiotherapy.

References

1. Shiryaeva ES, Baranova IA, Kiselev GO, Morozov VN, Belousov AV, Sherstiuk AA, Kolyvanova MA, Krivoshapkin PV, Feldman VI (2019) Hafnium oxide as a nanoradiosensitizer under x-ray irradiation of aqueous organic systems: a model study using the spin-trapping technique and monte carlo simulations. J Phys Chem C 123(45):27375–27384. https://doi.org/10.1021/acs.jpcc.9b08387
2. Lim EK, Kim T, Paik S, Haam S, Huh YM, Lee K (2015) Nanomaterials for theranostics: recent advances and future challenges. Chem Rev 115(1):327–394. https://doi.org/10.1021/cr300213b
3. Sun H, Wang X, Zhai S (2020) The rational design and biological mechanisms of nanoradiosensitizers. Nanomaterials 10(3):1–33. https://doi.org/10.3390/nano10030504
4. Chen G, Roy I, Yang C, Prasad PN (2016) Nanochemistry and nanomedicine for nanoparticle-based diagnostics and therapy. Chem Rev 116(5):2826–2885. https://doi.org/10.1021/acs.chemrev.5b00148
5. Liu Y, Zhang P, Li F, Jin X, Li J, Chen W, Li Q (2018) Metal-based NanoEnhancers for future radiotherapy: radiosensitizing and synergistic effects on tumor cells. Theranostics 8(7):1824–1849. https://doi.org/10.7150/thno.22172
6. Schmähl D, Arturson G (1985) Book reviews. Agents Actions 16(6):585–587. https://doi.org/10.1007/bf01983666
7. Li N, Xia T, Nel AE (2008) The role of oxidative stress in ambient particulate matter-induced lung diseases and its implications in the toxicity of engineered nanoparticles. Free Radical Biol Med 44(9):1689–1699. https://doi.org/10.1016/j.freeradbiomed.2008.01.028
8. Huang CC, Aronstam RS, Chen DR, Huang YW (2010) Oxidative stress, calcium homeostasis, and altered gene expression in human lung epithelial cells exposed to ZnO nanoparticles. Toxicol In Vitro 24(1):45–55. https://doi.org/10.1016/j.tiv.2009.09.007
9. Buzea C, Pacheco II, Robbie K (2007) Nanomaterials and nanoparticles: sources and toxicity. Biointerphases 2(4):MR17–MR71. https://doi.org/10.1116/1.2815690
10. Cooper DR, Bekah D, Nadeau JL (2014) Gold nanoparticles and their alternatives for radiation therapy enhancement. Front Chem 2(OCT):1–13. https://doi.org/10.3389/fchem.2014.00086
11. Cheng K, Sano M, Jenkins CH, Zhang G, Vernekohl D, Zhao W, Wei C, Zhang Y, Zhang Z, Liu Y, Cheng Z, Xing L (2018) Synergistically enhancing the therapeutic effect of radiation therapy with radiation activatable and reactive oxygen species-releasing nanostructures. ACS Nano 12(5):4946–4958. https://doi.org/10.1021/acsnano.8b02038
12. Geng F, Song K, Xing JZ, Yuan C, Yan S, Yang Q, Chen J, Kong B (2011) Thio-glucose bound gold nanoparticles enhance radio-cytotoxic targeting of ovarian cancer. Nanotechnology 22(28). https://doi.org/10.1088/0957-4484/22/28/285101
13. Na, Li, Yu L, Wang J, Gao X, Chen Y, Pan W, Tang B (2018) A mitochondria-targeted nanoradiosensitizer activating reactive oxygen species burst for enhanced radiation therapy. Chem Sci 9(12):3159–3164. https://doi.org/10.1039/c7sc04458e
14. Wu H, Lin J, Liu P, Huang Z, Zhao P, Jin H, Ma J, Wen L, Gu N (2016) Reactive oxygen species acts as executor in radiation enhancement and autophagy inducing by AgNPs. Biomaterials 101:1–9. https://doi.org/10.1016/j.biomaterials.2016.05.031
15. Bouras A, Kaluzova M, Hadjipanayis CG (2015) Radiosensitivity enhancement of radioresistant glioblastoma by epidermal growth factor receptor antibody-conjugated iron-oxide nanoparticles. J Neurooncol 124(1):13–22. https://doi.org/10.1007/s11060-015-1807-0
16. Gara PMD, Garabano NI, Portoles MJL, Moreno MS, Dodat D, Casas OR, Gonzalez MC, Kotler ML (2012) ROS enhancement by silicon nanoparticles in X-ray irradiated aqueous suspensions and in glioma C6 cells. J Nanoparticle Res 14(3). https://doi.org/10.1007/s11051-012-0741-8
17. Choi BJ, Jung KO, Graves EE, Pratx G (2018) A gold nanoparticle system for the enhancement of radiotherapy and simultaneous monitoring of reactive-oxygen-species formation Nanotech. 29:504001

18. Jia TT, Yang G, Mo SJ, Wang ZY, Li BJ, Ma W, Guo YX, Chen X, Zhao X, Liu JQ, Zang SQ (2019) Atomically precise gold-Levonorgestrel nanocluster as a radiosensitizer for enhanced cancer therapy. ACS Nano 13(7):8320–8328. https://doi.org/10.1021/acsnano.9b03767
19. Chen F, Zhang XH, Hu XD, Liu PD, Zhang HQ (2018) The effects of combined selenium nanoparticles and radiation therapy on breast cancer cells in vitro. Artif Cells Nanomed Biotechnol 46(5):937–948. https://doi.org/10.1080/21691401.2017.1347941
20. Friedberg EC (2003) DNA damege and repair. Nature 421(January):436–440
21. Lomax ME, Folkes LK, O'Neill P (2013) Biological consequences of radiation-induced DNA damage: relevance to radiotherapy. Clin Oncol 25(10):578–585. https://doi.org/10.1016/j.clon.2013.06.007
22. Zhang P, Qiao Y, Wang C, Ma L, Su M (2014) Enhanced radiation therapy with internalized polyelectrolyte modified nanoparticles. Nanoscale 6(17):10095–10099. https://doi.org/10.1039/c4nr01564a
23. Joh DY, Sun L, Stangl M, Al Zaki A, Murty S, Santoiemma PP, Davis JJ, Baumann BC, Alonso-Basanta M, Bhang D, Kao GD, Tsourkas A, Dorsey JF (2013) Selective targeting of brain tumors with gold nanoparticle-induced radiosensitization. PLoS ONE 8(4). https://doi.org/10.1371/journal.pone.0062425
24. Yu D, Zhang Y, Lu H, Zhao D (2017) Silver nanoparticles coupled to anti-EGFR antibodies sensitize nasopharyngeal carcinoma cells to irradiation. Mol Med Rep 16(6):9005–9010. https://doi.org/10.3892/mmr.2017.7704
25. Shetake NG, Kumar A, Pandey BN (2019) Iron-oxide nanoparticles target intracellular HSP90 to induce tumor radio-sensitization. Biochim Biophys Acta Gen Subj 1863(5):857–869. https://doi.org/10.1016/j.bbagen.2019.02.010
26. Xiao F, Zheng Y, Cloutier P, He Y, Hunting D, Sanche L (2011) On the role of low-energy electrons in the radiosensitization of DNA by gold nanoparticles. Nanotechnol 22(46). https://doi.org/10.1088/0957-4484/22/46/465101
27. Sun L, Joh DY, Al-Zaki A, Stangl M, Murty S, Davis JJ, Baumann BC, Alonso-Basanta M, Kao GD, Tsourkas A, Dorsey JF (2016) Theranostic application of mixed gold and superparamagnetic iron oxide nanoparticle micelles in glioblastoma multiforme. J Biomed Nanotechnol 12(2):347–356. https://doi.org/10.1166/jbn.2016.2173
28. Roa W, Zhang X, Guo L, Shaw A, Hu X, Xiong Y, Gulavita S, Patel S, Sun X, Chen J, Moore R, Xing JZ (2009) Gold nanoparticle sensitize radiotherapy of prostate cancer cells by regulation of the cell cycle. Nanotechnology 20(37). https://doi.org/10.1088/0957-4484/20/37/375101
29. Cho S, Lee B, Park W, Huang X, Kim DH (2018) Photoperiodic flower mimicking metallic nanoparticles for image-guided medicine applications. ACS Appl Mater Interfaces 10(33):27570–27577. https://doi.org/10.1021/acsami.8b09596
30. Ruan J, Wang Y, Li F, Jia R, Zhou G, Shao C, Zhu L, Cui M, Yang DP, Ge S (2018) Graphene quantum dots for radiotherapy. ACS Appl Mater Interfaces 10(17):14342–14355. https://doi.org/10.1021/acsami.7b18975
31. Pan W, Gong S, Wang J, Yu L, Chen Y, Li N, Tang B (2019) A nuclear-targeted titanium dioxide radiosensitizer for cell cycle regulation and enhanced radiotherapy. Chem Commun 55(56):8182–8185
32. Kim EH, Kim MS, Song HS, Yoo SH, Sai S, Chung K, Sung J, Jeong YK, Jo YH, Yoon M (2017) Gold nanoparticles as a potent radiosensitizer in neutron therapy. Oncotarget 8(68):112390–112400. https://doi.org/10.18632/oncotarget.19837
33. Kim SR, Kim EH (2018) Feasibility study on the use of gold nanoparticles in fractionated kilovoltage X-ray treatment of melanoma. Int J Radiat Biol 94(1):8–16. https://doi.org/10.1080/09553002.2018.1393579
34. Liu J, Liang Y, Liu T, Li D, Yang X (2015) Anti-EGFR-conjugated hollow gold nanospheres enhance radiocytotoxic targeting of cervical cancer at megavoltage radiation energies. Nanoscale Res Lett 10(1). https://doi.org/10.1186/s11671-015-0923-2
35. Szegezdi E, Logue SE, Gorman AM, Samali A (2006) Mediators of endoplasmic reticulum stress-induced apoptosis. EMBO Rep 7(9):880–885. https://doi.org/10.1038/sj.embor.7400779

36. Su N, Dang Y, Liang G, Liu G (2015) Iodine-125-labeled cRGD-gold nanoparticles as tumor-targeted radiosensitizer and imaging agent. Nanoscale Res Lett 10(1). https://doi.org/10.1186/s11671-015-0864-9
37. Press D (2016b) Silver nanoparticles outperform gold nanoparticles in radiosensitizing U251 cells in vitro and in an intracranial mouse model of glioma, pp 5003–5014
38. Yamaguchi H, Hayama K, Id IS, Okada Y (2018) HER2-Targeted multifunctional silica nanoparticles specifically enhance the radiosensitivity of HER2-overexpressing breast cancer cells. https://doi.org/10.3390/ijms19030908
39. Zhang H, Sun Q, Tong L, Hao Y, Yu T (2018) Biomedicine & Pharmacotherapy Synergistic combination of PEGylated selenium nanoparticles and X-ray- induced radiotherapy for enhanced anticancer e ff ect in human lung carcinoma. Biomed Pharmacother 107(August):1135–1141. https://doi.org/10.1016/j.biopha.2018.08.074
40. Chen N, Yang W, Bao Y, Xu H, Qin S, Tu Y (2015) BSA capped Au nanoparticle as an efficient sensitizer for glioblastoma tumor radiation therapy. RSC Adv 5(51):40514–40520. https://doi.org/10.1039/c5ra04013b
41. Mirrahimi M, Hosseini V, Shakeri-Zadeh A, Alamzadeh Z, Kamrava SK, Attaran N, Abed Z, Ghaznavi H, Hosseini Nami SMA (2019) Modulation of cancer cells' radiation response in the presence of folate conjugated Au@Fe_2O_3 nanocomplex as a targeted radiosensitizer. Clin Transl Oncol 21(4):479–488. https://doi.org/10.1007/s12094-018-1947-8
42. Liu S, Piao J, Liu Y, Tang J, Liu P, Yang D, Zhang L, Ge N, Jin Z, Jiang Q, Cui L (2018) Radiosensitizing effects of different size bovine serum albuminlated gold nanoparticles on H22 hepatoma-bearing mice. Nanomedicine 13(11):1371–1383. https://doi.org/10.2217/nnm-2018-0059
43. Mizushima N, Levine B, Cuervo AM, Klionsky DJ (2008) Autophagy fights disease through cellular self-digestion. Nature 451(7182):1069–1075. https://doi.org/10.1038/nature06639
44. Gewirtz DA (2014) The four faces of autophagy: implications for cancer therapy. Can Res 74(3):647–651. https://doi.org/10.1158/0008-5472.CAN-13-2966
45. Liu Z, Xiong L, Ouyang G, Ma L, Sahi S, Wang K (2017) Investigation of copper cysteamine nanoparticles as a new type of radiosensitiers for colorectal carcinoma treatment. Sci Rep October 2016:1–11. https://doi.org/10.1038/s41598-017-09375-y
46. Jiang YW, Gao G, Jia HR, Zhang X, Zhao J, Ma N, Liu JB, Liu P, Wu FG (2019) Copper oxide nanoparticles induce enhanced radiosensitizing effect via destructive autophagy [Research-article]. ACS Biomater Sci Eng 5(3):1569–1579. https://doi.org/10.1021/acsbiomaterials.8b01181
47. Liu Z, Tan H, Zhang X, Chen F, Zhou Z, Hu X, Chang S, Liu P, Zhang H (2018) Enhancement of radiotherapy efficacy by silver nanoparticles in hypoxic glioma cells. Artif Cells Nanomed Biotechnol 46(sup3):S922–S930. https://doi.org/10.1080/21691401.2018.1518912
48. Zhang X, Liu Z, Lou Z, Chen F, Chang S, Miao Y, Zhou Z, Hu X, Feng J, Ding Q, Liu P, Gu N, Zhang H (2018) Radiosensitivity enhancement of Fe_3O_4 @Ag nanoparticles on human glioblastoma cells. Artif Cells Nanomed Biotechnol 46(sup1):975–984. https://doi.org/10.1080/21691401.2018.1439843
49. Li F, Li Z, Jin X, Liu Y, Li P, Shen Z, Wu A, Zheng X, Chen W, Li Q (2019) Radiosensitizing effect of gadolinium oxide nanocrystals in NSCLC cells under carbon ion irradiation. Nanoscale Res Lett 14(1). https://doi.org/10.1186/s11671-019-3152-2
50. Ma S, Miao H, Luo Y, Sun Y, Tian X, Wang F, You C, Peng S, Tang G, Yang C, Sun W, Li S, Mao Y, Xu J, Xiao Y, Gong Y, Quan H, Xie C (2019) FePt/GO nanosheets suppress proliferation, enhance radiosensitization and induce autophagy of human non-small cell lung cancer cells. Int J Biol Sci 15(5):999–1009. https://doi.org/10.7150/ijbs.29805
51. Zhang X, Zhang C, Cheng M, Zhang Y, Wang W, Yuan Z (2019) Dual pH-responsive "charge-reversal like" gold nanoparticles to enhance tumor retention for chemo-radiotherapy. Nano Res 12(11):2815–2826. https://doi.org/10.1007/s12274-019-2518-1
52. Kunoh T, Takeda M, Matsumoto S, Suzuki I, Takano M, Kunoh H, Takada J (2018) Green synthesis of gold nanoparticles coupled with nucleic acid oxidation. ACS Sustain Chem Eng 6(1):364–373. https://doi.org/10.1021/acssuschemeng.7b02610

53. Ahmed BS, Rao AG, Sankarshan BM, Vicas CS , Namratha K, Umesh TK, Somashekar R, Byrappa K (2016) Evaluation of gold, silver and silver–gold (Bimetallic) Nanoparticles as radiosensitizers for radiation therapy in cancer treatment. Cancer Oncol Res 4(3):42–51. https://doi.org/10.13189/cor.2016.040302
54. Zheng Y, Hunting DJ, Ayotte P, Sanche L (2008) Radiosensitization of DNA by gold nanoparticles irradiated with high-energy electrons (Radiation Research (2007) 169, 1 (19–27)). Radiat Res 169(4):481–482. https://doi.org/10.1667/0033-7587(2008)169[481:E]2.0.CO;2
55. Jim G, Maury P, Stefancikova L, Laurent G, Chateau A, Hoch FB, Denat F, Pinel S, Porcel E, Lacombe S, Bazzi R (2019) Fluorescent radiosensitizing gold nanoparticles *Int. J. Mol. Sci. 20*(18):4618
56. Ma N, Liu P, He N, Gu N, Wu F, Chen Z (2017). Action of gold nanospikes-based nanoradiosensitizers: cellular. https://doi.org/10.1021/acsami.7b09599
57. Zhang P, Qiao Y, Xia J, Guan J, Ma L, Su M (2015). Enhanced radiation therapy with multilayer microdisks containing radiosensitizing gold nanoparticles. https://doi.org/10.1021/am506866a
58. Yi X, Chen L, Zhong X, Gao R, Qian Y, Wu F, Song G, Chai Z, Liu Z, Yang K (2016) Core–shell Au@MnO2 nanoparticles for enhanced radiotherapy via improving the tumor oxygenation. Nano Res 9(11):3267–3278. https://doi.org/10.1007/s12274-016-1205-8
59. Nicol JR, Harrison E, O'Neill SM, Dixon D, McCarthy HO, Coulter JA (2018) Unraveling the cell-type dependent radiosensitizing effects of gold through the development of a multifunctional gold nanoparticle. Nanomed Nanotechnol Biol Med 14(2):439–449. https://doi.org/10.1016/j.nano.2017.11.019
60. Moreau N, Michiels C, Masereel B, Feron O, Gallez B, Vander Borght T, Lucas S (2009) PVD synthesis and transfer into water-based solutions of functionalized gold nanoparticles. Plasma Processes Polym 6(SUPPL. 1):888–892. https://doi.org/10.1002/ppap.200932210
61. Li S, Bouchy S, Penninckx S, Marega R, Fichera O, Gallez B, Feron O, Martinive P, Heuskin AC, Michiels C, Lucas S (2019) Antibody-functionalized gold nanoparticles as tumor-Targeting radiosensitizers for proton therapy. Nanomedicine 14(3):317–333. https://doi.org/10.2217/nnm-2018-0161
62. Liang G, Jin X, Zhang S, Xing D (2017) RGD peptide-modified fluorescent gold nanoclusters as highly efficient tumor-targeted radiotherapy sensitizers. Biomaterials 144:95–104. https://doi.org/10.1016/j.biomaterials.2017.08.017
63. Fathy MM, Mohamed FS, Elbialy NS, Elshemey WM (2018) Multifunctional Chitosan-Capped gold Nanoparticles for enhanced cancer chemo-radiotherapy: an invitro study. Physica Med 48(April):76–83. https://doi.org/10.1016/j.ejmp.2018.04.002
64. Mulgaonkar A, Moeendarbari S, Silvers W, Hassan G, Sun X, Hao Y, Mao W (2017) Hollow gold nanoparticles as efficient in vivo radiosensitizing agents for radiation therapy of breast cancer. J Biomed Nanotechnol 13(5):566–574. https://doi.org/10.1166/jbn.2017.2367
65. Ghorab MM, Ragab FA, Heiba HI, Youssef HA, El-gazzar MG (2010) Bioorganic & Medicinal Chemistry Letters Synthesis of novel pyrrole and pyrrolo [2, 3- d] pyrimidine derivatives bearing sulfonamide moiety for evaluation as anticancer and radiosensitizing agents OH. Bioorg Med Chem Lett 20(21):6316–6320. https://doi.org/10.1016/j.bmcl.2010.08.005
66. El Ella DAA, Ghorab MM, Heiba HI, Soliman AM (2012) Synthesis of some new thiazolopyrane and thiazolopyranopyrimidine derivatives bearing a sulfonamide moiety for evaluation as anticancer and radiosensitizing agents. Med Chem Res 21(9):2395–2407. https://doi.org/10.1007/s00044-011-9751-9
67. Ghorab MM, Ragab FA, Heiba HI, Youssef HA, El-Gazzar MG (2012) Synthesis of novel pyrazole and pyrimidine derivatives bearing Sulfonamide moiety as antitumor and radiosensitizing agents. Med Chem Res 21(7):1376–1383. https://doi.org/10.1007/s00044-011-9653-x
68. Ghorab MM, Ragab FA, Heiba HI, El-Gazzar MG, Zahran SS (2015) Synthesis, anticancer and radiosensitizing evaluation of some novel sulfonamide derivatives. Eur J Med Chem 92:682–692. https://doi.org/10.1016/j.ejmech.2015.01.036

69. Gul HI, Yamali C, Sakagami H, Angeli A, Leitans J, Kazaks A, Tars K, Ozgun DO, Supuran CT (2018) New anticancer drug candidates sulfonamides as selective hCA IX or hCA XII inhibitors. Bioorg Chem 77:411–419. https://doi.org/10.1016/j.bioorg.2018.01.021
70. Soliman AM, Alqahtani AS, Ghorab M (2019) Novel sulphonamide benzoquinazolinones as dual EGFR/HER2 inhibitors, apoptosis inducers and radiosensitizers. J Enzyme Inhib Med Chem 34(1):1030–1040. https://doi.org/10.1080/14756366.2019.1609469
71. Meidanchi A, Akhavan O, Khoei S, Shokri AA, Hajikarimi Z, Khansari N (2015) ZnFe2O4 nanoparticles as radiosensitizers in radiotherapy of human prostate cancer cells. Mater Sci Eng, C 46:394–399. https://doi.org/10.1016/j.msec.2014.10.062
72. Generalov R, Kuan WB, Chen W, Kristensen S, Juzenas P (2015) Radiosensitizing effect of zinc oxide and silica nanocomposites on cancer cells. Colloids Surf, B 129:79–86. https://doi.org/10.1016/j.colsurfb.2015.03.026
73. Wahab R, Siddiqui MA, Saquib Q, Dwivedi S, Ahmad J, Musarrat J, Al-Khedhairy AA, Shin HS (2014) ZnO nanoparticles induced oxidative stress and apoptosis in HepG2 and MCF-7 cancer cells and their antibacterial activity. Colloids Surf, B 117:267–276. https://doi.org/10.1016/j.colsurfb.2014.02.038
74. Klein S, Sommer A, Distel LVR, Neuhuber W, Kryschi C (2012) Superparamagnetic iron oxide nanoparticles as radiosensitizer via enhanced reactive oxygen species formation. Biochem Biophys Res Commun 425(2):393–397. https://doi.org/10.1016/j.bbrc.2012.07.108
75. Fathy MM, Fahmy HM, Saad OA, Elshemey WM (2019) Silica-coated iron oxide nanoparticles as a novel nano-radiosensitizer for electron therapy. Life Sci 234(July):116756. https://doi.org/10.1016/j.lfs.2019.116756
76. Klein S, Sommer A, Distel LVR, Hazemann J, Kro W, Neuhuber W, Mu P, Proux O, Kryschi C (2014). Superparamagnetic Iron oxide nanoparticles as Novel X - ray enhancer for low-dose radiation therapy. https://doi.org/10.1021/jp5026224
77. Massart R (1981) Preparation of aqueous magnetic liquids in alkaline and acidic media. IEEE Trans Magn 17(2):1247–1248. https://doi.org/10.1109/TMAG.1981.1061188
78. Girdhani S, Ahmed MM, Mishra KP (2009) Enhancement of gamma radiation-induced cytotoxicity of breast cancer cells by curcumin. Mol Cell Pharmacol 1(4):208–217. https://doi.org/10.4255/mcpharmacol.09.25
79. Sebastià N, Montoro A, Hervás D, Pantelias G, Hatzi VI, Soriano JM (2014) Mutation research / fundamental and molecular mechanisms of mutagenesis curcumin and trans -resveratrol exert cell cycle-dependent radioprotective or radiosensitizing effects as elucidated by the PCC and G2-assay. Mutat Res Fundam Mol Mech Mutagenesis 766–767:49–55. https://doi.org/10.1016/j.mrfmmm.2014.05.006
80. Xu H, Wang T, Yang C, Li X, Liu G, Yang Z, Singh PK, Krishnan S, Ding D (2018) Supramolecular nanofibers of curcumin for highly amplified radiosensitization of colorectal cancers to ionizing radiation. Adv Func Mater 28(14):1–11. https://doi.org/10.1002/adfm.201707140
81. Minafra L, Porcino N, Bravatà V, Gaglio D, Bonanomi M, Amore E, Cammarata FP, Russo G, Militello C, Savoca G, Baglio M, Abbate B, Iacoviello G, Evangelista G, Gilardi MC, Bondì ML, Forte GI (2019) Radiosensitizing effect of curcumin-loaded lipid nanoparticles in breast cancer cells. Sci Rep 9(1):1–16. https://doi.org/10.1038/s41598-019-47553-2
82. Pietzsch J (2017) Nitric Oxide-releasing selective Cyclooxygenase-2 inhibitors as promising Radiosensitizers in Melanoma Cells In Vitro. Ann Radiat Ther Oncol 1(2):1010
83. Cook T, Wang Z, Alber S, Liu K, Watkins SC, Vodovotz Y, Billiar TR, Blumberg D (2004) Nitric oxide and ionizing radiation synergistically promote apoptosis and growth inhibition of cancer by activating p53. Can Res 64(21):8015–8021. https://doi.org/10.1158/0008-5472.CAN-04-2212
84. Korde S, Sridharan G, Gadbail A, Poornima V (2012) Nitric oxide and oral cancer: a review. Oral Oncol 48(6):475–483. https://doi.org/10.1016/j.oraloncology.2012.01.003
85. Munaweera I, Shi Y, Koneru B, Patel A, Dang MH, Di Pasqua AJ, Balkus KJ (2015) Nitric oxide- and cisplatin-releasing silica nanoparticles for use against non-small cell lung cancer. J Inorg Biochem 153:23–31. https://doi.org/10.1016/j.jinorgbio.2015.09.002

86. Jiang YW et al (2019) Copper oxide nanoparticles induce enhanced radiosensitizing effect via destructive autophagy. ACS Biomater Sci Eng 5(3):1569–1579
87. Rajaee A, Wang S, Zhao L, Wang D, Liu Y, Wang J, Ying K (2019) Multifunction bismuth gadolinium oxide nanoparticles as radiosensitizer in radiation therapy and imaging. Phys Med Biol 64(19). https://doi.org/10.1088/1361-6560/ab2154
88. Nosrati H, Charmi J, Salehiabar M, Abhari F, Danafar H (2019) Tumor targeted albumin coated bismuth sulfide nanoparticles (Bi_2S_3) as radiosensitizers and carriers of curcumin for enhanced chemoradiation therapy. ACS Biomater Sci Eng 5(9):4416–4424. https://doi.org/10.1021/acsbiomaterials.9b00489
89. Liang Y, Liu J, Liu T, Yang X (2017) Anti-c-Met antibody bioconjugated with hollow gold nanospheres as a novel nanomaterial for targeted radiation ablation of human cervical cancer cell 5:2254–2260. https://doi.org/10.3892/ol.2017.6383
90. Teraoka S, Kakei Y, Akashi M, Iwata E, Hasegawa T (2018) Gold nanoparticles enhance X-ray irradiation-induced apoptosis in head and neck squamous cell carcinoma in vitro, pp 415–420. https://doi.org/10.3892/br.2018.1142
91. Ngwa W, Korideck H, Kassis AI, Kumar R, Sridhar S, Makrigiorgos GM, Cormack RA (2013) In vitro radiosensitization by gold nanoparticles during continuous low-dose-rate gamma irradiation with I-125 brachytherapy seeds. Nanomed Nanotechnol Biol Med 9(1):25–27. https://doi.org/10.1016/j.nano.2012.09.001
92. Penninckx S, Heuskin A, Michiels C (2021) Gold nanoparticles as a potent radiosensitizer : a transdisciplinary approach from physics to patient, pp 1–36
93. Ma N et al (2017) Action of gold nanospikes-based nanoradiosensitizers : cellular ACS *Appl. Mater. Interfaces*, 9(37):31526–31542
94. Zhang P et al (2015) Enhanced radiation therapy with multilayer microdisks containing radiosensitizing gold nanoparticles ACS *Appl. Mater. Interfaces* 7(8):4518–4524
95. Li S, Bouchy S, Penninckx S, Marega R, Fichera O (2019) Antibody-functionalized gold nanoparticles as tumor targeting radiosensitizers for proton therapy Nanomedicine (Lond) 14(3):317-333
96. Liang G, Jin X, Zhang S, Xing D (2017) Biomaterials RGD peptide-modi fi ed fl uorescent gold nanoclusters as highly ef fi cient tumor-targeted radiotherapy sensitizers 144:95–104. https://doi.org/10.1016/j.biomaterials.2017.08.017
97. Mahmoud M, Elshemey WM (2018) Physica Medica Multifunctional Chitosan-Capped Gold Nanoparticles for enhanced cancer chemo-radiotherapy : an invitro study. Physica Medica 48(November 2017):76–83. https://doi.org/10.1016/j.ejmp.2018.04.002
98. Zhu C, dong, Zheng, Q., Wang, L. xue, Xu, H. F., Tong, J. long, Zhang, Q. an, Wan, Y., & Wu, J. qing. (2015) Synthesis of novel galactose functionalized gold nanoparticles and its radiosensitizing mechanism. J Nanobiotechnol 13(1):1–11. https://doi.org/10.1186/s12951-015-0129-x
99. Moradi Z, Mohammadian M, Saberi H, Ebrahimifar M, Mohammadi Z, Ebrahimpour M, Behrouzkia Z (2019) Anti-cancer effects of chemotherapeutic agent; 17-AAG, in combined with gold nanoparticles and irradiation in human colorectal cancer cells. DARU J Pharmaceutical Sci 27(1):111–119
100. Zhang C, Yan L, Wang X, Dong X, Zhou R, Gu Z, Zhao Y (2019) Tumor microenvironment-responsive $Cu_2(OH)PO_4$ nanocrystals for selective and controllable radiosentization via the X - ray-triggered fenton-like reaction. 2. https://doi.org/10.1021/acs.nanolett.8b04763
101. HER2-targeted multifunctional silica nanoparticles specifically enhance the radiosensitivity of HER2-overexpressing breast cancer cells Int J Mol Sci. 19(3):908
102. Generalov R et al (2015) Radiosensitizing effect of zinc oxide and silica nanocomposites on cancer cells. Colloids Surf, B 129:79–86. https://doi.org/10.1016/j.colsurfb.2015.03.026
103. Press D (2016a) RGD-conjugated mesoporous silica-encapsulated gold nanorods enhance the sensitization of triple- negative breast cancer to megavoltage radiation therapy, pp 5595–5610
104. Klein S, Dell ML, Wegmann M, Distel LVR, Neuhuber W, Gonzalez MC, Kryschi C (2013) Bioch emical and biophysical research com munications Oxidized silicon nanoparticles for radiosensitization of cancer and tissue cells. Biochem Biophys Res Commun 434(2):217–222. https://doi.org/10.1016/j.bbrc.2013.03.042

105. Wardman P (2007) Chemical Radiosensitizers for Use in Radiotherapy *. https://doi.org/10.1016/j.clon.2007.03.010
106. Mina L, Po N, Valentina B, Gaglio D, Bonano M, Erika A, Paolo F, Giorgio R, Militello C, Savo G, Baglio M, Boris A, Irma G (2019) Radiosensitizing effect of curcumin- loaded lipid nanoparticles in breast cancer cells. January, 1–16. https://doi.org/10.1038/s41598-019-47553-2
107. Nosrati H, Charmi J, Salehiabar M, Abhari F, Danafar H (2019a) Tumor targeted albumin coated bismuth sul fi de nanoparticles (Bi_2S_3) as radiosensitizers and carriers of curcumin for enhanced chemoradiation therapy. https://doi.org/10.1021/acsbiomaterials.9b00489
108. Sebastià N, Montoro A, Hervás D, Pantelias G, Hatzi VI, Soriano JM (2014) Mutation Research / Fundamental and Molecular Mechanisms of Mutagenesis Curcumin and trans - resveratrol exert cell cycle-dependent radioprotective or radiosensitizing effects as elucidated by the PCC and G2-assay. Mutat Res Fundam Molecular Mech Mutagenesis 766–767:49–55
109. Jiang Y, Gao G, Jia H, Zhang X, Zhao J, Liu J, Liu P, Wu F (2019). Copper oxide nanoparticles induce enhanced radiosensitizing effect via destructive autophagy. https://doi.org/10.1021/acsbiomaterials.8b01181
110. Klein S et al (2012) Superparamagnetic iron oxide nanoparticles as radiosensitizer via enhanced reactive oxygen species formation. Biochem Biophys Res Commun 425(2):393–397. https://doi.org/10.1016/j.bbrc.2012.07.108
111. Klein S, Sommer A, Distel LVR, Hazemann JL, Kröner W, Neuhuber W, Müller P, Proux O, Kryschi C (2014) Superparamagnetic iron oxide nanoparticles as novel x-ray enhancer for low-dose radiation therapy. J Phys Chem B 118(23):6159–6166. https://doi.org/10.1021/jp5026224
112. Meidanchi A et al (2015) $ZnFe_2O_4$ nanoparticles as radiosensitizers in radiotherapy of human prostate cancer cells. Mater Sci Eng C 46:394–399. https://doi.org/10.1016/j.msec.2014.10.062
113. Mirrahimi M, Hosseini V, Zadeh AS, Kamrava ZASK, Abed NAZ (2019) Modulation of cancer cells ' radiation response in the presence of folate conjugated Au @ Fe_2O_3 nanocomplex as a targeted radiosensitizer. Clin Transl Oncol 21(4):479–488. https://doi.org/10.1007/s12094-018-1947-8

Harnessing the Power of Nanomaterials to Alleviate Tumor Hypoxia in Favor of Cancer Therapy

Hamid Rashidzadeh, Faezeh Mozafari, Mohammadreza Ghaffarlou, Murat Barsbay, Ali Ramazani, Morteza Abazari, Mohammad-Amin Rahmati, Hafeez Anwar, Surender K. Sharma, and Hossein Danafar

Abstract Cancer hypoxia is considered a hallmark of almost all solid malignancy and is responsible for diminishing the efficacy of some important cancer therapy modalities, particularly for those dependent on oxygen, including phototherapy, radiotherapy, and chemotherapy. Tumor hypoxia not only contributes to tumor progression and metastasis, but also augments tumor recurrence and resistance to conventional tumor treatments, ultimately leading to unsuccessful therapeutic outcomes. To this end, researchers have put a lot of effort into developing nanotechnology-based strategies to treat tumor hypoxia. Herein, we have classified the emerging strategies into two main types: (i) nanosystems with the ability to support oxygen content in hypoxic tumors to enhance oxygen-dependent tumor therapy, and (ii) nanomaterials with diminished oxygen dependence for hypoxic tumor therapy. In this chapter, we summarize all the exciting advances in nanomaterials and emerging smart strategies are making toward hypoxic tumor therapy.

Hamid Rashidzadeh and Faezeh Mozafari: These authors contribute equally to this work.

H. Rashidzadeh · F. Mozafari · M. Abazari · M.-A. Rahmati · H. Danafar (✉)
Zanjan Pharmaceutical Biotechnology Research Center, Zanjan University of Medical Sciences, Zanjan, Iran
e-mail: danafar@zums.ac.ir

H. Rashidzadeh · F. Mozafari · A. Ramazani · H. Danafar
Cancer Gene Therapy Research Center, Zanjan University of Medical Sciences, Zanjan, Iran

M. Ghaffarlou · M. Barsbay
Department of Chemistry, Hacettepe University, Beytepe, Ankara 06800, Turkey

H. Anwar
Department of Physics, University of Agriculture Faisalabad, Faisalabad 38040, Pakistan

S. K. Sharma
Department of Physics, Central University of Punjab, Bathinda 151401, India

Department of Physics, Federal University of Maranhao, Sao Luis, MA 65080-805, Brazil

S. K. Sharma et al. (eds.), *Harnessing Materials for X-ray Based Cancer Therapy and Imaging*, Nanomedicine and Nanotoxicology,
https://doi.org/10.1007/978-3-031-04071-9_5

Keywords Nanomaterials · Hypoxic tumor · Oxygenation · Tumor therapy · Cancer

1 Introduction

Cancer is a disease caused when cells divide uncontrollably and spread into surrounding tissues and it negatively affects the quality of human life and imposes significant burdens on public health worldwide. This complex disease has a very harsh and intricate microenvironment that is regarded as a major obstacle to current cancer therapy [1]. The cancer microenvironment is characterized by vascular anomalies and malformation, which leads to altered blood flow and thus fails to provide adequate oxygen and nutrients to further growing tumor mass [2]. Such a condition arises because the balance between oxygen consumption and supply is disturbed due to the rapid progression and proliferation of tumor tissues [3, 4]. This imbalance in consumption and delivery of oxygen impairs its diffusion into the deep tumors layers, results in a very low oxygen level (below 5–10 mmHg) compared to normal tissues with an oxygen level of 40–60 mmHg, which is known as tumor hypoxia [5]. It has been well documented that cancer hypoxia is considered as a distinctive feature of almost all solid malignancies and is responsible for reducing the efficacy of some important cancer treatment methods, especially for oxygen-dependent ones [6]. Hypoxia can actively contribute to tumor metastasis, invasion, deterioration, progression and proliferation by regulating hypoxia-inducible-factor-1 (HIF-1) [7]. In fact, on the one hand, hypoxia is closely associated with tumor multi drug resistance to chemotherapeutics. On the other hand, the efficacy of oxygen-dependent cancer treatments such as chemotherapy, photodynamic therapy (PDT) and radio therapy (RT) has been significantly hindered by tumor hypoxia. Also, resistant tumor cells associated with hypoxia may be emerged after RT and PDT therapy, since the effectiveness of these two methods of cancer therapy is closely dependent on accessible oxygen molecules to produce reactive oxygen species (ROS) to stimulate apoptosis of cancer cells [8, 9]. Accordingly, tumor hypoxia may be exacerbated due to the consumption of oxygen molecules present in tumors with hypoxia during RT or PDT, ultimately leading to lower therapeutic potential or greater tomural cell resistance [10]. Within the framework of these criteria, tumor oxygenation or raising the oxygen levels in hypoxic tumors can be considered as an effective strategy to overcome all the challenges associated with tumor hypoxia and increase the sensitivity of hypoxic tumor cells to the oxygen-dependent cancer treatments [11, 12]. In addition, several attempts have been conducted to date aimed at improving and modifying the tumor hypoxia and its microenvironment, e.g. with the use of inspiratory hyperoxia, which is considered hyperbaric oxygen therapy [13–15]. But despite all its benefits, unfortunately this technique is still far from being perfect because of its intrinsic side effects, e.g. barotrauma and hyperoxic seizures as a result of overproduced ROS in healthy tissues and difficulty of applying this technique in a hypoxic microenvironment due to severe structural malformation of microvessels in tumors [16]. Besides, several

angiogenesis inhibitors have been employed to diminish oxygen consumption and also to temporarily normalize the tumor vessels. However, normalization of vessels may lead to oxygenation of the tumor microenvironment for only a few days, not any more [17]. Over the past few decades, the development and production of novel nanomaterials have rapidly increased, and researchers have also dedicated substantial efforts to convert scientific discoveries associated with all classes of nanomaterials into clinical use [18]. In this regard, a great number of nanocarrier-based platforms have been reached to the clinical trials and some of them have been approved by FDA. These nano-sized materials are also opening up new and eccentric research areas in biomedical applications, including tumor therapy, targeted drug delivery and bioimaging to tackle cancer-related disease [19–21]. It has been well documented that nanomaterials tend to settle in tumor tissues, which is attributed to enhanced permeability and retention (EPR) effect [22]. Moreover, nano-based materials have been recruited as a viable drug carrier to deliver drugs (DNA, proteins, small molecules, etc.) through encapsulation, conjugation, entrapping and surface attachment over the past few decades [20, 21]. Nanocarrier-based platforms possessed excellent properties owing to their unique features such as high drug loading capacity, ease of functionalization, controllable drug release and delivery, different size, shape and flexibility to meet a variety of therapeutic requirements [23–25]. This chapter sheds light on the application of novel nanocarrier-based platforms to overcome tumor hypoxia.

2 Targeting Hypoxia by Nanomedicine

In recent years, great attention has been paid to addressing the dilemma of hypoxia in cancer treatment. Once nanotechnology merges with medicine, which is so-called nanomedicine, copious strategies and intelligent ideas would be emerged as time demands. In this context, we tried to shed new light on approaches specifically targeting tumor hypoxia with the use of nanomedicine. Herein, we classified the emerging strategies into three main types (i) HIF-1 inhibitors, (ii) hypoxia-responsive nanomaterials, e.g. hypoxia-activated linkers/prodrugs, (iii) exploiting hypoxia to facilitate tumor therapy. Each of them is discussed in the following subsection.

2.1 Hypoxia-Inducible Factor-1(HIF-1) as a Potential Therapeutic Target

One of the most common clinical conditions associated with tumor tissue is hypoxia. Such a condition occurs in the tumor microenvironment as a result of inadequate oxygen supply and results in augmented metastatic potential of tumor cells as well as altered their metabolism [26]. Due to the dynamic tumor microenvironment and

low level of oxygen in tumor tissue, cancer cells rapidly adapt their metabolism and growth to this hypoxic condition, which is influenced mainly by hypoxia-inducible factors (HIFs), predominantly HIF-1 [27, 28]. A growing body of evidence indicates that HIF-1 plays direct and vital roles in tumor metastasis, metabolism and proliferation, Fig. 1. HIF-1 mainly encompasses two subunits, there are HIF-1α and HIF-1β. Expression of HIF-1α has been widely identified as the major transcriptional regulator of numerous cellular responses to the low oxygen condition of tumor tissues. Moreover, the undeniable role of HIF-1 in the development of multi-drug resistance (MDR), invasion and migration of tumoral cells, promotion of tumor cell motility, maintenance and development of cancer stem cells, poor prognosis, glucose metabolism and tumor angiogenesis, indicates that tumor hypoxia is an ideal target for cancer therapy [26, 29–31]. Lamentably, bioactive administered to target HIF-1α currently exhibit low chances of reaching therapeutic concentration. Accordingly, combination of HIF-1α inhibitors with other modalities such as smart nanovehicles might result in boosted therapeutic potential, as these two approaches could produce synergistic/additive effects.

Recently, piceatannol, an active natural polyhydroxylated stilbene, has shown great anti-tumor and chemo-preventive properties through inhibition of HIF-1α expression particularly in colorectal cancer cells. In this respect, Aljabali et al. developed a bovine serum albumin (BSA)-based nanovehicle with piceatannol as a bioactive agent to boost the in vitro anti-cancer potential of free piceatannol and confine the colony formation, invasion and migration against HT-29 (human colon cancer cell lines). Accordingly, the BSA-loaded piceatannol was more effective in down-regulating HIF-1 compared to bare piceatannol. In addition, in vivo results

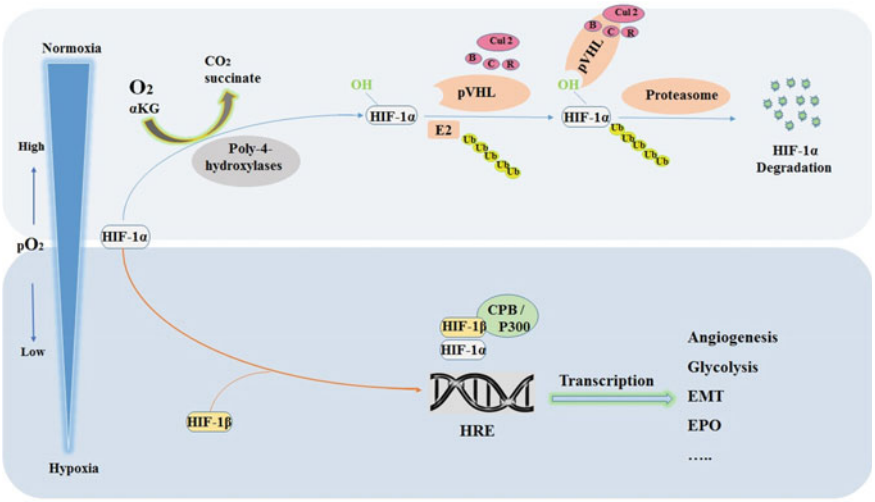

Fig. 1 Oxygen-dependent HIF-1α pathway. CPB: CREB-binding protein; Ub: ubiquitin; Cul2: cullin 2; R: ring-box 1; C: elongin C; B: elongin-B; αKG: α-ketoglutarate; HRE: hypoxia response element; EPO: erythropoietin; EMT: epithelial–mesenchymal transition

in tumor-bearing mice revealed that the produced nanomaterials could potentially reduce tumor size and be used as a safe and effective therapeutic for colon cancer [32]. HIF-1α siRNA has been considered as a potential tool to suppress cancer cell proliferation and growth. Ilhan et al. prepared biogenic silver nanoparticles using *Piper longum* fruit extract and investigated its potential anticancer activity against human prostate cancer cells. In conclusion, the developed nanosystem with an average particle size of less than 100 nm exhibited significant anti-cancer activity in a concentration-dependent manner. Moreover, the biosynthesized nanoparticle could actively restrict the expression of HIF-1α and vascular endothelial growth factor (VEGF) and inhibit cell migration as well [33].

Montigaud et al. fabricated reverse micelle containing acriflavine (ACF), a promising HIF inhibitor, and then prepared micellar suspension was introduced into the lipid nanocapsules. According to their results, the prepared nanoparticles exhibited high encapsulation efficiency of about 80% and presented great cytotoxicity against 4T1 cells by down-regulating HIF expression.

It was found that the in vivo anti-tumor activity of ACF-loaded nanoparticles at a dose of 5 mg/kg ACF was found to be notably higher than that of free ACF, and similar results were observed for ACF-loaded nanoparticles at a lower frequency of administration in comparison with bare ACF [34].

In another study, Izadi et al. developed carboxylated graphene oxide (CGO)-based nanocomposites for dual dinaciclib and HIF-1α siRNA delivery to suppress different cancer cells. It was reported that this nanocomposites-based combinational therapy could considerably suppressed the expression of HIF-1α and Cyclin-Dependent Kinase (CDK), resulting in reduced colony formation, angiogenesis, migration and proliferation in tumor cells [35].

Similar research was conducted by Wan et al. They constructed folic acid- functionalized graphene oxide nanoparticles containing HIF-1α siRNA to precisely deliver their payload to Patu8988 cells. The prepared nanovehicle was able to suppress cells growth, metastasis, invasion, and proliferation by silencing of the HIF-1α gene. Furthermore, glucose transporter-1 expression was also reduced by administration of HIF-1α siRNA-loaded graphene oxide nanoparticles in Patu8988 cancer cells, resulting in tumor cell death and prolonging the survival rate of tumor-bearing mice [36]. Tzeng and colleagues fabricated pterostilbene nanoparticles by nanoprecipitation with the aid of polyvinyl alcohol (PVA) and Eudragit® e100 (EE). This nanovehicle presented superior anti-cancer activity against HepG2 cells compared to free drug. The obtained results indicated that pterostilbene nanoparticles could effectively hamper the proliferation of HepG2 cells by down-regulating antiapoptotic and hypoxia-induced proteins, including BCL-2, CAV-3, CAV-1, and HIF-1α [37].

In the research conducted by Kang et al., a novel nanobody based on VHH212 [a single-domain antibody (nanobody)] was prepared to reduce gemcitabine resistance in the treatment of cancer. In addition, anti-HIF-1α VHH212 nanobody was implemented to suppress angiogenesis. Notably, in vivo results in the xenograft model demonstrated that combination therapy using VHH212 nanobody and gemcitabine

could substantially restrict tumor growth with tumor inhibition of 80.44% compared to free gemcitabine [38].

In order to vanquish hypoxia-induced drug resistance as well as to sensitize tumor cells to the chemotherapy, Xie et al. created stimulus-responsive pegylated dendrimer nanoparticles containing HIF-1α siRNA and DOX. Under hypoxic microenvironment, the azobenzene linkage between PEG and the dendrimer could be cleaved, thereby reducing the particle size, and altering the surface charge into positive zeta potential. The anti-tumor potential of the co-loaded drug/gene was notably enhanced, furthermore, the expression of HIF-1α was effectively suppressed by the incorporated siRNA [39]. Similar research was carried out by Huang and colleagues, who developed a metal–organic framework with azoreductase linker (MOFs) using 4,4′-azobisbenzoic acid and Fe (III). HIF-1α siRNA and DOX were co-loaded within AMOFs. They reported that the introduction of HIF-1α siRNA could significantly inhibit the expressions of P-glycoprotein, multidrug resistance gene 1 and HIF-1α, enhancing the anti-cancer potential of DOX against MCF-7 cells [40]. Chen et al. created chitosan nanoparticles containing 5-fluorouracil and HIF-1α siRNA to overcome multidrug resistance in SGC-7901 cells. In their research, co-treatment based approaches revealed a promising strategy for gene silencing. In addition, the combined treatment could not only restrict the expression of HIF-1α proteins, but also promote apoptosis of SGC-7901 cells [41]. Zhang et al. designed and fabricated nano self-assembled micelles based on two drugs with amphipathic features to suppress the VEGF and HIF-1α proteins. This nanosystem composed of hydrophilic irinotecan (Ir) block and hydrophobic block of HIF-1α inhibitor (YC-1). Accordingly, this nanosystem could also enhance the water solubility of irinotecan drug. Expression of VEGF and HIF-1α proteins was significantly down-regulated by the fabricated nanomicelle, and antitumor activity was increased 5.7-fold in comparison with free Ir in A549 cells [42].

Cancer therapy with co-treatment modalities such as photodynamic therapy and HIF-1α inhibitors can be considered as an effective treatment option. It has been fully clarified that photodynamic therapy entails oxygen molecules for consumption to induce cellular damages, which may exacerbate the tumor hypoxia. As a result, the HIF-1α is upregulated and provokes resistance to the photodynamic therapy [43, 44]. Accordingly, suppression of HIF-1α could potentially improve photodynamic therapy efficacy. To make this clear, Sun and colleagues designed and fabricated multifunctional nanovehicles based on cationic porphyrin-grafted lipid microbubble containing HIF-1α siRNA. These unique drug/gene carriers could be self-assembled into microbubbles and converted into nanoparticles at tumor sites using ultrasound. The results revealed that porphyrin were preferentially accumulated within tumor tissues and the expression of HIF-1α was actively inhibited, which augmented photodynamic therapy efficacy [45]. In another research study, Chen et al. employed lipid–calcium–phosphate nanoparticles loaded HIF-1α siRNA for the treatment of head

and neck tumors. In addition, intravenous administration of fabricated nanovehicles containing HIF-1α siRNA into the tumor-bearing mice was found to significantly suppress HIF-1α expression. Remarkably, the use of the prepared nanosystem in combination with photodynamic therapy exhibited superior tumor inhibition compared to either photodynamic therapy or HIF-1α siRNA alone [46]. Some similar studies have confirmed that the combination of photodynamic therapy with HIF-1α inhibitors exerts a synergistic effect in suppressing tumor growth [47, 48]. A summary of hypoxia-inducible factor-1 (HIF-1) targeting with selected nanoparticles is given in Table 1.

2.2 Hypoxia-Activated Linkers/Prodrugs

Conventional drug delivery systems based on physical entrapment of chemotherapeutics suffer from drug leakage, toxicity, unwanted side effects, broad biodistribution, low efficacy, poor bioavailability, low stability, drug resistance and, etc. The use of prodrugs in treatment of cancer is potentially superior to conventional therapy due to the aforementioned drawbacks. In addition, prodrugs can potentially lead to accumulation of drugs at tumor sites, resulting in decreased drug index and more targeted treatment [52].

Various parameters have been exploited in drug delivery formulation, such as enzyme utilization, temperature, pH and redox potential, to liberate drugs at the intended site of action via stimuli-cleavable linkage [20, 21, 23].

The hypoxic tumor microenvironment has proven to be reductive, so bioreductive-based prodrugs can be considered a cornerstone in cancer therapy. Typically, two forms of prodrugs have been exploited to diminish tumor hypoxia problems: (i) hypoxia-responsive linkers (HRLs) and (ii) hypoxia-responsive prodrugs (HRPs) [53]. Prodrugs are not toxic under normoxia condition, whereas they become toxic through redox reactions in hypoxic tumor microenvironment [54]. Moreover, glutathione (GSH) as a reducing agent in the hypoxic tumor microenvironment was found to be in high concentration compared to that of present in normoxic cells. Therefore, redox-responsive linkage, such as disulfide bonds, has often been considered in the design and fabrication of nanovehicles for drug delivery to the hypoxic microenvironment. In other words, both redox-responsive nanosystems and hypoxia-activated prodrugs (HAPs) are potential tools for smart drug delivery to the hypoxic microenvironment, with effective outcomes (Fig. 2) [55, 56].

Besides, there are several other types of hypoxia-activated prodrugs based on their skeletal structure such as transition metal complexes, N-oxide analogs, nitro-groups and quinones (Fig. 3) [57]. Altogether, the implementation of HRLs/HRPs in conjunction with nanomedicine can be harnessed for boosting the efficacy of cancer therapy by effectively delivering various chemotherapeutics to hypoxic tumor tissue. Herein, we summarized some recent advances in hypoxia-activated prodrugs and redox-responsive nanocarriers and discuss their potential application in cancer treatment.

Table 1 Hypoxia-inducible factor-1(HIF-1) targeting with selected nanoparticles

Selected nanoparticles	Encapsulated Drugs/genes	Cancer/cell line	Brief outcomes	References
Metal nanoparticles	*Biogenic silver*	PC-3 (ATCC, CRL-1435) and DU-145 (ATCC, HTB81)	Inhibited cell migration Suppression of VEGF and HIF-1α expression	[33]
Liposomes	Zinc phthalocyanine and acriflavine	SK-ChA-1	Induced apoptosis Downregulated VEGF and HIF-1α Reduced tumor volume	[47]
Lipid microbubble nanoparticles	Porphyrin and HIF-1α siRNA	HUVECs	Suppression of VEGF and HIF-1α expression	[45]
Graphene oxide nanocomposites	Dinaciclib and HIF-1α siRNA	TM3, 4 T1, B16-F10 and CT26	Suppression of HIF-1α and Cyclin-Dependent Kinase (CDK) expression	[35]
Lipid–calcium–phosphate (LCP) nanoparticles	Photosan and HIF-1α siRNA	SCC4	Reduced tumor volume Suppression of HIF-1α expression	[46]
ZnPc@Cur-S-OA nanoparticles	Curcumin	B16F10	Downregulated HIF-1α and depleted GSH	[48]
Chitosan nanoparticles	5-fluorouracil and HIF-1α siRNA	SGC-7901	Reduced drug resistance, Induced apoptosis Downregulated VEGF and HIF-1α	[41]
MnO_2 nanoparticles	Acriflavine	CT26	Suppression of the expression of MMP-9, VEGF and HIF-1α	[49]
Micelle	Irinotecan and HIF-1α inhibitor (YC-1)	A549	Suppression of the expression of VEGF and HIF-1α Reduced tumor volume	[42]

(continued)

Table 1 (continued)

Selected nanoparticles	Encapsulated Drugs/genes	Cancer/cell line	Brief outcomes	References
MOFs	DOX and HIF-1α siRNA	MCF-7	Reduced tumor volume Suppression of the expression of HIF-1α	[40]
Nanobody	VHH212 nanobody	MIA PaCa-2, BxPC-3, and PANC-1	Suppression of the expression of VEGF and HIF-1α Reduced tumor volume	[38]
CdTe quantum dots	DOX and HIF-1α siRNA	HepG2, U87MG, SGC-7901 and MCF-7	Reduced tumor volume, Reduced GLUT-1 receptor, Suppression of the expression of VEGF and HIF-1α	[50]
Pterostilbene nanoparticles	Pterostilbene	HepG2	Down-regulation of antiapoptotic and hypoxia-induced proteins, including BCL-2, CAV-3, CAV-1, and HIF-1α	[37]
PAMAM dendrimer	DOX and H IF-1α siRNA	MCF-7	Increased ROS Suppression of the expression of HIF-1α Reduced tumor volume	[39]
Graphene oxide nanoparticles	HIF-1α siRNA	Patu8988	Reduced tumor volume Suppression of the expression of 18F-fluorodeoxyglucose Glut-1 and HIF-1α	[36]
BSA nanoparticles	Piceatannol	HT-29 and CaCo-2	Reduced tumor volume, Downregulated HIF-1α and p65	[32]
Chitosan nanoparticles	HIF-1α siRNA	OVK18#2	Suppression of the expression of VEGF and HIF-1α	[51]

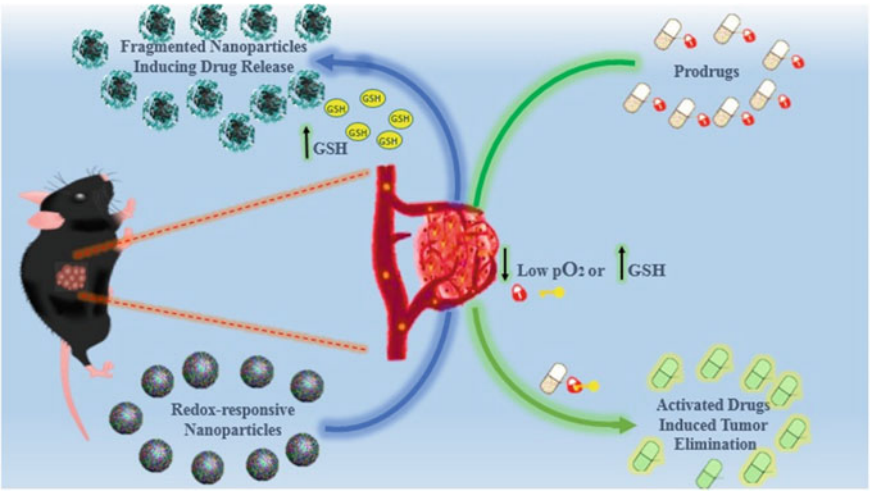

Fig. 2 Schematic representation of redox-responsive nanoparticles and hypoxia-activated prodrugs

Recently, Guo et al. fabricated redox-responsive nanosized prodrugs based on Au nanorods for the smart delivery of Pt as an effective cancer treatment modality. The results showed that fabricated Pt-based prodrugs displayed the advantages of minimized sever side effect, triggered drug release, and high drug encapsulation efficiency. Immunohistochemistry and live animal imaging results revealed that expression of VEGF and HIF-1α was upregulated under mild hyperthermia, resulting in induction of angiogenesis. The prepared nanosized prodrugs with accelerating angiogenic vessel and increasing blood flow exhibited a positive impact on accumulation of prodrugs in the tumor tissue. The higher accumulation of prodrugs in cancer cells resulted in boosting the efficacy of cancer therapy. Additionally, this stimuli-responsive prodrug disclosed an outstanding regression and inhibition of tumor growth, indicating the fact that tumor accumulation as well as long blood circulation time were the crucial factors for cancer treatment. In some mice, tumors were completely eradicated under short-term NIR irradiation due to the synergistic effect [58]. In addition, the same research group developed nanogel poly-drugs based on Pt(IV) loaded with hypoxia-activated and bioreductive prodrug tirapazamine for hypoxia-activated synergistic chemotherapy (Fig. 4). As a result of activation of Pt and TPZ under hypoxia and redox microenvironment, extremely cytotoxic radicals were generated, potentiating the efficacy of chemotherapy. Moreover, this unique nanosized prodrug represented the advantages of prolonged blood circulation, superior tumor accumulation, and redox-responsive drug release [59]. In another study, Zhao et al. created self-assembled polymeric micelles containing PR104A as a hypoxia-activated prodrug for synergistic photodynamic cancer therapy. These polymeric nanoparticles had zeta potential of around −30 mV and average particle size ranging from 90 to 100 nm in diameter. It was found that this nanosystem exhibited stimuli trigger drug release pattern which minimized drug side effects and was

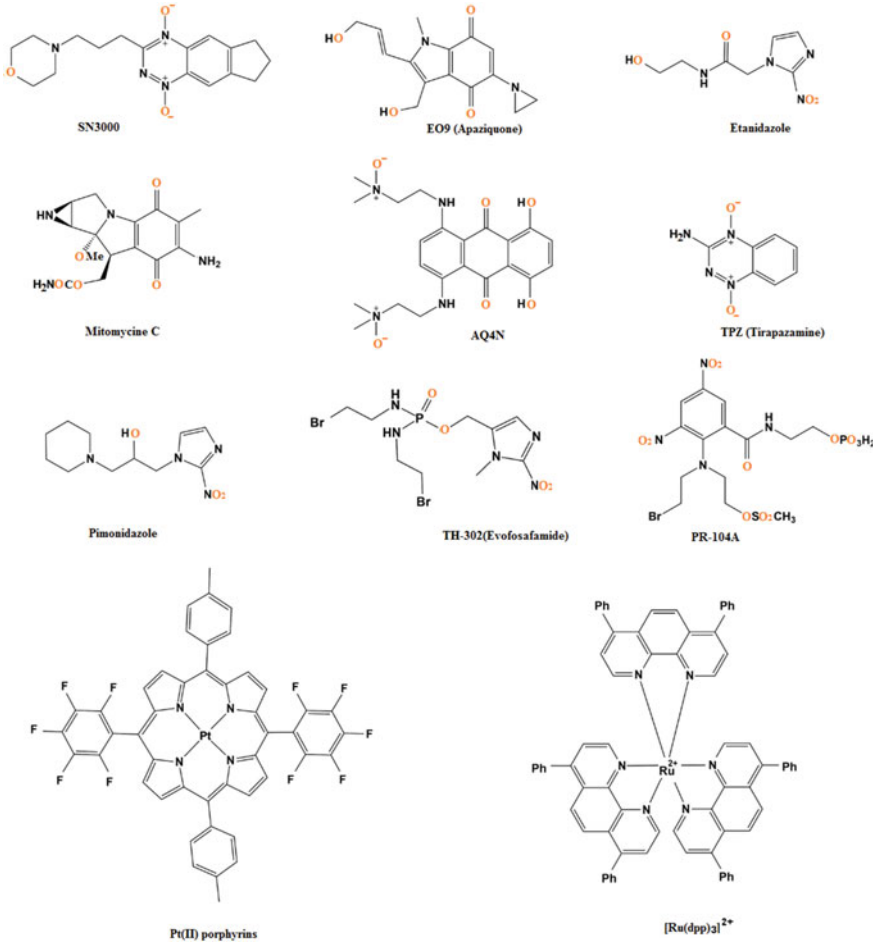

Fig. 3 Structures of typical HAPs including transition metal complexes, aliphatic N-oxides, aromatic N-oxides, quinones and nitroimidazoles/nitroaromatics

favored in cancer therapy. In addition, this was confirmed by an in vivo pharmacokinetic study where the majority of prodrugs (>90%) were intact in the bloodstream, resulting in a reduction of adverse effects on normal tissues. Fluorescence quantitative analysis revealed that the developed prodrugs were not broadly distributed in the major organs of the mice after 36 h of prodrug administration. Pegylation and EPR effects caused the prodrug nanoparticles to be more localized in tumor sites rather than other organs, primarily the spleen and liver. In vivo results demonstrated that this nano-prodrugs could potentially inhibit tumor growth as well [60].

Unfortunately, to date, hypoxia-activated prodrugs have failed to reach clinics, regardless of all promising results achieved in vitro. This is largely because of insufficient accumulation of HAPs within tumor sites as the tumor hypoxia is not adjacent

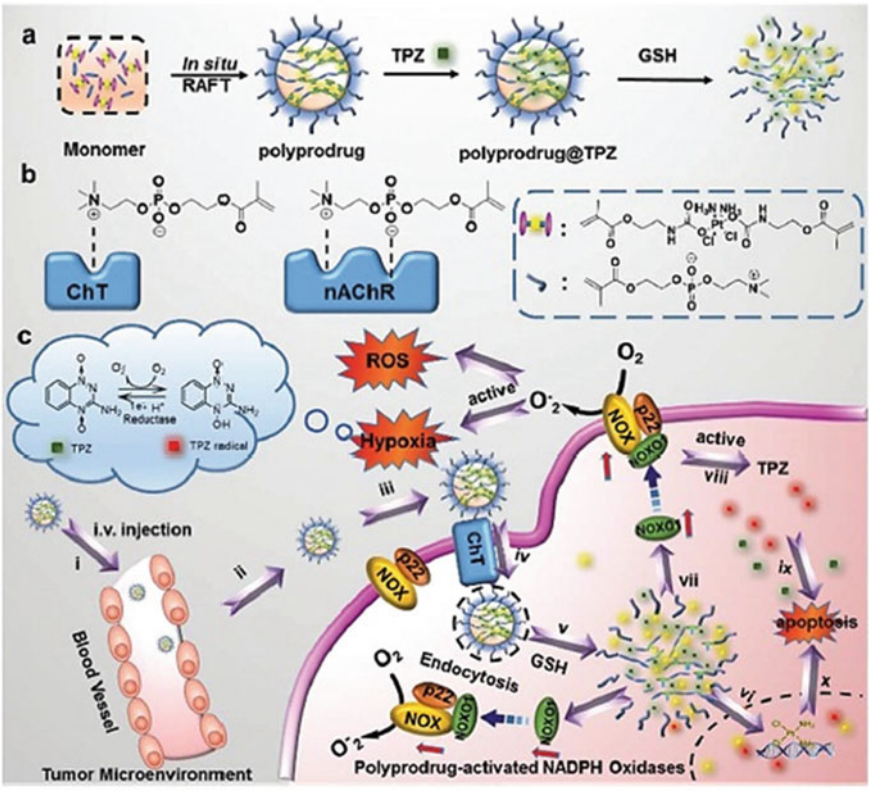

Fig. 4 Schematic representation of the fabricated prodrugs based-nanogel for Hypoxia-Activated Synergistic Chemotherapy **a** fabrication and stimuli trigger drug release. **b** Diagram of the interactions of 2-methacryloyloxyethyl phosphoryl-choline (MPC) with nicotinic acetylcholine receptor (nAChR) and choline transporter (ChT). **c** Activation of the embedded prodrug TPZ after internalization into cancer cells for enhanced synergistic anticancer efficacy. Reproduced with permission from Ref. [59]. Copyright 2020, with permission from RSC

to blood vessels. In this regard, Evans et al. developed a drug delivery system based on macrophage nanoparticles to augment the accumulation and penetration of HAPs to the tumors site. This drug carrier took advantage of phagocytic and chemotactic capacities of macrophages to boost hypoxia-activated prodrug efficiency of tirapazamine loaded nanoparticles. Some in vitro assessments were employed to elucidate the potential of the developed drug vehicles by maximizing therapeutic efficacy while minimizing carrier cell toxicity. This system was found to improve and facilitate drug accumulation within the hypoxic microenvironment of tumors and caused more DNA double-strand breaks in the hypoxic regions of tumors. These results were also observed and repeated by in vivo experiments, which demonstrated that the created drug vehicle increased accumulation of tirapazamine in hypoxic areas of 4T1 breast tumors and suppressed the tumor growth. Overall, Evans et al. claimed

that macrophage-based delivery systems could considerably enhance the efficacy and transport of HAPs through high drug concentration at the tumor site, pointing to a potential strategy to harness these nanoparticles to diminish the hypoxia-activated prodrug problems [61].

In another study, Yang and colleagues prepared a novel combinational treatment modality using vascular disrupting agent (VDA) combretastatin A4 (CA4) nanoparticles and bioreductive tirapazamine for killing hypoxic cells. Hypoxia probe immunofluorescence staining and PA imaging revealed that the produced CA4 nanoparticles were able to selectively eradicate blood vessels as well as induced intense hypoxia within tumors. Accordingly, this profound hypoxia level could activate prodrugs, enhancing the therapeutic and antimetastatic effects of tirapazamine in metastatic 4T1 breast tumors. Combination therapy based on CA4 nanoparticles and tirapazamine demonstrated superior antitumor efficacy on each modality where complete ablation of the tumor was observed for mice with moderate tumor volume ($\approx$180 mm^3). In addition, this system also showed remarkable antimetastatic effects and significantly shrunk large tumors ($\approx$500 mm^3) [62]. Dai et al. designed and synthesized multifunctional liposomes containing hypoxia-activated prodrugs tirapazamine and indocyanine green for imaging and cancer therapy (Fig. 5). This theranostic liposome was modified with cRGD and gadolinium. It was found that the fabricated system could potentially reach the tumor site by cRGD-mediated active targeting ability and EPR effects. Additionally, PDT exacerbated the hypoxia condition, which altered tirapazamine to its active form and kill the tumor hypoxia cells. Overall, Dai et al. showed that this system can be used for multiple purposes, such as imaging, tumor hypoxia therapy, and intelligent nanotheranostics owing to its optimized therapeutic efficiency [63]. A summary of the hypoxia-activated linkers/prodrugs and selected nanoparticles is given in Table 2.

2.3 Taking Advantage of Hypoxia to Modulate Tumor Therapy

Although the hypoxic tumor microenvironment is responsible for failure of most oxygen-dependence therapies, the intrinsic features of tumor microenvironment can also assist tumor treatment through different strategies. Due to the low oxygen content within the tumor, the use environmentally sensitive drugs or other bioactive agents with low oxygen content may facilitate tumor therapy. Moreover, there are certain components that are overexpressed in hypoxic condition, thus chemotherapeutics sensitive to these agents have great potential to modulate tumor therapy. Some of these strategies enable the nano-based drug delivery system to specifically target the hypoxic tumor microenvironment, whereas the others induce cell death /injury [71–73]. Therefore, herein we divided the strategies of hypoxia that assist to treatment into two classes: (i) controlled release of the cargo under a tumor hypoxia condition; (ii)

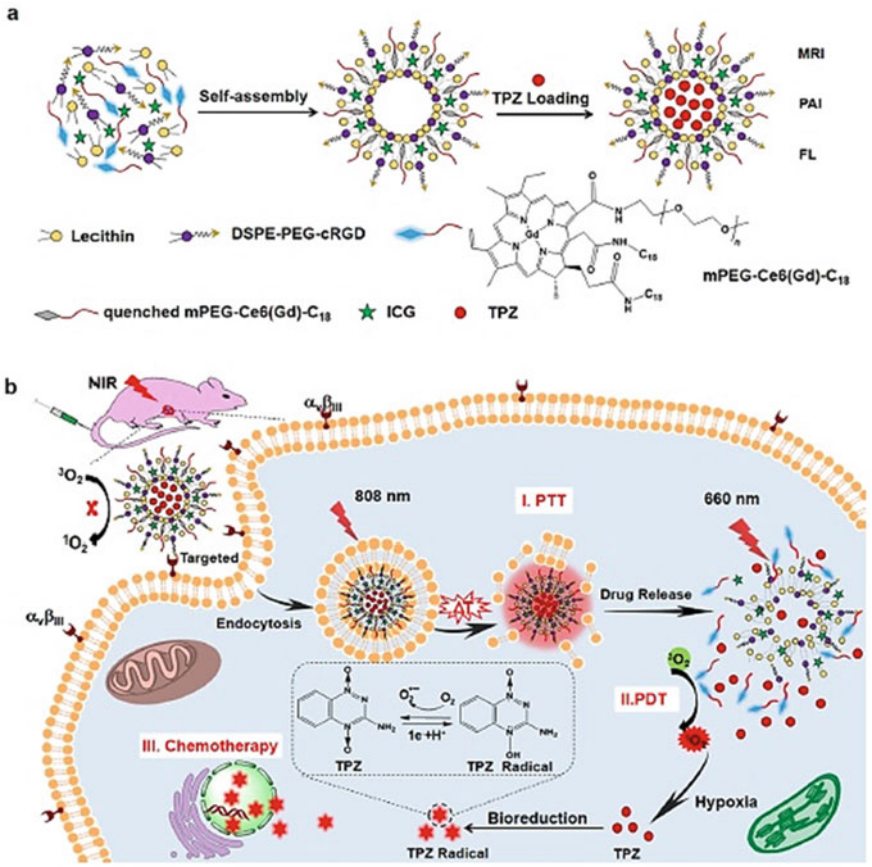

Fig. 5 Schematic illustration of developed multifunctional Nano liposomes for hypoxia activated prodrugs and therasontics **a** Synthesis of liposomes loaded tirapazamine and indocyanine green; **b** activation of prodrugs by PDT induced hypoxia. Reproduced with permission from Ref. [63]. Copyright 2019, with permission from ACS

inducing cell toxicity for synergistic therapy via taking advantages of tumor hypoxia (Table 3).

One of the promising approaches in cancer therapy is to harness the power of bacteria, specifically anaerobic bacteria or facultative anaerobic bacteria, in favor of tumor hypoxia treatment. Luo and colleagues used two strains of anaerobic bacterial to enhance drug accumulation within tumor sites. In this context, B. *breve* UCC2003 was used as a targeting agent to guide nanoparticles directly into the hypoxic tumor tissues, while another bacterium (C. *difficile* CCUG 37,780) was applied to increase the efficacy of tumor therapy and indirectly target tumor tissue. These strategies were recruited to provide the treatment of hypoxia with excellent outcomes as well as imaging capability [81]. Similarly, Chen and colleagues

Table 2 Hypoxia-activated linkers/prodrugs and selected nanoparticles

Selected nanoparticles/prodrugs	Conjugated drugs	Size(nm)	Cancer/cell line	Brief outcomes	References
Gold nanorod	Cisplatin	~200	A549	Inhibited tumor growth High level of drug accumulation within tumor cell	[58]
Nanogel	Cisplatin-Tirapazamine	98–123	A549	Inhibited tumor growth High level of drug accumulation within tumor cell Increased blood half-life	[59]
Self-assembeled nanoparticles	PR104A	~100	4T1	Great cell cytotoxicity High blood circulation, higher tumor accumulation Suppressed tumor growth	[60]
PLGA nanoparticles	Tirapazamine	~ 250	4 T1	Higher tumor accumulation Suppressed tumor growth Safe and potent	[61]
Phthalocyanine/albumin Supramolecular complexes	AQ4N	–	In vivo breast cancer model	Completely eradicated tumor Activated $CD8^+$ T cells Destroyed tumor resistance	[64]
Core/Shell-Structured Mesoporous Silica	AQ4N	100–600	4T1	Destroyed tumor Microcirculation Eradicated tumors without recurrence	[65]
Nanoparticles based on ITTC	Tirapazamine	120–125	–	High synergistic tumor ablation Great passive targeting ability to the tumor tissue	[66]
Micelle	Tirapazamine	50–100	4T1	Suppressed tumor growth Great cell cytotoxicity	[67]

(continued)

Table 2 (continued)

Selected nanoparticles/prodrugs	Conjugated drugs	Size(nm)	Cancer/cell line	Brief outcomes	References
Liposomes	AQ4N	>100	Breast cancer 4T1	Suppressed tumor growth Excellent cell cytotoxicity	[68]
Micelle	Tirapazamine	~ 58	4T1	Completely suppressed tumor volume Great synergistic effect	[62]
Nanogel	Tirapazamine	–	–	Self-fluorescence for cell imaging Improved cytotoxicity	[69]
Micelle	Tirapazamine	~ 100	A549	Minimized side effects Great in vivo/vitro efficacy	[63]
Hybrid polymeric-MOF nanoparticles	AQ4N	95	U87MG	Synergistic effect Excellent cellular uptake Great in vivo/vitro results	[70]

Table 3 Strategies of hypoxia facilitate tumor therapy

Assistance	Nano-systems	Approaches	References
Hypoxic condition of tumor tissue	HCHOA	Azobenzene linkage dissociation under hypoxic condition	[74]
	CAGE	Fabrication of hypoxia-sensitive linker to control the release of payloads	[75]
	Hybrid PEG-FTn	Development of ferritin-based nanosystem to be sensitive to hypoxic condition	[76]
	Polymeric nanoparticles with semiconducting properties	Control release of chemodrug induced by the hypoxic microenvironment	[77]
	CA IX-C4.16	Enabling nanoparticles to target the hypoxic tumor by overexpression of CA IX within tumor microenvironment	[78]
	WOACC	CCL-28 chemokine overexpression as well as targeting tumor tissue with propitious targeting agents	[79]
	DOX/CP-NI	Targeting tumor via polymeric nanoparticles containing DOX and 2-nitroimidazole as hypoxia-sensitive agents	[80]
	Bacteria-UCNRs	Targeting hypoxic tumor microenvironment using facultative anaerobic bacterial	[81]
	pDA-VNP	Targeting hypoxic tumor microenvironment using VNP20009 strains as an anaerobic bacteria	[82]
Synergistic effects	Hs-IMQ + CA4	Activation of IMQ by overexpression of nitroreductase within hypoxia tumor, resulting in potentiate immunological responses	[83]
	Polyoxometalate cluster based on Mo	Photothermal effect of polyoxometalate improved by hypoxia condition	[84]

(continued)

Table 3 (continued)

Assistance	Nano-systems	Approaches	References
	Mg_2Si	Application as a deoxygenating agent for tumor-starving therapy	[85]
	HMBRN-GOx/TPZ	Cytotoxicity of prodrug activated by hypoxia condition	[86]
	BCETPZ@(GOx + CAT)	Activation of cytotoxicity of prodrug by hypoxia condition	[87]
	liposome-AQ4N	Hypoxia induce cytotoxicity of prodrug	[88]
	AQ4N-hCe6-liposome	Hypoxia induce cytotoxicity of prodrug	[89]
	PM-coated MTD@P	Cytotoxicity of TPZ induced by hypoxia condition	[90]
	PPPPB-CO-TPZ	Cytotoxicity of TPZ caused by hypoxia condition	[91]
	CD133/TAT/TPZ-Fe_3O_4@ $mSiO_2$	Induction of TPZ cytotoxicity using hypoxia condition	[92]
	iNP/IT	Induction of TPZ cytotoxicity using hypoxia condition	[93]
	TPZ-UC/PS	Induction of TPZ cytotoxicity using hypoxia condition	[94]

developed dopamine nanoparticles decorated with a facultative anaerobic bacterium (VNP20009). The results showed that the fabricated nanosystem could potentially improve the photothermal therapy owing to its targeting features [82]. Regardless of all these benefits associated with anaerobic bacteria, potential side effects and toxicity have hindered their application, consequently, hypoxia-sensitive nanosystems possess superiorities in terms of safety. It has been reported that carbonic anhydrase IX (CA IX) is overexpressed within hypoxic tumor tissue. Accordingly, Alsaab et al. combined this targeting agent along with other modalities such as apoptosis inducer (CFM 4.16) and monoclonal antibody (Sorafenib) to diminish drug resistance in renal cancer, and the results revealed a potent effect [78]. Some linkages and bonds are prone to dissociate under specific condition, thereby enabling drug loaded nanoparticles to liberate its cargo at their intended site of action, ultimately minimizing drug side effects and toxicity while boosting treatment efficacy. Yang et al. developed hypoxia sensitive nanosystem based on albumin (HCHOA) to potentiate tumor therapy and drug accumulation within the tumor site. They used

hypoxia-sensitive linkage based on azobenzene groups to bind both the oxaliplatin prodrug and photosensitizer Ce6 (Fig. 6a). Once the prepared nanosytems reached the hypoxic microenvironment, the azobenzene bond dissociated, and consequently, the fabricated HCHOA (100–150 nm) decreased in size and shrunk to a smaller size (10 nm). Tumor penetration and diffusion were enhanced by decreasing in size. They also developed an indissociable nanosystem (HCHOH) as a contrast agent for imaging as well. HCHOA was found to represent large tumor accumulation and therapeutics efficacy (Fig. 6 c–d) [74].

It has been well documented that the potential toxicity of various drugs is highly dependent on the hypoxia condition, making them excellent candidates to specifically addressing tumor cells while ensuring the safety of healthy tissues. TPZ is a kind prodrug that can be activated via several reductase agents inside cells to generate cytotoxic radical species. However, these radicals can readily return to their

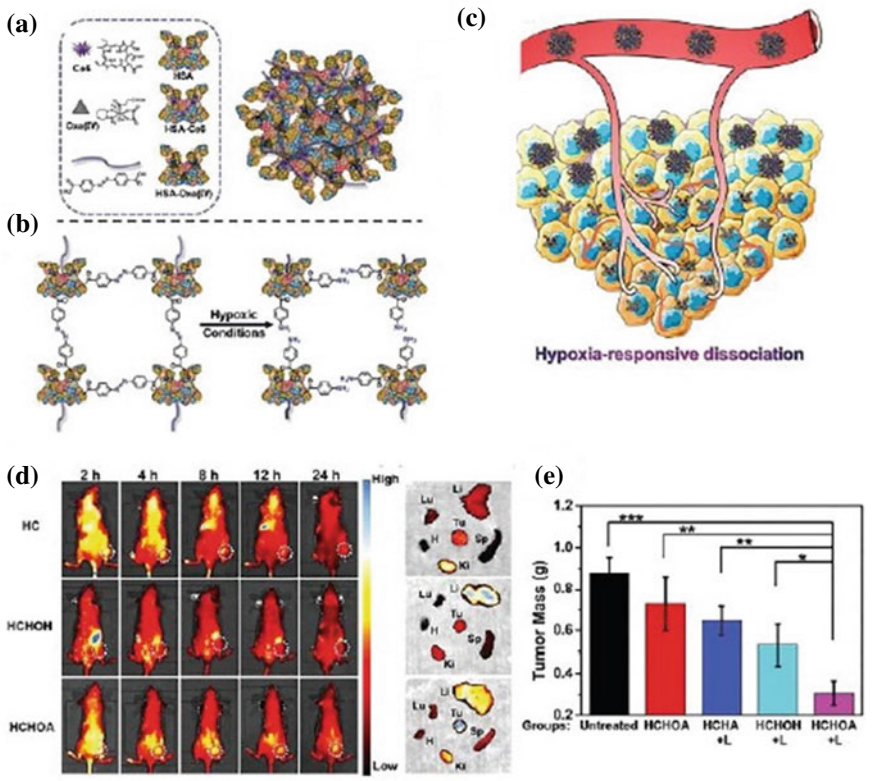

Fig. 6 Hypoxia responsive nano-systems for cancer therapy. **a** Components for fabrication of HCHOA. **b** Dissociation mechanism of HCHOA under hypoxia condition. **c** Deep tumor penetration of HCHOA after dissociation by tumor hypoxia. **d** Fluorescence images of different fabricated nano-systems in mouse models. **e** Tumor masses after treatment with different groups. Reproduced with permission from Ref. [74]. Copyright 2019, with permission from Wiley

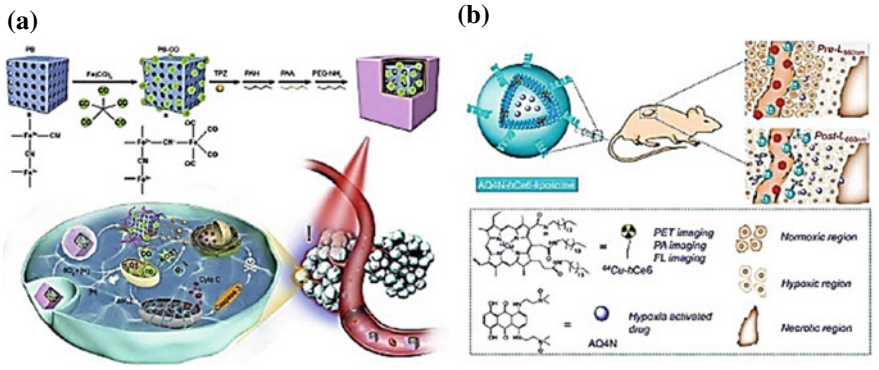

Fig. 7 Treatment of cancer using photodynamic therapy by employing AQ4N-64Cu-hCe6-liposome and PPPPB-CO-TPZ nanoparticles. **a** Fabrication of PPPPB-CO-TPZ NP as well as mechanism of activation. Reproduced with permission from Ref. [91]. Copyright 2019, with permission from Elsevier. **b** Activation mechanism related to AQ4N-64Cu-hCe6-liposome and its components. Reproduced with permission from Ref. [89]. Copyright 2017, with permission from ACS

origin molecules in the normal oxygen condition. Moreover, these cytotoxic radical species can damage macromolecules found in hypoxic tumors by removing their hydrogen atoms. Li and colleagues created polymer-conjugated TPZ nanoparticles (PPPPB-CO-TPZ NPs) compassing different components, such as pentacarbonyl iron to generate carbon monoxide (CO), PB nanoparticles as photothermal therapy reagent, and TPZ to kill cells. By introducing the fabricated nanoparticles, the PB nanoparticles induced local hyperthermia by NIR radiation (808 nm) and promoted pentacarbonyl iron to produce carbon monoxide for hypoxia augmentation and mitochondria exhaustion, which ultimately activated TPZ to induce cytotoxicity (Fig. 7a) [91]. In addition, another prodrug (AQ4N) is also known to induce cytotoxicity through the hypoxia condition. In this regard, Feng and colleagues fabricated liposomal nano-formulation termed AQ4N-^{64}Cu-*h*Ce6 containing AQ4N prodrug, ^{64}Cu as contrast agent and Ce6 as photosensitizer to efficiently eradicate hypoxic tumors (Fig. 7b) [89].

It can be concluded that the hypoxic microenvironment may also assist tumor therapy through hypoxia-activated toxicity or the controlled-release of drugs. In general, some challenges and issues such as complete protection of normal tissue from these anaerobia and cytotoxic drugs have not been fully elucidated and it is strongly recommended to consider these difficulties in the design and fabrication of such nanosystems.

3 Tumor Oxygenation by Nanomedicine

Over the decades, several strategies have been conducted to treat cancer disease, including immunotherapy [95, 96], photodynamic therapy [97], radiotherapy [98,

99], and chemotherapy [100], either alone or in combination with other modalities. However, all these strategies to treat tumors need oxygen. Tumor hypoxia has impeded the efficacy of the aforementioned strategies in cancer therapy. To address these challenges, various approaches have been undertaken to modulate the oxygen level in the hypoxic microenvironment [101]. In this context, oxygen-generating nanomaterials and oxygen-loaded nanomaterials have been utilized as promising strategies to improve the therapeutic effects of such oxygen-dependent treatments by supplying oxygen at the hypoxic tumor sites. Moreover, oxygen content can be temporarily enhanced by inhibiting respiration to economize oxygen in tumor cells [102]. Applications of oxygen-loaded and oxygen-generating nanosystems are discussed separately below.

3.1 Oxygen-Loaded Nanocarriers

The use of oxygen-loaded nanocarriers has shown great potential in relieving tumor hypoxia and mitigating challenges associated with hypoxic tumors [103]. Although this approach cannot deliver and supply oxygen to all tumor sites, it provides adequate amount of oxygen for radiotherapy and photodynamic therapy. Promising examples of nanomaterials for oxygen delivery to the hypoxic microenvironment are summarized Table 4.

Core–shell nanobubbles, as oxygen loaded nanovehicles, are comprised of a gas core and a stabilized mono layer shell [115, 116]. It has been reported that this oxygen-loaded nanovehicle could potentially carry oxygen molecules to the hypoxic microenvironments such as tumors, thereby increasing the efficacy of tumor therapy [117, 118]. The shell layer of such oxygen-loaded nanovehicles is commonly prepared with gas vesicles, dextran, polymer and lipid, while the core is made of oxygen [119, 120]. In addition, chemotherapeutic agents can be loaded within the oxygen-loaded nanovehicles either in the shell or the core depending on the intrinsic features of drugs (hydrophobicity or hydrophilicity).

Oxygen-loaded nanovehicles have been employed to improve the therapeutic effects of chemotherapy and radiotherapy by suppressing HIF-1α expression [121]. Furthermore, stimuli-responsive oxygen release in hypoxic tumor sites may limit the unpleasant side effects associated with premature oxygen release. In this regard, Song and colleagues developed pH-responsive oxygen-loaded nanovehicles enclosed by an acetylated dextran shell, thus enabling burst release of oxygen to alleviate hypoxia within weakly acidic tumor tissue [118]. However, with all the progress in this era, some problems such as storage and stability of oxygen-loaded nanovehicles to prevent premature oxygen release remain an unresolved concern [122]. As one of the main components of blood, erythrocytes play a vital role in the modulation of oxygen inside the living organisms such as mammals. Erythrocytes or red blood cells (RBCs) can assist cell breathing due to the ability of their hemoglobin (Hb) to bind or release of oxygen as the oxygen partial pressure changes. Hb facilitates the efficient binding of oxygen under high oxygen pressure, while modulating the rapid release

Table 4 Promising nanomaterial for delivery of oxygen to the hypoxic microenvironment

Vehicles	Nanoparticles	Approaches	References
Hemoglobin	LIH	Utilizing hemoglobin to carry oxygen	[104]
	BP@RB-Hb 92	Utilizing hemoglobin to supply oxygen	[105]
	ICG-loaded artificial red cells (I-ARCs)	Utilizing hemoglobin to Elevate oxygen concentration in tumor	[106]
Fluorocarbon	IR780@O_2-FHMON	Using perfluorocarbon to supply oxygen	[107]
Perfluoropentane	O_2 − PFP@HMCP	Using perfluoropentane to deliver oxygen	[108]
CuTz-1	CuTz-1-O_2@F127	Implementation of CuTz-1-O2@F127 to carry oxygen	[109]
	TaOx@PFC-PEG	Promotion of oxygen concentration in tumor by using perfluorocarbon	[110]
	PFC	Applying perfluorocarbon to supply oxygen	[111]
Perfluorocarbon	PFC@PLGA-RBCM	Utilizing perfluorocarbon to elevate oxygen concentration in tumor	[112]
	Oxy-PDT agent	Utilizing perfluorocarbon to promote oxygen level in tumor	[113]
	PEG-Bi_2Se_3@PFC@O_2	Utilizing perfluorocarbon to supply oxygen	[114]

of oxygen under hypoxia condition. To put it briefly, the tumor hypoxia microenvironment induces Hbs or RBCs to dismiss their oxygen to assist therapy [123]. Consequently, RBCs have been extensively exploited as safe biological vehicles for the delivery of drugs as well as oxygen shuttles for cancer therapy owing to their long circulation time and unique biocompatibility [124–126]. Tang and colleagues developed a ferritin-based nanocapcule conjugated with ZnF16Pc as photosensitizer on the surface of RBCs for co-delivery of photosensitizers and oxygen to enhance photodynamic therapy [127]. This was achieved by the sustained release of oxygen adjacent to photosensitizers by RBCs, even under low level of oxygen concentration. However, despite all the benefits, the size of large RBCs (micrometer) may limit their ability to diffuse deep into hypoxic tumor tissue. On the contrary, as the main compartment of erythrocytes, Hb has an ideal size for oxygen supply and delivery. However, the clinical translation and in vivo use of Hb is far from perfect due to its undesirable biocompatibility features such as poor stability, potential side effect, and short half-life. Hb-based oxygen vehicles enclosed with biodegradable nanomaterials

or chemical modifications can overcome the disadvantages associated with cell-free Hb [105, 128–130]. Compared to micron-sized RBCs, Hb-based nano sized vehicles can profoundly diffuse into the hypoxic tumor microenvironment, thereby providing more oxygen supply [106, 131, 132]. Among bio-inspired nano sized vehicles, RBC-based oxygen/drug carriers have gained substantial attention, accordingly, Liu and colleagues fabricated a universal oxygen-self-supply system based on aggressive man-made erythrocytes called AmmRBCs to diminish photodynamic tumor resistance caused by the hypoxia microenvironment. Such biomimetic aggressive pseudo-RBCs systems were constructed by entrapping polydopamine (PDA), polydopamine-adsorbed photosensitizer, and methylene blue (MB) in biovesicle engineered from recombined RBC membranes. This novel platform represented excellent biocompatibility owing to the identical outer layer to erythrocytes. Hb is susceptible to oxide when it encounters to blood stream, so there are some antioxidant agents within biological RBCs, such as superoxide dismutase (SOD), catalase (CAT), and glutathione (GSH). Thus, in this case, PDA was also applied as an enzyme-mimicking agent capable of simulating the functions of SOD and CAT to protect Hb from the oxidation damage during the circulation. Overall, this bioengineered platform was proposed as a potential self-oxygenating system to diminish limitations of oxygen-dependent therapy modalities such as radiotherapy, chemotherapy, and photodynamic therapy, because PDA can embed a variety of desired active agents [133]. Recently, as an artificial blood product, perfluorocarbon (PFC), which possesses great oxygen and carbon dioxide solubility along with good hemocompatibility, has been widely utilized as oxygen vehicles to moderate tumor hypoxia as well as contrast agents [134–136]. Cheng and colleagues synthesized an oxygen-self-supplied nanoplatform (Oxy-PDT) based on PFCs nanodroplets loaded with IR780 (a near-infrared photosensitizer) for photodynamic therapy. This nanoplatform exhibited longer singlet oxygen lifetime and great oxygen capacity, so the photodynamic efficacy of fabricated PFC nanodroplets loaded with IR780 increased significantly [113]. In another study, Gao et al. fabricated artificial RBCs based on PFC nanoparticles enclosed by erythrocyte membrane to potentially carry oxygen and improve radiation response [112]. Although PFC exhibits high oxygen solubility, oxygen release is controlled by the diffusion process caused by the oxygen level gradient, which results in a low delivery efficacy. To solve this weakness point, several approaches have been implemented, such as the use of ultrasound (US) or near-infrared (NIR) light, which could promote the oxygen release and facilitate tumor oxygenation [107, 114]. Song and colleagues synthesized hollow Bi_2Se_3 nanosized particles containing PFC to accelerate oxygen release induced by NIR laser irradiation to suppress hypoxia-mediated radio-resistance by promoting more oxygen to hypoxic tumors [114]. Similarly, Song et al. applied an external low-power/low-frequency US modality to accelerate burst oxygen release from the fabricated nano-PFC to modulate hypoxia-related challenges to improve the efficiency of radiotherapy and photodynamic therapy [111].

Several other studies have demonstrated that PFC can be fabricated by self-assembly of polymers or proteins (e.g. PLGA, HA, HSA) to form nanosized micelles to accelerate cancer therapy. In this regard, Hu et al. prepared oxygen self-supplied

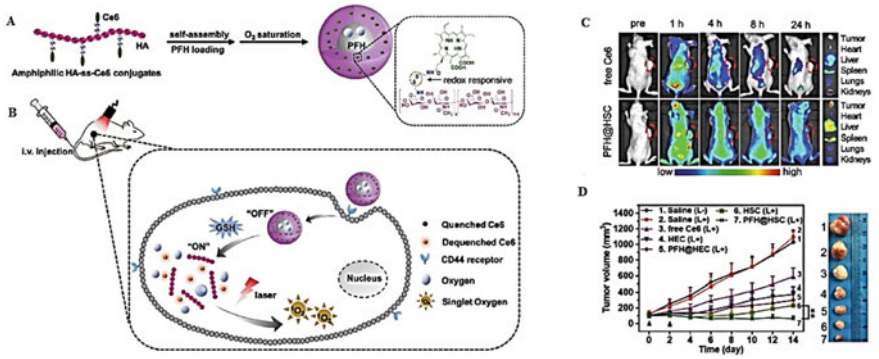

Fig. 8 Schematic representation of PFH@HSC nanoparticles fabrication (**a**), The mechanism of PFH@HSC nanoparticles in promoting efficiency of photodynamic therapy to relieve hypoxia (**b**), Fluorescence images of tumor-bearing mice (**c**), Tumor growth curves of mice treated with various groups (**d**) Reproduced with permission from Ref. [137]. Copyright 2019, with permission from Wiley

nanoplatforms (PFH@HSC) by conjugating chlorin e6 (Ce6) to HA via redox responsive linkages (HSC) and entrapping PFC inside micelles for selective tumor targeting (Fig. 8 a–d). Due to the presence of HA in the construction of these nanoparticles, their endocytosis was fascinated, resulting in high accumulation of PFH@HSC at tumor sites. Afterwards, PFH@HSC was fragmented under redox microenvironment of tumor tissue and supplied oxygen by PFC, resulting in the promotion of ROS products for cancer therapy [137]. In another study, Guo et al. created liposomes containing Hb/photosensitizer to enhance the efficacy of photodynamic therapy, which successfully downregulates the expression of VEGF and HIF-1α as well [104].

In recent years, among various PFC formulations, emulsion has reached the late-phase clinical trials as either an artificial blood constitute or clinical translation. In conclusion, nano-PFC could be considered as potential tool in addressing cancer-associated challenges and have a promising approach for future clinical translation. Of note, PFCs are not completely safe, it has been reported that extensive exposure to these agents may cause several unpleasant problems such as chest tightness, pulmonary hypertension, elevated central venous pressure, fever, cutaneous flushing, and hypotension [138].

3.2 Oxygen Generators

In situ oxygen generation within the tumor microenvironment serves as a promising approach to modulate tumor hypoxia. This strategy will also minimize toxicity and side effects associated with oxygen in the blood during circulation. Recent studies have revealed that there is a high concentration of hydrogen peroxide in tumor microenvironment due to abnormal metabolic processes. The catalytic degradation

of hydrogen peroxide in the tumor microenvironment is local. This phenomena may also be accompanied by the generation of oxygen, which can be used to relieve hypoxia and facilitate tumor therapy.

Nanomaterials/nanozymes with catalytic activity features have great potential for in situ oxygenation of hypoxic tumor, thus providing better tumor therapy efficacy for oxygen-dependent modalities such as radiotherapy, chemotherapy and photodynamic therapy. These nanomaterials with above-mentioned properties are mostly based on CAT/CAT like nanoenzymes that can potentially decompose hydrogen peroxide to produce oxygen. Although natural-based CAT can boost catalyzes of hydrogen peroxide, its poor half-life and in vivo instability have significantly hampered the biomedical applications of CAT [139]. To address these challenges, researchers have devoted their great efforts to the renovation of CAT. In this context, to prevent CAT from being affected by the degradation process, Zhang's research group fabricated MOFs containing CAT [140, 141]. MOFs containing CAT and other chemotherapeutics such as doxorubicin and AlPcS4 were developed to enhance the efficacy of chemotherapy and photodynamic therapy, respectively (Fig. 9a). Also, covalent conjugation of CAT with polymers can improve the biological efficacy of CAT. In order to promote the oxygen level in tumor microenvironment as well as enhance photo/sonodaynamic therapy, both fluorinated polyethyleneimine (PEI) and HA have been applied to carry CAT [142–144]. In another study, Meng et al. synthesized hydrogel encapsulating CAT to supply oxygen to tumor sites to improve photo-immunotherapy [145]. It has been well documented that with overwhelming hypoxia, tumor radiotherapy could be significantly enhanced. Accordingly, Song and colleagues created tantalum oxide (TaOX) nanoshells containing CAT to promote the efficacy of tumor radiotherapy. The results indicated that radiation-induced DNA damage was achieved by tantalum as a high-Z element and hypoxia was relieved by decomposition of hydrogen peroxide at tumor sites [146]. As noted above, natural

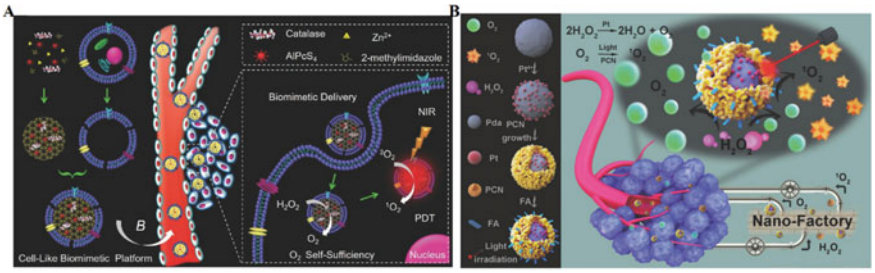

Fig. 9 Nanomaterials with oxygen-generating properties to alleviate hypoxic tumor. **a** MOFs containing CAT with cell-like biomimetic membrane for highly efficient tumor-targeted photodynamic therapy. Reproduced with permission from Ref. [140] Copyright 2016, with permission from Wiley. **b** Preparation of core–shell nanoplatforms based on Pt for generation of oxygen to boost the efficacy of photodynamic therapy. Reproduced with permission from Ref. [170]. Copyright 2018, with permission from Wiley

CAT exhibits high activity and specificity, but suffers from instability and is vulnerable to degradation in vivo due to the availability of some physiological proteases, especially during circulation. Additionally, large-scale production and extraction of this active agent is costly. Nanozymes are defined as nanosized materials with enzyme-like features as well as the ability to mimic key biologically relevant natural enzymes properties [147, 148]. In recent years, design and fabrication of nanozymes has been rapid as our knowledge of catalytic science and nanotechnology related era has been promoted. Compared to natural enzymes, nanozymes exhibited several superior benefits such as longer durability, tunable activity, high stability, low cost and easy mass production. Various nanosized enzymes have been fabricated so far, but among them only CAT-like nanozymes containing metal oxides/metals or Prussian Blue (PB) could effectively catalyze the decomposition of hydrogen peroxides to generate oxygen and water [149]. Accordingly, we highlight these classes of nanozymes as potential agents for in situ oxygenation of hypoxic tumor hypoxia for mitigating challenges and enhancing tumor therapy efficacy. Manganese, as an essential ion, has demonstrated a fundamental role in a wide range of biological processes. This ion also occupies the active sites of several enzymes, including CAT, photosystem II oxygen-evolving complex, manganese SOD, etc. The design and development of manganese-based catalysts has gained considerable attention in recent years due to their great ability to generate water and especially oxygen by decomposing hydrogen peroxides. Accordingly, different forms of nanosized materials made of manganese can be designed with diverse structures and constituents. Among them, manganese dioxide (MnO_2) nanoparticles has been the most widely utilized manganese-based nanomaterials to generate oxygen in hypoxia tumor therapy [150–152]. In this regard, several studies have been conducted on manganese dioxide nanosheets, manganese dioxide nanodots and hollow manganese dioxide nanoparticles, for catalyzing hydrogen peroxides and consequently oxygen generation to enhance tumor therapy [153–156]. The hollow manganese dioxide nanoparticles can act as dual sward as well, besides catalyzing the decomposition of hydrogen peroxides to relieve the hypoxic tumor microenvironment by oxygen production. Due to its acid-responsive characteristics, it can also be used as a drug vehicle with specifically controlled release of its payload. In addition, manganese ions released from nanoparticles can be utilized in MRI for both treatment and diagnosis. . Hollow manganese dioxide nanoparticles are uniform and have great potential for biomedical application [157]. The combination of manganese dioxide nanoparticles with other materials may result in higher therapeutic efficacy, called synergistic effects. For example, manganese dioxide nanosheets anchored by calcinated titanium dioxide-coated upconversion nanoparticles (UCNPs) were fabricated by Zhang et al. to alleviate hypoxic condition of tumor microenvironment through generation of oxygen and ROS [158]. Both bare metal ions and metal ion complexes are frequently conducted as dopant agents to modify manganese-based nanosized particles. Liu and colleagues fabricated mesoporous copper/manganese silicate nanospheres to promote the GSH-activated Fenton reaction and ROS generation, and ultimately improved the chemo/photodynamic synergistic therapy [159]. In another study,

mesoporous silica nanoparticles doped with ceria and manganese ferrite were fabricated to generate oxygen as well as scavenge ROS for the treatment of rheumatoid arthritis [160]. Numerous manganese-based nanoparticles have been designed and fabricated, but there are still no clinically approved manganese-based nanoparticles, indicating that most of them remain at the lab stage and have not yet reached clinical use. Moreover, the biodegradation of manganese-based nanoparticles may impose human tissues and cells to high concentrations of manganese ions that can damage tissues and cells. The faith of manganese ions released after biodegradation still remains unclear as well. Therefore, further investigation should be implemented to verify their potential toxicity and biocompatibility before reaching to the clinical translation. Prussian Blue (PB) is a deep blue dye applied to textiles and is produced by oxidation of ferrous ferrocyanide salts. The most striking application of this pigment in medicine is the detoxification of patients in case of poisoning by metals/elements. PB is considered as an antidote for thallotoxicosis and has already been approved by the FDA, indicating its potential biocompatibility for further clinical use. In 2016, Zhang and colleagues revealed for the first time that PB exhibits multienzyme-like activity such as SOD, peroxidase (POD) and CAT [161]. Afterwards, it has been emerged as a new multienzyme mimetic and has been applied to generate oxygen for enhanced tumor therapy, especially due to its CAT-like activity. Nanosized PB particles were enclosed by mesoporous organosilicon containing photosensitizer to enhance the efficacy of photodynamic therapy [162, 163]. In recent years, hollow nanoparticles have gained special interest due to their high drug loading capacity. In addition, PB-containing hollow structure nanoparticles could efficiently promote the oxygen generation by catalyzing hydrogen peroxides, and by loading glucose oxidase the efficacy of tumor hypoxia therapy was boosted as well [164]. Additionally, PB-containing hollow nanoparticles can be used for generation of heat by NIR light irradiation, providing a potential approach to potentiate photothermal therapy by boosted starvation therapy. Despite all these unique features of PB, such as catalytic activity for oxygen generation by hydrogen peroxide decomposition and highly desired biocompatibility, the weakly acidic condition in the tumor microenvironment limited the catalytic activity of PB. Over the past years, nanomaterials with the ability to absorb NIR light, such as Platinum (Pt) nanoparticles, have received much attention in biomedical applications of tumor treatment and diagnosis [165–167]. Depending on the pH and temperature of the microenvironment, Pt nanoparticles may represent POD-like or CAT-like activity [168]. Different forms of Pt have been applied to relieve hypoxic tumor microenvironment using of Pt's ability to induce tumor oxygenation [12, 169]. Accordingly, Zhang and colleagues designed and fabricated a promising nanoplatform based on Pt core–shell nanoparticles to promote ROS generation and relieve tumor hypoxia and ultimately restrict tumor invasion and metastasis. The use of Pt in construction of this hybrid nanoplatform augmented tumor therapy by catalyzing hydrogen peroxide to oxygen (Fig. 9b) [170]. Similarly, Liu et al. developed a novel Pt-based nanozyme termed PtFe@Fe_3O_4 with dual enzyme-like activities. PtFe@Fe_3O_4 could operate even under the acidic tumor microenvironment, therefore, in this challenging condition, it displayed dual enzyme-like activities, including POD-like activities and CAT-like activities. This Pt-based

nanozyme can successfully alleviate hypoxia and suppress the pancreatic cell growth [171]. Besides the dual CAT/POD enzyme activities of Pt, its combination with Au nanoparticles can lead to generation of a new type of enzyme like-activity called glucose oxidase-like nanozyme [172]. Xu et al. synthesized Pt and oxygen self-supplied micelles to alleviate hypoxia-triggered photodynamic resistance. Upon NIR irradiation, this self-assembled nanocomposite released Pt(II) and oxygen by generating oxygen and ROS, consequently enhancing photochemotherapy and antitumor efficiency [173].

In addition to Pt-based nanoparticles, their complexes such as *cis, trans, cis*-$[Pt(N3)_2(OH)_2(NH3)_2]$, were fabricated for generation of oxygen to relieve hypoxia tumor under light irradiation [173]. Regardless of the ability of these nanozymes in catalyzing hydrogen peroxide to oxygenate of hypoxic tumor sites, the amount of hydrogen peroxide present in tumor microenvironment is limited, thus limiting adequate generation of oxygen for efficient tumor therapy [174–176]. Liu and colleagues independently fabricated liposomes to carry and deliver CAT and hydrogen peroxide to tumor tissue. This approach produced adequate oxygen, overcoming the restrictions of endogenous hydrogen peroxide contents. It also augmented the therapeutic efficacy of radiotherapy and facilitated antitumor immunity by restricting the immunosuppressive tumor microenvironment [177]. However, this novel approach encountered with some challenges. Hydrogen peroxide has been reported to exhibit strong oxidizing features, so direct introducition of this agent into the bloodstream to compensate for the insufficient content of endogenous hydrogen peroxide in the tumor microenvironment can cause severe toxicity to tissues. To address this issue, researchers sought to find an alternative agent for hydrogen peroxide to generate oxygen. Among the potential solutions, dihydrogen monoxide (H_2O) was selected as an abundant agent at tumor sites, considering the above-mentioned problem. In recent years, water-splitting materials (from water to hydrogen and oxygen) have received substantial attention due to their potential applications in a variety of industrial fields, particularly in the energy and environment applications. Advances in materials science and engineering have expanded the demand for water-splitting materials into biomedical applications as well. As a natural material, thylakoid has been utilized to provide efficient oxygen generation. The thylakoid membrane could efficiently generate oxygen by participating in some complex reactions called photosynthetic electron-transfer reactions upon laser irradiation at 660 nm. Synthetic nanoparticles enclosed by the thylakoid membrane could suppress anaerobic respiration and re-oxygenate the hypoxic microenvironment to alleviate tumor hypoxia for improved treatment efficacy (Fig. 10a) [178]. However, there are still some problems in the implementation of thylakoid for biomedical use, as its preservation and extraction is intricate and some physiological parameters affect the efficiency of oxygen generation. As a water-splitting material, C_3N_4 (Carbon nitride) has attracted significant attention due to its potential in biomedical applications without requiring any metal elements. Unfortunately, this attractive agent is also far from being perfect, as its absorption is in the ultraviolet and visible range, indicating low penetration depth which is responsible for any skin damage and associated side effects. Considering this problem, carbon dots were introduced

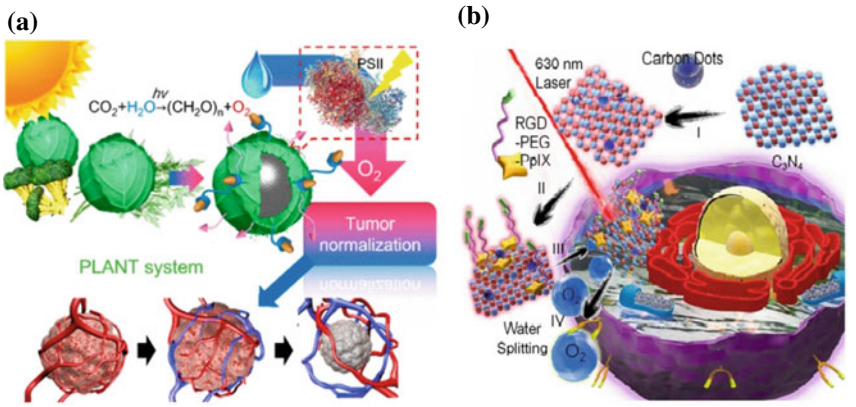

Fig. 10 Nanomaterials with oxygen-generating properties based on water decomposition to relieve hypoxic tumor. **a** Normalization of tumor microenvironment using thylakoid membrane-coated nanoparticles to generate oxygen. Reproduced with permission from Ref. [178]. Copyright 2018, with permission from ACS. **b** The mechanism of light-induced water splitting based nanocomposite to generate oxygen and sensitizing tumor cells to photodynamic therapy. Reproduced with permission from Ref. [179]. Copyright 2016, with permission from ACS

into carbon nitride to enhance red light absorption and consequently modulate water decomposition for oxygen generation [179]. Furthermore, by introducing photosensitizer into carbon nitride, tumor hypoxia was potentially restricted and the efficiency of photodynamic therapy was enhanced (Fig. 10b).

The combination of with iron (Fe) has also been exploited under two-photon irradiation because of its potential to generate oxygen to diminish oxygen dependency of photodynamic therapy [180]. As noted above, the absorption of red-shift by carbon nitride can be achieved by applying some modifications, but this is intricate and time-consuming. Apart from carbon nitride, tungsten nitride (WN) is another promising material that can operate at a wavelength of 765 nm and has water-splitting properties. This water-splitting material has been used directly to raise the oxygen level in the hypoxic microenvironment to treat tumor [181]. However, there is insufficient data on the biocompatibility of these water-splitting materials and should not be overlooked before their clinical use. Table 5 provides a summary of selective strategies based on nanomaterials to decompose hydrogen peroxide or water to generate oxygen.

4 Challenges and Conclusion

The natural hypoxic microenvironment within tumor sites is often responsible for failure of most oxygen-dependence therapies, such as chemotherapy, radiotherapy and photodynamic therapy. Herein we provide a brief overview of current strategies to modulate hypoxic tumor condition in favor of cancer therapy. Different

Table 5 Selective strategies based on nanomaterials to decompose hydrogen peroxide or water to generate oxygen

Decomposing agent	Nanoparticles	Approaches	References
Water (H_2O)	GDYO@i-RBM	Ultrathin graphdiyne oxide (GDYO) catalyzes the oxidation of water to release oxygen	[182]
	PCCN	Decomposing of water by carbon nitride (C_3N_4)	[179]
	PLANT	Oxygen generation by mimicking photosynthesis	[178]
	iOCOMs	Using manganese dioxide to catalyze the decomposition of hydrogen peroxide	[183]
	WS2-IO/S@MO-PEG	Decomposition of hydrogen peroxide by applying manganese dioxide	[184]
	H-MnO_2-PEG/C&D	Utilizing manganese dioxide to assist hydrogen peroxide decomposition	[157]
	SPN-Ms	Manganese dioxide to facilitate decomposition of hydrogen peroxide	[185]
	ACF@MnO_2	Applying manganese dioxide to supply oxygen by catalyzing hydrogen peroxide	[49]
	Ce6@MnO_2-PEG	Elevating oxygen concentration by using manganese dioxide to decompose hydrogen peroxide	[186]
	HSA-MnO_2-Ce6&Pt (HMCP)	Employing manganese dioxide to promote oxygen level by catalyzing hydrogen peroxide	[187]
Hydrogen peroxide (H_2O_2)	^{131}I-HSA-CAT	Catalyze to decompose hydrogen peroxide	[188]
	PLGA-R837@ Cat	Accelerating decomposition of hydrogen peroxide	[176]

(continued)

Table 5 (continued)

Decomposing agent	Nanoparticles	Approaches	References
	CAT@S/Ce6-CTPP/DPEG	Catalyze to decompose hydrogen peroxide	[189]
	Ce6-CAT/PEGDA	Facilitate decomposition of hydrogen peroxide	[145]
	CAT@liposome	Catalyze to decompose hydrogen peroxide	[177]
	CACH-PEG	Accelerating decomposition of hydrogen peroxide	[190]
	HAOP NP	Facilitate decomposition of hydrogen peroxide	[191]
	HSA-Ce6-Cat–PTX	Catalyze to decompose hydrogen peroxide	[192]
	TaOx@Cat-PEG	Accelerating decomposition of hydrogen peroxide	[146]

approaches/strategies based on nanomaterials are also summarized with typical examples for increasing the oxygen concentration in tumor microenvironment or reducing the oxygen dependence of therapies. Low oxygen level within the tumor microenvironment can be alleviated through nanomaterials that provide oxygen directly or indirectly. In direct way, tumor oxygenation can be achieved by applying oxygen-carrying nanomaterials, while indirectly oxygen-generating nanomaterials or in situ oxygen-generating nanomaterials can be used. In addition to the strategies mentioned above, due to the convolution of the tumor microenvironment, some researchers have recently been fascinated by strategies using nanomaterials with reduced oxygen-dependent properties, HIF-1 inhibitory effects, and hypoxia activated linkers/prodrugs for enhanced hypoxic tumor therapy. Despite all these unique characteristics and positive outcomes associated with nanomaterials, some challenges and unresolved concerns, such as long-term biosafety, validity, biodistribution, and biocompatibility of nanomaterials for the treatment of hypoxic tumors have impaired their clinical applications. In addition, the negative impact of nanomaterials containing heavy metals on human health is recognized as a growing concern, limiting their biological and clinical applications. But, since implantable nanomaterials exhibited good biocompatibility through surface modification, we believe that many of these nanomaterials can achieve clinical translation by simply changing their surface chemically or physically. The release of oxygen from oxygen-carrying nanomaterials into the bloodstream may cause severe toxicity to host tissues, which should not be overlooked in their design and fabrication. Accordingly, the development of nano-based oxygen carriers with the ability to release their payload in a controllable manner can efficiently diminish the premature release of oxygen during blood circulation. Fortunately, over the last decades, numerous nanocarrier-based platforms have

been developed to release their payload via endogenous or exogenous stimulation, so these strategies can also be utilized for controllable release of oxygen. Additionally, another promising approach to address any concerns about oxygen-related nanomaterials is to use nanomaterials with diminished oxygen-dependency. However, these nanoscale agents require some modification for specific eradication of tumor cells. In this case, nanomaterials with diminished oxygen dependency should be tuned and functionalized with appropriate targeting moieties. Furthermore, laser irradiation is considered an integral part of the treatment of hypoxic tumors based on nanomaterials, but its low penetration depth in the body limits its efficacy. Therefore, strategies based on nanomaterials with diminished laser irradiation dependency are required for treatment of hypoxic tumors. Overall, nanocarrier-based platforms for effective treatment of the hypoxic tumor microenvironment are novel approaches that remain in its infancy and requires further attention. In conclusion, endeavors should be continued to hasten the clinical translation of these systems in hypoxic tumor therapy.

References

1. Nejad AE et al (2021) The role of hypoxia in the tumor microenvironment and development of cancer stem cell: a novel approach to developing treatment. Cancer Cell Int 21(1):1–26
2. Roy S et al (2020) Hypoxic tumor microenvironment: Implications for cancer therapy. Exp Biol Med 245(13):1073–1086
3. Jin M-Z, Jin W-L (2020) The updated landscape of tumor microenvironment and drug repurposing. Signal Transduct Target Ther 5(1):1–16
4. Brown JM, Wilson WR (2004) Exploiting tumour hypoxia in cancer treatment. Nat Rev Cancer 4(6):437–447
5. Kim Y et al (2009) Hypoxic tumor microenvironment and cancer cell differentiation. Curr Mol Med 9(4):425–434
6. Jahanban-Esfahlan R et al (2018) Modulating tumor hypoxia by nanomedicine for effective cancer therapy. J Cell Physiol 233(3):2019–2031
7. Greijer A, Van der Wall E (2004) The role of hypoxia inducible factor 1 (HIF-1) in hypoxia induced apoptosis. J Clin Pathol 57(10):1009–1014
8. Graham K, Unger E (2018) Overcoming tumor hypoxia as a barrier to radiotherapy, chemotherapy and immunotherapy in cancer treatment. Int J Nanomed 13:6049
9. Hu D et al (2020) Application of nanotechnology for enhancing photodynamic therapy via ameliorating, neglecting, or exploiting tumor hypoxia. View 1(1):e6
10. Huang L et al (2021) Photodynamic therapy for hypoxic tumors: Advances and perspectives. Coord Chem Rev 438:213888
11. Yang B, Chen Y, Shi J (2019) Reactive oxygen species (ROS)-based nanomedicine. Chem Rev 119(8):4881–4985
12. Wei J et al (2018) A novel theranostic nanoplatform based on Pd@ Pt-PEG-Ce6 for enhanced photodynamic therapy by modulating tumor hypoxia microenvironment. Adv Func Mater 28(17):1706310
13. Wang X et al (2021) Boosting nanomedicine efficacy with hyperbaric oxygen therapy. Bionanomedicine for cancer therapy. Springer, pp 77–95
14. Zhang L et al (2021) Hyperbaric oxygen therapy represses the Warburg effect and epithelial–mesenchymal transition in hypoxic NSCLC cells via the HIF-1α/PFKP axis. Front Oncol 11:691762

15. Liu X et al (2021) Hyperbaric oxygen regulates tumor microenvironment and boosts commercialized nanomedicine delivery for potent eradication of cancer stem-like cells. Nano Today 40:101248
16. Moen I, Stuhr LE (2012) Hyperbaric oxygen therapy and cancer—a review. Target Oncol 7(4):233–242
17. Liu J-N, Bu W, Shi J (2017) Chemical design and synthesis of functionalized probes for imaging and treating tumor hypoxia. Chem Rev 117(9):6160–6224
18. Rashidzadeh H et al (2021) Recent advances in targeting malaria with nanotechnology-based drug carriers. Pharm Dev Technol (just-accepted):1–40
19. Cheon J, Chan W, Zuhorn I (2019) The Future of nanotechnology: cross-disciplined progress to improve health and medicine. Acc Chem Res 52(9):2405–2405
20. Rashidzadeh H et al (2021) pH-sensitive curcumin conjugated micelles for tumor triggered drug delivery. J Biomater Sci Polym Ed 32(3):320–336
21. Rezaei SJT et al (2020) pH-triggered prodrug micelles for cisplatin delivery: preparation and in vitro/vivo evaluation. React Funct Polym 146:104399
22. Huang D et al (2021) Nanodrug delivery systems modulate tumor vessels to increase the enhanced permeability and retention effect. Journal of Personalized Medicine 11(2):124
23. Yoozbashi M et al (2021) Magnetic nanostructured lipid carrier for dual triggered curcumin delivery: Preparation, characterization and toxicity evaluation on isolated rat liver mitochondria. J Biomater Appl 36(6):1055-1063
24. Liu Y et al (2018) Modulating hypoxia via nanomaterials chemistry for efficient treatment of solid tumors. Acc Chem Res 51(10):2502–2511
25. Rahmati M-A et al (2021) Self-assembled magnetic polymeric micelles for delivery of quercetin: Toxicity evaluation on isolated rat liver mitochondria. J. Biomater Sci Polym Ed. (just-accepted):1–14
26. Choudhry H, Harris AL (2018) Advances in hypoxia-inducible factor biology. Cell Metab 27(2):281–298
27. Semenza GL (2010) Defining the role of hypoxia-inducible factor 1 in cancer biology and therapeutics. Oncogene 29(5):625–634
28. Semenza GL, Wang GL (1992) A nuclear factor induced by hypoxia via de novo protein synthesis binds to the human erythropoietin gene enhancer at a site required for transcriptional activation. Mol Cell Biol 12(12):5447–5454
29. Semenza GL (2008) Hypoxia-inducible factor 1 and cancer pathogenesis. IUBMB Life 60(9):591–597
30. Semenza GL (2009) Regulation of cancer cell metabolism by hypoxia-inducible factor 1, in Seminars in cancer biology. Elsevier
31. Ma Z et al (2021) Targeting hypoxia-inducible factor-1-mediated metastasis for cancer therapy. Antioxid Redox Signal 34(18):1484–1497
32. Aljabali AA et al (2020) Albumin nano-encapsulation of piceatannol enhances its anticancer potential in colon cancer via down regulation of nuclear p65 and HIF-1α. Cancers 12:113. (Correction: Aljabali AAA et al, Cancers, 2020. 12(12): 3587)
33. Ilhan S, Pulat ÇÇP (2021) Biogenic silver nanoparticles synthesized from Piper longum fruit extract inhibit HIF-1α/VEGF mediated angiogenesis in prostate cancer cells. Cumhur Sci J 42(2): 236–244
34. Montigaud Y et al (2018) Optimized acriflavine-loaded lipid nanocapsules as a safe and effective delivery system to treat breast cancer. Int J Pharm 551(1–2):322–328
35. Izadi S et al (2020) Codelivery of HIF-1α siRNA and dinaciclib by carboxylated graphene oxide-trimethyl chitosan-hyaluronate nanoparticles significantly suppresses cancer cell progression. Pharm Res 37(10):1–20
36. Wan R et al (2019) The target therapeutic effect of functionalized graphene oxide nanoparticles graphene oxide–polyethylene glycol–folic acid-1–pyrenemethylamine hydrochloride-mediated RNA interference of HIF-1α gene in human pancreatic cancer cells. J Biomater Appl 34(2):155–177

37. Tzeng W-S et al (2021) Pterostilbene nanoparticles downregulate hypoxia-inducible factors in hepatoma cells under hypoxic conditions. Int J Nanomed 16:867
38. Kang G et al (2021) VHH212 nanobody targeting the hypoxia-inducible factor 1α suppresses angiogenesis and potentiates gemcitabine therapy in pancreatic cancer in vivo. Cancer Biol Med 18(3):772
39. Xie Z et al (2018) Targeting tumor hypoxia with stimulus-responsive nanocarriers in overcoming drug resistance and monitoring anticancer efficacy. Acta Biomater 71:351–362
40. Huang C et al (2019) Azoreductase-responsive metal–organic framework-based nanodrug for enhanced cancer therapy via breaking hypoxia-induced chemoresistance. ACS Appl Mater Interfaces 11(29):25740–25749
41. Chen Y et al (2017) Co-delivery of hypoxia inducible factor-1α small interfering RNA and 5-fluorouracil to overcome drug resistance in gastric cancer SGC-7901 cells. J Gene Med 19(12):e2998
42. Zhang B et al (2019) Promoting antitumor efficacy by suppressing hypoxia via nano self-assembly of two irinotecan-based dual drug conjugates having a HIF-1α inhibitor. J Mater Chem B 7(35):5352–5362
43. Ji Z et al (2006) Induction of hypoxia-inducible factor-1α overexpression by cobalt chloride enhances cellular resistance to photodynamic therapy. Cancer Lett 244(2):182–189
44. Lamberti MJ et al (2017) Transcriptional activation of HIF-1 by a ROS-ERK axis underlies the resistance to photodynamic therapy. PLoS ONE 12(5):e0177801
45. Sun S et al (2018) Ultrasound-targeted photodynamic and gene dual therapy for effectively inhibiting triple negative breast cancer by cationic porphyrin lipid microbubbles loaded with HIF1α-siRNA. Nanoscale 10(42):19945–19956
46. Chen W-H et al (2015) Nanoparticle delivery of HIF1α siRNA combined with photodynamic therapy as a potential treatment strategy for head-and-neck cancer. Cancer Lett 359(1):65–74
47. Weijer R et al (2016) Inhibition of hypoxia inducible factor 1 and topoisomerase with acriflavine sensitizes perihilar cholangiocarcinomas to photodynamic therapy. Oncotarget 7(3):3341
48. Zhang Z et al (2020) Self-delivered and self-monitored chemo-photodynamic nanoparticles with light-triggered synergistic antitumor therapies by downregulation of HIF-1α and depletion of GSH. ACS Appl Mater Interfaces 12(5):5680–5694
49. Meng L et al (2018) Tumor oxygenation and hypoxia inducible factor-1 functional inhibition via a reactive oxygen species responsive nanoplatform for enhancing radiation therapy and abscopal effects. ACS Nano 12(8):8308–8322
50. Zhu H et al (2015) pH-responsive hybrid quantum dots for targeting hypoxic tumor siRNA delivery. J Control Release 220:529–544
51. Li TSC, Yawata T, Honke K (2014) Efficient siRNA delivery and tumor accumulation mediated by ionically cross-linked folic acid–poly (ethylene glycol)–chitosan oligosaccharide lactate nanoparticles: For the potential targeted ovarian cancer gene therapy. Eur J Pharm Sci 52:48–61
52. Fattahi N et al (2021) Enhancement of the brain delivery of methotrexate with administration of mid-chain ester prodrugs: In vitro and in vivo studies. Int J Pharm 600:120479
53. Anduran E et al (2021) Hypoxia-activated prodrug derivatives of anti-cancer drugs: a patent review 2006–2021. Expert Opin Ther Pat (just-accepted)
54. Meaney C, Rhebergen S, Kohandel M (2020) In silico analysis of hypoxia activated prodrugs in combination with anti angiogenic therapy through nanocell delivery. PLoS Comput Biol 16(5):e1007926
55. Thomas RG, Surendran SP, Jeong YY (2020) Tumor microenvironment-stimuli responsive nanoparticles for anticancer therapy. Front Mol Biosci 7:414
56. Zeng Y et al (2018) Hypoxia-activated prodrugs and redox-responsive nanocarriers. Int J Nanomed 13:6551
57. Denny WA (2010) Hypoxia-activated prodrugs in cancer therapy: progress to the clinic. Future Oncol 6(3):419–428

58. Guo D et al (2021) A Redox-Responsive, in-situ polymerized polyplatinum (IV)-coated gold nanorod as an amplifier of tumor accumulation for enhanced thermo-chemotherapy. Biomaterials 266:120400
59. Guo D et al (2020) Tirapazamine-embedded polyplatinum (iv) complex: a prodrug combo for hypoxia-activated synergistic chemotherapy. Biomater Sci 8(2):694–701
60. Zhao D et al (2020) Light-triggered dual-modality drug release of self-assembled prodrug-nanoparticles for synergistic photodynamic and hypoxia-activated therapy. Nanoscale Horiz 5(5):886–894
61. Evans MA et al (2020) Macrophage-mediated delivery of hypoxia-activated prodrug nanoparticles. Adv Ther 3(2):1900162
62. Yang S et al (2019) Selectively potentiating hypoxia levels by combretastatin A4 nanomedicine: toward highly enhanced hypoxia-activated prodrug tirapazamine therapy for metastatic tumors. Adv Mater 31(11):1805955
63. Dai Y et al (2019) Multifunctional theranostic liposomes loaded with a hypoxia-activated prodrug for cascade-activated tumor selective combination therapy. ACS Appl Mater Interfaces 11(43):39410–39423
64. Li X et al (2021) In Vivo-assembled phthalocyanine/albumin supramolecular complexes combined with a hypoxia-activated prodrug for enhanced photodynamic immunotherapy of cancer. Biomaterials 266:120430
65. Yin H et al (2021) 2D Core/shell-structured mesoporous silicene@ silica for targeted and synergistic NIR-II-induced photothermal ablation and hypoxia-activated chemotherapy of tumor. Adv Funct Mater 2102043
66. Zhang G et al (2021) Novel semiconducting nano-agents incorporating tirapazamine for imaging guided synergistic cancer hypoxia activated photo-chemotherapy. J Mater Chem B **9**, 5318-5328
67. Zhong Y et al (2021) A light and hypoxia-activated nanodrug for cascade photodynamic-chemo cancer therapy. Biomater Sci **9**, 5218-5226
68. Wang C et al (2021) Photodynamic creation of artificial tumor microenvironments to collectively facilitate hypoxia-activated chemotherapy delivered by coagulation-targeting liposomes. Chem Eng J 414:128731
69. Hong X et al (2021) Hyaluronan-fullerene/AIEgen nanogel as CD44-targeted delivery of tirapazamine for synergistic photodynamic-hypoxia activated therapy. Nanotechnology
70. He Z et al (2019) Hybrid nanomedicine fabricated from photosensitizer-terminated metal-organic framework nanoparticles for photodynamic therapy and hypoxia-activated cascade chemotherapy. Small 15(4):1804131
71. Wilson WR, Hay MP (2011) Targeting hypoxia in cancer therapy. Nat Rev Cancer 11(6):393–410
72. Kumari R, Sunil D, Ningthoujam RS (2020) Hypoxia-responsive nanoparticle based drug delivery systems in cancer therapy: an up-to-date review. J Control Release 319:135–156
73. Sharma A et al (2019) Hypoxia-targeted drug delivery. Chem Soc Rev 48(3):771–813
74. Yang G et al (2019) A hypoxia-responsive albumin-based nanosystem for deep tumor penetration and excellent therapeutic efficacy. Adv Mater 31(25):1901513
75. Im S et al (2018) Hypoxia-triggered transforming immunomodulator for cancer immunotherapy via photodynamically enhanced antigen presentation of dendritic cell. ACS Nano 13(1):476–488
76. Huang X et al (2018) Hypoxia-tropic protein nanocages for modulation of tumor-and chemotherapy-associated hypoxia. ACS Nano 13(1):236–247
77. Cui D et al (2019) A semiconducting polymer nano-prodrug for hypoxia-activated photodynamic cancer therapy. Angew Chem 131(18):5981–5985
78. Alsaab HO et al (2018) Tumor hypoxia directed multimodal nanotherapy for overcoming drug resistance in renal cell carcinoma and reprogramming macrophages. Biomaterials 183:280–294
79. Huo D et al (2017) Hypoxia-targeting, tumor microenvironment responsive nanocluster bomb for radical-enhanced radiotherapy. ACS Nano 11(10):10159–10174

80. Qian C et al (2016) Light-activated hypoxia-responsive nanocarriers for enhanced anticancer therapy. Adv Mater 28(17):3313–3320
81. Luo C-H et al (2016) Bacteria-mediated hypoxia-specific delivery of nanoparticles for tumors imaging and therapy. Nano Lett 16(6):3493–3499
82. Chen W et al (2018) Bacteria-driven hypoxia targeting for combined biotherapy and photothermal therapy. ACS Nano 12(6):5995–6005
83. Shen N et al (2019) Combretastatin A4 nanoparticles combined with hypoxia-sensitive imiquimod: a new paradigm for the modulation of host immunological responses during cancer treatment. Nano Lett 19(11):8021–8031
84. Zhang C et al (2016) A polyoxometalate cluster paradigm with self-adaptive electronic structure for acidity/reducibility-specific photothermal conversion. J Am Chem Soc 138(26):8156–8164
85. Zhang C et al (2017) Magnesium silicide nanoparticles as a deoxygenation agent for cancer starvation therapy. Nat Nanotechnol 12(4):378–386
86. Shan L et al (2019) Organosilica-based hollow mesoporous bilirubin nanoparticles for antioxidation-activated self-protection and tumor-specific deoxygenation-driven synergistic therapy. ACS Nano 13(8):8903–8916
87. Ma Y et al (2019) Nanoclustered cascaded enzymes for targeted tumor starvation and deoxygenation-activated chemotherapy without systemic toxicity. ACS Nano 13(8):8890–8902
88. Zhang R et al (2018) Glucose & oxygen exhausting liposomes for combined cancer starvation and hypoxia-activated therapy. Biomaterials 162:123–131
89. Feng L et al (2017) Theranostic liposomes with hypoxia-activated prodrug to effectively destruct hypoxic tumors post-photodynamic therapy. ACS Nano 11(1):927–937
90. Zhang M et al (2019) Platelet-mimicking biotaxis targeting vasculature-disrupted tumors for cascade amplification of hypoxia-sensitive therapy. ACS Nano 13(12):14230–14240
91. Li Y et al (2019) Carbon monoxide (CO)-Strengthened cooperative bioreductive anti-tumor therapy via mitochondrial exhaustion and hypoxia induction. Biomaterials 209:138–151
92. Li H et al (2019) Nucleus-targeted nano delivery system eradicates cancer stem cells by combined thermotherapy and hypoxia-activated chemotherapy. Biomaterials 200:1–14
93. Wang Y et al (2017) Tumor-penetrating nanoparticles for enhanced anticancer activity of combined photodynamic and hypoxia-activated therapy. ACS Nano 11(2):2227–2238
94. Liu Y et al (2015) Hypoxia induced by upconversion-based photodynamic therapy: towards highly effective synergistic bioreductive therapy in tumors. Angew Chem 127(28):8223–8227
95. Palazón A et al (2012) Molecular pathways: hypoxia response in immune cells fighting or promoting cancer. Clin Cancer Res 18(5):1207–1213
96. Ruf M, Moch H, Schraml P (2016) PD-L1 expression is regulated by hypoxia inducible factor in clear cell renal cell carcinoma. Int J Cancer 139(2):396–403
97. Lu J et al (2019) Photodynamic therapy for hypoxic solid tumors via Mn-MOF as a photosensitizer. Chem Commun 55(72):10792–10795
98. Li J et al (2018) Advanced nanomaterials targeting hypoxia to enhance radiotherapy. Int J Nanomed 13:5925
99. Yang Y et al (2019) NIR-II driven plasmon-enhanced catalysis for a timely supply of oxygen to overcome hypoxia-induced radiotherapy tolerance. Angew Chem 131(42):15213–15219
100. Tian H et al (2017) Cancer cell membrane-biomimetic oxygen nanocarrier for breaking hypoxia-induced chemoresistance. Adv Func Mater 27(38):1703197
101. Xu M et al (2020) Smart strategies to overcome tumor hypoxia toward the enhancement of cancer therapy. Nanoscale 12(42):21519–21533
102. Zou M-Z et al (2021) Advances in nanomaterials for treatment of hypoxic tumor. Natl Sci Rev 8(2):nwaa160
103. Ruan C et al (2021) Nanomaterials for tumor hypoxia relief to improve the efficacy of ROS-generated cancer therapy. Front Chem **9**
104. Guo X et al (2018) Synchronous delivery of oxygen and photosensitizer for alleviation of hypoxia tumor microenvironment and dramatically enhanced photodynamic therapy. Drug Delivery 25(1):585–599

105. Cao H et al (2018) An assembled nanocomplex for improving both therapeutic efficiency and treatment depth in photodynamic therapy. Angew Chem 130(26):7885–7889
106. Luo Z et al (2016) Self-monitoring artificial red cells with sufficient oxygen supply for enhanced photodynamic therapy. Sci Rep 6(1):1–11
107. Chen J et al (2017) Oxygen-self-produced nanoplatform for relieving hypoxia and breaking resistance to sonodynamic treatment of pancreatic cancer. ACS Nano 11(12):12849–12862
108. Lu N et al (2018) Biodegradable hollow mesoporous organosilica nanotheranostics for mild hyperthermia-induced bubble-enhanced oxygen-sensitized radiotherapy. ACS Nano 12(2):1580–1591
109. Cai X et al (2019) Monodispersed copper (I)-based nano metal-organic framework as a biodegradable drug carrier with enhanced photodynamic therapy efficacy. Adv Sci 6(15):1900848
110. Song G et al (2017) TaOx decorated perfluorocarbon nanodroplets as oxygen reservoirs to overcome tumor hypoxia and enhance cancer radiotherapy. Biomaterials 112:257–263
111. Song X et al (2016) Ultrasound triggered tumor oxygenation with oxygen-shuttle nanoperfluorocarbon to overcome hypoxia-associated resistance in cancer therapies. Nano Lett 16(10):6145–6153
112. Gao M et al (2017) Erythrocyte-membrane-enveloped perfluorocarbon as nanoscale artificial red blood cells to relieve tumor hypoxia and enhance cancer radiotherapy. Adv Mater 29(35):1701429
113. Cheng Y et al (2015) Perfluorocarbon nanoparticles enhance reactive oxygen levels and tumour growth inhibition in photodynamic therapy. Nat Commun 6(1):1–8
114. Song G et al (2016) Perfluorocarbon-loaded hollow Bi2Se3 nanoparticles for timely supply of oxygen under near-infrared light to enhance the radiotherapy of cancer. Adv Mater 28(14):2716–2723
115. Iijima M et al (2018) Development of single nanometer-sized ultrafine oxygen bubbles to overcome the hypoxia-induced resistance to radiation therapy via the suppression of hypoxia-inducible factor-1α. Int J Oncol 52(3):679–686
116. Khan MS et al (2019) Anti-tumor drug-loaded oxygen nanobubbles for the degradation of HIF-1α and the upregulation of reactive oxygen species in tumor cells. Cancers 11(10):1464
117. Bhandari PN et al (2017) Oxygen nanobubbles revert hypoxia by methylation programming. Sci Rep 7(1):1–14
118. Song R et al (2019) pH-responsive oxygen nanobubbles for spontaneous oxygen delivery in hypoxic tumors. Langmuir 35(31):10166–10172
119. Owen J et al (2016) Reducing tumour hypoxia via oral administration of oxygen nanobubbles. PLoS ONE 11(12):e0168088
120. Song R et al (2018) Lipid-polymer bilaminar oxygen nanobubbles for enhanced photodynamic therapy of cancer. ACS Appl Mater Interfaces 10(43):36805–36813
121. Song L et al (2020) Biogenic nanobubbles for effective oxygen delivery and enhanced photodynamic therapy of cancer. Acta Biomater 108:313–325
122. Cavalli R, Soster M, Argenziano M (2016) Nanobubbles: a promising efficienft tool for therapeutic delivery. Ther Deliv 7(2):117–138
123. Jensen FB (2009) The dual roles of red blood cells in tissue oxygen delivery: oxygen carriers and regulators of local blood flow. J Exp Biol 212(21):3387–3393
124. Wang P et al (2017) Orthogonal near-infrared upconversion co-regulated site-specific O2 delivery and photodynamic therapy for hypoxia tumor by using red blood cell microcarriers. Biomaterials 125:90–100
125. Sun X et al (2015) Remotely controlled red blood cell carriers for cancer targeting and near-infrared light-triggered drug release in combined photothermal-chemotherapy. Adv Func Mater 25(16):2386–2394
126. Wang L-Y et al (2013) Versatile RBC-derived vesicles as nanoparticle vector of photosensitizers for photodynamic therapy. Nanoscale 5(1):416–421
127. Tang W et al (2016) Red blood cell-facilitated photodynamic therapy for cancer treatment. Adv Func Mater 26(11):1757–1768

128. Hu J et al (2020) Polydopamine-based surface modification of hemoglobin particles for stability enhancement of oxygen carriers. J Colloid Interface Sci 571:326–336
129. Jansman MM, Hosta-Rigau L (2018) Recent and prominent examples of nano-and microarchitectures as hemoglobin-based oxygen carriers. Adv Coll Interface Sci 260:65–84
130. Paciello A et al (2016) Hemoglobin-conjugated gelatin microsphere as a smart oxygen releasing biomaterial. Adv Healthcare Mater 5(20):2655–2666
131. Zhao P et al (2016) Oxygen nanocarrier for combined cancer therapy: oxygen-boosted ATP-responsive chemotherapy with amplified ROS lethality. Adv Healthcare Mater 5(17):2161–2167
132. Jia Y, Duan L, Li J (2016) Hemoglobin-based nanoarchitectonic assemblies as oxygen carriers. Adv Mater 28(6):1312–1318
133. Liu WL et al (2018) Aggressive man-made red blood cells for hypoxia-resistant photodynamic therapy. Adv Mater 30(35):1802006
134. Liang X et al (2020) Perfluorocarbon@ porphyrin nanoparticles for tumor hypoxia relief to enhance photodynamic therapy against liver metastasis of colon cancer. ACS Nano 14(10):13569–13583
135. Que Y et al (2016) Enhancing photodynamic therapy efficacy by using fluorinated nanoplatform. ACS Macro Lett 5(2):168–173
136. Wu L et al (2018) Local intratracheal delivery of perfluorocarbon nanoparticles to lung cancer demonstrated with magnetic resonance multimodal imaging. Theranostics 8(2):563
137. Hu D et al (2019) Perfluorocarbon-loaded and redox-activatable photosensitizing agent with oxygen supply for enhancement of fluorescence/photoacoustic imaging guided tumor photodynamic therapy. Adv Func Mater 29(9):1806199
138. Zhou Z et al (2016) Reactive oxygen species generating systems meeting challenges of photodynamic cancer therapy. Chem Soc Rev 45(23):6597–6626
139. Gu Z et al (2011) Tailoring nanocarriers for intracellular protein delivery. Chem Soc Rev 40(7):3638–3655
140. Cheng H et al (2016) An O2 self-sufficient biomimetic nanoplatform for highly specific and efficient photodynamic therapy. Adv Func Mater 26(43):7847–7860
141. Zou MZ et al (2018) A multifunctional biomimetic nanoplatform for relieving hypoxia to enhance chemotherapy and inhibit the PD-1/PD-L1 axis. Small 14(28):1801120
142. Li G et al (2020) Fluorinated chitosan to enhance transmucosal delivery of sonosensitizer-conjugated catalase for sonodynamic bladder cancer treatment post-intravesical instillation. ACS Nano 14(2):1586–1599
143. Li G et al (2019) Fluorinated polyethylenimine to enable transmucosal delivery of photosensitizer-conjugated catalase for photodynamic therapy of orthotopic bladder tumors postintravesical instillation. Adv Func Mater 29(40):1901932
144. Phua SZF et al (2019) Catalase-integrated hyaluronic acid as nanocarriers for enhanced photodynamic therapy in solid tumor. ACS Nano 13(4):4742–4751
145. Meng Z et al (2019) Light-triggered in situ gelation to enable robust photodynamic-immunotherapy by repeated stimulations. Adv Mater 31(24):1900927
146. Song G et al (2016) Catalase-loaded TaOx nanoshells as bio-nanoreactors combining high-Z element and enzyme delivery for enhancing radiotherapy. Adv Mater 28(33):7143–7148
147. Wu J et al (2019) Nanomaterials with enzyme-like characteristics (nanozymes): next-generation artificial enzymes (II). Chem Soc Rev 48(4):1004–1076
148. Wong EL, Vuong KQ, Chow E (2021) Nanozymes for environmental pollutant monitoring and remediation. Sensors 21(2):408
149. Liang M, Yan X (2019) Nanozymes: from new concepts, mechanisms, and standards to applications. Acc Chem Res 52(8):2190–2200
150. Yang G,Ji J, Liu Z (20214) Multifunctional MnO2 nanoparticles for tumor microenvironment modulation and cancer therapy, in Wiley interdisciplinary reviews: nanomedicine and nanobiotechnology, p e1720
151. Zhang L et al (2021) MnO 2-capped silk fibroin (SF) nanoparticles with chlorin e6 (Ce6) encapsulation for augmented photo-driven therapy by modulating the tumor microenvironment. J Mater Chem B 9(17):3677–3688

152. Chang C-C et al (2020) Nanoparticle delivery of MnO2 and antiangiogenic therapy to overcome hypoxia-driven tumor escape and suppress hepatocellular carcinoma. ACS Appl Mater Interfaces 12(40):44407–44419
153. Yu M et al (2019) Multifunctional nanoregulator reshapes immune microenvironment and enhances immune memory for tumor immunotherapy. Adv Sci 6(16):1900037
154. Zhang X et al (2019) Gold cube-in-cube based oxygen nanogenerator: a theranostic nanoplatform for modulating tumor microenvironment for precise chemo-phototherapy and multimodal imaging. ACS Nano 13(5):5306–5325
155. Gordijo CR et al (2015) Design of hybrid MnO2-polymer-lipid nanoparticles with tunable oxygen generation rates and tumor accumulation for cancer treatment. Adv Func Mater 25(12):1858–1872
156. Zhang W et al (2018) Oxygen-generating MnO2 nanodots-anchored versatile nanoplatform for combined chemo-photodynamic therapy in hypoxic cancer. Adv Func Mater 28(13):1706375
157. Yang G et al (2017) Hollow MnO 2 as a tumor-microenvironment-responsive biodegradable nano-platform for combination therapy favoring antitumor immune responses. Nat Commun 8(1):1–13
158. Zhang C et al (2017) An O2 self-supplementing and reactive-oxygen-species-circulating amplified nanoplatform via H2O/H2O2 splitting for tumor imaging and photodynamic therapy. Adv Func Mater 27(43):1700626
159. Liu C et al (2019) Biodegradable biomimic copper/manganese silicate nanospheres for chemodynamic/photodynamic synergistic therapy with simultaneous glutathione depletion and hypoxia relief. ACS Nano 13(4):4267–4277
160. Kim J et al (2019) Synergistic oxygen generation and reactive oxygen species scavenging by manganese ferrite/ceria co-decorated nanoparticles for rheumatoid arthritis treatment. ACS Nano 13(3):3206–3217
161. Zhang W et al (2016) Prussian blue nanoparticles as multienzyme mimetics and reactive oxygen species scavengers. J Am Chem Soc 138(18):5860–5865
162. Hu J-J et al (2019) Augment of oxidative damage with enhanced photodynamic process and MTH1 inhibition for tumor therapy. Nano Lett 19(8):5568–5576
163. Yang ZL et al (2018) Oxygen-evolving mesoporous organosilica coated prussian blue nanoplatform for highly efficient photodynamic therapy of tumors. Adv Sci 5(5):1700847
164. Zhou J et al (2018) Engineering of a nanosized biocatalyst for combined tumor starvation and low-temperature photothermal therapy. ACS Nano 12(3):2858–2872
165. Song Y et al (2021) Fabrication of the biomimetic DOX/Au@ Pt nanoparticles hybrid nanostructures for the combinational chemo/photothermal cancer therapy. J Alloys Compd 160592
166. Yang X et al (2021) Platinum nanoenzyme functionalized black phosphorus nanosheets for photothermal and enhanced-photodynamic therapy. Chem Eng J 409:127381
167. Sathiyaraj G et al (2021) Bio-directed synthesis of Pt-nanoparticles from aqueous extract of red algae Halymenia dilatata and their biomedical applications. Colloids Surf A 618:126434
168. Fan J et al (2011) Direct evidence for catalase and peroxidase activities of ferritin–platinum nanoparticles. Biomaterials 32(6):1611–1618
169. Liang S et al (2019) Intelligent hollow Pt-CuS janus architecture for synergistic catalysis-enhanced sonodynamic and photothermal cancer therapy. Nano Lett 19(6):4134–4145
170. Wang XS et al (2018) A versatile Pt-based core-shell nanoplatform as a nanofactory for enhanced tumor therapy. Adv Func Mater 28(36):1801783

171. Li S et al (2019) A nanozyme with photo-enhanced dual enzyme-like activities for deep pancreatic cancer therapy. Angew Chem 131(36):12754–12761
172. Liu C et al (2019) Nanozymes-engineered metal–organic frameworks for catalytic cascades-enhanced synergistic cancer therapy. Nano Lett 19(8):5674–5682
173. Xu S et al (2018) Oxygen and Pt (II) self-generating conjugate for synergistic photo-chemo therapy of hypoxic tumor. Nat Commun 9(1):1–9
174. Huo M et al (2017) Tumor-selective catalytic nanomedicine by nanocatalyst delivery. Nat Commun 8(1):1–12
175. Zhang L et al (2018) An adenosine triphosphate-responsive autocatalytic fenton nanoparticle for tumor ablation with self-supplied H2O2 and acceleration of Fe (iii)/Fe (ii) conversion. Nano Lett 18(12):7609–7618
176. Chen Q et al (2019) Nanoparticle-enhanced radiotherapy to trigger robust cancer immunotherapy. Adv Mater 31(10):1802228
177. Song X et al (2018) Self-supplied tumor oxygenation through separated liposomal delivery of H2O2 and catalase for enhanced radio-immunotherapy of cancer. Nano Lett 18(10):6360–6368
178. Zheng D et al (2018) Normalizing tumor microenvironment based on photosynthetic abiotic/biotic nanoparticles. ACS Nano 12(6):6218–6227
179. Zheng D-W et al (2016) Carbon-dot-decorated carbon nitride nanoparticles for enhanced photodynamic therapy against hypoxic tumor via water splitting. ACS Nano 10(9):8715–8722
180. Li R-Q et al (2019) A two-photon excited O2-evolving nanocomposite for efficient photodynamic therapy against hypoxic tumor. Biomaterials 194:84–93
181. Wang SB et al (2019) A tungsten nitride-based O2 self-sufficient nanoplatform for enhanced photodynamic therapy against hypoxic tumors. Advanced Therapeutics 2(6):1900012
182. Jiang W et al (2019) Tumor reoxygenation and blood perfusion enhanced photodynamic therapy using ultrathin graphdiyne oxide nanosheets. Nano Lett 19(6):4060–4067
183. Revuri V et al (2019) In situ oxygenic nanopods targeting tumor adaption to hypoxia potentiate image-guided photothermal therapy. ACS Appl Mater Interfaces 11(22):19782–19792
184. Yang G et al (2018) Manganese dioxide coated WS2@ Fe3O4/sSiO2 nanocomposites for pH-responsive MR imaging and oxygen-elevated synergetic therapy. Small 14(2):1702664
185. Zhu H et al (2018) Oxygenic hybrid semiconducting nanoparticles for enhanced photodynamic therapy. Nano Lett 18(1):586–594
186. Zhu W et al (2016) Modulation of hypoxia in solid tumor microenvironment with MnO2 nanoparticles to enhance photodynamic therapy. Adv Func Mater 26(30):5490–5498
187. Chen Q et al (2016) Intelligent albumin–MnO2 nanoparticles as pH-/H2O2-responsive dissociable nanocarriers to modulate tumor hypoxia for effective combination therapy. Adv Mater 28(33):7129–7136
188. Chen J et al (2019) Hybrid protein nano-reactors enable simultaneous increments of tumor oxygenation and iodine-131 delivery for enhanced radionuclide therapy. Small 15(46):1903628
189. Yang G et al (2018) Smart nanoreactors for pH-responsive tumor homing, mitochondria-targeting, and enhanced photodynamic-immunotherapy of cancer. Nano Lett 18(4):2475–2484
190. Yang Y et al (2018) G-quadruplex-based nanoscale coordination polymers to modulate tumor hypoxia and achieve nuclear-targeted drug delivery for enhanced photodynamic therapy. Nano Lett 18(11):6867–6875
191. Chen H et al (2015) H2O2-activatable and O2-evolving nanoparticles for highly efficient and selective photodynamic therapy against hypoxic tumor cells. J Am Chem Soc 137(4):1539–1547
192. Chen Q et al (2017) Drug-induced co-assembly of albumin/catalase as smart nano-theranostics for deep intra-tumoral penetration, hypoxia relieve, and synergistic combination therapy. J Control Release 263:79–89

Application of Nanoradioprotective Agents in Cancer Therapy

Faezeh Mozafari, Hamid Rashidzadeh, Murat Barsbay, Mohammadreza Ghaffarlou, Marziyeh Salehiabar, Ali Ramazani, Morteza Abazari, Mohammad-Amin Rahmati, Gopal Niraula, Surender K. Sharma, and Hossein Danafar

Abstract Radiotherapy (RT) has been widely employed in health centers and hospitals for the treatment of several malignant tumors. The main goal of RT is to augment the therapeutic efficacy of treatment by delivering supreme dose of ionizing radiation to tumor sites while diminishing undesirable radiation dose to healthy tissues to restrict the severe adverse effects. However, despite all the advances and progressions in radiation therapy technology, irradiation of surrounding normal tissues always occurs and results in damage and side effects. Accordingly, radiation protectors with the ability to protect healthy tissue can be a promising approach for radiation escalation, thereby expanding the therapeutic ratio. Although several radiation protectors are available for clinical use to protect healthy tissue from the deleterious effects of radiation, some drawbacks such as short plasma half-life and rapid clearance greatly hamper sustainable biological applications. Over the past few years, multifunctional nanomaterials have emerged as very promising tools in the biological and medical field, opening a new route for developing potential nanoradioprotective agents as some nanoparticles exhibit intrinsic radioprotective properties. Accordingly, within

F. Mozafari and H. Rashidzadeh—These authors contribute equally to this work

F. Mozafari · H. Rashidzadeh · M. Abazari · M.-A. Rahmati · H. Danafar (✉)
Zanjan Pharmaceutical Biotechnology Research Center, Zanjan University of Medical Sciences, Zanjan, Iran
e-mail: danafar@zums.ac.ir

F. Mozafari · H. Rashidzadeh · A. Ramazani · H. Danafar
Cancer Gene Therapy Research Center, Zanjan University of Medical Sciences, Zanjan, Iran

M. Barsbay · M. Ghaffarlou
Department of Chemistry, Hacettepe University, Beytepe, Ankara 06800, Turkey

M. Salehiabar
ERNAM—Nanotechnology Research and Application Center, Erciyes University, Kayseri 38039, Turkey

G. Niraula · S. K. Sharma
Department of Physics, Federal University of Maranhao, Sao Luis, MA 65080-805, Brazil

S. K. Sharma
Department of Physics, Central University of Punjab, Bathinda 151401, India

S. K. Sharma et al. (eds.), *Harnessing Materials for X-ray Based Cancer Therapy and Imaging*, Nanomedicine and Nanotoxicology,
https://doi.org/10.1007/978-3-031-04071-9_6

the framework of these criteria, this chapter summarizes some exciting advances in protection of normal tissue from inevitable radiation during RT by multifunctional nanomaterials. In addition, this review highlights an outlook of nanomaterial designs for potential radioprotection applications and also discusses the challenges followed.

Keywords Radioprotection · Radiotherapy · Nanomaterials · Healthy tissue · Ionizing radiation

1 Introduction

Radiotherapy is one of the most common (more than 50%) treatments for cancer patients. It exploits high-energy radiations that generate ions to destroy tumor cells [1, 2]. But like any other treatment, it has its drawbacks; nearby healthy tissues are also damaged. Serious side effects occur by damaging healthy tissue [3], so there is an urge to shield healthy cells; that's where radioprotectors come into play. Molecular radioprotectors are mostly organic and insoluble in water. They have a short half-life, short circulation time and fast metabolism. Therefore, these organic molecules are not as efficient as expected [4, 5]. As promising drug delivery tools to overcome the mentioned challenges, nanocarriers can be utilized to increase blood circulation time and molecule stability to enhance bioavailability [6]. Thus, it is advantageous to use a carrier to achieve a higher bioavailability [7–9]. As a paradigm, poly(lactide-*co*-glycolide) (PLGA) microspheres loaded with a radioprotector demonstrate improved stability and slower drug release, giving higher radioprotection efficacy to PLGA-drug-loaded nanosystems compared to bare drug [10]. Meanwhile, novel radioprotectors should be considered as a great substitute for conventional molecular radioprotectors.

Nanocarriers may be intrinsically radioprotective -called multifunctional nanomaterials- or they may carry molecular radioprotectors and indirectly help radioprotection. For instance, modified C_{60} fullerene nanomaterials can scavenge radiation-induced free radicals and protect healthy tissue from radical-mediated damages. Thus, nanosystems can serve radioprotection of healthy tissue directly or indirectly [11]. In this context, nanoradioprotectors are potential substitutes for conventional radioprotective drugs as they exhibit better characteristics. Beside these advantages, if the nanomaterial itself can function as a radioproctective agent, then the superiority of the system would be undeniable.

2 Delivery of Molecular Radioprotectors by Nanocarriers

Molecular radioprotectors utilize different cardinal mechanisms to defend healthy tissue. They can scavenge free radicals, prevent DNA double strand damage, improve DNA repair or cause hypoxia in normal cells. Some of these molecules are widely

used in clinical practice, such as amifostine. Curcumin, methylproamine, and sesamol are examples of molecular radioprotectors that use different mechanisms for radioprotection; that is, by scavenging free radicals [10], preventing double-strand DNA (dsDNA) break and improving DNA repair [12], respectively. Amifostine employs all of the above mechanisms [13] but other molecules may use only one of the mechanisms to become a radioprotector. The therapeutic efficacy of these molecules cannot reach to its potential because of their natural counter-effect in the body, water insolubility, fast metabolism rate and short half-life. To overcome this problem, nanotechnology can intervene. Biocompatible nanomaterials with high drug loading capacity provide better stability, higher drug circulation time, attenuated metabolism rate and eventually a controlled release feature. Thus, improved bioavailability and efficacy can be achieved by using nanomaterials as nanocarriers for molecular radioprotectors.

2.1 Organic Polymeric Carriers

Biodegradability is a major advantage of such carriers, making them the most frequently used carrier for different molecular radioprotectors, as demonstrated in case of oral controlled delivery of amifostine by biodegradable PLGA microcapsules [4, 5, 10]. PLGA nanocarriers in particular are in the center of focus due to the biodegradability of PLGA. After loading the PLGA microspheres with **curcumin**, the stability of this radioprotector was increased, its release was prolonged, and the overall radioprotective efficacy of curcumin increased [10]. When PLGA nanocarriers were administered orally 1 h before exposure to gamma radiation, PLGA-loaded **amifostine-**nanoparticles appeared to significantly promote jejunal crypt cell survival and hematopoietic progenitor cell survival for 30 days compared to the untreated group [14]. Morover, in another study, oral administration (1 h before radiation exposure) of PLGA nanoparticles loaded with N-(2-mercaptoethyl)1,3-diaminopropane (**WR1065**) were able to remarkably attenuate bone marrow suppression, increase survival over 30 days, and decrease intestinal damages. As an active metabolite of amifostine, WR1065 is widely employed in cancer radiotherapy to protect untransformed cells [15]. **Potassium iodide** and **penicillamine**, conventional radioprotective drugs, were loaded separately on PLGA nanoparticles, resulting in longer circulation in blood and improved efficacy compared to implementation of the same dose of free drug in gamma-exposed mice [16]. Chitosan, a natural, biocompatible and non-toxic polymer, was designed as a nanocarrier for **ferulic acid**, a radioprotective agent, to improve its circulation time [15]. **Green tea polyphenols** have been proved to alleviate post-radiation injuries in several experiments. Three-day oral pretreatment with Bovine serum albumin-Green tea polyphenol-Chitosan Nanoparticles (BGCN) significantly mitigated gamma-radiation-induced mortality in mice, Fig. 1 [17]. According to pathological data, BGCN also caused increased cell count of bone marrow, hematological parameters and spleen index in irradiated mice. Furthermore, BGCN plays a role in attenuating the unbalance of the intracellular redox system following radiation exposure resulting from the green tea polyphenol's

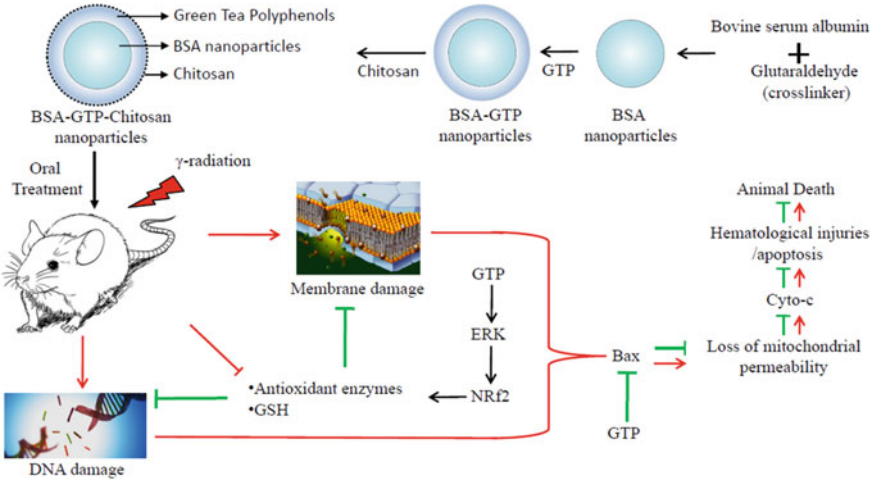

Fig. 1 Fabrication of BSA-green tea polyphenols-chitosan nanoparticles and its role in radioprotection. Reproduced with permission from Ref. [17]. Copyright 2016, with permission from ACS

ability to affect Nrf2-ERK pathway, reduce Bax expression, and consequently alleviate oxidative stress damage as well as restoring cell's redox balance. Finally, it is noteworthy that chitosan can improve bioavailability of molecular radioprotective drugs, as radioprotective efficacy of BGCNs is greater than that of free green tea polyphenols, Fig. 2.

Solid lipid nanoparticles (SLNs) can also encapsulate and deliver these molecules, such as trans-resveratrol (RVL) [5]. SLNs can significantly increase the solubility, blood circulation time, and radioprotection and antioxidant ability of RVL compared to the group that received RVL without any carrier.

Du and colleagues developed novel versatile theranostics based on poly(vinylpyrollidone)- and selenocysteine-modified Bi_2Se_3 nanoparticles (PVP-Bi_2Se_3@Sec NPs) to enhance radiotherapy efficacy of tumors while promoting the radioprotection of healthy tissues. In vivo results indicated that the radioprotection of the developed system was dependent on the release of selenium moiety and its entry into the bloodstream [18]. Nosrati et al. fabricated Bi_2S_3–Au hybrid nanoparticles containing methotrexate (MTX) and curcumin (CUR) for complete ablation of tumors. Due to the presence of CUR as a component of designed hybrid system, the fabricated nanoparticles not only served as nutritional supplement for chemotherapy, but also displayed a key role in radioprotection of healthy cells [19]. This research group also exploited radioprotective effect of CUR-conjugated BSA nanoparticles. It was found that the fabricated nanoparticles could serve as proficient carriers to promote the potential radioprotective effect of CUR [20]. Lagoda et al. exploited the radioprotective efficiency of sugar-containing compounds. In this context condensation products of thiol-containing hydrazides with mono- and

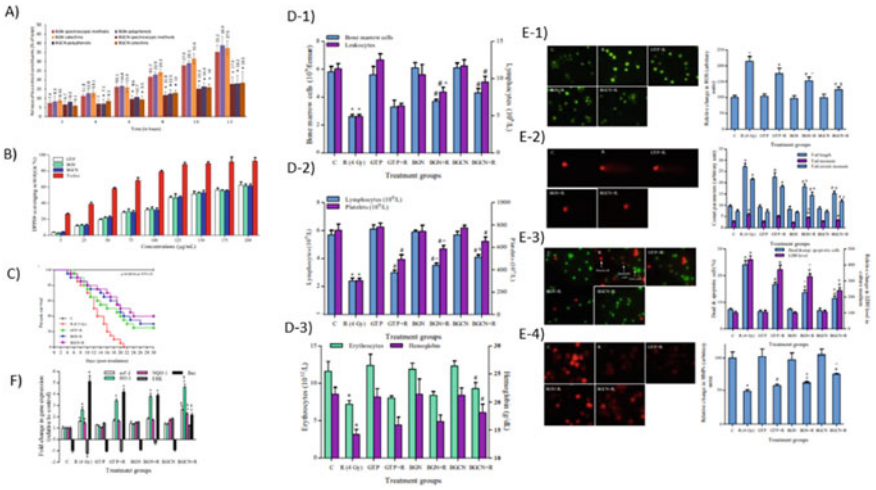

Fig. 2 **a)** Sustained release polyphenols and stability in PBS (PH = 7.4). **b)** Free radical scavenging activity. DPPH scavenging activity of BGCN, green tea polyphenols (GTP) and BGN. **c)** Effect of BGCN, green tea polyphenols (GTP) and BGN on survival rate. **D-1)** Bone marrow cell count in peripheral blood. **D-2)** Lymphocytes and platelets count. **D-3)** Erythrocytes count and hemoglobin content. **E-1)** Reactive oxygen species (ROS), **E-2)** DNA damage, **E-3)** Apoptosis and **E-4)** mitochondrial membrane potential (MMP) in splenocytes of irradiated mice. **F)** Effect of BGCN, BGN and GTP on the mRNA expression of NQO-1, HO-1, nrf-2, ERK and Bax. Reproducedwith permission from Ref. [17]. Copyright 2016, with permission from ACS

disaccharides were fabricated. Results showed that implementation of monosaccharides D-glucose-thioglycolic and D-maltose-thiosalicylic preparations promoted the survival rate of lethally irradiated animals by 25% when administered 1 h before irradiation, and 40% when administered 24 h before irradiation [21]. Liu et al. fabricated polymeric nanoparticles based on WR-1065 loaded PEG-PCL conjugated CUR as an efficient carrier for co-delivery of CUR and WR-1065 (the active ingredient of amifostine) and investigated its potential synergistic radioprotection capability. In vivo results revealed that the developed polymeric nanosystem exhibited great radioprotective activity on the hematopoietic system and prevented intestinal injury. Interestingly, all mice survived after exposure to the half-lethal dose (7.2 Gy) of total body irradiation for time periods of 30 days [22].

2.2 Inorganic Carriers

In recent years, several inorganic carriers have been employed and have exhibited promising results. As an example, melanin, an insoluble radioprotective pigment, was loaded into silica nanoparticles. To ensure their radioprotective properties, melanin precursors were polymerized and decorated on the surface of silica nanoparticles

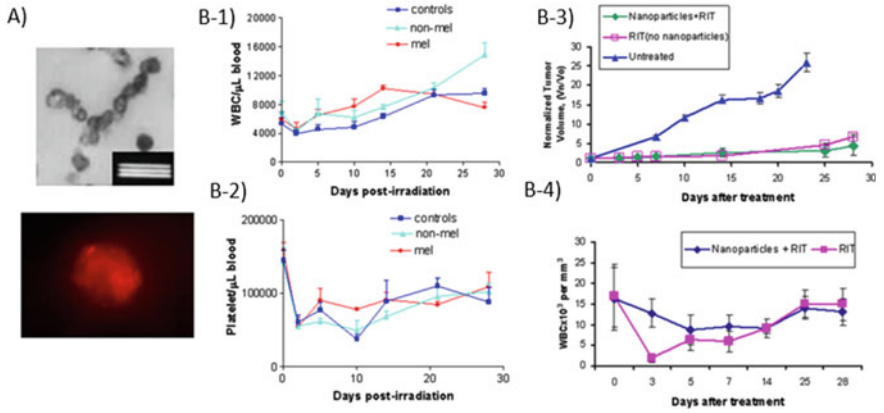

Fig. 3 **a)** TEM (Transmission electron microscopy) (up) and immunofluorescence (down) image of MNs (melanin-covered nanoparticles) made with L-DOPA. The bar is 200 nm. **b)** Shielding effects of MNs on the bone marrow of mice during whole-body irradiation and radioimmunotherapy (RIT). **b-1)** WBC and **b-2)** platelet counts for CD-1 mice irradiated with 125 cGy. **b-3)** Change of tumor volume and **b-4)** WBC count after RIT in nude mice bearing A2058 melanoma tumors pretreated with MNs. Reproduced with permission from Ref. [23]. Copyright 2010, with permission from Elsevier

for IV administration. These melanin-covered nanoparticles minimized hematological toxicity and showed no protection against tumor cells in mice exposed to external beam radiation or undergone radio-immunotherapy (Fig. 3) [23]. Melanin-silica nanoparticles inhibited radical formation and consequently protected the bone marrow from ionizing radiation. Glycyrrhizic acid (known as a radioprotector) was complexed with silver nanoparticles (SN-GLY), which was also employed in mice for radioprotection before/after exposure to ionizing radiation. The nanoparticles were effective when administered orally both before and after irradiation by accelerating DNA repair, demonstrated by micronucleus formation and reduction of chromosomal aberrations [24–26].

Silver nanoparticles were also exploited by Chandrasekharan et al. to deliver another radioprotector, PasAG (6-palmitoyl ascorbic acid-2-glucoside), which is a vitamin C derivative. PAsAG-silver nanoparticles (SN-PAsAG complex) were demonstrated to protect DNA as shown in comet assay during ex-vivo, in vivo and in vitro irradiation following oral administration. The complex with promising radioprotection enhanced radiation-induced DNA breakage in various tissues and DNA repair [27]. To enhance the radioprotective properties of curcumin and increase its cancer therapeutic efficacy through synergistic therapy and radioprotection of healthy cells, Xie et al. tailored curcumin to BCNP-TPGS (bamboo charcoal nanoparticles-D-α-tocopherol polyethylene glycol 1000 succinate) and consequently effectively alleviated DNA damage in HUVECs (human umbilical vein endothelial cells) following radiation. Curcumin is known for its shortcomings, such as low solubility in water, high metabolism, and being a P-gp substrate, which limit its application in biomedicine. TPGS was functionalized with bamboo charcoal, which responds

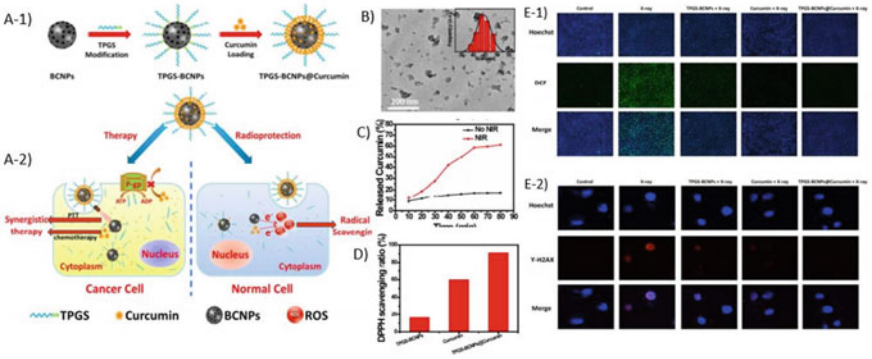

Fig. 4 **a-1)** Schematic illustration of loading curcumin onto functionalized TPGS with BCNPs. **a-2)** Utilizing TPGS-BCNPs@Curcumin as a multifunctional delivery system for synergic therapy of cancer cells and protecting normal tissue from ionizing radiation at the same time. **b)** TEM image and DLS analysis of size distribution (inset). **c)** Curcumin release from TPGS-BCNPs@Curcumin in ethanol media (60%) with or without NIR laser radiation. **d)** Radical scavenging ratio. **e-1)** Fluorescence images of HUVEC intracellular ROS and **e-2)** confocal fluorescence images of HUVEC cells DNA fragmentation after different treatments. Reproduced with permission from Ref. [28]. Copyright 2017, with permission from ACS

to NIR radiation (808 nm) and generates heat as a result. NIR-triggered heat generated by bamboo charcoal nanoparticles promotes radioprotector release from TPGS-BCNP@Curcumin. The rapid and significant release of curcumin after NIR exposure is due to attenuated drug-vehicle interaction, which is a consequence of the heat generated by TPGS-BCNPs. The nanocarrier (TPGS), which considerably increased drug accumulation in cancer cells due to its size, triggered drug release and inhibited the P-gp efflux pomp. Both curcumin and BCNP (carbon materials such as graphene and carbon nanotubes scavenge free radicals) have been used in the structure of this mesoporous nanoparticles for their radical scavenging ability and protecting normal tissue (Fig. 4) [28].

Cao et al. fabricated metal–organic frameworks (MOFs) for the co-delivery of radioprotective agents. In this regard, they developed a novel nanovehicle based on MIL-101(Fe) and containing both glutathione (GSH) and WR-1065. Afterwards, the prepared nanoparticles were decorated with PEG moieties to enhance stability and permeability. The results showed that modification with PEG promoted the radioprotection properties of MIL-101(Fe) nanoparticles. Moreover, both in vitro and in vivo results indicated that the developed MOF-based radioprotector could potentially improve cell viability through scavenging accumulated ROS and resisting DNA damage after irradiation. Additionally, these systems could ameliorate the hematopoietic injury of mice caused by radiation [29]. Similarly, this group also produced MIL-101(Cr) nanoparticles decorated with PEG chains for hematopoietic radioprotection. In conclusion, inorganic nanocarriers can be counted as promising tools for the delivery of molecular radioprotectors to ameliorate their bioavailability and thus their efficacy in radioprotection.

3 Nanoradioprotectors

Nanomaterials are widely used as carriers for radioprotective molecules. In addition to their ability to roleplay as carriers, multifunctional nanomaterials with intrinsic radioprotective characteristic are endowed with the ability to circulate longer in blood stream due to their lower metabolism rate, in contrast to molecular radioprotectors. Thus the term 'nanoradioprotectors' indicates specific multifunctional nanoparticles with radioprotective nature, also called new generation of radioprotectors [30].

3.1 Principle

Regarding the rational comprehension of the design of nanoradioprotectors, there is an impulse to discern the destructive mechanisms of ionizing radiation to the cells. There are two ways in which the radiation can damage healthy tissue: it can directly damage DNA or indirectly damage macromolecules and cell structure by generating excessive amounts of ROS through water decomposition, ultimately leading to cell dysfunction and death [31, 32, 35, 34]. Discussing the indirect pathway in greater depth, radiation interacts with water molecules, which ultimately generates ROS and strongly damages cell macromolecules including RNA, DNA, protein, cell membrane and other cell constitutions. DNA damage, macromolecular impairment, and cellular organization disruption all together lead to the transformation of healthy cells into dysfunctional, dead cells. Assuming that 60% of the total body weight is composed of water, it can be concluded that the indirect pathway involves major damage caused by irradiation [33, 34, 35, 36]. Therefore, the most common principle pursued in nanoradioprotector design is based on the free radical scavenging ability of nanomaterials. By neutralizing ROS, the goal of decreasing damage to normal cells as a result of free radical production can be achieved.

The common nanoradioprotectors

The discussion in the following section will focus on the development of various nanosized radioprotectors, including carbon-based, cerium-based and noble metal nanoradioprotectors.

Carbon-based nanoradioprotectors

The most widely investigated and cutting-edge carbon-based nanomaterials for radiation protection, along with their mechanisms and applications, are discussed below.

3.2 Based on C_{60} Fullerene

Fullerenes, a category of molecules with a spherical structure, are composed of sp^2 carbon atoms, where each carbon is directly bonded to three other carbons, forming a hollow cage construction in an arrangement of five- and six-carbon rings. Since their discovery in 1985, C_{60} has been widely investigated due to its I_h-symmetrical structure [37]. Among fullerenes, C_{60} can be reduced 6 times reversibly [38], but in practice this cannot happen. Pristine Fullerenes, the only soluble form of carbon [39], exhibit very low solubility in water [40] due to their highly hydrophobic properties. Medical applications of fullerenes have been limited by their cytotoxicity due to their poor solubility in water which is generally associated with elevated toxicity of substance. Although singlet oxygen toxicity leading to membrane damage and cell death was observed in C_{60} aqueous solution, no toxic effects were observed in Chinese-hamster V79 cells following administration of C_{60} aqueous solution [41]. Cytotoxicity, which may be necessary as in cancer therapy, was magnified over 7 orders by decreasing exohedral functionalization [42]. The addition of polar, hydrophilic groups capable of forming hydrogen binding to fullerenes is necessary to achieve medicinal application of fullerenes. Streaming blood consists mainly of water in which drugs are administered intravenously to be delivered [43]. Because water solubility causes reduced recognition of fullerenes as foreign bodies by the immune system, and higher drug solubility in the blood leads to a longer retention time of fullerenes [44]. A number of water solubilizing methods of fullerenes were discussed by *Rašović et al.*, such as covalent functionalization including exohedral (amination, hydrohylation, prato and bingel reaction) and endohedral functionalization, encapsulation in water soluble carriers, and incorporation of fullerenes into water-soluble polymers [44]. Due to the lack of substantial functional groups, previous C_{60}-based vectors were solubilized in organic solvents, leading to undesired cytotoxicity. Therefore, in response to the need for a safer transfection vector for DNA, 6 new C_{60} fullerene derivatives were synthetized in 2008 in order to be used as non-viral vectors for gene delivery [45]. Based on the evidence, lipid peroxidation was halted by C_{60} after radical initiation. Additionally, C_{60} could act as a liposolube antioxidant with potency equal to or greater than that of vit E. The antioxidant ability of these compounds is related to the number of their reactive sites [46]. C_{60} fullerene was coupled with solubilizing agents with different types of linkages to form water-soluble C_{60} derivatives. Depending on their surface functional groups and interactions with the cells, neuroprotection effect in neural stem cell or antitumor activity in glioma cells was seen by depleting or increasing ROS, respectively. Moreover, in zebrafish, CNS damage could be rescued without tumor growth, and glioblastoma formation was attenuated without slowing neural repair [47].

Biocompatible fullerenes such as water-soluble C60-PEG conjugates and fulleropeptides were synthetized in 2014 [48]. Special chemical properties, including the large number of π –conjugated bonds and the LUMO that endows them with the ability of easily reacting with electrophiles, make them superior candidates for radioprotection, as irradiation leads to free radical production, a nucleophile. Thus, free

radicals formed in a radiolysis study can easily react with fullerenes [49]. Fullerenes are capable of scavenging ROS effectively. As antioxidants, water-soluble fullerene derivatives are counted as potential candidates as they provide proper bioavailability [50]. The ability to quench free radicals makes fullerenes a good candidate for radioprotection in addition to being an antioxidant. Due to ROS scavenging ability, water-soluble derivatives of C_{60} have attracted considerable attention among others. Most of the studies reporting the radioprotective ability of water-soluble C_{60} derivatives have focused on fullerenols and DF-1 (dendro-C_{60}-(fullerene)-1). Thus, these two types of C_{60} derivatives will be reviewed mainly in the following sections. In brief, it should be noted that fullerenes are insoluble in water, but can be dissolve in aqueous media when functionalized with suitable groups. Also, organofullerens can biologically interact with living cells, proteins and DNA, and quench free radicals [51]. Besides being a promising antioxidant, fullerenes can be exploited for HIV-1 protease inhibition, PDT and chemotherapy. In 1993, a water soluble fullerene derivative with an inhibitory effect on HIV 1 protease, as the hydrophobic, spherical-shaped fullerene core that could interact with the receptor site of the enzyme, was designed and investigated [52]. In 2002, C_{60} was functionalized by diphosphonate group to target bone mineralized tissue [53]. Fullerenes can also be used for drug delivery and thus play a multifunctional role. As an example, paclitaxel can be conjugated with fullerene, which slows paclitaxel release from aerosol liposome and demonstrates a significant cytotoxicity in human epithelial lung carcinoma A549 cells [54].

PHF (polyhydroxyl fullerenes, fullerenols or fullerol) such as C_{60} $(OH)_{24}$ is both water-soluble and biodegradable and thereby desirable for application in biological environments, making fullerenols potential radioprotectors. Fullerenols may also contain other oxygen groups ($C_n(OH)_XO_Y$) or salt-typed groups ($C_n(OH)_XO_Y](ONa)_Z$). An excellent review on the physicochemical properties and applications of PHF is covered by Semenov et al. [55]. Hydroxylated fullerenol ($C_{60}(OH)_{30}$) is well tolerated after IV administration of these water-soluble carbon nanoparticles, as evidenced by histology, blood and urine chemical analysis in female rats [56]. Fullerenols were first described as an antioxidant in ROS-induced injuries such as reversible in vitro hippocampus injury [57], small bowel transplantation in dogs [58] and in vivo ischemia–reperfusion of the intestines in dogs [59]. Recently the antioxidant effect of C_{60} $(OH)_{24}$ has been shown to be associated with Nrf2-induced enhanced expression of antioxidants in phase 2. Nrf2 binds to antioxidant response element and regulates gene expression of several anti-oxidants. Translocation of Nrf2 as a crucial factor for defending against oxidative stress can be enhanced to increase the phase 2 antioxidant expression in A549 cells. P38 MAPK, extracellular signal-regulated kinases, and c-Jun-N-terminal kinase phosphorylation were the results of C_{60} $(OH)_{24}$ treatment. Pre-trearment of A549 with specific P38 MAPK inhibitor (SB203580) halted Nrf2 translocation and enhanced fullerenol-induced HO-1 expression, indicating p38 MAPK pathway involvement in Nrf2/HO-1 activation by fullerenol. This result is in line with diminished protective effect of $C_{60}(OH)_{24}$ as a result of Nrf2 knock-down by si-RNA. Furthermore, hydrogen

peroxide-induced A549 apoptosis was attenuated as a result of fullerenol pretreatment. On the contrary, fullerenol was found cytotoxic in mili-molar concentration ranges [60].

Fullerenols are considered potent ROS scavengers, as experimented in small bowel transplantation. Since there are numerous studies investigating the radioprotective properties of fullerenols, the researchers compared efficiency of amifostine, an FDA-approved radioprotector, with fullerenols to provide a view of their clinical application. The performance of $C_{60}(OH)_{24}$ and amifostine in radiation protection was compared with each other by evaluating survival rate and body mass gain for 30 days. The whole body of the rat was irradiated by lethal dose of X-ray (8 Gy) and animals were pretreated with aforementioned radioprotectors 30 min before exposure. The same procedure was performed for an X-ray dose of 7 Gy to evaluate the protection of healthy tissue and the impact of ionizing radiation on hematopoiesis (by histopathological analysis) and blood cell count, respectively. Overall, 100 mg/kg of fullerenol manifested better radioprotection than that of 10 mg/kg dosage, which was comparable to the effect of amifostine (300 mg/kg). While fullerenol provided better protection against WBC count, both radioprotectors showed promising results in different organs. According to the results of pathophysiology research, amifostine showed better protection for heart, kidney and liver, while fullerenol performed better in the small intestine, spleen and lung. The overall results of fullerenol radioprotection was satisfactory and comparable to amifostine [61].

The radioprotective activity of fullerenol ($C_{60}(OH)_{24}$) was also investigated in whole body irradiation in mice. Based on these results, the radioprotective ability of fullerene was found to be dependent on its concentration. An i.p injection of 100 mg/kg fullerene showed satisfactory effect on rats irradiated 30 min prior to exposure, while 10 mg/kg fullerene showed little protection and even intensified irradiation detrimental effects. Therefore, when appropriate concentration and radiation dose are applied, $C_{60}(OH)_{24}$ can be recommended as a good radioprotector [62]. Later in vitro radioprotection efficiency of $C_{60}(OH)_{24}$ against X-rays on human erythroleukemia cell line (K562) was also investigated. Pretreatment with fullerenol significantly increased cell count and antioxidative enzymes activity (SOD and GPX) against X-ray-induced oxidative damage to the cell, while decreasing GGT(γ-glutamyltransferase) in exposed cells [63]. In a study conducted by Cai *et al.* in 2010, animals were treated for 2 weeks before whole body γ-irradiation (lethal dose). Pretreatment with fullerenol (a daily IP injection of 40 mg/kg fullerene) could effectively reduce irradiation-induced mortality, defend liver and spleen, and significantly protect the immune system and mitochondrial dysfunction [11].

High polarity, electron affinity and reactivity with nucleophiles and free radicals, which are required for good radioprotectors, are noteworthy properties of water soluble fullerenes, as proved by radiolysis studies of fullerene and hydroxyl radicals in case of highly hydroxylated fullerene ($C_{60}(OH)_{36}$) [49]. The radioprotection properties of C_{60} fullerenols ($C_{60}(OH)_x$,x = 18–22) was studied by Zhao *et al.* in 2005 on *stylonychia mytilus* cells (protozoan) exposed to γ-rays [64]. Radioprotection effectiveness was found to be dependent on γ-radiation dose and C_{60} derivative concentration. Increased survival fraction, improved catalase (CAT) and superoxide

dismutase (SOD) activity of liver, attenuated harmful MDA products (as a result of lipid peroxidation, MDA=malondialdehyde) and lipofusion were demonstrated at a fullerene concentration of 0.10 mg/mL, demonstrating effective radiation protection response. By increasing the irradiation dose (from 100 to 2000 Gy), cell line survival rate decreased. While fullerenols could enhance cell survival fraction, they were not able to protect the cells at the highest irradiation dose. Maximum protection was observed at the concentration of 0.10 mg/mL, while the cell survival fraction was less than that of the control sample at 0.25 mg/mL. Thus, at higher fullerenol concentration and irradiation dose, little radiation protection was observed. In this study, the radioprotection effect of fullerenol seemed to be (at least partially) mediated through radical scavenging and anti-oxidative properties [64]. Wang and colleagues developed a fullerenol@nano-montmorillonite (FNMT) nanocomposite as a potent radioprotective system to ameliorate duodenal injury caused by X-ray irradiation in radiation therapy. The results showed that the prepared nanocomposite could efficiently diminish DNA and mitochondrial damage as well as alleviating duodenum tissue pathological damage in mice by utilizing both nano-montmorillonite (NMMT) and fullerenol [65]. Zhao *et al.* synthesized scalable and eco-friendly synthesis method of fullerenols for efficient radioprotection of skin. Fullerenols have been shown to acts as radioprotectant agents due to their high free radical scavenging capability. *In vitro* experiments showed that these nanosized radioprotectors could notably block the ROS-induced damage and promote the viability of irradiated human keratinocyte cells. Additionally, in vivo results revealed that medical sodium hyaluronate hydrogels containing fullerenols are applicable for skin administration and remarkably mitigate radiodermatitis by protecting epidermal stem cells meritoriously [66].

Synthesis of dendritic fullerene (C_{60} mono-adduct) by Bingel reaction showed the highest water solubility (12 mM), which signifies utilizing dendritic decoration to represent numerous polar groups instead of adding many similar polar groups [44, 67]. For effective superoxide scavenging, lower doses of first and second generation of dendrofullerens (than C_3 and D_3) are required, possibly confirming that the antioxidant ability of mono-adducts is better due to the more intact conjugation system [68].

In another study (2006), zebrafish embryos were used to evaluate the radioprotective ability of DF-1 nanoparticles (containing 18 carboxyl groups) and the results were compared with amifostine radioprotection. Amifostine protection of zebrafish and human embryos were previously demonstrated by McAleer *et al.* [69]. The studied fullerene had no toxic effect on the morphology and survival of embryos less than 1000 μM/L. Neurotoxicity, impaired excretion (kidney defect), diminished survival of irradiate embryos, and defective development of the midline (resulting in curly-up) were observed when embryos were irradiated (10–40 Gy) without any radioprotection. At a concentration of 100 μM/L, DF-1 could significantly attenuate toxicity when administered 3 h before to 15 min after exposure, but no protection was observed when given 30 min after exposure. DF-1 protection against the lethal effects of irradiation is associated with significant omission of ionizing radiation-induced ROS, in which irradiated embryos were not distinguished from non-irradiated controls. DF-1 (100 μM/L) could alleviate radiation toxicity in an

in vivo model of the zebrafish embryo, similar to the FDA-approved radioprotector, amifostine (4 mM/L) [70].

Zebrafish (*Danio rerio*), as a vertebrate, is suitable for testing therapeutic agents (radiosensitizers or radioprotectors) because of its easy accessibility, genetic similarity to human and optical clarity of organs [69]. In 2010, in vitro protection of DF-1 nanoparticles along with its uptake by the cell was investigated at the genetic level. DF-1 was administered in mice crypt cells and human lymphocyte cells, two mammalian cell lines relatively sensitive to irradiation, and protected them by intrinsic antioxidant properties and attenuating free radical level. While DF-1 exhibited no toxicity for both cell lines (in biological dose ranges), it was more effective at scavenging radicals at a concentration ten-fold less than amifostine. The micronucleus is the condensed chromosomal fraction seen as extra cellular bodies formed through cell division and known as reliable markers for radiation induced damage [71]. The presence of DF-1 resulted in attenuated micronucleus formation, protection of cells from DNA damage or enhanced DNA repair and increased cell viability in both cell lines [72]. Consequently, DF-1 was rated as a promising radioprotector.

Despite lack of specificity, fullerene hydroxylation is a very popular solubilization method. Carboxylic acid C_{60} derivatives were able to inhibit the death of cultured neurons when exposed to excitotoxic materials. They could also postpone death and functional deterioration in transgenic mice carrying the human mutant (G93A), the superoxide dismutase gene responsible for a type of familial amyotrophic lateral sclerosis. This study suggested that these polar derivatives could be a neuroprotective agent in neurodegenerative diseases; acute or chronic [73]. Besides the chemical modification of fullerenes, the antioxidant and radioprotective properties of the hydrated form of pristine fullerene C_{60} were investigated. The aqueous solution of C_{60} donor–acceptor complex with H_2O ($C_{60}@(H_20)$ n, n = 22–24) manifested strong hydroxyl radical scavenging properties, inversely correlated with fullerene concentration in the tested concentration range (10^{-11}–10^{-6} M). The anti-radical effect of fullerene was due to a non-stoichiometric mechanism. In the 10^{-7}–10^{-6} concentration range, the protective effect of fullerene on nucleic acids from hydroxyl radicals in aqueous solution was evident thanks to the DNA oxidative marker, 8-oxoguanine. Significantly prolonged lifespan of whole body-irradiated mice (lethally, 7 Gy) was observed with fullerene IP administration (1 mg/kg, 1 h prior to exposure). The In vivo protective effect of fullerene was determined by its considerable ROS scavenging ability. High efficacy at low doses and non-toxicity in the hydrated form makes the hydrated C_{60} a considerable novel radioprotector. It is noteworthy that the fullerene structure is stable after irradiation and the supermolecule withstand radical effects and shows long-lasting antiradical properties [74].

3.3 Based on Graphene and CNT

This group of nanoradioprotectors are capable of neutralizing free radicals due to their special chemical structure [75]. Thus, it can be inferred that these structures

could be promising nanoprotectives that could be used either in the development of therapeutic agents or in radiation protection through occupational procedures. Two dimensional nanomaterials, graphene and derivatives, provide very high surface area to scavenge free radicals. Graphene and CNTs are similar except that if a graphene sheet is rolled into a cylinder shape, a CNT is formed in which the carbons are in hexagonal arrangement [76]. Graphene, as a few atomic layers of graphite, has drawn a lot of attention due to its special characteristics such as strong electrical field [77]. Carbon nanotubes (CNT) can have single-, double- or multiple walls or form nanofibers. Due to the outstanding superiority of single-walled carbon nanotubes (SWCNTs) over multi-walled ones (MWCNTs), such as high electrical conductivity, high capacity to carry electrone and structural uniformity, SWCNTs can be employed in electrodes. SWCNTs possess unique electrical properties as they can carry 10^9 amp/cm^2 electrons, which is higher than copper or gold capacity [78, 79]. CNTs can either be pristine or functionalized depending on their functional groups. By functionalizing SWCNTs, they may also be eligible to be applied in medical approaches. It has been demonstrated that functionalized SWCNTs can increase the population of irradiated survived crypt cells of the rat small intestine. In an in vivo experiment, the alleviative effect of SWCNTs was demonstrated on radiation-induced severe curling in zebrafish. They were also able to protect against occupational hazards caused by irradiation [80]. SWCNTs, whose potential ability was modelled by density functional calculations, showed to be free radical sponge for hydroxyl radicals, the most dangerous and reactive radical species. The properties of CNTs can be manipulated by controlling the OH proportion on the nanotubes [81]. It was evident that the electron transfer reaction of ultrashort SWCNTs was dependent on the nature of CNTs and properties of free radicals. [82]. In 2010, MWCNTs were covalently grafted with gallic acid (an anti-oxidant polyphenol) by Cirillo *et al.*, which further demonstrated good antioxidant and radical scavenging ability in vitro. In contrast to pristine CNTs, GA-CNTs inhibited lipid peroxidation and exhibited good hydroxyl radical neutralizing ability while tests demonstrated its biocompatibility [83]. Many studies have investigated the reduced toxicity of CNTs by preparing water-soluble derivatives of CNTs. Gallic acid has been found to be a free radical scavenger and a cell protector from radiation-induced damage [84]. MWCNTs were functionalized with fundamental amino-acids as well, including lysine, arginine, cysteine, histidine, and aspartic acid, which escalated their antioxidant ability and water dispersity, noting that each pristine MWCNTs and amino acids are good antioxidants themselves [85].

Graphene-based nanomaterials protected target molecules from oxidation by effectively scavenging free radicals such as hydroxyl radicals. Despite their lower surface area, few layers of graphene showed more radical scavenging activity compared to monolayer graphene oxide (GO), because the radical scavenging sites are carbons with sp^2 network, not oxygen-containing functional groups. It has also been demonstrated that TiO_2 nanoparticle encapsulation by graphene can reduce photo-oxidative damage by UV, suggesting a new approach for managing the redox state of the cell environment [86].

Due to expensive preparation method of graphene [87, 88], graphene oxide (GO) has been chosen as an alternative to be processed to graphene-like materials. While

GO shows semi-conductivity depending on temperature, its conductivity can be increased by 10,000 fold using various reduction methods [89]. GO can also be employed for catalytic oxidation and in the field of biotechnology [90, 91, 92, 93]. Interestingly, it has been proved that GO can be considered as an effective radioprotector at low concentration (10 μg/mL) and X-ray intensity (1.25 Gy). Because GO effectively scavenges ROS, it reduces X-ray-induced DNA damage and cell apoptosis in healthy human fibroblast cells, while at higher concentration (500, 100 μg/mL) it causes higher DNA damage and cell death (apoptosis) by 48% and 39%, respectively (Fig. 5) [94].

Graphene-encapsulated metal nanoshields (M@C, M = Fe, CoNi, Co, Ni, FeNi) were introduced in 2018 to serve as nanoradioprotector. Radioprotection principle and mechanism of these nanomaterials are as followed.

Inorganic chemistry is mainly on the basis of electron transfer in chemical reactions. These nanohybrids catalyze the neutralizing reactions of · OH, H_2O_2 and · O^{2-} radicals through extensive electrolytic activity. These reactions involve electron transfers between encapsulated metals and the single layer graphene. Thus, these nanohybrids can consume the excessive ROS produced as a result of high

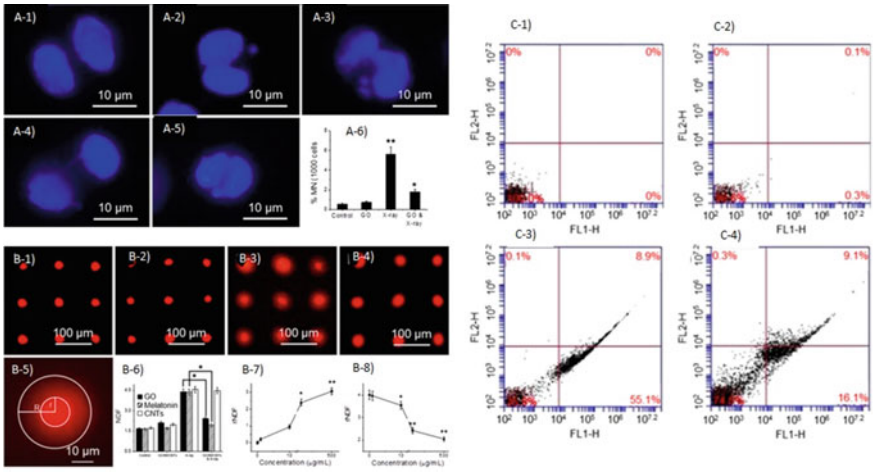

Fig. 5 Fluorescence images of X-ray irradiated binucleutid fibroblast cells with 0 (**a-1**), 1 (**a-2**), 2 (**a-3**) micronucleus, a neoplasmic bridge (NPB) (**a-4**) and a nuclear bud (NBUD) (**a-5**). Micronucleus appearance frequency where cells are arrested at stage of inter-phase (**a-6**). **b-1)** Fluorescent images of arrayed cells. Halo assay for assessing cell genotoxicity when **b-2)** treated with 10 μg/mL GO, **b-3)** exposed to X-ray (1.25 Gy), **b-4)** pre-treated with GO and exposed to X-ray (1.25 Gy), **b-5)** enlarged image of halo and nucleus. **b-6)** NDF values of cells after different treatment, the rNDF values of cells treated with different concentration of GO **b-7)** without and **b-8)** with 1.25 Gy X-ray radiations. **c)** Cell flowcytometry for evaluating cell apoptosis of **c-1)** non-treated cells, **c-2)** GO-treated cells, **c-3)** X-ray irradiated cells, **c-4)** cells pre-treated with GO (10 μg/mL) and exposed to X-ray (1.25 Gy). Reproduced with permission from Ref. [94] with the permission of the Creative CommonsAttribution 4.0 International License (http://creativecommons.org/licenses/by/4.0/). Copyright 2014, MDPI

energy irradiation and manifest radioprotection. In case of specific redox reactions involving metals complex of metals, cyclic voltammetry can be applied for measuring and monitoring electron flow through electrochemical processes. For cyclic voltammetry simple guild for beginners, see [95]. Cyclic voltammograms show the current generated by electron flow between electrodes and redox molecules in the electrochemical cell medium, versus the applied potential (current = y, potential = x) [96]. The greater the electron flow in an electrochemical cell, the greater the current. To assess the electron flow in graphene-encapsulated metal nanoshields, cyclic voltammograms of GCE (glassy carbon electrodes) modified with Fe@C and CoNi@C were compared to that of unmodified GCE (glassy carbon electrodes are physically and chemically inert [97]) in an electrolyte medium riched with O_2•, H_2O_2 and O_3•. The reducing current density in the cyclic voltammetry diagram of Fe@C and CoNi@C-modified GCE had a sharp increase in comparison to unmodified GCE with an ignorable reduction in current density, indicating superior catalytic ability of graphene-encapsulated metal nanoparticles to convert ROS into O_2 and H_2O effectively. This demonstrates high potential of modified graphene's ability to protect healthy tissues against radiation. Density functional theory (DFT) was also employed to simulate the atomic perspective of the ROS scavenging catalytic process on the surface of CoNi@C and Fe@C. An in vitro study of Fe@C and CoNi@C ROS scavenging ability was performed on Chinese Hamster Ovary (CHO) cell line. After exposing to X-ray radiation, DNA damage was reduced and survival rate increased. In vivo pretreatment of Fe@C and CoNi@C in exposed C57BL/6 mice revealed alleviated cell apoptosis in intestine tissue, enhanced survival, increased SOD level and elevated total bone marrow DNA amount. To summarize, highly active graphene-encapsulated metallic nanoparticles containing Fe or CoNi as metal core manifested promising radioprotection by effective ROS scavenging [98].

3.4 Based on Cutting-Edge Carbon-Based Radioprotectors

Carbon-based nanoparticles (BCNPs) such as graphdiyne-BSA appear to be next promising candidates for radioprotection. Low cost and toxicity [98, 99], easy preparation, and proven ability to scavenge free radicals in radioprotection [28] are substantial characteristics of BCNPs. TPGS-BCNPs, another example of carbon-based nanoparticles, were applied to HUVECs cells (normal cells) to explore their properties in the context of radioprotection activity. The radioprotection results were promising as a reduction in DNA damage and a significant attenuation in intracellular radiation-induced ROS level were demonstrated.

Graphydiyne-BSA nanoparticles can potently quench intracellular ROS strongly by using their reactive diacetylen bonds and strong delocalized π bonds, which endow graphydiyne-BSA with significant radioprotective ability. According to the fluorescent signals of HUVECs cell line administered with graphydiyne-BSA NP

+ X-ray showed effective free radical scavenging (2′,7′-dichlorofluorescein (DCF) immunofluorescence images), decreased cellular DNA double-stand damage (γ-H2AX immunofluorescence images), and improved cell viability compared to the group treated only with X-rays. Animal studies indicated bone marrow DNA protection and normalized SOD and MDA levels in the liver of pretreated mice. Therefore, graphdiyne-BSA NPs can be considered as an ideal candidate to be employed for radioprotection [100].

Recently, Wang and colleagues investigated the potential features of clinically approved carbon nanoparticles for efficient radioprotection of intestinal crypt by maintaining the balance of the intestinal flora as well as protecting small intestinal crypt stem cells. Furthermore, these nanoparticles exhibited high ROS scavenging activities, successfully restricting the DNA double-strand breaks and mitochondrial dysfunction to protect cells against radiation-induced damage [101].

3.5 Cerium-Based Nanoradioprotectors

Cerium Oxide Nano Particles (CeONPs) were found to be flexible in terms of electron configuration with rapid change of valance state between Ce^{4+} and Ce^{3+} due to its enzymatic role or oxygen vacancies enabling cerium-based NPs to participate in the redox-coupled reaction. Because of their catalytic activities by losing their electron or oxygen atoms, they can mimic multi enzyme activity such as SOD, CAT and oxidase. This character ends up with neutralizing nearly all intracellular ROS, which makes it a potential candidate for radioprotection. In addition to their application in industry, biomedicine and bioscaffolding, interestingly, they can also be used for drug delivery [102].

Oxygen vacancies can induce mixed valance states of cerium on the surface of CeO NPs. Radioprotection of vacancy engineered CeONPs on tumor breast cancer cell line and normal cells was examined, showing 99% protection against irradiation for normal cells, while no protection was observed for MCF-7 cell line at the same concentration [103]. Therefore, these NPs have great potential to serve as radioprotectors while maintaining radiotherapy efficacy. CeONPs can also reduce immunological neurodegeneration associated with oxidative damage when administered IV in mice and can further penetrate the brain and finally reduce ROS level by switching between 3 + and 4 + valance states as reported in murine multiple sclerosis model. Thus, CeONPs may be efficient in reducing tissue damage caused by free radical accumulation in tissues [104].

The onset of high dose radiation-induced pneumonitis was prevented by radioprotection of CeONPs studied in murine animals. In vitro studies on normal lung fibroblast cells suggested increased cell viability, in line with results obtained from in vivo investigations. A visible pneumonitis associated with microphage invasion was evident in irradiated animals, while no visible pneumonitis was observed in the group treated with CeONPs. This study suggests a new way for protecting human

health from the harmful effects of radiotherapy with oxidized form of the rare earth element, cerium [105].

Also, pretreatment of normal human colon cells (CRL 1541) with CeO (24 h, single injection) could significantly decrease cell death in a dose-dependent manner by reducing the level of radiation-induced ROS and increasing SOD2 expression. Thus gastrointestinal epithelium could be effectively protected from radiation, as shown in murine colonic crypt case, where CeONPs (IP) can predominantly attenuate TUNEL (terminal deoxynucleotidyl transferase dUTP nick end labeling) and caspase 3-positive crypt cells in irradiated mice. CeO_2NPs could protect GI epithelial cells against radiation biohazard by scavenging free radicals and inducing SOD2 expression [106]. The radioprotection of citrate stabilized CeO_2 NPs results from 3 different mechanisms upon exposure to ionizing radiation; (i) chemically, the nanoparticles effectively reduce the level of hydroxyl radicals and hydrogen peroxide in the aqueous media, (ii) physically, they play the role of shielding against radiation, and (iii) biologically, they can regulate the expression of some antioxidant enzymes and proinflammatory cytokines as was indicated in vivo. Ultra-small citrate-stabilized nanoceria could remarkably increase primary mouse fibroblast cell viability in vitro, then decreased ROS level (high level of dehydrogenase activity) and improved survival of irradiated mice in vivo (cytogenetic damage to bone marrow was declined). These findings confirmed nanoceria protection at the molecular, cellular and organismal stages [107].

Despite the good radioprotection observed in bare NPs, they must be protected from surfactants to maintain their bioavailability. To optimize the chemical and physical characteristics of cerium-based NPs and enhance their radioprotection, surface modifier (PEG) was adopted to improve stability and bioavailability while reducing cytotoxicity. PEG-Ce NPs were employed for radioprotection of normal human liver cells (L-02) when higher radioprotection was observed in comparison to bare ceria NPs due to elevated expression of SOD2. Also, excellent stability and dispersity, enhanced radioprotection and reduced cytotoxicity were observed in the modified nanoparticles. Therefore, optimizing the physiochemical properties of ceria NPs is urgent to achieve improved radioprotection efficacy, Fig. 6 [108]. In brief, oxidative damage after irradiation can be mitigated by converting between valance states and thus reacting with free radicals. Engineered CeONPs are potential free radical scavengers that can protect a variety of cells and animal models from radiation-induced cell death, including cancer radiotherapy [109]. Bahreinipour and colleagues investigated the radioprotection properties of flower-like Fe_3O_4 microparticles (FIOMPs) and ceria nanoparticles (CNPs) in the presence of bovine serum albumin (BSA) at a radiation dose of 3 Gy. Both FIOMPs and CNPs were found to have great radioprotective property. The radioprotective features of the former nanoparticles arises from their catalase mimetic activity (CAT) as well as their porous structure, so that ROS recombination occurs to terminate the free radicals. Moreover, CNPs represent excellent radioprotection capability owing to their antioxidant potential toward hydroxyl radicals and their enzyme mimetic activities (e.g. peroxidase, dismutase, superoxide and catalase) [110]. Han *et al.* investigated the radioprotective potential of metal-based nanocrystals

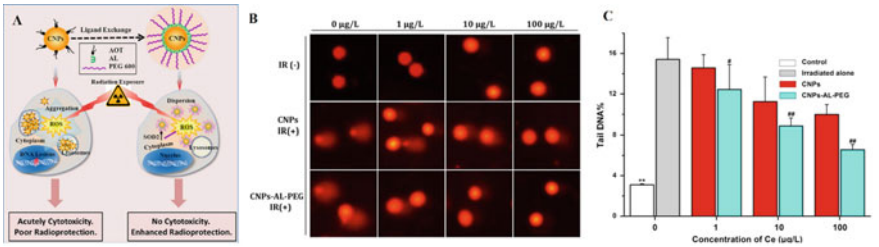

Fig. 6 **a)** PEG-Al-Ce NP enhanced Ce^{3+}/Ce^{4+} ratio that decreased cellular uptake, changed Ce dispersion and distribution and resulted in reduced cytotoxicity while elevating SOD2 expression and protecting cell from oxidative stress-mediated DNA damage. **b)** Comet assay in L-02 cells cultured with/without 10 μg/L of nanoparticle for 24 h. then exposed to 20 Gy γ-ray. **c)** Tail DNA % calculation with CASP software for 100 cells. Reproduced with permission from Ref. [108] Copyright 2010, with permission from Elsevier

of CeO_2/Mn_3O_4. The results revealed that CeO_2/Mn_3O_4 nanocrystals were able to promote the survival rate of mice treated with a lethal dose of total body irradiation as well as preventing acute radiation syndrome owing to their antioxidant capability even at low doses of administration [111]. Moreover, CeO_2 nanoparticles produced by Popova and colleagues efficiently protected NCTC L929 murine fibroblast cells upon irradiation by X-rays. The results indicated that these nanoparticles exhibited excellent radioprotective properties through modulation of gene expression [112].

3.6 Noble Metal Nanoradioprotectors

The noble metals are a specific group of metals including Rh, Pd, Pt, Ag, etc,. which represent certain catalytic features and outstanding resistance to oxidation. Nanoparticles, nanoclusters and nanocubes composed of these group of metals have been developed and represented radioprotective characteristics [66, 113]. In vivo results of administration of silver (Ag) nanoparticles (AgNPs) to swiss albino mice showed that these nanoparticles can enhance DNA repair of peripheral leukocytes, which was demonstrated by the comet test [24]. Post irradiation administration of these nanoparticles can also attenuate micronucleus formation. It has been demonstrated that the administration of silver nanoparticles 1 h before exposure may be beneficial as it reduces the damage in spleen, bone marrow and peripheral blood leukocyte cells [27]. Pre-irradiation administration of AgNPs can also effectively reduce the formation of micronucleus and chromosomal aberration, protect gastrointestinal system and hemopoietic cells. Pretreatment with AgNPs can:

- Enhance bone marrow regeneration and colony formation in the spleen
- Attenuate WBC reduction, intracellular antioxidant consumption, lipid peroxidation (LPO) and crypt and villus damages (intestinal structures) [26].

Thus, silver nanoparticles are promising nanoradioprotectors that operate efficiently for shielding healthy tissues against radiation-induced damages.

Nano-catalytic research is directed towards obtaining the smallest size nanoparticles, as demonstrated by the effect of size on the catalytic activity of gold nanoparticles [114]. Ultra-small (2 nm) nanoparticles of platinum (Pt) were employed to neutralize $\cdot OH$ and $\cdot O^{2-}$ radicals (cause by UVA) and ultimately prevented HeLa cell death as a result of ROS production after irradiation [115]. No toxicity was observed after exposure to adherent normal cell lines (MRC-5, TIG-1, WI-38, HepG2, and HeLa) with Pt concentrations as high as 50 mg/L. Later, the very low particle sizes of Pt clusters demonstrated reduced injuries in vitro and in vivo by scavenging free radicals, and eventually could:

- Reduce DNA damage
- Recover bone marrow DNA content and Super Oxide Dismutase(SOD) activity
- Increase the survival rate in the irradiated mouse by up to 30%, while the non-treated mouse died after 15 days.

Of note, no long-term toxicity was caused, since ultra-small Pt clusters can be rapidly excreted by the kidneys.

Nanocubes of PtPdRh covered with poly(vinyl pyrrolidone) (PVP) are able to scavenge $O_2 \cdot^-$ and $OH \cdot$(radicals of potential radioprotection issue) and also react with H_2O_2 via a catalytic mechanism in parallel. When comparing the catalytic strength, the ternary protected nanocube can change H_2O_2 to H_2O more efficiently than its Pt and PtPd counterparts. By neutralizing ROS effectively, PtPdRh nanocube exhibits promising responses in every aspect of important indicators for radioprotection:

- Cell viability and mice survival rate enhancement
- Repairing DNA damage
- Activating antioxidant enzymes.

Thus, it can be concluded that Pt and Pt-based nanoparticles are momentous materials for radioprotection, Fig. 7.

4 Challenges and Conclusion

In radiation-induced cancer therapy, there is a large gap in differentiation of tumor cells from normal cells, as tumor tissue usually surrounded by healthy tissue. Accordingly, it is of utmost urgency to develop novel and effective multifunctional nanomaterials for radioprotection of healthy tissue against radiation-induced side effects. Herein we summarized the power of multifunctional nanomaterials and all the exciting advances nanomaterials have made towards the protection of normal cells in RT. Multiplatform nanomaterials can be harnessed either as a carrier to augment the bioavailability of radioprotective agents or as next-generation radioprotectors

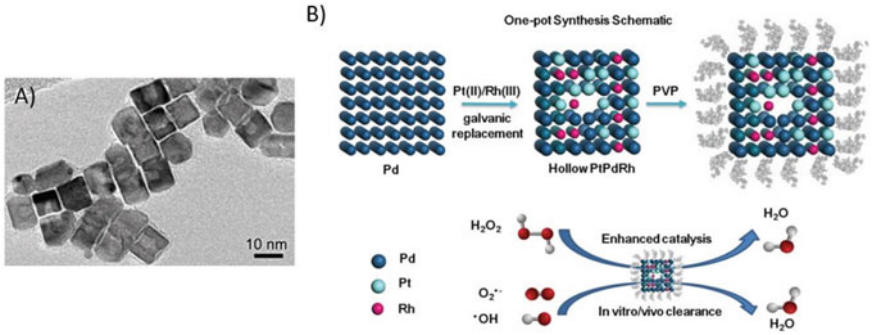

Fig. 7 **a)** Characterization of nanocubes with TEM image. **b)** Schematic design and catalytic/therapeutic mechanism of hollow PtPdRh nanocubes with improved catalytic properties. Reproduced with permission from Ref. [113] Copyright 2018, with permission from Wiley

as some nanomaterials have been reported to exhibit great intrinsic radioprotective features.

It is worth noting that despite all the benefit, significant progresses and achievements associated with multiplatform nanomaterials, research on their potential radioprotection is still in its infancy and there are some challenges and unresolved concerns that need attention before they reach clinical use. One of the main concerns regarding the use of nanomaterials in clinical trials and in vivo is their biosafety and biodistribution, which can greatly influence the biological applications of nanomaterials. Besides, numerous studies have reported short-term biosafety evaluation of nanomaterials, and insufficient data are available for their long-term safety. Thereby, exploiting their prolonged biosafety would facilitate their clinical utility. Remarkably, a massive number of papers have focused on demonstrating the radioprotective phenomenon of nanomaterials, whereas their radioprotective mechanisms are completely overlooked or only discussed superficially. Hence, a deep understanding of the radioprotective mechanisms of nanoradioprotectors is desired. To date, a lot of literature regarding nanoradioprotectors has emerged, but unfortunately very few of them have been able to reach the clinic. Therefore, endeavors should be continued to hasten the clinical application of these systems. Moreover, some physicochemical properties of nanomaterials such as surface group composition modification, size and shape need to be optimized in order to develop nanoradioprotectors with efficient radioprotective activity. In the context of former one, for instance, modification of ceria nanoparticles with PEG moieties exhibited superior radioprotective activity in comparison with bare nanoparticles [108]. It is also a rapidly expanding field, and researchers are having great success in utilizing nanoradioprotectors in RT, and progress in nanotechnologies not only have broaden the horizon of this field, but also facilitated the development of potent nanoradioprotectors. We anticipate that in the near future, researchers will develop more efficient nanoradioprotectors and exploiting multiplatform novel radioprotectors would open a new avenue in radiation-induced tumor therapy.

References

1. Her S, Jaffray DA, Allen C (2017) Gold nanoparticles for applications in cancer radiotherapy: Mechanisms and recent advancements. Adv Drug Deliv Rev 109:84–101
2. Song G et al (2017) Emerging nanotechnology and advanced materials for cancer radiation therapy. Adv Mater 29(32):1700996
3. Shirazi A, Ghobadi G, Ghazi-Khansari M (2007) A radiobiological review on melatonin: a novel radioprotector. J Radiat Res 48(4):263–272
4. Mandal TK et al (2002) Development of biodegradable microcapsules as carrier for oral controlled delivery of Amifostine. Drug Dev Ind Pharm 28(3):339–344
5. Ahmad I et al (2016) Supercritical fluid technology-based trans-resveratrol SLN for long circulation and improved radioprotection. J Pharm Innov 11(4):308–322
6. Rashidzadeh H et al (2021) Recent advances in targeting malaria with nanotechnology-based drug carriers. Pharm Dev Technol 26(8):807–823
7. Rezaei SJT et al (2020) pH-triggered prodrug micelles for cisplatin delivery: preparation and in vitro/vivo evaluation. React Funct Polym 146:104399
8. Fattahi N et al (2021) Enhancement of the brain delivery of methotrexate with administration of mid-chain ester prodrugs: in vitro and in vivo studies. Int J Pharm 600:120479
9. Yoozbashi M et al. (2021) Magnetic nanostructured lipid carrier for dual triggered curcumin delivery: Preparation, characterization and toxicity evaluation on isolated rat liver mitochondria. J Biomater Appl 08853282211034625
10. D'Souza R et al (1997) Curcumin-loaded PLGA microspheres with enhanced radioprotection in mice. Pharmaceut Sci 3(9):439–441
11. Cai X et al (2010) The polyhydroxylated fullerene derivative C60(OH)24 protects mice from ionizing-radiation-induced immune and mitochondrial dysfunction. Toxicol Appl Pharmacol 243(1):27–34
12. Protection of cellular dna and membrane from γ-radiation–induced damages and enhancement in DNA repair by Sesamol. Cancer Biotherapy Radiopharmaceut 25(6):629–635
13. Kouvaris JR, Kouloulias VE, Vlahos LJ (2007) Amifostine: the first selective-target and broad-spectrum radioprotector. Oncologist 12(6):738–747
14. Pamujula S et al (2005) Radioprotection in mice following oral delivery of amifostine nanoparticles. Int J Radiat Biol 81(3):251–257
15. Zhou Y et al (2015) A strategy for effective radioprotection by chitosan-based long-circulating nanocarriers. J Mater Chem B 3(15):2931–2934
16. Mohamed A (2013) Role of PLGA-nanoparticles formulation to improve drug radioprotective activity in gamma-irradiated mice. Chem J. ISSN 2049–954X: 97–104
17. Kumar S, Meena R, Rajamani P (2016) Fabrication of BSA–green tea polyphenols-chitosan nanoparticles and their role in radioprotection: a molecular and biochemical approach. J Agric Food Chem 64(30):6024–6034
18. Du J et al (2017) Poly (Vinylpyrollidone)-and selenocysteine-modified Bi2Se3 nanoparticles enhance radiotherapy efficacy in tumors and promote radioprotection in normal tissues. Adv Mater 29(34):1701268
19. Nosrati H et al (2022) Complete ablation of tumors using synchronous chemoradiation with bimetallic theranostic nanoparticles. Bioact Mater 7:74–84
20. Nosrati H et al (2020) Evaluation radioprotective effect of curcumin conjugated albumin nanoparticles. Bioorg Chem 100:103891
21. Lagoda I et al (2020) Investigation of the radioprotective efficiency of condensation products of thiol-containing hydrazides with mono-and disaccharides. Biol Bull 47(12):1680–1685
22. Liu Y et al. (2021) Oral codelivery of WR-1065 using curcumin-linked ROS-sensitive nanoparticles for synergistic radioprotection. ACS Biomater Sci Eng 7(6):2496–2507
23. Schweitzer AD et al. (2010) Melanin-covered nanoparticles for protection of bone marrow during radiation therapy of cancer. Int J Radiat Oncol* Biol* Phys 78(5):1494–1502

24. Chandrasekharan DK, Nair CKK (2010) Effect of silver nanoparticle and glycyrrhizic acid (SN-GLY) complex on repair of whole body radiation-induced cellular DNA damage and genomic instability in mice. Int J Low Radiat 7(6):453–466
25. Chandrasekharan DK, Khanna PK, Nair CKK (2011) Cellular radioprotecting potential of glyzyrrhizic acid, silver nanoparticle and their complex. Mutat Res/Genet Toxicol Environ Mutagen 723(1):51–57
26. Chandrasekharan DK, Nair CKK (2012) Studies on silver nanoparticle–glycyrrhizic acid complex as a radioprotector and an adjuvant in radiotherapy under in vivo conditions. Cancer Biother Radiopharm 27(10):642–651
27. Chandrasekharan DK et al (2011) Synthesis of nanosilver using a vitamin C derivative and studies on radiation protection. Cancer Biother Radiopharm 26(2):249–257
28. Xie J et al (2017) Therapeutic nanoparticles based on curcumin and bamboo charcoal nanoparticles for chemo-photothermal synergistic treatment of cancer and radioprotection of normal cells. ACS Appl Mater Interfaces 9(16):14281–14291
29. Cao J et al (2021) Ultrasound-assisted continuous-flow synthesis of PEGylated MIL-101 (Cr) nanoparticles for hematopoietic radioprotection. Mater Sci Eng, C 129:112369
30. Xie J et al (2018) Application of multifunctional nanomaterials in radioprotection of healthy tissues. Adv Healthcare Mater 7(20):1800421
31. Kwatra D, Venugopal A, Anant S (2013) Nanoparticles in radiation therapy: a summary of various approaches to enhance radiosensitization in cancer. Transl Cancer Res 2(4):330–342
32. Linji Gong JX, Zhu S, Gu Z, Zhao Y (2018) Application of multifunctional nanomaterials in tumor radiosensitization. Acta Phys -Chim Sin 34(2):140–167
33. Nair CKK, Parida DK, Nomura T (2001) Radioprotectors in radiotherapy. J Radiat Res 42(1):21–37
34. Goswami N et al (2017) Engineering gold-based radiosensitizers for cancer radiotherapy. Mater Horiz 4(5):817–831
35. Mathew J, Sankar P, Varacallo M (2021) Physiology, blood plasma, in StatPearls. 2021, StatPearls Publishing. Copyright © 2021, StatPearls Publishing LLC.: Treasure Island (FL)
36. Ramachandran L, Nair CKK (2011) Therapeutic potentials of silver nanoparticle complex of α-lipoic acid. Nanomater Nanotechnol 1:14
37. Mateo-Alonso A, Bonifazi D, Prato M (2006) Chapter 7 - Functionalization and applications of [60]fullerene. In: Dai L (ed) Carbon nanotechnology. Elsevier, Amsterdam, pp 155–189
38. Xie Q, Perez-Cordero E, Echegoyen L (1992) Electrochemical detection of C606- and C706-: enhanced stability of fullerides in solution. J Am Chem Soc 114(10):3978–3980
39. Singh H, Srivastava M (1995) Fullerenes: synthesis, separation, characterization, reaction chemistry, and applications—a review. Energy Sources 17(6):615–640
40. Heymann D (1996) Solubility of fullerenes C60 and C70 in seven normal alcohols and their deduced solubility in water. Fullerene Sci Technol 4(3):509–515
41. Kyzyma EA et al. (2015) Structure and toxicity of aqueous fullerene C60 solutions. J Surface Investig. X-ray, Synchrot Neutron Tech 9(1):1–5
42. Sayes CM et al (2004) The differential cytotoxicity of water-soluble fullerenes. Nano Lett 4(10):1881–1887
43. Krätschmer W et al (1990) Solid C60: a new form of carbon. Nature 347(6291):354–358
44. Rašović I (2017) Water-soluble fullerenes for medical applications. Mater Sci Technol 33(7):777–794
45. Sitharaman B et al (2008) Water-soluble fullerene (C60) derivatives as nonviral gene-delivery vectors. Mol Pharm 5(4):567–578
46. Wang IC et al (1999) C60 and water-soluble fullerene derivatives as antioxidants against radical-initiated lipid peroxidation. J Med Chem 42(22):4614–4620
47. Hsieh F-Y et al (2017) Water-soluble fullerene derivatives as brain medicine: surface chemistry determines if they are neuroprotective and antitumor. ACS Appl Mater Interfaces 9(13):11482–11492
48. Aroua S, Schweizer WB, Yamakoshi Y (2014) C60 pyrrolidine bis-carboxylic acid derivative as a versatile precursor for biocompatible fullerenes. Org Lett 16(6):1688–1691

49. Grebowski J et al. (2014) Rate constants of highly hydroxylated fullerene C60 interacting with hydroxyl radicals and hydrated electrons. Pulse radiolysis study. Radiat Phys Chem 103:146–152
50. Beuerle F, Lebovitz R, Hirsch A (2008) Antioxidant properties of water-soluble fullerene derivatives, in medicinal chemistry and pharmacological potential of fullerenes and carbon nanotubes, Cataldo F, Da Ros T (eds). Springer Netherlands, Dordrecht, pp 51–78
51. Nakamura E, Isobe H (2003) Functionalized fullerenes in water. The first 10 years of their chemistry, biology, and nanoscience. Accounts Chem Res 36(11):807–815
52. Friedman SH et al (1993) Inhibition of the HIV-1 protease by fullerene derivatives: model building studies and experimental verification. J Am Chem Soc 115(15):6506–6509
53. Mirakyan AL, Wilson LJ (2002) Functionalization of C60 with diphosphonate groups: a route to bone-vectored fullerenes. J Chem Soc, Perkin Trans 2(6):1173–1176
54. Zakharian TY et al (2005) A fullerene−paclitaxel chemotherapeutic: synthesis, characterization, and study of biological activity in tissue culture. J Am Chem Soc 127(36):12508–12509
55. Semenov KN et al (2016) Fullerenols: physicochemical properties and applications. Prog Solid State Chem 44(2):59–74
56. Monteiro-Riviere NA et al (2012) Lack of hydroxylated fullerene toxicity after intravenous administration to female sprague-dawley rats. J Toxicol Environ Health A 75(7):367–373
57. Tsai M-C, Chen YH, Chiang LY (2011) Polyhydroxylated C60, fullerenol, a novel free-radical trapper, prevented hydrogen peroxide- and cumene hydroperoxide-elicited changes in rat hippocampus in-vitro. J Pharm Pharmacol 49(4):438–445
58. Lai H-S et al (2000) Free radical scavenging activity of fullerenol on grafts after small bowel transplantation in dogs. Transpl Proc 32:1272–1274
59. Lai H-S, Chen W-J, Chiang L-Y (2000) Free radical scavenging activity of fullerenol on the ischemia-reperfusion intestine in dogs. World J Surg 24(4):450–454
60. Ye S et al (2014) Polyhydroxylated fullerene attenuates oxidative stress-induced apoptosis via a fortifying Nrf2-regulated cellular antioxidant defence system. Int J Nanomedicine 9:2073–2087
61. Trajković S et al (2007) Tissue-protective effects of fullerenol C60(OH)24 and amifostine in irradiated rats. Colloids Surf, B 58(1):39–43
62. Djordjević A, Bogdanović G, Dobrić S (2006) Fullerenes in biomedicine. J BU ON: Offic J Balkan Union Oncol 11(4):391–404
63. BogdanoviĆ V et al (2008) Fullerenol C60(OH)24 effects on antioxidative enzymes activity in irradiated human erythroleukemia cell line. J Radiat Res 49(3):321–327
64. Zhao Q et al (2005) Radioprotection by fullerenols of Stylonychia mytilus exposed to γ-rays. Int J Radiat Biol 81(2):169–175
65. Wang C et al (2022) Fullerenol@ nano-montmorillonite nanocomposite as an efficient radioprotective agent for ameliorating radioactive duodenal injury. Chem Eng J 427:131725
66. Zhao M et al. (2021) Eco-friendly and scalable synthesis of fullerenols with high free radical scavenging ability for skin radioprotection. Small 2102035
67. Brettreich M, Hirsch A (1998) A highly water-soluble dendro[60]fullerene. Tetrahedron Lett 39(18):2731–2734
68. Witte P et al (2007) Water solubility, antioxidant activity and cytochrome C binding of four families of exohedral adducts of C60 and C70. Org Biomol Chem 5(22):3599–3613
69. McAleer MF et al (2005) Novel use of zebrafish as a vertebrate model to screen radiation protectors and sensitizers. Int J Radiat Oncol Biol Phys 61(1):10–13
70. Daroczi B et al (2006) In vivo radioprotection by the fullerene nanoparticle DF-1 as assessed in a zebrafish model. Clin Cancer Res 12(23):7086–7091
71. Cornforth MN (2006) Perspectives on the formation of radiation-induced exchange aberrations. DNA Repair 5(9):1182–1191
72. Theriot CA et al (2010) Dendro[C60]fullerene DF-1 provides radioprotection to radiosensitive mammalian cells. Radiat Environ Biophys 49(3):437–445
73. Dugan LL et al (1997) Carboxyfullerenes as neuroprotective agents. Proc Natl Acad Sci 94(17):9434–9439

74. Andrievsky GV et al (2009) Peculiarities of the antioxidant and radioprotective effects of hydrated C60 fullerene nanostuctures in vitro and in vivo. Free Radical Biol Med 47(6):786–793
75. Xia W et al (2016) Functionlized graphene serving as free radical scavenger and corrosion protection in gamma-irradiated epoxy composites. Carbon 101:315–323
76. Galano A (2010) Carbon nanotubes: promising agents against free radicals. Nanoscale 2(3):373–380
77. Novoselov KS et al (2004) Electric field effect in atomically thin carbon films. Science 306(5696):666–669
78. Tans SJ et al (1997) Individual single-wall carbon nanotubes as quantum wires. Nature 386(6624):474–477
79. Jansen R, Wallis P (2009) Manufacturing, characterization and use of single walled carbon nanotubes. Mater Matters 4(1):23–27
80. Tour JM et al. (2010) Radiation protection using single wall carbon nanotube derivatives. Google Patents
81. Galano A (2008) Carbon nanotubes as free-radical scavengers. J Phys Chem C 112(24):8922–8927
82. Martínez A, Galano A (2010) Free radical scavenging activity of ultrashort single-walled carbon nanotubes with different structures through electron transfer reactions. J Phys Chem C 114(18):8184–8191
83. Cirillo G et al (2010) Antioxidant multi-walled carbon nanotubes by free radical grafting of gallic acid: new materials for biomedical applications. J Pharm Pharmacol 63(2):179–188
84. Jang A et al (2009) Biological functions of a synthetic compound, octadeca-9,12-dienyl-3,4,5-hydroxybenzoate, from gallic acid–linoleic acid ester. Food Chem 112(2):369–373
85. Amiri A et al (2013) Influence of different amino acid groups on the free radical scavenging capability of multi walled carbon nanotubes. J Biomed Mater Res, Part A 101A(8):2219–2228
86. Qiu Y et al (2014) Antioxidant chemistry of graphene-based materials and its role in oxidation protection technology. Nanoscale 6(20):11744–11755
87. Mattevi C, Kim H, Chhowalla M (2011) A review of chemical vapour deposition of graphene on copper. J Mater Chem 21(10):3324–3334
88. Li X et al (2009) Large-area synthesis of high-quality and uniform graphene films on copper foils. Science 324(5932):1312–1314
89. Gilje S et al (2007) A chemical route to graphene for device applications. Nano Lett 7(11):3394–3398
90. Yeh T-F et al (2010) Graphite oxide as a photocatalyst for hydrogen production from water. Adv Func Mater 20(14):2255–2262
91. Song Y et al (2011) Selective and quantitative cancer cell detection using target-directed functionalized graphene and its synergetic peroxidase-like activity. Chem Commun 47(15):4436–4438
92. Guo Y et al (2011) Hemin−graphene hybrid nanosheets with intrinsic peroxidase-like activity for label-free colorimetric detection of single-nucleotide polymorphism. ACS Nano 5(2):1282–1290
93. Sanchez VC et al (2012) Biological interactions of graphene-family nanomaterials: an interdisciplinary review. Chem Res Toxicol 25(1):15–34
94. Qiao Y et al (2014) Reducing X-ray induced oxidative damages in fibroblasts with graphene oxide. Nanomaterials 4(2):522–534
95. Elgrishi N et al (2018) A practical beginner's guide to cyclic voltammetry. J Chem Educ 95(2):197–206
96. Brett C, Oliveira Brett AM (1993) Electrochemistry: principles, methods, and applications
97. Zittel HE, Miller FJ (1965) A glassy-carbon electrode for voltammetry. Anal Chem 37(2):200–203
98. Wang J et al (2018) Highly efficient catalytic scavenging of oxygen free radicals with graphene-encapsulated metal nanoshields. Nano Res 11(5):2821–2835

99. Dong X et al (2016) Mesoporous bamboo charcoal nanoparticles as a new near-infrared responsive drug carrier for imaging-guided chemotherapy/photothermal synergistic therapy of tumor. Adv Healthcare Mater 5(13):1627–1637
100. Xie J et al (2019) Graphdiyne nanoparticles with high free radical scavenging activity for radiation protection. ACS Appl Mater Interfaces 11(3):2579–2590
101. Xu C, Qu X (2014) Cerium oxide nanoparticle: a remarkably versatile rare earth nanomaterial for biological applications. NPG Asia Mater 6(3):e90–e90
102. Tarnuzzer RW et al (2005) Vacancy engineered ceria nanostructures for protection from radiation-induced cellular damage. Nano Lett 5(12):2573–2577
103. Heckman KL et al (2013) Custom cerium oxide nanoparticles protect against a free radical mediated autoimmune degenerative disease in the brain. ACS Nano 7(12):10582–10596
104. Colon J et al. (2009) Protection from radiation-induced pneumonitis using cerium oxide nanoparticles. Nanomed: Nanotechnol, Biol Med 5(2):225–231
105. Colon J et al. (2010) Cerium oxide nanoparticles protect gastrointestinal epithelium from radiation-induced damage by reduction of reactive oxygen species and upregulation of superoxide dismutase 2. Nanomed: Nanotechnol, Biol Med 6(5):698–705
106. Popov AL et al (2016) Radioprotective effects of ultra-small citrate-stabilized cerium oxide nanoparticles in vitro and in vivo. RSC Adv 6(108):106141–106149
107. Li H et al (2015) PEGylated ceria nanoparticles used for radioprotection on human liver cells under γ-ray irradiation. Free Radical Biol Med 87:26–35
108. Baker CH (2013) Harnessing cerium oxide nanoparticles to protect normal tissue from radiation damage. Transl Cancer Res 2(4):343–358
109. Bahreinipour M et al (2021) Radioprotective effect of nanoceria and magnetic flower-like iron oxide microparticles on gamma radiation-induced damage in BSA protein. AIMS Biophys 8(2):124–142
110. Han SI et al (2020) Epitaxially strained CeO2/Mn3O4 nanocrystals as an enhanced antioxidant for radioprotection. Adv Mater 32(31):2001566
111. Popova NR et al. (2019) Cerium oxide nanoparticles provide radioprotective effects upon X-ray irradiation by modulation of gene expression. Наносистемы: физика, химия, математика 10(5).
112. Wang J-Y et al (2018) Hollow PtPdRh nanocubes with enhanced catalytic activities for in vivo clearance of radiation-induced ROS via surface-mediated bond breaking. Small 14(13):1703736
113. Astruc D (2020) Introduction: nanoparticles in catalysis. Chem Rev 120(2):461–463
114. Hamasaki T et al (2008) Kinetic analysis of superoxide anion radical-scavenging and hydroxyl radical-scavenging activities of platinum nanoparticles. Langmuir 24(14):7354–7364
115. Xu F et al (2017) Ultrasmall Pt clusters reducing radiation-induced injuries via scavenging free radicals. J Biomed Nanotechnol 13(11):1512–1521

X-ray Triggered Photodynamic Therapy

Ifrah Kiran, Naveed Akhtar Shad, Muhammad Munir Sajid, Hafiz Zeeshan Mahmood, Yasir Javed, Muhammad Sarwar, Hamed Nosrati, Hossein Danafar, and Surender K. Sharma

Abstract Photodynamic therapy (PDT) is an auspicious cancer treatment technique, however, have limitations due to inadequate penetration of visible light. In this scenario, X-ray inducible PDT has been evolved in which treatment is regulated by X-rays. Upon X-ray irradiation, the injected nano-system comprising nanoscintillator core and material loaded with photosensitizers, transform X photons to visible photons that stimulate the photosensitizers and induce effective tumor shrinkage. In this chapter, we have reviewed limitation of traditional PDT, principles of X-ray induced PDT, and different nano-system being applied for X-ray PDT.

I. Kiran · Y. Javed (✉)
Magnetic Materials Laboratory, Department of Physics, University of Agriculture, Faisalabad, Pakistan
e-mail: myasi60@hotmail.com

N. A. Shad · M. Sarwar
National Institute of Biotechnology and Genetic Engineering, Government College University, Jhang Road, Faisalabad, Pakistan

M. M. Sajid
Henan Key Laboratory of Photovoltaic Materials, School of Physics, Henan Normal University, Xueyuan Road 30th, Haidian District, Xinxiang 453007, China

H. Z. Mahmood
University of Central Punjab, Faisalabad Campus, Faisalabad, Pakistan

H. Nosrati
ERNAM—Nanotechnology Research and Application Center, Erciyes University, Kayseri 38039, Turkey

H. Nosrati · H. Danafar
Zanjan Pharmaceutical Biotechnology Research Center, Zanjan University of Medical Sciences, Zanjan, Iran

Joint Ukraine-Azerbaijan International Research and Education Center of Nanobiotechnology and Functional Nanosystems, Drohobych, Ukraine

S. K. Sharma
Department of Physics, Central University of Punjab, Bathinda 151401, India

Department of Physics, Federal University of Maranhao, Sao Luis, MA 65080-805, Brazil

S. K. Sharma et al. (eds.), *Harnessing Materials for X-ray Based Cancer Therapy and Imaging*, Nanomedicine and Nanotoxicology,
https://doi.org/10.1007/978-3-031-04071-9_7

Keywords X-ray PDT · Nano-scintillator · Nanomaterials · Singlet oxygen · Cancer treatment

1 Introduction

Photodynamic therapy is functional treatment based on the use of light energy with the photosensitizing chemical material known as photosensitizer [1]. The photosensitizing agent can be light sensitive medicine that gets activated with the light of specific wavelength usually obtained through a laser. The two-stage treatment is explicitly designed to destroy the abnormal cancerous and precancerous cells using the photosensitizer in conjunction with molecular oxygen causing the cell death. This therapy has been clinically approved and is extensively used for treating various skin diseases i.e. treatment of acne, eye conditions and some particular kinds of cancer. The Photodynamic therapy (PDT) has shown its extensive ability to kill various microbial cells including fungi, bacteria and viruses [2]. The conventional strategies of PDT are primarily focused on the superficial lesions. The reason behind the illumination light is the activation of most of the clinically approved photosensitizers with light of the wavelength lying in ultraviolet/visible range. This shows limited ability of light in tissue penetration resulting into ineffectual therapeutic response in case of deep-seated tumors. The problem can be resolved by combining the PDT technique with nanotechnology. The combination leads to a promising approach help in curing deep tumors. The advancements in the field introduced new PDT modalities in treating deep tumors on the basis of actively designed nanocomposites [3].

The Photodynamic therapy is termed as a non-invasive clinical oncologic therapeutic modality using photosensitizers which generate reactive oxygen species (ROS) [4] under illumination of particular wavelength of light aiming in toxicity of cancer cells. The non-invasion factor of photodynamic therapy [5] provides intrinsic safety which is its major advantage over all the other traditional cancer therapies such as clinical surgery, chemotherapy, and radiotherapy. The three key components of photodynamic therapy [6] are functioned in a proper manner; when the photosensitizers are irradiated to light of certain wavelength, they get excited and react with the neighboring biomolecules present in cellular microenvironment. The reaction occurs through electron transfer [7] generating the radical and radical anion species. The other way is the direct transfer of energy to neighboring triplet oxygen resulting in production of singlet oxygen. It is accepted from both the ways to occur simultaneously. The singlet oxygen produced by second way is the basic cytotoxic component for the biological effect of photodynamic therapy [8]. The singlet oxygen is extremely reactive specie, able to induce substantial damage to tissues and cells. The illumination with certain wavelength of light is necessary for activation of photosensitizers to produce toxicity of cells and tissues. Therefore, the photosensitizers exhibit no generation of toxicity component in a dark environment. The advantages of photodynamic therapy involve the use of excitation lasers with appropriate power that

can be modestly tuned to safe threshold values for operative activation of photodynamic therapy [9]. The high selectivity is another positive aspect of this therapeutic modality. In other therapeutic modalities, the photosensitizers get distributed without any selective targeting delivery throughout the body. In this technique, the selective tumor therapeutic operation can be performed by focusing the illumination of light specifically on the malignant lesion region [10]. So the process only is initiated in the tumor tissue regions supplying plenty of singlet oxygen to destroy the cancer cells. Therefore, the other organs of the body do not get affected even at high concentrations of photosensitizers because no excitation light is present. This minimal damaging impact of photodynamic therapy on the normal tissues of the body makes it advantageous over radiotherapy and chemotherapy [11].

2 Limitations of Photodynamic Therapy

Despite of all the favorable features, there is a limitation of the photodynamic therapy due to which its application has been restricted in clinical aspect. The low tissue penetration ability of light used to be a major constraint. The tissue penetration of the visible light is even less than 1 cm which suppresses the use of PDT in treatment of tumors present deep inside the organs [12]. In the early periods, the UV–Vis light used to activate the photosensitizers produced lethal damage to the tumor vasculature and cancerous cells, whereas, the non-transparency of the tissues to the UV/Vis light appeared to be a major downside of PDT [13] (Fig. 1). Due to this limitation, the light cannot be accurately supplied to photosensitizers accrued in deeply seated tumors. The photodynamic therapy is restricted to be applied to endoscope and peripheral accessible regions such as neck, skin and oral cavity cancers [14].

3 X-ray Triggered Photodynamic Therapy

The limitations of photodynamic therapy can be overcome by innovative light delivering technologies that make some internal cavities to illuminate definite tumor cites i.e. lung, prostate, bladder and esophagus. The conventional PDT techniques are unable to treat large sized tumors or multi loci [16]. The novel PDT techniques are aiming to less tissue interference and resulting to improve penetration depth, all are controlled by light since treatment efficiency can be extremely surface weighted. There is an innovative methodology named X-ray inducible photodynamic therapy which purposes activation of the photosensitizers by X-rays [17]. The technique exhibits advantage over visible and NIR light as the photons of X-rays possess higher penetration ability in the body tissues [18]. The photodynamic therapy leads to the process of treating deep tissues using X-rays as irradiation source. The X-ray triggered PDT possesses promising potential in treating the tumors present in the internal organs. The X-rays are extensively used in the clinical field [19] for the diagnosis

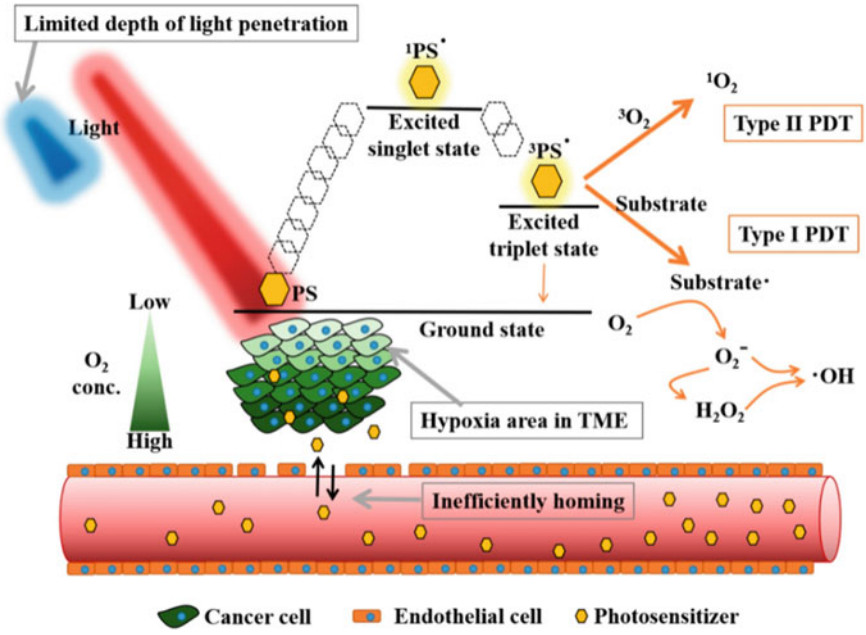

Fig. 1 Reaction mechanisms of photodynamic therapy and limitation for deep seated tumor treatment, PS: Photosensitizer, TME: Tumor microenvironment [15]

as well as therapeutic purposes. X-rays can perform different functions according to the activity i.e. X-rays may cover comparatively small area in dental and external radiotherapy and a larger area during a CT or chest X-ray. Both of the functions of X-rays are favorable to empower X-ray PDT. The narrow X-ray beam is proposed to result more selective and effectual damage. The X-rays given to cover larger area may empower the X-ray PDT to treat tumor metastasis or multiple loci tumors [20]. The approach is promising for finding extensive applications in the medical field especially in case of tumors that cannot be treated by radiation therapy. The X-ray PDT leads to combination of both radiotherapy and conventional photodynamic therapy [21]. However, practicing the X-ray PDT in medical field can give a risky feedback as the X-ray alone could have shown serious damaging effects to the treated body. Therefore, the nanostructures [22] were found to be effective in this manner to be integrated with X-ray illuminance and delivered to the cancerous sites. There have been a great number of photosensitizers loaded nano-sensitizers reported which perform function of converting the X-rays to optical luminescence. This function results into synergistic properties of conventional photodynamic therapy and radiotherapy under the action of low dose x-ray irradiation. The nano-sensitizers functioning as photosensitizers [23] include nanoscale metal–organic layers, inorganic scintillators based on rare-earth elements and inorganic insistent luminescent nanoparticles. The navigation of treatment with accuracy using external irradiation was ambiguous which is being resolved by integrating the systematically injected nanoparticles. This results

the emission of the NIR X-ray luminescence [24], allowing optical imaging of deep sighted tissues used to guide irradiation. There is a transducer essential to connect the energy transfer from X-ray to photosensitizers. This technique makes effective use of external X-ray irradiation and delivers nanoparticles to the cancerous sites [25]. Hence, X-ray triggered photodynamic therapy is an encouraging technique leading to advancements in the field of cancer treatment.

4 Principle of X-ray Triggered Photodynamic Therapy

To track the estimation of X-ray triggered PDT efficacy and for the nano-sensitizers development, numerous models have been theoretically developed. The fundamental principle of X-ray PDT is based on the activation of an energy transducer which converts X-ray photons to optical luminescence [26]. In this way, radiotherapy and photodynamic procedures get initiated. The X-rays used in the practical radiotherapy possess the energy ranging from hundreds of KeV to MeV [27]. Due to this reason, most conventional photosensitizers work in the photodynamic therapy, cannot be effectually triggered by X-rays. Regarding the issue, there is need of a physical transducer which may has ability to absorb X-ray radiation and transfer it to the used photosensitizers to generate cytotoxic singlet oxygen ($^1O_2$) essential for the tumor destruction [28]. Focusing on conventional X-ray PDT, the process of energy transfer is attained by conversion of absorbed X-rays into optical photons. The optical photons possess the specific wavelength suitable for effective absorption by the photosensitizers [29]. The transducers thus used are known as scintillators and demonstrate X-ray Excited Optical Luminescence (XEOL) [30]. Some other mechanisms are also presented for the transfer of energy between the X-ray irradiation absorbers and the photosensitizers. The practical example of the other mechanisms is the use of acridine orange which is a good photosensitizer [31]. The acridine orange has been employed in the tumor models and sarcoma patient and demonstrated effective results under small X-ray irradiation dosages, without any need of additional scintillator transducer.

The classical X-ray induced PDT mechanism can be divided into three major steps [32]. First of all, the nanoscintillators are exposed to X-rays and generate XEOL. The generated XEOL is then lead to be absorbed by nearly present and well-suited photosensitizer to generate the lethal $^1O_2$, has tendency to directly destruct the cell membrane phospholipids of the tumors. On the other hand, the deeply immersed ionizing radiation can eventually produce the radical species leading to ultimate breakage of DNA double strands. However, the generated ROS results into expiry of cancer cells [33] by an operative combination of Radiotherapy and Photodynamic therapy. Hence, there is a well-designed mechanism to generate interaction between X-rays and X-ray sensitive materials. In this manner, the active energy transfer between nanoscintillators and the photosensitizer leads to a potential therapeutic success by using the X-rays as excitation light source for triggering the PDT to treat particularly deeply seated tumors (Fig. 2) [34]. It is pertinent that exploiting mecha-

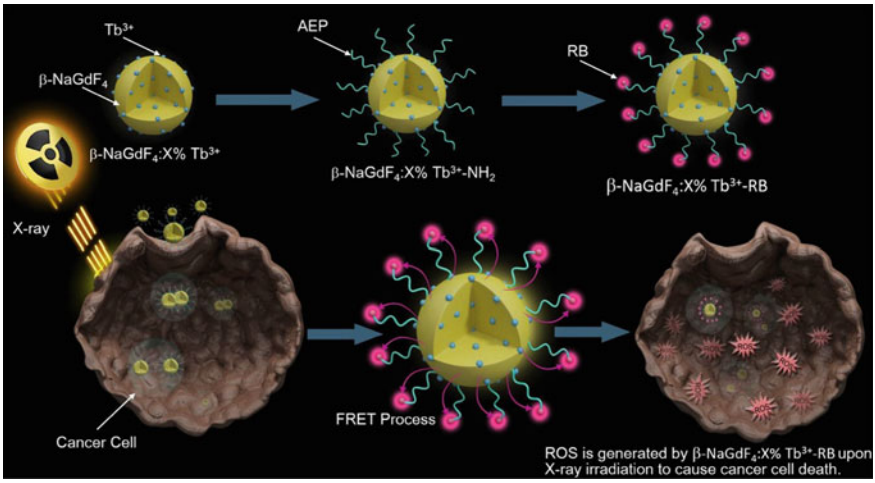

Fig. 2 Graphical abstraction of materials synthesis and mechanism in X-ray based PDT [34]

nisms to enhance the energy conversion process and safety of the scintillators are the basic points to induce effective X-PDT. The designed nanosensitizers should have certain characteristics for effective operation [35]. The scintillators constructed for employing in X-PDT should have large cross-section for X-ray absorption, possess great conversion capability of X-ray photons to visible photons and involve the optimized spatial positioning of molecular entities. Reduction of overall size distribution of transducers is required [36] for balancing the loss of efficacy of energy conversion. It is notable that conventionally stated transducers normally have large size [37] that is not optimal for the tumor targeting. There should be a definite balance between the short-term stability of the scintillators and their fast biodegradation. Owing to the therapeutic tactic, it must involve the transducers possessing high XEOL efficiency [38] under small X-ray dosages. Furthermore, the transducers having controlled size distribution ranging from 50 to 200 nm should demonstrate elongated blood circulation, an enhancement in the tumoral uptake rate by the enhanced permeability, high retention effects and comparatively low uptake rate by the mononuclear phagocyte systems [39]. In addition to all these aspects, the stealth components modification onto the nanoparticles' surface can produce reduction in the nonspecific protein corona formation [40].

The most important factor is that the nanosensitizers are required to be non-toxic [41] and should be smoothly metabolized with low toxicity for longer period [42]. Most of the proficiently used scintillators such as all the inorganic perovskites possess hydrolytic nature [43] and simply go on breakage into their constituent ions on exposure to water. This problem can be addressed by using the coating materials which can decorate the hydrolytic scintillator cores and improve the physiological stability of the scintillators in the media [44]. The energy transfer from the employed scintillators to the photosensitizers is influenced by amount of photosensitizers incorporated

in scintillators and the separating distance between both the species. Therefore, the physical loading mechanism should be overcome by a covalent conjugation strategy [45] in order to conjoin the scintillators and photosensitizers with a well-regulated intra-component distance. Many scintillators consist of high Z-elements [46] and it is appreciative to use these scintillators to guide the X-ray irradiation leading to minimal damaging effect on the normal tissues of the body. Overall the X-ray triggered PDT can overcome the restrictions of conventional photodynamic and radiotherapy tactics, providing high tumor ablation under lesser irradiation condition.

5 Different Nanomaterials-Based Systems for X-ray Triggered Photodynamic Therapy

The gold-based nanoparticles as photosensitizers to instigate the photodynamic therapy have been under consideration due to their bio-inertness and optical nature [47]. The gold nanoparticles have been considered much valuable photo-sensitizers but these admiring features need specific design considerations for being fully harnessed. The bio-inertness of gold nanoparticles makes them highly suitable and can also be instigated through the UV–Visible radiation and X-ray radiation exposure [48]. This makes them highly applicable to be used in different biological applications especially in the cancer therapies. The confinement of the gold particles to the single carrier [49] usually shows more advantageous effects than the unconfined gold particles moving freely in physiological environment due to impending haphazardness of non-restricted nanoparticles that could give rise to collateral damage, destroying the healthy tissues. The gold nanoparticles structured in the pollen morphology, behave more efficiently in producing the ROS (Fig. 3) [50]. The design of the pollen shape gold nanoclusters is proposed in such a manner that it may exhibit the good practicability in playing the role of photosensitizers [51]. As upon the irradiation by the light source, the photosensitizers get activated and produce cytotoxic ROS like singlet oxygen (O_2), superoxide radicals (O_2^-), hydroxyl radicals (·OH), hydrogen peroxide (H_2O_2) [52] and through the energy transfer or the electron transfer to the neighboring oxygen molecule. These extremely reactive oxygen species are directed towards the cancer cells [53] or persuade to the damaging effect on the tumor microvessels, giving rise to ultimate tissue ischemia. The pollen shape gold nanoclusters possess larger surface area in the same proportion of size in comparison to the gold nanoparticles, makes them more efficient to produce the ROS and instigate the X-ray PDT. The ROS levels generated under the action of X-ray irradiation is quantified using a fluorescent probe for O_2 [54]. The pollen shape gold nanoclusters exhibited the most effective results under the X-ray irradiation dosages in between 2-5 Gy. This is the fractional value of the radiation dosage employed in the conventional cancer radio-therapeutic technique. The oxidative stress generated during the therapeutic discourse of X-ray PDT has been renowned as the primary reason of the cellular DNA double breaks [55]. On comparison among the gold nanoparticles,

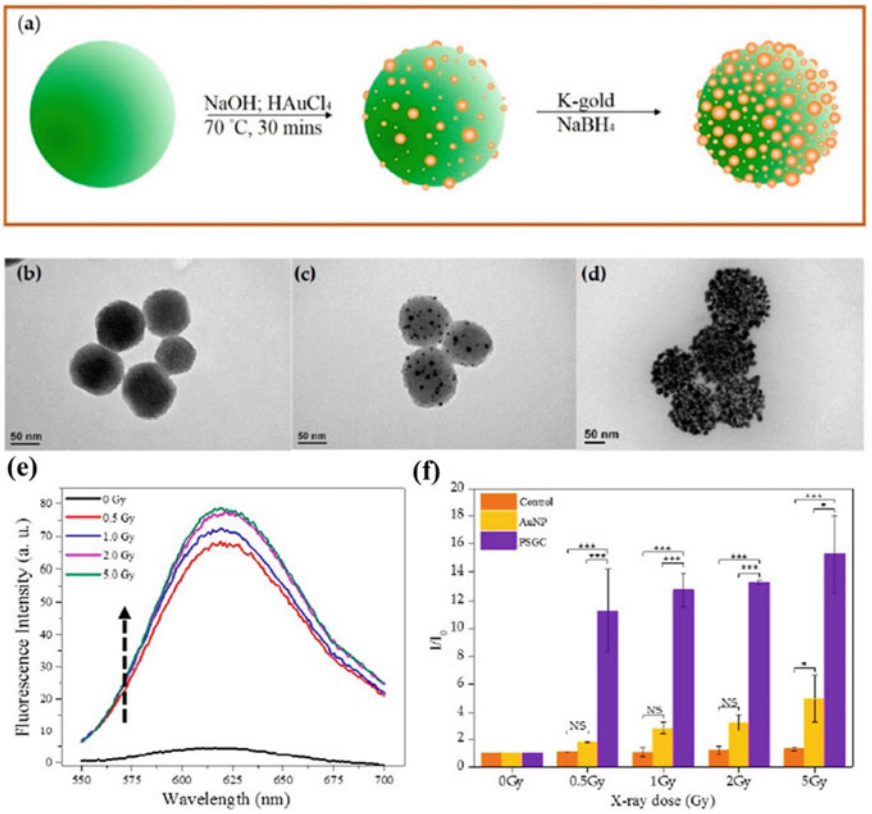

Fig. 3 **a** Graphical growth mechanism of pollen structure gold clusters. **b–d** TEM micrographs of silica, seed particles and pollen type structures respectively. **e** Fluorescence emission spectrums of dihydroethium in pollen structured gold NPs aqueous solution under different X-ray doses. **f** Fluorescence improvement in different aqueous solutions i.e. control = water, gold NPs and Pollen structured gold NPs at variable X-ray irradiation (0–5 Gy) [50].

pollen shaped gold nanoclusters and the controlled cells, the highest cellular DNA damage is recorded in the pollen shaped gold nanoclusters treated cells with the same X-ray dose.

Remarkably, there is another material suitable for the cancerous therapeutic techniques i.e. mesoporous silica nanoparticles [56]. Mesoporous silica nanoparticles are used in the drug delivery due to their high surface area and exceptional bio-inertness [57]. These particular properties make them capable of delivering stimulating drug molecules specifically possessing high solubility. The intentional hybridization between gold and silica materials can converse two aspects in the drug delivery; first, the gold nanoparticles are capable of generating enough amount of ROS to be activated on the cancer targets and give required platform for bioimaging, On the other hand, the mesoporous silica facilitates the drug with a dynamic control

release profile. The protection of the drug molecule encapsulated in the core is extended to provide better efficiency. Therefore, these nanostructures offer great future aspects in the in vivo treatments of cancer.

The $SrAl_2O_4$:Eu_2, stated as SAO-mediated X-ray triggered PDT is reported. The SAO material possesses remarkable optical properties [58] but the most important features which made it highly advantageous for this application; firstly, it produces exceptional energy pair with MC540 which leads to effective intraparticle energy transfer resulting to high $^1O_2$ production. Secondly, the SAO is exceedingly hydrolytic material [59] and the hydrolytes are comparatively non-toxic. The SAO core possesses a protection shell due to which it remains undamaged for the period sufficient for the therapy. This property reduces the long-term toxic effect to the hosting body, a basic problem that occurs in nanoparticle centered imaging and therapeutic techniques (Fig. 4) [60]. The synthesized SAO nanoparticles were coated with inner solid silica layer and outer mesoporous silica layer. Consequently, silica coated SAO nanoparticles formed, sustained strong photoluminescence. The cellular uptake of the SAO@SiO_2 nanoparticles was examined by using U87MG cells. The assumption was made that on X-ray irradiation, MC540-loaded SAO@SiO_2 nanoparticles would release energy to MC540 cells in form of visible photons and generates $^1O_2$. The $^1O_2$ generation in the solution or cells was determined by measuring the fluorescence change. The results did not show significant increased signal during the X-ray irradiation intervals. The cells nurtured with M-SAO@SiO_2 nanoparticles and triggered by X-ray radiation showed substantial enrichment in the fluorescence. This proved that the incorporation of all the three components SAO, MC540, and X-ray is essential for the $^1O_2$ generation.

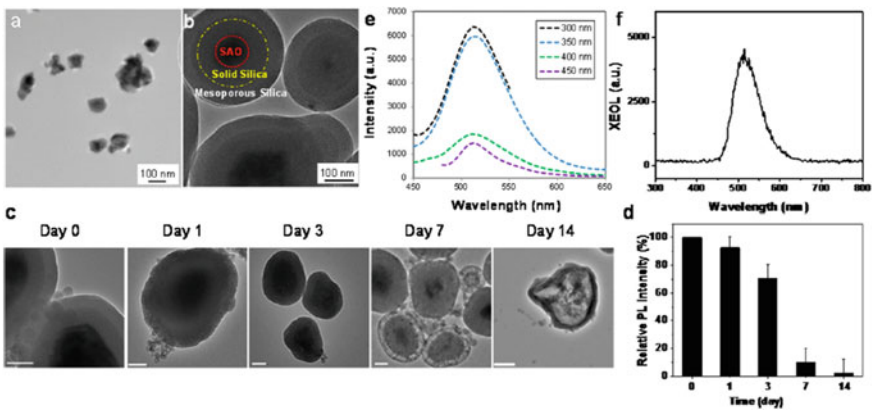

Fig. 4 **a**, **b** TEM micrographs of Bare and SiO_2 coated SAO NPs. **c** Stability studies of composite system in simulated body fluid for two weeks. **d** Photoluminescence variation of SAO@SiO_2 composite system during the incubation in body fluid. **e** Photoluminescence of the NPs at different excitation wavelengths, **f** XEOL spectrum of the NPs showing peak at 520 nm. Reproduced with permission from [60]. Copyright @American Chemical Society.

The selective tumor eradication needs the highly accurate navigation of both nanosensitizers and irradiation to the tumors. A novel $LiGa_5O_8$:Cr (LGO:Cr)-based nanoscintillator was introduced and employed in X-ray PDT due to its property of emitting near-infrared X-ray luminescence [61]. The LGO:Cr nanoparticles emit NIR insistent X-ray luminescence leading to the deep tissue optical imaging [62], which helps in directing the external irradiation. The X-ray excited optical luminescence (XEOL) peaks of the earlier scintillators take place in visible spectrum. Whereas, the LGO:Cr undergoes strong optical emission. The afterglow properties of the scintillator and unique NIR produced by it render the imaging with low luminescence background and facilitates with good tissue penetration which increases the exposure capacity to deep tissues. In a study by [63], the LGO:Cr nanoparticles were encapsulated with a photosensitizer, 2,3-naphthalocyanine. The nanoparticles were conjugated along with cetuximab and systematically inoculated into H1299 orthotopic lung cancer tumor models. The therapy turns out to be highly selective and efficient, producing minimal collateral damage to the normal tissues.

FR-mediated targeting is presented as an effective approach to spare healthy tissues present near around the tumors during the treatment. Clement et al. [64] studied the therapeutic impact of the PLGA-encapsulated photosensitizers, in combination with verteporfin (VP) under the condition of 6 meV X-ray radiation externally applied along with light illumination of 690 nm. The verteporfin is a therapeutically approved photosensitizer employed in treating the macular degeneration with high absorption band lying in blue region, closer to the ultraviolet (UV) region and a weaker band around 700 nm. The loading capability of PLGA nanoparticles combined with diverse VP concentrations was examined. The ability of the photosensitizer molecules to produce singlet oxygen by the illumination through visible light was evaluated. The FA conjugate (FA-PLGA-VP) exhibited great attraction towards the folate receptors present on most of the tumor cells surface in humans. The In vitro PDT revealed that corresponding conjugated nanoparticles effectually destroyed the HCT116 cells under action of 6 meV X-ray irradiation. The combined X-ray PDT technique provided stronger cytotoxic effect. In this way, the X-ray triggered PDT taking advantage of the tremendous targeting ability of FA-PLGA-VP nanostructures (Fig. 5) [65].

Another novel nano-agent is Tb-doped Gd-W-nano-scintillator. This multifunctional nano-agent is based on the novel Merocyanine 540-coupled $Gd_2(WO_4)_3$:Tb (GWOT) nano-scintillators. These nanoscintillators have encouraging properties favorable for the magnetic resonance imaging guided synergistic radiotherapy, dual modal computed tomography and X-ray induced photodynamic therapy [66]. The singlet oxygen production due to scintillator GWOT@MC540 was examined using SOSG probe. X-ray PDT using scintillator nanoparticles was then analyzed on the mice bearing tumors. The therapeutic impact was examined by both intravenous (i.v) injection and intrathecal (i.t) injection. The low cytotoxicity of the GWOT@MC540 nanoparticles had no effect on the tumors growth and the tumors kept growing rapidly. On exposing to the X-ray radiation, the GWOT nanoparticles proficiently increased the radiotherapy efficiency and inhibited the further growth of tumor. There was no change in the blood parameters using these nanoagents and no hepatic or kidney

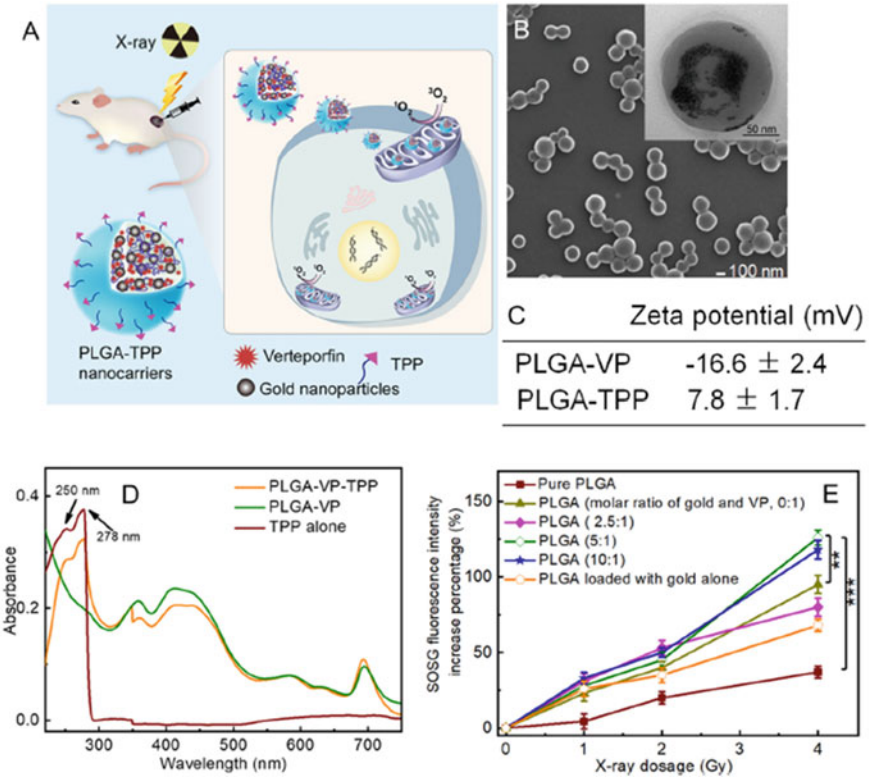

Fig. 5 **a** Graphical representation of PLGA nanocarriers containing verteporfin and gold NPs. **b** SEM image of nanocarrier. **c** Surface charge on nanocarriers. **d** UV vis spectrums PLGA samples with and without triphenylphosphonium. **e** Percentage rise in fluorescence intensities of different PLGA samples under different X-ray doses. Reprinted with permission from [65]. Copyright@ American Chemical Society

disorder was observed. Radiotherapy and X-ray PDT combinely induced higher suppression on the tumor cells in existence of GWOT@MC540 and X-ray radiations.

Mitochondria has been receiving attention as a target site of singlet oxygen to enhance the therapeutic effect of PDT since they are highly exposed to the oxidative damage produced by $^1O_2$. There are various targeting moieties presented for mitochondrial targeting such as triphenylphosphonium (TPP) and cationic peptides [67]. The mitochondria-targeted liposomes directed the verteporfin to mitochondria, because a small dose of X-ray radiation is enough to induce the cytotoxic $^1O_2$ generation from verteporfin there. The TEM imaging revealed that the 10 nm gold particles were deeply incorporated in hydrophilic core of liposomes. The exploration of $^1O_2$ generation by the VP gold NPs incorporated liposomes demonstrated that the samples containing 10 nm gold nanoparticles exhibited the highest $^1O_2$ generation. The increase in $^1O_2$ generation with the 10 nm gold under action of X-ray radiation at 4 Gy was approximately 186% which was only 129% in case of 5 nm VP gold

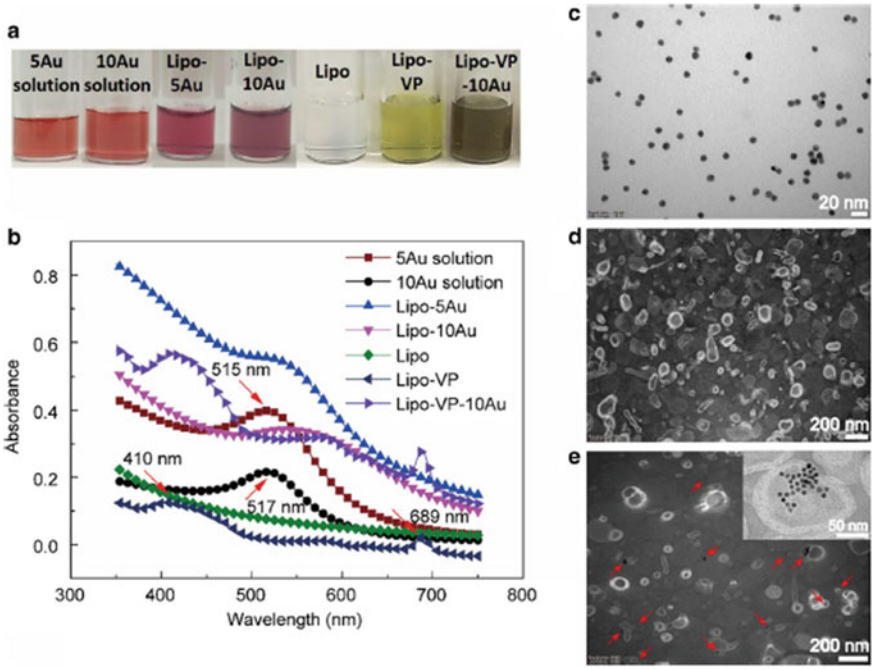

Fig. 6 VP and gold NPs incorporated liposomes: **a** Visual images of liposomes and gold colloidal solution. **b** Absorption spectra of different samples. Arrows indicate the absorption edge of VP, 5 nm and 10 nm gold NPs. **c**–**e** TEM micrographs of 10 nm gold NPs, pure liposomes, 10 nm gold NPs loaded in liposomes respectively [68]

liposome sample. The VP molecules integrated with gold nanoparticles showed more interaction with ionizing radiation, resulting to enhanced $^1O_2$ generation (Fig. 6) [68].

6 Radio-Sensitizing Materials Operation in X-ray Induced Photodynamic Therapy

The evolving era of conventional photodynamic therapy went through a variety of studies on the sensitizing materials specifically porphyrins and its relationship with X-rays and gamma radiations. In order to increase penetration depth, X-rays having wavelength less than red lasers are presented for exciting the sensitizing materials. The investigations in this modality presented the unique radiosensitizers triggered by X-rays. On the basis of similar excitation mechanism of scintillators, photocatalysts and specific semiconductors on exposure to X-rays, the viability of the radiosensitization for CeF_3, ZnS:Ag, TiO_2 and CeSe quantum dots are examined. For all the materials which were dispersed in the aqueous solution, ROS was determined as a

function of X-ray doses. The ROS generation by these sensitizing materials demonstrated that the CdSe quantum dots to be the most inspiring material for giving the highest yield. On the other hand, CeF_3 gave the lowest yield irrespective of lower concentrations by three orders of magnitude comparatively [69]. In the experimental setup, polychromatic X-rays obtained from a diagnostic x-ray generator were functioned at a tube voltage of 100 kV. The soft X-ray components were eliminated in the system with the help of aluminum filters for the objective of diagnosis. The analysis suggested the internalized quantum dots to act as more operative radiosensitizers. The resulting parameters demonstrated that for the photon range from 20 to 170 keV, incident intensity was reduced to 90% through path length of 3 cm in aqueous solutions at the varying concentrations from 0.01 to 100 wt%. The survival function of HeLa cells was calculated by WST-1 assay instantly after the X-ray irradiation. The measurements did not show any significant impact of the sensitizing materials on the cell viability.

7 Conclusion

In X-ray PDT, the X-ray excitation put forward ultimate solution of the fundamental limitation of conventional PDT. The basic difference in both the therapeutic tactics is the photon energy employed. The high penetration ability of X-rays proposed a groundbreaking success in treating the deep seated tumors. X-ray PDT provides quantum and ROS generation through definite grouping of complex elemental content, particular shaping and precise structuring of nanoparticles. This gives rise to their enhanced biocompatibility, making them highly applicable for clinical applications. The hypermetabolic rate of tumor cells results is lower oxygen concentration in comparison to the normal cells. The co-delivery of oxygenic compounds along with the photosensitizers through nanocarriers in X-ray PDT reverses the hypoxic condition, providing efficient therapeutic effects.

References

1. Bown SG (2013) Photodynamic therapy for photochemists. Philos Trans R Soc Math Phys Eng Sci 371(1995):20120371
2. Zeina B et al (2001) Killing of cutaneous microbial species by photodynamic therapy. Br J Dermatol 144(2):274–278
3. Hu J et al (2015) Nanocomposite-based photodynamic therapy strategies for deep TUMOR treatment. Small 11(44):5860–5887
4. Kim MM et al (2017) On the in vivo photochemical rate parameters for PDT reactive oxygen species modeling. Phys Med Biol 62(5):R1
5. Cheng X et al (2021) Multi-functional liposome: a powerful theranostic nano-platform enhancing photodynamic therapy. Adv Sci, 8(16):2100876
6. Kholin VV et al (2016) Methods and fiber optics spectrometry system for control of photosensitizer in tissue during photodynamic therapy. In: Photonics applications in astronomy,

communications, industry, and high-energy physics experiments 2016. International Society for Optics and Photonics
7. Jiménez-Mancilla NP et al (2021) Electron transfer reactions in rhodamine: potential use in photodynamic therapy. J Photochem Photobiol Chem 409:113131
8. Moore JV, West CM, Whitehurst C (1997) The biology of photodynamic therapy. Phys Med Biol 42(5):913
9. Pérez-Pérez L, García-Gavín J, Gilaberte Y (2014) Daylight-mediated photodynamic therapy in Spain: advantages and disadvantages. Actas Dermo-Sifiliográficas (English Edition) 105(7):663–674
10. Mang TS (2004) Lasers and light sources for PDT: past, present and future. Photodiagn Photodyn Ther 1(1):43–48
11. Kusuzaki K et al (2000) Total tumor cell elimination with minimum damage to normal tissues in musculoskeletal sarcomas following photodynamic therapy with acridine orange. Oncology 59(2):174–180
12. Zhang JY et al (2017) NaYbF 4 nanoparticles as near infrared light excited inorganic photosensitizers for deep penetration in photodynamic therapy. Nanoscale 9(8):2706–2710
13. Wang HJ, Shrestha R, Zhang Y (2014) Encapsulation of photosensitizers and upconversion nanocrystals in lipid micelles for photodynamic therapy. Part Part Syst Charact 31(2):228–235
14. Musani AI et al (2018) Photodynamic therapy via navigational bronchoscopy for peripheral lung cancer in dogs. Lasers Surg Med 50(5):483–490
15. Li W-P et al (2021) Recent advances in photodynamic therapy for deep-seated tumors with the aid of nanomedicine. Biomedicines 9(1):69
16. Toussaint M et al (2015) How nanoparticles can solve resistance and limitation in pdt efficiency. In: Resistance to photodynamic therapy in cancer. Springer, p 197–211
17. Larue L et al (2018) Using X-rays in photodynamic therapy: an overview. Photochem Photobiol Sci 17(11):1612–1650
18. Wang GD et al (2016) X-ray induced photodynamic therapy: a combination of radiotherapy and photodynamic therapy. Theranostics 6(13):2295
19. Lewis R (1997) Medical applications of synchrotron radiation X-rays. Phys Med Biol 42(7):1213
20. Ma L, Zou X, Chen W (2014) A new X-ray activated nanoparticle photosensitizer for cancer treatment. J Biomed Nanotechnol 10(8):1501–1508
21. Xu J, Gao J, Wei Q (2016) Combination of photodynamic therapy with radiotherapy for cancer treatment. J Nanomater 2016:8507924
22. Cline B, Delahunty I, Xie J (2019) Nanoparticles to mediate X-ray-induced photodynamic therapy and Cherenkov radiation photodynamic therapy. Wiley Interdiscip Rev Nanomed Nanobiotechnol 11(2):e1541
23. Olivo M et al (2011) Nano-sensitizers for multi-modality optical diagnostic imaging and therapy of cancer. In: European conference on biomedical optics. Optical Society of America
24. Xu J et al (2019) Recent advances in near-infrared emitting lanthanide-doped nanoconstructs: mechanism, design and application for bioimaging. Coord Chem Rev 381:104–134
25. Shrestha S et al (2019) X-ray induced photodynamic therapy with copper-cysteamine nanoparticles in mice tumors. Proc Natl Acad Sci 116(34):16823–16828
26. Zou X et al (2014) X-ray-induced nanoparticle-based photodynamic therapy of cancer. Nanomedicine 9(15):2339–2351
27. Kurudirek M (2014) Effective atomic numbers and electron densities of some human tissues and dosimetric materials for mean energies of various radiation sources relevant to radiotherapy and medical applications. Radiat Phys Chem 102:139–146
28. Juarranz Á et al (2008) Photodynamic therapy of cancer. Basic principles and applications. Clin Trans Oncol 10(3):148–154
29. Gu B et al (2017) Precise two-photon photodynamic therapy using an efficient photosensitizer with aggregation-induced emission characteristics. Adv Mater 29(28):1701076
30. Novais S, Valerio M, Macedo Z (2012) X-ray-excited optical luminescence and X-ray absorption fine-structures studies of CdWO4 scintillator. J Synchrotron Radiat 19(4):591–595

31. Yslas EI, Durantini EN, Rivarola VA (2007) Zinc-(II) 2, 9, 16, 23-tetrakis (methoxy) phthalocyanine: potential photosensitizer for use in photodynamic therapy in vitro. Bioorg Med Chem 15(13):4651–4660
32. Sun W et al (2020) Nanoscintillator-mediated X-ray induced photodynamic therapy for deep-seated tumors: from concept to biomedical applications. Theranostics 10(3):1296
33. Suvorov N et al (2021) Derivatives of natural chlorophylls as agents for antimicrobial photodynamic therapy. Int J Mol Sci 22(12):6392
34. Zhang W et al (2018) Ultra-high FRET efficiency NaGdF4: Tb3+-Rose Bengal biocompatible nanocomposite for X-ray excited photodynamic therapy application. Biomaterials 184:31–40
35. Hu H et al (2021) Emerging nanomedicine-enabled/enhanced nanodynamic therapies beyond traditional photodynamics. Adv Mater 33(12):2005062
36. Fromme P et al (2006) On the development and testing of a guided ultrasonic wave array for structural integrity monitoring. ieee Trans Ultrason Ferroelectr Freq control 53(4):777–785
37. Dahlin AB (2012) Size matters: problems and advantages associated with highly miniaturized sensors. Sensors 12(3):3018–3036
38. Fan W et al (2019) Breaking the depth dependence by nanotechnology-enhanced X-ray-excited deep cancer theranostics. Adv Mater 31(12):1806381
39. Goos JA et al (2020) Delivery of polymeric nanostars for molecular imaging and endo-radiotherapy through the enhanced permeability and retention (EPR) effect. Theranostics 10(2):567
40. Kang B et al (2015) Carbohydrate-based nanocarriers exhibiting specific cell targeting with minimum influence from the protein corona. Angew Chem Int Ed 54(25):7436–7440
41. Generalov R et al (2009) Generation of singlet oxygen and other radical species by quantum dot and carbon dot nanosensitizers. In: Photodynamic therapy: back to the future. International Society for Optics and Photonics
42. Xing C et al (2020) Engineering mono-chalcogen nanomaterials for omnipotent anticancer applications: progress and challenges. Adv Healthcare Mater 9(14):2000273
43. Zhao J et al (2016) Investigation of the hydrolysis of perovskite organometallic halide CH 3 NH 3 PbI 3 in humidity environment. Sci Rep 6(1):1–6
44. Du Z et al (2018) X-ray-controlled generation of peroxynitrite based on nanosized LiLuF4: Ce3+ scintillators and their applications for radiosensitization. Adv Mater 30(43):1804046
45. Aryal S et al (2013) Erythrocyte membrane-cloaked polymeric nanoparticles for controlled drug loading and release. Nanomedicine 8(8):1271–1280
46. Perego J et al (2021) Composite fast scintillators based on high-Z fluorescent metal–organic framework nanocrystals. Nat Photonics 15(5):393–400
47. Błaszkiewicz P, Kotkowiak M (2018) Gold-based nanoparticles systems in phototherapy-current strategies. Curr Med Chem 25(42):5914–5929
48. Falahati M et al (2020) Gold nanomaterials as key suppliers in biological and chemical sensing, catalysis, and medicine. Biochimica et Biophysica Acta (BBA)-Gen Sub 1864(1):129435
49. Ostovar B et al (2020) Increased intraband transitions in smaller gold nanorods enhance light emission. ACS Nano 14(11):15757–15765
50. Tew LS et al (2018) Pollen-structured gold nanoclusters for X-ray induced photodynamic therapy. Materials 11(7):1170
51. Dixit S et al (2015) Transferrin receptor-targeted theranostic gold nanoparticles for photosensitizer delivery in brain tumors. Nanoscale 7(5):1782–1790
52. Chekulayeva LV et al (2006) Hydrogen peroxide, superoxide, and hydroxyl radicals are involved in the phototoxic action of hematoporphyrin derivative against tumor cells. J Environ Pathol Toxicol Oncol 25(1–2)
53. Manda G, Nechifor MT, Neagu T-M (2009) Reactive oxygen species, cancer and anti-cancer therapies. Curr Chem Biol 3(1):22–46
54. Ruiz-González R et al (2017) NanoSOSG: a nanostructured fluorescent probe for the detection of intracellular singlet oxygen. Angew Chem Int Ed 56(11):2885–2888
55. Fisher AM et al (1997) Increased photosensitivity in HL60 cells expressing wild-type p53. Photochem Photobiol 66(2):265–270

56. Li Z et al (2012) Mesoporous silica nanoparticles in biomedical applications. Chem Soc Rev 41(7):2590–2605
57. Manzano M, Vallet-Regí M (2020) Mesoporous silica nanoparticles for drug delivery. Adv Func Mater 30(2):1902634
58. Gültekin S et al (2019) Structural and optical properties of SrAl2O4: Eu2+/Dy3+ phosphors synthesized by flame spray pyrolysis technique. J Lumin 206:59–69
59. Chen I-C, Chen T-M (2001) Sol-gel synthesis and the effect of boron addition on the phosphorescent properties of SrAl2O4: Eu2+, Dy3+ phosphors. J Mater Res 16(3):644–651
60. Chen H et al (2015) Nanoscintillator-mediated X-ray inducible photodynamic therapy for in vivo cancer treatment. Nano Lett 15(4):2249–2256
61. Maiti S, Sen KK (2019) Bio-targeted nanomaterials for theranostic applications. In: Drug discovery and development. CRC Press, pp 99–117
62. Kirsanova DY et al (2021) Nanomaterials for deep tumor treatment. Mini Rev Med Chem 21(6):677–688
63. Chen H et al (2017) $LiGa_5O_8$: Cr-based theranostic nanoparticles for imaging-guided X-ray induced photodynamic therapy of deep-seated tumors. Mater Horiz 4(6):1092–1101
64. Clement S et al (2018) X-ray radiation-induced and targeted photodynamic therapy with folic acid-conjugated biodegradable nanoconstructs. Int J Nanomed 13:3553
65. Deng W et al (2020) Application of mitochondrially targeted nanoconstructs to neoadjuvant X-ray-induced photodynamic therapy for rectal cancer. ACS Cent Sci 6(5):715–726
66. Yu X et al (2019) CT/MRI-guided synergistic radiotherapy and X-ray inducible photodynamic therapy using Tb-doped Gd-W-nanoscintillators. Angew Chem 131(7):2039–2044
67. Gu X et al (2020) X-ray induced photodynamic therapy (PDT) with a mitochondria-targeted liposome delivery system. J Nanobiotechnol 18(1):1–13
68. Gu X et al (2020) X-ray induced photodynamic therapy (PDT) with a mitochondria-targeted liposome delivery system. J Nanobiotechnol 18(1):87
69. Takahashi J, Misawa M (2007) Analysis of potential radiosensitizing materials for X-ray-induced photodynamic therapy. NanoBiotechnology 3(2):116–126

Nanoparticle Based CT Contrast Agents

Jalil Charmi, Marziyeh Salehiabar, Mohammadreza Ghaffarlou, Hossein Danafar, Taras Kavetskyy, Soodabeh Davaran, Yavuz Nuri Ertas, Surender K. Sharma, and Hamed Nosrati

Abstract The increasing significance of computed tomography (CT) which is one of the most widely used radiological methods in biomedical imaging, has accelerated the development of nanoparticles as next-generation CT contrast agents. Nanoparticles are predicted to play a significant role in the future of medical diagnostics due to

J. Charmi · M. Salehiabar · Y. N. Ertas (✉) · H. Nosrati (✉)
ERNAM—Nanotechnology Research and Application Center, Erciyes University, Kayseri 38039, Turkey
e-mail: yavuzertas@erciyes.edu.tr

H. Nosrati
e-mail: nosrati.hamed2020@gmail.com

M. Ghaffarlou
Department of Chemistry, Hacettepe University, Beytepe, Ankara 06800, Turkey

H. Danafar · H. Nosrati
Zanjan Pharmaceutical Biotechnology Research Center, Zanjan University of Medical Sciences, Zanjan, Iran

H. Danafar · T. Kavetskyy · S. Davaran · H. Nosrati
Joint Ukraine-Azerbaijan International Research and Education Center of Nanobiotechnology and Functional Nanosystems, Drohobych, Ukraine, Baku, Azerbaijan

T. Kavetskyy
Department of Materials Engineering, The John Paul II Catholic University of Lublin, 20-950 Lublin, Poland

Drohobych Ivan Franko State Pedagogical University, Drohobych 82100, Ukraine

S. Davaran
Drug Applied Research Center, Tabriz University of Medical Sciences, 51656-65811 Tabriz, Iran

Y. N. Ertas
Department of Biomedical Engineering, Erciyes University, Kayseri 38039, Turkey

S. K. Sharma
Department of Physics, Central University of Punjab, Bathinda 151401, India

Department of Physics, Federal University of Maranhao, Sao Luis, MA 65080-805, Brazil

S. K. Sharma et al. (eds.), *Harnessing Materials for X-ray Based Cancer Therapy and Imaging*, Nanomedicine and Nanotoxicology,
https://doi.org/10.1007/978-3-031-04071-9_8

their several benefits over conventional contrast agents, such as longer blood circulation time, regulated biological clearance pathways, and precise molecular targeting capabilities. The basic design concepts of nanoparticle-based CT contrast agents will be described in this chapter in comparison to iodine and other commercial products with in vivo and in vitro experiment.

Keywords CT contrast agent · Nanoparticles · X-ray · Medical imaging

1 Introduction

Discovery of X-ray, a milestone in the history of science, has largely been attributed to images from organs to molecules scale in both treatment and diagnosis [1]. Medical application of X-ray is divided into two main categories: structural and functional imaging. Structural imaging reveals anatomical structures, while functional imaging measuring changes in biological functions including metabolism, blood flow, regional chemical composition and biochemical processes [2]. Skipping the various applications of X-ray in non-medical fields such as material science to determine sample structure and physical properties, this chapter is devoted to introducing the benefits of contrast agents and the magnificent role of nanotechnology in developing agents of interest for imaging scope.

Upon X-ray beam incidence and followed interaction with sample, due to the weak X-ray absorption (low attenuation coefficient) with light atoms such as carbon, hydrogen and nitrogen as organic phosphors elements, fluorescence is generated from singlet excitons. Upon X-ray beam incidence and interaction with sample, electrons either attenuation or secondary X-ray/luminescence optical excitation occurs [3, 4]. X-ray may be scattered or absorbed by cells and as a result, X-ray radiation intensity attenuates until it reaches the scintillator. The difference or contrast between different X-ray absorption ability of tissues make it possible to distinguish them [5, 6], whereas the transmitted X-ray generates the background noise [7].

Absorption of X-ray energy by electrons provides a situation for every element to emit a unique X-ray fluorescence spectrum at a specific angle which can be detected by a detector [8]. This spectrum behaves like a fingerprint for identifying the element.

Despite the limitation of imaging techniques, they can be used to complete image information. Contrast agents can also be applied in vivo molecular imaging such as tracking kinetics of drugs, cancer diagnosis and beta-amyloid plaques [9, 10].

X-ray attenuation is detected by projection and computed tomography imaging techniques. The contrast between tissues is determined by relative attenuation of objects which itself depends on atomic number and tissue density [11]. Thus, soft tissues (e.g., tumors, muscle, and fat) and materials containing hydrocarbon backbone with low density and atomic number produce less contrast in comparison to tissues like bone [12].

Computed tomography provides 3D images through mathematical back projection algorithms by converting sinograms to tomograms [13]. This highly efficient imaging

technique apart from many other applications has been used for diagnosis as high resolution data can be analyzed easily. Exposure period must neither be long nor short but long enough to prevent poor resolution, mainly in soft tissue. To increase the quality of the image, several imaging techniques or contrast agents can be employed. Contrast agent material should have a high atomic number to attenuate X-ray intensity to the desired level and consequently, create the appropriate contrast. Commercial contrast agents for examining soft tissue such as iohexol, iodixanol and barium sulfate contain iodine and barium with atomic numbers of 53 and 56 respectively, which enables them to reduce X-ray density more than the soft tissue does.

Disadvantages of conventional X-ray:

- Soft tissues are not distinguished from each other. Although contrast agents are able to enhance the contrast but it has been shown that it is not sufficient for detection of tumors in early stages and in deep anatomical regions.
- Low sensitivity is observed when X-ray intensity decreases, because noise which is caused by transmitted X-ray, lowers the contrast.

Contrast agents can be used for highlighting a specific part of tissue or functionalized to target the expressed proteins on the surface of specific cells such as tumor cells. Not all contrast agents attenuate X-ray intensity at the same level, but proportional to their mass attenuation coefficient. This is the reason why different doses of X-ray are employed for different contrast agents. Toxicity and circulation time of the contrast agent should be taken into consideration for specific applications.

The significance of CT as one of the principal radiology techniques which is frequently used in biomedical imaging, has experienced a significant growth with the development of various nanoparticles (NPs) as next generation CT contrast agents. Because of their numerous benefits over traditional contrast agents, such as longer blood circulation period, regulated biological clearance pathways, and precise molecular targeting capabilities, NPs are going to play a substantial role in the future of medical diagnostics. This section outlines different NPs, which play a significant role in X-ray techniques and imaging applications as contrast agents. Traditionally, iodine-based components were employed as contrast agents in CT scans, however after development of NPs with high atomic number, K-absorption edge (K-edge), and appropriate coefficient absorption, iodine started to lose its importance in the literature. The iodine-based elements were compared to modern NPs such as gold, silver, bismuth, thorium, tantalum, and lanthanides. These series of NPs have usually better performance in comparison to the iodine or iohexol in terms of toxicity, and coefficient parameters. However, thorium-based NPs had a malignancy effect as a long-term side effect. Following sections will provide in-depth information regarding these benefits and deficiencies.

2 Nanoparticle Based Contrast Agents

2.1 Gold Nanoparticle Based Contrast Agents

Gold, one of the chemical elements with high atomic number (79), has been identified as a metaphysical and healing power source since ancient times, and it attracted attention of many researchers in traditional medicine and many of recent investigators were also fascinated by its different applications in nanomaterial and biomedical sciences [14]. In 2004, Smilowitz and his colleagues utilized the high atomic number of gold in the field of X-ray imaging, which has since acquired significant attraction across the world [15]. Since 2004, it is clearly seen that most of the research on inorganic nanoparticles based X-ray contrasting media have focused on gold nanoparticles or their hybrids. Aside from the fact that gold particles exhibit great attenuation in X-ray, research has also concentrated on the significant control of their physical, chemical, and biological characteristics, making it one of the most appropriate candidates for X-ray CT and multimodal imaging [16]. AuNPs are not only stable and inert, but they also exhibit a variety of intriguing characteristics, including self-assembly in conjugation with organization motifs and templates, size-related electrical and optical properties, and uses as catalyst and biological processes. The following points highlight the uses of AuNPs for medical diagnostics and X-ray CT imaging: (i) radiopacity characteristics that have been shown to be superior to standard CT contrast agents (e.g., iodinated), (ii) a highly adaptable and simple surface chemistry that allows for a broad flexibility in surface functionalization for in vivo stability or coating, as well as conjugation with specific functional molecules for active targeting to specific organs and cancerous cells. (iii) and biocompatible properties.

In 1847, Faraday described the production of red gold solutions by reduction of gold chloride and phosphorus in carbon disulfide. Similarly, synthesis process of gold NPs is based on the reduction of gold salt by a variety of reduction agents and chemical methods. Citrate reduction is one of the methods which are introduced by J. Turkevich. This is the simplest protocol which allows the synthesis of monodisperse and spherical shape, citrate stabilized AuNPs with a size range of 10–20 nm [17–19]. However, size of NPs can be changed from 16 to 147 nm using improved methods and adding amphiphilic items into the synthesis reaction [20–23]. In the previous decade, AuNPs were used as X-ray contrast agents due to their high stability against oxidation, exceptional absorption coefficient (5.16 cm^2g^{-1}) and high Z-number (79) instead of traditional iodine-based alternatives with low absorption coefficient (1.94 cm^2g^{-1}) and lower Z-number (53) where Au exhibits 2.7 times more contrast per unit weight in comparison to iodine at 100 keV. Furthermore, gold imaging at 80–100 keV minimizes interferences from bone and soft tissue absorption and finally lowers the overall radiation dosage and exposure [24].

When AuNPs are used as blood pool contrast agents (BPCA), it is worth noting these three factors: (i) stabilization of AuNPs suspensions in bulk media is required which is related to the synthesis steps, (ii) AuNPs should demonstrate proper in vivo

pharmacokinetics properties and good in vivo stability which need suitable coating, for example PEG-coatings which show poor interactions with plasma proteins [19, 20], (iii) active targeting should be achieved by surface modifications to enable site-specific targeting between AuNPs and receptors of tumor cells. Active targeting usually links the functionalized NPs and receptor-specific target using three distinct biomarkers that are highly expressed in cancer cells site which include epidermal growth-factor receptor, matrix metalloprotease and oncoproteins that are related to the human papillomavirus infection [25]. Figure 1 depicts the surface functionalization of AuNPs as well as their potential for surface coating and nano encapsulation. Table 1 shows different applications of AuNPs in BPCA and CT applications. In

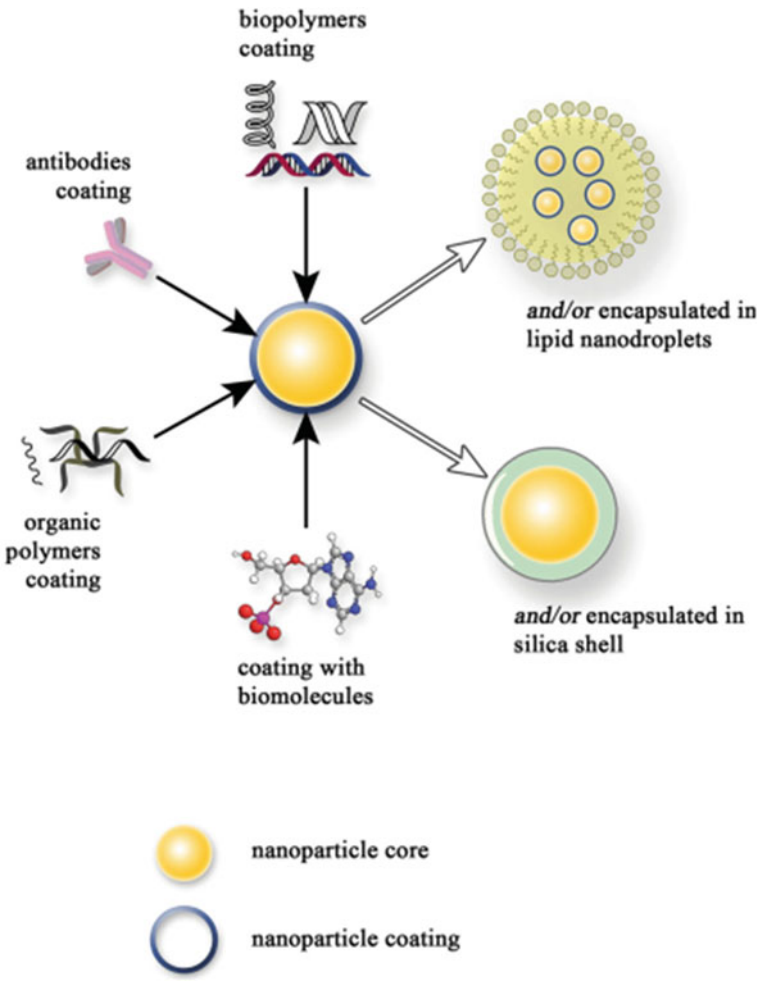

Fig. 1 Schematic illustration of surface functionalization of inorganic NPs with different materials. Reproduced with permission from Ref. [27]. Copyright 2012, with permission from Wiley

Table 1 Main results regarding the use of AuNPs as X-ray contrast agent and imaging

Reducing agent	Coating	Targeting	Application	Main results	References
Citrate	PEG coating	–	BPCA	$t_{1/2}$∼12 h	[19]
Commercial product	Heparin coating	–	Contrast agent	Stable, biocompatible	[28]
THPAL (phosphino animoacid)	Gum Arabic coating	–	Contrast agent	Enhanced contrast in juvenile swine & Good tolerance to administration	[29]
Citrate	2-mercaptosuccinic acid (MSA)	–	Contrast agent	Surface-enhanced Raman spectroscopy (SERS) and CT	[21]
Citrate	PEG-COOH coating	Antibody: CD4	Imaging	Contrast enhancement stronger with large AuNPs	[22]
Growth method	Poly(acrylic acid) (PAA) coating	Antibody: UM-A9	Imaging	CT imaging allows reliable and sensitive detection of lymph nodes	[16]
$NaBH_4$	Dendrimer G5-NH2	Folic-Acid and FITC	Imaging	Efficiency in targeting (and thus imaging) KB cells	[30]

addition, Table 1 shows that citrate reduction is obviously the preferable method for the production of AuNPs core because it is the simplest approach to provide a stable dispersion in aqueous media. Besides, PEGylation of AuNPs can also be beneficiary in BPCA applications and imaging processes, and it can mitigate the effect of reticuloendothelial system (RES) by minimizing the accumulation of AuNPs in liver and spleen. Targeted CT contrast agents using AuNPs have achieved global success ranging from long circulation vascular contrast to targeting tumor cells [19, 20, 22, 26].

To increase contrast effect and better surface modification, gold NPs can be used with gadolinium to provide hybrid NPs. Gadolinium is in the middle of the lanthanide family and it contains seven unpaired electrons, producing a strong signal in magnetic resonance imaging (MRI). Coupling gold with gadolinium illustrates a suitable detectable dual nanosystem both by X-Ray CT and MRI. The core of this hybrid nanosystem is made up of AuNPs and the shell layer is gadolinium where disulfide bonds keep them together. The reduction of gold salt in the presence of dithiolated derivatives of diethylenetriaminepentaacetic acid was followed by the addition of Gd^{3+}. Through disulfide connections, the two thiol groups were critical in the creation of the multilayered ligand shell. Favorably, modest concentrations of

gold (10 mg/mL) and gadolinium (5 mg/mL) could be easily identified and tracked using MRI and X-ray imaging [31]. Presence of cysteine [32], penicillamine [33] and 4-aminothiophenol [34] on Gd added AuNPs demonstrated high r_1 relaxivity [33].

Furthermore, Jon et al. also evaluated the ability of coupled superparamagnetic iron oxide with AuNPs [35, 36]. In 2009, synthesis of PEG coated iron oxide core and gold shell hybrid NPs were also reported. The particle surfaces were coated with PEG to assure biocompatibility and a lengthy circulation duration in the bloodstream even at high concentrations. Amphiphilic poly(DMA-r-mPEGMA-r-MA) prevent aggregation and increasing water solubility [35]. Mulder and colleagues demonstrated another method for developing multifunctional probes for fluorescence imaging, CT, and MRI. They coated a fluorescent and paramagnetic lipid layer containing a Gd conjugation and a special dye Cy5.5 over gold/silica core-shell NPs which exhibited highly sensitive signal enhancements of 24 and 50% for MRI and CT in mice liver, respectively [37].

In another study, Salehi et al. used PEGylated AuNPs with deoxycholic acid (DCA-PEG-GNPs) (Fig. 2c) in comparison to commercially available contrast agent Visipaque. DCA-PEG-GNPs with the size of 17 nm in an oval-like shape as shown in Fig. 2a demonstrated significant stability in a various range of pHs (2.5–11) and

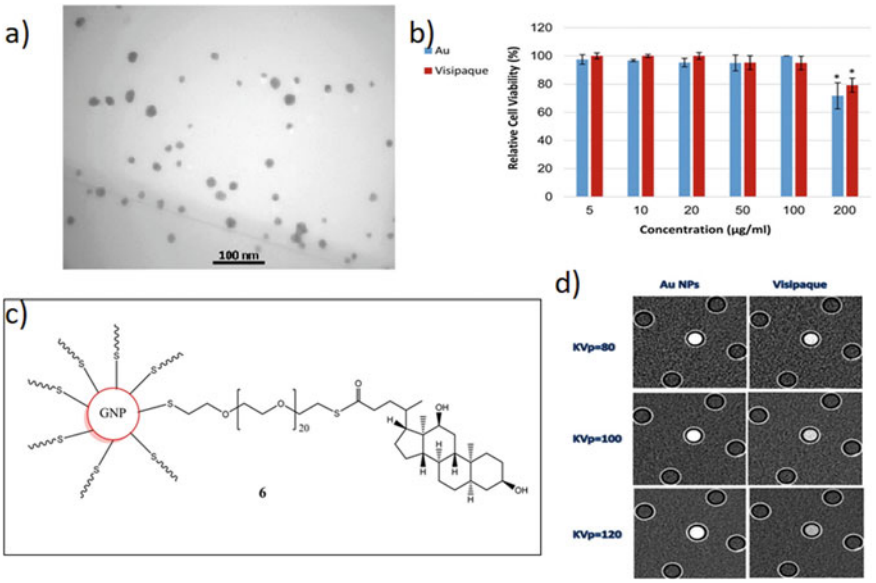

Fig. 2 **a** TEM image of DCA-PEG-GNPs, **b** MTT assay on A549 cells in different concentrations of DCA-PEG-GNPs and Visipaque, **c** Structure of DCA-PEG-GNPs, **d** In vitro X-ray CT images at different kVp values, the vials contained 1.0 mg ml^{-1} AuNPs or iodine. Reproduced with permission from Ref. [38]. Copyright 2020, with permission from Wiley

temperatures (−78–48 °C). Also, AuNPs had similar cell viability with Visipaque in the concentration value of under 100 μg/ml on A549 lung cells. MTT assay also suggested that in the high concentration (200 μg/ml), AuNPs showed low cell viability than Visipaque as shown in Fig. 2b. Notably, CT performance of DCA-PEG-GNPs were higher than Visipaque. This result is also comparable with the iodine. For example, at kVp = 120 keV, the attenuation value of 0.8 mg ml^{-1} for iodine was close to the attenuation value of 0.49 mg ml^{-1} for gold as shown in Fig. 2d [38]. In addition, Wang and his colleagues designed Au nanocage@PEG nanoparticles (AuNC@PEGs) as shown in Fig. 3 in different concentrations (0, 50, 100, 200, 500, and 1000 μg/ml) and compared with iodine and showed that Au nanocages were possible alternative CT contrast agents to iodine [39]. Park et al. synthesized gold@silica NPs, and their cytotoxicity studies displayed that they were not hazardous, and while tiny deformations on the silica shell had no effect on the stability of gold@silica NPs, larger deformations on the silica shell resulted in agglomeration. However, in vivo applications revealed effective contrast enhancement in CT imaging [40]. Real-time in vivo X-ray images showed that gold@silica NPs with folic acid (FA) as a targeting agent can visualize MGC803 gastric cancer after intravenous injection in nude mice as show in Fig. 4 [41, 42].

Interestingly, Guo et al. designed multifunctional core–shell tecto dendrimers (CSTDs) with AuNPs core and β-cyclodextrin modified generation 5 poly(amidoamine) dendrimers for dual-mode CT and MRI of tumors. Au CSTDs with the size of 11.61 nm displayed excellent stability, strong X-ray attenuation and good r_1 relaxivity (9.414 mM^{-1} s^{-1}), and desirable cytocompatibility as well. They also showed that CSTDs act as suitable CT/MRI dual mode imaging probe (Au/Gd) in cancer diagnosis applications as shown in Fig. 5 [43].

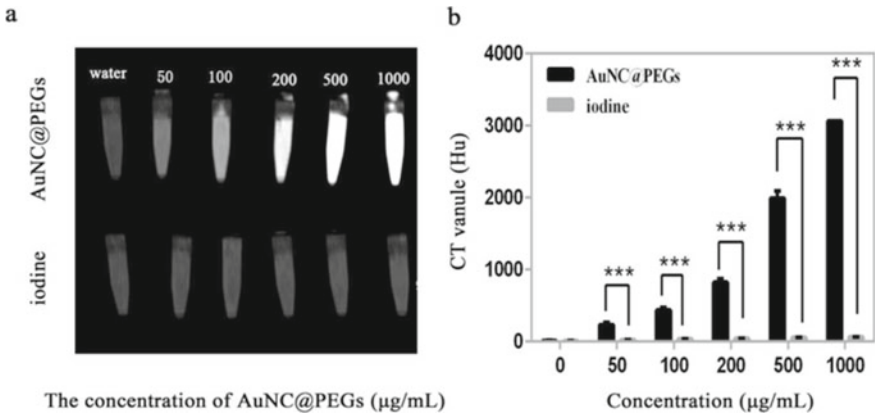

Fig. 3 **a** In vitro CT images of AuNC@PEGs and iodine-based at different concentrations. **b** Hu values for AuNC@PEGs and iodine-based contrast agents, ***P < 0.001. Reproduced from Ref. [39] with the permission of the Creative Commons Attribution 4.0 International License http://creativecommons.org/licenses/by/4.0/). Copyright 2020, Springer

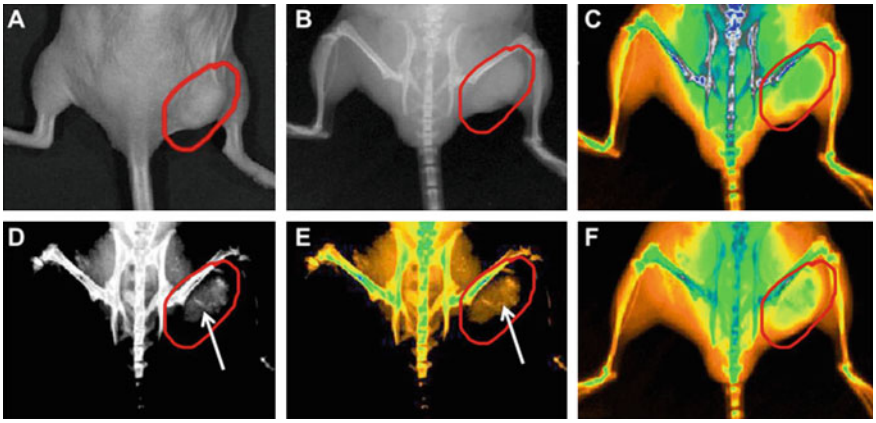

Fig. 4 Real-time in vivo X-ray images. **a** The tumor tissue, **b** X-ray image at 0 h, **c** X-ray image at 0 h (in color), **d** X-ray image at 12 h, **e** X-ray image at 12 h (in color). **f** X-ray image at 24 h (in color). Reproduced with permission from Ref. [41]. Copyright 2011, with permission from Elsevier

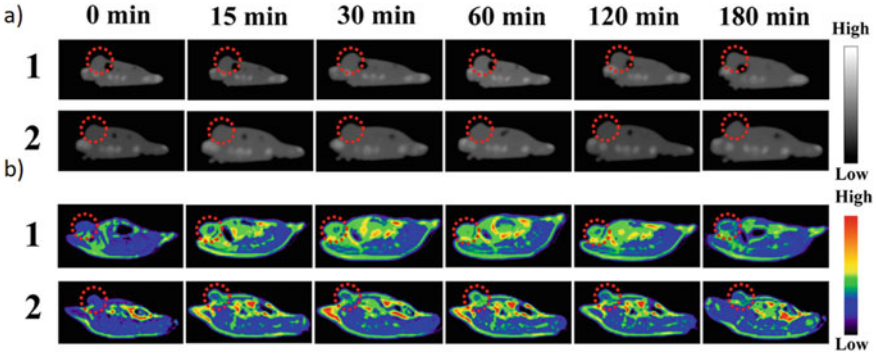

Fig. 5 **a** CT images and **b** T1-weighted MR image of Gd@Au CSTDs in vivo. Reproduced with permission from Ref. [43] Copyright 2021, with permission from ACS

2.2 Silver Nanoparticle Based Contrast Agents

Silver, a metal with atomic number of 47, is recognized as fascinating NPs in different applications such as biomedical sciences, food, textiles, consumer products and industrial purposes, due to their unique physical and chemical properties.

Image processing at two separate energy windows is known as dual-energy imaging (low and high) where images with reduced contrast between background tissues is achieved by weighting variables. Because of good X-ray attenuation properties of Ag as appealing contrast material with k-edge[1] of 25.5 keV and average

[1] The K-absorption edge (K-edge) is the sudden rise in photoelectric absorption of x-ray photons observed at an energy level slightly above the binding energy of the absorbing atom's k-shell

diameter of 2–6 nm by Brust method demonstrate slight cellular toxicity in T6-17 fibroblast cells. AgNPs, stabilized with PEG, can provide similar or better contrast in comparison to the iodine [44].

Silver iodide (AgI) and silver oxide (Ag_2O) were introduced as contrast agents in the earlier twentieth century. However, their usage was immediately halted due to the significant toxicity and reported deaths [45–47]. Yet, silver was maintained in the liver for a long enough period of time to allow CT scanning with a contrast difference of 4–5 times that of the background [48]. Lui et al. showed the X-ray contrasting properties of generation 5 poly(amidoamine) dendrimer which is appropriate for the stabilization of silver nanoparticles for in vivo CT imaging. Size and concentration of AgNPs are two main parameters for the X-ray absorption coefficient. They were not only able to readily control the size of AgNPs from 8.8 to 23.2 nm by changing the molar ratio of dendrimer/Ag salt, but also kept AgNPs stable in the phosphate buffered saline, fetal bovine serum and water at pH range of 5–8 in room temperature conditions. It is quite interesting to note that X-ray attenuation behavior of particles with a diameter of around 16 nm were identical to those of an iodine-based contrast agent and in vivo studies with mice revealed that the AgNPs provided sustained contrast enhancement while having no severe toxicity. In another study, Cormode and his colleagues explored potential of silver telluride (Ag_2Te) NPs in an in vivo setting at a low dose (2 mg Ag per kg) for X-ray imaging. An astonishing contrast agent performance was observed compared to the $AgNO_3$, Na_2TeO_3 and iodine which were frequently used in the previous studies as shown in Fig. 6 [49].

Luo et al. produced heterostructure samples with bismuth and silver NPs conjugated with poly(vinylpyrrolidone) (PVP) to design Bi-Ag@PVP NPs for

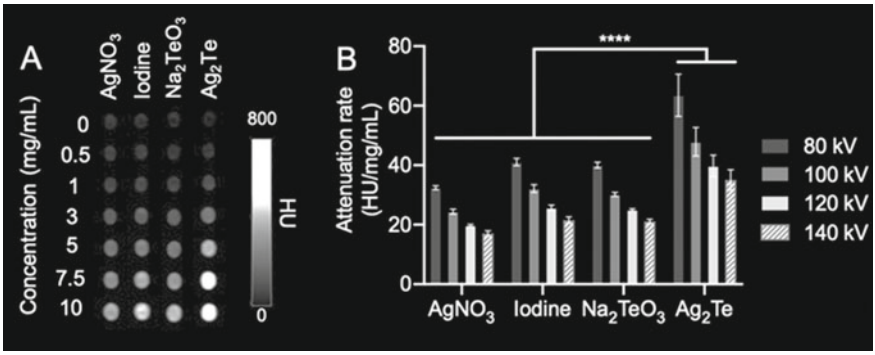

Fig. 6 In vitro imaging with CT. **a** CT phantom images, **b** CT attenuation rate of the different samples at various energies (80,100, 120, and 140 kV). Reproduced with permission from Ref. [49]. Copyright 2020, with permission from RSC

electrons. Each element's K-shell binding energies are unique. As an element's atomic number (Z) grows, so does its corresponding k-shell binding energy, and therefore the photon energy at which the K-edge occurs. The K-edges of the most common elements in human tissue (hydrogen, carbon, oxygen, and nitrogen) are too low to be detected (1 keV). Elements with larger K-edge values, are within the useful portion of the x-ray spectrum, are of greater interest in radiology.

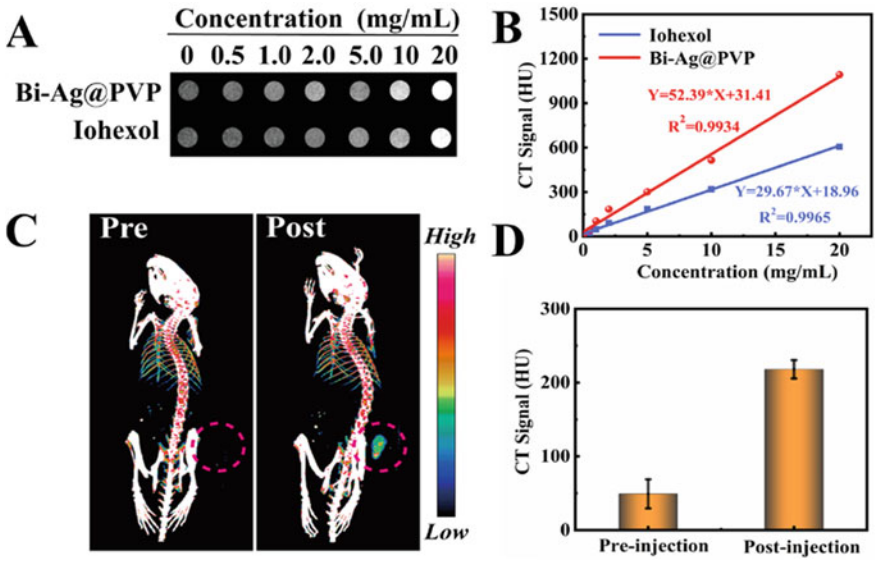

Fig. 7 **a** CT images of Bi-Ag@PVP and iohexol, **b** CT signals-concentration fitting curves, **c** CT imaging capability of Bi-Ag@PVP NPs in tumor site (red), and **d** CT signal intensity before and after injection. Reproduced from Ref. [50] with the permission of the Creative Commons Attribution 4.0 International License http://creativecommons.org/licenses/by/4.0/. Copyright 2021, ACS

quadra applications including CT, photoacoustic imaging, photodynamic therapy and photothermal therapy (PDT/PTT) into one nanotheranostic platform. They also compared Bi-Ag@PVP with the commercial contrast agent, iohexol, in different range concentrations from 0 to 20 mg ml^{-1} as shown in Fig. 7 [50].

2.3 Bi Nanoparticle Based Contrast Agents

Bismuth is a heavy metal with a high atomic number of 83. Bismuth was one of the first X-ray contrast agents used on human gastrointestinal tract before the 1990s [51–53]. The surface of Bi_2S_3 NPs was modified with poly(vinylpyrrolidone) (PVP), a biocompatible polymer, and a rectangular flat plate morphology, size range of 10–50 nm and 4 nm in thickness was obtained. These NPs were highly soluble in water, inert and had a longer blood half-life. Noticeably, the X-ray opacity of Bi_2S_3–PVP NPs was about fivefold higher than the commercial iodine. In vivo experiment revealed the temporal evolution of the blood after injection where NPs accumulated in liver and spleen after 24 h [53].

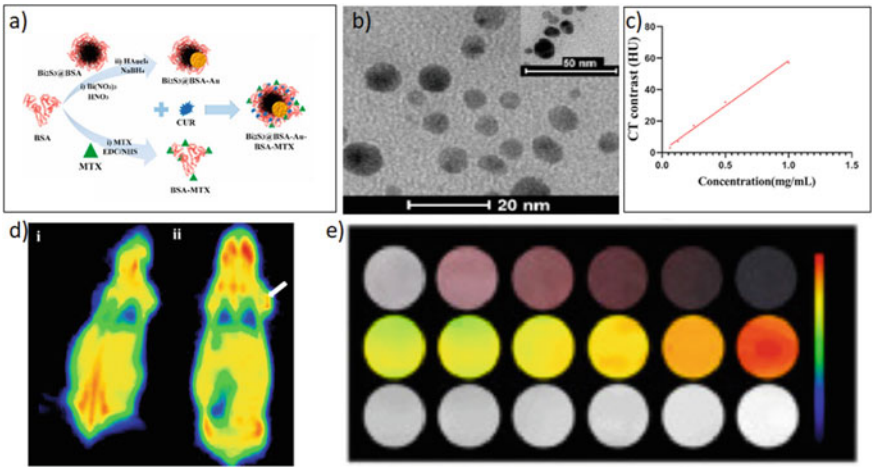

Fig. 8 **a** Schematics of designed nano drug delivery system of Bi_2S_3@BSA-Au-BSA-MTX-CUR, **b** TEM image of Bi_2S_3@BSA-Au-BSA-MTX-CUR, **c** CT contrast value curve of Bi_2S_3@BSA-Au-BSA-MTX-CUR at different concentrations, **d** CT images of mice with a 4T1 tumor recorded at (i) pre and (ii) post intravenous injection of Bi_2S_3@BSA-Au-BSA-MTX-CUR, and **e** First row: Typical photograph of each concentration; Second and Third rows: CT images of each concentration. Reproduced from Ref. [10] with the permission of the Creative Commons Attribution 4.0 International License (http://creativecommons.org/licenses/by/4.0/). Copyright 2022, Elsevier

Radiopaque[2] objects block radiation rather than allow it to pass through. This concept was cleverly employed in a study where Bi_2S_3 NPs with the inner core layer covered with alginate-poly-L-lysine-alginate were used to avoid toxic effects in the X-ray process. Results displayed microcapsules were not only visualized individually in the rabbit and mice, but also kept their contrast properties for two weeks due to low water solubility [54].

Nosrati et al. evaluated the ability of Bi_2S_3-Au semiconductor heterojunction NPs which can improve the contrast of CT images and free radical generation via the Schottky barrier in addition to their intrinsic radiosensitizing ability [10]. As it is declared earlier, under X-ray irradiation, NPs with high-Z number (here bismuth) components produce secondary and Auger electrons via the photoelectric and Compton processes, resulting in the generation of large quantities of reactive oxygen species (ROS) within the cells [10, 55, 56]. Figure 8 shows successful targeting and

[2] **Radiopaque**: Opaque to one or another form of radiation, such as X-rays. Radiopaque Metal, for instance, is radiopaque, so metal objects that a patient may have swallowed are visible on X-rays. Radiopaque dyes are used in radiology to enhance X-ray pictures of internal anatomic structures. The opposite of radiopaque is radiolucent.

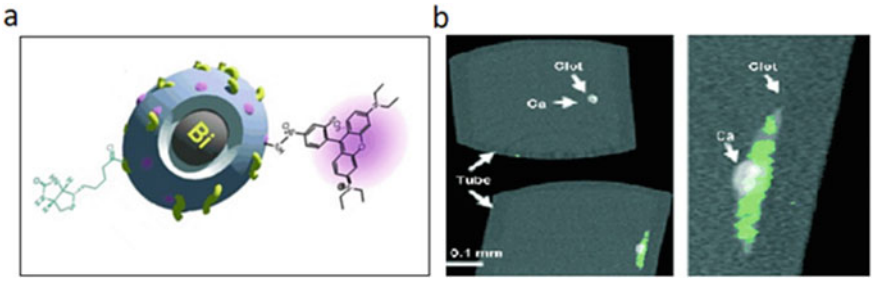

Fig. 9 **a** Structure of Bi-based NanoK, **b** Cross-sectional slices of fibrin clot targeted with NanoK presenting calcium. Reproduced with permission from Ref. [57]. Copyright 2020, with permission from ACS

effective tumor accumulation of drug loaded heterojunction NPs (Bi_2S_3@BSA-Au-BSA-MTX-CUR). It increase the Hounsfield units (HU)[3] in the tumor site from 15 to 81 (white arrow). They also showed that CT contrast intensity directly depended on the concentration of the final sample (Bi_2S_3@BSA-Au-BSA-MTX-CUR) as shown in Fig. 8c and e.

In a study, Pan et al. demonstrated CT contrast effect for detection of clot with thrombus-targeted NanoK with a diameter of 180 and 250 nm (Fig. 9b) [57].

Zhang et al. explored ultrasmall FA and bovine serum albumin-modified Bi–Bi_2S_3 heterostructure NPs (Bi–Bi_2S_3/BSA&FA NPs) as CT contrast agents. Bi–Bi_2S_3/BSA&FA NPs with the size of 10 nm showed not only an appropriate stability due to formation of Bi_2S_3 NPs on the surface of Bi without any agglomeration even after the one month, also displayed photothermal conversion efficiency (35%). As demonstrated in Fig. 10, the X-ray absorption coefficient of Bi–Bi_2S_3/BSA&FA NPs (50.4 HU L g^{-1}) is higher than commercial contrast agent iohexol (24.1 HU L g^{-1}), therefore, Bi–Bi_2S_3/BSA&FA NPs can be a candidate CT contrast agent [58].

Yang et al. explored bismuth functionalized S-nitrosothiol (Bi–SNO NPs) with a size of 36 nm for the combination therapy (X-ray radiotherapy and 808 nm PTT). X-rays can break down the S–N bond and commence a large amount of NO-release which is a cancer killing agent at concentrations above 60 μM [59]. CT value increased from 47.52 HU to 232.21 HU at a NP concentration of 2 mg.mL^{-1} after the injection [59]. Shan et al. designed Bi/Se NPs loaded with Lenvatinib (Len) in a simple reduction reaction for in vivo CT imaging of mice. They showed that Bi/Se-Len NPs can increase CT value from 27 to 638 HU after the injection in mice [60]. Luo and his colleagues also designed hybrid NPs containing bismuth and lanthanide conjugated PVP as BiF_3Ln@PVP as a CT contrasting agent. CT value increased from 48.9 HU to 194.58 HU post-injection, as shown in Fig. 11 [61].

[3] **Hounsfield unit (HU)** is a relative quantitative measurement of radio density that radiologists use to analyze computed tomography (CT) images. During CT reconstruction, the absorption/attenuation coefficient of radiation within a tissue is utilized to generate a grayscale image.

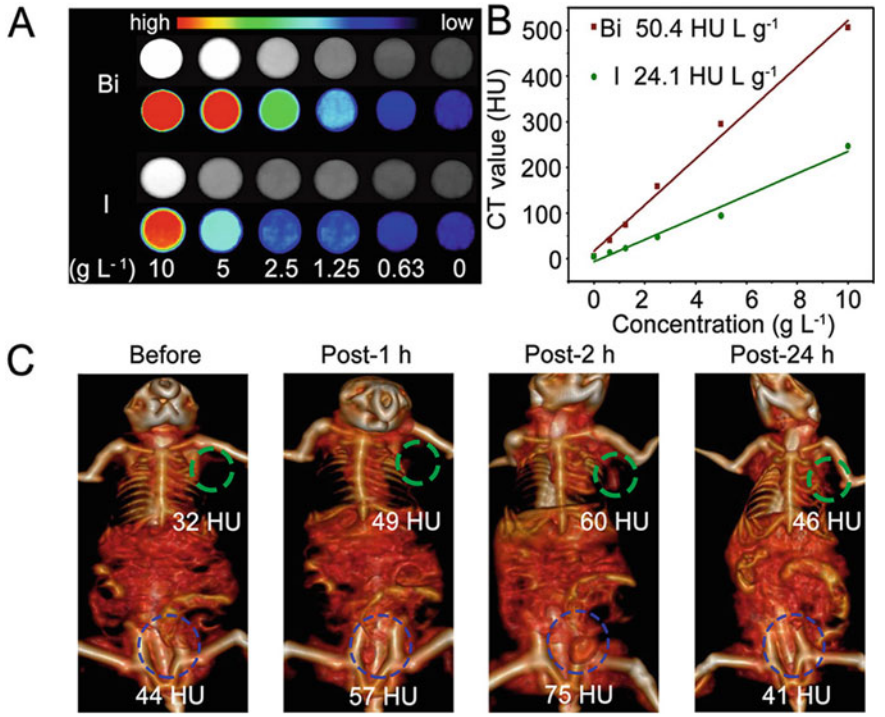

Fig. 10 **a** CT images of Bi and iohexol (I) for different concentrations from 0 to10 $g.L^{-1}$, **b** Quantification of CT value for Bi–Bi_2S_3/BSA&FA NPs and iohexol samples, **c** In vivo CT images of tumor (green circles) and bladder (blue circles). Reproduced with permission from Ref. [58]. Copyright 2019, with permission from ACS

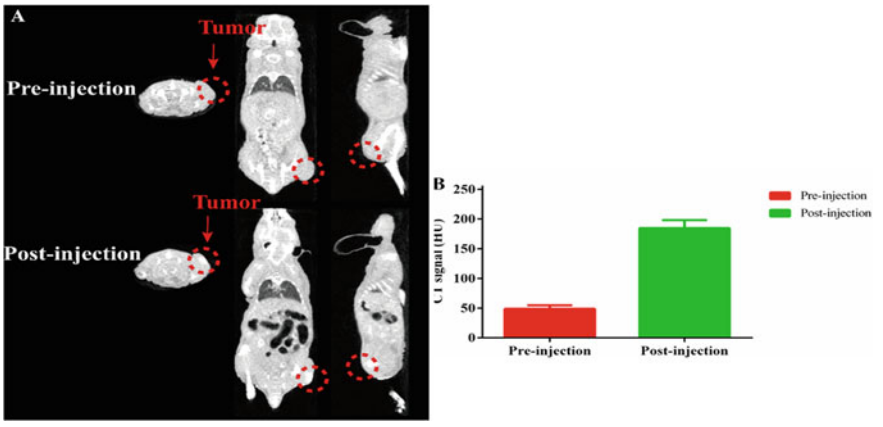

Fig. 11 In vivo CT imaging of BiF_3Ln@PVP NPs, **a** CT images before and after the injection of BiF_3Ln@PVP NPs (tumor site is shown in red circle), **b** Corresponding CT values (HU). Reproduced from Ref. [61] with the permission of the Creative Commons Attribution 4.0 International License (http://creativecommons.org/licenses/by/4.0/). Copyright 2021, Springer

Table 2 Risk of malignancy after thorotrast administration

Type of tumor	Related organ	Model of injection	Human or animal	References
Angiosarcoma[4]	Liver	Intravenous	Human	[69–71]
Plasmacytoma[5]	Blood	–	Human	[72–74]
Anaplastic[6]	Lung	–	Human	[74]
Sarcoma	–	Intraperitoneal	Guinea pigs	[75]
Cholangiocarcinoma[7]	Liver	Intravenous	Hamsters	[75]
Fibrosarcoma[8]	Local	Subcutaneous	Mice	[75]
Hemangioendotheliosarcoma[9]	Liver	Intravenous	Rabbits	[76]
Adenomas[10]	Liver	Intravenous	Rats	[77]

2.4 Thorium Oxide Nanoparticle Based Contrast Agents

Thorium, one of the actinide group element (group 4, period 7) with a high atomic number of 90 is represented with the symbol Th. In 1828, Jöns Jacob Berzelius, a Swedish scientist, discovered Th in the mineral thorite ($ThSiO_4$). Heyden chemical company produced colloidal thorium oxide (ThO_2) as a radiological contrast agent in 1920s [62, 63]. Favorably, ThO_2 or Thorotrast (trade label) does not aggregate after intravenous administration with a size of 3–10 nm and showed appropriate contrast agent performance due to the high atomic weight. ThO_2 was also used as oral administration in gastric mucosa and upper part of gut for imaging applications. However, it is found that ThO_2 not only deposits lifelong in the RES of many organs such as spleen, liver, lymph nodes and bone marrow, but also causes formation of malignant tumors, blood dyscrasias, liver fibrosis and leukemia [64–68]. Table 2 shows some of these problems which cause malignant effects in human and animal models [65]. Later, the usage of colloidal ThO_2 was eventually abandoned due to the severe toxicity.

[4] Angiosarcoma is a rare cancer that develops in the inner lining of blood vessels and lymph vessels. This cancer can occur anywhere in the body but most often is in the skin, breast, liver and spleen.

[5] Plasmacytoma is a plasma cell dyscrasia in which a plasma cell tumor grows within soft tissue or within the axial skeleton.

[6] A term used to describe cancer cells that divide rapidly and have little or no resemblance to normal cells.

[7] Cholangiocarcinoma is a type of cancer that forms in the slender tubes (bile ducts) that carry the digestive fluid bile. Bile ducts connect your liver to your gallbladder and to your small intestine.

[8] Fibrosarcoma is a rare type of cancer that affects cells known as fibroblasts. Fibroblasts are responsible for creating the fibrous tissue found throughout the body. Tendons, which connect muscles to bones, are made up of fibrous tissue.

[9] A malignant tumor arising from vascular tissue.

[10] Adenoma is a benign tumor of glandular tissue, such as the mucosa of stomach, small intestine, and colon, in which tumor cells form glands or gland like structures.

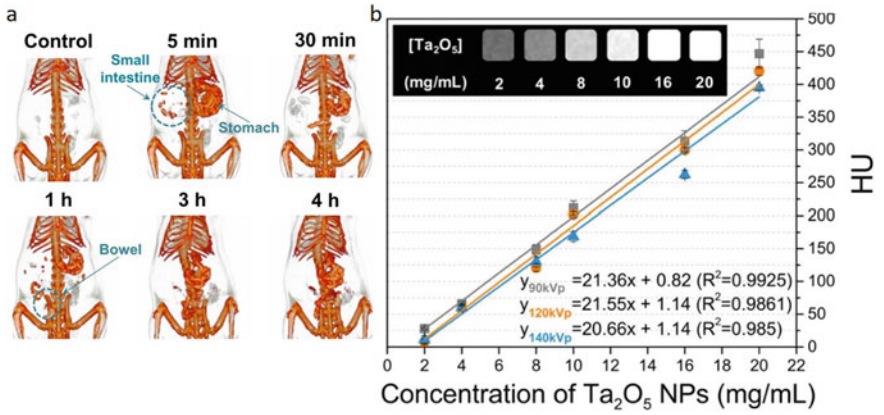

Fig. 12 **a** CT image of Ta_2O_5 NPs from the coronal views in GI tract, **b** CT images and values of Ta_2O_5. Reproduced with permission from Ref. [84]. Copyright 2020, with permission from RSC

2.5 Tantalum Nanoparticle Based Contrast Agents

Tantalum is a chemical element with the atomic number of 73 and the symbol Ta in the periodic table. Tantalum has demonstrated certain benefits over traditional iodinated contrast agents as a X-ray contrast agent due to the high radiopacity with a density of 16.6 g/mL [78–80]. Tantalum oxide (Ta_2O_5) is a biocompatible material and used in gastrointestinal imaging and angiography [81–83]. Bonitatibus et al. designed a tantalum-based NP in the form of a core–shell structure with the total size of less than 6 nm. Silica was used as a coating layer to make NPs stable and water soluble. In vivo experiment showed that tantalum-based NPs displayed appropriate contrast compared to iodine [84]. Krivoshapkin and his colleagues also showed Ta_2O_5 NPs, at a concentration of 20 $mg.ml^{-1}$, can increase CT value from 47.1 ± 5.7 HU to 426.1 ± 2.8 HU at tumor site in 10 min Fig. 12 [85].

2.6 Rare Earth Nanoparticles Based Contrast Agents

Rare earth elements display very complex luminescence activity which arises from f-f transitions of the 4f shell and f-d transitions in the 4f-5d shell. Upconversion nanoparticles (UCNPs) and downconversion nanoparticles (DCNPs) are the two primary types of rare-earth based NPs. UCNPs can convert low energy with long-wavelength light to high energy with short wavelength while DCNPs convert high energy to low energy. Rare-earth NPs have been widely employed in vitro and in vivo imaging of biomolecules due to the outstanding properties of rare-earth ions, such as their low energy losses, different absorption and emission wavelengths, and low

photobleaching [86]. Below, two rare-earth NPs are introduced as contrast agents in imaging applications.

2.6.1 Gadolinium Based Nanoparticles

Gadolinium (Gd) is an appropriate contrast agent for MRI [87] and CT imaging due to its high atomic number (64), large number of unpaired electrons and high K-edge (52 keV) which is greater than iodine. Havoron et al. evaluated Gd oxide as a contrast agent in 1970s. Their animal test resulted that there were no observable toxic effects when poly(vinylpyrrolidone) was used to stabilize the Gd_2O_3 microparticles [88, 89]. In a study, Prosser et al. used Gd NPs in both CT and MRI applications. Their data indicated that $NaGdF_4$ (with a low polydispersity and 20–22 nm size) and 50:50 mixture of GdF_3 and CeF_3 (with the 10–12 nm size) not only displayed high relaxivities at 1.5 and 3 T (35–40 $mL.s^{-1}$ mg^{-1}) in MRI which was better than Gd^{3+}-DTPA (gadopentetate dimeglumine, Magnevist®) complex but also could be functionalized with folic acid for targeting purpose in human cancer cells [90].

In another study, Watkin et al. described Gd_2O_3-albumin NPs with a diameter of 20–40 nm and embedded them within protein microspheres as CT contrast agent, which had 40 to 100 times higher contrast effect than iopamidol[11] at the same concentration [91, 92]. In a similar approach, Ru(bpy):Gd(III)@SiO_2 NPs were developed as a contrast agent for CT imaging, MRI and diffuse optical tomography. Ru(bpy) can act as a dye to prohibit photo bleaching and Gd has paramagnetic properties which is useful in enhancing MR contrast for both longitudinal (T_1) and transverse (T_2) proton relaxation rate measurements. NPs displayed higher contrast enhancement than the commercial contrast agent, Gadoteridol, however, the contrast effect was less than the trade mark Omnipaque® at the same concentration [27, 93].

Qui et al. explored fabrication of neodymium (Nd)-doped and gadolinium tungstate NPs with a hydrophilic layer ($NaGd(WO_4)_2$:Nd@PDA–HA NPs) for CT, MRI and fluorescence imaging. Their result demonstrated that NPs displayed a higher CT contrast (11.67 ± 0.46 $HU.mM^{-1}$) compared to the commercial contrast agent, iohexol (4.31 ± 0.09 $HU.mM^{-1}$). NPs were proposed as an appropriate CT contrast agent in breast tumor at a concentration of 2.5 $mg.mL^{-1}$ [94].

2.6.2 Holmium Based Nanoparticles

Holmium with electron configuration of [Xe] 4f11 6s2 is soft and stable in the room temperate but it oxidizes rapidly in moisture. Similar to gadolinium, it exhibits an effective contrasting agent for both MRI and CT imaging due to its paramagnetic nature, high atomic number (67) and high attenuation coefficient [95–98]. Bult et al. synthesized HoAcAc NPs (Fig. 13a) by dissolving holmium acetylacetonate

[11] Iopamidol, sold under the brand name Isovue among others, is a nonionic, low-osmolar iodinated contrast agent, developed by Bracco Diagnostics.

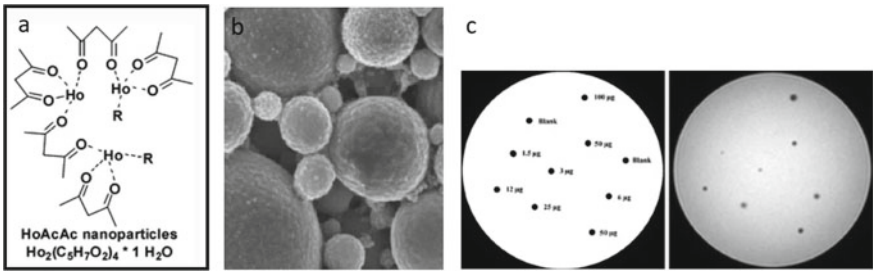

Fig. 13 **a** Structure of HoAcAc NPs, **b** STEM image of HoAcAc NPs with the size of 78 ± 10 nm, **c** Phantom image (left) and photograph of HoAcAc NPs at different concentration. Reproduced from Ref. [99] with the permission of the Creative Commons Attribution Noncommercial License (https://creativecommons.org/licenses/by-nc/2.0). Copyright 2010, Springer

in chloroform, followed by emulsifying in an aqueous surfactant solution, and stabilizing with polyvinyl alcohol and didodecyldimethylammonium bromide. Spherical HoAcAc NPs had a diameter of 78 ± 10 nm (Fig. 13b) and had higher CT contrast effect (15.6 HU·mg^{-1}) in comparison to the iodine. Figure 13c shows agarose MRI phantom images for different NP concentration, where increase in the amount of NPs resulted in an increase in the degree of darkness [99].

Ocana et al. explored the role of dysprosium vanadate ($DyVO_4$) and holmium vanadate ($HoVO_4$) NPs functionalized with poly(acrylic acid) (PAA) with a diameter of 60 nm for contrast agent application. Such NPs displayed (Fig. 14) 2.4 fold more contrast than the commercial agent iohexol [98].

Cormode et al. used cerium oxide NPs as a CT contrast agent with k-edge of 40.4 keV for imaging the gastrointestinal tract (GIT) and inflammatory bowel disease (IBD). Dextran was used to increase the accumulation in the IBD inflammation sites.

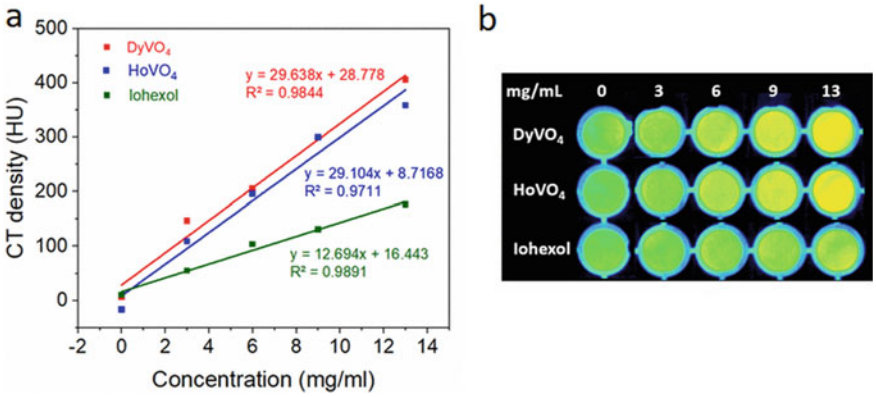

Fig. 14 **a** Quantification of HU for HVO_4 and $DyVO_4$ NPs functionalized with PAA in comparison to the iohexol, **b** CT phantom images for different NP concentrations. Reproduced with permission from Ref. [98]. Copyright 2020, with permission from ACS

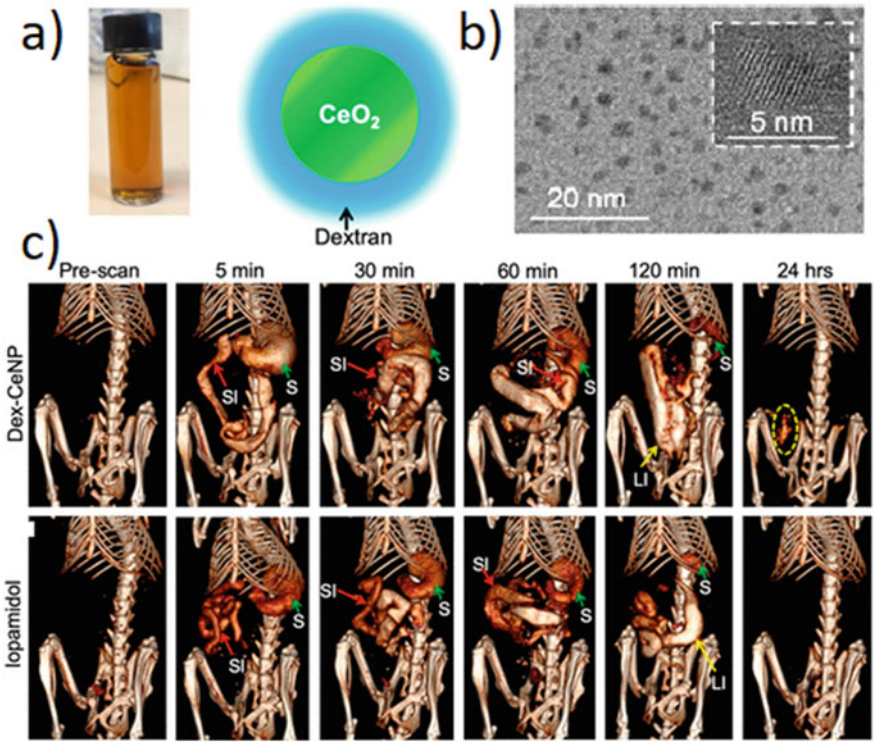

Fig. 15 **a** Photograph of a solution of Dex-CeNP, and schematic illustration of Dex-CeNF, **b** TEM image of Dex-CeNP, and **c** Micro-CT images of colitis mice, before and after oral administration of Dex-CeNP and iopamidol where "S", "SI" and "LI" are the stomach, small intestine, and large intestine, respectively. The yellow arrow shows Dex-CeNP accumulation in a colitis site. Reproduced with permission from Ref. [100]. Copyright 2020, with permission from ACS

Dextran-coated cerium oxide NPs (Dex-CeNP) was compared to the FDA-approved commercial contrast agent iopamidel (Fig. 15). More than 97% of oral dosage of Dex-CeNP was eliminated from the body within 24 h. Therefore, Dex-CeNP has the potential to be used as a CT contrast agent for GIT imaging in IBD [100].

3 Conclusion and Future Perspective

Advances in CT equipment, along with better CT contrast formulations are propelling the field of CT imaging forward in both laboratory and clinic throughout the world. Contrast enhancement and high-resolution CT images, as well as the low cost and widespread availability of clinical CT scanners facilitate the diagnosis process. High atomic number based NP based contrast agents can be a prosperous milestone in the CT imaging to decrease the radiation doses while maintaining sensitivity and

specificity, simultaneously. The reviewed studies displayed novel metal NPs can be appropriate candidates as contrast agents in CT imaging and MRI applications in compared to the traditional iodine-based contrast agent as long as long-term side effects are evaluated precisely in the clinical phase to prevent possible health concerns. Furthermore, the ability to integrate imaging and treatment as a theranostic approach in a single nanoplatform is another promising approach in biomedical applications. Appropriate design and functionalization of nanostructures can target specific tissue/cell for imaging and therapy aims. Future research and development of novel CT contrast agents is expected to result in new chemical structures, modes of different functionality, and improved image resolution, and nanoparticle based commercial CT contrast agents could be possible as long as long term in vivo concerns are well documented.

References

1. Lu L, et al (2021) High energy X-ray radiation sensitive scintillating materials for medical imaging, cancer diagnosis and therapy. Nano Energy 79:105437
2. Chen H, Rogalski MM, Anker JN (2012) Advances in functional X-ray imaging techniques and contrast agents. Phys Chem Chem Phys 14(39):13469–13486
3. Terao Y, et al (2021) X-ray induced luminescence spectroscopy for DNA damaging intermediates aided by a monochromatic synchrotron radiation. Int J Radiat Biol 1–6
4. Wang X et al (2021) Organic phosphors with bright triplet excitons for efficient X-ray-excited luminescence. Nat Photonics 15(3):187–192
5. Sy S et al (2010) Terahertz spectroscopy of liver cirrhosis: investigating the origin of contrast. Phys Med Biol 55(24):7587
6. Ji Z et al (2012) Three-dimensional thermoacoustic imaging for early breast cancer detection. Med Phys 39(11):6738–6744
7. Ma J, et al (2012) Variance analysis of x-ray CT sinograms in the presence of electronic noise background. Med Phys 39(7Part1):4051–4065
8. Cheong S-K et al (2010) X-ray fluorescence computed tomography (XFCT) imaging of gold nanoparticle-loaded objects using 110 kVp x-rays. Phys Med Biol 55(3):647
9. Bonekamp D, Hammoud DA, Pomper MG (2010) Molecular imaging: techniques and current clinical applications. Appl Radiol 39(5):10
10. Nosrati H et al (2022) Complete ablation of tumors using synchronous chemoradiation with bimetallic theranostic nanoparticles. Bioactive Mater 7:74–84
11. Birnbacher L et al (2018) Accurate effective atomic number determination with polychromatic grating-based phase-contrast computed tomography. Opt Express 26(12):15153–15166
12. Spiers F (1946) Effective atomic number and energy absorption in tissues. Br J Radiol 19(218):52–63
13. Lu W, Mackie TR (2002) Tomographic motion detection and correction directly in sinogram space. Phys Med Biol 47(8):1267
14. Meija J et al (2016) Atomic weights of the elements 2013 (IUPAC Technical Report). Pure Appl Chem 88(3):265–291
15. Hainfeld JF, Slatkin DN, Smilowitz HM (2004) The use of gold nanoparticles to enhance radiotherapy in mice. Phys Med Biol 49(18):N309
16. Popovtzer R et al (2008) Targeted gold nanoparticles enable molecular CT imaging of cancer. Nano Lett 8(12):4593–4596
17. Turkevich J, Stevenson PC, Hillier J (1951) A study of the nucleation and growth processes in the synthesis of colloidal gold. Discuss Faraday Soc 11:55–75

18. Watson KJ et al (1999) Hybrid nanoparticles with block copolymer shell structures. J Am Chem Soc 121(2):462–463
19. Kim D et al (2007) Antibiofouling polymer-coated gold nanoparticles as a contrast agent for in vivo X-ray computed tomography imaging. J Am Chem Soc 129(24):7661–7665
20. Cai Q-Y et al (2007) Colloidal gold nanoparticles as a blood-pool contrast agent for X-ray computed tomography in mice. Invest Radiol 42(12):797–806
21. Xiao M et al (2009) Gold nanotags for combined multi-colored Raman spectroscopy and x-ray computed tomography. Nanotechnology 21(3):035101
22. Eck W et al (2010) Anti-CD4-targeted gold nanoparticles induce specific contrast enhancement of peripheral lymph nodes in X-ray computed tomography of live mice. Nano Lett 10(7):2318–2322
23. Yonezawa T, Kunitake T (1999) Practical preparation of anionic mercapto ligand-stabilized gold nanoparticles and their immobilization. Colloids Surf, A 149(1–3):193–199
24. Hainfeld J et al (2006) Gold nanoparticles: a new X-ray contrast agent. Br J Radiol 79(939):248–253
25. Sokolov K et al (2003) Optical systems for in vivo molecular imaging of cancer. Technol Cancer Res Treat 2(6):491–504
26. Hainfeld JF et al (2011) Micro-CT enables microlocalisation and quantification of Her2-targeted gold nanoparticles within tumour regions. Br J Radiol 84(1002):526–533
27. Jakhmola A, Anton N, Vandamme TF (2012) Inorganic nanoparticles based contrast agents for X-ray computed tomography. Adv Healthcare Mater 1(4):413–431
28. Sun IC, et al (2009) Heparin-coated gold nanoparticles for liver-specific CT imaging. Chem A Europ J 15(48):13341–13347
29. Boote E et al (2010) Gold nanoparticle contrast in a phantom and juvenile swine: models for molecular imaging of human organs using x-ray computed tomography. Acad Radiol 17(4):410–417
30. Shi X et al (2007) Dendrimer-entrapped gold nanoparticles as a platform for cancer-cell targeting and imaging. Small 3(7):1245–1252
31. Alric C et al (2008) Gadolinium chelate coated gold nanoparticles as contrast agents for both X-ray computed tomography and magnetic resonance imaging. J Am Chem Soc 130(18):5908–5915
32. Park J-A et al (2010) Gold nanoparticles functionalized by gadolinium–DTPA conjugate of cysteine as a multimodal bioimaging agent. Bioorg Med Chem Lett 20(7):2287–2291
33. Kim H-K et al (2010) Gold nanoparticles coated with gadolinium-DTPA-bisamide conjugate of penicillamine (Au@ GdL) as a T1-weighted blood pool contrast agent. J Mater Chem 20(26):5411–5417
34. Shaikh MN (2013) Thiolated Gd (III) chelate coated gold nanoparticles: synthesis, characterization, x-ray CT and MRI relaxivity studies. In: Materials Science Forum. 2013. Trans Tech Publ
35. Kim D et al (2011) Amphiphilic polymer-coated hybrid nanoparticles as CT/MRI dual contrast agents. Nanotechnology 22(15):155101
36. Kim D-K et al (2009) Antibiofouling polymer coated gold@ iron oxide nanoparticle (GION) as a dual contrast agent for CT and MRI. Bull Korean Chem Soc 30(8):1855–1857
37. van Schooneveld MM, Hart DC't, Fayad ZA, Mulder WJM, Meijerink A (2010) Contrast Media Mol. Imaging 5:231–236
38. Mohajeri M et al (2020) Pegylated deoxycholic acid coated gold nanoparticles as a highly stable CT contrast agent. ChemistrySelect 5(29):9119–9126
39. Gao Y et al (2020) Use of the highly biocompatible Au nanocages@ PEG nanoparticles as a new contrast agent for in vivo computed tomography scan imaging. Nanoscale Res Lett 15(1):1–9
40. Park Y-S et al (2007) Concentrated colloids of silica-encapsulated gold nanoparticles: colloidal stability, cytotoxicity, and X-ray absorption. J Nanosci Nanotechnol 7(8):2690–2695
41. Huang P et al (2011) Folic acid-conjugated silica-modified gold nanorods for X-ray/CT imaging-guided dual-mode radiation and photo-thermal therapy. Biomaterials 32(36):9796–9809

42. Aslan N, et al (2020) Metallic nanoparticles as X-Ray computed tomography (CT) contrast agents: a review. J Mol Struct 1219:128599
43. Liu R et al (2021) Multifunctional core-shell tecto dendrimers incorporated with gold nanoparticles for targeted dual mode CT/MR imaging of tumors. ACS Appl Bio Mater 4(2):1803–1812
44. Karunamuni R, et al (2012) An examination of silver as a radiographic contrast agent in dual-energy breast X-ray imaging. In: International Workshop on Digital Mammography. Springer
45. Voelcker F, Von Lichtenberg A (1906) Pyelographie (Röntgenographie des Nierenbeckens nach Kollargolfüllung). Munch Med Wochenschr 53:105–106
46. Swick M (1978) Radiographic media in urology: the discovery of excretion urography: historical and developmental aspects of the organically bound urographic media and their role in the varied diagnostic angiographic areas. Surg Clin North Am 58(5):977–994
47. Skrepetis K, Siafakas I, Lykourinas M (2001) Evolution of retrograde pyelography and excretory urography in the early 20th century. J Endourol 15(7):691–696
48. Seltzer SE, Adams DF, Davis MA, Hessel SJ, Paskins-Hurlburt AJ, Havron A, Hollenberg NK (1979) Invest Radiol 14:356
49. Nieves LM et al (2021) Silver telluride nanoparticles as biocompatible and enhanced contrast agents for X-ray imaging: an in vivo breast cancer screening study. Nanoscale 13(1):163–174
50. Zhou Z et al (2021) Construction of smart nanotheranostic platform Bi-Ag@ PVP: multimodal CT/PA imaging-guided PDT/PTT for cancer therapy. ACS Omega 6(16):10723–10734
51. Yu S-B, Watson AD (1999) Metal-based X-ray contrast media. Chem Rev 99(9):2353–2378
52. Rumpel T (1897) The clinical diagnosis of fusiform dilatation of the esophagus. Muenchen Med Wschr 44:420–421
53. Rabin O et al (2006) An X-ray computed tomography imaging agent based on long-circulating bismuth sulphide nanoparticles. Nat Mater 5(2):118–122
54. Barnett B et al (2006) Radiopaque alginate microcapsules for X-ray visualization and immunoprotection of cellular therapeutics. Mol Pharm 3(5):531–538
55. Liu Q et al (2021) Pharmacological ascorbate promotes the tumor radiosensitization of Au@ Pd nanoparticles with simultaneous protection of normal tissues. ACS Appl Bio Mater 4(2):1843–1851
56. Fu W et al (2020) Stimuli-responsive small-on-large nanoradiosensitizer for enhanced tumor penetration and radiotherapy sensitization. ACS Nano 14(8):10001–10017
57. Pan D et al (2010) Computed tomography in color: NanoK-enhanced spectral CT molecular imaging. Angew Chem 122(50):9829–9833
58. Dong L et al (2019) Renal clearable Bi–Bi2S3 heterostructure nanoparticles for targeting cancer theranostics. ACS Appl Mater Interfaces 11(8):7774–7781
59. Zhang F et al (2020) X-ray-triggered NO-released Bi–SNO nanoparticles: all-in-one nano-radiosensitizer with photothermal/gas therapy for enhanced radiotherapy. Nanoscale 12(37):19293–19307
60. Liu J et al (2021) Bi/Se-based nanotherapeutics sensitize CT image-guided stereotactic body radiotherapy through reprogramming the microenvironment of hepatocellular carcinoma. ACS Appl Mater Interfaces 13(36):42473–42485
61. Xie J et al (2021) Facile fabrication of BiF3: Ln (Ln= Gd, Yb, Er)@ PVP nanoparticles for high-efficiency computed tomography imaging. Nanoscale Res Lett 16(1):1–10
62. Abbatt JD (1979) History of the use and toxicity of thorotrast. Environ Res 18(1):6–12
63. Wickleder MS, Fourest B, Dorhout PK (2008) Thorium. The chemistry of the actinide and transactinide elements. Springer, pp 52–160
64. Ritter J, Rattner I (1932) Umbrathor in urography. Am J Roentgenol Rad Ther 28:629–633
65. Lipshutz GS, Brennan TV, Warren RS (2002) Thorotrast-induced liver neoplasia: a collective review. J Am Coll Surg 195(5):713–718
66. Cannon WB (1898) The movements of the stomach studied by means of the Rontgen rays. Am J Physiol Legacy Content 1(3):359–382

67. Lambrianides A, Askew A, Lefevre I (1986) Thorotrast-associated mucoepidermoid carcinoma of the liver. Br J Radiol 59(704):791–792
68. Md YI et al (1988) Pathomorphologic characteristics of 102 cases of thorotrast-related hepatocellular carcinoma, cholangiocarcinoma, and hepatic angiosarcoma. Cancer 62(6):1153–1162
69. MacMahon HE, Murphy AS, Bates MI (1947) Endothelial-cell sarcoma of liver following thorotrast injections. Am J Pathol 23(4):585
70. Andersson M et al (1994) Primary liver tumors among Danish patients exposed to Thorotrast. Radiat Res 137(2):262–273
71. Lee FI et al (1996) Malignant hepatic tumours associated with previous exposure to Thorotrast: four cases. Eur J Gastroenterol Hepatol 8(11):1121–1124
72. Kamiyama R et al (1988) Clinicopathological study of hematological disorders after Thorotrast administration in Japan. Blut 56(4):153–160
73. Mole R (1986) Leukaemia induction in man by radionuclides and some relevant experimental and human observations. Radiobiol Radium Thorotrast
74. Silva IDS, et al (1999) Mortality in the Portuguese thorotrast study. Radiat Res 152(6s): S88–S92
75. Wegener K (1979) Systematic review of thorotrast data and facts: animal experiments. Virchows Archiv A 381(3):245–268
76. Johansen C (1967) Tumors in rabbits after injection of various amounts of thorium dioxide. Ann NY Acad Sci 145:724–727
77. Wegener K, Hasenöhrl K, Wesch H (1983) Recent results of the German Thorotrast study–pathoanatomical changes in animal experiments and comparison to human thorotrastosis. Health Phys 44:307–316
78. Dilley RB, Nadel JA (1970) Powdered tantalum: its use as a roentgenographic contrast material. Ann Otol Rhinol Laryngol 79(5):945–952
79. Gamsu G, Nadel JA (1972) New technique for roentgenographic study of airways and lungs using powdered tantalum. Cancer 30(5):1353–1357
80. Gamsu G et al (1973) Powdered tantalum as a contrast agent for tracheobronchography in the pediatric patient. Radiology 107(1):151–157
81. Hallouard F, Lahiani-Skiba M, Skiba M (2015) Nanometric carriers or metallic nanoparticles: promising platforms for computed tomography applications. American Scientific Publishers
82. Goldberg HI, Dodds WJ, Jenis EH (1970) Experimental esophagitis: roentgenographic findings after insufflation of tantalum powder. Am J Roentgenol 110(2):288–294
83. Chakravarty S et al (2020) Tantalum oxide nanoparticles as versatile contrast agents for X-ray computed tomography. Nanoscale 12(14):7720–7734
84. Bonitatibus PJ Jr et al (2010) Synthesis, characterization, and computed tomography imaging of a tantalum oxide nanoparticle imaging agent. Chem Commun 46(47):8956–8958
85. Koshevaya E et al (2020) Surfactant-free tantalum oxide nanoparticles: synthesis, colloidal properties, and application as a contrast agent for computed tomography. J Mater Chem B 8(36):8337–8345
86. Yu Z, Eich C, Cruz LJ (2020) Recent advances in rare-earth-doped nanoparticles for NIR-II imaging and cancer theranostics. Front Chem 8:496
87. Ertas YN et al (2015) Oxide-free gadolinium nanocrystals with large magnetic moments. Chem Mater 27(15):5371–5376
88. Havron A et al (1980) Heavy metal particulate contrast materials for computed tomography of the liver. J Comput Assist Tomogr 4(5):642–648
89. Lu R et al (2020) Gadolinium-hyaluronic acid nanoparticles as an efficient and safe magnetic resonance imaging contrast agent for articular cartilage injury detection. Bioactive Mater 5(4):758–767
90. Cheung ENM et al (2010) Polymer-stabilized lanthanide fluoride nanoparticle aggregates as contrast agents for magnetic resonance imaging and computed tomography. Chem Mater 22(16):4728–4739
91. McDonald MA, Watkin KL (2003) Small particulate gadolinium oxide and gadolinium oxide albumin microspheres as multimodal contrast and therapeutic agents. Invest Radiol 38(6):305–310

92. Watkin KL, McDonald MA (2002) Multi-modal contrast agents: a first step. Acad Radiol 9(2):S285–S289
93. Santra S, walter GA, tan W, Moudgil BM, Mericle RA, et al (2005) Synthesis and characeterization of fluorescent, radio-opaque, and paramagnetic silica nanoparticles for multimodal bioimaging applications. Adv Mater 17:2165–2169
94. Yu X et al (2021) Integrating the second near-infrared fluorescence imaging with clinical techniques for multimodal cancer imaging by neodymium-doped gadolinium tungstate nanoparticles. Nano Res 14(7):2160–2170
95. Chang X et al (2020) Graphene oxide/BaHoF5/PEG nanocomposite for dual-modal imaging and heat shock protein inhibitor-sensitized tumor photothermal therapy. Carbon 158:372–385
96. Marasini S, et al (2021) Synthesis, characterizations, and 9.4 Tesla T2 MR images of polyacrylic acid-coated terbium (III) and holmium (III) oxide nanoparticles. Nanomaterials 11(5):1355
97. Zhai T et al (2020) Hollow bimetallic complex nanoparticles for trimodality imaging and photodynamic therapy in vivo. ACS Appl Mater Interfaces 12(33):37470–37476
98. Gómez-Gónzalez E et al (2020) Dysprosium and holmium vanadate nanoprobes as high-performance contrast agents for high-field magnetic resonance and computed tomography imaging. Inorg Chem 60(1):152–160
99. Bult W et al (2010) Holmium nanoparticles: preparation and in vitro characterization of a new device for radioablation of solid malignancies. Pharm Res 27(10):2205–2212
100. Naha PC et al (2020) Dextran-coated cerium oxide nanoparticles: a computed tomography contrast agent for imaging the gastrointestinal tract and inflammatory bowel disease. ACS Nano 14(8):10187–10197

Natural Radioprotectors

Zahra Gharari, Parichehr Hanachi, Hossein Danafar, Hamed Nosrati, Surender K. Sharma, and Ali Sharafi

Abstract Given the widespread use of radiation in the therapy and diagnosis of different illnesses and its side effects on normal tissues, it is essential to protect healthy cells from ionizing-induced damages. Ionizing radiation can damage directly to DNA, proteins and lipids, resulting to molecular and cellular dysfunctions. In addition, it can hydrolyze water molecules, resulting enhanced production of free radicals with strong oxidation ability in the body, which can indirectly cause to tissue degeneration, necrosis and possibly leads to cancer. Since, there is no ideal and safe synthetic radio-protective agent to protect healthy cells and tissues from radiation-induced damage, the search for alternative safe and effective radio-protective sources such as plants, is still ongoing worldwide. Naturally occurring compounds are given largely as the secondary products in herbs and have been shown to be easily accessible, affordable, less or non-toxic, inexpensive and effective. In this chapter, we have presented an overview of the key molecular mechanisms implicated in radio-protective properties of natural compounds ranging from free radical scavenging, protecting against DNA and auto-immune damage and also hematopoietic system protection and inflammation reduction.

Keywords Natural compounds · Radiation · Radioprotective mechanisms · Radioprotectors · Signaling pathway · Toxicity

Z. Gharari · P. Hanachi
Department of Biotechnology, Faculty of Biological Sciences, Alzahra University, Tehran, Iran
e-mail: z.gharari@alzahra.ac.ir

H. Danafar · H. Nosrati (✉) · A. Sharafi (✉)
Zanjan Pharmaceutical Biotechnology Research Center, Zanjan University of Medical Sciences, Zanjan, Iran
e-mail: nosrati.hamed2020@gmail.com

A. Sharafi
e-mail: sharafi.a@gmail.com

S. K. Sharma
Department of Physics, Central University of Punjab, Bathinda 151401, India

Department of Physics, Federal University of Maranhao, Sao Luis, MA 65080-805, Brazil

S. K. Sharma et al. (eds.), *Harnessing Materials for X-ray Based Cancer Therapy and Imaging*, Nanomedicine and Nanotoxicology,
https://doi.org/10.1007/978-3-031-04071-9_9

1 Introduction

Radiotherapy is one of the key and primary therapeutic methods for patients with malignant carcinoma. Over 50% of carcinoma patients receive therapeutic radiology as part of their treatment scheme during course of treatment [1, 2]. While radiotherapy accounts as one of the most powerful treatments for cancer therapy, it may have serious side effects on healthy normal tissues. Recent studies have shown that ionizing radiation (IR) interacts directly or indirectly with cellular components and causes significant damage to the human body [3]. Generally, direct damages occur through interaction of IR with DNA, proteins and lipids. DNA is the primary objective of IR via direct interaction, which results in DNA strand destruction, base mutation, DNA-DNA intra and inter connection, DNA–protein connection and dimer formation, leading to mutagenesis, chromosomal aberrations, and organism death [4]. However, most radiation-induced cellular damages are through indirect interaction. Indirect damage involves the indirect interaction between IR and water molecules in the body, which lead to formation of free radicals such as oxygen and nitrogen radicals and neighboring DNA molecules [5], resulting to structural variations in the cells, tissue degeneration, necrosis and basically result in cancer [6]. The most degenerative ROSs are among ·OH: hydroxyl radicals, hydrogen atoms and solvated electrons, among which ·OH is sufficiently long-lived, highly reactive with powerful oxidizing effects which can lead to structural changes in biomolecules such as DNA and other cell constituents [7]. In the human body, the main attack targets for ·OH are DNA, protein and lipids. IR-induced DNAdamages include point mutations, DNA crosslinking, single-strand breaks (SSBs), double-strand breaks (DSBs), dimer formation and chromosome aberrations [4]. DSBs are the most severe and common form of IR-induced DNAdamages, which can trigger a succession of enzymatic processes cause to DNA repair or apoptosis [8]. The immune system activates in response to IR-induced secretion of cytokines, ROS generation, and apoptosis, which cause to inflammation reaction. Immune system activation in exposure to high levels of ionizing radiation can result in functional impairment of the immune system, disorder in antibody production, failure in cytokine network regulation and even death due to degeneration and necrosis in tissue cells which lead to decrease in the number of immune cells [9]. Several diseases such as organ inflammation, which caused by acute phase damage and also atrophy, infertility, fibrosis, vascular damage and secondary malignancies, resulting from chronic phase damage, are the most common IR- associated responses [10]. Regarding to significant utilization of radiotherapy in the therapy and diagnosis of several health disorders, on the contrary its adverse effects on healthy tissues, there is increased importance in protecting individual at risk from the radiation in the field of radiation therapy [11]. Several strategies such as technological progress in IR delivery and accuracy, the use of natural radioprotectors (pharmacological agents) have been proposed as an alternative to alleviate toxicity to healthy tissue in the field of radiation protection [12]. Natural radioprotectors are nontoxic plant-derived compounds with proven therapeutic properties which are known to possess potential radio-protective effect on normal cells (noncancerous)

against radiation [12]. An optimal radioprotective agent should be easily accessible, affordable, and nontoxic and also prevents the occurrence of acute or chronic injuries on healthy tissues without affecting the efficacy of the radiation [12, 13]. Currently, a number of compounds, including radioprotectors, mitigators and therapeutic agents have been approved by the U.S. Food and Drug Administration (FDA) for administration before, during or after exposure to IR. Radioprotective agents are administered prior to exposure to IR to provide protection on normal tissues against either acute or chronic effects. Mitigators are administrated before or shortly after radiation therapy and decline the side effects of radiation on healthy tissues. Generally, therapeutic agents are administered after emergence of symptoms following IR treatment [14]. Over the last 50 years, many naturally occurring and synthetic compounds have been studied for their efficacy as radioprotective agents in biological systems. However, due to inherent cytotoxicity, high cost, limited administration routes, side effects, and also limited protection of organs against ionizing radiation by synthetic chemicals, the use of natural products has gained increased awareness and immense attention [15].

Therefore, investigators are searching for natural source of radioprotectors that have preferable radioprotective activities with less cytotoxicity. Considering radioprotective potential of pharmaceutical agents, so far about 74 plant-derived natural products including flavonoids, alkaloids, anthocyanidins and carotenoids have been screened by different in vitro and in vivo studies [16]. The purpose of this chapter is to present the radioprotective efficacy of natural agents that are currently under study for the prevention of radiation-induced adverse effects and the molecular mechanisms underlying these effects.

2 Damage Due to Ionizing Radiation

In biological systems, different forms of IR, such as electromagnetic radiation (X-rays or γ- rays) and particles (alpha, beta, or neutrons) occur both naturally or artificially [17].

Artificial radiation comes from by utilizing of radiation in medical diagnosis (X-rays), radiotherapy and radiology. The use of IR on the human organs may cause to a sequence of several biochemical and pathological variations including cellular apoptosis and necrosis and organ dysfunction [18]. Regardless of the numerous advantages of ionizing radiation in medical and industrial applications, they cause to several adverse effects on integrity and functionality of the cell through both direct and indirect biological corruptions [19]. Direct radiation effect includes the absorption of high linear energy transfer (high-LET) radiation (alpha -particles and carbon ions) by biomolecules like nucleic acids (DNA or RNA), proteins, and lipids, which cause to the decomposition of these macromolecules [20]. Generally, indirect damage of the ionizing radiation occurs when Low-LET radiation (γ- and X-rays) alter macromolecules indirectly via reactions with free radicals which are derived from water radiolysis [21]. Ionizing radiation stimulates the generation of active

oxidizing free radicals such as hydroxyl radical ($^{\bullet}OH$), hydrogen atom ($H^{\bullet}$), superoxide ($O_2^{-\bullet}$), H_2O_2 and $NO^{\bullet}$ in radiated body. The most reactive oxygen species i.e., $^{\bullet}OH$ interfere with the biomolecules, which lead to serious physiological and functional destructions of body's biological macromolecules, leading to serious tissue damage [22]. Cellular DNA and immune and hematopoietic systems destruction is considered as the considerable damages caused by radiotherapy [23]. Studies have shown that damage of DNA through ionizing radiation occurs in the form of loss of biological information and deterioration of normal cell action, which may result in cells death and ultimately development of cancer [24]. With regards to the immune system and hematopoietic cells, because of very high sensitivity of these cells to radiotherapy, in addition to a reduction in the immune and blood cells number, IR damage can also possibly cause to a reduction in the specific and non-specific immune functions and suppression of bone marrow microcirculation, respectively [24].

3 Radioprotectors

Ionizing radiation in different kinds, including natural and artificial (for diagnosis and medical purposes) has the potential to cause prolonged damage to human health. Although radiation therapy (RT) is one of the key strategies for the treatment or control of malignant diseases, on the other hand, the use of these approach causes cancer in 50% of people who receive some kind of radiation therapy as part of their cancer treatments [25]. Additionally, it is expected that cancer rates will increase further as underdeveloped countries get permission to radiation therapy procedures. Hence, there are increased efforts in the field of radiation protection to advance small molecules that act as radio-protectors. In this regard, identification and validation of efficient and nontoxic molecules from natural sources in both in vitro and in vivo samples is a vital goal. Table 1 gives an overview of the various radioprotective natural compounds with their group, natural source, and mechanism of action, respectively.

4 Radio-Protective Agents of Natural Origin

Natural radio-protectors refer to the nontoxic or less-toxic plant products with recognized therapeutic benefits and without adverse side effects, which can be applied before or after radiotherapy to reduce injury caused by IR exposure on normal (noncancerous) cells [68]. Over the past 25 years, nearly 710 new drugs have been developed from natural sources as radio-protective agents [16]. Due to the critical dose-limiting toxicities of radiation therapy on normal tissue, the use of radiotherapy is limited. Both acute and chronic injuries caused by radiation are improved through the action of these natural agents by prevention of apoptosis, altering the proportion between profibrotic and antifibrotic regulators or promoting proliferating of critical

Table 1 List of natural radioprotective agents and their activities

No	Radioprotective agents	Group	Natural sources	Activity	References
1	Amentoflavone	Biflavonoid	*Selaginella tamariscina*, *Cupressus sempervirens*	Free radical clearing ability	[26]
2	Apigenin	Flavonoid	Parsley, thyme, celery, and chamomile tea	Reduce micronuclei formation; Protect of bone marrow	[27, 28]
3	Baicalein	Flavonoid	*Paeonia lactiflora, Scutellaria baicalensis*	Decrease DNA rupture; P-MAPKs and p-Akt ↓	[29, 30]
4	Baicalin	Flavonoid	*Scutellaria bacalensis*	Scavenging reactive oxygen	[31]
5	Bergenin	Polyphenol	*Caesalpinia digyna*	Protects against DNA damage	[32]
6	Breviscapine	Flavonoids	*Erigeron breviscapus*	Hemopoietic function protection	[33]
7	Caffeine	Alkaloid	Tea, coffee	Reduction in inflammation	[34]
8	Ascorbic acid	Vitamin	Fruits and vegetables	Free radical scavenging	[35]
9	Chlorogenic acid/quinic acid	Phenolic compounds	*Hibiscus sabdariffa*	Protects against X-ray induced DNA damage	[36]
10	Coniferyl aldehyde	Phenolic compound	*Eucommia ulmoides*	Increasing the stability of heat shock protein	[37]
11	Curcumin	Polyphenolic compound	*Curcuma longa*	Reduction in inflammation	[38]
12	Delphinidin	Anthocyanidin	Tomato, Carrot, Cranberries, Red onion, Concord grapes	The induction of apoptosis	[39]
13	Ferulic acid	Phenolic acid	Green tea, Rice, Coffee beans	Reduction in inflammation	[40]
14	Genistein	Isoflavone	*Genista tictoria*	Regeneration of the hematopoietic stem cells ↑	[41, 42]
15	Hesperidin	Flavanone glycoside	Citrus fruit	Reduction in inflammation	[43]

(continued)

Table 1 (continued)

No	Radioprotective agents	Group	Natural sources	Activity	References
16	Lycopene	Carotenoid	Watermelon, Tomato, Papaya, Pink grapefruit	Protects against IR-induced DNA damage	[44]
17	Mangiferin	Gluosylxanthone	*Mangifera indica*	Reduced the radiation-induced sickness and mortality	[45]
18	Melatonin	Hormone	*Tanacetum parthenium;Hypericum perforatum;* banana; grape; rice; wheat and oat	Protection against radiation-induced nephrotoxicity	[46]
19	N-Acetyl tryptophan glucopyranoside	Bacterium secondary metabolite	bacterium *Bacillus* sp	Apoptosis inhibition	[47]
20	Naringin	Biflavonoid	Citrus	Protects against IR-induced DNA damage	[48]
21	Orientin	Flavone	Indian Holy Basil	Free radical scavenging, reduction of DNA damage	[49]
22	Pentoxifylline	Alkaloid	Tea, coffee	Protection effects on hematopoietic, gastrointestinal and vascular Systems	[50]
23	Polydatin	Stilbenoid glucoside	Grape; *Picea sitchensis* bark; *Reynoutria japonica*	Clearing free radicals and enhancing the antioxidant capacity of cells	[51]
24	Procyanidin	Polymers of flavonoids	*Psoralea corylifolia*	Decreasing the levels of complex cytogenetic DNA damage	[52]
25	Psoralidin	Phenolic coumarin	*Psoralea corylifolia*	Reduction in inflammation	[53]
26	Quercetin	Flavonoid	Apples, buckwheat, onions, and citrus fruits	Scavenging free radicals	[51, 54]
27	Resveratol	Polyphenol	Soy, grapes, red wine, and peanuts	Genotoxic effects	[55]

(continued)

Table 1 (continued)

No	Radioprotective agents	Group	Natural sources	Activity	References
28	Rutin	Flavonoid	Buckwheat, Japanese pagoda tree, Eucalyptus	Decreasing the amount of base damage	[56]
29	s-allyl cysteine sulphoxide	Allyl sulfur compound	Garlic	Reduction the radiation induced mortality	[57]
30	Sesamol	Phenolic compound	Sesame and sunflower oil	Scavenging free radicals	[58]
31	Silibinin	Flavonolignan	*Silybum marianum*	Reduce micronuclei formation	[59]
32	Troxerutin	Flavonol	*Sophora japonica*	Protective effects on the hematopoietic system	[60]
33	Vanillin	Phenolic aldehyde	Vanilla bean	Protects against IR-induced single-strand breaks	[61]
34	Zingerone	Polyphenol	Ginger	Mitigating radiation-induced mortality and cytogenetic damage	[62]
35	Zymosan A	Polysaccharide	*Saccharomyces cerevisiae*	Protecting the hematopoietic system	[63]
36	Biscoclaurine	Alkaloid	*Stephania cepharantha*	Protecting the immune and hematopoietic systems	[64]
37	Epigallocatechin gallate (EGCG)	Catechin	Tea, *Camellia sinensis*	Immune system protection	[65, 66]
38	Indirubin	Bis-indole alkaloid	*Isatis indigotica*, *Indigofera indica*, *Isatis tinctoria*	Hematopoietic system protection	[67]

dose-limiting systems. Recent studies have shown that the use of natural radioprotectors jointly with radiation can enhance cancer killing by radiosensitizing cancerous cells in turn protection normal cells against radiation [69].

4.1 Radioprotective Mechanisms of Natural Radioprotectors

In general, the main radio-protective mechanisms of natural radioprotectors action include (1) DNA protection by triggering cellular DNA repair pathways, (2) antioxidant activity by suppressing the formation of free radicals or activating the cellular radioprotectors, (3) protection the immune system, (4) protection the hematopoietic system, and (5) the reduction of inflammation, which are discussed below.

4.1.1 Reduction of DNA Damage and Genotoxicity

DNA is one of the critical targets of IR damage. Both direct and indirect actions of IR can damage genomic DNA. DNA exposure to ionizing radiation can lead to numerous adverse consequences on human health. During IR exposure, IR-induced free radicals are generated, which causes DNA damage by:

1. Introducing base damage, resulting from covalently linking between adjacent pyrimidines in DNA, this referred as cyclobutane pyrimidine dimer (CPD) such as formation link between adjacent thymines [70] (Fig. 1),
2. DNA Single Strand Breaks (SSBs) are discontinuities in one strand of the dna double helix caused by radiation induced damage to a single nucleotide at the site of the break,

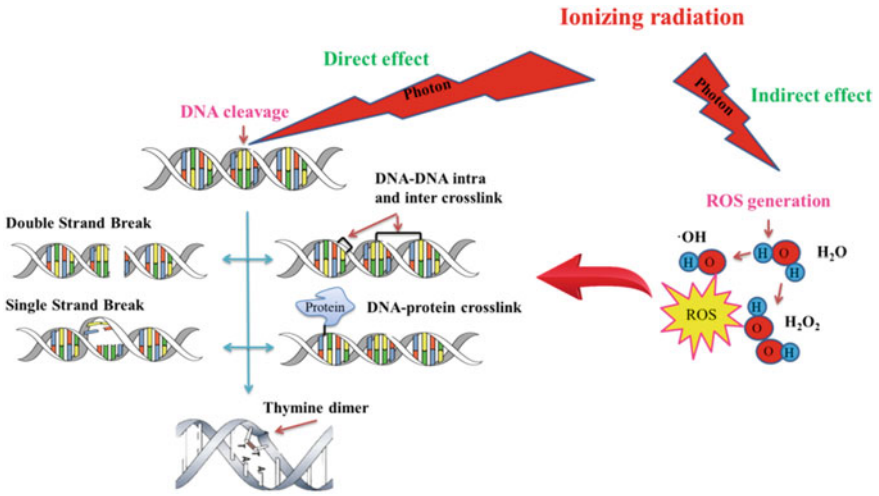

Fig. 1 Ionizing radiation disrupts the structure of the DNA both directly and indirectly. Radiation directly results in DNA strand breaks (double and single strand breaks), crosslinking (DNA-DNA and DNA–protein crosslinks), and dimer formation. Indirectly, radiation radiolysis of water molecules generates additional cell-damaging molecules (ROS), by which damages DNA directly

3. DNA double strand breaks (DSBs), which is considered as highly lethal consequence of ionizing radiation arises from the cleavage of both strands of the double helix and classically defined as broken chromosomes,
4. Upon exposure to ionization radiation, DNA–DNA cross-links forms through covalently linkage between two nucleotides of DNA, which can occur within the same strand (intrastrand) or between opposite strands of double-stranded DNA (interstrand), and,
5. Exposure to IR may also cause to dna–protein cross-links, resulting from covalently trapped of cellular proteins on DNA strands [71].

Hall and Giaccia reported that exposure to medical radiation dose of IR on average leads to 3000 damaged bases, 1000 SSBs and 40 DSBs per Gray (Gy) [72]. These effects are responsible for altered gene expression and protein modifications, cell death, senescence, and genomic instability, which may also cause to mutations, carcinoma and birth defects. Hence, one of the most important issues in protecting of body cells against IR is reduction of IR-induced adverse effects on DNA structure [73]. Gakova and colleagues investigated the radiation protection effects of the oral administration of silymarin to mice one hour prior to whole-body irradiation with a 5.7 Gy dose of gamma radiation (^{60}Co) and showed that silymarin administration significantly influenced the concentration and total content of RNA and DNA in the spleen and bone marrow [74]. Several investigations have revealed the ameliorative effects of quercetin on gamma radiation-induced biochemical changes in human peripheral blood lymphocytes, DNA damage and scavenging of free radicals [75, 76]. Devipriya et al. [75] used alkaline comet MN and DC assays to disclose the radio-protective properties of quercetin on the radiation-induced DNA destruction in irradiated human peripheral blood lymphocytes. Quercetin (24 μM) pre-incubation of lymphocytes with 4 Gy γ-radiation demonstrated a significant reduction in damage to DNA without any genotoxic effects at mentioned concentration [75]. It has been shown that quercetin treating Sprague–Dawley rats whole-abdominal expose to 8 Gy ionizing radiation significantly prevent the DNA oxidative damage [76]. Alkaline comet assay technology was applied by Gandhi to consider the radio-protective advances of bailcalein on DNA repair in mice in exposure to radiation. The results revealed that the administration of this flavonoid, prior to radiation exposure, causes significant protective effect against DNA damage [30]. The radiation protection of apigenin was investigated in cellular experiments. Begum and colleagues assessed the radiation protection effects of apigenin on human lymphocytes and showed that apigenin can reduce the injuries to the chromosome in exposure to ionizing radiation by prompted reduction in the rate of micronuclei (MN) formation [27]. Xu et al. [77] used water extraction and alcohol precipitation method to obtain the flavonoid rich extract of Guipi Pill to administrate the mice for 8 days before whole body-γ-exposure (8 Gy). Their results showed that oral administration of Guipi Pill extract leads to a significant increase in survival rate of mice after exposure to lethal dose of γ-radiation [77]. Tiwari et al. investigation showed that when lymphocyte cells were exposed to γ-radiation (3 Gy), silibinin alleviated the DNA damage and microcrystalline formation in lymphocytes. In addition when mice were oral administrated

with silibinin prior to IR exposure (7.5 Gy), DNA damage was significantly reduced in blood leukocytes and therefore the death caused by these beams was attenuated [59]. In addition to the radioprotective effects of the above mentioned flavonoids, the flavonoids isolated from Ocimum such as narigin, procyanidins and hesperidin, and also flavonoids purified from Propolis and Gentianella families can successfully decrease the genetic toxicity induced by radiation, and can secure DNA from the radiation damage [48, 52, 78, 79].

4.1.2 Scavenging Free Radicals and Antioxidant Effect

During radiation exposure, IR stimulates the production of large number of free radicals and ROS i.e., $^{1}O_2$ and $^{\cdot}OH$, which decreases superoxide dismutase (SOD), catalase (CAT) and glutathione peroxidase (GSH-Px) activities in vivo, resulting to lipid peroxidation and a rise in malondialdehyde (MDA) content, which is capable for significant injuring to all biological molecules including cell membranes, DNA structure and protein. Natural agents including flavonoids, alkaloids, anthocyanidins and carotenoids play an important role as radioprotectors by prevention of these reactions through destroying free radicals and inhibition their formation. Free radicals are generally short-lifetime molecules and react quickly with cellular organic molecules [80]. Therefore, providing effective agents in the cellular systems is necessary for proper radioprotection at the time of IR exposure. Flavonoids are a group of effective and nontoxic natural compounds with great antioxidant effects [81]. These metabolites are accepted as the most potent radio-protective compounds on human cells in exposure to ionizing radiations, which is due to their ability for scavenging and eliminating of oxygen radicals and removing the indirect radiation damage by in vivo and in vitro experiments [82, 83]. In terms of radioprotective properties, the most investigations have been performed on phenolic compounds including flavonoids; biflavonoids; phenylethanoid gelycosids and their derivatives. Investigation has revealed that flavonoids such as amentoflavone, apigenin, baicalein, quercetin, and rutin could significantly remove reactive oxygen radicals and remove the indirect effects of radiotherapy on human cells [82]. The biflavonoid amentoflavone demonstrated to possess interesting radio-protective effects on guinea pig pulmonary fibroblast cells [84]. Treatment with amentoflavone for 1 day before γ-IR-exposure (8 Gy) from ^{60}Co remarkably reduced the concentration of ROS, inhibited apoptosis, decreased the relative mitochondrial mass and promoted the G2 phase [84]. Malakyan and colleagues reported the effective antioxidant and radioprotective role of hop (*Humulus lupulus*) aqueous extracts on protecting of rat erythrocytes in exposure to X-ray irradiation (4.0 and 7.6 Gy) [85]. The oral administration of extract to white rats 3 days prior to X-ray irradiation showed significant potential of *H. lupulus* aqueous extracts to inhibit the radiation induced H_2O_2-enhanced erythrocyte oxidative damage in rats [85]. It has been shown that pretreatment of human keratinocyte cell line HaCaT with quercetin, polydatin, and genistein in exposure to UVB rays increased the activity of SOD, which was accompanied by a reduction in the levels of tumor necrosis factor (TNFα), ·OH free radicals and MDA level [51]. In

a similar study, Zhu and colleagues were investigated the quercetin radioprotective activity and its mechanism of action on UVB-injured keratinocyte (HaCaT) cells. The findings of the investigation revealed that quercetin considerably arrested the intracellular ROS generation and protected cell membrane and mitochondria against ROS attack. Moreover, the reduction of cell membrane fluidity and mitochondrial membrane depolarization was inhibited in the presence of quercetin [54]. It has been demonstrated that the pre-incubation of the cancerous PC12 cells of the rat with different concentrations of breviscapine before X-rays exposure (4 Gy), in addition to an increase in the activity of SOD and T-AOC in PC12 cells,significantly reduced the level of ROS and MDA in irradiated-cells [86]. In addition to radioprotective effects, quercetin has potential radiomitigator effects on human lymphocyte cells [87]. De Siqueira and colleagues studied the radiomitigator effect of quercetin on chromosome aberration yield in lymphocytes of in vitro-irradiated human peripheral blood. The results showed that quercetin decreased the frequency of chromosomal abnormalities, probably by reducing cytokines (INF-γ, PGE2, IL-1β, IL6, IL-8) release, down-regulation of NF-kB and reduction of expression TGF-β [87]. The study by He and colleagues showed that breviscapine, a crude extract of several flavonoids of *Erigeron breviscapus*, when pre-incubated with human kidney 293 T cells prior to irradiation exposure in different doses prompted cell survival, in vitro. They also examined the radio-protective effects of breviscapine by examining survival rate and hemopoietic function of mice in exposure to different doses of total-body irradiation (TBI) including: sub-lethal (4 Gy), lethal (7 Gy) or supra- lethal (13 Gy) dose. The results demonstrated that breviscapine flavonoids effectively alleviated bone marrow suppression, decreased the bone marrow cells reduction after sub-lethal TBI and also mitigated the TBI-induced reduction in granulocyte–macrophage colony-forming units [33].

4.1.3 Protection the Immune System

The cells of the immune system are among the most vulnerable cells in the body in terms of radiation damage. Exposure to IR, the numbers and functions of immune system cells can alter in irradiated organs, an issue that may even lead to death. In terms of immune system, Ionizing radiation also is able to disrupt the production of antibodies and impair cytokine network regulation in the body [9]. Among alkaloids, biscoclaurine alkaloids, which are extracted from *Stephania cepharantha* Hayata, have a certain protective role in protecting the immune and hematopoietic systems of irradiated mice [64]. Wang and colleagues have found that when mice were oral administered with biscoclaurine alkaloids 3 days before the IR and 15 days after radiation, biscoclaurine alkaloids could increase the white blood cells and reduce the platelets in the peripheral blood. It also significantly promoted serum levels of vascular cell adhesion molecule 1 (VCAM-1), and interferon-c (IFN-c) in ^{60}Co-γ Radiated mice [64]. Epigallocatechin gallate (EGCG) is a type of catechin known as an excellent natural radioprotective compound which abundantly found in tea [65]. Recent study by Juanjuan and colleagues on radioprotection of EGCG

in 60Coγ radiatied mice, showed the valid protection effect of EGCG on immune system of ^{60}Coγ-radiated mice via ameliorating the immune organ index, enhancing the conversion of spleen cells into T- and B-cells, and increasing the macrophage phagocytosis, by comparison with control group [65]. Several class of flavonoids have been found to display a diverse range of useful pharmaceutical activities such as immune system protection against ionizing radiation [88]. Isoflavones generally are polyphenolic compounds which are produce particularly by the members of the family Fabaceae (Soybeans) in their main forms, as genistein, daidzein, and glycytine bound to sugar molecules. Due to their plant origin and estrogenic-like activity, isoflavones are categorized as phytoestrogens. The immune system protection against ionizing radiation has been reported as major role of isoflavones [89]. Mice receiving only 4 Gy radiation have been shown to significantly reduce immune function in thymus and the spleen by means of laboratory animals [89]. It has been shown that when mice were feeding with soy isoflavones for 2-weeks before exposure to 4 Gy gamma-radiations, the cell apoptosis rate and cell cycles rate of G0-G1 phase in splenocytes were increased. However the cell cycles rate of S phase and the proliferation index in spleen were remarkably reduced [89]. At the similar study by Jia and colleagues showed that feeding with soybean isoflavones significantly increase the macrophage phagocytosis, serum level of hemolysin and immunoglobulin, IgA, IgG, and IgM levels in gamma-irradiated group of mice [90]. These results indicate that isoflavones could significantly increase immune system protection in irradiated mice. Zhang and colleagues have reported that when male workers were pretreated with resveratrol as dietary supplements prior to high-voltage electricity lines, resveratrol could reverse the adverse impacts of high-voltage electricity on workers by reconstruction of the nuclear factor-kappa B (NFkappa B) and IL-6 expression and function, and finally avoid the deterioration of the immune system [91].

4.1.4 Hematopoietic System Protection

Hematopoietic cells are blood and bone marrow originated cells, which produce through process known as hematopoiesis. These cells give rise to various forms of blood cells such as red blood cells (RBCs), platelets and white blood cells (WBCs). Due to high metabolic and proliferative rate of hematopoietic cells, they are largely susceptible to direct and indirect radiation-induced damages, which can dramatically decrease their number and function [92]. Hence, in order to provide valuable protecting agents against IR -induced damages, numerous studies have been published on hematopoietic cells biology and their protective mechanisms against radiation with the participation of natural plant compounds. Wang et al. [64] treated mice intraperitoneally with baicalein 1 h prior to radiation exposure and then a day post-IR. Findings of the survey revealed that baicalein can improve the intestinal structure, the regeneration and proliferation ability of mice by inhibiting apoptosis and rebalancing gut microbiota after exposure to IR. It also could ameliorate the IR induced damages to hematopoietic system [93]. These results support the potential

of baicalein as a radioprotective constituent. Liu et al. [94] reported the radioprotective effects of chemically synthesized 6,7,3',4'-tetrahydroxyisoflavone (T3) on irradiated mice with gamma rays from ^{60}Co. Their results revealed that the subcutaneous administration of T3 considerably increased the survival rate and improved the recovery of hematopoietic function in lethally γ-irradiated mice [94]. Similar studies which conducted by Benković and colleagues on readioprotective effects of quercetin from Propolis demonstrated its positive effects on enhancing the number of WBC and RBCs and also platelets and hemoglobins in gamma-irradiated cells [95, 96]. The radioprotective effects of genistein on hematopoietic system have been investigated both in the form of free flavonoids and in the form of genistein nanoparticles suspensions [42, 97]. Zhou et al. pre-treated mice with genistein prior to radiation and found that it increased the survival rate, improved the mice hematopoietic system and stimulated the reconstruction of erythrocytes, leukocytes, lymphocytes and thrombocytes [42]. Ha et al. [97] studied the radioprotective effect of genistein nanoparticles suspensions on survival rate and hematopoietic system recovery of total-body gamma-irradiated mice. A pre- intramuscular injection of genistein nanoparticles suspensions one day before 9.25 Gy ^{60}Co exposures, improved the 30-day survival rate from 25% in vehicle-treated animals to 95% in genistein nanoparticles suspensions treated mice. In addition it increased the survival rate of IR-treated hematopoietic stem cells from 43 to 77% and on the other hand it attenuated the suppression of pro-inflammatory factors such as cyclooxygenase-2 (COX-2), interleukin 1 beta (IL-1β), and IL-6 in mice bone marrow and spleen cells [97]. Ping et al. (2012) assessed the radioprotection effects of the oral administration of troxerutin to mice for six days prior to whole-body irradiation with different doses (6, 7, 8, and 10 Gy) of gamma radiation (^{60}Co) and showed that troxerutin administration significantly improved the survival rate and also biochemical parameters [98]. Qi et al. investigated the role of *Astragali complanali* flavonoids (ACFs) in the radiation protection of whole-body of mice. The research findings showed that ACFs can improve the survival rate, increase the number of RBCs, WBCs, platelets, and hemoglobin in peripheral blood of mice in exposure to radiation [99].

4.1.5 Reduction in Inflammation

Intense exposures to ionizing radiation can strongly stimulate the inflammation reaction. Proinflammatory cytokines are signaling molecules such as IL-1, IL-12 and IL-18, TNF-α and IFNγ, which can cause damage to each part of body. Excessive production of these cytokines most commonly can cause injuries to the lungs and kidneys. Indirubin, is natural valuable bis-indole alkaloid used in traditional Chinese medicine, which is derived from various natural sources such as *Isatis indigotica*, *Indigofera indica* and *Isatis tinctoria.* It most often produced as a byproduct of bacterial metabolism and has shown remarkable pharmaceutical activities such as anticancer, anti-inflammatory and antibacterial [67, 100, 101]. In mice, You et al. investigated the role of *Isatis indigotica* indole alkaloids in the radiation protection of hematopoietic system, serum cytokines, and intestinal toxicity [102]. The mice

were post-administered with Indigowood root extract immediately after exposure to 7-days 5.4 Gy radiation. The results of this study showed that *Isatis indigotica* indole alkaloids are potential radiomitigators by protecting the hematopoietic cells, reducing the tissue damage and modulating the inflammatory serum cytokines such as TNF-α, IL-1β, and IL-6 after total-body irradiation [102]. Phenolic compounds and flavonoids are among the most studied natural agents for their radioprotective properties. Caffeic acid is a natural phenolic compound with inherent antioxidant, anti-cancer, anti-inflammatory and antimicrobial properties [103]. Caffeic acid has the capacity to reduce radiation toxicity on radiation-induced pneumonitis [104]. Chen et al. [104] pre administered the mice with caffeic acid prior to whole body exposure to the single dose of 10 Gy and 20 Gy radiation. Their results showed that Caffeic acid was able to alleviates pneumonitis via reducing the expression of inflammatory cytokines such as IL-1α, IL-1β, IL-6, NF-κB, TGF- beta and TNF-α after exposure to radiation [104]. Ascorbic acid (vitamin C) is a natural water-soluble vitamin, which functions as a potent reducing radiation toxicity and antioxidant agent in biological systems [105]. Sato et al. investigated the radioprotective effect of ascorbic acid on survival rate of whole body irradiated mouse [105]. The mice which were administered with a single dose of 3 g/kg ascorbic acid after whole body exposure to 7–8 Gy radiation, showed increased survival rate, suppression inflammatory cytokines production, as well as decreased radiation-induced apoptosis in bone marrow cells and restored hematopoietic function following treatment with ascorbic acid [105]. Şener et al. results showed that when rats were exposed to whole-body IR (800 cGy) immediately after pre-treatment with *Ginkgo biloba* extract (EGb), their TNF-α and Lactate dehydrogenase serum and tissues level were down regulated by EGb following irradiation [106]. Intraperitoneal administration of hesperidin prior to exposing mice to 2 Gy gamma irradiation caused notable reduction in the inflammatory cytokines levels such as IL-1β, IL-6, and TNF-α and accordingly reduced inflammatory damage in the exposed mice [107]. Baicalein is a natural flavonoid, which originally isolate from the *Scutellaria radix* (the root of *Scutellaria baicalensis*) and possesses a multitude of pharmacological activities such as anti-inflammatory activity [108]. It can suppress the radiation-induced inflammatory responses in mouse kidney by down-regulating of NF-κB and up-regulating of the FOXO transcription factors activation, catalase and SOD activities [29]. It also can inhibit the radiation-induced phosphorylation of mitogen-activated protein kinase (MAPK) and Akt, which are the upstream kinases of NF-κB and FOXOs. In respect to these declarations, it can be assume that baicalein is a prominent natural radioprotectant that act against NF-κB-mediated inflammatory responses via MAPKs and the Akt pathway, which leads to protective effects on FOXO and its target genes [108]. Quercetin is a plant pigment that belongs to a group of plant compounds called flavonoids and found in different types of fruits, vegetables and foods, such as red wine, skin of onions, green tea, apples, berries and Ginkgo biloba. In irradiated rats, Guven et al. investigated the radioprotective role of hesperidin and quercetin on the intestinal damage. Their results showed that the administration of quercetin and hesperidin in rat could considerably inhibit intestinal injury by declining TNF-α

levels and increasing IL-10, leading to radioprotection [109]. Additionally, in irradiated mice, oral administration of *Astragalus complanatus* flavonoids both before and after exposure to IR, alleviated the lung injury induced by radiation and reduced the serum content of TGF-β1, TNF-α and IL-6 [110].

5 Molecular-Based Radioprotection

The important role of natural agents in ameliorating various damages induced by radiation exposure has long been recognized. Among these, flavonoids are demonstrated to have promising results for mitigation of ionizing radiation-induced toxicities, management of inflammatory responses, detoxification of free radicals and diminution of apoptosis signaling pathways in radiosensitive tissues. Currently, perception the signaling and apoptotic pathways involved in IR damage, as well as identifying the events that occur late in these pathways are the major parts of studies. Most of these studies are focus on the protein molecules and signaling pathways which are involved in apoptosis induction. For example, protein p53, a tumor suppressor and ATM/ATR, a sensing protein respond to DNA breaks induced by ionizing irradiation (IR) [111]. Together with ATM, ATR plays a key role in the regulation of the phosphorylation of apoptotic proteins such as p53 (Ser15), which in turn activates the transcription of the p21 involved in the induction of apoptosis [112]. p53, the Guardian of the genome, plays an important role in the response to IR. After exposure to IR, p53 is stabilized and activated, which results to induce the growth arrest and DNA-damage repair. Recent study by Strom and colleagues demonstrated the inhibition role of pifithrin-l on p53 activation. They injected pifithrin-l into mice before IR exposure which results to protection of thymocytes from IR-induced apoptosis and cell death by p53 protein [111]. In a similar study by Liu et al. which used RT-PCR and Western techniques to investigate the radiation protection effect of blueberry anthocyanins on UV-irradiated HepG2 cells, it was found that blueberry anthocyanins are able to inhibit the cell apoptosis and diminish the IR-induced damage by reducing the gene expression of p53 and p21 proteins [113]. Overexpression of Bcl2, another inhibitor of pro-apoptotic proteins, in irradiated transgenic mice increased the survival rate by protecting against IR-induced apoptosis in hematopoietic cells [114]. Granulocyte colony stimulating factor (G-CSF) and IL-6 are major serum hematopoietic factors. Singh et al. treated mice with single subcutaneous (sc) administration of genistein 24 h before IR exposure (7 Gy ^{60}Co) [115] and showed that genistein administration could significantly stimulate serum G-CSF and IL-6 after γ-irradiation. Considering G-CSF and IL-6 as the main hematopoietic factors, these results suggest that radioprotective efficacy of genistein through its role in enhancing production of G-CSF and IL-6, can lead to early recovery of hematopoietic cells [115]. It revealed that the signal transducer and activator of transcription 3 (STAT3), a latent cytoplasmic transcription factor, is activated by several growth factors and protects against IR-induced damages. For instants, Xu et al. study indicated that CBLB502, STAT3 activator, stimulates the phosphorylation of STAT3, which in turn activate NF-κB signaling

pathway and protect hair cells from IR-induced cell death [116] (Fig. 2). Nuclear factor-erythroid 2-related factor 2 (Nrf2), is an important transcriptional factor, which regulates the activity of antioxidant and anti-inflammatory enzymes. It has been shown that when Nrf2 is activated by genetic or pharmacologic agents, it can reduce the expression of the pro-inflammatory factors IL6 and IL1β, and COX2 in the skin of SKH-1 hairless mice to protect against IR damage [117]. Importantly, the agonists of peroxisome proliferator-activated receptor-c (PPAR-c), a member of the nuclear hormone receptor family, is able to prevent effectively from collagen deposition and TGFb1-induced collagen secretion in bleomycin-induced pulmonary fibrosis [118]. Mangoni et al. study showed that Rosiglitazone which is a PPAR-c synthetic activator is able to enhance the IR induced apoptosis signaling in human cells [119]. Moreover,

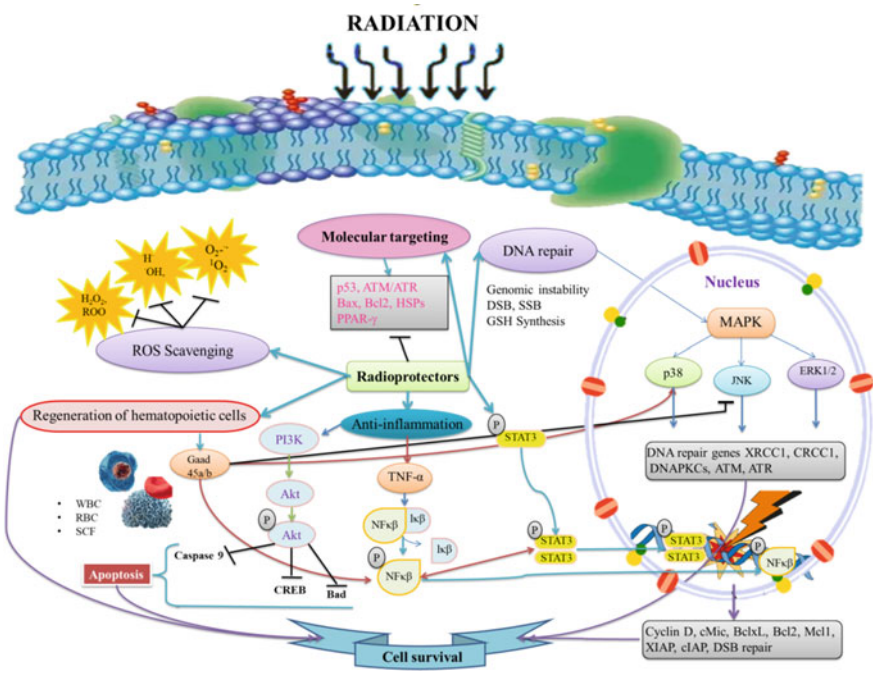

Fig. 2 Summary of the cellular mechanisms of natural radioprotectors. Natural products with radioprotective effects apply their activity through different mechanisms, such as free radical scavenging, anti-inflammation, regeneration of hematopoietic cells, facilitation of repair activity, and affecting to molecular levels. The main radioprotective mechanisms of natural compounds are involved in radiation response and tissue damage repair, which can be considerable pharmacological targets for advancement of excellent bio-radioprotectors. STAT3: signal transducer and activator of transcription 3; NF-κB: nuclear factor kappa-light-chain-enhancer of activated B cells; HSPs: heat shock proteins; SSB: single strand break; DSB: double strand break; RBC: red blood cells; WBC: white blood cells; O_2^-: Superoxide anions; OH^-: Hydroxyl radicals; H_2O_2 Hydrogen peroxide; TNF-α: Tumor necrosis factor α; ROS: Reactive oxygen species; MAPK: Mitogen-activated protein kinases; ATM: A-T mutated; ATR: ATM and Rad3-related; JNK: Jun-N-terminal kinases; P13K: Phosphatidylinositol-3-kinase; AKT: Serine-threonin protein kinase; GSH: Glutathione

it has been suggested that PPAR-c act as important fibroblast/myofibroblast activation regulator, which propose the PPAR-c ligands as potential treating ingredient for IR-induced fibrotic lung diseases. Another group of proteins that can determine in cell and tissue repair after IR exposure are heat shock proteins (HSPs) [120]. It has been shown that up-regulation of HSP genes could be sufficient to protect against IR exposure via apoptotic pathway interferences [121].

6 Challenges and Conclusion

Clearly, a key challenging in the success or failure of radiotherapy is interplay between cancerous and normal cells in sufficient doses in the clinic. In order to better discriminate between normal and tumor tissues, it is necessary to find new strategies to optimize the therapeutic index, either by increasing the radiation sensitivity of malignant cells compared to normal cells or by physically improving target conformity, which would not only be a quantum improvement to the patient, but it would also be useful as a means of enabling appropriate dose delivery to eliminate the tumor. Recent studies have led to the development of numerous radio protective agents with the aim of improving clinical outcomes. Although more than a dozen radio-protective agents have received FDA Animal Rule approval for radioprotection of normal tissues from radiation-induced adverse effects, but with the exception of amifostine and palifermin which received FDA approval in 1995 and 2004 for use in radiation therapy, no anew identified and developed product has received fully approval of FDA as a radioprotector for radiotherapy [122]. Despite these advances, a number of newer, still-under-developments, radiation-countering agents should be developed to specifically target healthy cells from radiation without conferring protection to cancerous cells. This is possible by large-scale screening of new sources of natural agents, investigation of existing medicines for radioprotection effect (drug repositioning) and reconstitution of former radioprotector drugs with small dosage combinations of inherently toxic but effectual agents.

In general, an ideal radioprotectors or radiomitigators for use as an adjunct in radiotherapy should be stable, easily available, easily dispensed without toxicity, economically affordable and orally administered. It should act selectively in protecting normal tissues from direct acute or chronic effects of IR without protecting tumor tissue. It also should be delivered with relative ease and possess an ability to act through multiple mechanisms. Finally, the agent should have minimum interference with other therapies [123]. A large number of drugs which were evaluated for treatment, prevention or mitigation of IR induced toxicities are among natural products. Although the use of radioprotectors is a beneficial way to protect the healthy cells from harmful effects of radiotherapy, unexpected radiation accidents and also terrorist incidents, there are no safe, effective and completely preventing IR-related toxicities radio-protectors available for human use [12]. Therefore an extensive search to find an ideal radio-protector among naturally occurring compounds can be a good strategy.

Naturally occurring compounds offer a variety of beneficial properties including mitigation the IR-induced injuries by scavenging or destroying of free radicals, repairing of DNA breaks, protecting the hemopoietic and immune systems, reduction in inflammation and also interaction with proteins in signaling pathways. These compounds have more advantages than synthetic chemical compounds, including their increased safety, non-toxicity to healthy cells in mild doses, having considerable toxicity to tumor cells by induction of apoptosis and being more effective in curing of IR-symptoms. Despite great advances, future efforts are required to explore the mechanisms underlying the protective effects and to develop natural radioprotectors which are medicinally safe on healthy tissues.

References

1. Moding EJ, Kastan MB, Kirsch DG (2013) Strategies for optimizing the response of cancer and normal tissues to radiation. Nat Rev Drug Discov 12:526–542
2. Prasad K (2005) Rationale for using multiple antioxidants in protecting humans against low doses of ionizing radiation. Br J Radiol 78:485–492
3. Wideł M, Przybyszewski W, Rzeszowska-Wolny J (2009) Radiation-induced bystander effect: the important part of ionizing radiation response. Potential clinical implications. Postepy higieny i medycyny doswiadczalnej 63:377–88
4. Hall E (1994) DNA strand breaks and chromosomal aberrations. Radiobiol Radiol 15–27
5. Wang H, Mu X, He H, Zhang X-D (2018) Cancer radiosensitizers. Trends Pharmacol Sci 39:24–48
6. Sankaranarayanan K (2006) Estimation of the genetic risks of exposure to ionizing radiation in humans: current status and emerging perspectives. J Radiat Res 47:B57–B66
7. Andersen MH, Becker JC, thor Straten P (2005) Regulators of apoptosis: suitable targets for immune therapy of cancer. Nat Rev Drug Discov 4:399–409
8. Mavragani IV, Nikitaki Z, Souli MP, Aziz A, Nowsheen S, Aziz K et al (2017) Complex DNA damage: a route to radiation-induced genomic instability and carcinogenesis. Cancers (Basel). 9:91
9. Norval M (2001) Effects of solar radiation on the human immune system. In: Comprehensive Series in Photosciences. Elsevier, pp 91–113
10. Mun G-I, Kim S, Choi E, Kim CS, Lee Y-S (2018) Pharmacology of natural radioprotectors. Arch Pharmacal Res 41:1033–1050
11. Greenberger JS (2009) Radioprotection. In Vivo 23:323–336
12. Citrin D, Cotrim AP, Hyodo F, Baum BJ, Krishna MC, Mitchell JB (2010) Radioprotectors and mitigators of radiation-induced normal tissue injury. Oncologist 15:360
13. Hosseinimehr SJ (2007) Trends in the development of radioprotective agents. Drug Discov Today 12:794–805
14. Bourgier C, Levy A, Vozenin M-C, Deutsch E (2012) Pharmacological strategies to spare normal tissues from radiation damage: useless or overlooked therapeutics? Cancer Metastasis Rev 31:699–712
15. Cheki M, Mihandoost E, Shirazi A, Mahmoudzadeh A (2016) Prophylactic role of some plants and phytochemicals against radio-genotoxicity in human lymphocytes. J Cancer Res Ther 12:1234

16. Kuruba V, Gollapalli P (2018) Natural radioprotectors and their impact on cancer drug discovery. Radiat Oncol J 36:265
17. Crump KS, Duport P, Jiang H, Shilnikova NS, Krewski D, Zielinski JM (2012) A meta-analysis of evidence for hormesis in animal radiation carcinogenesis, including a discussion of potential pitfalls in statistical analyses to detect hormesis. J Toxicol Environ Health Part B 15:210–231
18. Friedman DA, Tait L, Vaughan AT (2016) Influence of nuclear structure on the formation of radiation-induced lethal lesions. Int J Radiat Biol 92:229–240
19. Bala M (2014) Concerted action of Nrf2-ARE pathway, MRN complex, HMGB1 and inflammatory cytokines-implication in modification of radiation damage. Redox Biol 2:832–846
20. Phaniendra A, Jestadi DB, Periyasamy L (2015) Free radicals: properties, sources, targets, and their implication in various diseases. Indian J Clin Biochem 30:11–26
21. Azzam EI, Jay-Gerin J-P, Pain D (2012) Ionizing radiation-induced metabolic oxidative stress and prolonged cell injury. Cancer Lett 327:48–60
22. Nakano T, Xu X, Salem AM, Shoulkamy MI, Ide H (2017) Radiation-induced DNA–protein cross-links: mechanisms and biological significance. Free Radical Biol Med 107:136–145
23. Srinivasan M, Sudheer AR, Pillai KR, Kumar PR, Sudhakaran P, Menon V (2007) Lycopene as a natural protector against γ-radiation induced DNA damage, lipid peroxidation and antioxidant status in primary culture of isolated rat hepatocytes in vitro. Biochim Biophys Acta (BBA) Gen Subj 1770:659–65
24. Zhang X, Ma C, Sun X, Zhang K (2004) Research progress of natural drug antiradiation effect. Chinese J Radiol Health 13:228–230
25. Ringborg U, Bergqvist D, Brorsson B, Cavallin-Ståhl E, Ceberg J, Einhorn N et al (2003) The Swedish Council on Technology Assessment in Health Care (SBU) systematic overview of radiotherapy for cancer including a prospective survey of radiotherapy practice in Sweden 2001–summary and conclusions. Acta Oncol 42:357–365
26. Xu P, Jiang E-J, Wen S-Y, Lu D-D (2014) Amentoflavone acts as a radioprotector for irradiated v79 cells by regulating reactive oxygen species (ROS), cell cycle and mitochondrial mass. Asian Pac J Cancer Prev 15:7521–7526
27. Begum N, Prasad NR, Kanimozhi G, Hasan AQ (2012) Apigenin ameliorates gamma radiation-induced cytogenetic alterations in cultured human blood lymphocytes. Mutat Res/Genet Toxicol Environ Mutagen 747:71–76
28. Rithidech KN, Tungjai M, Whorton EB (2005) Protective effect of apigenin on radiation-induced chromosomal damage in human lymphocytes. Mutat Res/Genet Toxicol Environ Mutagen 585:96–104
29. Lee EK, Kim JM, Choi J, Jung KJ, Kim DH, Chung SW et al (2011) Modulation of NF-κB and FOXOs by baicalein attenuates the radiation-induced inflammatory process in mouse kidney. Free Radic Res 45:507–517
30. Gandhi NM (2013) Baicalein protects mice against radiation-induced DNA damages and genotoxicity. Mol Cell Biochem 379:277–281
31. Wang S-C, Chen S-F, Lee Y-M, Chuang C-L, Bau D-T, Lin S-S (2013) Baicalin scavenges reactive oxygen species and protects human keratinocytes against UVC-induced cytotoxicity. In Vivo 27:707–714
32. Veerapur V, Prabhakar K, Parihar VK, Kandadi MR, Ramakrishana S, Mishra B, et al (2009) Ficus racemosa stem bark extract: a potent antioxidant and a probable natural radioprotector. Evid Based Complement Alternat Med 6
33. He X, Long W, Dong H, Wang C, Chu X, Zheng Q et al (2017) Evaluation of the protective effects of 13 traditional Chinese medicine compounds on ionizing radiation injury: bupleurum, shenmai, and breviscapine as candidate radioprotectors. RSC Adv 7:22640–22648
34. Hebbar S, Mitra A, George K, Verma N (2002) Caffeine ameliorates radiation-induced skin reactions in mice but does not influence tumour radiation response. J Radiol Prot 22:63
35. Kim JK, Kim JH, Lee BH, Yoon YD (2003) Comparison of radioprotective effects of caffeine and ascorbic acid in male mice proceedings of the 18th KAIF/KNS 34(37):34063898

36. Cinkilic N, Cetintas SK, Zorlu T, Vatan O, Yilmaz D, Cavas T et al (2013) Radioprotection by two phenolic compounds: chlorogenic and quinic acid, on X-ray induced DNA damage in human blood lymphocytes in vitro. Food Chem Toxicol 53:359–363
37. Kim S-Y, Lee H-J, Nam J-W, Seo E-K, Lee Y-S (2015) Coniferyl aldehyde reduces radiation damage through increased protein stability of heat shock transcriptional factor 1 by phosphorylation. Int J Radiat Oncol Biol Phys 91:807–16
38. Verma V (2016) Relationship and interactions of curcumin with radiation therapy. World J Clin Oncol. 7:275
39. Jeong M-H, Ko H, Jeon H, Sung G-J, Park S-Y, Jun WJ et al (2016) Delphinidin induces apoptosis via cleaved HDAC3-mediated p53 acetylation and oligomerization in prostate cancer cells. Oncotarget 7:56767
40. Das U, Manna K, Sinha M, Datta S, Das DK, Chakraborty A et al (2014) Role of ferulic acid in the amelioration of ionizing radiation induced inflammation: a murine model. PLoS One 9:e97599
41. Ahmad IU, Forman JD, Sarkar FH, Hillman GG, Heath E, Vaishampayan U et al (2010) Soy isoflavones in conjunction with radiation therapy in patients with prostate cancer. Nutr Cancer 62:996–1000
42. Zhou Y, Mi M-T (2005) Genistein stimulates hematopoiesis and increases survival in irradiated mice. J Radiat Res 46:425–433
43. Fardid R, Ghorbani Z, Haddadi G, Behzad-Behbahani A, Arabsolghar R, Kazemi E et al (2016) Effects of hesperidin as a radio-protector on apoptosis in rat peripheral blood lymphocytes after gamma radiation. J Biomed Phys Eng 6:217
44. Kelkel M, Schumacher M, Dicato M, Diederich M (2011) Antioxidant and anti-proliferative properties of lycopene. Free Radical Res 45:925–940
45. Jagetia G, Baliga M (2005) Radioprotection by mangiferin in DBAxC57BL mice: a preliminary study. Phytomedicine 12:209–215
46. Canyilmaz E, Uslu GH, Bahat Z, Kandaz M, Mungan S, Haciislamoglu E et al (2016) Comparison of the effects of melatonin and genistein on radiation-induced nephrotoxicity: results of an experimental study. Biomedical reports. 4:45–50
47. Malhotra P, Adhikari M, Singh SK, Kumar R (2015) N-acetyl tryptophan glucopyranoside (NATG) provides radioprotection to murine macrophage J774A. 1 cells. Free Radic Res 49:1488–1498
48. Jagetia GC, Venkatesha V, Reddy TK (2003) Naringin, a citrus flavonone, protects against radiation-induced chromosome damage in mouse bone marrow. Mutagenesis 18:337–343
49. Satyamitra M, Mantena S, Nair C, Chandna S, Dwarakanath B (2014) The antioxidant flavonoids, orientin and vicenin enhance repair of radiation-induced damage. SAJ Pharm Pharmacol 1:1
50. Berbée M, Fu Q, Garg S, Kulkarni S, Kumar KS, Hauer-Jensen M (2011) Pentoxifylline enhances the radioprotective properties of γ-Tocotrienol: differential effects on the hematopoietic, gastrointestinal and vascular systems. Radiat Res 175:297–306
51. Zhang D, Wang J-B, Li W-F, Xu B (2013) Study on antioxidant activities of quercetin, polydain and genisten and the protection on HaCa T cells against damage from UVB irradiation. Chinese J Clinic 45
52. Benkovic V, Knezevic AH, Orsolic N, Basic I, Ramic S, Viculin T et al (2009) Evaluation of radioprotective effects of propolis and its flavonoid constituents: in vitro study on human white blood cells. Phytother Res Int J Devoted Pharmacol Toxicol Eval Nat Prod Deriv 23:1159–1168
53. Chiou W-F, Don M-J, Liao J-F, Wei B-L (2011) Psoralidin inhibits LPS-induced iNOS expression via repressing Syk-mediated activation of PI3K-IKK-IκB signaling pathways. Eur J Pharmacol 650:102–109
54. Zhu X, Li N, Wang Y, Ding L, Chen H, Yu Y et al (2017) Protective effects of quercetin on UVB irradiation-induced cytotoxicity through ROS clearance in keratinocyte cells. Oncol Rep 37:209–218

55. Agbele AT, Fasoro OJ, Fabamise OM, Oluyide OO, Idolor OR, Bamise EA (2020) Protection against ionizing radiation-induced normal tissue damage by resveratrol: a systematic review. Euras J Med 52:298
56. Sunada S, Fujisawa H, Cartwright IM, Maeda J, Brents CA, Mizuno K et al (2014) Monoglucosyl-rutin as a potential radioprotector in mammalian cells. Mol Med Report 10:10–14
57. Jaiswal S, Bordia A (1996) Radio-protective effect of garlic *Allium sativum* Linn. in albino rats. Indian J Med Sci 50:231–3
58. Mishra K, Srivastava P, Chaudhury N (2011) Sesamol as a potential radioprotective agent: in vitro studies. Radiat Res 176:613–623
59. Tiwari P, Kumar A, Ali M, Mishra K (2010) Radioprotection of plasmid and cellular DNA and swiss mice by silibinin. Mutat Res/Genet Toxicol Environ Mutagen 695:55–60
60. Maurya DK, Salvi VP, Nair CKK (2004) Radioprotection of normal tissues in tumor-bearing mice by troxerutin. J Radiat Res 45:221–228
61. Kumar SS, Ghosh A, Devasagayam TP, Chauhan PS (2000) Effect of vanillin on methylene blue plus light-induced single-strand breaks in plasmid pBR322 DNA. Mutat Res/Genet Toxicol Environ Mutagen 469:207–214
62. Ahmad B, Rehman MU, Amin I, Arif A, Rasool S, Bhat SA, et al (2015) A review on pharmacological properties of zingerone (4-(4-Hydroxy-3-methoxyphenyl)-2-butanone). Sci World J 2015:816364
63. Du J, Cheng Y, Dong S, Zhang P, Guo J, Han J et al (2017) Zymosan-a protects the hematopoietic system from radiation-induced damage by targeting TLR2 signaling pathway. Cell Physiol Biochem 43:457–464
64. Wang M, Xie X, Du Y, Ma G, Xu X, Sun G, et al (2020) Protective effects of biscoclaurine alkaloids on leukopenia induced by 60Co-γ radiation. Evid Based Complement Alternat Med 2020:2162915
65. Yi J, Chen C, Liu X, Kang Q, Hao L, Huang J et al (2020) Radioprotection of EGCG based on immunoregulatory effect and antioxidant activity against 60Coγ radiation-induced injury in mice. Food Chem Toxicol 135:111051
66. Zhu W, Jia L, Chen G, Zhao H, Sun X, Meng X et al (2016) Epigallocatechin-3-gallate ameliorates radiation-induced acute skin damage in breast cancer patients undergoing adjuvant radiotherapy. Oncotarget 7:48607
67. Qi T, Li H, Li S (2017) Indirubin improves antioxidant and anti-inflammatory functions in lipopolysaccharide-challenged mice. Oncotarget 8:36658
68. Dobrzynska M (2013) Resveratrol as promising natural radioprotector. A review. Roczniki Pa´nstwowego Zakładu Higieny Rocz Panstw Zakl Hig. 64(4):255-62
69. Jagetia GC (2007) Radioprotective potential of plants and herbs against the effects of ionizing radiation. J Clin Biochem Nutr 40:74–81
70. Urbach F (1989) The biological effects of increased ultraviolet radiation: an update: introduction. Photochem Photobiol 50:439–441
71. Barker S, Weinfeld M, Murray D (2005) DNA–protein crosslinks: their induction, repair, and biological consequences. Mutat Res/Rev Mutat Res 589:111–135
72. Hall EJ, Giaccia A (2012) Radiobiology for the Radiologist. Seventh. Lippincott, Williams and Wilkins, Wolter Kluwer Philadelphia
73. Hall J, Angèle S (1999) Radiation, DNA damage and cancer. Mol Med Today 5:157–164
74. Gakova N, Mishurova E, Kropachova K (1992) Effects of flavobion on nucleic acids in tissues of rats irradiated with gamma rays. Biulleten'eksperimental'noi biologii i meditsiny. 113:275
75. Devipriya N, Sudheer AR, Srinivasan M, Menon VP (2008) Quercetin ameliorates gamma radiation-induced DNA damage and biochemical changes in human peripheral blood lymphocytes. Mutat Res/Genet Toxicol Environ Mutagen 654:1–7
76. Özyurt H, Çevik Ö, Özgen Z, Özden A, Çadırcı S, Elmas M et al (2014) Quercetin protects radiation-induced DNA damage and apoptosis in kidney and bladder tissues of rats. Free Radic Res 48:1247–1255

77. Xu P, Jia J-Q, Jiang E-J, Kang L-P, Wu K-L (2012) Protective effect of an extract of Guipi Pill (归脾丸) against radiation-induced damage in mice. Chin J Integr Med 18:490–495
78. Hosseinimehr SJ, Mahmoudzadeh A, Ahmadi A, Mohamadifar S, Akhlaghpoor S (2009) Radioprotective effects of hesperidin against genotoxicity induced by γ-irradiation in human lymphocytes. Mutagenesis 24:233–235
79. Moon H-I, Jeong MH, Jo WS (2014) Protective activity of C-Geranylflavonoid analogs from *Paulownia tomentosa* against DNA damage in 137Cs irradiated AHH-1Cells. Nat Prod Commun 9:1934578X1400900919
80. Lobo V, Patil A, Phatak A, Chandra N (2010) Free radicals, antioxidants and functional foods: Impact on human health. Pharmacogn Rev 4:118
81. Gharari Z, Bagheri K, Khodaeiaminjan M, Sharafi A (2019) Potential therapeutic effects and bioavailability of Wogonin, the Flavone of Baikal Skullcap. J Nutri Med Diet Care 5:039
82. Ma X, Deng D, Chen W (2017) Inhibitors and activators of SOD, GSH-Px, and CAT. Enzyme Inhibit Activat 29:207
83. Gvilava I, Ormotsadze G, Chkhikvishvili I, Giorgobiani M, Kipiani NV, Sanikidze T (2018) Radioprotective activity of polymetoxy-lated flavonoids of citrus extract. Georgian Med News 119–124
84. Xu P, Zhang W-B, Cai X-H, Lu D-D, He X-Y, Qiu P-Y et al (2014) Flavonoids of *Rosa roxburghii* Tratt act as radioprotectors. Asian Pac J Cancer Prev 15:8171–8175
85. Malakyan M, Bajinyan S, Vardevanyan L, Yeghiazaryan D, Mairapetyan SK, Tadevosyan A (2008) Anti-radiation and anti-radical activity of hydroponically produced hop extract vol 848. In: *II International Humulus Symposium.* pp 253–258
86. Yu J (2012) Flavonoids protection against ionizing radiation induced PC12 cell injury and its machine system research. Hubei, Hubei University of Chinese Medicine
87. de Siqueira WN, Dos Santos FTJ, de Souza TF, de Vasconcelos LM, Silva HAMF, de Oliveira PSS et al (2019) Study of the potential radiomitigator effect of quercetin on human lymphocytes. Inflammation 42:124–134
88. Li Y-N, Zhang W-B, Zhang J-H, Xu P, Hao M-H (2016) Radioprotective effect and other biological benefits associated with flavonoids. Trop J Pharm Res 15:1099–1108
89. Liu L, Jin H, Wang X, Xu Z, Nan W, Li P (2006) Effects of soybean isoflavones on the cell cycles, the cell apoptosis and the proliferation of spleen in radiated mice. Chinese J Appl Physiol 22:497–500
90. Jia H, Jin H, Li P, Wu J, Nan W, Wang Y et al (2011) Effects of soybean isoflavones on immune function in irradiation mice. J Prev Med Chin PLA 06:402–404
91. Zhang D, Zhang Y, Zhu B, Zhang H, Sun Y, Sun C (2017) Resveratrol may reverse the effects of long-term occupational exposure to electromagnetic fields on workers of a power plant. Oncotarget 8:47497
92. Shao L, Luo Y, Zhou D (2014) Hematopoietic stem cell injury induced by ionizing radiation. Antioxid Redox Signal 20:1447–1462
93. Wang M, Dong Y, Wu J, Li H, Zhang Y, Fan S et al (2020) Baicalein ameliorates ionizing radiation-induced injuries by rebalancing gut microbiota and inhibiting apoptosis. Life Sci 261:118463
94. Liu C, Liu J, Hao Y, Gu Y, Yang Z, Li H et al (2017) 6, 7, 3′, 4′-Tetrahydroxyisoflavone improves the survival of whole-body-irradiated mice via restoration of hematopoietic function. Int J Radiat Biol 93:793–802
95. Benković V, Knežević A, Đikić D, Lisičić D, Oršolić N, Bašić I et al (2009) Radioprotective effects of quercetin and ethanolic extract of propolis in gamma-irradiated mice. Arch Ind Hyg Toxicol 60:129–138
96. Benković V, Kopjar N, Kneževic AH, Đikić D, Bašić I, Ramić S et al (2008) Evaluation of radioprotective effects of propolis and quercetin on human white blood cells in vitro. Biol Pharm Bull 31:1778–1785
97. Ha CT, Li X-H, Fu D, Xiao M, Landauer MR (2013) Genistein nanoparticles protect mouse hematopoietic system and prevent proinflammatory factors after gamma irradiation. Radiat Res 180:316–325

98. Ping X, Junqing J, Junfeng J, Enjin J (2012) Radioprotective effects of troxerutin against gamma irradiation in mice liver. Int J Radiat Biol 88:607–612
99. Qi L, Liu C, Wu W, Yang J, Sheng W (2008) Effects of flavonoids of Astragali Complanali against damage induced by 60 Co γ-ray irradiation. Suzhou University J Med Sci 28:26–29
100. Nguyen DT, Truong GN, Van Vuong T, Van TN, Manh CN, Dao CT et al (2019) Synthesis of new indirubin derivatives and their in vitro anticancer activity. Chem Pap 73:1083–1092
101. Ponnusamy K, Ramasamy M, Savarimuthu I, Paulraj MG (2010) Indirubin potentiates ciprofloxacin activity in the NorA efflux pump of Staphylococcus aureus. Scand J Infect Dis 42:500–505
102. You WC, Lin WC, Huang JT, Hsieh CC (2009) Indigowood root extract protects hematopoietic cells, reduces tissue damage and modulates inflammatory cytokines after total-body irradiation: does Indirubin play a role in radioprotection? Phytomedicine 16:1105–1111
103. Michaluart P, Masferrer JL, Carothers AM, Subbaramaiah K, Zweifel BS, Koboldt C et al (1999) Inhibitory effects of caffeic acid phenethyl ester on the activity and expression of cyclooxygenase-2 in human oral epithelial cells and in a rat model of inflammation. Cancer Res 59:2347–2352
104. Chen M-F, Keng PC, Lin P-Y, Yang C-T, Liao S-K, Chen W-C (2005) Caffeic acid phenethyl ester decreases acute pneumonitis after irradiation in vitro and in vivo. BMC Cancer 5:1–9
105. Sato T, Kinoshita M, Yamamoto T, Ito M, Nishida T, Takeuchi M et al (2015) Treatment of irradiated mice with high-dose ascorbic acid reduced lethality. PLoS One 10:e0117020
106. Şener G, Kabasakal L, Atasoy BM, Erzik C, Velioğlu-Öğünç A, Çetinel Ş et al (2006) Ginkgo biloba extract protects against ionizing radiation-induced oxidative organ damage in rats. Pharmacol Res 53:241–252
107. Hosseinimehr S, Nemati A (2006) Radioprotective effects of hesperidin against gamma irradiation in mouse bone marrow cells. Br J Radiol 79:415
108. Zhang J, Teng C, Li C, He W (2020) Deliver anti-inflammatory drug baicalein to macrophages by using a crystallization strategy. Front Chem 8:787
109. Guven B, Can M, Piskin O, Gulhan Aydin B, Karakaya K, Elmas O et al (2019) Flavonoids protect colon against radiation induced colitis. Regul Toxicol Pharmacol 104:128–132
110. Wang J, Xu H-W, Li B-S, Zhang J, Cheng J (2012) Preliminary study of protective effects of flavonoids against radiation-induced lung injury in mice. Asian Pac J Cancer Prev 13:6441–6446
111. Strom E, Sathe S, Komarov PG, Chernova OB, Pavlovska I, Shyshynova I et al (2006) Small-molecule inhibitor of p53 binding to mitochondria protects mice from gamma radiation. Nat Chem Biol 2:474–479
112. Sullivan KD, Gallant-Behm CL, Henry RE, Fraikin J-L, Espinosa JM (202) The p53 circuit board. Biochim Biophys Acta (BBA)-Rev Cancer 1825:229–44
113. Liu W, Lu X, He G, Gao X, Li M, Wu J et al (2013) Cytosolic protection against ultraviolet induced DNA damage by blueberry anthocyanins and anthocyanidins in hepatocarcinoma HepG2 cells. Biotechnol Lett 35:491–498
114. Erlacher M, Michalak EM, Kelly PN, Labi V, Niederegger H, Coultas L et al (2005) BH3-only proteins Puma and Bim are rate-limiting for γ-radiation–and glucocorticoid-induced apoptosis of lymphoid cells in vivo. Blood 106:4131–4138
115. Singh VK, Grace MB, Parekh VI, Whitnall MH, Landauer MR (2009) Effects of genistein administration on cytokine induction in whole-body gamma irradiated mice. Int Immunopharmacol 9:1401–1410
116. Xu Y, Dong H, Ge C, Gao Y, Liu H, Li W, et al (2016) CBLB502 administration protects gut mucosal tissue in ulcerative colitis by inhibiting inflammation. Ann Trans Med 4
117. Knatko EV, Ibbotson SH, Zhang Y, Higgins M, Fahey JW, Talalay P et al (2015) Nrf2 activation protects against solar-simulated ultraviolet radiation in mice and humans. Cancer Prev Res 8:475–486
118. Milam JE, Keshamouni VG, Phan SH, Hu B, Gangireddy SR, Hogaboam CM et al (2008) PPAR-γ agonists inhibit profibrotic phenotypes in human lung fibroblasts and bleomycin-induced pulmonary fibrosis. Am J Physiol-Lung Cell Mol Physiol 294:L891–L901

119. Mangoni M, Sottili M, Gerini C, Desideri I, Bastida C, Pallotta S et al (2017) A PPAR-gamma agonist protects from radiation-induced intestinal toxicity. United Europ Gastroenterol J 5:218–226
120. Lee S-J, Choi S-A, Lee K-H, Chung H-Y, Kim T-H, Cho C-K et al (2001) Role of inducible heat shock protein 70 in radiation-induced cell death. Cell Stress Chaperones 6:273
121. Åkerfelt M, Morimoto RI, Sistonen L (2010) Heat shock factors: integrators of cell stress, development and lifespan. Nat Rev Mol Cell Biol 11:545–555
122. Singh VK, Garcia M, Wise SY, Seed TM (2016) Medical countermeasures for unwanted CBRN exposures: part I chemical and biological threats with review of recent countermeasure patents. Expert Opin Ther Pat 26:1431–1447
123. Cheki M, Shirazi A, Mahmoudzadeh A, Bazzaz JT, Hosseinimehr SJ (2016) The radioprotective effect of metformin against cytotoxicity and genotoxicity induced by ionizing radiation in cultured human blood lymphocytes. Mutat Res/Genet Toxicol Environ Mutagen 809:24–32

ROS-Based Cancer Radiotherapy

Faezeh Mozafari, Hamid Rashidzadeh, Mohammadreza Ghaffarlou, Marziyeh Salehiabar, Yavuz Nuri Ertas, Ali Ramazani, Morteza Abazari, Mohammad-Amin Rahmati, Yasir Javed, Surender K. Sharma, and Hossein Danafar

Abstract Reactive oxygen species (ROS) in cancer cells play a crucial role in metabolic reprogramming, altering tumor microenvironment, regulating cell death, repairing DNA and other physiological functions of living organisms. The unique features of ROS, which underlie the mechanisms indispensable for the aging, fitness, or growth of cells, have opened new route for researchers to take all benefits of these potential species in order to potentiate treatment efficacy and boost medical advances. Radiation therapy (RT) as a common method of cancer treatment, destroys malignant tumors and cells through both direct and indirect mechanisms. In the context of indirect mechanism, radiation could induce the generation of ROS and free radicals, resulting in the induction of cellular stress, injuring biomolecules, and ultimately altering cellular signaling pathways. Accordingly, adjusting ROS generation and elimination in favor of killing cancer cells without impairing normal cells

Faezeh Mozafari and Hamid Rashidzadeh. These authors contribute equally to this work.

F. Mozafari · H. Rashidzadeh · M. Abazari · M.-A. Rahmati · H. Danafar (✉)
Zanjan Pharmaceutical Biotechnology Research Center, Zanjan University of Medical Sciences, Zanjan, Iran
e-mail: danafar@zums.ac.ir

F. Mozafari · H. Rashidzadeh · A. Ramazani · H. Danafar
Cancer Gene Therapy Research Center, Zanjan University of Medical Sciences, Zanjan, Iran

M. Ghaffarlou
Department of Chemistry, Hacettepe University, Beytepe, Ankara 06800, Turkey

M. Salehiabar · Y. N. Ertas
ERNAM—Nanotechnology Research and Application Center, Erciyes University, Kayseri 38039, Turkey

Y. Javed
Magnetic Materials Laboratory, Department of Physics, University of Agriculture, Faisalabad, Pakistan

S. K. Sharma
Department of Physics, Central University of Punjab, Bathinda 151401, India

Department of Physics, Federal University of Maranhao, Sao Luis 65080-805, MA, Brazil

S. K. Sharma et al. (eds.), *Harnessing Materials for X-ray Based Cancer Therapy and Imaging*, Nanomedicine and Nanotoxicology,
https://doi.org/10.1007/978-3-031-04071-9_10

hold promising approach in achieving favorable results in cancer radiotherapy. Over the past few years, nanotechnology-based materials have driven notable progress in medical and biological fields, a large number of nanomaterials with unique ROS-regulating features or nanomaterial-induced ROS formation have been exploited for its potential in modulating the tumor microenvironment and in more particular cancer cells, which contributes to the emergence of a new therapeutic modality. In order to use ROS as a potent weapon in cancer therapy, we need to eludicate its corresponding biology and chemistry as well. Herein, this chapter summarized some recent advances in ROS-based RT in detail to harness the innate powers of ROS for effective tumor therapy. Our demonstration on this emerging field will be very useful to further development of ROS-based fundamental researches and clinical applications in favor of mitigating the burden of cancer treatment.

Keywords Radiotherapy · ROS · Nanomaterials · Cancer · Tumor therapy

1 Introduction

Since late 90s, chemistry has been tightly linked with biology which led to role verification of chemical molecules in biological mechanisms. This matter along with endeavors to discover Reactive Oxygen Species (ROS) and their redox chemistry over last 50 years, have opened new doors toward development of new therapeutic agents and approaches (Fig. 1). Free radicals are molecules with one or more unpaired electrons. Incomplete reduction of oxygen (O_2) mainly forms reactive chemical species in the cell [1]: (bold ones are the major ROS products).

I. Radical ROS: **Superoxide anion ($O_2^{\cdot -}$)**, **hydroxyl radical (·OH)**, nitric oxide (NO·), peroxyl radicals (ROO·) and peroxyl radicals (RO·), organic radicals (R·), alkoxyl radicals (RO·), sulfonyl radicals (ROS·), thiyl peroxyl radicals (RSOO·), thiyl radicals (RS·), and disulfides (RSSR)
II. Non-radical ROS: **hydrogen peroxide (H_2O_2)**, **singlet oxygen ($^1O_2$)**, organic hydroperoxides (ROOH), hypochlorous acid (HOCl), hypobromous acid (HOBr), and ozone (O_3) [2–5], organic hydroperoxides (ROOH), peroxynitrite (ONO^-), nitrosoperoxycarbonate anion ($O{=}NOOCO_2^-$), dinitrogen dioxide (N_2O_2), nitronium (NO_2^+), nitrocarbonate anion ($O_2NOCO_2^-$), and highly reactive carbonyl compounds derived from lipid or carbohydrate.

ROS is generated inside the cell through oxidative phosphorylation of mitochondria or cell interaction with exogenous-sourced materials such as xenobiotics. Electron transport chain (ETC) of mitochondria and nicotinamide adenine dinucleotide phosphate oxidases (NOXs) are the major sources of endogenous ROS production. Superoxide major source is endoplasmic reticulum and mitochondria in which respiratory chain is placed. Leakage of ~2% electrons from mitochondria chain carriers and joining with O_2 develop superoxide [6]. Genomic stability and cellular macromolecular function is properly preserved from random radical damages by an arranged complex antioxidant system; prominently by GSH and SOD system. Super Oxide

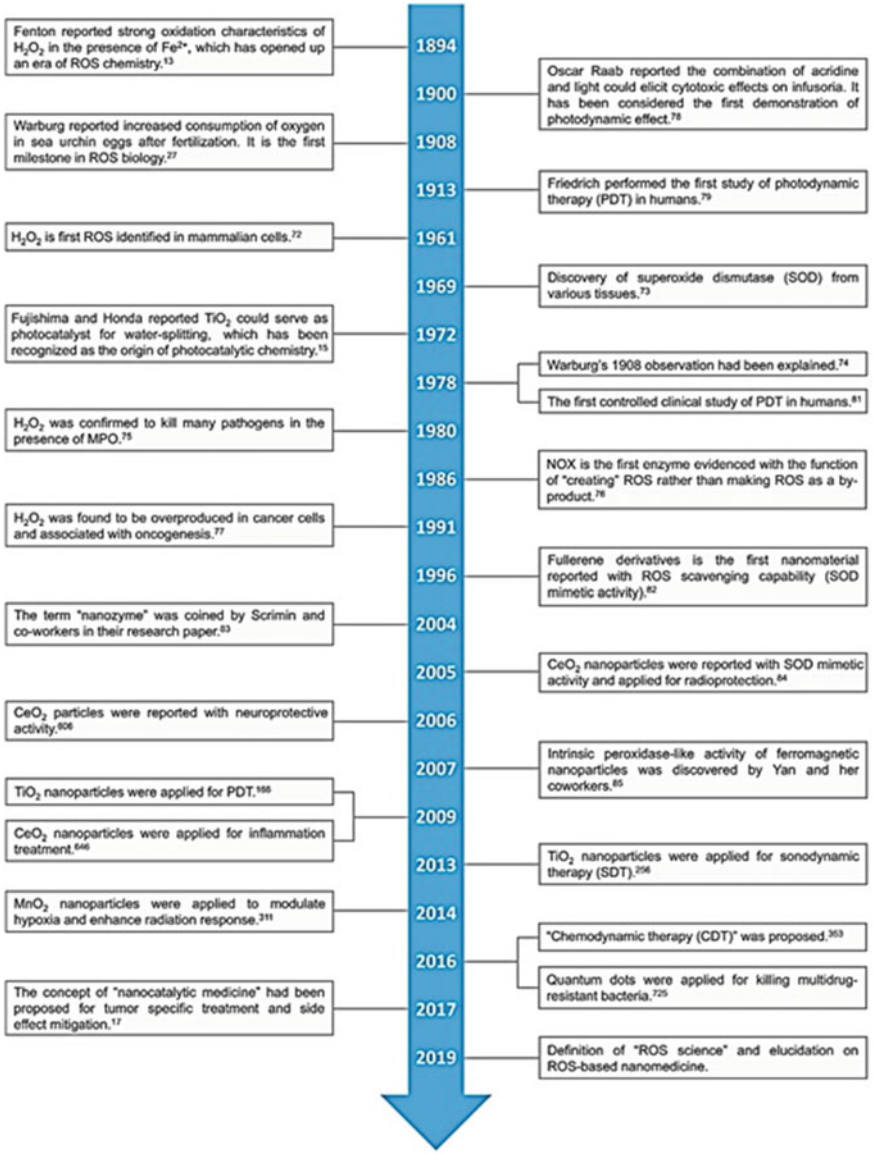

Fig. 1 Historical trend of ROS science at a glance. Reproduced with permission from Ref. [9]. Copyright 2019, with permission from ACS

Dismutase (SOD) enzyme is evolved for scavenging superoxide specifically. Important role of ROS in controlling body functions is undeniable. It involves both in cell proliferation and differentiation mechanisms [7]. Oxidative stress (which is known as a major problem in various diseases) occurs if excess amount of ROS production, more than cell antioxidant capacity, happens or if cell antioxidant storage is decreased. Cell should be able to defense against extra production of ROS because if oxidative stress occurs, proteins, lipids and nucleic acids may be damaged and subsequently involve in diabetes (i/ii), atherosclerosis, neurodegeneration, aging and carcinogenesis physiopathology [8]. ROS are involved in diseases' mechanisms both by damaging macro molecules and signaling alternation; for example by activating genes responsible for tumor metastasis.

- ROS are *produced* endogenously:
  - by the lack of oxygen, metabolic defects, physical agents (UV, heat, X-ray, γ-ray)
  - in endoplasmic reticulum (ER), mitochondria and peroxisomes where fatty acid ß-oxidation and electron transportation are conducted.
  - by enzymatic reactions: **lipoxygenase enzymes**, cyclooxygenase enzymes, **NADPH oxidases (NOX)** [10], **xanthine oxidase**, **cytochrome P450** and redox metals like Fe^{2+} and Cu^{2+} in Fenton reaction.

- ROS are *eliminated* by antioxidants inside the cell by:
  - Antioxidative enzymes: superoxide dismutase (SOD), catalase (CAT), **peroxiredoxins (PRXs)**, thioredoxine, **glutathione peroxidases (GPXs)**, glutathione reductase (GR).

Nuclear factor erythroid 2-related factor 2 (NRF2) (transcription factor which provokes antioxidant response in cancer cells), glutathione (GSH), NADPH, **vitamin C, and vitamin E** and many other antioxidant compounds are part of our food regimen components (e.g. selenium, etc.) [11]. Bold ones participate closely in redox system. SOD exists in cytoplasm, mitochondria and extra cellular matrix (ECM) with different bounded metal ions (Zn/Cu, Mn) [12].

Diseases associated with ROS toxicity and associated signaling have been investigated for either prevention or therapy. Innovative therapeutics, regarding disease pathogenesis and ROS regulation role can be developed. Although reducing ROS level is considered to be an approach for disease prevention or control like in neurodegenerative diseases and cancer therapy, the vice versa can be another useful approach for designing novel therapeutic agents. Looking from another perspective, molecules involved in ROS signaling pathways can be targeted for prevention or treatment of related diseases [13, 14]. Cancer, a deadly disease worldwide, is caused by tumorigenesis. Dysregulation of proliferation and apoptosis by ROS regulators lead to tumorigenesis. Oxidative stress involves closely in cancer pathophysiology which is caused by high level of ROS. Excessive concentration of ROS may damage pivotal macromolecules such as DNA and proteins. Cancer radiotherapy is being used as

adjuvant or monotherapy depending specially on tumor radiosensitivity. Basically, ionizing radiations such as high-energy photons (for instance X and γ ray) and particle photons (alpha–beta, electron-proton-neutron particles) are used depending on clinical necessity to interact with intracellular components and cause damage to macromolecules especially DNA, directly (cell proliferation in tumor cells will be stopped and necrosis or apoptosis may happen by damaging DNA) or indirectly by inducing ROS production as main product of water radiolysis [15]. Further, chemical reactions cause biomolecular damage which leads to structural damage, directing cell elimination. Meanwhile solid tumors with hypoxic conditions (oxygen itself acts as a radiosensitizer and fixes the induced damage) manifest more resistance to radiotherapy, thus require higher dose of radiation for treatment. Radiosensitizers can be implemented to overcome this issue with different mechanisms and attenuate subsequent side effects [16]. For oxygen concentration less than 1%, cancer cells begin to resist (mild hypoxia), and at 0.01%, they fully resist to ionizing radiation. Hypoxia intensity, cell survival and repopulation after RT within 6–7 weeks and tumor radioresistance are the three main key factors determining RT outcome [17, 18]. ROS are able to regulate specific signaling pathways involved in tumorigenesis. Specific pathways are altered in various types of cancer cells and regulate cell proliferation/growth, glucose metabolism, protein synthesis, differentiation and inflammation. It's a challenging to control ROS concentration in favor of medical purposes, considering their unstable nature. Additionally, ROS-related therapies could initiate unwanted biological reactions which makes this approach more peculiar [9]. Due to recent advancement in nanotechnology, various nanomaterials have been synthesized with the ability to regulate ROS concentration in biological environments through manipulating chemical reactions associated with ROS. New therapeutic advancements can be made considering the effect of nanomaterials on biochemistry of the living cell. Biochemical regulation of ROS modifying nanomaterials could direct us into manipulating ROS production, transformation and decrement-associated processes in order to achieve therapeutic effect. In this regard, forecasting innate ROS-regulating properties of these nanomaterials is of essence which affect ROS dynamic behavior. ROS chemistry and biology are required to be studied to design new therapeutic protocols by means of novel nano-scale materials; which can be fabricated to aim ROS production/decrement [9].

In addition to cancer, ROS can be employed for a variety of therapeutic purposes including cardiovascular diseases [19] (e.g., myocardial infarction), inflammatory diseases (such as periodontal disease [20]and intestinal inflammation)), brain diseases (such as neuroprotective therapy, PD and treatment and ischemic stroke), bacterial infection and myopia [21, 22].

2 ROS Chemistry

Chemistry of ROS has been studied for more than 50 years. The dawn of ROS chemistry investigations was the time that strong oxidation characteristics of H_2O_2 in Fe^{2+} presence was reported in 1894 (Fenton reaction) [23]. Since the beginning,

chemical properties of ROS have been investigated in different environments; nature, biology and matters. ROS are synthetized in various compartments in the nature with different mechanisms. For instance, in higher altitudes of troposphere, ·OH radicals are produced by photolysis of O_3 gas [24]. Materials can control ROS production by catalytic reactions; these reactions convert external energy to internal energy of ROS' chemical bonds. In 1972, semiconducting TiO_2 was found to be play photocatalyst role in water electrolysis [25]. Further, ·OH-involving processes were recognized in which ·OH was a photocatalyst [26]. The study of ROS generating catalysts is of importance as they can be employed for medical purposes to treat diseases such as cancer [27]. Mechanisms underlying ROS production by means of various materials will be discussed further. ROS are also produced in viable cells in different subcellular sections, especially in mitochondria. Some electrons can escape from mitochondrial respiratory chain, react with O_2 and produce $O_2^{\cdot -}$ (primary ROS) which can be further changed into H_2O_2, ·OH, ClO^-, etc. (secondary ROS) by different catalytic reactions [28]. In some types of cancer cells, ROS are produced in proliferated cell membranes by NADPH oxidase (NOX) complexes activation. Studies have shown NOX oxidase impact on cancer hall marks such as metastasis, cell survival, uncontrolled growth and angiogenesis [29]. Endoplasmic reticulum (ER) is another organelle which produces $H_2O_2$by O_2 oxidation through Flavoenzyme ERO1. This phenomenon causes a tense flux in subcellular level. Some enzymes like xanthine oxidase (XO), lipoxygenases (LOX) and cyclooxygenases (COX) and several metal ions such as Fe^{2+} and Cu^{2+} could participate in catalytic ROS production as well [11]. ROS properties are high instability and therefore high reactivity in liquid media; this results in several reactions such as reduction, oxidation or dismutation. Depending on reaction mechanism, radicals (such as $O_2\cdot^-$ and ·OH) or neuter (such as H_2O_2) oxidant molecules can be produced. Reactivity of these molecules differ from each other. Distinguishing between ROS species, based on oxidative strength is crucial, so we can comprehend the mechanisms better; for instance it enables us to anticipate which kind of ROS species take part in a specific reaction. The oxidizing capabilities of one-electron ROS radicals in a reaction can be evaluated on the basis of one-electron reduction potential as the energy necessary for activation is relatively low [30]. Activation energy is a practical tool to predict a reaction possibility to happen. For instance, in case of ROS-associated reactions, standard activation energy required to convert $O_2\cdot^-$ to H_2O_2 is lower than that of H_2O_2 to ·OH; so, former reaction is more favorable in pH = 7. In comparison, activation energy of neuter molecules of ROS (non-radical ROS) in association with kinetic factors determines their oxidative reactivity where the former is more dominant. Higher activation energy correlates with lower reaction rate [30]. In a biological setting, ROS reactivity establishes which reaction they participate in. ROS intercedes various types of redox reactions with macromolecules, right after their production. ROS can modify biomolecules in a sequence-specific or temporal manner [31, 32]. As the oxidizing strength declines, the power of specific species to discriminate between different reactions declines; so $O_2^{\cdot -}$ or H_2O_2 are capable of targeting specific biological molecules while ·OH and $^1O_2$ are not. Such a preference was first observed in E.coli in which superoxide specific reactivity with Fe-S clusters was identified. Further release of H_2O_2 and

Fe^{2+} is responsible for superoxide mediated toxicity as it leads to ·OH generation by Fenton reaction [1, 33, 34]. Other observation in E.coli provided the mechanism of high reactivity of H_2O_2 with Cys residues of macromolecules to manipulate cellular signaling pathway [35]. $^1O_2$ biochemistry has been rarely investigated as it commonly is produced by exogenous reactions rather than biological reactions. The ROS reactions has been assumed to be conducted in a homogenous media, therefore steric hindrance has not been contemplated and is ignored in above discussion. Moreover, all unit components of an organism such as organelles and cells, and in whole the organism itself are systems which have the following characteristics: heterogeneous, dynamic architecture relating to time and space. As ROS are naturally transitory and reactive, redox reactions take place in the site they are produced and subsequently localized. ROS can barely move farther than the cell diameter, except in the case of H_2O_2 which can move approximately for 1.5 mm [30]. Hence, in biology context, ROS should be compartmentalized considering ROS-involved reactions. Theoretically, some redox reactions may happen but taking time and space restrictions into account, they will not be practically probable in a physiological environment [30]. In physiochemical environment, reaction characteristics that determine ROS biochemical reactions are as follows; reactivity, specificity, and the ability to diffuse. Study on the ROS chemistry can lead us to clearly understand complicated chemical processes and develop tools in order to investigate ROS biology (for instance its role in oxidative stress and pathology).

3 ROS Biology—ROS Modulation to Radiotherapy Efficacy Improvement

Physiological roles of ROS has been a subject of study since 1908 when, for the first time, the role of H_2O_2 was discovered [11, 36]. There are controversial data on the role of ROS as intracellular signaling molecules. ·OH and $^1O_2$ cannot contribute in intracellular signaling by redox pathway as they are localized due to their more relatively transient nature and less ability to travel farther than the site of production. $O_2^{\cdot -}$ cannot penetrate cell membrane while is unstable thus, is not a strong candidate for cell signaling. H_2O_2 can be a potent candidate with the opposite characteristics of above-mentioned molecules along with its high specificity and more capability to travel longer [1]. In 1981, insulin potency for promoting tumor growth was demonstrated; the underlying mechanism was elevating intracellular H_2O_2 level [37]. In 2003, it was observed that ROS production by NOX can facilitate plant growth by further activation of Ca^{2+} channels [38]. Then, it was discovered that H_2O_2 has a regulatory role in cell migration by modulating cytoskeleton structure in which the mechanism was NOX-derived H_2O_2 production [39]. As investigations followed, H_2O_2 concentration gradient in healthy cells near the wound was found to be associated in migration of leukocytes to the injured tissue [40]. Intracellular crosstalk mediated by ROS can help us improve our comprehension about

other areas of science such as circadian cycle and cell biology. In circadian cycle studies, red blood cells (RBCs) has been discovered to have a significant role in circadian regulation by redox reactions of peroxiredoxin proteins in a 24-h cycle which may continue for several days [41]. Despite molecular structure and reaction ambiguity, it is clear that ROS contribute in circadian regulation; it was detected by observing fluctuations of adenosine triphosphate (ATP) and nicotinamide adenine dinucleotide phosphate hydrogen (NADPH) in relation to each other [32]. Phagocytosis mechanism depends on superoxide generation as leucocytse are not able to kill infectious organism without this reactive molecule [42, 43]. As such, glial cells are able to protect CNS from infectious diseases, but higher than necessity production of radicals leads to radical induced damages [44]. ROS role in regulation of cell signaling is accomplished by interacting with signaling molecules thereby, regulating cell processes. In an intracellular cross talk, H_2O_2 mostly targets reactive cysteine residues for reversible oxidization. It is noteworthy that cysteine amino acid is part of a regulation system for numerous physiological events [45].

In brief, ROS regulates signaling pathway by modifying redox state of Cys (Cystein) residues on proteins which leads to function and/or structure alternation of aforementioned proteins. Detailed pathways in which ROS affects signaling are reviewed by Ray et al. [46].

Several enzymes like ribonucleotide reductase and cytochrome 450 use iron for their function. Excess amount of free iron involves in Fenton reaction and develops ROS and causes oxidative stress. Thus, maintaining normal function of cell and prevention of iron induced oxidative stress are owed to iron balance. Iron can express genes which regulate its storage and transportation in post transcriptional level. ROS can regulate iron regulation. Cellular iron hemostasis (IRE–IRP regulatory system) is regulated by both intra cellular iron and ROS to prevent cell from undergoing iron-induced oxidative stress [46].

ROS need to be neutralized to maintain redox homeostasis. That is of importance, as overwhelming antioxidant capacity can lead to pathological events like aging and cancer. So, with regard to their role as intracellular messengers in moderate concentration, ROS production and elimination should be balanced as excessive amounts can cause cell death [47].

Anti-oxidant system retains cell's redox balance. Upon exposure of normal cell to continuous exogenous stimuli and activation of endogenous oncogene, the redox balance fails to be maintained and normal cell turns to a cancer cell. Nascent cancer cell's ROS level should adapt with redox system to survive. High level of ROS and defective antioxidant defense system of cell make it (more than normal cell) susceptible to ROS modulation. While the same concentration of ROS makes cancer cells undergo apoptosis, normal cells can tolerate the condition [48].

Normal cells detoxify themselves from radicals by molecules or enzymatic reaction as shown in Fig. 2:

- Superoxide dismutase: a group of metalloenzymes which convert superoxide to oxygen and hydrogen peroxide and regulate biology processes specifically.

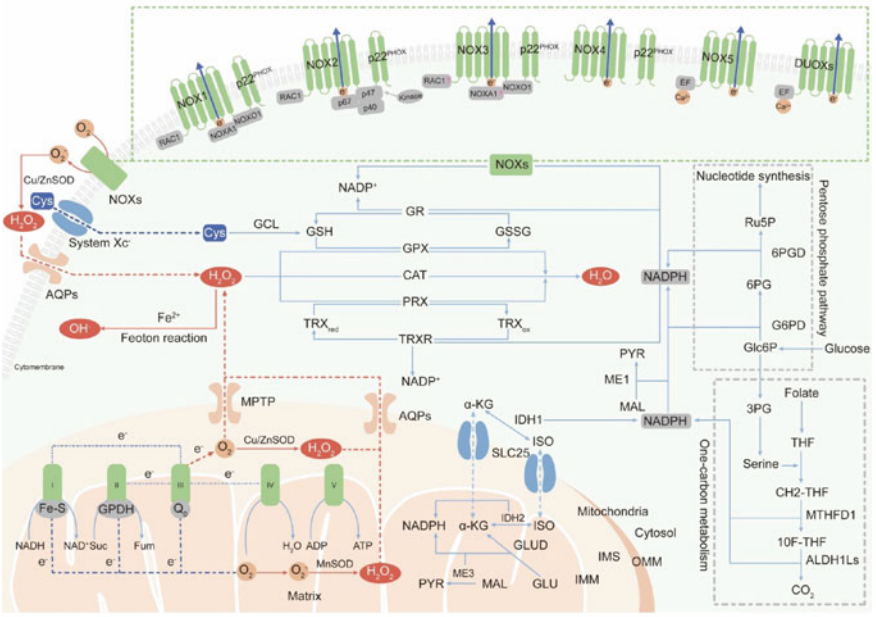

Fig. 2 Intracellular primary ROS generation and elimination mechanisms. Reproduced with permission from Ref. [52], with the permission of the Creative Commons Attribution 4.0 International License (http://creativecommons.org/licenses/by/4.0/). Copyright 2021, Ivyspring

- Catalase, which converts hydrogen peroxide to water and oxygen, and it mostly resides in cytosol and peroxisomes in eukaryotes [49, 50].
- Glutathione system consists of glutathione, glutathione reductase, glutathione peroxidases (GPX) and glutathione S-transferases (GST). Glutathione shields the cell from oxidative stress by transforming disulfide bonds of proteins to cysteine and changes into GSSG (oxidized form) which further is converted to GSH (reduced form) by the involvement of glutathione reductase. Glutathione transferase facilitates the covalent bond construction between S atom of GSH and the electrophile compounds [47, 51].

Investigations have exhibited that aging is a result of oxidative stress which itself is caused by ROS over production [53, 54]. Although ROS production as long as its amount is lower than cell capability to overcome oxidants, seems to elevate lifespan of living creatures; as manifested recently in case of drosophila, low amounts of oxidants leverage its life time [55]. Different levels of ROS lead to different effects:

- Basal level of ROS maintains normal cell hemostasis.
- Continuous and low level of ROS is associated with cell mitosis and elevated gene instability which induces tumor initiation and progression [56].
- Cell cycle arrest (temporary or permanent) and differentiation are related to moderate concentration of ROS [57].

- Macromolecule damage and induced apoptosis, necrosis and ferroptosis are related to acute elevation of ROS concentration [58, 59].

As radiation passes through cells, induced ROS causes unrepairable damage to gene stability and causes death. Of note, cancer cells are not efficient as normal cells to repair radiotherapy-induced damage. Subsequently, killing cells is relatively differential [60]. Many strategies in cancer therapy focused on increasing intracellular ROS level to promote irreversible damage and trigger apoptosis of tumor cells [59]. Regulating intracellular ROS level to efficiently kill cancer cell is a fundamental approach to treat cancer and decrease radiotherapy side effect. Radiation affects cancer prognosis which is dependent on ROS regulation directly or indirectly [59]. Cells can protect themselves from oxidative stress by activation of autophagy program. This is achieved by phosphorylation of proteins involved in cell survival/death/proliferation and DNA repair [61]. Elevated ROS level has been identified in many kinds of cancer cells afterwards, but the correlation between ROS overproduction and its tumorigenesis ability is still controversial. Several factors related to cancer cells and tumor environment facilitate ROS overproduction and influence cellular equilibrium to control radical species. Conversely, some strong evidence propose that raising levels of ROS provokes presence of cancer hallmarks. When provided level of ROS is medium, they involve in pro-oncogenic processes or boost DNA mutation and as a result, assist tumorigenesis [48]. High amounts of ROS are produced in cancer cells from different sources; high metabolism, peroxisome activity and mitochondrial dysfunction, mainly. H_2O_2 is the second messenger as it passes easily from membrane aquaporine-8. Besides, cytokines like IL-1 and growth factors like EGF provoke ROS production in tumor cells. Incidence of several cancers depends on generation of superoxide radical [62–64]. Inflammation has an essential role in progression of tumor [65–67]. Inflammation-activated macrophage produces nitric oxide that converts superoxide to peroxinitrite radical which can contribute to apoptosis of tumor cells similar to hydroxyl radicals. Macrophages and neutrophils stimulate ROS production inside cancer cells and the burst generation of superoxide, which changes into hydrogen peroxide and kills tumor cells [43, 68]. This contradictory role of ROS in cancer cells, in which ROS level is raised and detoxified simultaneously, implies the existing ROS balance inside cancer cells [51]. Redox hemostasis is regulated by oxidative stress sensitive transcription factors which include Nrf2/Keap1 complex (Fig. 3), nuclear factor-κB (NF-κB), p53, and hypoxia inducible factor 1 (HIF-1). After sensing oxidative stress, Nrf2/Keap1 activates downstream antioxidant elements such as glutathione-S-transferases (GST), PRXs, GPXs, and CAT and NAD (P)H: quinone oxidoreductase (NQO1). Other transcription factors rise ROS scavenger enzymes (such as GSH and SOD), inhibit cell death associated factors and activate survival factors (such as B-cell lymphoma-2 (Bcl-2) and myeloid cell leukaemia-1 (Mcl-1)) [47, 69, 70].

Following oxidative stress, ROS regulate specific tumor cell signaling pathways which determine cell fate (Fig. 4).

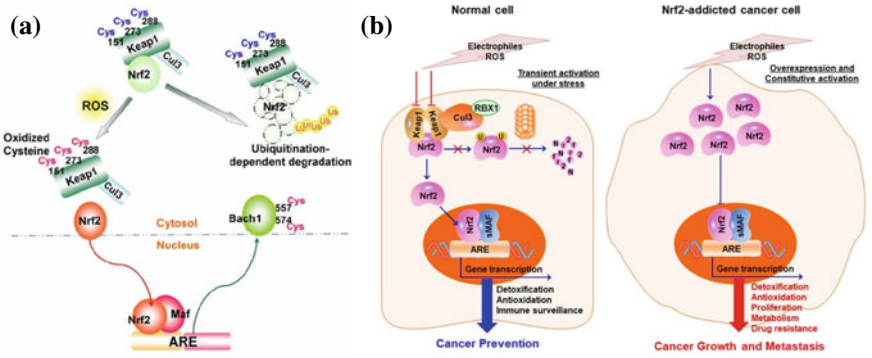

Fig. 3 **a)** Redox regulation of the Nrf2–ARE pathway. Reproduced with permission from Ref. [46]. Copyright 2012, with permission from Elsevier. **b)** Dual roles of Keap1-Nrf2 signaling pathway studied in pancreatic cancer. Reproduced with permission from Ref. [71], with the permission of the Creative Commons Attribution 4.0 International License (http://creativecommons.org/licenses/by/4.0/). Copyright 2019, BMC

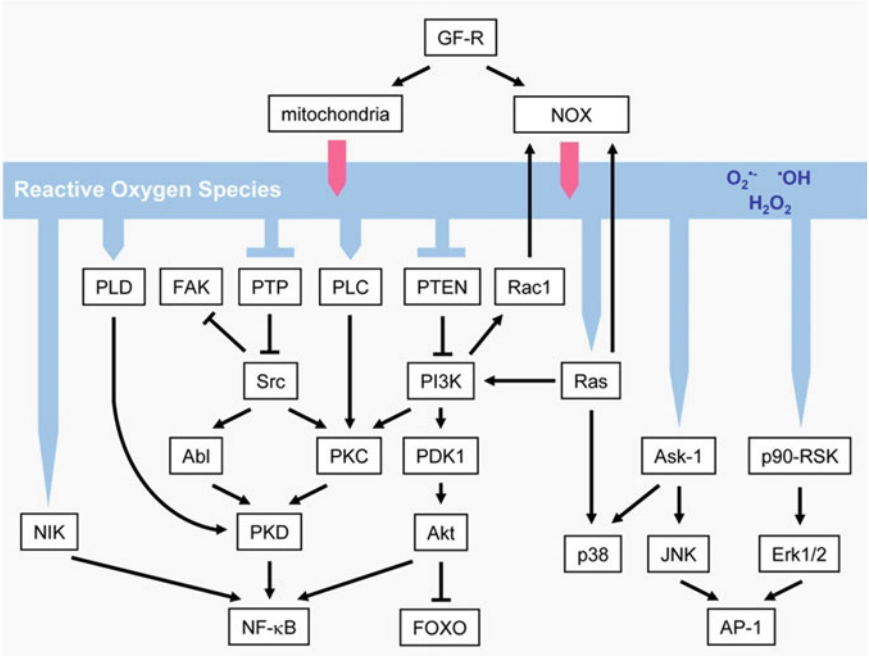

Fig. 4 ROS-mediated cell signaling pathways. Reproduced with permission from Ref. [51]. Copyright 2010, with permission from Taylor and Francis

1. MAPK/Erk 1/2: Activation of this pathway by growth factors leads to cell proliferation. The key role of this pathway activation by ROS increment is well established in proliferation of tumor cells, motility and cell growing without adhesion (anchorage-independent) [72–74]. ROS ability to regulate this pathway is due to their impact on upstream activator/kinases of Erk 1/2 [73, 75]. As demonstrated in ovarian cancer cells, the suppression of negative regulators mediated by elevated endogenous ROS leaded to increased activation of this pathway [73, 75]. ROS effect on cell survival is dependent on cell type and Erk1/2 signaling role, activated by ROS, is evident [73, 75–77]. In breast cancer cell, decreased ROS concentration results in higher apoptosis rate while in human pancreatic and glioma tumor cells, elevated level of ROS concentration is responsible for cell death [78, 79]. MAPK (mitogen-activated protein kinase)- Erk1/2 (extracellular regulated kinase 1/2).
2. PI3K/Akt: PIK3, a key signaling pathway that determines cell survival or proliferation, following hormone secretion, growth factor and cytokine effects, is regulated by ROS (Fig. 5). Cell survival is influenced by phosphorylation of Akt substrates as found in ovarian, breast and human pancreatic cell lines. ROS production activates Akt and upstream kinases including PDK-1 (3′-phosphoinositide-dependent kinase-1) and mTOR which control (increase) Akt activity along with PTEN as a phosphatase (decreased activity) [80–82]. PTEN

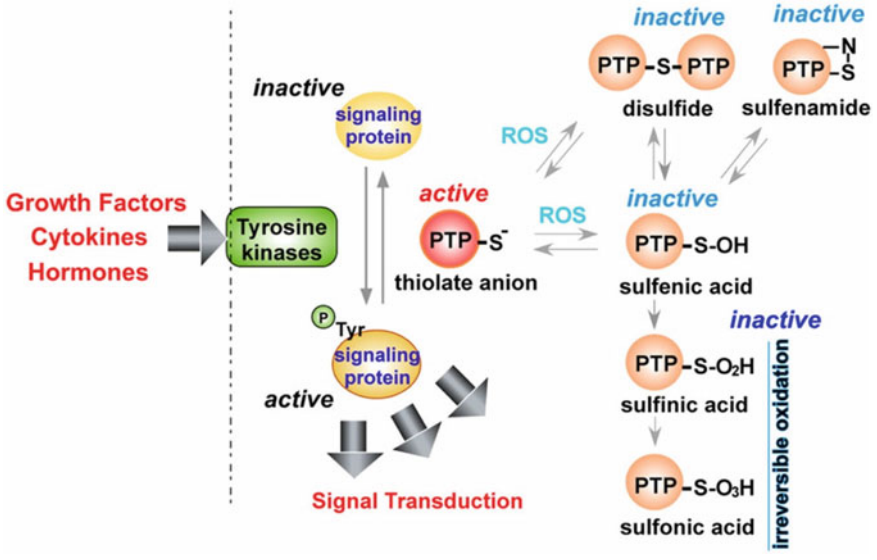

Fig. 5 ROS-mediated protein tyrosine phosphatase inactivation. Protein tyrosine phosphatases (PTP) can reverse phosphorylation; ROS inactivates oxidation of catalytic cysteine residues by PTP, eventually resulting in formation of relatively irreversible sulfinic ($-SO_2H$) or sulfonic acid ($-SO_3H$). Reproduced with permission from Ref. [46]. Copyright 2012, with permission from Elsevier

loss (phosphatase and tensin homolog delete on chromosome 10) leads to constant activation of Akt by enhancing ROS production as well as inducing upstream activating kinases by oxidative stress as basal level of superoxide and H_2O_2 increases due to depleted expression of several antioxidant enzymes including Cu/Zn-SOD and peroxiredoxins.

3. IKK/NF-κB: Increased activity of NF-κB transcription factor following increased cellular oxidative stress and its essential role is discovered in survival, cycle regulation, adhesion and drug resistance of tumor cells [83–86]. Low doses of hydrogen peroxide are able to activate NF-κB (redox-regulation) [87]. Cytokines like TNF-α and IL-1 induce translocation of NF-κB and consequently anti-apoptotic and anti-inflammatory genes will be expressed [88, 89]. As observed in MCF-7 breast cancer (following TNF-α and IL-1ß treatment) and oral squamous carcinoma cells (following SOD silencing), increased ROS concentration and activated NF-κB resulted in cell proliferation and increasing NIK/NF-κB activity, respectively [90, 91].

Specific role of ROS in tumorigenesis and cancer cells are categorized as follows:

1. **Proliferation**: In various cancer cell types, low doses of superoxide and hydrogen peroxide are capable of stimulating cell proliferation [51, 92]. For instance, increased mitochondrial ROS in breast cancer cells, either by estrogen translocation or decreased MnSOD activity and hydrogen peroxide attenuation simultaneously, directs the cell toward proliferation. Therefore, the role of mitochondrial induced tumor growth is well-known [93]. Upregulated level of cyclins' mRNA by ROS indicates that loss of cell redox balance of cell cycle in normal cell like MCF-10A causes abnormal proliferation which can be treated by NAC antioxidant and as a result postpone G1 to S phase progression [94, 95]. As mentioned before, it has been shown that antioxidants can halt proliferation in vivo and in vitro in pancreatic cancer cell line and ATM knocked-out mice, respectively (Fig. 6) [96–98]. Taken together, ROS positively regulate tumor proliferation by modifying crucial proteins that control cell cycle [46].
2. **Cell survival and apoptosis**: Off-balanced intracellular ROS and incremental oxidative stress in mitochondria predispose the process of senescence, cell cycle arrest and apoptosis (including Rac-1/NADPH oxidase pathway) [99, 100]. Chemotherapy, antioxidant deprivation and immune system are capable of inducing of ROS overproduction. Bcl-2 and Bcl-XL have the ability to disaffect ROS-induced apoptosis in the cell [100–102]. Mitochondrial H_2O_2 and NO release eventually, downregulating the production of these two anti-apoptotic proteins [99, 103]. Furthermore, alternation of Bax/Bcl-2 complex conformation dissipates integrity of mitochondrial membrane [104–106]. ROS elevation affects JNK, p38, Ask-1, forkhead transcription factors and p66Shc in the process of apoptosis induction (Fig. 7) [107, 108]. It is hypothesized that continuous oxidative stress status may result in selection of p53 deficient colony of cells which are resistant to apoptosis [51]. ROS production is also induced by death receptors like TNF receptor I, mediating several pathways. Of note, anti-apoptotic signals are also involved after oxidative stress is induced by TNFα.

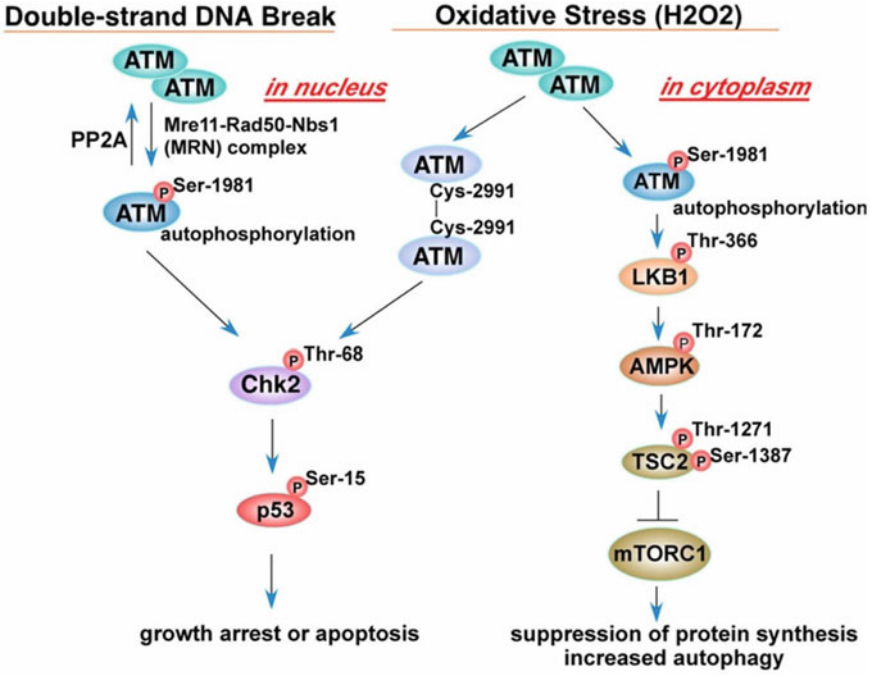

Fig. 6 ATM signaling following oxidative stress and double-strand DNA breaks. Reproduced with permission from Ref. [46]. Copyright 2012, with permission from Elsevier

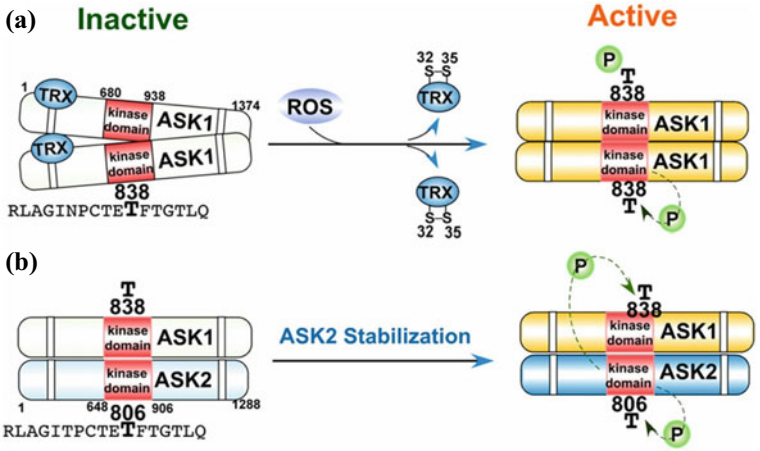

Fig. 7 ASK kinases activation in response to oxidative stress. **a)** Oxidation of thioredoxin (TRX) and its subsequent dissociation. **b)** Hetero-oligomerization of ASK1 and ASK2. Reproduced with permission from Ref. [46]. Copyright 2012, with permission from Elsevier

MnSOD and catalase are expressed after NF-κB pathway involvement [109, 110]. Inconsistently, low levels of oxidative stress and increased generation of mitochondrial ROS develop signaling pathways associated with cell survival and upregulate the generation of antioxidants and anti-apoptotic proteins (such as Akt which is activated by ROS, respectively [51, 111–113]. The elimination of related pathway matters in sensitizing tumor cells to ROS-induced cell death [114–117].

3. **Metastasis**: Higher concentration of intracellular ROS level is detected in metastatic and motile subpopulations of non-or low- motile MCF-7 cell line [118]. Also, a decreased level of MnSOD activity was detected in metastatic breast and highly invasive pancreatic cancer [119–121]. This implies that a crucial part of metastatic process relies on intracellular redox status. Metastatic processes include lower cell adhesion to extracellular matrix, elevated potential for migration and invasion, independency of anchorage for cell survival and eventually intra-vasation. In contrast, mitosis of normal cells require to be anchored to extra cellular matrix (ECM) and similar to tumor cells, mediation of ROS is required; increased mitochondrial ROS increases normal cell adhesion to ECM and proliferation [122, 123]. In the case of a normal cell detaching from ECM, anoikis will be triggered and cell life will be terminated while tumor cells are immune to this effect and are able to form new colonies distant from initial site of tumorigenesis. Tumor cells' independency of anchorage signals to proliferate and terminating apoptosis signals after losing contact with ECM owes most likely to increased level of intracellular ROS generation [124, 125]. Other processes ROS involves in to direct metastasis include epithelial-mesenchymal transition of cell membrane to degrade basal membrane protein composition, DNA damage and instability of genome, actin reorganization and cell shape change, increased cell migration, induction and maintenance of tumorigenic state of cell, ECM degradation and reorganization, losing cell–cell adhesion and probably increased permeability of vasculature. It is noteworthy that mitochondrial ROS are capable of enhancing cancer cell metastasis by contributing to tumor progression [51, 126, 127].
4. **Tumor progression**: As tumor grows, limited oxygen supply happens and activates the transcription of several transcriptional factors including HIF-1 where its expression is suppressed by MnSOD under hypoxic condition [128–130]. This implies the involvement of superoxide and H_2O_2 in the accumulation of HIF-1α [131]. As HIF-1 regulates genes related to glycolysis and halts mitochondrial respiration, tumor cell energy metabolism shifts to anaerobic glycolysis by transactivation of glucose transporter (GLUT-1) and lactate dehydrogenase (LDH). As a consequent of inhibiting mitochondrial activity, H_2O_2 production decreases and the survival rate of oxygen-deprived cells enhances [132]. Thus, tumor cells' metabolism is shifted to anaerobic after oncogenic transformation assuming even normal oxygen supply [130, 133]. Ultimately, this adaption to hypoxia invokes the expression of genes related to metastasis which breeds tumor malignancy and subsequent poor prognosis. Furthermost, HIF-1 prevents intracellular acidic condition (increased formation of lactate and CO_2)

and both molecules favor cell motility with degradation of extra cellular matrix [134, 135].

5. **Angiogenesis**: As tumor grows, oxygen and nutrition need are increases [136, 137]. New blood vessels should develop to accomplish this. Oxygen and nutrition shortage induce expression of intracellular ROS and VEGF (vesicular epithelial growth factor), increasing the intracellular level of ROS [138–141]. Chaotic blood flow in newly formed micro-vasculature assists oxidative stress condition by hypoxia and re-oxygenation fluctuation which augments ROS concentration [142]. ROS elevation provokes angiogenesis with upregulating HIF-1 which initiates gene expression of angiogenesis mediators (growth factors) especially, VEGF [143, 144]. Similarly, intracellular ROS decrease caused by mitochondrial suppressors or glutathione peroxidase decreases HIF-1 induction and VEGF expression in cancer cells [135]. ROS-induced matrix metalloproteinase formation corporates in angiogenesis as well [145]. Additionally, ROS can trigger vasodilation and increases blood supply through heme oxygenase-1 activation leading to formation of CO and NO [146].
6. **Redox status regulation of cancer stem cells (CSC)**: Cancer stem cells are responsible for recurrence initiation of treated tumor with radio- or chemotherapy because CSCs can resist to radiotherapy-induced damage or chemotherapy drugs oppositely to their more mature progeny [147, 148]. Increased HIF-1α inside CSCs causes poor prognosis and radiotherapy resistance. As reviewed earlier, normal cells transform to cancer cells through genome instability, enhanced motility, anchorage independency to grow and oncogenic growth. The level of ROS in CSCs is lower that of in normal cells and more mature tumor cells. This feature of stem cells are due to higher anti-oxidant capacity, anti-apoptotic proteins (such as Bcl-2), DNA repair enzymes and increased expression of ROS scavenging enzymes, especially those involved in glutathione synthesis which induce a moderate level of ROS inside the cell [47, 149]. ROS scavenger depletion leads to lower colony forming ability of CSCs and increased radio sensitivity [149]. By continuous exposure to low level of oxygen, CSCs undergo epithelial to mesenchymal transition (EMT) and make the tumor invasive and metastatic. Ionizing radiation will cause cell death by means of ROS production, but cancer stem cells are immune to this effect due to high anti-oxidant expression [150, 151]. For instance, pharmacological reduction of GSH in epithelial cancer stem cells leads to attenuated growth and enhanced radio sensitization [149]. Characteristics lower DNA damage (double strand and single strand DNA break) in the population (higher the stem cell count, lower the total damage will be) following radiotherapy and the survival chance rises. Due to self-renewal and differentiation capability of CSCs, they are more inclined to form resistant, aggressive and heterogeneous tumors, especially when tumor is not vascularized enough to deliver oxygen [152]. Thus, resistance of stem cells to chemotherapy drugs, which target redox system and elevate intracellular ROS level, may occur. In order to reduce recurrence following conventional treatments, stem cell special redox state should be considered (Fig. 8) [51].

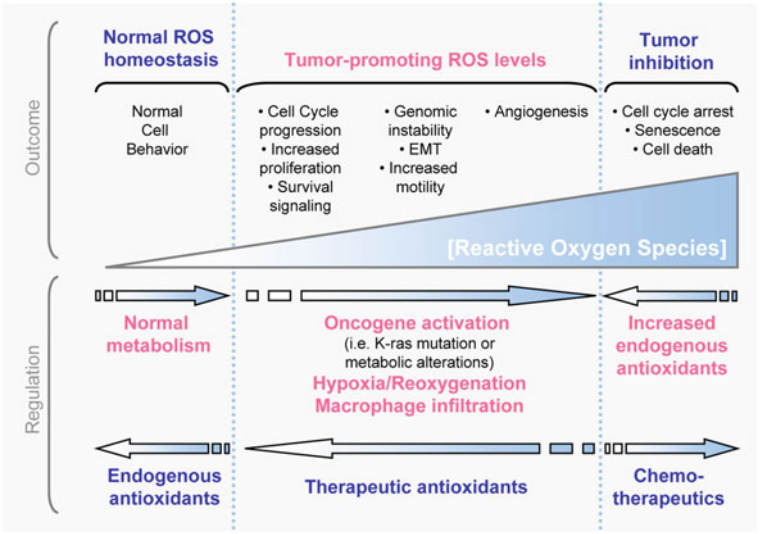

Fig. 8 Cellular ROS regulation and the corresponding response in different ROS levels. Reproduced with permission from Ref. [51]. Copyright 2010, with permission from Taylor and Francis

Oxygen is a crucial enhancer of radiotherapy efficacy for fixing the damage and subsequently killing cancer cell. Increasing oxygen in tumor site is possible by following approaches. Although implementation of hyperbaric oxygen elevates oxygen level directly, in some cases causes complications as well [153, 154]. Also, hydrogen peroxide can be used intra-tumorally and increase oxygen production to boost irradiation efficacy [155]. Hemoglobin level or oxygen binding modification could be another useful approach seemingly beneficial to the patient [156–158]. **DNA damage fixation**, **cell death programing**, CSC features and tumor microenvironment condition significantly impact radiotherapy outcome in which the bold ones are the most influenced by cell redox condition.

ROS balance can be altered in favor of cancer therapy by affecting involving pathways (Figs. 9 and 10). These pathways can precede to initiate cell apoptosis and autophagy. This phenomenon results in altering ROS balance in favor of apoptosis and consequently killing the cancer cell. Other pathways can affect inflammation responses and iron hemostasis in cancer therapy. Changing ROS concentration, production and elimination should be carried out by xenobiotics and materials implementation. Next section will focus on nanomaterials which are promising tools for ROS production/elimination interventions.

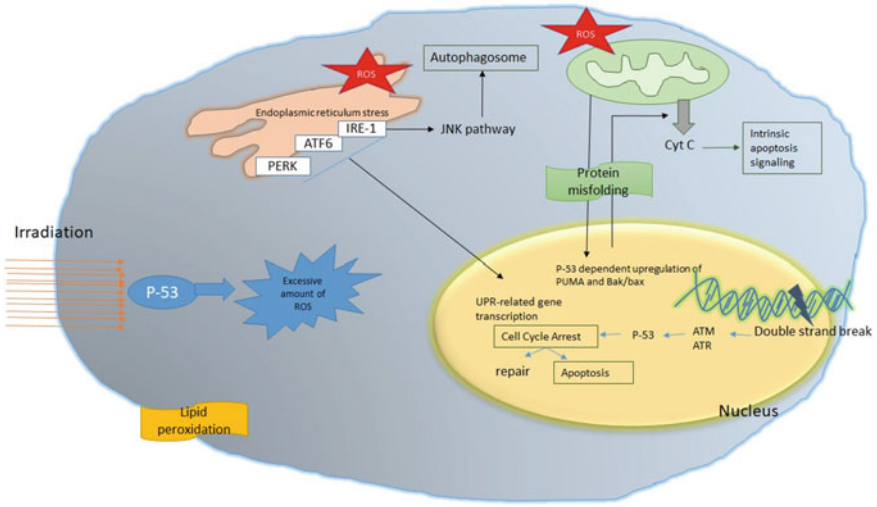

Fig. 9 ROS-induced events following irradiation

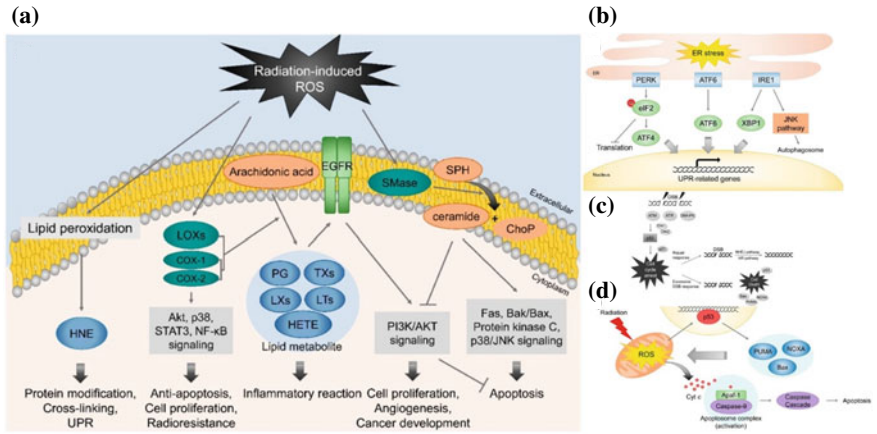

Fig. 10 Detailed cell responses to radiation. **a** lipid peroxidation and ceramide signaling, **b** ER stress, **c** Double strand break and **d** Mitochondrial response induced by radiation. Reproduced with permission from Ref. [159] with the permission of the Creative Commons Attribution 4.0 International License (http://creativecommons.org/licenses/by/4.0/). Copyright 2019, MDPI

4 ROS Nanotechnology

Various underlying pathological mechanisms are connected to ROS generation more than cell capacity to handle. In recent era, numerous nanomaterials have been synthesized that can be both multifunctional and ROS-regulating at the same time, owing to nanotechnology. The utilization of functional nanomaterials has been widely

expanded over the past few years [160–166]. Nanomaterials are capable of affecting biology of cell by generation, transition or depletion of ROS levels; thereby they can apply their therapeutic effects by regulating cellular redox hemostasis. Thus, ROS regulating nanomaterials can be counted as therapeutic modalities with unique chemistry to intervene pathological abnormalities [2].

Temporo-spatial characteristics of nanomaterials are determined by two innate features: Biophysics and biomedical features.

- Biophysical features include thermodynamics, 2D surface topography, 3D stereoscopic geometry etc.
- Biochemical features include interfacial reactivity, enzymatic interaction etc.
- ROS research in nanotechnology should consider nanomaterials' chemistry (ROS production, transition and depletion) and biology (bioavailability, biodegradability, and biocompatibility) (Fig. 11).

There are two different methods for nanomaterial synthesis: Top-down (making bulk materials smaller to reach a nanoscale) and bottom-top (reaching nanoscale from atoms' angstrom scale dimension). These two methods make it possible to synthesize nanomaterials with distinct dimensions.

Dimensions of nanomaterial	Nanomaterial specific name
0	Nanoparticle
1	Nanowires
2	Nanosheets
3	Nanoformulations

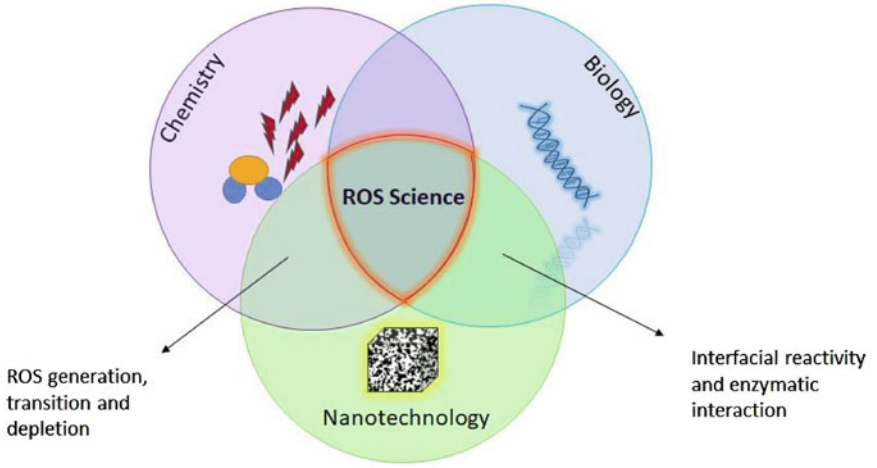

Fig. 11 Nanotechnology interface with biology and chemistry

Why nano-scale? Not micro? For designing ROS-based therapeutic agents, size impact and surface area to volume ratio are of importance.

$$\text{Surface Area (SA)/Volume} = \text{Specific SA}$$

Nanomaterials are equipped with unique features because of their nanoscale size. For instance, for inorganic nanoparticles, when the size is less than 20–30 nm, crystallographic properties regulate kinetics of interfacial reactions including kinetics of ROS reactions which occur at the surface of nanoparticles [167]. With nanotechnology, large specific surface area (SA) and small volume are useful features that come in the territory. Large specific surface area creates plenty of anchoring sites available for ambient reactive species which improves the chemical reactivity. In addition, small volume provides easier tissue penetration and cellular uptake and possibility of intracellular transportation of these nanosystems. As investigated before, size of ROS based nanomaterials determines their physiochemical role and consequently regulates biological responses [168]. To acquire the best ROS-regulating properties and also achieving better in vivo therapeutic effect, extrinsic (e.g. particle size, volume and specific SA) and intrinsic factors (physiochemical features) concerning nanomaterial performance should be considered given that nanomaterials have acquired magnificent in vivo ROS regulating behavior for therapeutic applications due to aforementioned characteristics. We will discuss nanomaterial modulation from the chemical and biological perspectives.

In chemical view, due to recent advancements, reaction characteristics of nanomaterials can be modulated feasibly. This can be achieved by:

- Precise topographic modulation by increasing quantity of localized action sites on nanomaterial surface
- Combining nanomaterials with other functional materials; this integration enhances nanoparticle activity, selectivity and versatility in biological systems.

Developing ROS based nanomaterials with ROS generating/scavenging ability effectively modulates reactions to further benefit therapeutic results. As an example, heterogeneous nanocomposite catalysts can intervene effectively in cancer therapy by in situ ROS production through catalytic enzymatic reactions [169, 170]. In biological view, comprehending systematic effect of the materials is mandatory. Due to nanomaterials' large SA, strong adsorption of biomolecules such as DNA, proteins and phospholipids occurs to stabilize surface area by attenuating excessive surface energy [171]. These interactions can affect how the cell and the nanoparticle affect each other which further influence how cellular substructure and cellular biochemistry can change [172]. Thus, in ROS research field, nanomaterial's biological systematic effect should be examined to achieve a better therapeutic result. Taking TiO_2 as an example, it was revealed that size determines physiochemical properties, ROS-induced toxicity, shape, efficacy and subsequently its biological effect, as studied theoretically [173]. In this context, quantitative optimal parameters should be considered to be evaluated extensively along with nanomedicine efficacy evaluation.

In a unique pathological region, investigating nanotechnology and biology interaction may enhance the outcome of ROS-based nano-therapeutics significantly. For instance, pores of tumor blood vessels enhances nanomedicine delivery of smaller nanoparticles (~12 nm). Notably, hydrodynamic diameter and steric hindrance are responsible for difficult entrance of larger nanoparticles (125 nm) into tumors [172]. Thus, for treating cancer, nanomaterials should be designed small enough to acquire the capability of transportation (within vessels), accumulation (inside the tumor) and excretion (from kidney) [174]. To achieve improved ROS-regulating efficacy and enhanced therapeutic outcome, integrating chemistry and biology at nanoscale is essential for designing ROS-based nanomedicines.

In cancer treatment, ROS-based nanoplatforms can push forward redox regulating therapeutic modalities such as RT [2].

(1) **ROS-based nanomaterial chemistry**: It is essential to elucidate nanomaterial chemistry to determine biological behavior and in vivo chemical features. Unique chemical characteristics of representative materials that involve in cell redox status will be overviewed (such as nanozyms, photosensitizers, radiosensitizers). In this context, utilizing ROS detectors as developing tools can improve our understanding of chemistry of nanomaterials in which provided biomedical assays respond quantitatively to ROS level changes [175, 176].

1.1. **ROS-generating nanomaterials**: Excessive ROS generation in tumor is considered a general therapeutic approach in which intracellular redox status upregulation occurs by exo-/endogenous interventions [48]. ROS-generating nanosystems utilize their intrinsic chemistry to extract and transit energy of exogenous sources into ROS internal chemical energy. Similar to radiotherapy, which employs ionizing radiation, photodynamic (PDT), sonodynamic (SDT) and chemodynamic therapy (CDT) employ optical, mechanical and chemical energies, respectively, to evoke remote-controlled ROS generation in site of pathology.

1.2. ROS-scavenging nanomaterials: Various materials have enzyme mimicking activity (such as SOD-CAT). These nanoenzymes down-regulate deviant amount of ROS to level which is compatible with cell function [177]. Fullerene derivatives are counted as a great achievement in nanozyms. They behave like SOD and electrostatically stabilize superoxide with their electron deficient regions. Fullerene derivatives are extensively exploited as antioxidants due to their unique ROS detoxifying capability [178]. Next eye catching improvement in nanozyme field was discovering SOD and CAT mimicking activity of inorganic nanomaterials, such as CeO_2 nanoparticles [179–181]. Mixed valance state of cerium (Ce^{3+} and Ce^{4+}) and presence of spare oxygen vacancies are the reasons behind CeO_2 nanoparticle capability of efficiently scavenging superoxide and H_2O_2 [182, 183]. Thus, it is clear that cerium nanoparticle has a vital role in radiation protection, despite their role in cancer cell sensitization to RT [184, 185]. Next generation of ROS

scavengers are inorganic nanomaterials with intrinsic catalytic activity such as Pt, NiO and Prussian blue (PB) nanoparticles [186–188].

(2) **ROS-based cancer therapy-nanomaterials**: Cancer cell retains its high reproducibility by activating potent endogenous antioxidant defense system equal to induced oxidative damage. In new steady state of cancer cell redox hemostasis with upregulated antioxidant and ROS level, total ROS concentration is remained below toxic level. This mechanism of adaption to new redox status makes the cell resistant to excessive ROS-induced toxicity and the cell can escape from high oxidative stress damages [47]. Therefore, if oxidative stress is further intensified, endogenous antioxidant system cannot maintain cellular redox hemostasis and cancer cell becomes much more vulnerable. Thus, to disrupt cancer cell redox adaption, ROS-generating nanomedicine can overwhelm cell antioxidant system by excessive ROS production, beyond cell tolerance. This highly qualified and feasible approach for cancer therapy is based on cancer redox biology and employed ROS-based nanomaterials. Another complementary and feasible approach is exploiting elevated intracellular ROS level to activate ROS-sensitive nanomaterials for releasing drug, on site of neoplasm. On-demand drug release can be considered beside aforementioned approaches [2]. Oxidative stress and aerobic glycolysis are two main characteristics of cancer cell that can be utilized for designing therapeutic strategies [47].

(3) **Radiotherapy efficacy enhancement**

3.1. **Radiotherapy physiochemical basis**: RT, as a mainstream therapeutic modality for cancer, utilizes ionizing radiation to suppress tumor progression by causing water ionization and subsequently elevating ROS level [189–191]. The source of radiation can be external (such as high-energy X-ray which radiates on pathological site), or internal (such as sources from radioisotopes like ^{131}I, that are already located in pathological site by systematic administration and on-site tumor accumulation) [192]. These two techniques are named External Beam Radiotherapy (EBRT) and Internal Radioisotope Therapy (IRT), respectively. Nevertheless, EBRT is the most common RT (which is discussed here assuming X-ray is used), and IRT is the competent therapeutic way for metastatic tumors [193]. Considering high energy X-ray is the most commonly used radiation for RT, specific physical processes during nanomaterial and X-ray interaction lead to Auger electron, Compton electron and photoelectron generation which react with surrounding H_2O and produce ROS to induce cell death. Although X-ray therapeutic efficacy is compromised because of low mass energy absorption coefficient (LEAC) of tumors, increased dose leads to serious side effects [191, 194]. ROS-based nanomaterials enhance therapeutic result of X-ray-based RT which will be discussed further along with existing approaches.

3.2. **Tumor Radiosensitization**: Lack of oxygen in tumor cells necessitates means to fix the damage. Radiosensitizers can fix radiotherapy-induced damage and by lowering required radiotherapy dosage, thereby minimizing potential side effects. Radiosensitizers enhance intratumoral ROS generation under X-ray irradiation and improve RT efficacy. Organic molecules like porphyrins are known as radiosensetizers, but their main drawback is rapid degradation and wide distribution which ends up with limited therapeutic outcomes [195]. That is where nanotechnology can propose strategies to modify material properties. The mechanisms involved in boosting tumor radiotherapy by radiosensitizers include:

1. Reducing intracellular radioprotectors-enhancing biomolecular damage fixation
2. Cytotoxic material production subsequent to radiosensitizer radiolysis to free radicals (preferentially in hypoxic cells)
3. Inhibition of biomolecular damage repair-suppressing cellular radioprotectors and oxidoreductases
4. Incorporation of thymine analogs into DNA strand
5. Mimics of oxygen
6. Chemicals modulating vital pathways; Apoptosis, DNA repair, metastasis and protein degradation [196].

Radiosensitizers might involve in production of ROS and affect subsequent signaling pathways. Considerably, specific chemical radiosensitizers are capable of regulating important cellular pathways which can boost RT impact on tumor cells. Nano radio sensitizers in some cases are able to elevate ROS production through various mechanisms. Nanoscale radiosensitizers are divided into two categories based on chemical and action nature:

1. Containing high Z (atomic number) elements: these materials attenuate X-ray strongly and focus the energy inside the tumor cell.
2. NO-generators: when requested, they release NO (radiosensitizer) in response to X-ray exposure [196].

Energy conversion of X-ray after interaction with nanomaterial is attributed to the Z of atoms which nanomaterial is composed of. With increased Z, capacity of photoelectric absorbtion and electron ejection (Auger and photoelectron) is intensified and ROS generation is enhanced which is followed by improved RT outcome. Efficient inorganic nanoradiosensitizers including Au, Bi_2Se_3, TaO_x, W-based materials, Hf^{4+} containing MOF and UCNPs, can serve radiotherapy by focusing ionizing radiation energy [197–202]. For instance, ultrathin Bi_2Se_3 nanosheets (2 nm by 30 nm) decorated with RGD peptide and chitosan, were evaluated as a strong theranostic agent and it exhibited high stability and enhanced HELA cells sensitivity to RT. RGD was used as targeting agent and the nanosheet could inhibit TrXR activity and activate ROS-ralated signaling pathway. Further, release of Si could reduce liver, lung and

prostate cancer occurrence. Considering Bi_2O_3-coated mesoporous silica nanoparticle (BMSN) conjugation with radiotherapy, tumor growth was suppressed tremendously in comparison to radiotherapy alone. Notably, this pH-responsive nanoparticle could encapsulate high load of doxorubicin and develop a significant therapeutic consequence against multi drug resistant cancer cells versus using doxorubicin alone. Thus, BMSN is considered a multifunctional nanosystem with high efficiency for tumor eradication in simultaneous chemo- and radio-therapy [198]. Controlled drug release and RT can synergistically develop this enhanced therapeutic outcome against multi drug resistant cancer cells, showing that RT plays a complementary role for conventional chemotherapy in removing therapy limitations. To overcome radioresistance which is responsible for treatment failure, Gd-containing polyoxometalates-conjugated chitosan nanosphere (GdW10@CS) with HIF-1α siRNA (to prevent DNA damage reconstruction) was fabricated for tumor hypoxia attenuation and response induction. The significant radiosensitization of hypoxic tumor due to high atomic number of Gd and W elements, W6+-mediated GSH oxidization and as a result sufficient level of ROS production was observed [200]. X-ray energy transfers to nanomaterial containing high Z atoms and then to semiconductor. Ejected electron from nanomaterial can interact with adjacent semiconductors (at the interface) as well as surrounding tissue. This interaction facile hole and electron motility and consequently electron generation to amplify ROS production efficiency. Enhancing RT outcome is possible by coupling nanomaterials (containing high Z atoms) and nano semiconductors. Au@TiO_2 anisotropic nanostructure was first proposed for radiosensetization and the synergistic therapeutic outcome in contrast to other Au nanoparticles suggested the coupling at the interface, the main reason. Tumor model depicted suppression in growth and survival improvement. High energy electrons emitted from Au, generate ROS inside the cancer cell and low-energy electrons are responsible for electric coupling and further ROS generation [197]. The most important gasotransmitter with several pathophysiological functions, NO, is another important tumor radiosensetizer in high levels which efficiently generate ROS and react to produce peroxynitrite (ONOO–) that is a biocide and highly reactive molecule [203]. X-ray-responsive NO-releasing nanosystems can kill cancer cells directly in synergistic therapy when demanded. On-demand release of NO of these nanosystems provide less side effects, and enhanced RT outcome. In 2015, X-ray responsive nano theranostic system (PEG-USMSs-SNO) was architected to release NO in a dose-controlled manner in response to X-ray irrediation after breaking the bond S–N (even in RT of deep solid tumors) [204]. Previously in 2008, nitrite was proven to be converted to bioactive NO under specific condition in tumor cell [205]. Then in 2017, remotely triggering NO release from nitro imidazole (nitro imidazole-Au-CPP-PEG NP) upon responding to exogenous stimuli (X-ray) proved to enhance hypoxic cancer cell sensitivity, in vitro [206]. These nanosystems are highly desirable for enhancing RT efficacy.

3.3. **Tumor Microenvironment (TME) Modulation**

Radioresistance is a great clinical concern for radiotherapy of solid tumors with hypoxic nature. Under hypoxic condition, thiol compounds neutralize produced DNA

radical and prevent its cytotoxic effect and cell apoptosis. Furthermore, VEGF expression induced by HIF-1 activation (Hypoxia hallmark) compensates for its pleiotropic effect on tumor cell and cell apoptosis which is not desired in RT. Thus, TME should be re-oxygenated to conquer hypoxic-induced radioresistance [128]. Three categories of nanosystems are synthetized to attenuate hypoxic condition of tumors:

i) O_2 generating nanomaterials: These nanosystems convert endogenous H_2O_2 of tumor cell to O_2 and reduce hypoxia. Nanoshells of CAT-loaded TaO_x enhances RT therapeutic effect as this bioreactor can focus radiation energy inside the cell by high atomic number of Ta, CAT can generate O_2 and attenuate hypoxia, and mesoporous architecture guarantees high level of enzyme activity [128]. MnO_2 nanoparticles like albumin coated MnO_2 nanoparticles react with H_2O_2 and H^+ which consequently produce O_2 (by 45%) and increase cell pH. This nanosystem has considered hypoxia, ROS production and low pH interplay effect on outcome of treatment with considering Mn reactivity for peroxide and downregulation of two major factors in cancer progression, HIF-1alpha and VEGF expression. RT and nanoparticle combination therapy inhibited the growth of breast tumor, increased dsDNA breakage and cancer cell death compared to radiotherapy alone [207]. Notably, complete HIF-1 degradation which is dependent on O_2, is possible by re-oxygenation and remaining HIF-1 function inhibition (by acriflavine or other hydrophilic cationic drugs) simultaneously. HIF inhibitor@MnO_2 ROS-responsive nano materials release Mn^{2+} from MnO_2 for MRI and activate tumor immune response (T-cell) which leads to efficient inhibit the tumor growth. The risk of metastasis is lowered when VEGF and MMP-9 expressions are decreased [208]. Further, Au@MnO_2 core–shell nanoparticle with PEG coating was developed. Au, in the core, interacted with X-ray to produce charged particles (radiosensitizer) and MnO_2, in the shell, reacted with H_2O_2 to reduce hypoxia-associated radioresistance. The nanoparticle could effectively radiosensitize hypoxic cancer cell to RT in vitro and in vitro with no obvious side effect [209].

ii) O_2 Delivering Nanomaterial: High capacity of these nanosystems for oxygen loading modulates TME. Nanosystems have used oxygen transporters such as perfluorocarbon (PFC) (commonly used as artificial blood), hemoglobin and oxygen microbubbles. Erythrocyte membrane-PFC@PLGA (PFC is located in the core) nanoparticle plays the role as artificial RBC and transfers oxygen to tumor site while the RBC coating membrane increases blood circulation time. Nanoscale size of these nanoparticles enables them to penetrate into tumor tissue properly, in contrast to natural micro-scaled RBCs, and greatly compensates for tumor hypoxia after intravenous injection to refine RT efficacy. In addition to RT, this nanosystem can potentially improve therapeutic outcome of other modalities such as PDT and SDT while the radioresistance is due to tumor hypoxia [210]. Oxygen delivery with hemoglobin or oxygen micro-bubble nanocomposites are comparable with PFC-containing nanomaterials in modulating TME and improving RT. Hemoglobin containing liposome (10 ml/kg) administered in mice 30 min before radiation lowered HIF-1α

accumulation in treated tumor and enhanced RT efficacy [211]. Independent of hemoglobin transport, oxygen was delivered to not-vascularized regions of solid tumor by ultrasound-sensitive oxygen loaded microbubbles, tripling radiosensitization when administered immediately before RT exposure [212].

iii) Photothermal therapy (PTT) + Radiotherapy (RT): As blood flow increases, oxygen delivery rises. Photothermal agents, in response to light, produce mild heat which leads to higher blood flow and higher intratumoral O_2 level to vanquish radioresistance and sensitize the tumor. For instance, 2D MoS_2-Bi_2S_3 nanosheet was synthesized for RT/PTT synergistic therapy and tumor eradication. MnO_2 nanosheet, a famous transition metal dichalcogenide (TMD), performs its role in PTT and Bi_2O_3 role is radiosensitizing due to extensive ability to attenuate X-ray. This theranostic nanosystem is also suitable for tumor imaging (photo-acoustic and computed tomography) and diagnosis [213]. Above discussion declared the role of nanosystems in ameliorating radioresistance caused by hypoxia.

3.4. **Normal tissue radioprotection**

Unfavorable RT side effects including activity alternation of apoptotic proteins, mitosis inhibition, mitochondria dysfunction and cell hemostasis dysregulation, are the results of unavoidable ROS production in adjacent healthy cells [184]. Although cellular antioxidant system defends against oxidative stress, the counterbalance is not successful to encounter all radiation-induced cell damages. Consequently, side effects such as vomiting, nausea and hair loss can occur which emphasize the urgency of considering applicable strategies for radioprotection. Diverse science of nanotechnology proposes three categories of efficient radioprotective nanoplatforms:

1. **Inorganic nano enzymes**

   CeO_2 nanoparticles with enzyme mimicking (SOD, CAT and oxidase) activity scavenge excessive ROS sequentially (superoxide to H_2O_2 to H_2O) by reverse binding to oxygen atoms in the molecules and alternating between reduced (3+) and oxidized (4+) form of Ce [181, 214, 215]. Its unique anti-oxidative feature has been investigated intensely in radioprotection. In 2005, radioprotective effect of vacancy-engineered CeO_2 nanoparticles on normal human breast cell was examined (99% protection) while no protection was seen on MCF-7 cell line, probably due to transmembrane pH difference [216]. This feature is beneficial because it does not compromise RT outcome as it depends on high ROS level while radioprotectors decline ROS concentration. Radioprotection of CeO_2 nanoparticles over normal gastrointestinal epithelium and lung fibroblast cells was further demonstrated [184, 217].

2. **Inorganic electro-catalysts**

   Inorganic nanomaterials with ROS scavenging properties reduce oxygen efficiently, and that are used for excessive ROS depletion in RT. Cys-MoS_2 quantum dots (below 5 nm in size) reported to exhibit radioprotection by increasing

survival percentage, cell viability and DNA recovery with striking properties including low toxicity, effective clearance from kidney and their role as radical scavenger which could be credited to excellent H_2O_2 reduction (electrocatalytic properties) and enabling electron transfer. High renal excretion (80%) after 24 h of administration and biocompatibility of these dots, make them appropriate for radioprotection applications [218]. WS_2 quantum dots presented DNA and hematopoietic system protection by neutralizing overproduced ROS and exhibited high renal clearance (80% in 24 h) due to their ultra-small size, resembling MoS_2 dots. Blue photo luminescent properties and scavenging ROS from whole biological system are other considerable advantages of these dots .With decreased size, extraordinary catalytic properties of these quantum dots make them favorable for medical purposes [219]. PVP-protected PtPdRh hollow nanocubes adsorb ROS in low energy active sites of pores and reduce oxygen in vivo. This modified electronic structure with catalytic activity and hollow structure bestow large surface area and more reachable active sites on H_2O_2 compared to solid counterparts. Galvanic replacement of Pt lattice with Rh and Pd leaded to synthesis of Pt-based alloys with better catalytic characteristics. This tertiary alloy breaks superoxide bond on the surface and produce oxygen through radioprotection. Bone marrow cells containing nucleus showed increased SOD activity, lowered DNA damage and malondialdehyde (MDA) level which indicates Pt-based alloys mimic SOD, CAT and peroxidase activity [220]. More catalysts with Oxygen Reduction Reaction (ORR) are expected to be in the pipeline for protection against RT-induced oxidative damage.

3. **Organic nanomaterials**

As biodegradable ROS scavengers' representative, melanin nanoparticle has a pleiotropic effect in neutralizing excessive ROS. Combination of physical (shielding) and chemical (scavenging) properties of melanin are responsible for its effects as first realized that melanized fungal response to high dose of radiation was enhanced growth [221]. A generated Compton recoil electron slowly loses energy while passing through melanin, until it reaches a low enough energy that it can be trapped by stable free radicals of the pigment. Controlled dissipation of high-energy recoil electrons by melanin inhibits secondary ionizations and the generation of damaging free radical species [222]. Treatment of Balb/C mice with melanin nanoparticles pre- or post- irradiation provided protection to hematopoietic tissues and enhanced the survival (40% in post radiation treatment) [223]. Considering double sword edge effect of ROS, radioprotector overdose may result in attenuation of RT outcome by encountering excessive ROS cell toxicity in tumor cells. Therefore, investigations on involved mechanisms are still necessary. Wise inspection of discussed strategies—**radio protection/sensitization and TME modulation**—is of importance to develop conventional RT further and overcome limitations of this therapeutic modality in clinic.

5 RT Synergic Therapy

Tumor cell diversity and complexity make it laborious to contend with cancer, despite development of redox-based modalities (RT, PDT, CDT, CDR, and SDT) which may still not be capable of reaching considered therapeutic goal when applied alone due to probable existence of specific resistant cancer cell subpopulations. The shift from monotherapy to multiple modality synergic therapy is the current approach for improving treatment outcome [224]. Coalescence of strategies based on nanomaterials and their responsiveness to stimulus should be designed to improve the synergistic therapeutic effect of monotherapies such as RT, PDT and immunotherapy. Ineffective treatment of solid hypoxic tumors and distant metastasis from tumor location hinder broader RT application. The solution to this obstacles is application of nanotechnology in integrating RT with other therapeutic modalities for alleviating side effects while enhancing efficacy. Three strategies in synergic therapy with RT are considered:

i) RT+ Chemotherapy: To surmount radioresistant malignancies and improve cancer therapeutic efficacy, chemotherapy was implemented besides RT. By inhibiting DNA damage repair and changing cell phenotype from radioresistant to radiosensitive, chemotherapy collaboration with RT has been estimated to improve cancer therapy significantly. Cisplatin-loaded UCNP@SiO_2 nanoparticles (up-converting core and porous silica shell) were employed for RT + chemo/synergic therapy in which cisplatin plays two roles, a radio sensitizer and a chemotherapeutic drug. In vivo experiment on Balb/C nude mice bearing HeLa tumor demonstrated a higher therapeutic effect when this rattle-structured nanotheranostic system was utilized besides RT rather than employing one therapeutic strategy. UCNP favors dual (magnetic—luminescent) mode imaging in addition to delivering cisplatin which is more effective than cisplatin alone as radiosensitizer [225]. Hollow TaO_x (tantalum oxide)-based theranostic platform was designed to deliver chemotherapeutic drug and enhance RT effect simoultanously. 7-ethyl-10-hydroxy-camptothecin (SN38) was efficiently loaded in mesoporous shell and large cavities of its hollow structure, and Ta with high atomic number was used to attenuate X-ray radiation. PEG-modified TaO_x nanoshells by intrinsic binding tendency with metal ions upon mixing qualify for single photon emission computed tomography (PET) imaging and magnetic resonance imaging (MRI) which enable locating the tumor and tracking its distribution in biosystems. With SN38 inducing cell cycle arrest into a radiosensitive phase, and Ta depositing X-ray energy inside the tumor cell, this nanocomposite (TaOx-PEG@SN-38) unveiled synergistic therapeutic effect, in vivo and in vitro [199]. Thus, chemo/RT corporation can improve cancer therapeutic efficacy as shown by mitomycin C-SiO_2@UCNP nanotheranostic system design

which could efficiently treat multi drug resistance cancer cell efficiently both in vivo and in vitro [226].

Recently, nitrosylated tubulin targeted DM-1 loaded in PLGA-b-PEG nanoparticles showed enhanced drug delivery to tumor via increased permeability and retention effect. By increased oxidative stress as a result of tumor irradiation, S-N bond cleavage occurs which leads to the release of NO and DM-1. DM-1 inhibits cell polymerization of microtubules and arrests the cell cycle at G2/M which is relatively more radiosensitive, and simultaneously NO forms toxic radicals which both contribute in tumor suppression. Synergistically enhanced RT outcome in head and neck cancer was confirmed by in vivo and in vitro experiments (H1299 tumor-bearing mouse and clonogenic assay). The promising results of DM1-NO PLGA nanoparticles demonstrated enhanced RT outcome for NSCLC (non-small cell lung cancer) and potentially other types of cancer. It is noteworthy that DM-1 toxicity was suppressed by nitrosylation and encapsulation [227].

ii) RT + PTT: To diminish hypoxia-induced radioresistance by modulation of tumor environment, mild hyperthermia can be induced during PTT which boosts blood flow of tumor tissue and consequently mitigates hypoxia. For instance, PVP-Bi_2Se_3@selenocysteine nanotheranostic system was proposed for enhancing RT therapeutic outcome and shielding healthy tissue from radiation by enhanced generation of ROS and high capability of absorbing NIR laser beam. Bi_2Se_3 strongly absorbed and performed photothermal conversion and subsequently modulated hypoxia and provided a complementary effect during RT. No considerable in vivo or in vitro toxicity was observed, demonstrating its high biocompatibility. In vivo release of selenium to the blood flow protects whole body from irradiation and enhance immune responses [228]. Another proposed nanotheranostic system with the same mechanism of action used CuS-modified mesoporous organosilica nanoparticles to specifically deliver O_2-saturated perfluoropentane (PFC) to tumor site which is gasified by hyperthermia, which was induced by NIR laser. Also, this nanotheranostic system was ^{64}Cu-labeled which enabled multimodality imaging of tumor while oxygenating the area to increase radiosensitivity [229]. In the recent decade, enormous investigations have been performed on nanosystems with capability of simultaneous X-ray attenuation and photothermal conversion. First, a core/satellite theranostic platform based on silica@UCNP decorated with CuS ultra-small nanoparticles was synthetized to absorb NIR energy and transform it to local heat (by photothermal feature of CuS) and to enhance the radiation dose around nanoparticles to radiosensitize the tumor cell (by high Z elements such as Gd, Er and Yb in UCNP). The synergistic effect of combining PTT and RT was confirmed when administered intratumorally, and a distinct therapeutic effect was observed when administered intravenously. Eradication of tumor was observed within 120 days by integrating PTT and enhanced RT in this

powerful and biodegradable platform [202]. MnSe@Bi_2O_3 core/shell was fabricated to overcome RT resistance by combining RT/PTT and implementing a synergistic effect. Bi_2O_3 is capable of absorbing X-ray strongly and concentrate its energy locally while NIR-triggered PTT favors hypoxia attenuation [230]. Another effective theranostic platform, BiOI@Bi_2S_3@BSA had the capability of concurrent application of RT/PDT/PTT synergistically. Bismuth Oxyiodide (BiOI) plays two roles simultaneously, as a radiosensitizer (containing high Z elements such as Bi and I) and as a photosensitizer (upon X-ray irradiation, this photocatalytic semiconductor forms electron-hole pair and generates ROS which causes X-ray excited PDT). Bi_2S_3 coating presents increased ROS generation (by forming a heteroconjunction structure at the interface of dissimilar BiOI semiconductor to decrease recombination of electron-hole and further enhance the electron-hole generation) along with NIR photothermal conversion for photothermal tumor ablation where the phenomenon also aids improved oxygen level of TME by increasing local blood flow and enhance RT outcome. Synergistic RT/PDT/PTT therapy demonstrated more significant effect than RT or PTT or PDT alone based on in vivo tumor ablation experiments. Such corporation among these modalities can be a promising approach for cancer therapy in the future [194].

iii) RT+ Immunotherapy: Clinical studies have revealed the role of RT in provoking crucial responses locally (in site of treatment) and remotely which is called abscopal effect. Immune system's major role in abscopal effect is elucidated which provides a way for integrating RT and immunotherapy for synergistic therapeutic strategies [231]. Inflammatory response-induced dendritic cell (DC) maturation and upregulation of chemokine receptors occur after RT exposure. Upon tumor antigen processing by DCs, they migrate to lymphatic nodes to express tumor antigen peptide and present it to $CD8^+$ cytotoxic T lymphocytes (CTL) which further reside in tumor and kill (phagocytosis) tumor cells, mediated by the proteins expressed on the surface of plasma membrane [232].

Immunomodulatory effect of RT by altering microenvironment of irradiation site, when administered alone, rarely leads to rejection of tumor systematically, while the RT-augmented immunotherapy enhances the therapeutic effect. At a glance, tumor may prevent immunization, cause wrong immune response or enable accumulation/expansion of T regulator (preventing cytotoxic T lymphocyte function) in tumor location. Effector T cell can undergo anergy if PD-1 receptors connect with specific surface molecules of tumor cells such as PD-L1 and PD-L2. MHC I molecules or target tumor antigen expression may be downregulated to prevent effector T cell response as well. Molecules with immunosuppressive function which are released from tumors such as indole amine 2,3-dioxygenase (IDO) enzyme (by consuming tryptophan) are capable of limiting T effector. Similarly, adenosine which is produced as a result of TME, hypoxia inhibits T cell function. Hypoxia emphasizes the presence of regulator T cells by producing CCL28. As a conclusion, several factors inhibit effector T cell function to avoid systemic response against tumor tissue.

This is where immunotherapy is employed for provoking immune responses and preventing tumor escape from immune attack as a result of immunosuppression [233–236]. High IDO expression, which is responsible for immune tolerance and poor prognosis of various types of cancer cells, can be inhibited by small molecules that has displayed a moderate effect in anticancer monotherapy [237]. In 2018, aiming to combine RT and immunotherapy for systematic tumor rejection after local radiation exposure, two engineered nano-metal organic framework (MOFs) were designed. After irradiation of X-ray at low doses, the crystalline structure of 5,15-di(p-benzoato)-porphyrin-Hf (DBP-Hf) and 5,10,15,20-tetra(p-benzoato)-porphyrin-Hf (TBP-Hf) acted as strong photosensitizers which produced ROS, especially $^1O_2$, killing malignant cells efficiently and enhancing the presentation of tumor specific antigens to T cells by stimulating immune system [238]. PDT might produce acute inflammation and subsequently attract leukocytes to the treated location, increase immunogenicity of dead tumor cells by exposing or creating new tumor antigens and inducing heat shock protein (HSP) expression which consequently increase antigen presentation to cytotoxic T cells. DC migration and maturation may be promoted by pro-inflammatory effect of PDT. According to in vivo tumor models, PDT has produced long lasting immunity memory [149]. Hf clusters with strong X-ray absorption favors RT with production of hydroxyl radicals which excite porphyrine- based photosensetizers for treatment of remote tumors. In vivo and in vitro eradication of various types of tumors were observed by employing nano-MOFs. Loading of small molecules (IDO inhibitors) in porous structure of DBP-Hf demonstrated enhanced therapeutic efficacy (including checkpoint blockade) and 100 % abscopal effect, rejecting both irradiated and non-radiated, treated and non-treated tumors in breast and colorectal mouse cancer models. In this nanoplatform, RT, PDT and immunotherapy were integrated for systematic and local tumor treatment [201]. Considering intrinsic immunomodulatory effect of RT and PDT, complementary role of these three modalities is beneficial for treating metastatic tumors. Again in 2018, immunomodulatory effect of IRT was combined with immunotherapeutic systemic checkpoint blockade by anti CTLA-4 antibody. Catalase was labeled with ^{131}I (which is employed as a source for internal excitation) to decompose overproduced H_2O_2 to O_2, relieve hypoxia and subsequently improve IRT efficacy with low doses of radioisotope. Intratumoral injection of ^{131}I-CAT/sodium alginate enabled tumor eradication and caused hypoxia elimination for a long period of time. Upon intratumoral injection, endogenous Ca^{2+} binds with alginate polysaccharide and forms hydrogel which causes ^{131}I-CAT fixation within the tumor and inhibits excessive radioisotope leakage to healthy tissues. CpG oligonucleotide role is stimulating intratumoral tumor specific antigen generation which leads to strong immune response. Checkpoint blockade and immunostimulation circumvent metastasis and tumor recurrence in advanced-stage patients [239]. RT and immunotherapy combination is a promising synergistic approach for promoting long term immunity

against tumor recurrence and treating hypoxic solid tumors along with remote metastatic cells when RT is inefficient as monotherapy.

Other approaches include:

I. Recently, platelets loaded with Au-hemoglobin complex (Au-Hb@ Plot) were fabricated to alleviate tumor hypoxia and penetrate deeply into tumor (due to small size). This nanosystem can be activated by cancer cells, where hemoglobin carries oxygen and Au potentiates tumor sensitivity to X-ray radiation. The enhanced in vivo RT therapeutic outcome was observed in tumor bearing mouse under low dose of radiation which was confirmed by in vitro experiments [240].

II. Full-process radiosensitizing hafnium-based nanoscale metal–organic frameworks (Hf-nMOFs) with uniform dispersion of Fe^{3+} ions were constructed to improve in vivo radiotherapy outcome by fenton reaction (due to Fe^{3+} presence) and X-ray energy conversion (due to Hf^{4+} presence) [241].

III. Other radiations can benefit radiotherapy efficacy by activating radioisotopes in the site of tumor. For instance, neutron irradiation can activate ^{152}Sm-filledcarbon nanocapsules inside the biological system after intravenous administration and turn it into ^{153}Sm radioactive form. This approach reduces nuclear waste, eliminates the need for nuclear facilities for nanoparticle preparation, increases stability of loaded in vivo radioactive content and can be used for imaging and RT simultaneously [242].

6 Challenges and Conclusion

Below a certain threshold, ROS assist cell survival but when elevated above cell antioxidant capacity, cell dies due to intolerance. Such balance is maintained in normal and tumor cells, but the level of toleration varies for different types of cells. Normal cells change into cancer cells when oncogenes are activated and cell redox hemostasis is in unbalanced state. ROS affect radiotherapy efficacy in both direct and indirect ways. Direct effect majorly results in lethal DNA damage, and indirect effects include cell death regulation, DNA damage repair, cancer stem cell (CSC) characteristics and tumor microenvironment (TME) modulation. Radiotherapy can be utilized based on tumor stage and type for curative or palliative purposes, and the underlying mechanism is increasing reactive species (ROS) inside the cell to damage macromolecules and shift the signaling pathways. Hypoxia is well-known for its association with radioresistance in which oxygen plays an important role in promoting induced cell damage. Low oxygen level and high antioxidant capacity are two major obstacles responsible for radiotherapy resistance which is a reason for poor prognosis of cancer. Radiosensitizers should be employed for enhancing cell sensitivity, and radioprotectors should be used for their ability to protect healthy tissue from radiation-induced damages. By using these tools, ROS concentration and

signaling pathways can be altered in favor of producing more ROS in tumor cells and lowering the ROS level in healthy cells. Despite engineering smart nanoplatforms to enhance/deplete ROS generation, modulating tumor microenvironment and synergistic therapy, ROS-based cancer therapeutics have been restricted to academic research, while there is an urge for more efficient cancer therapeutics, noting the severe cancer status across the world. So it is essential to:

- Acquire more advanced comprehension of intrinsic features of modalities which are based on ROS
- Determine the mechanism and extent of synergistic therapeutic effect in contrast to employing monotherapy [243].

Unique characteristics of ROS in biological mechanisms have been utilized for medical purposes. ROS regulating nanomaterials can be manipulated to direct temporospatial dynamic behaviors of these chemical species to develop advanced in vivo therapeutic approaches. Nanocatalytic medicine refers to catalytic nature of nanosystems in ROS-involving therapeutic approaches where nanomaterials attenuate energy barriers of ROS-related reactions for initiating therapeutic effects via ROS regulation. Exogenous stimuli can induce or accelerate these catalytic reactions in which therapeutic processes generally can be categorized as nanocatalytic medicine. Despite advancements in ROS science, the is in initial stages, and with development of advanced approaches, ROS-related biomedical research area will emerge. For development of ROS-based therapeutic materials, there are still scientific/technological issues remaining to be investigated:

1. **Biosafety:** In vivo application of ROS-generating nanomaterials with cytotoxic chemical feature may be associated with surrounding normal tissue impairment and degradability issue which causes continuous ROS generation and consequently oxidative damage [244, 245]. Precise characterization of ROS behavior and safety assessment of nanomaterials by developing cutting edge tools are steps needed to be taken in order to balance the benefit of ROS generating nanomaterials and their side effect [246].
2. **Chemical mechanism:** Computational chemistry has provided tools for prediction/exploration of chemical reactions including mechanisms of ROS-related reactions such as ROS generation and interaction with biomolecules which affect progression of disease pathology. Most investigations lack mechanism exploration of nanomaterial therapeutic processes [247]. Computational chemistry can come in handy in ROS investigations to unveil chemical role of ROS in therapeutic processes [220, 248]. Consequently, redox active nanomaterials can be discovered and fabricated noting the emergence of cheminformatics which can contribute greatly in ROS science and exploration of related molecular mechanisms.
3. **Therapeutic concept:** Precise fabrication of nanomaterials with unique compositions and structures for fulfilling the individual demands, is the opening of a new era [249–251]. Immunotherapy is considered a personalized therapeutic

modality for cancer. Thus, integrating immunotherapy with ROS-based modalities is of importance. For instance, combination of RT/PDT with immunotherapy leads to super additive therapeutic effect, given that PDT and RT initiate immunoregulatory responses. Immunoregulatory effect of cutting-edge therapeutic modalities such as SDT and CDT have to be investigated to answer the query whether these modalities are competent for synergic therapy and enhancing cancer therapeutic outcome.

4. **Catalytic efficiency:** Material's capability to scavenge/produce ROS determines its final therapeutic performance. The common focus is still synthesis and design to achieve significant redox-regulation in nanomaterials. Inorganic nanozyms has managed intracellular ROS concentration but their in vivo catalytic efficiency should be further improved due to strong demand for decreasing drug dosage as much as possible. Significant improvement of catalytic chemistry owes to recent advances which can be utilized for in vivo ROS regulation such as atomic catalytic modalities. In 2015, a pioneering work demonstrated catalytic oxidization of benzene by single iron atom catalysis of H_2O_2 which was confined in graphene matrix [252].

Clinical translation of these engineered nanomaterials is the last concern after addressing aforementioned design issues. Most FDA-approved nanomaterials are organic where certain types have been chosen for loading specific APIs (active pharmaceutical ingredients) for chemo/immuno/gene therapies but ROS-based modalities are not included. A clinical trial for RT enhancement of adult soft tissue carcinoma is ongoing phase I which involves one-time intratumoral implementation of hafnium oxide nanoparticles [253].

Clinical translation of ROS-based nanosystems may be hindered by several issues:

1. Increasing number of fabricated ROS-regulating nanomaterials claimed to be effective may cause difficulties in choosing optimized platform for clinical trials.
2. Generated ROS dose should be identified and managed, because ROS as double edge sword, can guide cells toward therapeutic or pathological effect.
3. Safety and efficacy of each component are hard to be assessed as design of nanomedicines has shifted to co-delivery of therapeutic agents to achieve multifunctional and efficient ROS-regulating nanomaterials.
4. Although preclinical studies provide therapeutic results in animal models, they lack mechanistic understanding of nanomedicine interaction with in vivo environment. Considering much different texture and physiological response between human and animal models, more strict evaluations of safety and efficacy are necessary before nanomedicine administration to patient's body.

Considering the efforts made so far, further acceleration to clinical translation by meeting aforementioned stringent requirements and patient specific approaches should be given attention to. In this regard, cancer nanomedicines should address problems associated with tumor heterogeneity. For instance, ROS-generating nanomedicines that respond to exogenous stimuli (RT, SDT and PDT) can be employed for localized treatment of skin malignancies whereas nanomedicines

which respond to tumor microenvironment should be utilized for treating deep tumors systematically. Optimized platform can be selected based on the unique chemistry of the nanomaterial and the stage of specific type of cancer. To determine appropriate dose and administration route, feasible diagnostic tools should be developed to monitor ROS level in pathological site in a real-time manner. Optimal clinical outcome can be achieved if these goals are achieved. To facilitate the clinical translation of nanomedicines, designs need to be simplified rather than getting more sophisticated to avoid potential biosafety issues. In this context, deep investigation of underlying mechanisms of long term biological effects induced by ROS-based nanomedicines should be undertaken (in both animal and human body) which necessitates close collaboration of university, hospital and industry with each other.

References

1. D'Autréaux B, Toledano MB (2007) ROS as signalling molecules: mechanisms that generate specificity in ROS homeostasis. Nat Rev Mol Cell Biol 8(10):813–824
2. Foote C (1968) Accts. Chem. Res. 1:104. CrossRef| CAS| Web of Science® Times Cited: 781 DR Kearns (1971) Chem. Rev. 71:395
3. Schweitzer C, Schmidt R (2003) Physical mechanisms of generation and deactivation of singlet oxygen. Chem Rev 103(5):1685–1758
4. Hayyan M, Hashim MA, AlNashef IM (2016) Superoxide ion: generation and chemical implications. Chem Rev 116(5):3029–3085
5. Nosaka Y, Nosaka AY (2017) Generation and detection of reactive oxygen species in photocatalysis. Chem Rev 117(17):11302–11336
6. Zorov DB, Juhaszova M, Sollott SJ (2014) Mitochondrial reactive oxygen species (ROS) and ROS-induced ROS release. Physiol Rev 94(3):909–950
7. Zuo L et al (2015) Biological and physiological role of reactive oxygen species–the good, the bad and the ugly. Acta Physiol 214(3):329–348
8. Snezhkina AV et al (2019) ROS generation and antioxidant defense systems in normal and malignant cells. Oxidative Med Cellul Longevity
9. Yang B, Chen Y, Shi J (2019) Reactive oxygen species (ROS)-based nanomedicine. Chem Rev 119(8):4881–4985
10. Superoxide-forming enzyme from human neutrophils: evidence for a flavin requirement Blood 50(3):517-24
11. Nathan C, Cunningham-Bussel A (2013) Beyond oxidative stress: an immunologist's guide to reactive oxygen species. Nat Rev Immunol 13(5):349–361
12. Ighodaro O, Akinloye O (2018) First line defence antioxidants-superoxide dismutase (SOD), catalase (CAT) and glutathione peroxidase (GPX): their fundamental role in the entire antioxidant defence grid. Alexandria J Med 54(4):287–293
13. García-Sánchez A, Miranda-Díaz AG, Cardona-Muñoz EG (2020) The role of oxidative stress in physiopathology and pharmacological treatment with pro-and antioxidant properties in chronic diseases. Oxidat Med Cellul Longevity 2020:2082145
14. Yang S, Lian G (2020) ROS and diseases: role in metabolism and energy supply. Mol Cell Biochem 467(1):1–12
15. Barhoi D et al (2021) Extract of Tagetes Erecta could be used as a potential drug candidate against cancer: a study on the anticancer efficacy of medicinal plants involving in vitro and in vivo approach Phytomedicine Plus 2(1):100187
16. Wardman P (2007) Chemical radiosensitizers for use in radiotherapy. Clin Oncol 19(6):397–417

17. Nordsmark M et al (2005) Prognostic value of tumor oxygenation in 397 head and neck tumors after primary radiation therapy. An international multi-center study. Radiotherapy Oncol **77**(1):18–24
18. Kim JJ, Tannock IF (2005) Repopulation of cancer cells during therapy: an important cause of treatment failure. Nat Rev Cancer 5(7):516–525
19. Han J et al (2018) Dual roles of graphene oxide to attenuate inflammation and elicit timely polarization of macrophage phenotypes for cardiac repair. ACS Nano 12(2):1959–1977
20. Bao X et al (2018) Polydopamine nanoparticles as efficient scavengers for reactive oxygen species in periodontal disease. ACS Nano 12(9):8882–8892
21. Liu S et al (2018) Electrochemiluminescence for electric-driven antibacterial therapeutics. J Am Chem Soc 140(6):2284–2291
22. Wang C et al (2018) Femtosecond laser crosslinking of the cornea for non-invasive vision correction. Nat Photonics 12(7):416–422
23. Fenton H (1876) Chem. News 190; Fenton HJH (1894) J Chem Soc (London) 65:899
24. Rohrer F, Berresheim H (2006) Strong correlation between levels of tropospheric hydroxyl radicals and solar ultraviolet radiation. Nature 442(7099):184–187
25. O'regan B, Grätzel M (1991) A low-cost, high-efficiency solar cell based on dye-sensitized colloidal TiO_2 films. Nature 353(6346):737–740
26. Nosaka Y, Nosaka A (2016) Understanding hydroxyl radical (·OH) generation processes in photocatalysis. ACS Energy Lett 1(2):356–359
27. Huo M et al (2017) Tumor-selective catalytic nanomedicine by nanocatalyst delivery. Nat Commun 8(1):1–12
28. Sabharwal SS, Schumacker PT (2014) Mitochondrial ROS in cancer: initiators, amplifiers or an Achilles' heel? Nat Rev Cancer 14(11):709–721
29. Block K, Gorin Y (2012) Aiding and abetting roles of NOX oxidases in cellular transformation. Nat Rev Cancer 12(9):627–637
30. Winterbourn CC (2008) Reconciling the chemistry and biology of reactive oxygen species. Nat Chem Biol 4(5):278–286
31. Bachi A, Dalle-Donne I, Scaloni A (2013) Redox proteomics: chemical principles, methodological approaches and biological/biomedical promises. Chem Rev 113(1):596–698
32. Dickinson BC, Chang CJ (2011) Chemistry and biology of reactive oxygen species in signaling or stress responses. Nat Chem Biol 7(8):504–511
33. Gray JM et al (2004) Oxygen sensation and social feeding mediated by a C. elegans guanylate cyclase homologue. Nature 430(6997):317–322
34. Gardner PR, Fridovich I (1991) Superoxide sensitivity of the Escherichia coli aconitase. J Biol Chem 266(29):19328–19333
35. Toledano MB et al (1994) Redox-dependent shift of OxyR-DNA contacts along an extended DNA-binding site: a mechanism for differential promoter selection. Cell 78(5):897–909
36. Warburg O (1908) Roebachtungen über die Oxydationsprozesse im Seeigelei. Zeitschr f Physiol Chem 57:1–16
37. Overley L (1998) Free radical and diabetes. Free Radical Biol Med 5:113–124
38. Foreman J et al (2003) Reactive oxygen species produced by NADPH oxidase regulate plant cell growth. Nature 422(6930):442–446
39. Kim J-S, Huang TY, Bokoch GM (2009) Reactive oxygen species regulate a slingshot-cofilin activation pathway. Mol Biol Cell 20(11):2650–2660
40. Niethammer P et al (2009) A tissue-scale gradient of hydrogen peroxide mediates rapid wound detection in zebrafish. Nature 459(7249):996–999
41. O'Neill JS, Reddy AB (2011) Circadian clocks in human red blood cells. Nature 469(7331):498–503
42. Zhong H et al (2021) Macrophage ICAM-1 functions as a regulator of phagocytosis in LPS induced endotoxemia. Inflamm Res 70(2):193–203
43. Segal AW, Shatwell KP (1997) The NADPH oxidase of phagocytic leukocytes a. Ann N Y Acad Sci 832(1):215–222

44. Kreutzberg GW (1996) Microglia: a sensor for pathological events in the CNS. Trends Neurosci 19(8):312–318
45. Holmström KM, Finkel T (2014) Cellular mechanisms and physiological consequences of redox-dependent signalling. Nat Rev Mol Cell Biol 15(6):411–421
46. Ray PD, Huang B-W, Tsuji Y (2012) Reactive oxygen species (ROS) homeostasis and redox regulation in cellular signaling. Cell Signal 24(5):981–990
47. Trachootham D, Alexandre J, Huang P (2009) Targeting cancer cells by ROS-mediated mechanisms: a radical therapeutic approach? Nat Rev Drug Discovery 8(7):579–591
48. Gorrini C, Harris IS, Mak TW (2013) Modulation of oxidative stress as an anticancer strategy. Nat Rev Drug Discovery 12(12):931–947
49. Litwin J et al (1987) Immunocytochemical localization of peroxisomal enzymes in human liver biopsies. Am J Pathol 128(1):141
50. Hashimoto F, Hayashi H (1990) Significance of catalase in peroxisomal fatty acyl-CoA β-oxidation: NADH oxidation by acetoacetyl-CoA and H_2O_2. J Bioch 108(3):426–431
51. Liou GY, Storz P (2010) Reactive oxygen species in cancer. Free Radic Res 44(5):479–496
52. Wang Y et al (2021) The double-edged roles of ROS in cancer prevention and therapy. Theranostics 11(10):4839
53. Ishii N et al (1998) A mutation in succinate dehydrogenase cytochrome b causes oxidative stress and ageing in nematodes. Nature 394(6694):694–697
54. Yan L-J, Sohal RS (1998) Mitochondrial adenine nucleotide translocase is modified oxidatively during aging. Proc Natl Acad Sci 95(22):12896–12901
55. Obata F, Fons C, Gould A (2018) Early-life exposure to low-dose oxidants can increase longevity via microbiome remodelling in Drosophila. Nat Commun. Nature Publishing Group.
56. Cui Q et al (2018) Modulating ROS to overcome multidrug resistance in cancer. Drug Resist Updates 41:1–25
57. Emanuele S et al (2018) The double-edged sword profile of redox signaling: oxidative events as molecular switches in the balance between cell physiology and cancer. Chem Res Toxicol 31(4):201–210
58. Panieri E et al (2013) Reactive oxygen species generated in different compartments induce cell death, survival, or senescence. Free Radical Biol Med 57:176–187
59. Perillo B et al (2020) ROS in cancer therapy: the bright side of the moon. Exp Mol Med 52(2):192–203
60. Begg AC, Stewart FA, Vens C (2011) Strategies to improve radiotherapy with targeted drugs. Nat Rev Cancer 11(4):239–253
61. Tan X, Azad S, Ji X (2018) Hypoxic preconditioning protects SH-SY5Y cell against oxidative stress through activation of autophagy. Cell Transplant 27(12):1753–1762
62. Aunoble B et al (2000) Major oncogenes and tumor suppressor genes involved in epithelial ovarian cancer. Int J Oncol 16(3):567–643
63. Minamoto T, Ougolkov AV, Mai M (2002) Detection of oncogenes in the diagnosis of cancers with active oncogenic signaling. Expert Rev Mol Diagn 2(6):565–575
64. Minamoto T, Mai M, Ronai ZE (2000) K-ras mutation: early detection in molecular diagnosis and risk assessment of colorectal, pancreas, and lung cancers-a review. Cancer Detect Preven 24(1):1–12
65. Xiao H, Yang CS (2008) Combination regimen with statins and NSAIDs: a promising strategy for cancer chemoprevention. Int J Cancer 123(5):983–990
66. Berasain C et al (2009) Inflammation and liver cancer: new molecular links. Ann N Y Acad Sci 1155(1):206–221
67. Balkwill FR (1992) Tumour necrosis factor and cancer. Prog Growth Factor Res 4(2):121–137
68. Suzuki N et al (2012) ROS and redox signalling in the response of plants to abiotic stress. Plant Cell Environ 35(2):259–270
69. Jaramillo MC, Zhang DD (2013) The emerging role of the Nrf2–Keap1 signaling pathway in cancer. Genes Dev 27(20):2179–2191
70. Wang X (2001) The expanding role of mitochondria in apoptosis. Genes Dev 15(22):2922–2933

71. Qin J-J et al (2019) Dual roles and therapeutic potential of Keap1-Nrf2 pathway in pancreatic cancer: a systematic review. Cell Commun Signaling 17(1):1–15
72. Roberts PJ, Der CJ (2007) Targeting the Raf-MEK-ERK mitogen-activated protein kinase cascade for the treatment of cancer. Oncogene 26(22):3291–3310
73. McCubrey J et al (2007) Terrian 416 DM, Milella M, Tafuri A, Stivala F, Libra M, Basecke J, Evangelisti C, Martelli AM, and Franklin RA. 417 Roles of the Raf/MEK/ERK pathway in cell growth, malignant transformation and drug resistance. 418. Biochim Biophys Acta, 1263–1284
74. Steelman L et al (2008) Contributions of the Raf/MEK/ERK, PI3K/PTEN/Akt/mTOR and Jak/STAT pathways to leukemia. Leukemia 22(4):686–707
75. Chan DW et al (2008) Loss of MKP3 mediated by oxidative stress enhances tumorigenicity and chemoresistance of ovarian cancer cells. Carcinogenesis 29(9):1742–1750
76. Rygiel TP et al (2008) The Rac activator Tiam1 prevents keratinocyte apoptosis by controlling ROS-mediated ERK phosphorylation. J Cell Sci 121(8):1183–1192
77. Kumar B et al (2008) Oxidative stress is inherent in prostate cancer cells and is required for aggressive phenotype. Can Res 68(6):1777–1785
78. Osada S et al (2008) Extracellular signal-regulated kinase phosphorylation due to menadione-induced arylation mediates growth inhibition of pancreas cancer cells. Cancer Chemother Pharmacol 62(2):315–320
79. Zhang Y et al (2002) Overexpression of copper zinc superoxide dismutase suppresses human glioma cell growth. Can Res 62(4):1205–1212
80. Chinnaiyan AM et al (2000) Combined effect of tumor necrosis factor-related apoptosis-inducing ligand and ionizing radiation in breast cancer therapy. Proc Natl Acad Sci 97(4):1754–1759
81. Higaki Y et al (2008) Oxidative stress stimulates skeletal muscle glucose uptake through a phosphatidylinositol 3-kinase-dependent pathway. Amer J Physiol-Endocrinol Metabolism 294(5):E889–E897
82. Sun H et al (1999) Mueller b, Liu X and Wu H: PTEN modulates cell cycle progression and cell survival by regulating phosphatidylinositol 3, 4, 5,-trisphosphate and Akt/protein kinase b signaling pathway. Proc Natl Acad Sci USA 96:6199–6204
83. BiswasDK SQ (2004) nF kappaBactiva tioninhu manbreastcancerspecimensanditsroleincell-proliferationand apoptosis. ProcNatlAcadSciUSA 101(27):10137–10142
84. Biswas DK, Iglehart JD (2006) Linkage between EGFR family receptors and nuclear factor kappaB (NF-κB) signaling in breast cancer. J Cell Physiol 209(3):645–652
85. Van der Heiden K et al (2010) Role of nuclear factor κB in cardiovascular health and disease. Clin Sci 118(10):593–605
86. Ahmed KM, Cao N, Li JJ (2006) HER-2 and NF-κB as the targets for therapy-resistant breast cancer. Anticancer Res 26(6B):4235–4243
87. Schreck R, Albermann K, Baeuerle PA (1992) Nuclear factor kB: an oxidative stress-responsive transcription factor of eukaryotic cells (a review). Free Radical Res Commun 17(4):221–237
88. Hacker H, Karin M (2006) Regulation and function of IKK and IKK-related kinases. Science's STKE
89. Karin M (2008) The IκB kinase–a bridge between inflammation and cancer. Cell Res 18(3):334–342
90. Parhar K et al (2007) Investigation of interleukin 1β-mediated regulation of NF-κB activation in colonic cells reveals divergence between PKB and PDK-transduced events. Mol Cell Biochem 300(1):113–127
91. Wang Y et al (2007) The endogenous reactive oxygen species promote NF-κ B activation by targeting on activation of NF-κ B-inducing kinase in oral squamous carcinoma cells. Free Radical Res 41(9):963–971
92. Burdon RH, Gill V, Rice-Evans C (1990) Oxidative stress and tumour cell proliferation. Free Radical Res Commun 11(1–3):65–76

93. Parkash J, Felty Q, Roy D (2006) Estrogen exerts a spatial and temporal influence on reactive oxygen species generation that precedes calcium uptake in high-capacity mitochondria: implications for rapid nongenomic signaling of cell growth. Biochemistry 45(9):2872–2881
94. Menon SG et al (2005) Differential susceptibility of nonmalignant human breast epithelial cells and breast cancer cells to thiol antioxidant-induced G1-delay. Antioxid Redox Signal 7(5–6):711–718
95. Felty Q, Singh KP, Roy D (2005) Estrogen-induced G 1/S transition of G 0-arrested estrogen-dependent breast cancer cells is regulated by mitochondrial oxidant signaling. Oncogene 24(31):4883–4893
96. Behrend L, Henderson G, Zwacka R (2003) Molecular mechanisms of signalling molecular mechanisms of signalling transformation. Biochem Soc Trans 31(6):1441–1444
97. Reichenbach J et al (2002) Elevated oxidative stress in patients with ataxia telangiectasia. Antioxid Redox Signal 4(3):465–469
98. Browne S, Levine RL (2004) Treatment with a catalytic antioxidant corrects the neurobehavioral defect in ataxia–telangiectasia mice. Free Radic Biol Med 36:938–942
99. Cadenas E (2004) Mitochondrial free radical production and cell signaling. Mol Aspects Med 25(1–2):17–26
100. Simon H-U, Haj-Yehia A, Levi-Schaffer F (2000) Role of reactive oxygen species (ROS) in apoptosis induction. Apoptosis 5(5):415–418
101. Gottlieb E, Vander Heiden MG, Thompson CB (2000) Bcl-xL prevents the initial decrease in mitochondrial membrane potential and subsequent reactive oxygen species production during tumor necrosis factor alpha-induced apoptosis. Molecul Cellul Biol 20(15):5680–5689
102. Abhari F et al (2020) Folic acid modified bismuth sulfide and gold heterodimers for enhancing radiosensitization of mice tumors to X-ray radiation. ACS Sustain Chem Eng 8(13):5260–5269
103. Storz P (2007) Mitochondrial ROS–radical detoxification, mediated by protein kinase D. Trends Cell Biol 17(1):13–18
104. Lee CH et al (2008) Novel 2-step synthetic indole compound 1, 1, 3-tri (3-indolyl) cyclohexane inhibits cancer cell growth in lung cancer cells and xenograft models. Cancer: Interdiscip Int J Ameri Cancer Soc 113(4):815–825
105. Zhang S et al (2011) In vitro and. Silico, 281–286
106. Shim H-Y et al (2007) Acacetin-induced apoptosis of human breast cancer MCF-7 cells involves caspase cascade, mitochondria-mediated death signaling and SAPK/JNK1/2-c-Jun activation. Molecul Cells (Springer Science & Business Media BV) 24(1)
107. Brunet A et al (1999) Akt promotes cell survival by phosphorylating and inhibiting a Forkhead transcription factor. Cell 96(6):857–868
108. You H, Yamamoto K, Mak TW (2006) Regulation of transactivation-independent proapoptotic activity of p53 by FOXO3a. Proc Natl Acad Sci 103(24):9051–9056
109. Wong GH, Goeddel DV (1988) Induction of manganous superoxide dismutase by tumor necrosis factor: possible protective mechanism. Science 242(4880):941–944
110. Xu YC et al (2002) Involvement of TRAF4 in oxidative activation of c-Jun N-terminal kinase. J Biol Chem 277(31):28051–28057
111. Xin M, Deng X (2005) Nicotine inactivation of the proapoptotic function of Bax through phosphorylation. J Biol Chem 280(11):10781–10789
112. Kawamura N et al (2007) Akt1 in osteoblasts and osteoclasts controls bone remodeling. PLoS ONE 2(10):e1058
113. Limaye V, Li X, Hahn C, Xia P, Berndt MC, Vadas MA, Gamble JR (2005) Sphingosine kinase-1 enhances endothelial cell survival through a PECAM-1-dependent activation of PI-3K/Akt and regulation of Bcl-2 family members. Blood 105:3169–3177
114. Song J et al (2009) PKD prevents H_2O_2-induced apoptosis via NF-κB and p38 MAPK in RIE-1 cells. Biochem Biophys Res Commun 378(3):610–614
115. Chiu TT et al (2007) Protein kinase D2 mediates lysophosphatidic acid-induced interleukin 8 production in nontransformed human colonic epithelial cells through NF-κB. Am J Physiol Cell Physiol 292(2):C767–C777

116. Storz P, Döppler H, Toker A (2005) Protein kinase D mediates mitochondrion-to-nucleus signaling and detoxification from mitochondrial reactive oxygen species. Mol Cell Biol 25(19):8520–8530
117. Zhang W et al (2005) Protein kinase D specifically mediates apoptosis signal-regulating kinase 1-JNK signaling induced by H_2O_2 but not tumor necrosis factor. J Biol Chem 280(19):19036–19044
118. Pelicano H et al (2009) Mitochondrial dysfunction and reactive oxygen species imbalance promote breast cancer cell motility through a CXCL14-mediated mechanism. Can Res 69(6):2375–2383
119. Lewis A et al (2005) Metastatic progression of pancreatic cancer: changes in antioxidant enzymes and cell growth. Clin Exp Metas 22(7):523–532
120. Hitchler MJ, Oberley LW, Domann FE (2008) Epigenetic silencing of SOD2 by histone modifications in human breast cancer cells. Free Radical Biol Med 45(11):1573–1580
121. Hitchler M et al (2006) Epigenetic regulation of manganese superoxide dismutase expression in human breast cancer cells. Epigenetics 1(4):163–171
122. Chiarugi P, Fiaschi T (2007) Redox signalling in anchorage-dependent cell growth. Cell Signal 19(4):672–682
123. Chiarugi P (2008) From anchorage dependent proliferation to survival: lessons from redox signalling. IUBMB Life 60(5):301–307
124. Werner E, Werb Z (2002) Integrins engage mitochondrial function for signal transduction by a mechanism dependent on Rho GTPases. J Cell Biol 158(2):357–368
125. Tiku M, Liesch J, Robertson F (1990) Production of hydrogen peroxide by rabbit articular chondrocytes. Enhancement by cytokines. J Immunol 145(2):690–696
126. Storz P (2005) Reactive oxygen species in tumor progression. Front Biosci 10(1–3):1881–1896
127. Ishikawa K et al (2008) ROS-generating mitochondrial DNA mutations can regulate tumor cell metastasis. Science 320(5876):661–664
128. Dewhirst MW, Cao Y, Moeller B (2008) Cycling hypoxia and free radicals regulate angiogenesis and radiotherapy response. Nat Rev Cancer 8(6):425–437
129. Hockel M, Vaupel P (2001) Tumor hypoxia: definitions and current clinical, biologic, and molecular aspects. J Natl Cancer Inst 93(4):266–276
130. Pani G et al (2009) Redox-based escape mechanism from death: the cancer lesson. Antioxid Redox Signal 11(11):2791–2806
131. Singh S, Darnay BG, Aggarwal BB (1996) Site-specific tyrosine phosphorylation of IκBα negatively regulates its inducible phosphorylation and degradation. J Biol Chem 271(49):31049–31054
132. Dang C (1999) SG Oncogenic alterations of metabolism. Trends in Biochemical Science 24:68–72
133. Hsu PP, Sabatini DM (2008) Cancer cell metabolism: Warburg and beyond. Cell 134(5):703–707
134. Poüysségur J, Dayan F, Mazure N (2006) Hypoxia signalling in cancer and approaches to enforce tumor regression. Nature 441:437–443
135. Rich JN (2007) Cancer stem cells in radiation resistance. Can Res 67(19):8980–8984
136. Claffey KP et al (1996) Expression of vascular permeability factor/vascular endothelial growth factor by melanoma cells increases tumor growth, angiogenesis, and experimental metastasis. Can Res 56(1):172–181
137. Senger D et al (1994) Vascular permeability factor, tumor angiogenesis and stroma generation. Invasion Metastasis 14(1–6):385–394
138. Brown L, Detmar M, Claffey K, Nagy JA, Feng D, Dvorak AM, Dvorak HF (1997) Vascular permeability factor/vascular endothelial growth factor: a multifunctional angiogenic cytokine. Regulation Angiogenesis, 233–269
139. Murakami M, Simons M (2008) Fibroblast growth factor regulation of neovascularization. Curr Opin Hematol 15(3):215

140. Wouters BG, Koritzinsky M (2008) Hypoxia signalling through mTOR and the unfolded protein response in cancer. Nat Rev Cancer 8(11):851–864
141. Spitz DR et al (2000) Glucose deprivation-induced oxidative stress in human tumor cells: a fundamental defect in metabolism? Ann N Y Acad Sci 899(1):349–362
142. Brown NS, Bicknell R (2001) Hypoxia and oxidative stress in breast cancer Oxidative stress-its effects on the growth, metastatic potential and response to therapy of breast cancer. Breast Cancer Res 3(5):1–5
143. Bertout JA, Patel SA, Simon MC (2008) The impact of O 2 availability on human cancer. Nat Rev Cancer 8(12):967–975
144. Gardner L, Corn PG (2008) Hypoxic regulation of mRNA expression. Cell Cycle 7(13):1916–1924
145. Wartenberg M et al (2003) Inhibition of tumor-induced angiogenesis and matrix-metalloproteinase expression in confrontation cultures of embryoid bodies and tumor spheroids by plant ingredients used in traditional chinese medicine. Lab Invest 83(1):87–98
146. Milligan SA, Owens MW, Grisham MB (1996) Augmentation of cytokine-induced nitric oxide synthesis by hydrogen peroxide. Am J Physiol 271(1 Pt 1):L114–L120
147. Bao S et al (2006) Glioma stem cells promote radioresistance by preferential activation of the DNA damage response. Nature 444(7120):756–760
148. Scott PD et al (2009) Results of laparoscopic Heller myotomy for extreme megaesophagus: an alternative to esophagectomy. Surgical Laparoscopy Endoscopy & Percutaneous Techniques 19(3):198–200
149. Diehn M et al (2009) Association of reactive oxygen species levels and radioresistance in cancer stem cells. Nature 458(7239):780–783
150. Shackleton M et al (2006) Generation of a functional mammary gland from a single stem cell. Nature 439(7072):84–88
151. Ward J (1985) Biochemistry of DNA lesions. Radiat Res 104(2s):S103–S111
152. Mohr M, Zänker KS, Dittmar T (2015) Cancer (stem) cell differentiation: An inherent or acquired property? Med Hypotheses 85(6):1012–1018
153. Overgaard J, Horsman MR (1996) Modification of hypoxia-induced radioresistance in tumors by the use of oxygen and sensitizers. In Seminars in radiation oncology. Elsevier
154. Dische S (1991) What have we learnt from hyperbaric oxygen? Radiother Oncol 20:71–74
155. Takaoka T et al (2017) Biological effects of hydrogen peroxide administered intratumorally with or without irradiation in murine tumors. Cancer Sci 108(9):1787–1792
156. Hoff CM et al (2011) Does transfusion improve the outcome for HNSCC patients treated with radiotherapy?–results from the randomized DAHANCA 5 and 7 trials. Acta Oncol 50(7):1006–1014
157. Welsh L et al (2017) Blood transfusion during radical chemo-radiotherapy does not reduce tumour hypoxia in squamous cell cancer of the head and neck. Br J Cancer 116(1):28–35
158. Hirst DG, Wood PJ (1989) Altered radio sensitivity in a mouse carcinoma after administration of clofibrate and bezafibrate. Radiother Oncol 15(1):55–61
159. Kim W et al (2019) Cellular stress responses in radiotherapy. Cells 8(9):1105
160. Rashidzadeh H et al (2021) pH-sensitive curcumin conjugated micelles for tumor triggered drug delivery. J Biomater Sci Polym Ed 32(3):320–336
161. Rezaei SJT et al (2020) pH-triggered prodrug micelles for cisplatin delivery: preparation and in vitro/vivo evaluation. React Funct Polym 146:104399
162. Rashidzadeh H et al (2021) Recent advances in targeting malaria with nanotechnology-based drug carriers. Pharm Dev Technol 26(8):807–823
163. Fattahi N et al (2021) Enhancement of the brain delivery of methotrexate with administration of mid-chain ester prodrugs: In vitro and in vivo studies. Int J Pharm 600:120479
164. Yoozbashi M et al (2021) Magnetic nanostructured lipid carrier for dual triggered curcumin delivery: preparation, characterization and toxicity evaluation on isolated rat liver mitochondria. J Biomater Appl, 08853282211034625
165. Auffan M et al (2009) Towards a definition of inorganic nanoparticles from an environmental, health and safety perspective. Nat Nanotechnol 4(10):634–641

166. Chauhan VP et al (2012) Normalization of tumour blood vessels improves the delivery of nanomedicines in a size-dependent manner. Nat Nanotechnol 7(6):383–388
167. Lin H, Chen Y, Shi J (2018) Nanoparticle-triggered in situ catalytic chemical reactions for tumour-specific therapy. Chem Soc Rev 47(6):1938–1958
168. Shi J (2013) On the synergetic catalytic effect in heterogeneous nanocomposite catalysts. Chem Rev 113(3):2139–2181
169. Mu Q et al (2014) Chemical basis of interactions between engineered nanoparticles and biological systems. Chem Rev 114(15):7740–7781
170. Jiang W et al (2008) Nanoparticle-mediated cellular response is size-dependent. Nat Nanotechnol 3(3):145–150
171. Barnard AS (2010) One-to-one comparison of sunscreen efficacy, aesthetics and potential nanotoxicity. Nat Nanotechnol 5(4):271–274
172. Qian X, Gu Z, Chen Y (2017) Two-dimensional black phosphorus nanosheets for theranostic nanomedicine. Mater Horiz 4(5):800–816
173. Hawkins C, Davies M (2014) Biochim Bio-Phys Acta Gen Subj 1840:708–721
174. Kruid J, Fogel R, Limson JL (2017) Quantitative methylene blue decolourisation assays as rapid screening tools for assessing the efficiency of catalytic reactions. Chemosphere 175:247–252
175. Salvemini D, Riley DP, Cuzzocrea S (2002) SOD mimetics are coming of age. Nat Rev Drug Discovery 1(5):367–374
176. Markovic Z, Trajkovic V (2008) Biomedical potential of the reactive oxygen species generation and quenching by fullerenes (C60). Biomaterials 29(26):3561–3573
177. Nelson BC et al (2016) Antioxidant cerium oxide nanoparticles in biology and medicine. Antioxidants 5(2):15
178. Das S et al (2013) Cerium oxide nanoparticles: applications and prospects in nanomedicine. Nanomedicine 8(9):1483–1508
179. Li Y et al (2015) Acquired superoxide-scavenging ability of ceria nanoparticles. Angew Chem 127(6):1852–1855
180. Korsvik C et al (2007) Vacancy engineered ceria oxide nanoparticles catalyze superoxide dismutase activity. Chem Commun 35:1056–1058
181. Celardo I et al (2011) Ce3+ ions determine redox-dependent anti-apoptotic effect of cerium oxide nanoparticles. ACS Nano 5(6):4537–4549
182. Colon J et al (2009) Protection from radiation-induced pneumonitis using cerium oxide nanoparticles. Nanomed Nanotechnol Biol Med 5(2):225–231
183. Wason MS et al (2013) Sensitization of pancreatic cancer cells to radiation by cerium oxide nanoparticle-induced ROS production. Nanomed Nanotechnol Biol Med 9(4):558–569
184. Zhang J et al (2010) Synthesis and oxygen reduction activity of shape-controlled Pt3Ni nanopolyhedra. Nano Lett 10(2):638–644
185. Zhang W et al (2016) Prussian blue nanoparticles as multienzyme mimetics and reactive oxygen species scavengers. J Am Chem Soc 138(18):5860–5865
186. Mu J et al (2016) Novel hierarchical NiO nanoflowers exhibiting intrinsic superoxide dismutase-like activity. J Mater Chem B 4(31):5217–5221
187. Jagsi R (2014) Progress and controversies: radiation therapy for invasive breast cancer. CA: Cancer J Clinicians 64(2):135–152
188. Timmerman RD et al (2009) Local surgical, ablative, and radiation treatment of metastases. CA: Cancer J Clinicians 59(3):145–170
189. Song G et al (2017) Emerging nanotechnology and advanced materials for cancer radiation therapy. Adv Mater 29(32):1700996
190. Horwitz EM, Hanks GE (2000) External beam radiation therapy for prostate cancer. CA: Cancer J Clinicians 50(6):349–375
191. Sadeghi M, Enferadi M, Shirazi A (2010) External and internal radiation therapy: past and future directions. J Cancer Res Ther 6(3):239
192. Guo Z et al (2017) Synthesis of BSA-Coated BiOI@ Bi2S3 semiconductor heterojunction nanoparticles and their applications for radio/photodynamic/photothermal synergistic therapy of tumor. Adv Mater 29(44):1704136

193. Luksiene Z, Juzenas P, Moan J (2006) Radiosensitization of tumours by porphyrins. Cancer Lett 235(1):40–47
194. Wang H et al (2018) Cancer radiosensitizers. Trends Pharmacol Sci 39(1):24–48
195. Cheng K et al (2018) Synergistically enhancing the therapeutic effect of radiation therapy with radiation activatable and reactive oxygen species-releasing nanostructures. ACS Nano 12(5):4946–4958
196. Song Z et al (2017) Decorated ultrathin bismuth selenide nanosheets as targeted theranostic agents for in vivo imaging guided cancer radiation therapy. NPG Asia Materials 9(10):e439–e439
197. Song G et al (2016) All-in-one Theranostic Nanoplatform based on hollow TaOx for chelator-free labeling imaging, drug delivery, and synergistically enhanced radiotherapy. Adv Func Mater 26(45):8243–8254
198. Yong Y et al (2017) Polyoxometalate-based Radiosensitization platform for treating hypoxic tumors by attenuating radioresistance and enhancing radiation response ACS Nano 11(7):7164–7176
199. Jiang W et al (2021) Considerations for designing preclinical cancer immune nanomedicine studies. Nat Nanotechnol 16(1):6–15
200. Xiao Q et al (2013) A core/satellite multifunctional nanotheranostic for in vivo imaging and tumor eradication by radiation/photothermal synergistic therapy. J Am Chem Soc 135(35):13041–13048
201. Fan W, Yung BC, Chen X (2018) Stimuli-responsive NO release for on-demand gas-sensitized synergistic cancer therapy. Angew Chem Int Ed 57(28):8383–8394
202. Fan W et al (2015) X-ray radiation-controlled NO-release for on-demand depth-independent hypoxic radiosensitization. Angew Chem Int Ed 54(47):14026–14030
203. Quandt D et al (2011) B7–h4 expression in human melanoma: its association with patients' survival and antitumor immune response. Clin Cancer Res 17(10):3100–3111
204. Liu F, Lou J, Hristov D (2017) X-Ray responsive nanoparticles with triggered release of nitrite, a precursor of reactive nitrogen species, for enhanced cancer radiosensitization. Nanoscale 9(38):14627–14634
205. Preethy P et al (2014) Correction to multifunctional Albumin-MnO 2 nanoparticles modulate solid tumor microenvironment by attenuating Hypoxia, Acidosis, vascular endothelial growth factor and enhance radiation response. ACS Nano 8(6):3202–3212
206. Meng L et al (2018) Tumor oxygenation and hypoxia inducible factor-1 functional inhibition via a reactive oxygen species responsive nanoplatform for enhancing radiation therapy and abscopal effects. ACS Nano 12(8):8308–8322
207. Yi X et al (2016) Core–shell Au@ MnO_2 nanoparticles for enhanced radiotherapy via improving the tumor oxygenation. Nano Res 9(11):3267–3278
208. Gao M et al (2017) Erythrocyte-membrane-enveloped perfluorocarbon as nanoscale artificial red blood cells to relieve tumor hypoxia and enhance cancer radiotherapy. Adv Mater 29(35):1701429
209. Murayama C et al (2012) Liposome-encapsulated hemoglobin ameliorates tumor hypoxia and enhances radiation therapy to suppress tumor growth in mice. Artif Organs 36(2):170–177
210. Eisenbrey JR et al (2018) Sensitization of hypoxic tumors to radiation therapy using ultrasound-sensitive oxygen microbubbles. Inte J Radiat Oncol* Biology* Phys 101(1):88–96
211. Wang S et al (2015) A facile one-pot synthesis of a two-dimensional MoS2/Bi2S3 composite theranostic nanosystem for multi-modality tumor imaging and therapy. Adv Mater 27(17):2775–2782
212. Singh V et al (2012) A facile synthesis of PLGA encapsulated cerium oxide nanoparticles: release kinetics and biological activity. Nanoscale 4(8):2597–2605
213. Asati A et al (2009) Oxidase-like activity of polymer-coated cerium oxide nanoparticles. Angew Chem 121(13):2344–2348
214. Tarnuzzer RW et al (2005) Vacancy engineered ceria nanostructures for protection from radiation-induced cellular damage. Nano Lett 5(12):2573–2577

215. Colon J et al (2010) Cerium oxide nanoparticles protect gastrointestinal epithelium from radiation-induced damage by reduction of reactive oxygen species and upregulation of superoxide dismutase 2. Nanomed Nanotechnol Biol Med 6(5):698–705
216. Zhang X-D et al (2016) Highly catalytic nanodots with renal clearance for radiation protection. ACS Nano 10(4):4511–4519
217. Bai X et al (2017) Ultrasmall WS2 quantum dots with visible fluorescence for protection of cells and animal models from radiation-induced damages. ACS Biomater Sci Eng 3(3):460–470
218. Wang JY et al (2018) Hollow PtPdRh nanocubes with enhanced catalytic activities for in vivo clearance of radiation-induced ROS via surface-mediated bond breaking. Small 14(13):1703736
219. Dadachova E, Casadevall A (2008) Ionizing radiation: how fungi cope, adapt, and exploit with the help of melanin. Curr Opin Microbiol 11(6):525–531
220. Schweitzer AD et al (2009) Physico-chemical evaluation of rationally designed melanins as novel nature-inspired radioprotectors. PLoS ONE 4(9):e7229
221. Abou-Shady H et al (2015) Melanin Nanoparticles (MNPs) provide protection against whole-body ɣ-irradiation in mice via restoration of hematopoietic tissues. Molecul Cellul Biochem, 399
222. Fan W et al (2017) Nanotechnology for multimodal synergistic cancer therapy. Chem Rev 117(22):13566–13638
223. Fan W et al (2013) Rattle-structured multifunctional nanotheranostics for synergetic chemo-/radiotherapy and simultaneous magnetic/luminescent dual-mode imaging. J Am Chem Soc 135(17):6494–6503
224. Fan W et al (2015) Design of an intelligent sub-50 nm nuclear-targeting nanotheranostic system for imaging guided intranuclear radiosensitization. Chem Sci 6(3):1747–1753
225. Gao S et al (2020) Nanoparticles encapsulating nitrosylated maytansine to enhance radiation therapy. ACS Nano 14(2):1468–1481
226. Du J et al (2017) Poly (Vinylpyrollidone)-and selenocysteine-modified Bi2Se3 nanoparticles enhance radiotherapy efficacy in tumors and promote radioprotection in normal tissues. Adv Mater 29(34):1701268
227. Lu N et al (2018) Biodegradable Hollow Mesoporous Organosilica Nanotheranostics for Mild Hyperthermia-Induced Bubble-Enhanced Oxygen-Sensitized Radiotherapy ACS Nano 12:1580–1591
228. Liu J et al (2015) ACS Nano 9:696 CrossRef PubMed; (b) Song G, Liang C, Gong H, Li M, Zheng X, Cheng L, Yang K, Jiang X, Liu Z (2015) Adv Mater 27:6110
229. Herrera FG, Bourhis J, Coukos G (2017) Radiotherapy combination opportunities leveraging immunity for the next oncology practice. CA: Cancer J Clinicians 67(1):65–85
230. Mellman I, Coukos G, Dranoff G (2011) Cancer immunotherapy comes of age. Nature 480(7378):480–489
231. Curiel TJ et al (2004) Specific recruitment of regulatory T cells in ovarian carcinoma fosters immune privilege and predicts reduced survival. Nat Med 10(9):942–949
232. Kono K et al (2006) CD4 (+) CD25 high regulatory T cells increase with tumor stage in patients with gastric and esophageal cancers. Cancer Immunol Immunother 55(9):1064–1071
233. Kooi S et al (1996) HLA class I expression on human ovarian carcinoma cells correlates with T-Cell Infiltrationin Vivoand T-cell Expansionin Vitroin low concentrations of recombinant interleukin-2. Cell Immunol 174(2):116–128
234. Hamanishi J et al (2007) Programmed cell death 1 ligand 1 and tumor-infiltrating CD8+ T lymphocytes are prognostic factors of human ovarian cancer. Proc Natl Acad Sci 104(9):3360–3365
235. Liu X et al (2010) Selective inhibition of IDO1 effectively regulates mediators of antitumor immunity. Blood J Amer Soc Hematol 115(17):3520–3530
236. Garg AD et al (2010) Photodynamic therapy: illuminating the road from cell death towards anti-tumour immunity. Apoptosis 15(9):1050–1071

237. Chao Y et al (2018) Combined local immunostimulatory radioisotope therapy and systemic immune checkpoint blockade imparts potent antitumour responses. Nature Biomed Eng 2(8):611–621
238. Xia D et al (2020) Au–hemoglobin loaded platelet alleviating tumor Hypoxia and enhancing the radiotherapy effect with low-dose X-ray. ACS Nano 14(11):15654–15668
239. Gong T et al (2020) Full-Process Radiosensitization based on nanoscale metal-organic frameworks. ACS Nano 14(3):3032–3040
240. Wang JT-W et al (2019) Neutron activated 153Sm sealed in carbon nanocapsules for in vivo imaging and tumor radiotherapy. ACS Nano 14(1):129–141
241. Sun Q et al (2017) Rational design of cancer nanomedicine: nanoproperty integration and synchronization. Adv Mater 29(14):1606628
242. Peynshaert K et al (2014) Exploiting intrinsic nanoparticle toxicity: the pros and cons of nanoparticle-induced autophagy in biomedical research. Chem Rev 114(15):7581–7609
243. Fadeel B et al (2018) Advanced tools for the safety assessment of nanomaterials. Nat Nanotechnol 13(7):537–543
244. Bourquin J et al (2018) Biodistribution, clearance, and long-term fate of clinically relevant nanomaterials. Adv Mater 30(19):1704307
245. Zhou R et al (2020) Suppressing the radiation-induced corrosion of bismuth nanoparticles for enhanced synergistic cancer radiophototherapy. ACS Nano 14(10):13016–13029
246. Pan X et al (2018) Metal–organic-framework-derived carbon nanostructure augmented sonodynamic cancer therapy. Adv Mater 30(23):1800180
247. Dugger SA, Platt A, Goldstein DB (2018) Drug development in the era of precision medicine. Nat Rev Drug Discovery 17(3):183–196
248. Wang X et al (2018) A highly stretchable transparent self-powered triboelectric tactile sensor with metallized nanofibers for wearable electronics. Adv Mater 30(12):1706738
249. von Roemeling C et al (2017) Breaking down the barriers to precision cancer nanomedicine. Trends Biotechnol 35(2):159–171
250. Dehui D, Duchesne Paul N, Peng Z, Jigang Z, Litao S, Jianqi L, Xiulian P, Xinhe B (2015) A single iron site confined in a graphene matrix for the catalytic oxidation of benzene at room temperature. Science Adv 1(11):e1500462
251. Bonvalot S et al (2014) Phase I study of NBTXR3 nanoparticles, in patients with advanced soft tissue sarcoma (STS). Amer Soc Clin Oncol J. of Clinical Oncology 32(15):10563
252. Bonvalot S et al (2017) First-in-human study testing a new radioenhancer using nanoparticles (NBTXR3) activated by radiation therapy in patients with locally advanced soft tissue sarcomas. Clin Cancer Res 23(4):908–917
253. Bonvalot S et al (2019) NBTXR3, a first-in-class radioenhancer hafnium oxide nanoparticle, plus radiotherapy versus radiotherapy alone in patients with locally advanced soft-tissue sarcoma (Act. In. Sarc): a multicentre, phase 2–3, randomised, controlled trial. Lancet Oncol 20(8):1148–1159